INTERNATIONAL SOLVENT EXTRACTION CONFERENCE

ISEC'80

PROCEEDINGS

1

- Plenary lectures
1. Organic Reagents
2. Mass Transfer
3. Dispersion
4. Equipment
5. Modelling
6. Fundamentals and Chemistry of Solvent Extraction

INTERNATIONAL SOLVENT EXTRACTION CONFERENCE

ISEC´80

LIEGE-BELGIUM
6-12 september

1

ISEC'80

The International Solvent Extraction Conferences, in abbreviated form ISEC, became in two decennia an important scientific event : a great diversity of chemists and engineers from the industrial world and from universities are gathering every three years to discuss of an apparently simple subject : solvent extraction. Solvent extraction now covers a wide variety of topics : industrial processes for the separation of organic and inorganic materials, investigations in solution chemistry and analytical applications, a field which has been expanding lately with the development of high performance liquid chromatography. The considerable success of the ISEC Conferences shows itself in the ever increasing number of communications presented and in the growing diversity of applications proposed.

When delivering its welcome address to an audience of 450 delegates during ISEC'77 in Toronto, Dr. A.W. Ashbrook ended its speech with the few words which follows : "it is now up to you, the delegates, to determine the success of the Conference in providing the stimulus and directions in the field of solvent extraction for the next three years when the results can be reported at ISEC'80". This call for progress has been heard as can be judged by the vastness of the scientifif program : four plenary sessions, two panel discussions, more than two hundred contributed papers allocated to oral or poster sessions. The organizers of the Toronto Conference seemed to worry about the fact that specialists in the field of solvent extraction showed an exaggerated fondness for copper and the oximes. This situation appears to have evolued favourably : around half of the communicationd presented during ISEC'80 deal with the extraction of a great variety of metals. It must be pointed out however that a majority of these contributions are devoted, as in the past, to the nuclear field. This situation appears normal, and in fact desirable, because it should not be overlooked that the development of nuclear power plants is considerably hampered by security problems related to fuel reprocessing and waste disposal. Solvent extraction plays a role of prime importance in the solution of these problems.

It is traditional to publish the proceedings of the ISEC Conferences. The Organizing Committee of ISEC'80 wanted not only to keep this tradition but also to deliver to all participants at the outset of the meeting the three volume of proceedings containing the texts of the plenary lecture and of the contributed papers. It is for me both a duty and a pleasure to thank cordially on behalf of the Organizing Committee all those

who made a handsome contribution to the fruition of this plan : first of all, the authors of plenary papers and communications who had to comply with the prescribed delays, the Co-Chairmen because of the quality of the work they carried out in selecting and correcting the manuscripts, and last but not least, Mr. R. Deprez, Honorary General Secretary of the Association of Engineers of the University of Liège and Dr. J.F. Desreux, scientific secretary of the Conference. Both of them devoted all their energy to the planning of the Conference.

For my part, I have to ask the reader to forgive us for the imperfections he might find in the Proceedings. I am confident that the availablility of the proceedings will lead to more complete exchanges of views between the participants of the Conference. The advantage gained should offset the inconveniences caused by some imperfections in the presentation of the proceedings.

The organization of ISEC'80 in the City of Liège would have not been possible without the patronage and the financial support of the Association of the Engineers of the University of Liège, the Administration Council of the University of Liège, the Ministry of Education and of French Culture and the National Science Foundation of Belgium. The Belgian Chemical Society, the belgian section of the Society of Chemical Industry, Benelux Metallurgie, the Koninklije Vlaamse Ingenieursvereniging and the European Federation of Chemical Engineering also accepted to grant us their support.

The members of the International Advisory Committee and of the Belgian Advisory Committee were particularly helpful in planning the scientific program. I want to thank them all heartily.

Finally, I would like to offer my sincere thanks, on behalf of the Organizing Committee to professor C. Hanson who gave us the benefit of his advices in so many occasions.

Professor G. DUYCKAERTS

INTERNATIONAL SOLVENT EXTRACTION CONFERENCE ISEC'80 LIEGE-BELGIUM 6-12 SEPTEMBER 1980

Conference Chairmen

L. Delvaux (University of Liège)
G. Duyckaerts (University of Liège)
C. Ek (University of Liège)
A. Lefèbvre (University of Liège)
G. L'Homme (University of Liège)
A. Van Peteghem (Metallurgie Hoboken - Overpelt)

International Advisory Committee

R.B. Akell (du Pont de Nemours, Wilmington, U.S.A.)
A.W. Ashbrook (Eldorado Nuclear Ltd., Ottawa, Canada)
A. Chesné (Commissariat à l'Energie Atomique, Fontenay-aux-roses, France)
H. Freiser (University of Arizona, Tucson, U.S.A.)
C. Hanson (University of Bradford, U.K.)
S. Hartland (E.T.H., Zurich, Switzerland)
A.S. Kertes (the Hebrew University, Jerusalem, Israel)
P. Lloyd (Chamber of Mines, Research Organisation, Johannesbourg, South Africa)
T. Misek (Research Inst. of Chemical Equipment, Prague, Czechoslovakia)
H.R.C. Pratt (University of Melbourne, Australia)
K.H. Reissinger (Bayer, Leverkusen, West Germany)
G.M. Ritcey (Canada Center for Mineral and Energy Technology, Ottawa, Canada)
J. Rydberg (Chalmers University, Göteborg, Sweden)
T. Sato (Shizuoka University, Hamamatsu, Japan)
G. A. Yagodin (Mendeleev Institute, Moscow, U.S.S.R.)
Y. A. Zolotov (Vernadsky Institute, Moscow, U.S.S.R.)
M. Zifferero (Comitato Nazionale de l'Energia Nucleare, Rome, Italy)

Belgian Advisory Committee

F. Alderweireldt (University of Antwerpen)
J. Brach (Sover, Andrimont)
A. Cottenie (University of Gent)
J. De Cuyper (University of Louvain)
E. Detilleux (Eurochimie, Mol)
R. Jottrand (University of Bruxelles)
R. Nonnon (Centre d'Information du Cuivre, Bruxelles)
T. Pitance (Vieille Montagne, Angleur)
J. Roos (University of Leuven)
A.P. Van Peteghem (University of Gent)
S. Wajc (University of Brussels)
A. Winand (University of Brussels)

Association des Ingénieurs sortis de l'Université de Liège. A.I.Lg.

Ch. Massonnet - Président
A. Firket - Secretary
R. Deprez - Honorary Secretary
M. Read - Secretary of the section of Liège

Conférence Secretariat

R. Deprez
J.F. Desreux
J. Fuger (Poster sessions)
R. Lemaire (Meeting coordinator)

Edition : Association des Ingénieurs sortis de l'Université de Liège - A.I.Lg, 22, rue Forgeur, B-4000 Liège.

PLENARY LECTURES

SOLVENT EXTRACTION : WHERE NEXT?

Professor C. Hanson,
Schools of Chemical Engineering,
University of Bradford,
Bradford, West Yorkshire,
England.

It is not the object of this paper in any way to purport to predict the future of solvent extraction. ISEC '80, however, seems an appropriate time to take stock of the position of both the science and technology of the subject and to offer some thoughts on where attention might best be concentrated in the future so as to exploit the potentialities of the technique as effectively as possible.

What, then, have been the achievements of solvent extraction so far? One could answer, perhaps somewhat flippantly, that it has helped provide society with atomic bombs, colour televisions and kerosene which burns without a smoky flame. Yet the achievement of each of these, significant goals in themselves, has demanded much research. The utility of the resultant knowledge, however, has not been restricted to these areas. As is so often the case, once it was established, other applications arose. Looking back over the last twenty years, there has been a remarkable expansion of interest in solvent extraction, coupled with a rapid growth of its applications in industry. The same rate of growth cannot be expected to continue indefinitely. With any subject, the rate of initial growth is rapid but it later enters a more mature phase. The questions still requiring study may then appear more detailed or academic, although possibly remaining of economic significance.

Solvent extraction is complementary to most other separation techniques in achieving separations through molecular interactions and therefore on the basis of chemical type rather than molecular size. It exploits chemistry to a greater extent and its successful application on an industrial scale demands a collaborative effort between both chemists and chemical engineers. Unfortunately, there is a danger in the scientific community of compartmentalising different disciplines and one of the achievements of the ISEC conferences has been the provision of an effective meeting point for all those with a contribution to make in either the science or technology of solvent extraction.

There are three broad facets which have to be considered when approaching any potential application of the technique:

1. The development and design of the process. This involves selection or development of a solvent system, demanding consideration of both equilibrium and kinetic data.
2. The selection and design of the optimum contactor for the system, bearing in mind the degree of separation required, and the rate of interphase transfer and the need for stable operating characteristics.

3. Interaction of the solvent extraction unit with other parts of the overall plant and with the environment. It should aim to be a good neighbour.

These are all subject, of course, to the final overall criterion: the degree of economic success achieved. Even the most technically sophisticated and clever processes are bound to fail unless they offer economic advantage over alternatives. This economic theme figured in the panel discussion at the close of ISEC '66. Warner(1) pointed out then that the economics of many metals extraction processes are dominated by the cost of reagents necessary for chemical conditioning to provide reversal of the process for solvent recovery. An essentially analogous conclusion was reached by Jeffreys and co-workers(2,3) for those processes where solvent recovery is by distillation rather than chemical conditioning: the solvent recovery operation can be critical in terms of economic success. It is also relevant to recall a comment made by Lloyd(4) in the same panel discussion at ISEC '66. There is a cost involved in driving a mole of material from one phase to another, the cost per mole being relatively constant for different metals across a liquid-liquid interface. This means that metals high in the periodic table are at an advantage and also gives incentive for attempts to actually extract minority components, so minimising the moles of material needing to be transported between phases. The literature on solvent extraction economics remains limited but it is important to remember, when considering the many technical developments which have taken place, that this is the criterion of ultimate success or failure.

THE PROCESS

The Ideal Process

The selection or development of any real process is bound to demand compromise. While no actual case is likely to encompass them all, the attributes of an ideal process might include:

(a) Only a small number of contacting stages (or transfer units) required to extract the desired proportion of solute from the feed.

(b) High selectivity for the desired solute, thus eliminating the need for scrubbing or extract reflux.

(c) Operation with concentrated streams.

(d) Rapid extraction and phase separation.

(e) Easy reversal and solvent recovery with a low energy requirement (either chemical or thermal).

(f) Insensitivity to up-stream operations.

(g) Low solvent losses and an absence of need to provide for solvent recovery from exit streams.

(h) Operation at ambient temperature and pressure.

(i) High level of safety.

These suggested attributes are not in any order of relative importance. Most would contribute to a compact plant and to minimising capital cost. (b),(e),(g) and, possibly, (c),(f),(h) would also influence operating costs.

They lead to attributes for an ideal solvent. These would be both high capacity and selectivity (high values of distribution coefficient and separation factor) to meet points (a) and (b). The solvent should have a low solubility in the raffinate phase [a contribution to (g): losses also arise in the raffinate from entrainment] but a high solvency for the solute or solute-extractant complex to allow operation with concentrated streams without danger of third-phase formation. The importance of reversibility/recoverability has already been stressed. Chemical stability under the conditions of use is also important, not only because of the cost of replacement but also the deleterious effects the decomposition products might have on the process. Desirable physical properties for ease of phase interdispersion coupled with fast phase separation are low viscosity and medium interfacial tension (the latter obviously has to be a compromise between the two requirements). The rate of interphase transfer may also depend on the kinetics of any chemical interaction involved. This aspect will be considered in more detail later but one ideally seeks a high kinetic rate for the desired solute.

Turning to commercial considerations, an ideal solvent would be both cheap and readily available from a number of alternative sources. However, it must be stressed that purchase price is by no means the final arbiter between two possible solvents. Thus hydroxyoximes have been commercially successful as copper extractants despite their comparatively high price, while much cheaper carboxylic acids have not so far been adopted because of the greater reagent cost for chemical conditioning to achieve a reversible cycle(5). Safety is obviously of prime importance and demands both low toxicity and high flash point as features to be sought.

Operation at ambient temperature and pressure were listed amongst the attributes of an ideal process since they keep down both capital cost and operational complexity. Most industrial solvent extraction processes do currently operate under ambient conditions. While this is undoubtedly convenient, it must be remembered that temperature is a possible variable. There are instances in which the advantages of operating other than at ambient temperature outweigh the additional plant complexities introduced. In addition, even if a plant is to operate at ambient temperature, processes can be sufficiently sensitive to this parameter that consideration should be given to it at the design stage because of the variations which will arise with time of day and season.

Temperature can be expected to influence three factors: the position of equilibrium (the distribution coefficient), the rate of interphase transfer and the rate of phase separation. Increase in temperature is likely to increase both rates. Its effect on the position of equilibrium will depend on heat effects (if any) during interphase transfer. There often are such effects but there have been comparatively few attempts to date to exploit them. One exception is in some uranium purification plants(6). Forward extraction of uranium into tri-n-butyl phosphate is exothermic. Increase in temperature therefore favours the reverse reaction, depressing the distribution coefficient. This is exploited by operating the stripping section at an elevated temperature of 60^{o}C, allowing stripping to be achieved with a lower aqueous/organic flow ratio, so giving a more concentrated product.

Since the additional plant complexity is not great and heating to temperatures such as 60^{o}C only requires low pressure processes steam, the question arises whether operation at non-ambient temperature could be adopted

with advantage in other cases. This seems quite likely and optimum operating temperature is certainly a parameter to consider at the design stage. It provides interesting possibilities in respect of scrubbing operations where operation at elevated temperature may allow reduction in either the number of stages or the scrub/extract flow ratio. The latter would be particularly advantageous in cases where some of the product is recycled as scrub in that it would reduce the cost of solute/solvent separation per unit of solute produced.

The thermochemistry of solvent extraction has been comparatively neglected and appears to be a subject worthy of further study. Not only is there the potential exploitation of thermal effects in process design, as discussed above, but also the fact that such studies should be capable of throwing more light on the interactions involved in the extraction process and on the rate controlling mechanisms.

Equilibria

The study of equilibria is necessary for two reasons: the data are essential for flowsheet design and the form of the data can throw light on the interactions involved. For the former purpose, there would be great attraction in being able to predict or, at least, correlate equilibrium data. The winning of such data is a relatively time-consuming operation. In many systems, particularly involving metals, the distribution coefficient for one solute is a function of the concentrations of others. Process design demands a knowledge of the coefficient under the particular conditions applicable. A full matrix of experimental points to allow such data to be estimated with only minimal interpolation represents a large financial investment. The possibility of reducing the experimental work required gives commercial incentive to attempts at correlating such data. Such correlations are also essential for modelling the dynamics of commercial plants, either for their study or as a prelude to some more sophisticated control system.

Attempts at modelling equilibrium data can be divided into two broad categories: those applicable to systems with only physical interactions and those designed for systems involving clearly defined chemical complex formation.

The approach for systems involving only physical interactions is inevitably based on thermodynamic considerations, following analogous lines to those adopted for liquid-vapour equilibria, using activity coefficient models such as NRTL and UNIQUAC(7). A computerised data bank has been developed, incorporating parameters for these equations(8). The approach has been used with real success for binary and ternary systems. It has also been used for some multi-component systems. These are clearly more complex but there is promise that the approach will yield practicable methods.

For metals systems(9,10) involving chemical interactions, models have been proposed based on the interactions, although they have not so far been noticeably more successful than empirical or semi-empirical approaches.

While the above represent a really significant advance over the last decade, there is ample need for further work, particularly on multi-solute systems.

Kinetics

Until comparatively recently, chemical engineers viewed the rates of solvent extraction processes as being dependent only on diffusional resistances, subsequently applying methods of analysis analogous to those used for distillation or gas absorption. This is doubtless valid for those processes which depend on physical interactions. Yet a significant and important number of solvent extraction processes are based on a clearly defined and stoichieometric chemical interaction between the solute and either the solvent as such or an extractant within the solvent phase. Such processes are examples of mass transfer with simultaneous chemical reaction. Their rates may depend, to different degrees, on both diffusional resistances and the kinetics of the chemical reaction. Many processes involving metals extraction fall into this category, as was pointed out at an earlier solvent extraction conference in Belgium(11), and much interest has been expressed in the subject during the 1970s. Work has been concentrated primarily on copper and uranium.

Considering copper first, incentive for the study has come from the successful commercial use of hydroxyoxime-type extractants on a very large scale. Extraction rates with the original extractants are only modest, leading to the need for quite high residence times when using conventional mixer-settlers with single compartment mixers (3 minutes in a mixer is typical). The cost involved in providing such a residence time on this scale of operation gave ample incentive for seeking a better understanding of the rate limiting steps. The results of several major investigations are now available. Time does not allow a full review but a number of general points arise.

Except for a process taking place homogeneously throughout one phase at a rate determined solely by the kinetics of the solute-extractant interaction, the rate of interphase transfer will be a function of interfacial area. A full insight into the process therefore demands rate data for known interfacial areas. While early work with the AKUFVE and other stirred cell contactors gave interesting information on the dependence of rate on various concentration terms, it could not include interfacial area as a parameter. Other workers have sought to do this with a variety of alternative techniques, including single drops, fixed interfacial area cells of the Lewis type, laminar jets and the rotating disc electrode. All have contributed something to our knowledge but all have limitations if the ultimate aim is to produce data relevant to the performance or design of an industrial contactor. Thus with single drops rising or falling through a continuous phase, there is a degree of uncertainty as to the hydrodynamic regime, particularly in the drop phase. Devices operating under laminar conditions should give data which will fit models incorporating molecular diffusivities, the only diffusion data easily measured. However, work in the analogous field of aromatic nitration has shown how models incorporating molecular diffusivities do not correctly predict rates in stirred tanks typical of industrial reactors(12), although good agreement is obtained under laminar conditions. We still have a considerable way to go before we can truly quantify the relative importance of the various resistances involved in copper extraction in the situation of an industrial contactor.

It should be pointed out that the choice of experimental method and conditions can bias a system towards a particular rate controlling mechanism. Thus the single drop technique, particularly with relatively slow systems

such as copper, yields the initial rate. At the other extreme, the AKUFVE operates very close to equilibrium. It is not perhaps surprising that different results are sometimes obtained. The same is true of metal concentration. The relative magnitudes of the various resistances will not necessarily remain constant over wide ranges of metal concentration.

There is still apparent controversy over the actual locale of the copper-oxime reaction, some workers adopting the view of an interfacial reaction and others believing the reaction to take place in a zone in the aqueous phase adjacent to the interface. This may be due, at least to some extent, to different views of the interface. Some appear to view it as akin to a pseudo-crystalline boundary, while others consider it as a region with some finite thickness.

My own view remains that presented with colleagues at ISEC '77(13), postulating a reaction in a narrow zone in the aqueous phase immediately adjacent to the interface but with a significant (and possibly sometimes dominating) diffusional resistance in a zone (likely to be of greater thickness) on the organic side of the interface.

Moving away from areas of controversy, the kinetic studies have pinpointed at least two significant factors. The first is that the reagents as supplied by the various manufacturers do contain other materials, either added intentionally or present as unconverted intermediates or by-products. The most important of these appears to be nonyl phenol(14). This has a significant influence on both the kinetics and equilibria of complex formation. There are instances in which this can be turned to advantage but it also means that any scientific study of kinetics needs to be conducted with purified reagents.

Secondly, the degree of aggregation of the oxime molecules in the organic phase has been shown to be a significant factor. Dimerisation was suggested several years ago(14) but more recent work has demonstrated that aggregation must proceed beyond the dimer(13). It seems likely that it is only the monomer which takes part in the rate limiting part of the copper extraction process and so the extent of aggregation is an important parameter in determining kinetics. The actual degree of aggregation is a function of temperature, so giving the processes a higher apparent activation energy than would correspond with the rate limiting step itself. It must also be a factor behind the effect of diluent type on rate.

Uranium has been the subject of an interesting recent study on kinetics based on three different experimental methods(16). Despite the cautions expressed above, these appeared to give results in remarkably good agreement. However, the concentration ranges studied were modest.

Reference should also be made to work on nickel(17), again using the rising drop technique. This showed extraction to virtually cease before equilibrium was reached, apparently due to formation of a viscous shell of hydrated nickel-extractant complex within the drop which effectively encapsulated the remaining extractant. Later work(18) has revealed more information on the formation of such interfacial films in both this and other systems. These again can play a part in determining rates of extraction.

With neither copper nor uranium fully understood and with little yet reported on other metals, there remains much scope for further useful work on

kinetics. For example, little is known on differential kinetics. It has been shown that the selectivity of certain hydroxyoximes for copper over iron is helped by this feature: a greater proportion of iron is taken up at very long residence times(19-21). Similar effects could already exist or be exploitable elsewhere. It is another reason why choice of diluent could be important(22). The kinetics of any processes by which impurities are taken up are also of significance for the design of scrubbing operations. It is easy to concentrate all attention on the key solute and to overlook impurities. Yet the rates of their interphase transfer will determine the values of HTU or stage efficiency in any scrubbing section, quite apart from the take-up of the impurities in the extraction section.

While the emphasis above has been on metals extraction processes, chemical interaction is involved in several other applications of solvent extraction, dissociation extraction being an obvious example, and these again should be approached in terms of mass transfer with simultaneous chemical reaction. They do not yet appear to have been the subject of any kinetic studies.

Process Development

It would not be appropriate in this paper to attempt any detailed review of process development. The separation of aromatic from aliphatic hydrocarbons remains one of the largest industrial applications and the last decade has seen some new systems introduced, as well as many new plants based on established processes. However, in terms of large new applications, the 1970s must be seen as the decade for copper and phosphoric acid. In the case of the former, large scale plants have been built in North and South America, Zambia and Australasia to exploit hydroxyoxime extractants on feeds derived from the leaching of both oxide ores and tailings. Quite a significant proportion of the world's copper is now processed hydrometallurgically. The impact of solvent extraction on the phosphoric acid industry has been seen over very much the same period. Early applications were designed to allow acids other than sulphuric to be used for the digestion of phosphate rock. The major expansion, however, has come in the use of the technique to provide a pure fraction from conventional "wet" process acid. This is interesting in that only a proportion of the solute present in the feed is extracted, giving two product streams of markedly different purities. Plants are now in operation for a second purpose in the phosphoric acid industry, that of recovering uranium from impure acid streams. There are two incentives for this: an economic one in terms of the value of the uranium recovered and an environmental one since such acid is subsequently used in the manufacture of fertilizers.

Looking to the future, it seems likely that we will see an escalation of interest in the solvent extraction of uranium. The expansion of nuclear power generation in most industrialised countries will inevitably increase demand for the metal and, later, for nuclear fuel reprocessing. The 1980s will see significant new plant construction in this field. Some of these plants will doubtless involve novel features in terms of equipment, although it seems unlikely that the well-established processes will be challenged.

Elsewhere in the metals field, cobalt and nickel are elements in which much interest has been shown but with applications still limited. In contrast to uranium, this situation can be attributed to the limited systems available and there remains great incentive for the development of new and selective extractants for these metals.

Change in oxidation state provides the key to the separation of plutonium from uranium. The range of metals for which oxidation state can be changed is obviously limited but it nevertheless offers a process design parameter which, like temperature, should not be overlooked.

In terms of process development, metals have claimed much of the limelight over the last decade. However, other areas of potential application must not be neglected. The increasing cost of energy could well make solvent extraction economically attractive for some separations in the general organic chemical field currently achieved by distillation. Differential reactions, as in dissociation extraction, also appear to offer scope for more selective separations and the research which has been conducted during the 1970s could well come to fruition in the form of industrial processes during the 1980s.

While there are processes for the recovery or purification of individual inorganic acids, e.g. phosphoric acid, solvent extraction is also capable of achieving separations between such acids based on their relative strengths. Khan and Pratt(23) have shown how amine salts can be used as extractants for separations such as nitric from phosphoric and nitric from sulphuric acids, the process having the attraction that stripping of the loaded solvent is achieved with water alone, so avoiding the cost of any conditioning agents.

Looking ahead a decade or more, there must inevitably be a switch from oil as the basic raw material of the organic chemical industry. The only alternative likely to meet the needs of the industrialised countries is coal. The move to coal will bring tremendous challenges to all concerned. Quite apart from its potential use in the production of liquid feedstocks from coal(24), there is likely to be need for the versatility of solvent extraction in the processing routes.

THE EQUIPMENT

The Ideal Contactor

The ideal contactor would be compact, flexible, reliable in both design and operation, easily and reliably scaled-up, cheap and safe. As with the ideal process, real situations demand compromise and the concept of an ideal contactor can be an elusive mirage. In essence, there is no such thing as *the* ideal contactor, only the best for a particular system in a given situation. While various criteria have been discussed(25,26), the final choice is a commercial decision and matters such as the degree of confidence that a particular type can be designed and constructed to meet performance specifications or be available when required are likely to dominate the decision, probably taking precedence over considerations such as best performance in terms of minimum HTU or even minimum capital cost. Nevertheless, it is desirable that some reasonably scientific basis should exist for matching contactors to particular processes. Unfortunately, data on the performance of individual contactors published in the literature have been derived with particular systems. Attempts to compare performance of contactors can then be difficult because differences caused by different systems cannot be clearly separated from those inherent in the different equipment. The characterisation of liquid-liquid systems has recently been discussed elsewhere(27).

The overall performance of a particular contactor derives from three factors: its hydrodynamic characteristics, the nature of the system and the phase separation behaviour. In addition to the difficulty of comparing results when different systems have been used, it is important to recognise that both the hydrodynamic and phase separation characteristics are influenced by mass transfer itself. Thus, while it is often convenient to study hydrodynamic features using binary systems at equilibrium, the results may not give a realistic guide to performance under the conditions which would be met in industrial use. This has become increasingly recognised over the last few years, having been demonstrated with axial mixing studies(28).

Mixer-Settlers

Despite the obvious penalties of size (due to the need to separate the phases at each stage) and potential loss of reagents by evaporation (due to the large liquid-air interface), mixer-settlers have remained popular and some very large plants have been built, particularly for hydrometallurgical applications. They offer considerable flexibility in terms of only slow changes in performance with phase flow ratio and rates, thus allowing adaptation to changing feed compositions. They are suitable for systems involving significant chemical kinetic resistances since residence time in the mixer is a simple design parameter. While there is still much uncertainty surrounding the best criteria to adopt for scale-up, it is nevertheless possible to scale-up mixer-settlers with some confidence that the resultant plant will have a useful performance. The presence of solids in the feed has a considerable nuisance value through the creation of crud but the open nature of conventional mixer-settlers does allow for relatively simple clean-up, although at the cost of a plant shut-down.

There have essentially been three aims behind recent work on mixer-settlers: (a) to achieve a reduction in their size, (b) to reduce losses or impurity levels in exit streams caused by entrainment, (c) to obtain better control of phase continuity.

Attempts to reduce size have been aimed at both the mixer and settler compartments. It has been recognised that a single compartment mixer operating close to equilibrium will inevitably demand a long residence time, as with a single compartment continuous reactor. Developments have followed the reactor analogy, leading to interest in both multi-compartment mixers (equivalent to the multi-stage C.F.S.T.R.)(29) and static mixers (equivalent to tubular reactors)(30,31). Both allow some reduction in residence time for the same stage efficiency. The latter has the added attraction of offering a closed system, potentially reducing losses due to evaporation and increasing safety when handling flammable liquids. In the case of settlers, much effort has been put into the use of coalescence aids, particularly of mesh woven with alternate strands of hydrophilic and hydrophobic material (32). Various forms of baffles and trays are also applied(33). Electro-static aids are useful, provided the continuous phase has a low conductivity, and have found application in some types of mixer-settlers. This could well increase in the future.

A better understanding of the performance of mixer-settlers demands a knowledge of the drop size and drop size distribution. While much has been reported in this field, most data have been for much lower values of dispersed phase hold-up than are used in industrial plants. However, methods have been developed to enable measurements to be made at high

hold-ups(34). Similarly, attention has been drawn to the need for the power input to a mixer to exceed a critical value to ensure a uniform hold-up of dispersed phase(35,38). Non-uniformity due to inadequate power input can lead to phase inversion or instability.

Losses of solvent in raffinate streams are of concern for both economic and environmental reasons, while aqueous entrainment in organic extracts can cause enhanced impurity levels in products. Recent research has demonstrated that entrainment can be caused by the design or operation of both mixer and settler compartments.

Entrainment levels increase with increase in mixer impeller speed(36,37). In addition, however, any conditions which lead to formation of localised double dispersions are likely to give high entrainment levels(36) as such double dispersions are not easily separated in conventional gravity settlers. Hence the level of power input must not be reduced to the point where some stratification occurs, giving localised high hold-ups of dispersed phase and possible local inversions(35). Entrainment appears to be a function of phase ratio(36), being minimal in the region of 1:1. Provision is often made for recycle of one phase to maintain the phase flow ratio within a stage at this value. This does increase the total volumetric throughput and it is not clear whether it is always justified. The other purpose of recycle, of course, is to ensure a particular phase continuity since this is another parameter which, in practice, affects both entrainment levels and settler performance. Air entrainment into the dispersion appears to have a significant influence on liquid phase entrainment(37). It is also of interest that entrainment levels vary during the start-up of a mixer-settler, starting high and falling progressively to the steady-state value.

Entrainment can be caused in the settler as well as in the mixer. One source is at the entrance and arises if the dispersion is caused to flow through the coalesced dispersed phase. The other arises from high linear velocities in the coalesced phases, particularly the continuous(29). Such conditions prevent smaller droplets from sedimenting to the coalescence interface. This gives incentive for considering the best geometry of settlers for high capacity plants so as to minimise solvent inventory while keeping linear velocities low.

Column Contactors

The fundamental design basis for column (differential) contactors was thoroughly established in the 1950s. The most important development since then has been recognition of the importance of axial mixing in determining actual performance(39). From this comes a need for design methods which allow for the phenomenon and some useful new proposals have been made in recent years(40-42).

In terms of actual novel contactors, an interesting approach has been the use of gas agitation(43). While only preliminary results have been published to date, these are very encouraging and further developments could well be seen in the future. This also applies to a new mechanically agitated column recently described(44), which aims to reduce axial mixing while maintaining high throughputs.

One of the main challenges in the equipment area is that of scale-up. With most types of column, use of the slip-velocity concept allows fairly

reliable calculation of the diameter required to handle any particular throughput. However, prediction of height required for a given separation is less reliable since virtually no data are available on change in the extent of axial mixing with scale. The systematic investigations reported in the literature have been limited to columns no greater than some 20 cm in diameter. Our understanding of columns would certainly be enhanced if data could be measured and made available on some large scale industrial units (covering drop sizes, dispersed phase hold-up and concentration profiles in both phases) to compare with laboratory columns operating on the same systems.

The scale-up of mechanically agitated columns and the mixers of mixer-settlers is made more uncertain by the fact that the different criteria which might be employed are not compatible.

EXTERNAL INTERACTIONS

Sight must not be lost of the fact that a solvent extraction process will only be one component within a larger complex. It must interface smoothly both up-stream and down-stream, imposing the minimum constraints on the other sections.

Considering up-stream limitations, solvent extraction processes are sensitive to the presence of impurities in a feed, particularly if these are surface active in character. Because of this, it is always wise to undertake pilot plant work with real feeds rather than simulates prepared from pure materials. Looking again at hydrometallurgy, it is important to question whether any floatation agents or flocculents carried through from the early stages of the overall process will be compatible with the solvent extraction section. Solids in the feed to extraction tend to be a problem, certainly in creating crud and thereby increasing solvent losses. This imposes requirements up-stream which can be quite expensive to meet. The incentive for solvent-in-pulp operation remains, although the goal is still elusive in commercial terms.

Down-stream, the prime concern must be with the fate and possible effects of entrained or dissolved solvent. Thus carry-over of organic into electrolysis in a copper circuit produces "burn" on the cathodes. Again, the fact that the depleted electrolyte is used for stripping in the solvent extraction section places severe constraints on the use of smoothing agents to prevent acid mist, since such agents are inevitably surface active in nature and potentially incompatible with extraction. Concern has been expressed at the possible effects of entrained or dissolved solvent in raffinate streams which are discharged into water courses. Little is yet available on the toxicity of common extractants used in the metals field(45). In addition, most raffinates would be subject to some form of conditioning prior to discharge (e.g. neutralisation) which could well remove some or all of any extractant present. Nevertheless, it is an aspect to remember, particularly when considering the implications of possible fault conditions.

In terms of the actual safety of solvent extraction plants and their personnel, the most obvious hazards are toxicity and fire. Many solvents are flammable and there have been at least two major fires in solvent extraction plants in recent years(46,47). A full safety analysis at the design stage is not something to be neglected.

WHERE NEXT?

The purpose of this paper is to set the scene for ISEC '80 and indicate some of the areas of solvent extraction where further work appears justified. Some of the issues may well be clarified during the Conference. It will not be until after all the papers have been read and digested that the direction of future advance can be judged.

REFERENCES

1. Warner, B.F.: in "Solvent Extraction Chemistry", ed. Dyrssen, D. et al., p.635 (North-Holland, Amsterdam, 1967).
2. Jenson, V.G. and Jeffreys, G.V.: Brit.Chem.Eng., 6, 676 (1961).
3. Jeffreys, G.V., Mumford, C.J. and Herridge, M.H.: J.Appl.Chem.Biotechnol., 22, 319 (1972).
4. Lloyd, P.J.: in "Solvent Extraction Chemistry", ed. Dyrssen, D. et al., p.642 (North-Holland, Amsterdam, 1967).
5. Cahalan, M.J.: Chemy.Ind., 1590 (1967).
6. Page, H., Shortis, L.P. and Dukes, J.A.: Trans.Inst.Chem.Engrs., 38, 184 (1960).
7. Sørensen, J.M., Magnussen, T., Rasmussen, P. and Fredenslund, Aa.: Fluid Phase Equilibria, 2, 297 (1979); 3, 47 (1979) and 4, 151 (1980).
8. Sørensen, J.M. and Arlt, W.: "Liquid-Liquid Equilibrium Data Collection", Chemistry Data Series (DECHEMA, Frankfurt, 1979).
9. Forrest, C. and Hughes, M.A.: Hydrometallurgy, 1, 25 (1975).
10. Hughes, M.A., Andersson, S. and Forrest, C.: Internat.Jl.Min.Proc., 2, 267 (1975).
11. Hanson, C.: Het.Ingenieursblad., 41, 408 (1972).
12. Giles, J., Hanson, C. and Ismail, H.A.M.: Chapter 12 in "Industrial and Laboratory Nitrations", ed. Albright, L.F. and Hanson, C. (Am.Chem.Soc. Symposium Series, 1976).
13. Whewell, R.J., Hughes, M.A. and Hanson, C.: Proceedings ISEC '77, p.185 (C.I.M., Montreal, 1979).
14. Hanson, C., Hughes, M.A., Preston, J.S. and Whewell, R.J.: J.Inorg. Nucl.Chem., 38, 2306 (1976).
15. Price, R. and Tumilty, J.A.: Paper 18, Inst.Chem.Engrs. Symposium Series No.42 (London, 1975).
16. Horner, D., Mallen, J., Thiel, S., Scott, T. and Yates, R.: Ind.Eng. Chem.Fundam., 19, 103 (1980).
17. Durrani, K., Hanson, C. and Hughes, M.A.: Metallurgical Transactions, 8B, 169 (1977).
18. Hughes, M.A.: Hydrometallurgy, 3, 85 (1978).
19. Fleming, C.A.: Trans.Inst.Min.Metall., 85, C211 (1976).
20. Fleming, C.A.: Trans.Inst.Min.Metall., 88, C253 (1979).
21. Flett, D.S. and Melling, J.: Trans.Inst.Min.Metall., 88, C256 (1979).

22. Whewell, R.J., Hughes, M.A. and Hanson, C.: in "Advances in Extractive Metallurgy" (Inst.Min.Metall., London, 1977).

23. Khan, I., PhD Thesis, University of Bradford (1980); also U.K. Patent Application 7,911,855 (1979).

24. Davies, G.O.: Chemy.Ind., 560 (1978).

25. Hanson, C.: Chem.Engng., 75 (18), 98 (1968).

26. Reissinger, K.H. and Schröter, J.: Chem.Engng., 85 (25), 109 (1978).

27. Barnea, E.: Hydrometallurgy, 5, 15 (1979).

28. Komasawa, I. and Ingham, J.: Chem.Eng.Sci., 33, 41, 479 and 541 (1978).

29. Orjans, J.R., Notebaart, C.W., Godfrey, J.C., Hanson, C. and Slater, M.J.: Proceedings ISEC '77, p.340 (C.I.M., Montreal, 1979).

30. Godfrey, J.C. and Slater, M.J.: Chemy.Ind., 745 (1978).

31. Merchuk, J.C., Shal, R. and Wolf, D.: Ind.Eng.Chem.Proc.Des.Dev., 19, 91 (1980).

32. Jackson, I.D., Scuffham, J.B., Warwick, G.C.I. and Davies, G.A.: Proceedings ISEC '74, p.567 (S.C.I., London, 1974).

33. Stönner, H.M. and Wöhler, F.: Paper 14, Inst.Chem.Engrs. Symposium Series No.42 (London, 1975).

34. Godfrey, J.C. and Grilc, V.: Proceedings 2nd European Conference on Mixing (BHRA), Cambridge (1977).

35. Godfrey, J.C. and Grilc, V.: Proceedings 3rd European Conference on Mixing (BHRA), York (1979).

36. Rowden, G.A., Scuffham, J.B., Warwick, G.C.I. and Davies, G.A.: Paper 17, Inst.Chem.Engrs. Symposium Series No.42 (London, 1975).

37. Godfrey, J.C., Hanson, C., Slater, M.J. and Tharmalingam, S.: A.I.Ch.E. Symposium Series No.173, p.127 (1978).

38. Skelland, A.H.P. and Seksaria, R.: Ind.Eng.Chem.Proc.Des.Dev., 17, 56 (1978).

39. Ingham, J.: Chapter 8 in "Recent Advances in Liquid-Liquid Extraction", ed. Hanson, C. (Pergamon, Oxford, 1971).

40. Pratt, H.R.C.: Ind.Eng.Chem.Proc.Des.Dev., 14, 74 (1975).

41. Pratt, H.R.C.: Ind.Eng.Chem.Proc.Des.Dev., 15, 34 (1976).

42. Pratt, H.R.C. and Anderson, W.J.: Proceedings ISEC '77, p.242 (C.I.M., Montreal, 1979).

43. Priestley, R. and Ellis, S.R.M.: Chemy.Ind., 757 (1978).

44. Hartland, S.: Paper presented at A.I.Ch.E. Annual Meeting, Philadelphia, June 1980.

45. Ashbrook, A.W., Itzkovitch, I.J. and Sowa, W.: Proceedings ISEC '77, p.781 (C.I.M., Montreal, 1979).

46. Høy-Petersen, R.: "Loss prevention and safety promotion in the process industries", ed. Busch, C.E. (Elsevier, Amsterdam, 1974).

47. Collins, G., Cooper, J.H. and Brandy, M.R.: E/MJ, 59, Dec.1978.

KINETICS OF SOLVENT EXTRACTION OF METAL CHELATES

Henry Freiser
Department of Chemistry
University of Arizona
Tucson, Arizona 85721
U.S.A.

Study of extraction kinetics of a number of metal chelate systems under conditions of rapid phase mixing serve to show that the rate-determining step(s) in the overall extraction process is the formation of the metal chelate in the aqueous phase. This was observed in this chloroform extraction of Cd^{2+},Zn^{2+},Co^{2+}, and Ni^{2+} by diphenylthiocarbazone (dithizone) and a series of substituted analogues and of Ni by 2,2'-dipyridyl and 1,10-phenanthroline. In addition to these systems of primarily analytical interest, examination of the kinetics of the extraction of Cu^{2} by the hydroxyoximes, LIX65 and LIX63, used in process scale separation reveals that aqueous phase formation of the metal complex rather than interfacial phenomena, is the rate limiting part of the extraction. The significance of these findings in the design of new extractants is discussed.

INTRODUCTION

Extraction processes involving chelating extractants have long enjoyed an important role in metal ion separations. A great deal of research has been carried out devoted to both fundamental extraction equilibria as well as to analytical applications. Within the last twenty years, chelating extraction systems have also been employed in commercial process scale metal ion separations. Study of the kinetic aspects of metal chelate extractions, begun in our Laboratory almost twenty years ago, addresses itself to resolution of questions, of both fundamental and practical interest, all focussing on resolution of the ultimate problem of uncovering the important factors to consider in designing new extractants of improved characteristics? Some of the kinetic questions involved include:- Under conditions of reasonably vigorous phase mixing, are mass transfer processes or chemical reactions rate-limiting? How do mass transfer characteristics change with increasing molecular weight of extractant? Does the nature of the rate-limiting step, i.e. the mechanism, change as the molecular weight and, therefore, the hydrophobicity of the extractant increases? In this report, our efforts to answer these questions over the last two decades will be described.

DITHIZONES

Rates of extractions of divalent cadmium, zinc, cobalt, and nickel ions from buffered aqueous solutions by chloroform solutions of dithizone can be described by the following expression (1,2)

$$\frac{d[M^{2+}]}{dt} = \frac{k'[M^{2+}][HDz]_{org.}}{[H+]} \qquad (1)$$

The extractions were carried out at shaking rates such that the extent of extraction was independent of shaking rate. Also, in the case of zinc, when CCl_4 was substituted for $CHCl_3$ in one series of runs, the increase of extractions rate observed was quantitatively predicted from the change of the K_{DR} of dithizone in the two solvent [1]. Thus, it was established that a homogeneous chemical reaction, rather than mass transfer of either the dithizone or the chelate, was rate determining. The kinetics of these reactions were followed by both radioisotope tagging of the metal ion (Cd, Zn, Co) and spectrophotometric assay (Ni). It was deduced from eq. (1) that the formation of the 1 : 1 metal complex was rate determining:

$$M^{2+} + Dz^- \xrightarrow{k} MDz^+$$

and the second order rate constant, k, was evaluated from k' as

$$k = k' \frac{K_{DR}}{K_a}, \qquad (2)$$

where K_{DR} is the distribution coefficient of dithizone between $CHCl_3$ and the aqueous medium and K_a is the acid dissociation constant of dithizone.

That the mechanism of chelate formation is related to dissociation of water coordinates to the metal ion, can be seen from the comparison of our data with those obtained by Eigen (Table 1). The rates of these two reactions differ by an almost constant factor (approximately 1 log unit).

TABLE 1 - Comparison of second order rate constants for formation of 1 : 1 metal chelates of diphenylthiocarbazone (dithizone) and of di-(o-tolyl)-thiocarbazone with the first order rate constant of water dissociation of the hydrated metal ions.

Metal Ion	Rate Constant For Water Dissociation (3) (sec^{-1})	Rate Constant of ML^+ Formation ($M^{-1}sec^{-1}$)	
		Dithizone	o-Methyl Derivative
Cd^{2+}	6.0×10^8	$>10^7$	-
Zn^{2+}	5.0×10^7	6.1×10^6	7.5×10^6
Co^{2+}	5.0×10^5	6.7×10^4	-
Ni^{2+}	2.0×10^4	1.3×10^3	5.2×10^3

In the case of zinc ion, it is possible that the formation of the 1:1 complex first occurs rapidly with retention of the coordination number of six followed by a slow,rate-determining, loss of water as zinc becomes tetra-coordinate.

$$Zn(H_2O)_6^{2+} + Dz^- \underset{\leftarrow}{\overset{K}{\rightarrow}} Zn(H_2O)_4D^+z + 2H_2O,$$

$$Zn(H_2O)_4D\overset{+}{z} \overset{k}{\rightarrow} Zn(H_2O)_2D\overset{+}{z} + 2H_2O.$$

This postulated mechanism accounts for the unexpectedly rapid rate observed (2) with the di-(o-tolyl)-thiocarbazone whose 1 : 1 zinc chelate is almost 50 times less stable than that of dithizone (4). In a related study, the rate of formation of the zinc complex of di-(1-naphthyl)-thiocarbazone, about 100 times less stable than that with dithizone, was also found to be more rapid than that of dithizone (2). These findings strengthen the mechanism postulated above since the presence of sterically hindering methyl or aromatic ring substituents would be expected to weaken the metal-water bonds and facilitate the loss of water.

Alternatively, the reaction might involve a rapid ion association of the hydrated metal ion with the ligand anion:

$$M(H_2O)_q^{n+} + L^- \underset{\leftarrow}{\overset{K}{\rightarrow}} (M(H_2O)_q^{n+}, L^-),$$

which slowly loses water to form the 1:1 complex:

$$(M(H_2O)_q^{n+}, L^-) \overset{k}{\rightarrow} ML(H_2O)_{q-a}^{(n-1)+} + aH_2O.$$

This mechanism is attractive in that it does not require a net change in coordination number.

Because the extraction rates of the zinc and nickel of the o-methyl derivative were faster than that of dithizone itself, we decided to examine the extraction kinetic behavior of a series of both electron-withdrawing and-releasing substituted dithizones. (7).

The kinetics of extraction of zinc and nickel with $CHCl_3$ solutions of the following substituted diphenylthiocarbazones were investigated: di-p-fluoro-, di-p-chloro-, di-p-bromo-, di-p-iodo-. di-m-trifluoromethyl-, di-p-methyl-, di-p-methoxyphenylthiocarbazones. Each reaction was first - order in metal ion and reagent but inverse first-order in hydrogen ion, which signifies that the formation of the 1 to 1 metal-ligand complex in the aqueous phase is rate-determining.

The rate constants of the formation of the 1 to 1 metal complexes are all more rapid than that for the complex with the parent compound with zinc as well as with nickel. The higher rates observed can help distinguish between the mechanism proposed by McClellan and Freiser and that used by Margerum and Wilkins.

TABLE II - Distribution Characteristics of Dithizones and Rate Constants for Formation of 1 : 1 Chelates at 25° C. and μ = 0.10.

Diarylthiocarbazone	-log Ka/KDR	log k_1 ($M^{-1}sec^{-1}$) Ni	Zn
Di-p-fluorophenyl-	9.72	3.43	7.57
Di-p-chlorophenyl-	10.46	3.52	7.66
Di-p-bromophenyl-	11.01	4.30	8.28
Di-p-iodophenyl-	11.36	5.11	8.81
Di-p-methylphenyl-	11.89	4.38	8.84
Di-p-methoxyphenyl-	11.26	4.85	8.43
Di-m-trifluoromethylphenyl-	10.36	4.43	8.23

In both mechanisms, rate constant k is a composite quantity, the product of the formation constant of a rapidly formed initial complex and the first-order rate constant of the loss of water from this complex or ion pair. Inasmuch as the rate constants varied so widely in the series of substituted dithizones, it would appear more likely that the initial complex involves metal-ligand bonding of some sort. Simple ion-pair formation would not be expected to depend so strongly on the relatively minor variation in the large anion of the position of a methyl group, for example, yet the rate constants for the zinc complex of the o- and p- methyl derivatives varied by almost a hundredfold, and even those for nickel by fivefold.

The effect of the electronegativity of the substituent as reflected by its Hammett σ value on the rate of the formation of the metal complexes is similar to that observed by Joy and Orchin (8) in a study of the stability of a series of substituted platinum-styrene complexes. They reasoned from a molecular orbital point of view that an increase in stability arose from the strengthening of the sigma bond between metal and ligand by the action of electron-releasing substituents. The sigma bond weakening that arose from electron-withdrawing substituents was amply compensated by their beneficial effect on the extent of overlap of pi bonding integrals. Hence both types of substituents would increase stability. It might be possible to apply analogous reasoning to the case of the rate constants of the nickel complex formation, since back pi bonding would be feasible from a d^8 ion. It would seem highly unlikely however, that these arguments could apply to zinc ion with its d^{10} configuration. Yet, as may be seen in Table II, the effect of substituents on the rate of formation of both nickel and zinc complexes is similar.

Admitting the independence of the kinetic enhancement on electronic influences of the substituents, focuses attention on their size, which does correlate with the rate constant. This led us to the desire to determine the activation parameters of the formation, to see whether the role of the substituent size would be reflected in the entropy of activation.

TABLE III - Rate Constant and Activation Parameters of $NiDz^+$ Formation

Diaryl-Thiocarbazone ARYL =	$k_{288°}$ $(M^{-1}sec^{-1})$	$k_{298°}$ $(M^{-1}sec^{-1})$	$k_{308°}$ $(M^{-1}sec^{-1})$	$\Delta G^{\neq}_{298°}$ kcal/mol	$\Delta H^{\neq}$ kcal/mol	$\Delta S^{\neq}_{298°}$ e.u.
Phenyl	4.1×10^3	6.1×10^3	7.2×10^3	12.3	4.4	-27
p-Chlorophenyl	1.0×10^2	1.2×10^4	1.6×10^4	11.9	4.0	-26
p-Bromophenyl	4.6×10^4	5.3×10^4	9.0×10^4	11.0	2.8	-27
p-Iodophenyl	2.3×10^5	3.5×10^5	3.3×10^5	10.0	0.0	-33
P-Tolyl	4.3×10^5	4.7×10^5	3.7×10^5	9.7	0.6	-31
o-Tolyl	7.7×10^3	1.0×10^4	1.5×10^4	11.9	4.8	-24

Very small w.r.t normal value of nickel

It is interesting to note that the large negative activation entropy observed in all cases (Table III) is the dominant factor affecting the rate. While this may justify our interest in entropy, the relative constancy of $\Delta S^{\ddagger}$ (excluding the o-tolyl ligand, it averages as -29 ±3 e.u.) certainly minimizes its role in the substituent rate enhancement. Rather, the $\Delta H^{\ddagger}$ unusually small for all of the systems studied, is seen to decrease with increasingly substituent size (rather than electronegativity) and thus, to account for the observed rate enhancement.

While the reaction rate constants for the nickel dithizonates reported here are in general agreement with other nickel ligand substitution reactions (2), the activation enthalpies and entropies of the relatively few other nickel chelation systems studied are considerably different from those seen here. For a series of diverse ligands including oxalate, malonate, glycine, 2,2-bipyridyl, and 1,10-phenanthroline, the formation of the 1 : 1 complexes exhibited $\Delta H^{\ddagger}$ values of 13 to 15 kcal/mole and $\Delta S^{\ddagger}$ values of 0 to +14 e.u. (9). The very low $\Delta H^{\ddagger}$ exhibited in the systems reported here may well indicate that the formation of the 1 : 1 chelate is fairly complex. For example, it may involve a preassociation step having a ΔH of the order of -8 to -10 kcal/mole, which would largely compensate for the expected value of 13 to 15. Whether the similarities of the $\Delta G^{\ddagger}$ accompanied by large differences in $\Delta H^{\ddagger}$ and $\Delta S^{\ddagger}$ are attributable in large measure to sulfur containing ligands in general or to dithizone-like ligands in particular, awaits further study.

Because the rates of the formation of the 1:1 metal dithizonates were seen to closely follow the rate of loss of coordinated water from the hydrated metal ion, we decided to investigate the effect of replacing at least one water molecule by another auxiliary ligand and upon the rate of chelate formation (10).

The rate of extraction of zinc and nickel dithizonates can be either increased or decreased by the presence of auxiliary complexing agents which transform the hydrated metal ions to complexes in which at least part of the coordinated water has been replaced. If we consider the formation of complexes

$$M^{2+} + nL \rightleftarrows ML_n$$

which then react with dithizonate

$$ML_n + Dz^- \xrightarrow{k_2} MDz + nL$$

followed by rapid formation and extraction of MDz_2, (so that we can ignore the rate of the reverse reaction, k-2) then we would explain an increase of K_{app} with concentration of auxiliary ligand as signifying that first ML_n is formed in a rapid pre-equilibrium step and that it reacts faster than does the hydrated metal ion with dithizonate; no change in K_{app} with auxiliary ligand to mean that the ML_n and M^{2+} react equally rapidly with dithizonate; and, finally, a decrease in K_{app} with auxiliary ligand to mean that ML_n reacted very slowly with dithizonate and either dissociated slowly or not at all to give free M^{2+} from which the rate of reaction with dithizonate could be quantitatively predicted. The general rate expression in which the formation of 1:1 and higher complexes with the auxiliary ligand are considered can be written

$$-\frac{d[M]}{dt} = K_{app}C_m[Dz] = \{k_o[M^{2+}] + k_1[ML] + k_2[ML_2] + \ldots\}[Dz^-] \quad (3)$$

or, if it can be assumed that the complexes ML, ML_2, etc., are rapidly formed and dissociated,

$$-\frac{d[M]}{dt} = (k_o\mu_o + k_1\mu_1 + k_2\mu_2 + \ldots)C_m[Dz^-] \quad (4)$$

where the μi values are distribution fractions of the total aqueous metal ion concentration in each of the various species present (M^{2+}, ML, ML_2, etc.) and whose values depend solely on the equilibrium formation constants (K_j) of these complexes and the auxiliary ligand concentration:

$$\mu i = \frac{\beta_i[L]^i}{\sum_{i=0}^{N} \beta\,[L]^i} \quad (5)$$

where $\beta = K_{f1}K_{f2}\ldots K_{fi}$

Provided only that $k_o \neq k_1 \neq k_2$, then the variation of log k_{app} with log [L] can be used to determine the values of the stepwise equilibrium constants of formation of the series of ML complexes.

All of the systems studied here have been analyzed in this manner and both rate and equilibrium constants evaluated. Generally good agreement was obtained between a fit of equation 4 and the values of k_{app} calculated from the experimental data. Thus, it may be concluded that reliable values (±0.1-0.2) of stepwise formation constants of metal complexes can be obtained by this kinetic method. In a number of cases, particularly those involving weak complexes, there is considerable variation in the stability constant values reported in the literature, increasing the significance of the values obtained by an independent method such as that used in this study (Table IV).

TABLE IV - Equilibrium Constants of Zinc and Nickel Complexes at 25 °C

	Nickel(II)		Zinc(II)	
Ligand	log K_{f1}	log K_{f2}	log K_{f1}	log K_{f2}
Acetate	---	---	0.5(0.5-1.0)[a]	---
Thiocyanate	1.3(1.1-1.8)	---	1.5(0.5-2)	---
Mercaptoacetate	7.3(7.0)	5.5(6.5)	8.0(7.4-8.3)	7.6(6.9-7.6)
Oxalate	---	1.8(1.3-2.4)	---	3.0(2.2-2.5)
Tartrate	---	1.8	---	2.0

[a] Values in parentheses are taken from the literature (3).

The effect of replacing some of the coordinated water by other ligands on the rates of complex formation of metal ions has been investigated for some systems. Margerum (11) found $CuOH^+$ to react much faster with EDTA anion than did Cu^{2+} but that $CuOAc^+$ slower. Bydalek (12) found $CuOAc^+$ to react 2.9 times more slowly with Ni-EDTA than did hydrated Cu^{2+}. In a study of the rate of water loss from nickel complexes, Hammes (6) found the 1:1 ni-glycine complex released a water molecule 13 times faster than did the aqueous Ni^{2+}. Even the 1:2 complex was faster (3.3 fold) than the aqueous ion. Hammes explained the observed kinetic behavior on the basis of the reduced attraction for water in the primary hydration sphere resulting from the reduction of the net positive charge on the nickel ion. Although the rate of water release can be expected to be increased by the lowered net charge on the metal ion complexed by an anionic ligand, the case of reaction with another negatively charged species should also decrease. In the reactions with dithizonate reported here, it would seem that the first factor is of greater influence than the second in the cases of $ZnOAc^+$, $NiCNS^+$, $NiCNS^+$, $Zn(SCH_2COO)$, and $Ni(SCH_2\ COO)$, that the two factors are balanced in the case of $NiOAc^+$, as well as in the 1:1 Ni and Zn complexes of lactate, oxalate, and tartrate, and the second factor outweighs the first in each of the 1:2 complexes studied (Table V)

TABLE V - Rate Constants at 25 °C for the Reaction:

$$ML_i + Dz^- \rightarrow MDz^+ + iL(\text{or } ML_iDz)$$

	Nickel		Zinc	
	$\frac{k_1}{k_0}$	$\frac{k_2}{k_0}$	$\frac{k_1}{k_0}$	$\frac{k_2}{k_0}$
Ligand				
Acetate	1.0		25.0	--
Thiocyanate	2.5	--	10.0	~ 0
Mercaptoacetate	14.0	~ 0	7.0	~ 0
Oxalate	1.0	~ 0	1.0	~ 0
Tartrate	1.0	0.23	1.0	~ 0

Quite obviously, a simple electrostatic explanation of these observations is inadequate. With zinc, both acetate and thiocyanate accelerate the reaction with dithizone; the thiocyanate, forming a stronger zinc complex than does acetate, to a lesser extent. In contrast the thiocyanate complex of nickel, probably more stable than that with acetate, reacts more rapidly than either the hydrated or monoacetate nickel ions. Again, although mercaptoacetate forms much stronger complexes with nickel and zinc than does thiocyanate, the former set react more rapidly than do the hydrated metal ions. In the cases of the 1:2 complexes, all of which react much more slowly with dithizone than do the hydrated metal ions, there is a possibility that in addition to the deterrent effect of the added negative charge, the coordination sphere may be (almost) completely filled by the auxillary ligand further hindering reaction. One might speculate that because the 1:2 nickel complex has observable reactivity whereas the zinc does not, perhaps in these tartrate complexes zinc has a coordination number of 4 and nickel, 6. At this point it can be

seen that much useful information can be obtained about the kinetic as well as equilibrium aspects of auxiliary complex formation but that meaningful generalizations will have to await the accumulation of information about many more systems.

Recently, we decided to make a detailed study of the extraction of Cu(II) with LIX Reagents. These materials, which are hydroxyoximes, were introduced in the 1960's by General Mills for the hydrometallurgical refining of copper (13, 14). The kinetics of copper-LIX extractions are of great practical importance and have been the subject of some study.

Most of the theoretical studies have been performed with 2-hydroxy-5-nonylbenzophenone oxime (LIX65N) and 5,8-diethyl-7-hydroxy-dodecan-6-one oxime (LIX63), which are shown below.

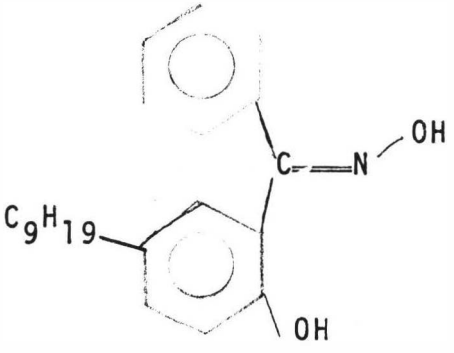

LIX 65N

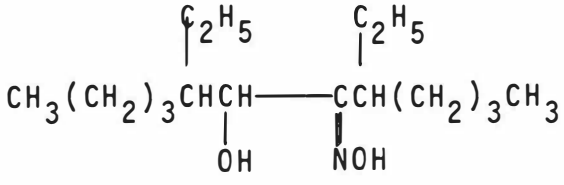

LIX 63

Previous workers, pointing to the low aqueous solubility of the LIX reagents, almost invariably discard the possibility of chelate formation in the aqueous phase and propose that interfacial reaction kinetics, rather than homogeneous chemically controlled rates, are dominant. Earlier methods of conducting rate studies involving Lewis cell (15), falling drops (16), and even AKUFVE apparatus (17,18) represent configurations having stirring intensities less than the ones we employ, and might, therefore, suffer from having some degree of diffusion limitation. In any event, the detailed mechanism study reported here should serve to resolve the controversy generated among other works as well as to help determine whether the limitations of the aqueous phase mechanism have been reached with the copper-LIX systems (19).

The distribution equilibrium of LIX65N between chloroform and water was determined to be $_{10}4.6\pm0.3$, which is significantly less than that of dithizone, an extractant whose kinetic behavior has been accepted as proceeding through an aqueous phase mechanism. On the basis of our kinetic data (Table VI), the rate expression for the extraction of copper by LIX65N can be quantitatively described by the following expression

$$-\frac{d[Cu^{2+}]}{dt} = k\frac{[Cu^{2+}][HL]_o^2}{[H^+]} \qquad (6)$$

where HL represents LIX65N. The reaction orders for this equation are taken from Table VII. It is noteworthy that all of theexperimentally observed orders are integers.

TABLE VI - Summary of Extraction Kinetics of Copper by 2-Hydroxy-5-nonylbenzophenone oxime (LIX65N) at 25°C.

$[LIX65N]_o$	pH	k'_1
7.50×10^{-4}M	3.00	8.53×10^{-4}
1.50×10^{-3}	3.00	3.31×10^{-3}
2.25×10^{-3}	3.00	7.99×10^{-3}
3.00×10^{-3}	3.00	1.23×10^{-2}
3.75×10^{-3}	3.00	2.06×10^{-2}
1.50×10^{-3}	3.00	3.95×10^{-3}
1.50×10^{-3}	3.20	5.20×10^{-3}
1.50×10^{-3}	3.62	1.98×10^{-2}
1.50×10^{-3}	4.00	4.65×10^{-2}

$[Cu^{2+}]_T = 1.00 \times 10^{-5}$M. I = 0.10 ($NaClO_4$0. Formic Acid/Formate Buffer at 0.010M.

TABLE VII - Summary of Kinetic Parameters for LIX65N-Cu^{2+} Extraction

Dependent Variable	Number of Determinations	Observed Orders
$[LIX65N]_o$	5	2.0 ±0.10
$[H^+]$	4	-1.1±0.08

The extraction of copper by LIX65N is unusual in that the observed second order dependence in ligand contrasts sharply with the nearly universally observed first order ligand dependencies (20). This behavior is not unique, however, and has also been observed in our laboratory for the extraction of copper by 8-quinolinol (21). From the observed second order ligand dependence on the rate of extraction, it follows that in this system the rate-determining step is that of the reaction of CuL^+ with a second molecule of neutral igand. Thus in the following extraction mechanism, since step (9) is the slowest

$$HL(o) \underset{\leftarrow}{\overset{K_D}{\rightleftarrows}} R\ HL \qquad \text{fast} \qquad (7)$$

$$Cu^{2+} + HL \underset{\leftarrow}{\overset{\beta_1 Ka}{\rightleftarrows}} CuL^+ + H^+ \qquad \text{fast} \qquad (8)$$

$$CuL^+ + HL \underset{\leftarrow}{\overset{k_1}{\rightarrow}} CuL_2 + H^+ \quad \underline{\text{slow}} \qquad (9)$$

$$CuL_2 \overset{K_{DC}}{\rightleftarrows} CuL_2(o) \qquad \text{fast} \qquad (10)$$

where K_{D_R} and K_{DC} represent the distribution constants of ligand and chelate, K_a the acid dissociation constant of LIX65 and β_1 the equilibrium formation constant of CuL^+ from Cu^{2+} and L^-. The overall extraction rate, under conditions where extraction is essentially complete at equilibrium, is determined by the rate of this step, i.e.,

$$-\frac{d[Cu^{2+}]}{dt} = k_1[CuL^+][HL] \qquad (11)$$

By substituting appropriate equilibrium expressions from (7) and (8) into (11), one obtains

$$-\frac{d[Cu^{2+}]}{dt} = \frac{k_1\beta_1 K_a}{K^2 D_R}\,\frac{[Cu^{2+}][HL]_o^2}{[H^+]} \qquad (12)$$

in which the observed dependence on metal ion, ligand and pH are explained. Further, the observed reaction rate constant, k' , is seen to be

$$k' = \frac{k_1\beta_1 K_a}{K^2 D_R} \qquad (13)$$

Although, unfortunately, the formation equilibria of Cu^{2+}-LIX65N have not been studied, a reasonable approximately of $\beta_1 K_a$ (to within about one order of magnitude) can be estimated from values obtained with salicylaldoxime, a closely related ligand. In fact, inasmuch as within a given ligand family changes in β_1 tend to be compensated by counter changes in K_a, the product tends to remain relatively constant (with a noticeable but small increase with increasing K_a). Hence from the measurement of $\beta_2 K_a^2$ of salicylaldoxime and Cu^{2+} of $10^{4.2}$ (23), we may take $\beta_1 K_a$ as $10^{2.0}$. Together with the value of K_{D_R} as $10^{4.6}$ and k' of 1.37,k' is $2.2 \times 10^7 M^{-1}s^{-1}$, a value that is quite similar to typical substitution reactions of Cu^{2+} (the corresponding rate constant for Cu and phenanthroline is only three times larger) (20).

This agreement with generally observed rate constant for copper substitution reactions in aqueous media represents strong evidence for the mechanism of the Cu-LIX65N extraction developed here. If chemical reactions at the interface were significant, far larger apparent rate constants would be calculated as a result of the incorporation of $[HL]_o$, the bulk organic phase ligand concentration, in the rate expression instead of the significantly larger concentration of the ligand, as a surface active material, at the interface.

Further studies of extractions with LIX reagents are underway. In preliminary work, we have examined the catalytic role of LIX63 on the LIX65N extraction of copper. Although our work serves to well characterize the empirical rate expression

$$-\frac{d[Cu^{2+}]}{dt} = \frac{k[Cu^{2+}][HL]_o^{0.97}[HR]_o^{0.99}}{[H^+]^{1.1}} \qquad (14)$$

where HR represents LIX63, the complexity of the copper coordination chemistry with LIX63 requires that additional work be conducted before elaborating further on the catalytic mechanism.

Finally, the role of experimental design, particularly regarding the nature of contact between the two phases, is quite important in obtaining readily interpretable results. Using our high speed stirring apparatus,(24) which gave highly efficient phase mixing, enabled us to achieve essentially integral reaction orders in our kinetic study. Fractional orders observed by earlier workers were at least in part responsible for their postulating interfacial mechanisms.

The results presented here not only clarify the extraction behavior of LIX65N, but are helpful as a guide to the design of new metal extractants for both analytical and hydrometallurgical applications. For example, if the extraction is already interfacially controlled, then no advantage would be gained with higher molecular weight homologs. As results presented here demonstrate, however, more highly hydrophobic extractants in conjunction with suitable catalysts do provide synthetic opportunities worth exploring. Furthermore, the work focuses on the appropriate variables to study with extraction systems of this type.

Acknowledgement

This work was conducted with financial assistance from the National Science Foundation.

REFERENCES

1. C.B. Honaker & H. Freiser, J. Phys. Chem. 66, 127 (1962)
2. B.E. McClellan & H.Freiser, Anal. Chem. 36, 2262 (1964)
3. M. Eigen, Pure & Appl. Chem., 6, 97 (1963)
4. K.S. Math, Q. Fernando & H. Freiser, Anal. Chem. 36, 1762 (1964)
5. R.K. Steinhaus & D.W. Margerum, J. Am. Chem. Soc. 88, 41 (1966)
6. R.G. Wilkins & M. Eigen, Advan. Chem. Ser. No. 49, 55 (1965)
7. J.S. Oh & H. Freiser, Anal. Chem. 39, 296 (1967)
8. J.R. Joy & M. Orchin, J. Am. Chem. Soc. 81, 305 (1959)
9. R.G. Wilkins, Accounts Chem. Res., 3, 408 (1970)
10. P.R. Subbaraman, M. Cordes & H. Freiser, Anal. Chem. 41, 1878 (1969)
11. D.W. Margerum, B.A. Zabin & D.L. Jones, Inorg. Chem., 5, 250 (1966)
12. T.G. Bydalek, Inor. Chem., 4, 232 (1965)
13. A.W. Ashbrook, Coord. Chem. Rev. 1975, 16, 285-307.
14. D.R.Spink &D.N. Okuhara, Intern. Symp. on Hydrometall., AIME, New York, 1972, p. 497
15. C.A. Fleming, "The Kinetics and Mechanism of the Solvent Extraction of Copper by LIX64N and Kelex 100," N.I.M. Report No. 1793, 1976 Johannesburg, S. Africa.
16. C. Hanson, R.J. Whewell, & M.A. Hughes, J. Inorg. Nucl. Chem. 1975, 37, 2303.
17. D.S. Flett, D.N. Okuhara, & D.R.Spink, J. Inorg. Nucl. Chem., 1973, 35, 2471.
18. D.S. Flett, J.A. Hartlage, D.R. Spink & D.N. Okuhara, J. Inorg. Nucl. Chem. 1975, 37, 1967.
19. S.P. Carter & H. Freiser, Anal. Chem. 52, 511 (1980)
20. R.G. Wilkins, "The Study of Kinetics and Mechanism of Reactions of Transition Metal Complexes", Allyn and Bacon: New York, 1974.
21. B. Budesinski, & H. Freiser, unpublished studies at Univ. of Arizona.
22. F.C. Chou, & H. Freiser, unpublished studies at Univ. of Arizona.
23. M. Bobtelsky & E. Jungries, J. Inorg. Nucl. Chem. 1956, 3, 38.
24. S.P. Carter & H. Freiser, Anal. Chem. 1979, 51, 1100.

SOLVENT EXTRACTION IN NUCLEAR FUEL REPROCESSING

A. Chesné

Commissariat à l'Energie Atomique
Boîte Postale No.6
92260 FONTENAY AUX ROSES
France

ABSTRACT

The author reviews the chief aspects of solvent extraction in reprocessing, including choice of the solvent, general description of the Purex process, and extractor technology, while emphasizing the specific character of nuclear fuels.

Irradiated fuel reprocessing is one of the major steps in the nuclear fuel cycle. During irradiation in reactors, the fuel undergoes changes in its composition - reduction of the fissile uranium content, appearance of fission products, plutonium and transuranium elements resulting from neutron capture - and also in its physical properties - the creation of defects, volume variations etc. Hence periodically, reactor loads must be renewed, but the frequencies depend on the type of reactor and the type of fuel.

Initially, this irradiated fuel is stored to allow decay of the short half-life isotopes with high specific activity and exhibiting highly penetrating radiation. This deactivation period is necessary to facilitate subsequent operations: transport and reprocessing.

In earlier years, reactor operation was oriented exclusively towards the synthesis of plutonium for military uses. Consequently, the reprocessing step was designed for the extraction and purification of this plutonium. The emergence of civil programs slightly changed this aspect. The objective remains the recovery of utilizable elements. The uranium can either be re-enriched (LWR) or used as a blanket (FBR). The plutonium forms part of the composition of mixed oxides used to load cores of fast breeder reactors.

In recovering these two elements, it is also very important to account for fission products and transuranium elements, which are long half-life α

emitters present in the fuel, in order to separate, concentrate and store them in a safe manner.

The composition of the irradiated fuel element is characterized by the presence of small amounts of plutonium and fission products in a large mass of uranium. The associated β γ activity is considerable.

To achieve quantitative recovery of the elements U and Pu, and sufficient purification of the β γ emitters (the decontamination factor required, which depends on the type of fuel reprocessed and the finished product specifications, is often in the range of 10^7), the chemical separation process must be highly selective, ideally adapted to trace chemistry, and preferably a multi-stage process so as to achieve the desired decontamination.

The first plutonium extraction process implemented at Hanford was based on precipitation (bismuth phosphate process). Very soon, however, process research was oriented towards solvent extraction. On the one hand, the extractive properties of ethyl ether to uranyl nitrate were known for a century, and furthermore, the similarity between the chemical properties of uranium and plutonium, demonstrated after the discovery of plutonium 239, encouraged simultaneous purification of both elements.

Many organic molecules were examined from the standpoint of their extraction capacity, particularly oxygenated compounds such as ethers, alcohol, ketones, esters etc. The Redox process, the first solvent extraction process used on an industrial scale, employed methyl-isobutylketone or hexone. Implemented at Hanford in 1951, it was based on the co-extraction of uranyl and plutonium nitrates from an aqueous nitric solution containing an unextractible nitrate, aluminum nitrate, acting as a salting out agent. The general purification flow sheet has become a standard. After transfer of the U and Pu substances into the organic solvent in countercurrent extraction, the solvent is scrubbed to improve decontamination. Separation of the uranium from plutonium is based on the reduction of the latter to the trivalent nitrate state, which is difficult to extract. The uranium is then re-extracted by using a slightly acidic aqueous phase. The operations, carried out in countercurrent flow in extractors featuring a large number of stages, serve to achieve high performance levels. To the extent that the two elements U and Pu must be recovered and separated, one of the following schemes is found in every process:

- co-extraction, scrubbing, re-extraction in aqueous phase corresponding to a co-decontamination cycle,

- co-extraction, scrubbing, partition, re-extraction corresponding to a partition cycle.

Among solvents of the ether type, dibutyl corbitol (dibutoxy-diethyl) ether has been used at Windscale since 1952, and then in 1969 in the first highly irradiated fuel reprocessing cycle, by the so-called Butex process. This process offers the advantage over the Redox process of not requiring salting out agent to perform uranium and plutonium extraction, as well as the drawback of higher cost and less favorable physical properties.

Very soon after implementation of the Redox process, tributylphosphate (TBP), an ester of phosphoric acid, was investigated and selected for future

industrial installations. TBP offers significant advantages over hexone and the Butex solvents. Like the latter, it does not require salting out agent, it exhibits greater chemical stability and selectivity, especially with respect to certain fission products such as Ru. On the other hand, owing to its viscosity and its density which is too close to that of water, it must be used diluted in an adequate solvent. A chemically inert compound, as non-inflammable as possible, is selected, whose physical properties allow easy emulsion settling. The paraffinic hydrocarbons derived from petroleum fractions, or possibly synthesized, are ideal: these include 'odorless kerosene', n-dodecane and hydrogenated tetrapropylene. CCl_4 has also been used. Unlike the former compound, which imparts to the TBP/diluent mixture a density lower than that of water, TBP/CCl_4 mixture has a higher density.

As a rule, the composition selected for the TBP/diluent mixture contains 30% TBP (good physical properties, sufficiently high value of partition coefficients).

An additional selection criterion is the resistance of the solvent to the combined effect of nitric acid and radiolysis. Chain splitting of organic compounds results in the formation of degradation products whose presence lowers chemical performance, makes settling more difficult, creates precipitates with certain fission products which accumulate at the interface and, in general, increases the β γ activity of the solvents to be recycled.

Hence TBP itself is degraded into a series of less and less substituted acids (dibutyl and monobutylphosphoric acids), whose complexes with certain fission products, especially Zr, are very stable and can be entrained in the solvent.

Similarly, diluents can be altered by irradiation, and while it is more difficult to identify the materials responsible for poor performance, it is generally considered that straight-chain hydrocarbons are more stable. Hence n-dodecane was selected as a diluent in the Savannah River plant at the start of the 1960s, replacing the commercial diluent used until then.

To the standard flow chart concerning U and Pu extraction and separation is added the chemical treatment of the solvent designed to bring it to constant purity. The acidic products discussed above are eliminated by alkaline scrubbing (solutions of Na_2CO_3, NaOH etc).

STEPS IN THE PUREX PROCESS

The use of TBP has spread, and its employment for reprocessing uranium fuels, by the Purex process, has entered into universal practice, since its description at the Conference on Peaceful Uses of Atomic Energy held at Geneva twenty-five years ago.

Slight changes have been made in the intervening twenty-five year period, but the general scheme has remained the same. We shall review the different steps in the process.

U-Pu CO-EXTRACTION

The nitric solution from dissolution is clarified and placed in countercurrent contact with the solvent, to co-extract U and Pu in the form of $UO_2(NO_3)_2 2TBP$ and $Pu(NO_3)_4 2TBP$, while the fission products, americium and curium, remain in the aqueous phase owing to their partition coefficient which is lower by several orders of magnitude than those of U and Pu. The success of this operation depends partly on the presence of plutonium in the tetravalent state, and also on the purity of the solvent throughout the operation.

With respect to the first point, the presence of hexavalent plutonium in non-negligible quantities has been noted in oxide fuel dissolutions. Pu (VI), which is less extractible, is liable to limit the recovery yield. A valency adjustment may become desirable if not necessary. As for solvent purity, it is important to consider the chemical or radiolytic degradation products, which are mainly butylphosphoric acids. They react with zirconium to give compounds which lower decontamination performance and yield precipitates at the organic phase/aqueous phase interface. The accumulation of these precipitates creates an irradiating source which accelerates solvent destruction. These effects are minimized by reducing the residence time of the solvent in the extractor, and by lengthening fuel deactivation time. The decontamination factor for β γ emitters obtained in this co-extracton is high, on the order of 10^3 to 10^4. It should be noted that the addition of controlled quantities of hydrofluoric acid to the solution to be extracted helps to limit considerably the formation of Zr compounds with phosphoric acids. The zirconium fluoride complex remains in the aqueous phase and is eliminated in the extraction raffinate with the fission products. This process has been used for more than ten years in the Marcoule facility.

In designing future installations, rather than altering the chemical conditions which impose constraints on downstream operations, such as fission product concentration and vitrification, preference is generally given to pulsed columns instead of mixer/settlers to perform this first step. This avoids the accumulation of solids, while reducing residence time and hence degradation of the solvent.

SOLVENT SCRUBBING

The impurities in the solvent are either entrained mechanically or bonded chemically to the TBP or to its degradation products. Placing of the solvent in countercurrent contact with the acidic aqueous phase serves to eliminate mechanical entrainment completely, and to reduce considerably the organic phase stability of TBP complexes formed with the various fission products. This operation is of limited effectiveness if the dibutylphosphate concentration in the solvent is high. Among the factors governing its efficiency are the acidity of the aqueous phase, solvent saturation, and contact time of the phases.

CO-RE-EXTRACTION

The stability of the complexes $UO_2(NO_3)_2 2TBP$ and $Pu(NO_3)_4 2TBP$ is heavily dependent on the acidity of the aqueous phase, so that co-re-extraction is carried out by placing the loaded solvent in countercurrent flow with a dilute nitric acid solution, into which the uranium and plutonium pass. This solution is easily hydrolysed, and the co-re-extraction step can be performed in two stages: re-extraction by 0.5 N HNO_3, by which all the plutonium and part of the uranium pass into the aqueous phase, followed by re-extraction by 0.01 N HNO_3, in which the residual uranium is re-extracted.

PARTITION

The principle of this operation is based on selective reduction of the plutonium present in the organic solvent in the trivalent state, which gives weak nitrate complexes which are difficult to extract, while the uranium remains in easily extractible hexavalent form.

One of the first Redox systems employed consists of ferrous sulfamate, in which the ferrous ion plays the role of a reducing agent to Pu^{4+} in accordance with $Pu^{4+} + Fe^{2+} \rightleftarrows Pu^{3+} + Fe^{3+}$, and the sulfamate ion reduces the ~~anta~~nitrite according to $HNH_2SO_3 + HNO_2 \rightarrow N_2 + H_2SO_4 + H_2O$. The presence of an antinitrite is necessary to avoid side reactions in which the Pu^{3+} is oxidized by the nitrous ions. Reagent in significant excess is required for complete reduction.

However, the sulfate and ferrous ions in the solutions raise problems, such as the corrosion risk during subsequent effluent concentrations, and increased solid wastes.

To avoid the addition of a foreign cation, tetravalent uranium salts have been used as a partition reagent, namely, the sulfate and especially the nitrate, stabilized by the presence of hydrazine, which performs the role of antinitrite. While ferrous sulfamate is a commercial product, uranous nitrate is produced on the very site of its use, by the electrolytic reduction of uranium from the purified stock, or by reduction by hydrogen in the presence of a catalyst. The isotopic composition of the reagent is thus the same as that of the material processed.

Uranous nitrate is valuable for two reasons: first, since it can be extracted by TBP, it acts not only in the aqueous phase but also in the organic phase; secondly, the reaction product makes no contribution to the increase of wastes. However, a large excess over stoichiometry is required to achieve quantitative reduction of the plutonium. This means that its use is accompanied by an increase in the amount of uranium flowing through the installation. For LWR fuels, in which the U/Pu ratio is around 100, this is not a major disadvantage. The same cannot be said of the reprocessing of fast breeder reactor cores, in which the U/Pu ratio is around 4. This drawback disappears if the uranous nitrate is produced on the spot, using the extractor itself to carry out electrolytic reduction of the uranium. In this case, the reagents are hydrazine and the electrons exchanged between the ions in solution and the electrodes.

Another possibility is the use of hydroxylamine nitrate which may be stabilized with hydrazine, which has hitherto been employed in certain industrial installations as a re-extraction reagent in plutonium purification cycles. Here again, the reagent leads to essentially gaseous products.

In all the foregoing cases, part of the uranium is entrained by the aqueous re-extraction solution containing trivalent plutonium and excess reducing agent. Scrubbing of the reacidified aqueous solution with 30% TBP allows recovery of this uranium and its recycling to reducing re-extraction.

The fission products still present in this partition stage are chiefly represented by ZrNb and RuRh pairs for $\beta\ \gamma$ activity, and by technetium and palladium for mass abundance, in the case of highly irradiated fuels. Another contaminant also present in non-negligible quantities is neptunium. In view of the stability of the complexes in weakly acidic medium, RuNb and ZrNb follow the plutonium flux preferentially. Technetium in the pertechnetate state and palladium, which are reducible by the Redox systems considered, also follow the plutonium flux. Neptunium, however, exhibits behavior which depends on the prevailing operating conditions. From Np VI in the solvent phase, it can be reduced to very poorly extractible Np V, or to medium-extractible Np IV, leading to more or less total U-Np or Pu-Np separation.

URANIUM RE-EXTRACTION

This is carried out with very dilute nitric acid in countercurrent flow. Operating at a temperature around 50 °C, the solution obtained is more concentrated than at room temperature, owing to the negative temperature coefficient affecting uranium partition.

URANIUM PURIFICATION CYCLES

The purpose of this cycle or cycles is to improve the decontamination of fission products and α emitters, chiefly Pu. This implies extraction in a reducing medium, in which Pu^{3+} remains in the aqueous phase with the fission products, and re-extraction of the type described in the previous section. The supplementary $\beta\ \gamma$ emitter decontamination factor is obtained, and may reach 10^3. If Np is to be separated, the operating conditions must be altered, for example by setting conditions to obtain unextractible Np V.

PLUTONIUM PURIFICATION CYCLES

Plutonium purification involves a scrubbing/reducing re-extraction extraction cycle, in which the feed solution's acidity is adjusted and the plutonium is oxidized quantitatively to valency 4. This is achieved by adding sodium nitrite, or preferably by bubbling nitrous vapors. This also avoids the introduction of a cation, which limits the subsequent effluent concentration. The extraction and scrubbing which follow achieve a decontamination factor for ruthenium and zirconium.

Reducing re-extraction involves either hydroxylamine nitrate or tetravalent uranium, and the reduced solution must undergo another organic scrubbing to separate Pu^{3+} from the uranium. A reflux system employed at the Marcoule facility serves to raise the decontamination factor and to obtain a more concentrated purified solution. The decontamination factors for $\beta\ \gamma$ emitters obtained in the purification cycle are generally around 10^2.

Formerly, this additional plutonium purification was performed by an anion exchange resin cycle. The finding of similar properties in amine type solvents, considered as liquid resins, led to the use of a plutonium purification cycle by extraction with trilaurylammonium nitrate at the La Hague facility, from 1966 to 1973. This compound, diluted in hydrogenated tetrapropylene, exhibits great affinity for tetravalent plutonium in nitric medium. High concentration factors can thus be achieved if the plutonium is very dilute. However, the capacity of the solvent is far lower than that of TBP. To offset this, re-extraction must be carried out using a complexing agent, sulfuric acid. While purification performance is good, the chemical stability of the solvent is poorer than that of TBP, but here the degradation products, secondary and primary amines, are only slightly complexing vis-à-vis the fission products, and their presence does not cause a lowering of the decontamination factors. Degradation is blocked by the addition of an antinitrite, sulfamic acid.

TREATMENT OF TBP

As we have seen above, acidic products are formed in the solvent. They are eliminated by scrubbing the solvent with a basic aqueous phase, preferably a carbonate which, if the cations U and Pu are present, helps to prevent hydroxide precipitation, thanks to the complexing power of the CO_3 ions. Owing to the different activity level, the decontamination cycle and purification cycles each feature their own specific solvent treatment.

Various investigations have been conducted to improve performance levels of these processes (oxidizing and reducing scrubbings etc).

It is worthwhile mentioning the development of a process based on the use of the hydrazinium ion instead of the sodium ion routinely used in carbonate solution. The advantage resides in the possibility of destroying this cation, and thus considerably reducing the volume of effluents.

***

Before setting aside the chemistry of the process, it is important to mention the research carried out in recent years concerning the means of minimizing the risks of proliferation, and chiefly the risk of theft of nuclear materials, especially plutonium. Three measures have been recommended with respect to the technical aspect:

- reduce the presence of materials which can be used for the fabrication of nuclear weapons, in separate form in the cycle,
- exploit radioactivity to protect these materials from diversion,
- protect them by physical barriers.

The implementation of these measures means the adaptation of existing techniques to create a diversion-proof civilian reprocessing plant called the Civex Plant. From the standpoint of extraction flow charts, this implies a complete re-assessment of extraction conditions. For example, we can take the case of plutonium breeder fuel reprocessing, in which the nitric dissolution solution of the cores and blankets is such that Pu/U + Pu = 12%. The final product desired is a U-Pu mixture containing 20% plutonium. In the Purex process, modified and adapted to the Civex concept, co-extraction is carried out without subsequent scrubbing to reduce fission product decontamination. Partition is performed in an incomplete manner: the aqueous reducing solution re-extracts the plutonium totally and the uranium partially. The uranium/plutonium combination, which may be adjusted by the introduction of additional uranium, is sent to fuel fabrication, which is remote-controlled due to the radioactivity level. In this new concept, the 'selectivity' aspect of solvent extraction, which formerly constituted the selection criterion, is no longer essential.

TECHNOLOGICAL ASPECTS

The extraction units employed in reprocessing plants are of three types: columns, mixer/settlers and centrifugal extractors. The first two were used in designing the earliest industrial installations (columns at Hanford, mixer/settlers at Savannah River), and today they still represent the large majority of extractors in service.

The operating principle of these units is well known and has formed the subject of many publications. It will not be discussed in detail here. However, we shall examine the constraints that the reprocessing industry applies concerning the choice of their design. Two specific nuclear aspects must be taken into account:

- the intense radioactivity of the aqueous solution to be processed,
- the presence, in this aqueous phase, of fissile isotopes which, if the right conditions are satisfied, are liable to give rise to a chain reaction.

The first aspect imposes the following.

(a) Personnel protection by thick shielding surrounding the units. Preference is given to minimum-sized units corresponding to lower investment. Hence pulsed columns with perforated plates have replaced packed columns, which are less efficient, hence more bulky. More compact mixer/settlers, of horizontal structure, can represent a smaller investment despite their larger holdup, and this factor is even more important for centrifugal extractors.

(b) Remote control and maintenance. Preference is given to reliable systems of simple design, in which all or part of the equipment can be replaced by remote-control. Air pulsation is preferable to mechanical agitation for pulsed columns. Mixer/settlers are equipped with automatic interphase control and independent agitation in each stage.

(c) Limitation of solvent residence time. As we have seen, solvent irradiation is accompanied by the formation of undesirable organic compounds. The average residence time is about one second in a centrifugal extractor stage, and by one or more orders of magnitude higher in pulsed columns and mixer/settlers. However, this advantage is largely offset by the fact that the precipitates formed accumulate at the aqueous/organic interphase, and are only eliminated in pulsed columns.

For future plant projects, a consensus is emerging with respect to co-extraction in the first cycle: the tendency is in favor of pulsed column extractors. This preference is also based on considerations relating to the second specific nuclear aspect: criticality risk.

In any given system, the risk that the presence of fissile isotopes may cause a chain reaction is estimated by a thorough analysis of many parameters: concentration of various substances, physical state, external environment etc. For the three types of equipment, a sub-critical geometry can be defined such that, irrespective of the concentration of fissile material, it leads to extractors with compact dimensions (cylinder diameters, liquid film thicknesses). Hence the reprocessing capacity is low. In operating or planned industrial facilities, the plutonium concentration and purification cycles are generally based on this concept. It would be highly constricting for the co-decontamination cycle, for example, in which the solutions to be processed have a low plutonium concentration. Control by concentration is preferable in this case, in other words, the units are designed to be 'safe' up to a predetermined concentration, which is never expected to be reached.

Very significant gains in scale can be achieved by poisoning the system in homogeneous or heterogeneous form, by using boronated steel, cadmium or hafnium plates. These systems have been especially recommended for pulsed columns: hafnium plates, compartmentation of the interplate space by boronated steel or hafnium plates.

Also developed, on the model of storage tanks, are annular geometry extractors with poisoned internal core. Both for columns and centrifugal extractors, they serve to achieve a very significant gain in capacity, making this concept highly attractive.

To conclude this overall review, it is worth noting that since the birth of the nuclear industry, solvent extraction, thanks to its flexibility, has served to reprocess fuels of very different types: metallic, alloy, oxide etc.

Owing to the importance of LWR reactors and, in the future, the fast breeder reactors, reprocessing facilities will mainly have to be adapted to growing capacity and the use of large plutonium fluxes. This implies the research and development of safe, high capacity nuclear extractors, for which physicochemical investigations must be intensified. The consequences of these plutonium fluxes on process chemistry will lead to the improvement of effluent decontamination in long half-life radioactive compounds, especially α emitters, and to the maximum recovery of fissile material. The technique of solvent extraction is ideal for the attainment of these objectives.

EXTRACTION OF METAL IONS BY LIQUID MEMBRANES

Dr. Norman N. Li
Exxon Research and Engineering Company
Linden, New Jersey 07036
U.S.A.

EXTENDED ABSTRACT

Liquid surfactant membranes (or liquid membranes) are made by forming an emulsion of two immiscible phases and then dispersing the emulsion in a third phase (continuous phase). Usually, the encapsulated phase and the continuous phase are miscible. For a given application, liquid membranes are usually tailor-made in order to meet all the specific requirements. When the emulsion is dispersed by agitation in a continuous phase (the third phase), many small globules of emulsion are formed. Thus, an enormously large membrane surface area is produced for rapid mass transfer from either the continuous phase to the encapsulated phase or vice versa. It should be noted that many much smaller droplets, such as those 1μ in diameters, are encapsulated within each globule.

The most effective use of the liquid membrane process is achieved when the flux through the membrane phase and the capacity for the diffusing species in the receiving phase are maximized. There are two types of facilitation mechanisms that can be used to maximize the flux and capacity:

Type (1) Facilitation: Minimization of the concentration of the diffusing species in the receiving phase. This is normally done by reacting the diffusing species with some other constituent in the receiving phase to form a product incapable of diffusing back through the membrane. For example, in the removal of phenol from water, the phenol diffuses through a hydrocarbon membrane to a receiving phase of caustic solution. The phenol reacts with caustic to form sodium phenolate which is insoluble in the hydrocarbon membrane and hence cannot diffuse back into the water phase. In this way, the concentration of phenol in the receiving phase is low, thus, facilitating its passage through the hydrocarbon membrane.

Type (2) Facilitation: Carrying the diffusing species across the membrane by incorporating "carrier" compounds in the membrane. This kind of carrier-mediated transport can be illustrated by the separation of metal ions from waste water and mine leaching solution by liquid membranes. In these cases, a liquid ion exchange reagent is incorporated in the membrane phase. Extraction of metal ions can then occur at the membrane/continuous phase interface while stripping can occur at the membrane/internal phase interface under proper process conditions.

In fitting with the Symposium, this paper will devote principally to the review of the work done on Type II facilitated transfer of metal ions through liquid membranes.

Organic reagents.
Session 1

Co-chairmen : A.S. Kertes (The Hebrew University, Jerusalem, Israël)
F. Alderweireldt (University of Antwerpen, Belgium)

1 A

80-10 Extraction of alkali metal dipicrylaminates into nitrobenzene in the presence of some linear polyethers.
E. Makrlik, P. Vanura, M. Kyrs and J. Rais, Nuclear Research Institute, Rez by Prague, Czechoslovakia.

80-11 Extraction of rare earth metals by carboxylic acids.
V.P. Gladyshev, F.I. Lobanov, N.N. Andreeva and A.K. Nurtaeva, Kazakh State University, Alma-Atta, U.S.S.R.

80-168 Some aspects of extraction by organic compounds.
Yu. I. Murinov, Yu. E. Nikitin and A.M. Rozen, Institute of Chemistry of the Bashkirian Branch of the Acad. of Sc., Ufa, U.S.S.R.

80-81 Some problems in chemical structures and properties of organic extractants.
Yuan Chengye, Shangai Institute of Organic Chemistry, Academia Sinica, China.

80-5 The design of selective reagents for liquid-liquid extractions of metal ions : a rational approach.
S. Högberg, Royal Institute of Technology, Stockholm, Sweden.

1B

80-3 Some observations on the extractibilities of univalent cations with dibenzo-18-crown-6 and picrate ion.
Y. Hasegawa and T. Sekine, Science University of Tokyo, Kagurazaka, Shinjuki-ku, Tokyo, Japan.

80-212 On the extraction and acceleration in hydroxyphenylketoxim systems.
K. Gloe, P. Mühl, J. Beger and H. Binte, Zentralinstitut für Festkörperphysik und Werkstofforschung, Dresden and Bergakademie, Freiberg, D.D.R.

80-179 Selective extraction of Mercury (II) with 4-Phenyl-5(4-Methylphenyl)-1,3,4-Thiadiazolium-2-Thiolate (PMPTD) from Brine solutions.
H.F. Aly and A.M. Kiwan, Chemistry Department, Kuwait University, Kuwait.

80-167 Synthesis ans extracting properties of ketosulfides.
Yu. E. Nikitin, Yu. I. Murinov, R.A. Khisamutdinov, V.I. Dronov and G.A. Tolstikov, Institute of Chemistry of the Baschkirian Branch of the Acad. of Sc., Ufa, U.S.S.R.

80-127 Synthesis and improvement of the properties of hydroxamic acids as a new extracting agents for metal ions.
H.N. Al-Jallo, S.S. Ahmed and F.I. Saleh, Nuclear Research Center, Tuwaitha, Baghdad, Iraq.

80-7 Schiff base of 2-Amino-3-Aminomethyl-4-Methoxymethyl-6-Methylpyri-dine with salicylic aldehyde as a promising extractant for copper.
Z. Cimerman, A. Deljac and Z. Stefanac, University of Zagreb, Yugoslavia.

80-4 The use of 4-Thiobenzoyl-2,4-Dihydro-5-Methyl-2-Phenyl-3H-Pyrazol-3-One (SBMPP) and Thiobenzoyl Trifluoroacetone (SBTA) as chelating extractants.
G.N. Rao and V.S. Chouhan, Indian Institute of Technology, New Delhi, India.

EXTRACTION OF ALKALI METAL DIPICRYLAMINATES INTO NITROBENZENE IN THE PRESENCE OF SOME LINEAR POLYETHERS.

E. Makrlík, P. Vaňura, M. Kyrš and
J. Rais
Nuclear Research Institute, Řež by
Prague
Czechoslovakia.

ABSTRACT

Extraction of alkali metal dipicrylaminates into nitrobenzene in the presence of six linear polyethers (glyme-2, glyme-3, glyme-4, polyethyleneglycol 200, 300 and 400) was studied. Experimental results were interpreted in terms of the extraction of the bare ions and the complexed cations (M^+/polyether ratio = 1). The stability constants for $\overline{ML}^+$ in nitrobenzene saturated with water are for all ligands studied the highest, in the case of the Na^+ ion. The influence of the ligand on the extraction selectivity is discussed.

In a previous paper (1) we reported on the large synergistic effect of polyethyleneglycols in extraction of alkaline earth cations into nitrobenzene in the presence of some hydrophobic anions such as the dipicrylaminate and the dicarbolide anions. Furthermore, we described a quantitative model accounting for the maxima occuring in the extraction of Sr^{2+} when D_{Sr} is plotted vs. the initial concentration of polyethyleneglycols - 400 in the aqueous phase (2). In the present work the investigation of the influence of acyclic polyethers on the extraction is extended to the alkali metal ions, the dipicrylaminate anions being present in the nitrobenzene phase in order to ensure sufficient extractability. The extraction equilibria of univalent cations in the systems investigated may be explained on the basis of the existence of the following species (species in the organic phase overlined) : M^+, A^-, $\overline{M}^+$, $\overline{A}^-$, $\overline{MA}$, $\overline{ML}^+$, $\overline{MLA}$, where A^- denotes the hydrophobic dipicrylaminate anion and L is a polyether. The concentrations of MA, MLA and ML^+ are considered as negligibly low because of the low values of the association constants of alkali metal dipicrylaminates in water (3) and because of the low values of the stability constants of the simple linear polyethers with alkali metal cations in water (3,4).

The present study can also be considered as a continuation of our work on the extraction of alkali metal dipicrylaminates into nitrobenzene (6) ; upon addition of linear polyethers the distribution ratios of the anion increase in all cases. As

ligands L, we used glyme-2, -3, and -4 and commercial polyethyleneglycol of mean molecular weights 200, 300, and 400 which will be denoted as PEG 200, 300, and 400.

Polyethyleneglycols, glyme-2, -3, -4 (di-, tri, and tetraethyleneglycol dimethylether- were Koch-Light chemical purity products.

Other experimental conditions were as described earlier (1, 6).

The main equilibria involved in the extraction can be expressed as :

$$M^+ + A^- + \bar{L} \rightleftarrows ML^+ + A^- \qquad K_{ex}(ML^+, A^-) \qquad (1)$$

$$M^+ + A^- \rightleftarrows \bar{M}^+ + A^- \qquad K_{ex}(M^+, A^-) \qquad (2)$$

$$\overline{MLA} \rightleftarrows \overline{ML}^+ + A^- \qquad K_d(MLA) \qquad (3)$$

$$\overline{MA} \rightleftarrows \bar{M}^+ + \bar{A}^- \qquad K_d(MA) \qquad (4)$$

The condition of electroneutrality is :

$$[\bar{M}^+] + [\overline{ML}^+] = [\bar{A}^-]$$

Note that reactions (2) and (4) have been observed previously (6) in similar systems without the presence of L. In all cases, equilibrium (3) can be omitted since the formation of $\overline{MLA}$ is negligible. This has been found in our laboratory where mathematical models taking into account the formation of $\overline{MLA}$ or neglecting it have been compared. We reached the conclusion that the more complete model is not superior in describing experimental data. The $K_{ex}(ML^+, A^-)$ values yielded by both models practically coincide. The formation of ML_2^+ at high L:M ratios was neglected because the simple model proposed agrees satisfactorily with experiments. The formation of only $\overline{ML}^+$ species was postulated also for other solvents (4,5).

For the calculation of the $K_{ex}(ML^+, A^-)$ values, the experimentally found values D_A and/or $[\bar{A}]$ were available the values v_a, v_o, C_L (initial concentration of the ligand in the aqueous phase) and $[OH^-]$ were deduced from the experiments, and the constants $K_{ex}(M^+, A^-)$, $K_D = [\bar{L}] / [L]$ and $K_d(MA)$ are known from previous work (6).

The main steps of the calculation follow the sequence :

$$[M^+] = [OH^-] + [A^-] \qquad (6)$$

$$[\bar{A}^-] = D_A [A^-] - K_{ex}(M^+, A^-).K_d^{-1}(MA) [M^+][A^-] \qquad (7)$$

$$[\bar{M}^+] = K_{ex}(M^+, A^-) [M^+] [A^-][\bar{A}^-]^{-1} \qquad (8)$$

$$[\overline{ML}^+] = [\bar{A}^-] - [\bar{M}^+] \qquad (9)$$

$$[\bar{L}] = (C_L v_a - v_o [\overline{ML}^+])/(v_o + v_a K_D^{-1}) \qquad (10)$$

Calculation of $K_{ex}(ML^+, A^-)$ where carried out according equation (1).

In the case of cesium, the above method of determining the $K_{ex}(CsL^+, A^-)$ value could not be used because the values of $[A^-]$ were too low to allow a reliable analytical determination. Therefore, only traces of ^{137}Cs were added to such systems for the determination of $K_{ex}(NaL^+, A^-)$ values and the distribution ratio D_{Cs} was measured. The distribution of A^- and L could not be altered by the introduction of trace amounts of ^{137}Cs so that in the above calculations the values of $[\overline{A^-}]$ and $[\overline{L}]$ remain constant.

Using eq. (1) and

$$\Sigma[\overline{Cs}] = [\overline{Cs^+}] + [\overline{CsA}] + [\overline{CsL^+}] \qquad (11)$$

where $\Sigma|\overline{Cs}| = D_{Cs} \cdot [Cs^+]$ = total equilibrium concentration of cesium in the organic phase, the relationship for the determination of $K_{ex}(CsL^+, A)$ value can be written as :

$$K_{ex}(CsL^+, A^-) = [\overline{A^-}][\overline{L}]^{-1} (D_{Cs} \cdot [A^-]^{-1} - K_{ex}(Cs^+, A^-) [\overline{A^-}]^{-1} - K_{ex}(Cs^+, A^-).K_d^{-1}(CsA) \qquad (12)$$

The values of $K_{ex}(ML^+, A^-)$ are practically independent of the initial concentration of A^- and L in the systems and are summarized in Table I. It can be seen that the $K_{ex}(ML^+, A^-)$ values increase from Li to Cs, whereas for other linear polyoxoethyenes the maximum was found for rubidium (13), dichloromethane being the solvent.

It is obvious that knowing the values of $K_{ex}(ML^+, A^-)$ and $K_{ex}(M^+, A^-)$ the stability constant of the complex ML^+ in the organic phase can be found ($\beta_o = K_{ex}(ML^+, A^-)/K_{ex}(M^+, A^-)$). It is also useful for some purposes to compute the ratio $K_{ML}^{Cs} = K_{ex}(CsL^+, A^-)/K_{ex}(ML^+, A^-)$ which corresponds to the equilibrium constant of the hypothetical reaction

$$M^+ + \overline{CsL^+} = Cs^+ + \overline{ML^+} \qquad (13)$$

The selectivity of the extraction is illustrated by the values of K_{ML}^{Cs} provided the ion in the organic phase is completely present in the form of its complex. The K_{ML}^{Cs} values may be compared with the constants $K_{ML}^{Cs} = K_{ex}(Cs^+, ML^+, A^-)/K_{ex}(M^+, A^-)$ which are obtained in the absence of the ligand. From Table II it may be seen that the selectivity of the extraction is always lower in the absence L. The selectivities for the pairs K/NH_4, K/Li, and NH_4/Li are practically the same in the presence of any type of L tested and in absence of ligand. The selecticity of the pair Na/Li increases upon addition of the polyethyleneglycols. The very similar behaviour of Li^+, K^+, and NH_4^+ is also apparent from β_o values.

Table I. Extraction constants $K_{ex}(ML^+, A^-)$ and other equilibrium constants for some linear polyethers and alkali metal cations.

M^+	log $K_{ex}(M^+, A^-)$[a]	$pK_d(MA)$[a]	log $K_{ex}(ML^+, L^-)$[b]					
			glyme-2	glyme-3	glyme-4	PEG 200	PEG 300	PEG 400
Li^+	0.16	1.43	3.49(17)	3.94(33)	4.48(29)	5.63(26)	6.34(18)	6.83(16)
Na^+	1.00	1.32	4.43(24)	5.07(29)	6.26(19)	6.98(30)	7.89(25)	8.51(21)
NH_4^+	2.41	1.45	5.34(15)	6.13(13	6.72(11)	7.67(21)	8.56(16)	9.26(14)
K^+	2.97	1.29	5.85(12)	6.64(13)	7.25(10)	8.32(16)	9.14(12)	9.91(10)
Cs^+	4.27	1.31	6.79(8)	7.14(8)	7.47(8)	9.34(10)	9.55(8)	9.96(8)
K_D			0.25	0.30	0.45	$1.6.10^{-3}$	$1.5.10^{-3}$	$1.3.10^{-3}$

a ... estimated by the method described in (6) for 3.10^{-3} M MOH.

b ... the number of experimental points is given in parentheses.

Table II. Extraction exchange constants K_{ML}^{Cs} (log K_{Li}^{Cs} = 4.01 ; log K_{Na}^{Cs} = 3.17 ; log $K_{NH_4}^{Cs}$ = 1.76 ; log K_{K}^{Cs} = 1.20).

L	log K_{LiL}^{Cs}	log K_{NaL}^{Cs}	log $K_{NH_4L}^{Cs}$	log K_{KL}^{Cs}
glyme-2	3.30	2.36	1.45	0.94
glyme-3	3.20	2.07	1.01	0.50
glyme-4	2.99	1.21	0.75	0.22
PEG 200	3.71	2.36	1.67	1.02
PEG 300	3.21	1.66	1.99	0.41
PEG 400	3.13	1.45	0.70	0.05

A short discussion of the dependence of β_o upon the type of ligand L and of cation seems interesting. For each ligand, the dependence of β_o on the crystallographic radius of the cation exhibits a maximum at $M^+ = Na^+$. The β_o value for the complex between H^+ and PEG 400 as deduced in our recent paper (2) is lower than for the Li^+ PEG 400 complex. On the basis of the literature data (Table III), it may be concluded that the presence of this type of maximum is a rather general feature of the complexing of alkali metal cations with linear polyethers in various solvents. However, the maximum in methanol is always found at $M^+ = K^+$. In this respect, the polyethyleneglycols parallel the behaviour of cyclic polyethers. The maximum displayed for dibenzo-18-crown-6 in nitrobenzene saturated with water lies again at $M^+ = Na^+$. This agreement seems to indicate that linear polyethers assume a cycle configuration around the complexed cations. The similar behaviour of the poly(ethylene oxide) ligands and of the cyclic ethers has already been noted by Fenton and coworkers (10) on the basis of the similarity of their infrared spectra. This is in agreement with the fact that for the lowest polyether used in this study, glyme-2, which hardly can form a complete ring around the cation, the difference between $\beta_o(\overline{LiL^+})$ and $\beta_o(\overline{NaL^+})$ is the lowest found. However, the discrimination between the individual cations is much stronger when using a rigid ring of the dibenzo-18-crown-6 type than with its linear analogs, probably due to the higher flexibility of the ring formed by the linear polyethers. The same conclusion can be reached from the data of Jaber and coworkers (11) who extracted alkali metal picrates into dichloromethane and found that the ratios of the extraction constants for the pairs Na/Li, K/Na and K/Cs are 20, 31 and 5.4 for dicyclohexyl-18-crown-6 (n = 6), whereas the same ratios for the linear nonylphenoxypoly (ethylenoxy)etanol (n = 20) are 5.5., 29 and 1.6.

In all cases the values of β_o increase with the number of ethylene oxide units (EOU). Comparing glyme-4 and PEG 200 which possess the same number of EOU, higher β_o values are found (by 0.7 - 1.8 log units) for PEG 200. Rather unexpected is the nearly identical behaviour of Li^+, K^+ and NH_4^+ ions (except for the combination Li^+ and glyme-2) reflected in the fact that log β_o for each polyether does not differ by more than 0.3 units.

TABLE III. Stability constants log β_o of the complexes of alkali metals with some polyethers in organic solvents.

nitrobenzene satd. with H_2O							methanol			
Ligand	Li^+	Na^+	NH_4^+	K^+	Cs^+	Ligand	Na^+	K^+	Rb^+	Cs^+
glyme-2	3.33	3.43	2.93	2.36	2.62	$RO(CH_2CH_2O)_6R$ [a]	1.18	1.58	1.52	-
glyme-3	3.78	4.07	3.72	3.61	2.97	$RO(CH_2CH_2O)_7R$ [a]	1.32	1.98	1.91	-
glyme-4	4.32	5.26	4.31	4.28	3.30	$RO(CH_2CH_2O)_8R$ [a]	1.57	2.47	2.36	-
PEG 200	5.47	5.98	5.26	5.35	5.17	$RO(CH_2CH_2O)_9R$ [a]	1.87	2.70	-	-
PEG 300	6.18	6.89	6.15	6.17	5.38	glyme-4 [b]	1.28	1.72	-	1.45
PEG 400	6.67	7.51	6.85	6.94	5.79	glyme-5 [b]	1.47	2.20	-	1.85
PEG 400 [c]	H^+ 5.69	-	-	-	-	glyme-6 [b]	1.60	2.55	-	2.17
dibenzo--18-crown--6 [d]	5.45	7.17	Rb^+ 5.78	6.89	4.79 4.5 [e]	glyme-7 [b]	1.67	2.87	-	2.41

a .... R = C_6H_5, from ref.(4)
b .... from ref. (5)
c .... from ref. (2)
d .... from ref. (7)
e .... from ref. (8)

The increase of β_o values in nitrobenzene with the number of EOU found herein can be compared with that in methanol found by other workers. Generally, the constants β_o are several orders of magnitude higher in nitrobenzene than in methanol. This is easily accounted for by the low basicity of nitrobenzene. Indeed, as reported previsouly by Matsura et al. (9), the values of β_o depend essentially on the competition between the solvent and dibenzo-18-crown-6 for the complexation of the metal ion. Methanol is well known to be much more basic than nitrobenzene.

REFERENCES

1. J. Rais, E. Šebestová, P. Selucký, M. Kyrš : J. Inorg. Nucl. Chem. 38, 1742 (1976).
2. P. Vaňura, J. Rais, P. Selucký, M. Kyrš : Coll. Czech. Chem. Comm. 44, 167 (1979).
3. J. Rais, M. Pacltová-Benešová, P. Selucký, M. Kyrš : J. Inorg. Nucl. Chem. 35, 633 (1973).
4. L. Favrette : Annali di Chim. 66, 621 (1976).
5. O. Chaput, G. Jeminet, J. Juillard : Can. J. Chem. 53, 2240 (1975).
6. J. Rais, M. Kyrš, M. Pivoňková : J. Inorg. Nucl. Chem. 30, 611 (1968).
7. P.R. Danesi, J. Meider-Gorican, R. Chiarizia, V. Capuano, G. Scibona : J. Inorg. Nucl. Chem. 37, 1479 (1975).
8. J. Rais, M. Kyrš, L. Kadlecová : Proceedings International Solvent Extraction Conference, Lyon, Sept. 1974, vol. II, p. 1705.
9. N. Mastura, K. Umemoto, Y. Takeda, A. Sasaki : Bull. Chem. Soc. Jap. 49, 1246 (1976).
10. D.E. Fenton, J.M. Parker, P.V. Kright : Polymer. 14, 589 (1973).
11. A.M.Y. Jaber, G.J. Moody, J.D.R. Thomas : J. Inorg. Nucl. Chem. 39, 1689 (1977).

EXTRACTION OF RARE EARTH METALS BY CARBOXYLIC ACIDS.

V.P. Gladyshev, F.I. Lobanov,
N.N. Andreeva, A.K. Nurtaeva
Kazakh State University

Alma-Ata, USSR.

Extraction of lanthanum, europium, gadolinium, erbium and ytterbium ions with melts of stearic acid and their mixtures with paraffin has been studied at 80°C.

An extraction scheme has been proposed, the constants ($lg\overline{K}_{ex}$) and the two phase stability constants ($lg\beta_3 K_{L,MA_3}$) have been determined.

For a number of years carboxylic acids have been used successfully in Analytical Chemistry and technology for isolating and concentrating some metals, the rare earth metals included (1-4). An increase in the number of carbon atoms of the acid molecule leads to a decrease in the solubility of carboxylic acids and their metal complexes in the aqueous phase. This facilitates metal ion transfer into the organic phase, but the application of long chain carboxylic acids (carbon atoms > 9) in the process of liquid-liquid extraction is not reasonable, since the solubility of metal salts decreases sharply (5).

It is possible, however, to use high-molecular weight carboxylic acids as extractants at high temperatures (6-10). The main merits of the method are : the possibility of achieving high degree of concentration, distinct phase separation and absence of emulsion and the possibility of direct determination of the elements in the solid organic phase by physical and physico-chemical methods (8).

Though there are no detailed in the literature on the extraction of rare earth metals by long chain carboxylic acids, the possibility of isolating microquantities of some elements (yttrium and cerium included) by palmitic acid has been shown (7).

In the present work some physico-chemical properties of stearic acid at high temperatures have been determined, and the formation of complexes of lanthanum, europium, erbium and ytterbium has been studied.

Dimerization of stearic acid has been investigated by the distribution method. Distribution of the acid between the aqueous and organic phases taking into account its possible ionization in the aqueous phase and polymerisation in the organic phase is described by the equation :

$$\underline{D}_c = \{\underline{K}_{D,HA} + 2\underline{K}_2\underline{K}^2_{D,HA}\,[HA]_{aq} + 3\underline{K}_2\underline{K}_3\underline{K}^3_{D,HA}\,[HA]^2_{aq} + \ldots + n\underline{K}_2\underline{K}_3 \ldots \underline{K}_n\underline{K}^n_{D,HA}\,[HA]^{n-1}_{aq}\} / \{1 + \underline{K}_{HA}/[H^+]\} \quad (1)$$

where $\underline{D}_c = C_{HA,org}/C_{HA,aq}$ is the distribution ratio of stearic acid between paraffin and water ;

$\underline{K}_n = [(HA)_n]_{org} / [HA]^n_{org}$ is the formation constant of the polymer ;

$\underline{K}_{D,HA} = [HA]_{org}/[HA]_{aq}$ is the partition coefficient of the acid monomer in the paraffin-water system.

Equation (1) is valid in the case of polymeric forms of the reagent in the aqueous phase and applies (11) to carboxylic acids at concentrations in the aqueous phase of $[HA]_{aq} < 0{,}065$M. Dependence of distribution ratios of stearic acid between the melt of carboxylic acids with paraffin and water at 80°C is shown in Fig. 1. From the experimental data of $\underline{D}_c = f([HA]_{aq})$

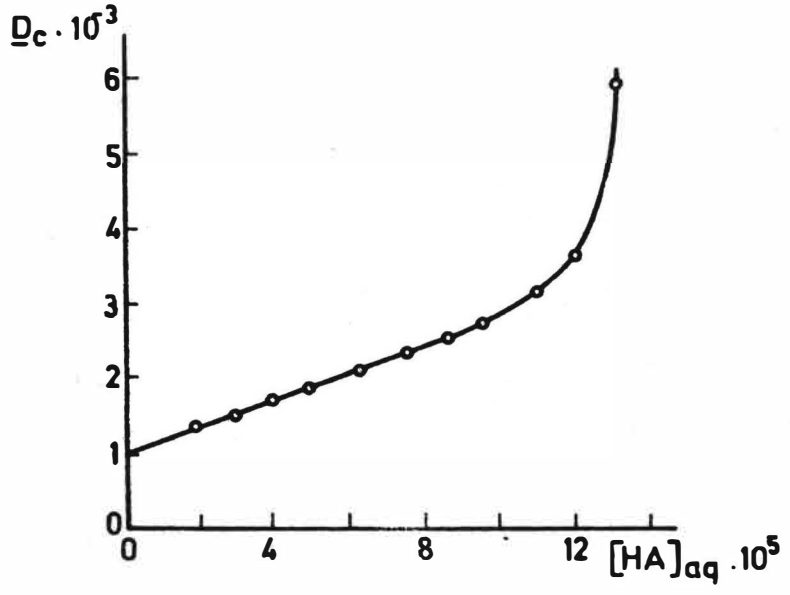

FIG. 1

Dependence of distribution ratios of stearic acid between paraffin and water on stearic acid concentration at 80°C ; $\underline{r}$ = 1:1.

dependence described by equation (1), if n = 2, dimerization constant of stearic acid in paraffin and partition coefficient of its monomer between paraffin and water at 80°C are estimated: $\underline{K}_2$ = (1,06 ± 0,07).10^3 and $\underline{K}_{D,HA}$ = 9,6 ± 0,6.

By increasing the stearic acid concentration in the paraffin phase the aqueous phase becomes saturated by the acid and the dependence of D_c upon $|HA|_{aq}$ is no longer linear. IR-spectra of the acid in paraffin confirmed that in the paraffin-stearic acid melt, the latter is predominantly in the dimeric form.

Extraction of rare earth elements by stearic acid were made as described previously (12). The equilibrium is achieved completely in 1-2 minutes. The phase ratio, r, was of 1:10 ; t = (80 ± 1)°C. The concentration of rare earth elements in the aqueous phase was determined spectrophotometrically using Arsenazo III, and radiometrically using isotope Eu^{154}. For the determination of the elements in the solid extracts, X-ray fluorescence was used.

Lanthanum, europium, gadolinium, erbium and ytterbium extraction is investigated in the wide range of aqueous phase acidity at different metal and stearic acid concentrations. Fig. 2 shows that stearic acid-paraffin mixtures quantitatively extract rare earth elements into the organic phase at pH 4,0-6,0. Investigation of the effect of metal concentration (Fig.2)

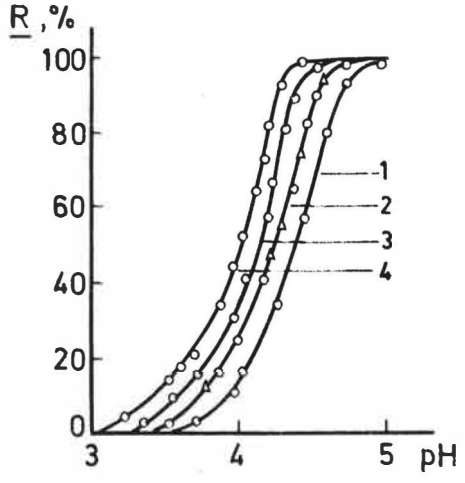

FIG. 2

Dependence of recovery factor of lanthanum (1), europium (2), gadolinium (3) and ytterbium (4) in the stearic acid-paraffin system on the initial metal concentration of the pH of the aqueous phase : O - 10^{-3}M ; Δ - 10^{-4}.

on the extraction of rare earth stearates shows that in the concentration range of metal 10^{-5}-10^{-3}M no hydration and polymerization phenomena of rare earth element ions occur. This is evidenced by coincidence of the curves on Fig. 2. However, further increase of metal concentration (10^{-3}-10^{-2}M) leads to a shift of the extraction curves toward the acidic region because of polymerization in the organic phase.

Experimental data obtained under conditions of existence of metal monomeric forms are presented in the Fig. 3. The slope of these lines is 3. This testifies to the displacement of

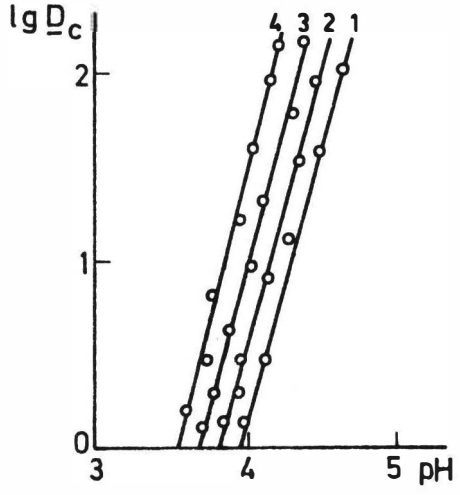

FIG. 3

Dependence of distribution ratios of stearates of lanthanum (1), europium (2), gadolinum (3) and ytterbium (4) on the pH of the aqueous phase.

three protons in the complex forming reaction. The slope of the dependence curve of distribution ratios of europium on the stearic acid in paraffin equals three (Fig. 4)

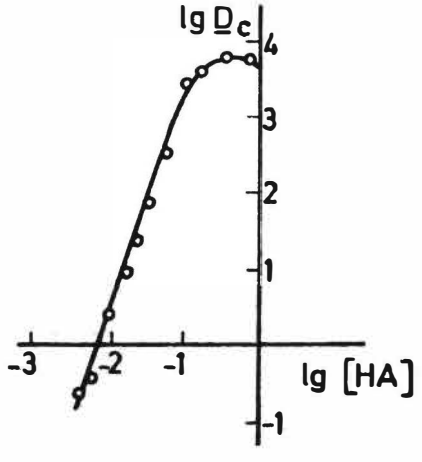

FIG. 4

Effect of stearic acid concentration on the extraction of europium stearate.

Thus on the basis of obtained results one can assume a transfer of EuA_3 compound into organic phase, and the process extraction scheme may be presented as :

$$Ln^{3+} + 3HA_{org} \rightleftarrows LnA_{3,org} + 3H^{+} \qquad (2)$$

Extraction constants of the rare earth element complexes with stearic acid is determined by the equation :

$$\lg \underline{K}_{ex} = \lg \underline{D}_c - 3hH - 3\log[HA]_{org} \qquad (3)$$

where $[HA]_{org}$ is the concentration of acid monomer form in paraffin, which can be found by the equation :

$$[HA]_{org} = C_{HA} - [HA]_{aq} - [A^-] - 2[(HA)_2]_{org} \qquad (4)$$

Taking into account the equilibria of ionisation and the distribution of the stearic acid monomer, one obtains :

$$\underline{K}_2 = [(HA)_2]_{org} / [HA]^2_{org} \; ; \; \underline{K}_{HA} = [H^+][A^-] / [HA]_{aq} \; ;$$
$$\underline{K}_{D,HA} = [HA]_{org} / [HA]_{aq} \qquad (5)$$

Neglecting stearic acid concentration in the aqueous phase in spite of a large value of $\underline{K}_{D,HA}$, one obtains :

$$[HA]_{org} = \{\sqrt{8\underline{K}_2 C_{HA} + 1} - 1\}/4\underline{K}_2 \qquad (6)$$

The calculated values of the extraction constants for La, Eu, Gd, Er and Yb are presented in Table 1. With decreasing ionic radius of the rare earth element, a regular increase of $\lg \underline{K}_{ex}$ is observed. However, the increase is not large and it speaks for unselectivity of stearic acid as extractant towards individual rare earth elements. Separation factor of the Yb-La pair is 10,0. Combining the present data with those in the literature (13), there appears to be an increase of the separation factor with the increase of the number of carbon atoms in the acid molecule (Fig. 5) : $\alpha_{Yb,La}$ for 50 % caproic acid in heptane is 3,9 ; for caprylic acid the corresponding value is 5,0. Two phase stability constants, calculated from extraction constants, increase monotonously in the rare earth series. Such phenomenon is related to a decrease in the basicity of the rare earth element ions. (Table 1).

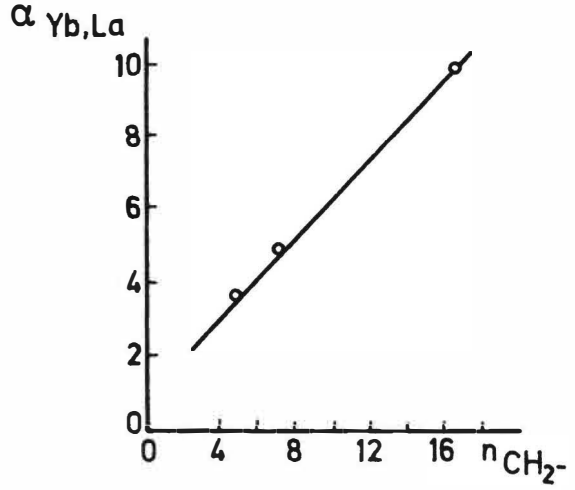

FIG. 5.

Dependence of separation factor $\alpha_{Yb,La}$ on the number of hydrocarbon units in fatty acid molecule.

Table 1. Quantitative characteristics of complexes of rare earth metals with stearic acid (0,1 M solution in paraffin).

Rare earth metal	La	Eu	Gd	Er	Yb
Ionic radius	1,22	1,13	1,11	1,04	0,99
$pH_{1/2}$	4,45	4,26	4,08	4,16	3,98
$lg\underline{K}_{ex}$	-8,16	-7,58	-7,39	-7,45	-7,17
$lg\ \beta_3\underline{K}_{D,MA_3}$	15,92	16,49	16,69	16,63	16,90

REFERENCES

1. Gindin L.M., Bobikov P.I., Couba E.F., Zh. Neorgan. Khimii, 5, 1868 (1960).
2. Fletcher A.W., Flett D.S. In "Khimiya Extraktsii Metallov Organicheskimi Rastvoritelyami" Atomizdat, Moscow, 1969, p. 263.
3. Merkin E.N. "Extraktsiya Metallov Nekotorymi Organicheskimi Kationoobmennymi Reagentami". Moscow, 1968.
4. Danilov N.A., Korpusov G.V., Krylov Yu. S., Zh. Neorgan. Khimii, 19, 194 (1974).
5. Korpusov G.V., Korpusova R.D., Vaks G.L. and Patrusheva E.N., Zh. Neorgan. Khimii, 14, 1912 (1969).
6. Kuznetsov V.I., Seryakova I.V., Zh. Analyt. Khimii, 14, 161 (1959).
7. Novak M., Havel A., J. Inorg. Nucl. Chem., 29, 531 (1967).
8. Lobanov F.I., Leonov V.A., Stefanov A.V. and Gibalo T.M., Zh. Neorgan. Khimii, 22, 3097 (1977).

9. Gladyshev V.P. et al. "Proceedings of the V Soviet Union Conference on the Extraction Chemistry". Novosibirsk, 1978, p. 202.
10. Lobanov F.I. et al. "Proceedings of the II Soviet Union Conference on the Concentration Methods". Moscow, 1977, p. 30.
11. Katchalsky A., Eisenberg H., Lifson S., J. Am. Chem. Soc., 73, 5889 (1951).
12. Lobanov F.I., Gladyshev V.P., Andreeva N.N., Koshevaya I.V., J. Radioanal. Chem., 51, 127 (1979).
13. Danilov N.A., Korpusov G.V. et al., Izv. Vys. Uch. Zav., Ser. Tsvet. Met., N5, 103 (1974).

SOME ASPECTS OF EXTRACTION BY ORGANIC COMPOUNDS

Yu. I. Murinov, Yu. E. Nikitin and
A.M. Rozen
Institute of Chemistry of the
Bashkirian Branch, Academy of
Sciences of the USSR
Ufa, USSR.

ABSTRACT

The synthesis of monodentate and polydentate organic sulphur compounds to be used as extractants is reported. Also, the extraction properties of these compounds are discussed. A quantitative interpretation of the extraction mechanism is presented. The ordering of the extractants with respect to the extraction of gold chloride and uranyl nitrate is given.

The range of metal extractants has so far been relatively narrow (mainly tributyl phosphate, di-2-ethyl-hexyl phosphoric acid and amines) and is less than adequate to ensure complete separation of the rare earths, the non-ferrous metals and the rare metals. Therefore, the search for new extractants of high extraction power, selectivity and chemical stability, which could be suitable for large scale production, is of interest. Furthermore, there is a need for extractants for the recovery of various organic compounds, such as carboxylic acids and sulfoacids. There is also a need for various absorbents able to trap sulfur and nitrogen dioxides, which are dangerous for the environment. Organic sulfur compounds are potential extractants. Among these compounds are the sulfides, the sulfoxides, the ketosulfides and the mercaptans. The synthesis of compounds with predetermined properties has been highly successful in the part. Organic sulfur compounds are of special interest because sulfur in these reagents, besides the vacant 3d-orbital, can act either as a π-electron donor or as an acceptor, depending on the nature of the extracted compound. The present paper deals with the chemistry of organic compounds of various classes. The following compounds have been synthesized and used as extractants : petroleum and synthetic sulfides and sulfoxides of various compositions, disulfides and disulfoxides with a wide range of substituents and featuring various aliphatic groups between the sulfur atoms (R-S-$(CH_2)_n$-S-R'), ketosulfides

and ketosulfoxides containing 1 to 4 sulfur atoms, as well as many polydentate extractants containing a variety of functional groups sulfur and oxygen, sulfur and nitrogen, etc.

ORGANIC SULFIDES

Neutral organic sulfur compounds form an important group of extractants for noble metals which is remarkable for its selectivity and its extraction power [1,2] . The influence of the compositions of organic sulfides on the extraction of noble metals has been studied. All the compounds studied have been synthesized in the laboratory.

All the sulfides, irrespective of their composition, do not extract mineral acids because sulfur barely protonizes. However, an electron-donor interaction exists between the sulfur atom of the sulfides which has a high electron density and the proton. By contacting ^{35}S labelled sulfide solutions in benzene, sulfide complexes have been shown to exist in the aqueous phase. Complexes such as $HCl.nH_2O.qR_2S$, $H_2SO_4.nH_2O.qR_2S$, $HNO_3.R_2S$ (where n = 1-3, q = 1-4) have been isolated. Concentrated nitric acid oxidizes sulfides into sulfoxides and sulfones. Sulfides do not extract water. Based on the soft and hard acid (base) concept, Pearson [3] showed that through a solvation mechanism, sulfides are able to extract metal salts of the soft acid type such as Ag, Hg, Pd and Ru from HNO_3 ; Pd and Ru from HCl. Other noble metals, Pt(IV), Ir(IV) and Rh(III) resist sulfide extraction because they exist in acid aqueous solutions as highly inert complexes. Sulfides do not extract salts of other metals. Therefore, they are suitable for concentrating and separating noble metals. The solvate numbers (q) have been determined by equilibrium shift and saturation methods in extracting silver nitrate (q = 1-3), gold nitrate and chloride (q = 1), platinum and palladium chlorides and nitrates (q = 2). With an increase in the acid concentration of the aqueous phase, the recovery of these metals sharply decreases.

Based on elemental analysis, the equilibrium shift method and IR and PMR spectra, the extraction reaction of noble metals by monodentate sulfides appears to be :

$$MeX_p^{n-p} + qR_2S \rightleftarrows MeX_n \cdot qR_2S + (p - n)x^- \qquad (1)$$

For polydentate sulfides, the saturation and equilibrium shift methods give different solvate numbers, i.e. complexes of various compositions can be present in the extraction phase. Therefore, to compare extraction properties of various sulfides, extraction isotherms for gold microconcentrations (from 10^{-5} to 10^{-7} mol/1) have been obtained, in conditions which are far from saturation of the organic phase (0.01 mol/1 in the extracted complex). The solvate number has been determined under these conditions for gold chloride (III) and found to be equal to 1 for all the species extracted. Therefore, the extraction properties of sulfides towards gold (III) chloride have been considered. The concentration constant K has been estimated

according to the relationship

$$K = \frac{[AuCl_3 \cdot S]_o \cdot Cl_w}{[AuCl_4^-]_w \cdot [S]} = \frac{Y_{Au} \cdot X_{Cl}}{X_{Au} \cdot [S]} \qquad (2)$$

where Y_{Au} and X_{Au} are gold equilibrium concentrations in the organic and aqueous phases, respectively ; Y_{Cl^-} is the chlorine ion concentration, [S] is the extractant equilibrium concentration, and w is water. According to their extraction power towards gold chloride, the sulfides investigated form the following series (concentration constants are given in parentheses) :

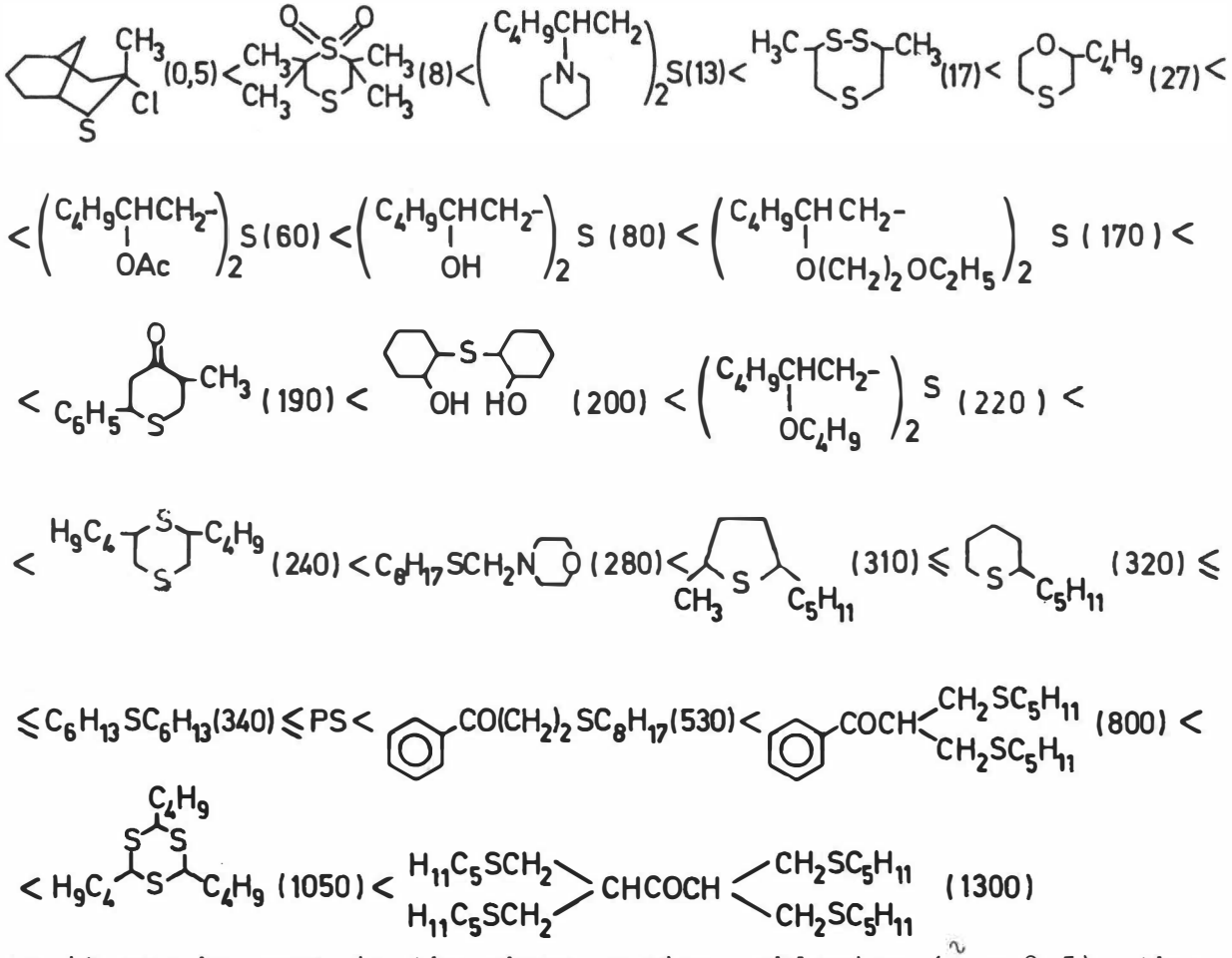

As it can be seen in the above series, chlorine ($\tilde{K}$ = 0.5), the sulfide complex ($\tilde{K}$ = 8) and tertiary nitrogen ($\tilde{K}$ = 13) have a most pronounced effect on the sulfur donor properties. It is to be noted that the nitrogen itself does not appear to be involved in bonding with the metal ion, obviously because of steric hindrances. The ether oxygen introduced in the β-position of dialkyl sulfides reduces donor properties only to a small extent while it sharply changes the extraction power of the sulfide ($\tilde{K}$ = 27) when it is introduced in a ring with the sulfuratom. Another sulfuratom in the para-position has a small effect on the extraction power, it increases the capacity of the extractant which is becoming bidentate.

Of all the reagents studied, trithian ($\tilde{K}$ = 1050) and the ketotetrasulfide ($\tilde{K}$ = 1300) were shown to be most interesting extractants.

In the extraction of silver nitrate by ketomonosulfides, the solvate numbers determined by a saturation method and by an equilibrium shift method greatly differ. Several types of complexes are present in the organic phase whose composition strongly depends on the activities of the species in the aqueous and organic phases. It is to be noted that with increase in the silver concentration and decrease in the free extractant concentration, the solvate number decreases from 3 to 1. The complexes $AgNO_3.3S$, $AgNO_3.2S$ and $AgNO_3.S$ have been isolated from the extraction phase.

SULFOXIDES

The extraction properties of petroleum sulfoxides and of individual sulfoxides were reported in detail in our previous paper [4,5] . Presently, studies of the oxidation-reduction properties of sulfoxides are continued. Also, the extraction of uranyl nitrate by new reagents of the sulfoxide series, hydrosulfoxides ($R-S-(CH_2)_n-OH$) and by ketosulfoxides of various compositions has been investigated. The recovery factors of the metal salts and acid complexes of 50 elements by petroleum sulfoxides from HCl, HNO_3, $HCl-HNO_3$ and $HCl-H_2SO_4$ media have been determined by reverse paper chromatography. Using petroleum sulfoxides as extractants, elements of similar properties, Zr/Hf (R = 9), Ta/Nb (R = 25), Fe/Cu (R = 60) etc. have been separated.

The extraction isotherms for uranyl nitrate at concentrations of uranium varying from 10^{-5} to 10^{-7} mol/l have been measured (aqueous phase : 0.1 mol/l, HNO_3 extractant 0.01 mol/l in o-xylol). The extraction at these concentrations can be described by the equation :

$$UO_2^{2+} + 2NO_3^- + 2S \rightleftarrows UO_2(NO_3)_2\ 2S \qquad (3)$$

whose effective extraction constant $\bar{K}$ is :

$$\bar{K} = \frac{[UO_2(NO_3)_2 \cdot 2S]}{[UO_2^{2+}]_w [NO_3^-]_w^2 [S]^2} = \frac{Y_U}{X_U (2X_U + X_H)^2 \gamma^{\pm}_{UO_2(NO_3)_2} \cdot [S]^2} \qquad (4)$$

where Y_U and X_U are equilibrium concentrations for uranyl nitrate in the organic phase and in the aqueous phases, respectively ; X_H is the nitric acid concentration ; $\gamma^{\pm}_u$ is the activity coefficient for uranyl nitrate.

On the basis of the $\bar{K}$ values, the following series of organic sulfur compounds has been obtained :

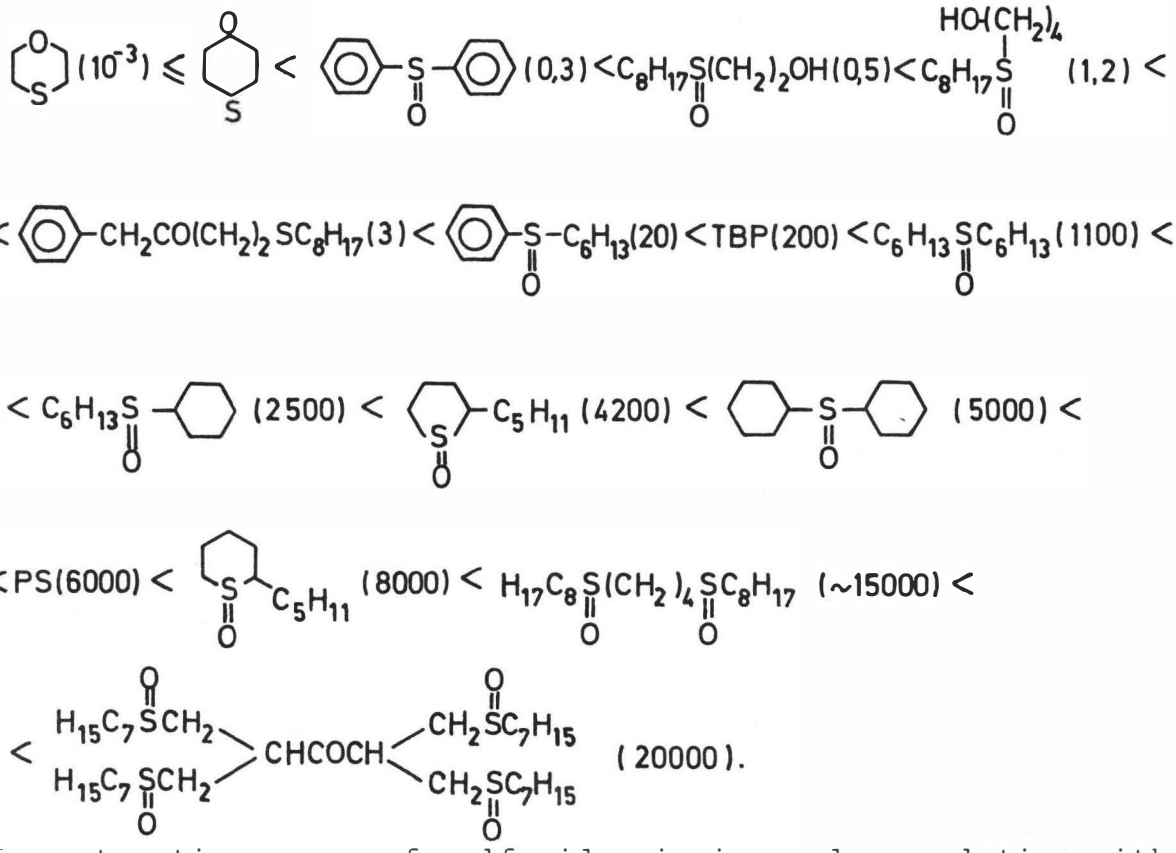

The extraction power of sulfoxides is in good correlation with the oxygen basicity and is described by the equations :

$$\log \overline{K}_U = 11.88 + 5.6\ pK \qquad (5)$$

For non-cyclic sulfoxides, correlation of the extraction power with the sum of the Taft constants for substituent electronegativities is also possible :

$$\log \overline{K}_U = 2.34 - 2.54\ \Sigma\sigma^* = 3.04 - 5.23\ \Sigma(X - 2) \qquad (6)$$

The oxidation-reduction properties of sulfoxides have been studied in the case of the extraction of chromium(VI) from sulfuric acid solutions by dioctylsulfoxide in o-xylol. The interpretation of the data obtained showed that extraction of chromium(VI) by sulfoxides proceeds according to the mechanism :

$$H^+ + HCr_2O_7^- + qR_2S \rightleftarrows H_2Cr_2O_7 \cdot qR_2SO \qquad (7)$$

Reaction (7) proceeds rapidly followed by a slower oxidation-reduction reaction

$$3H_2Cr_2O_7 + 3R_2SO \rightleftarrows Cr(CrO_4)_3 + 3R_2SO_2 + H_2CrO_4 + 2H_2O \qquad (8)$$

Various solvates are thus formed in the organic phase.

The participation of hydrogen ions in the oxido-reduction reaction taking place during the extraction of chromium(VI) has been shown with uranyl nitrate. In this case, reaction (8) is no longer absent. In the organic phase no trace of sulfones were found and no Cr(III) could be detected in the aqueous and organic phases. On studying the extraction of vanadium(V) from HCl and H_2SO_4 media, no oxido-reduction reactions leading to the formation of vanadium(IV) or sulfones has been observed.

Also, some synergic mixtures of extractants have been found : HDEHP + sulfoxides or sulfides ; picrolonic acid + sulfoxides or sulfides ; trioctyl amines + sulfoxides or sulfides and finally mixtures of sulfoxides of various compositions. With increase in the basicities of the donor additives, the extraction constant increases. All the systems are described by the following equations :

$$UO_2^{2+} + 2HA + 2S \rightleftarrows UO_2A_2 \quad 2S + 2H^+ \qquad (9)$$

The increased extraction power of petroleum sulfoxides (PSO) can be explained by a synergic effect since these compounds are in fact mixtures of sulfoxides of various compositions.

THE EXTRACTED COMPLEXES OF METAL SALTS WITH SULFOXIDES AND SULFIDES

All the complexes have been obtained by dilution of the extraction phase by isoalkanes at - 30°C. Under these conditions they precipitated or separated as a liquid phase. The composition of the complexes has been determined by elemental and functional analyses. Also IR, UV, PMR and mass spectra have been recorded to identify the complexes formed, to establish the extraction mechanism and to determine the symmetry of the internal coordination sphere and the type of the chemical bonding. The molecular weight of the extracted complexes has been determined by measuring condensation thermal effects in benzene and cyclohexane. For monodentate sulfides the following complexes have been isolated : $AuCl_3.R_2S$; $PdCl_2.2R_2S$; $PtCl_4.2R_2S$; $RhCl_3.3S$; $AgNO_3.R_2S$; $AgNO_3.2R_2S$; $AgNO_3.3R_2S$; $UO_2Cl_3.2R_2SO$; $UO_2(NO_3)_2.2R_2SO$; $Th(NO_3)_4.2R_2SO$; $Th(NO_3)_2.3R_2SO$; $NdCl_3.3H_2O.3R_2SO$; $Nd(NO_3)_3.3R_2SO$ etc. In the case of complexes where the metal cations have variable valences, oxidation-reduction reactions develop and the sulfides oxidize to sulfoxides. The scheme of the process can be shown as follows :

$$UO_2^{2+}\ 2R_2SO + h\nu \rightarrow (UO_2^{2+}\ 2R_2SO)^* \rightarrow UO^{2+}.\ R_2SO + R_2SO_2 \qquad (10)$$

From the values of the dipole moments for the isolated complexes and from UV spectra a cis-structure is assigned to most complexes. Strong association of the complexes in the organic phase is characteristic of the polydentate extractants, the following complexes form :

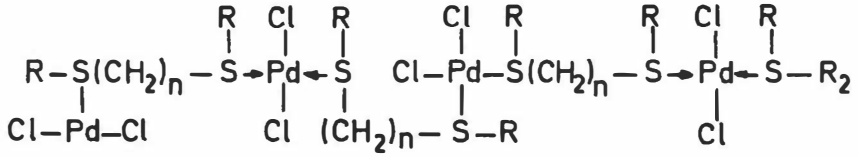

THERMODYNAMICS OF EXTRACTION BY ORGANIC SULFUR COMPOUNDS.

By calorimetric titration performed on a Calvet calorimeter, the enthalpies of dissolution of sulfoxides in various solvents (from - 4 to + 40 kJ/mol) and the enthalpies of mixing with water have been determined. The enthalpy of the 1:1 liquid diamylsulfoxide-water complex formation is 26 kJ/mol. The solubilities of the extractants in water increase with increase in the number of functional groups in the molecule. Formation of outer-sphere complexes have been noted in the organic phase, they are formed by the additional solvation of the extracted complex by the free extractant in the case of cobalt(II), chromium(III), uranium(VI), thorium(IV) and the rare earth chlorides as well as in the case of thorium(IV), cobalt(IV) and rare earth nitrates.

By GLC, the activity coefficients (γ^{o}) for the diluents have been measured in approximation to an infinite dilution state. The values of the activity coefficients are in good correlation with the values of the solubilities of the reported compounds $\log S = B_1 + B_o/\log \gamma^{o}$. The smaller the value of γ^{o} for the diluent in the complex, the greater is the solubility of the complex in the diluent, and consequently, the smaller is the probability of the mesophase in the extraction process. For all the organic sulfur compounds studied, aromatic and chlorinated hydrocarbons are most suitable as diluents.

From the temperature dependence $\log \overline{K}_{ex}$ from 1/T, thermodynamic functions of the extraction reactions (ΔH, ΔG, ΔS) have been calculated. For most systems, the value of the enthalpy change is negative, while in the case of extraction of noble metals (Au, Pd, Pt), it is positive. The positive value for these metals can be explained by the high activation energy spent by the substitution of chlorine ions by molecules of organic sulfide (+ 30-60 kJ/mol). For most extraction reactions, the effect of the entropy factor has been noted in the interaction of the extractant with the hydrated metal ions.

ABSORPTION OF GASES

Sorption properties of petroleum sulfoxides and sulfones have been investigated so as to contribute to the defence of the environment. Sorption of sulfur dioxide and nitrogen dioxide has been studied. Carbon dioxide, carbon monoxide and hydrogen sulfides are not sorbed by sulfoxides and sulfones. In the IR spectra of the NO_2/SO_2-sulfoxide adducts, a 20-30 cm^{-1} shift of

the adsorption bands of the SO group to the low frequency region has been observed which suggests formation of sulfoxide and NO_2/SO_2 complexes. The capacity of sulfoxides is 300-400 mg/g. After the regeneration, no change in the physicochemical properties of the extractant has been found.

REFERENCES

1. T.H. Handley, Talanta 12, 893 (1965).
2. V.A. Mikhailov, V.G. Torgov and A.V. Nikolaev, Izv. Sib. Otd. AN SSSR, 7, (3), 3 (1973).
3. R.G. Pearson, J. Am. Chem. Soc. 85, 3533 (1963).
4. Yu. E. Nikitin, Yu. I. Murinov and A.M. Rozen, Usp. Khim. 45, 2233 (1976).
5. Yu. E. Nikitin, Yu. I. Murinov and A.M. Rozen, Abstr. Int. Solvat. Extr. Conf. Toronto, 1977, p. 38.

SOME PROBLEMS IN CHEMICAL STRUCTURES AND PROPERTIES OF ORGANIC EXTRACTANTS

Yuan Chengye

Shanghai Institute of Organic Chemistry,
Academia Sinica, Peoples Republic of China.

ABSTRACT The molecular design of organic extractants based on the quantitative studies or structure-(re)activity relationships (QSAR) is one of the recent problems in extraction chemistry. This paper presents various aspects of the problem based on the experimental data from author's Laboratory.

1. Introduction.

Quantitative molecular design of organic extractants can, in very practical terms, contribute both to discovery of new selective extractants and to the progress of extraction chemistry in general. One understandable objective in the application of the process of solvent extraction to the separation of metals is to attain a maximum selectivity for a given metal. Development of such new extractants, up to now, is usually worked out by the screening method, which requires large amount of investment and labour. A much more effective way should be available if one knows both qualitatively and quantitatively relationship between chemical structure and the extraction properties of organic extractants. This is the basis for the quantitative molecular design.

2. HSAB PRINCIPLES IN SOLVENT EXTRACTION.

Metal extraction may be considered simply as the replacement reaction of water molecule in the hydration shells of metallic ions in aqueous solution by organic ligand (extractant).

$$M + nL \rightleftharpoons MLn \qquad (1)$$

Both metal ions (acceptor) and coordinating atoms (donor) are classified as hard, soft and borderline acids and bases according to Pearson's scale.

Oxygen-containing ligands (ether, alcohol, carboxylate, phosphate, phosphonate) are referred to hard bases, which prefer to coordinate with hard acids, such as lanthanides, actinides, Nb, Ta, Zr or Hf. As soft bases, sulfur-containing ligands (thioether, thiourea, thiocarboxylate or dithiophosphate) are preferred to combine with soft acid such as Cu, Au, Ag, Pt, Pd or Hg. A nitrogen-containing ligand e.g. aniline or pyridine, being a borderline base, reacts smoothly with a borderline acid (Fe, Co, Ni, Ru, Rh).

The hardness of donor atoms can be modified by the inductive or conjugative effect of the neighboring atoms and groups. An aliphatic hydroxy-oxime, being a hard base, posesses poor ability for extracting Cu (borderline acid) at pH 2. In an aromatic hydroxy-oxime, on the other hand, owing to the presence of a conjugated system, especially in the presence of an electron withdrawing group on the benzene ring, the hardness of the base is decreased and the extraction ability of Cu will be enhanced accordingly.

3. RELATIONSHIPS BETWEEN THE CHEMICAL STRUCTURE AND PROPERTIES OF ORGANIC EXTRACTANTS.

As shown by our early studies(1), the extraction properties of extractants are governed chiefly by three structural factors. First of all, the reactivity of the coordinating atom or group is one of the most important factors, which determines the extraction ability. In the meantime, steric effect plays an important role in the selectivity of solvent extraction. Beside these, appropriate range of molecular weight of extractant is necessary, in order to keep the extracted complex in organic diluents.

Influence of reactivity of the coordinating atom or group. It is well known that in the extraction of metals by neutral organophosphorus compounds,

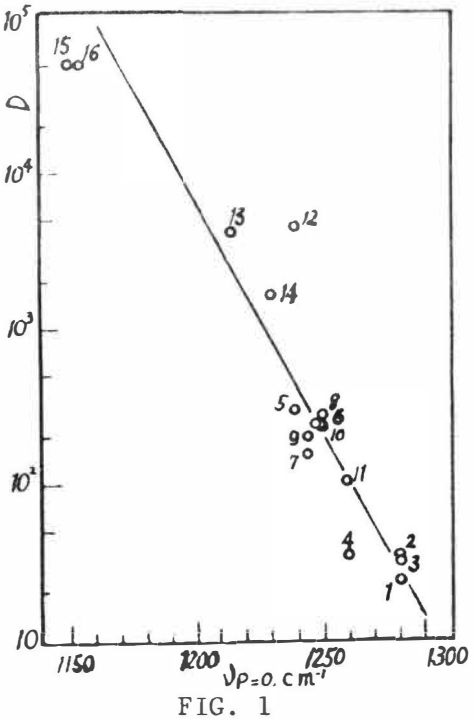

FIG. 1
Relationship between IR & Du of neutral organophosphorus compds(No. correspond to extractants in Table 1)

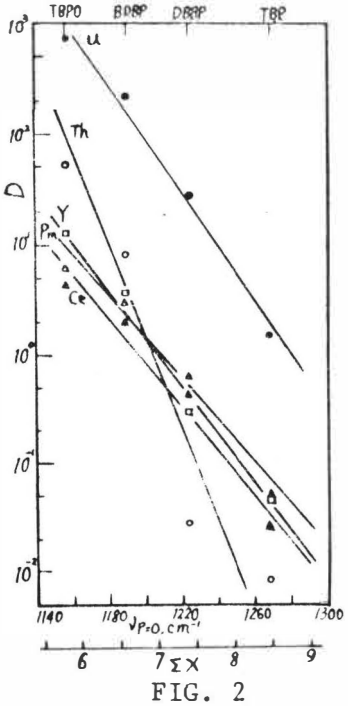

FIG. 2
Influence of group electronegativity on the extraction properties of phosphorus-based extractants. (aq. 3M HNO_3)

the phosphoryl oxygen serves as coordinating atom. As shown in Table 1 and FIG.1, the Maximum distribution ratios of uranium in extraction by such compounds is closely related to the phosphoryl stretching frequency ($\nu_{P=O}$) of extractants(2).

Table 1 Chemical Structure and Properties of Neutral Organophosphorus Compounds

No.	Structure	Du Max	$[HNO_3]$	$\nu_{P=O}$
1	$(n\text{-}C_4H_9O)_3PO$	24.3	5	1269
2	$(n\text{-}C_7H_{15}O)_3PO$	33.9	5	1280
3	$(C_4H_9CHEtCH_2O)_3PO$	31.8	5	1280
4	$(C_6H_{13}CHMeO)_3PO$	34.0	5	1265
5	$CH_3PO(OC_5H_{11}\text{-iso})_2$	298	3	1240
6	$n\text{-}C_4H_9P(O)(OC_4H_9)_2$	239	4	1224
7	$n\text{-}C_5H_{11}P(O)(OC_5H_{11})_2$	155	4	1245
8	$n\text{-}C_6H_{13}P(O)(OC_6H_{13})_2$	272	3	1250
9	$n\text{-}C_7H_{15}P(O)(OC_7H_{15})_2$	198	4	1245
10	$(C_4H_9CHEtCH_2)PO(OCH_2CHEtBu)_2$	226	4	1250
11	$(C_6H_{13}CHMe)PO(OCHMeC_6H_{13})_2$	107	4	1260
12	$(n\text{-}C_4H_9)_2P(O)OC_4H_9$	4500	1	1200
13	$(n\text{-}C_7H_{15})_2P(O)OC_7H_{15}$	4200	1	1215
14	$(C_4H_9CHEtCH_2)_2P(O)OCH_2CHEtBu$	1620	2	1230
15	$(n\text{-}C_7H_{15})_3PO$	>50000	0.5	1155
16	$(n\text{-}C_8H_{17})_3PO$	>50000	0.5	1150
17	$(C_4H_9CHEtCH_2)_3PO$	1200	1	1230

The group electronegativity (ΣX) of typical neutral phosphorus-based extractants as calculated from $\nu_{P=O}$ values by Bell-Rozen's equation: $\Sigma X=6.13+0.237(\nu_{P=O}-1170)$ is correlated linearly with distribution ratio of U, Th^{234}, Ce^{144}, Pm^{147} and Y^{90} from nitric acid system(3).(Table 2 & FIG.2)

Table 2 Influence of Lewis Basicity on the Properties of Extractants

Structure	$\Delta\nu_{OD}$	ΣX	Du	DTh	DCe	DPm	DY
$(BuO)_3PO$	111	8.48	1.48	8.3×10^{-3}	0.026	0.050	0.044
$BuPO(OBu)_2$	121	7.41	18.5	0.284	0.291	0.613	0.419
$Bu_2P(O)OBu$	151	6.60	220	7.78	1.96	2.95	3.61
Bu_3PO	161	5.82	743	49.4	4.25	6.00	12.3

0.1M Extractant in Benzene. Th^{234}, Ce^{144}, Pm^{147} and Y^{90}. $[HNO_3]$ 3M

The relationship between the extraction properties of uranium and the sub-structure of some organophosphorus compounds including neutral organophosphorus ligand ($R_1R_2R_3PO$) and N,N-disubstituted amino-alkylphosphonates $R_2N(CH_2)_nPO(OR)(OR')$ has been investigated by non-parametric method of pattern recognition(4). (Table 3)

Table 3 The Sub-structures Adopted for $R_1R_2R_3PO$

Order	Nature of Sub-structure	Wt. Factor
A	No. of C-atoms in shortest chain	0.2744
B	No. of C-atoms in longest chain	0.3388
C	Degree of branch of C-chain	0.3955
D	Total number of C-atoms	0.3271
E	Ratio of the length of C-chains	0.2117
F	No. of P-O-C bonds in R_1	0.3025
G	No. of P-O-C bonds in R_2	10000*
H	No. of P-O-C bonds in R_3	2.3725
I	Total No. of P-O-C bonds	2.7991

*The weigh factor for G is ∞. We take 10000 for calculation to avoid overflow.

In the nine sub-structures abstracted from seventeen neutral organophosphorus compounds it was found that, the distribution ratio of uranium is enhanced when the number of P-O-C bonds is decreased in the molecule. Such can be attributed to the increase of Lewis basicity of the phosphoryl oxygen, and it is in agreement with IR data. For the twenty eight N,N-disubstituted amino-alkylphosphonates, the extraction ability of uranuim is influenced either by the total carbon number of individual molecule, or by the length of ester alkyl group. In FIG. 3, the compounds examined are divided into groups I and II, according to the threshold value, which was taken as Du=500.

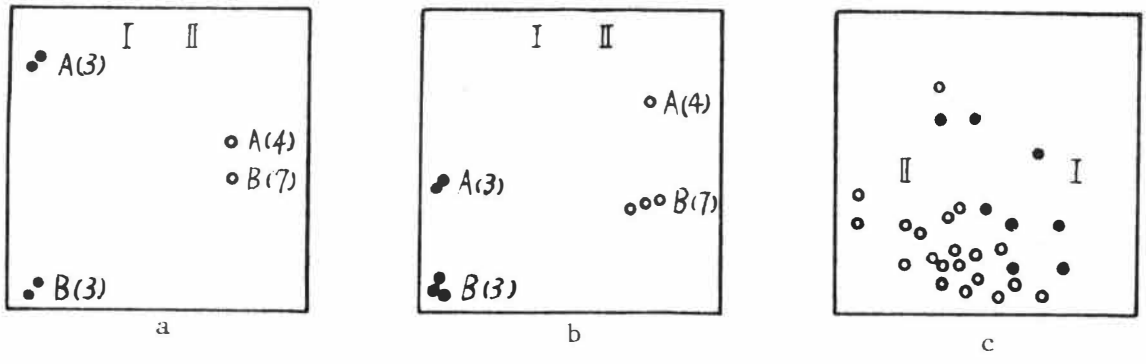

FIG. 3

Pattern recognition processing of relationship between chemical structure and extraction properties of organophosphorus compounds.

The influence of substitutents on the Lewis basicity of dialkyl p-substituted phenylphosphonates and their correlation to Du was studied. The Lewis basicity of these compounds, as measured by the degree of shift of OD vibration frequency ($\Delta\nu$OD) of deuterated methanol, owing to the association of the latter with compounds under investigation, correlates quantitatively to the nature of the nuclear substituents(5) (FIG 4a). The plot of Du value against either $\nu_{P=O}$ or $\Delta\nu$OD of these compounds gives straight lines in both cases(6)

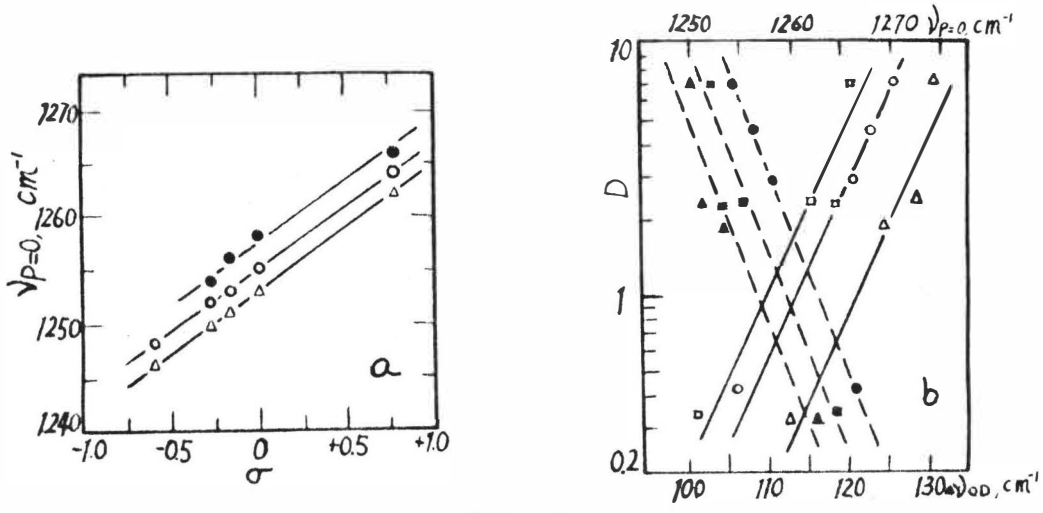

FIG. 4

Influence of substituents on the Lewis basicity of dialkyl p-substituted phenylphosphonates (a)▲ -C_2H_5,o-C_4H_9,●-C_8H_{17} & their correlation to Du (b). (Solidline: $\Delta\nu_{OD}$,o-C_8H_{17},□-C_4H_9,△-C_2H_5. dashedline: $\nu_{P=O}$, ●-C_8H_{17}, ■-C_4H_9, ▲-C_2H_5)

In extraction with acidic phosphates or phosphonates, grouping >P(O)OH acts as coordinating group, which can be measured quantitatively by pKa value. As shown in FIG. 5, there is free energy relationship between the pKa values of mono-ester of p-substituted phenylphosphonic acid and the σ values of the substituents. The pKa values of these compounds are closely related to the extraction properties (Du)(7).

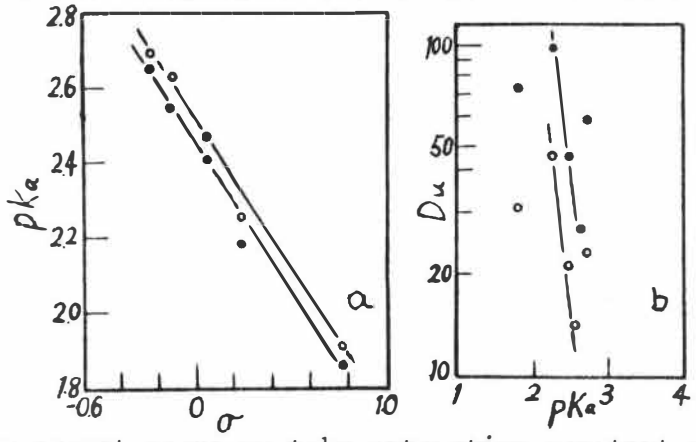

FIG. 5

Influence of substituents on the pKa of monoester of p-substituted phenylphosphonic acids (a) and their correlation to Du (b).

In recent years we take extraction constant as parameter in properties for the study of structure-activity relationship in solvent extraction. As indicated in Table 4 and FIG. 6, the reaction constants for Nd, Sm, Y and Yb extraction are increased, while the acidity of various acidic organophosphorus compounds is enhanced(8).

Table 4 Chemical Structure and Properties of Acidic Phosphates and Phosphonates

No.	Structure	pKa	$\Sigma\sigma$	Kex			
				Nd	Sm	Y	Yb
1	$(iso\text{-}C_8H_{17}O)_2P(O)OH$	2.47	-1.06	6.8×10^{-3}	4.9×10^{-2}	1.0×10^{1}	3.7×10^{1}
2	$(Sec\text{-}C_8H_{17}O)_2P(O)OH$	3.19		5.6×10^{-4}	6.4×10^{-3}	4.1×10^{-1}	3.3
3	$iso\text{-}C_8H_{17}PO(OC_8H_{17}\text{-}iso)OH$	4.09	-1.84	8.4×10^{-5}	8.8×10^{-4}	1.4×10^{-1}	8.9×10^{-1}
4	$C_6H_5P(O)(OC_8H_{17}\text{-}iso)OH$	2.99		2.2	4.2×10^{1}	1.7×10^{3}	2.2×10^{4}
5	$cyc\text{-}C_6H_{11}PO(OC_8H_{17}\text{-}iso)OH$	3.87		1.6×10^{-3}	2.8×10^{-2}	3.4	3.5×10^{1}
6	$(iso\text{-}C_8H_{17})_2P(O)OH$	5.45	-2.62	4.0×10^{-8}	3.2×10^{-7}	4.1×10^{-5}	6.1×10^{-4}
7	$(n\text{-}C_8H_{17})_2P(O)OH$	5.71		1.2×10^{-4}	1.8×10^{-3}	4.1×10^{-1}	1.8
8	$iso\text{-}C_8H_{17}OP(O)(OH)_2$	3.60 9.10	-0.53	6.7×10^{4}	2.2×10^{5}	6.4×10^{4}	2.0×10^{5}
9	$iso\text{-}C_{18}H_{37}OP(O)(OH)_2$*			3.8×10^{5}	4.1×10^{5}	2.9×10^{5}	9.8×10^{5}
10	$iso\text{-}C_8H_{17}P(O)(OH)_2$	4.72 10.41	-1.31	3.7×10^{3}	1.2×10^{4}	6.3×10^{3}	8.1×10^{3}
11	$iso\text{-}C_{18}H_{37}P(O)(OH)_2$	3.88 9.37		7.6×10^{2}	1.3×10^{3}	9.4×10^{2}	4.3×10^{3}

*$iso\text{-}C_{18}H_{37}$ is refered to $C_9H_{19}CH(C_7H_{15})CH_2$ group.

FIG. 7 tells us that the extraction constants for Nd, Sm, Y and Yb are correlated quantitatively with $\Sigma\sigma$ value or pKa of mono-basic phosphoric or phosphonic acids.

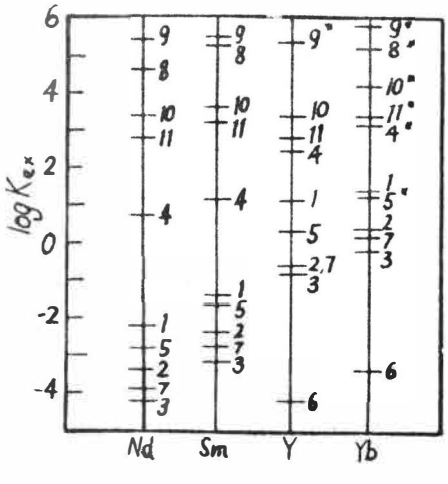

FIG. 6

Comparison of Kex. for Nd, Sm, Y & Yb extraction from chloride sol. with μ=1.0 by various acidic organophosphorus compds.(No.correspond to extractants in Table 4)

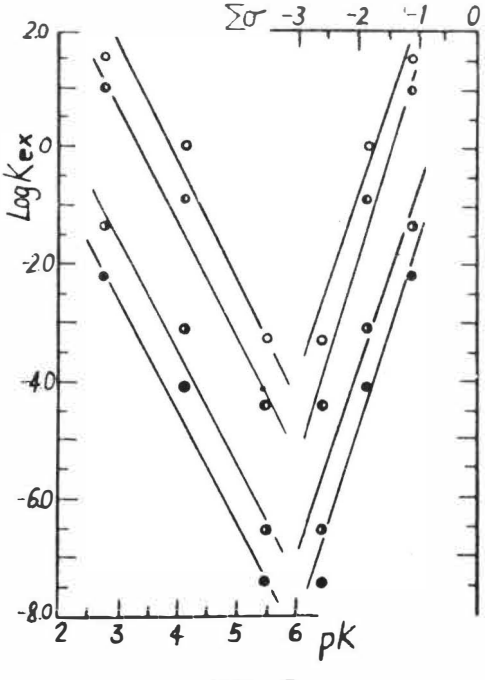

FIG. 7

Correlation of Kex for Nd (●), Sm (◑), Y (◐) & Yb (○) with Taft constants or pKa of acidic phosphorus based extractants.

Steric effects in solvent extraction. Solvent extraction may be regarded as complex formation between two phases. This thermodynamic process is evidently influenced by steric effects. This was examined experimentally on various types of phosphorus-based extractants. In the case of extraction of U and Th by dialkyl isopropylphosphonates, there are no obvious effects on the number of carbon atoms in ester alkyl groups, but the extraction ability is seriously influenced by the position of the side chain (FIG. 8), especially for the extraction of Th, since the formation of $Th(NO_3)_4.3S$ is necessary. The steric effect on extraction of rare earth elements by dialkyl phenylphosphonate(10) and dibutyl alkylphosphonates(11) have been studied. As shown in FIG. 9 (a) & (b) the steric effect of dialkyl phenylphosphonates is more evident than that in dibutyl alkylphosphonates, owing to the fact that there are two alkyl groups in the former case. On the other hand, the steric effect of the extractant is also influenced by the nature of the metal extracted. For example, the distribution ratio of heavy rare earth element (Y) is usually greater than that for light ones (Ce,Pm) due to the lanthanide contraction. We can, to a limited extent, design selective ligands for extraction of certain metals, utilizing the steric hindrance in solvent extraction.

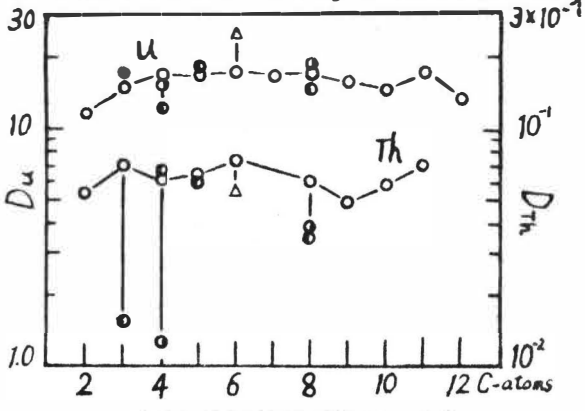

FIG. 8
Influence of structure of alkyl group of dialkyl isopropylphosphonates on the extraction properties of U & Th.(o n-,◐ iso-,● sec-)

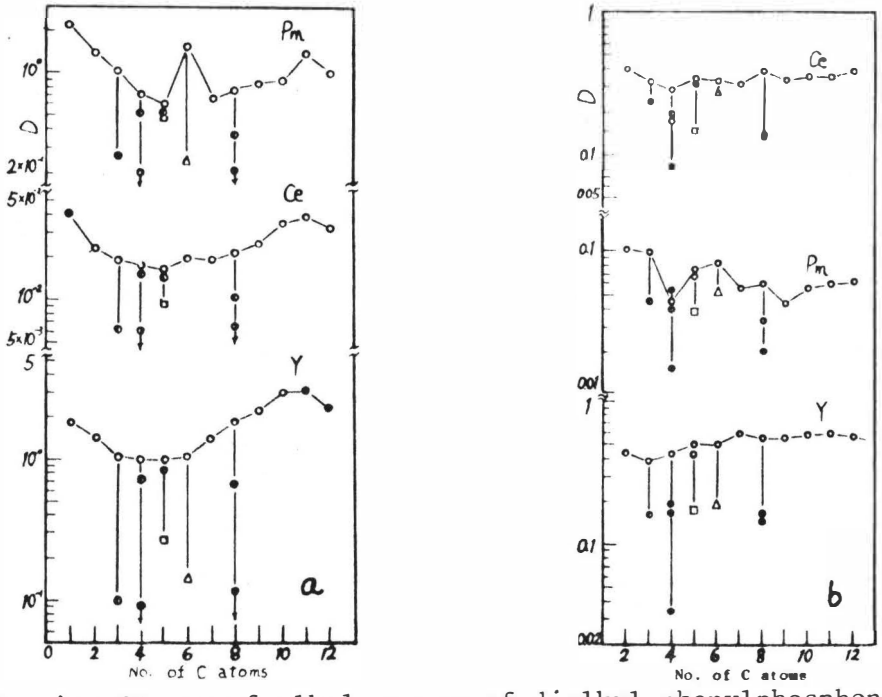

FIG. 9 Steric effects of alkyl groups of dialkyl phenylphosphonated (a) and dibutyl alkyl phosphonated (b) on their extraction behaviour of Ce, Pm and Y (O n-, ◐ iso-, ● sec-, ● ter-, □ Neo-, △ cyclo-)

Thus, the extraction properties, may be predicted by the expression (12).

$$\log K = \log K_0 + \rho\sigma + \delta Es + k\Sigma C \qquad (2)$$

Unfortunately, it is difficult to express the steric effect quantitatively owing to the fact that data on Es values are still insufficient(13).

4. APPLICATION OF MOLECULAR ORBITAL METHOD TO THE QUANTITATIVE STUDY OF STRUCTURE AND ACTIVITY RELATIONSHIP OF EXTRACTANTS

The PMO method. The relationship between the structure and the strength of intramolecular H-bonding of chelating agents was studied by PMO method(14) The charge density of the donating atom (qi) may be calculated simply as $q_i = 1 + a_{io}^2$ in isoconjugated systems of odd alternant hydrocarbons (AH) containing hetero-atoms, where a_{io} is the NEMO coefficient in ith atom. For even AH, $q_i = 1 + \pi_{ii}\delta\alpha$, $\pi_{ii} = \frac{1}{2}\beta\Sigma|a_{or}|$ where π_{ii} —self-polarizability of atom i, and $\delta\alpha$ — change in Coulomb integrals due to substitution of hetero-atoms.

The pKa values of various phenols (phenol —1, β - naphthol — 2, β - anthrol — 3, α - naphthol — 4 and α - anthrol — 5 in FIG. 10) or aromatic amines (aniline — 1, p-phenylaniline — 2, β - naphthylamine — 3, α- naphthylamine — 4, β - anthramine — 5, α - anthramine — 6, 1 - aminopyrene — 7 and 9-aminoanthracene — 8 in FIG. 11) are well correlated with qo and qN value calculated by PMO method. These results indicate that the strength of H-bonding is controlled by π -electrons in the conjugated system. As shown in FIG. 12, both ΔH(Kcal/mole), $\Delta\delta$OH(ppm) and $\Delta\nu$ co(cm^{-1}) are also correlated linearly with qco values in the molecules of methyl O-hydroxybenzene(naphthalene)carboxylates.

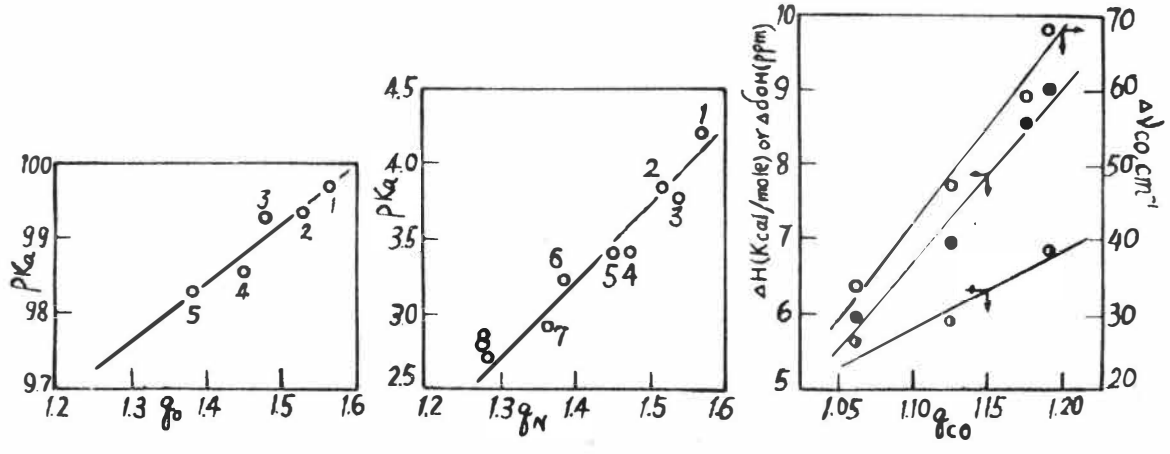

FIG. 10 Correlation of q_o values with pKa of phenols (numbers corresponded to phenols are shown in the text)

FIG. 11 Correlation of q_N value with pKa of aromatic amines(numbers corresponded to amines are shown in the text)

FIG. 12 The plot of ΔH, $\Delta\delta_{OH}$ and $\Delta\nu_{CO}$ versus the q_{CO} value of methyl O-hydroxybenzene(naphthalene) carboxylates.

The HMO method. The structure-activity relationship of nine different hydroxy-oximes has been studied by HMO method(15). These hydroxy-oximes may be considered as conjugated systems containing hetero atoms. In such a case the HMO calculation for the Coulomb and resonance integrals must be altered by expressions $\alpha_X = \alpha_C + h_X \cdot \beta_{C-C}$ and $\beta_{C-X} = k_{C-X}\,\beta_{C-C}$.

The characteristic roots of secular determinants was solved by Jacobi method. The program was made by method of Gauss and worked out on electronic computer CJ-719. The electron density of phenolic oxygen was taken in HOMO. As shown by our experiments the extraction ability of Cu is influenced by electron density of oxygen or nitrogen atoms. There are also certain correlations between bond order of C-N or N-O and extraction properties of hydroxyoximes.

The π bond energy of C=N in hydroxy-oximes was also estimated from expressions(16) $E_{C=N} = -(q_C\alpha_C + q_N\alpha_N) + 2P_{CN}\beta_{CN}$ The values of bond energy thus obtained are well correlated to the characteristic frequency of C=N bond in IR. The influence of these molecular parameters on the extraction properties of hydroxy-oximes was discussed in detail. (Table 5)

Table 5 Structure Parameters of Hydroxy - oximes

Hydroxy-oximes	Electron density			Bond order		
	-OH*	-N=	>N-OH	C - N	N - O	C - OH
$CH_3-\overset{NOH}{\overset{\|}{C}}-CH_2OH$	0.1707	0.8737	1.8898	0.7802	0.3508	0.4906
$CH_3-\overset{NOH}{\overset{\|}{C}}-CMeOH$	0.1330	0.9101	1.8981	0.8092	0.3169	0.4711
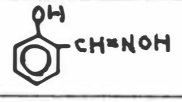	0.0928	1.2270	1.9494	0.8648	0.1960	0.2632
	0.0811	1.2797	1.9539	0.8429	0.1806	0.2630
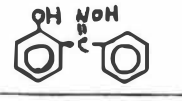	0.0481	1.2501	1.9470	0.7958	0.1992	0.2616
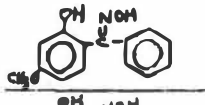	0.0400	1.2669	1.9489	0.7910	0.1914	0.2723
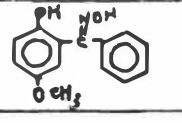	0.0804	1.2498	1.9470	0.7955	0.1972	0.2532
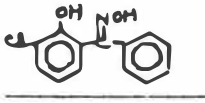	0.0489	1.2501	1.9470	0.7960	0.1968	0.2588
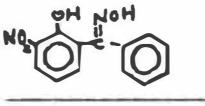	0.0393	1.2494	1.9474	0.7956	0.1974	0.3844

* Phenolic oxygen was taken in HOMO.

5. REACTIVITY-SELECTIVITY PRINCIPLES IN SOLVENT EXTRACTION.

A theoretical explanation for the reactivity-selectivity principle in solvent extraction has been deduced on the basis of the Leffler-Hammond postulate, which was applied in mechanistic studies in organic chemistry by Pross(17).

The schematic representation of FIG. 13 illustrates the fact that for reactive ligand L, the difference in the free energies of activation for reaction of L with M_1 and M_2 (selectivity) is relative small, while for a less reactive ligand L' the $\Delta G^{\ddagger}_{L'M_1} - \Delta G^{\ddagger}_{L'M_2}$ will be correspondingly larger. It shows that the selectivity (β) is inversely proportional to the reactivity (K) in solvent extraction.

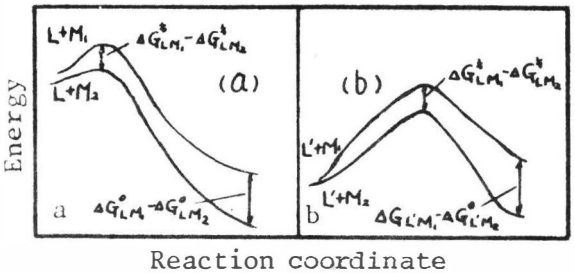

FIG. 13
The effect of a change in reactivity on selectivity of ligands, a highly reactive L (a) & an unreactive L'(b). Selectivity is proportional to $\Delta\Delta G^{\ddagger}$

Quantitative expression of the Hammond postulate may be derived from combination of the Hammett and Brönsted equations. As final expression, we gain $\sigma_M = c(\alpha_0 - \alpha_M)$ and $pK_{a_2} - pK_{a_1} = c(\rho_2 - \rho_1)$. These show that an in-crease of reactivity parameters (σ, pKa) will bring about a decrease in selectivity parameter (ρ, α).

REFERENCES

(1) Yuan Chengye, Nucl. Sci. & Technol. (1962) 908.
(2) Yuan Chengye, Si Lilan, Liu Xiyan, Ye Weizhen, Ma Enxin, Nucl. Sci. & Technol. (1963) 27.
(3) Yuan Chengye, Xie Jifa, Xu Qingren Yan Jinying, Nucl. Sci. & Technol. 2 (1975) 86.
(4) Hui Yongzheng, Wang Jizhong, Yuan Chengye, Kexue Tongbao,To be published.
(5) Yuan Chengye, Ye Weizhen, Ke Mingjuan, Zhou Liying Scientia Sinica, 13 (1964) 1510, Acta Chimica Sinica, 30 (1964) 458.
(6) Yuan Chengye, Si Lilan, Ye Weizhen, Cheng Zhichu, Nucl. Sci. & Technol. (1964) 668.
(7) Yuan Chengye, Cheng Zhichu, Ye Weizhen, Nucl. Sci. & Technol. (1965)870.
(8) Yuan Chengye, Xie Jifa, Ma Hengli, Wang Guoliang, Ye Weizhen, Qin Xiuqing, et.al. To be published.
(9) Yuan Chengye, Ye Weizhen, Yan Jinying, Cai Qixiu, Nucl. Sci. & Technol. 2 (1975) 47.
(10) Yuan Chengye, Xie Jifa, Yan Jinying, Wu Zhenzhong, Zhou Liying, Chen Dehua, Nucl. Sci. & Technol. 2 (1975) 59.
(11) Yuan Chengye, Ye Weizhen, Ke Mingjuan, Cheng Zhichu, Xie Jifa, Yan Jinying, Nucl. Sci & Technol. 2 (1975) 73.
(12) Yuan Chengye, Kexue Tongbao (1977) 465.
(13) S.H.Unger & C.Hansch in "Progress in Phys Org. Chem." (Ed.R.W.Taft) Vol. 12, J.Wiley, 1976, p.91.
(14) Li Shusen, Yuan Chengye, To be published.
(15) Zhou Chengming, Chen Kongchang, Yuan Chegye, To be published.
(16) M.A.Langau et.al. J. Struct. Chem. (1969) 335.
(17) A.Pross in "Advances in Phys. Org. Chem." (Ed. V.Gold) Vol.14, Acad. Press, 1977, P.69.

THE DESIGN OF SELECTIVE REAGENTS FOR LIQUID-LIQUID EXTRACTIONS OF METAL IONS: A RATIONAL APPROACH

Sverker Högberg, Department of Organic Chemistry, Royal Institute of Technology, S-100 44 STOCKHOLM, Sweden

The ability of liquid-liquid extraction processes to compete favourably with other collection and separation methods in the future, will be highly dependent on the successful development of a new generation of selective extraction reagents. The complexity of the factors responsible for the selectivity of a reagent makes a rational approach to the design and synthesis of metal specific reagents necessary in order to limit the time and cost requirements. The task is certainly one in which close interdisciplinary cooperation among organic and inorganic chemists and chemical engineers is important.

Recently a hydrometallurgical research program, HYMLE, was established at the Royal Institute of Technology at Stockholm under the sponsorship of the Swedish Board for Technical Development. The object of this program is to devise complete processes in which the collection, separation and recovery of heavy metal ions constitutes an important part, e.g. the processing of low grade ores or the recirculation of scrap metals. The design, synthesis and evaluation of new selective reagents is a key step in this program.

For the design of the reagents the following approach has been adopted. The coordination chemistry of the metal ions to be separated

is analyzed and characterized with respect to the following properties; charge, ionic radius, hardness-softness and preferred coordination geometry. The object of the design of a reagent is then to include discriminating factors, both steric and electronic, which stress the differences between the coordination requirements of the ionic species and thus enhance the selectivity of the reagent. The necessary control over both steric and electronic factors can only be achieved in highly structured reagents.

The structural components of a reagent may formally be divided into three classes, which from the standpoint of synthetic strategy may be dealt with fairly independently. They are (1) the ligand atoms (the active components of the reagent), (2) the carbon-skeleton (which determines the spatial arrangement of and the distances between the ligand atoms), and (3) the lipophilizing elements (usually alkane chains important for solubilizing the complexes in the organic phase).

How discriminatory factors may be applied on different levels of the metal ion-ligand interactions is discussed in the following both in general terms and with reference to a specific separation problem.

On ionic radius: The use of macrocyclic and macrobicyclic reagents possessing a cavity of fixed diameter have been successfully applied to the separation of different alkali and alkaline earth metal ions. In principle, other metal ions might be separated in the same way provided that their ionic radii are sufficiently different. The macrocyclic reagent generally exhibit slower rates of metal ion exchange and sometimes very high metal ion binding constants.

On hardness-softness: The choice of ligand atoms to match the hard-

ness-softness of the metal ion is one of the two most important ways to discriminating between two metal ions. The possible number of permutations (number and kind of donor atoms) is astronomical. A lot of basic data are still needed in this area.

On coordination geometry: Almost any suitable geometry of the ligand atoms can be established by suitable design of the reagent. For example, selection between square-planar and tetrahedral geometries can thus be achieved. The steric bulk of the reagent may also function as a discriminatory element by preventing the formation of complexes of higher coordination numbers.

The first specific case to which this general approach is being applied, is the separation of zinc (II) ions from iron (II) ions in sulfuric acid solution at low pH. This is a fairly general problem in many hydrometallurgical processes to which there is no general solution at present. The analysis of the coordination chemistry of the two metal ions results in the following Table.

	Zinc (II)	Iron (II)
Charge	+ 2	+ 2
Ionic radius	0.76 Å	0.76 Å
Hardness-softness	Intermediate	Intermediate
Preferred coordination geometry	Tetrahedral	Octahedral
Alternative - " - - " -	Octahedral, trigonal bipyramidal or square pyramidal	Tetrahedral, Trigonal bipyramidal

The design of a suitable reagent will have to concentrate on the fairly minor difference that seem to exist in the coordination geometry and the hardness-softness of the two metal ions. Although both are classified as intermediate cases, zinc (II) might be considered a somewhat softer ion than iron (II). A combination of sulfur and nitrogen donor atoms is expected to be more favourable for the complexation of zinc rather than ferrous ions. A reagent favouring a tetrahedral coordination geometry might likewise discriminate between the two ions. Geometric discrimination might be achieved in two different ways, either by using a flexible tetradentate reagent, which can not satisfy an octagonal coordination sphere, or by using a bulky bidentate which may form a ML_2 complex but not a $ML_2(HL)$ one due to the steric over-crowding that would take place around the metal ion.

A series of closely related bidentate and tetradentate ligands have been synthesized which makes it possible to evaluate the electronic and geometric discriminatory effects separately.

Using this approach, it has been possible to design new ligands which extract zinc but not ferrous ions from sulfate solutions at pH 2.

SOME OBSERVATIONS ON THE EXTRACTABILITIES OF UNIVALENT CATIONS WITH DIBENZO-18-CROWN-6 AND PICRATE ION

Yuko HASEGAWA and Tatsuya SEKINE

Department of Chemistry,
Science University of Tokyo

Kagurazaka, Shinjuku-ku, Tokyo
JAPAN, 162

The present paper summarizes our results of the extraction of ion-pairs formed by univalent metal complexes with dibenzo-18-crown-6(E) and picrate ion(L^-) into chloroform and benzene, and discusses several factors affecting the extractabilities of the complexes.

The extraction of a univalent metal ion with a crown-ether and an anion can be represented by $Kex_0 (=[ME^+L^-]_{org}/[M^+][L^-][E]_{org}=D([L^-][E]_{org})^{-1}$ when D is the distribution ratio of the metal ion, and $[M^+]>>[ME^+]$). The values of Kex_0 decrease in the following order; $K^+ \geq Tl^+ > Rb^+ > NH_4^+ \geq Ag^+ > Cs^+ > Na^+$.

The difference of the extraction can be explained mainly in terms of the difference of the stability of the cationic metal complex between the metal ion and the ether in aqueous solutions.

Actually, the extraction constant of the complex represented by Kex ($=[ME^+L^-]_{org}/[ME^+][L^-] = Kex_0 Kd\beta^{-1}$) is approximately the same for the different metals in a given organic solvent as seen in the table.

The extractability of the complex (ME^+) should be mainly affected by i) the hydrophobic tendency of the complex, ii) the counter ion, iii) the hydration in aqueous and organic solutions, iv) the interaction with organic solvents.

Since the molar volume of the complexes are approximately similar and the only anion used is the picrate ion, the hydrophobic tendency and the effect of anions may be excluded from the consideration of their extractability.

The poorer extraction of the sodium(I) and silver(I) complexes may be attributed to a stronger hydration of the central metal ions.

The extraction of the free crown ether is better into chloroform than into benzene. The same tendency is also observed for the extractions of the crown ether complexes except for the silver complex. This would be explained in terms of a stronger interaction of chloroform with the ethereal oxygens, most probably through the hydrogen atom of the solvent molecule . The different behavior of silver(I) complex may be explained in terms of the interactions of the central metal ion with the π-electrons of the benzene ring.

Table Summary of constants for univalent metals.

		Na*	Ag	K	NH_4	Rb	Tl	Cs*
$\log Kex_0$	C_6H_6	2.2	3.6	4.5	3.6	3.8	4.5	3.1
$\log Kex$	C_6H_6	3.9	5.1	5.7	6.2	5.6	5.9	5.0
$\log Kex_0$	$CHCl_3$	--	3.3	4.7	3.7	4.2	4.7	--
$\log Kex$	$CHCl_3$	--	5.8	6.9	7.3	7.0	7.1	--
$\log\beta$ **		1.2	1.4	1.7	0.3	1.1	1.5	0.8

$\log Kd (=[E]_{org}/[E])$: 2.9(C_6H_6)* , 3.9($CHCl_3$)

* A. Sadakane, T. Iwachido, and K. Toei, Bull. Chem. Soc. Jpn. 48, 60 (1975)
** E. Shchori, N. Nae, and J. J.- Grodzinski, J. Chem. Soc. Dalton 2381 (1975)

ON THE EXTRACTION AND ACCELERATION IN HYDROXYPHENYLKETOXIM SYSTEMS

K. Gloe, P. Mühl, J. Beger, H. Binte
Zentralinstitut für Festkörperphysik
und Werkstofforschung
Dresden - GDR
Sektion Chemie der Bergakademie
Freiberg - GDR

Several alkoxylated o-hydroxyphenylketoximes(I)have been synthesized and characterized by various methods (IR, UV, ^{1}H-NMR, TLC, HPLC). Solubilities of the oximes were determined in toluene, n-octane and water.

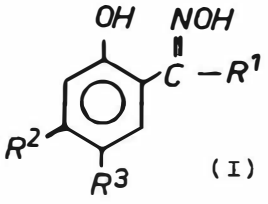

(I)

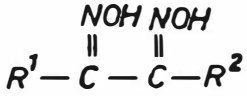

(II)

R^1 = CH_3, C_2H_5, C_6H_5
R^2 = CH_3, $C_6H_{13}O$, $C_{10}H_{21}O$, $C_{16}H_{33}O$, H
R^3 = H, $C_{10}H_{21}O$

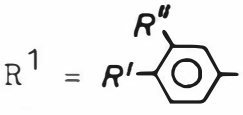

; R^2 = H, alkyl

R^1 = CH_3; R^2 = $-CONR_2$

The effect of substitution of(I) in the R^1, R^2 and R^3 positions on copper and iron extraction are systematic but small, in contrast to the influence of the aqueous phase composition or of the diluent.

Potential accelerators for the extraction of copper on the base of α, ß-dioximes(II) were prepared and in the above extraction system tested. The influence of the substitution of(II) on the acceleration of the copper extraction is significant. Remarkable effects has been obtained with dioximes substituted with cycloaliphatic groups in the R' position or with the tetramethylene group in the R', R'' position.

SELECTIVE EXTRACTION OF MERCURY(II) WITH 4-PHENYL-5(4-METHYL-PHENYL)-1,3,4-THIADIAZOLIUM-2-THIOLATE(PMPTD) FROM BRINE SOLUTIONS

H. F. ALY and A. M. KIWAN

Chemistry Department, Kuwait University

Kuwait

In the chlor-alkali industry, a significant amount of mercury is lost during the various stages of the process and eventually pollute the environment. Studies aimed at the removal of mercury from the waste brine solutions prior to discharging it to the environment are obviously desirable[1]

PMPTD is a mesoionic 1,3,4-thiodiazolium derivative with a selective ability to coordinate with mercury(II) compounds. Analogous derivatives have been recently found to form 1:1 and 1:2 complexes with $HgCl_2$ and 1:1 complex with PhHgCl[2]. The extraction of $HgCl_2$ by PMPTD was investigated radiometrically as a function of (a) nature of diluent (b) mineral acid concentration (c) nature of anions in the aqueous phase, and (d) extractant concentration. The extraction coefficient, D, for $HgCl_2$ from dilute (pH 3) hydrochloric acid by PMPTD (3.7×10^{-5}M) in various diluents was found to decrease in the order: chloroform (1.02) > ethyldichloroethylene (0.30) > kerosene (0.13) > toluene (0.07) > trichloroethylene (0.01) > cyclohexane (0.003) > n-hexane (0.003) > carbon tetrachloride (0.002). The values of D, was also found to depend on the concentration of HCl in the aqueous phase: it increased from 0.04 at 1.0 M HCl to 1.02 at 1×10^{-3}M HCl by using 3.73×10^{-5} M PMPTD/$CHCl_3$. Neither the presence of nitric acid (upto 2M), sulphuric acid (upto 4M), nor several metal salts (e.g. $CuSO_4$, $ZnSO_4$, Na_2SO_4 or $Al(NO_3)_3$) had any effect on the value of D. On the other hand, the presence of chlorides, bromides or iodides had lowered the values of D considerably. The lowering effect of the chloride ions however, are greatly compensated by increasing the concentration of PMPTD. Thus, by increasing the concentration of PMPTD from 3.73×10^{-5}M to 5.0×10^{-2}M, a corresponding increase in the values of D from 4×10^{-4} to 28.4 has been observed.

Preliminary investigation has been also indicated the feasibility of removing traces of mercury from brine solutions by extraction chromatography using silica loaded with PMPTD.

REFERENCES

1- M. Sitting. "Pollutent Removal Handbook", Noyes Data Coorporation, Park Ridge N.Y., p. 294 (1973).
2- A. M. Kiwan, A. Y. Kassim and H. M. Marafy, Proceeding of ISCE, 1977.

SYNTHESIS AND EXTRACTING PROPERTIES OF KETOSULFIDES

Yu.E.Nikitin, Yu.I.Murinov,
R.A.Khisamutdinov, V.I.Dronov,
G.A.Tolstikov
Institute of Chemistry of the
Baschkirian Branch of the Academy
of Sciences of the USSR
Ufa, USSR

Organic compounds containing a sulfur atom in the functional group are most effective extractants of noble metals. These are sulfides, sulphoxides, mercaptans, thiocarbamides etc. The search for new efficient agents to extract noble metals from poor solutions is of interest. We suggest ketosulfides for this purpose.

We have found that by interaction of excess ketones with a mixture of formaldehyde and a corresponding mercaptan in the presence of NaOH in the aqueous-alcoholic solution, various ketosulfides can be prepared:

$$R^1COCH_2R^2 + CH_2O + R^3SH \longrightarrow R^1COCHR^2CH_2SR^3 \qquad (1)$$

where R^1 is a lower alkyl, phenyl or cyclohexyl,
R^2 is a lower alkyl,
R^3 is an alkyl containing 1-12 atoms of carbon, or benzyl.

Based on the results of elemental analysis, the equilibrium shift method and IR and PMR spectra, the following mechanism for extraction of gold and palladium is suggested:

$$AuCl_4^- + S \longrightarrow AuCl_3 \cdot S + Cl^- \qquad (2)$$

$$PdCl_4^{=} + 2S \longrightarrow PdCl_2 \cdot 2S + 2Cl^- \qquad (3)$$

The extraction properties of ketosulfides of various structures have been evaluated, with silver nitrate as an example; they are increasing in the order: ketomonosulfide < keto-bis-sulfide < ketotetrasulfide. Since no agreement is observed for the solvate numbers by the saturation and dilution methods in ketomonosulfide extraction of silver nitrate, several species of complexes whose structure depends on the aqueous and organic phase activities exist in the organic phase: $AgNO_3 \cdot S$; $AgNO_3 \cdot 2S$; $AgNO_3 \cdot 3S$.

SYNTHESIS AND IMPROVEMENT OF THE PROPERTIES OF HYDROXAMIC ACIDS AS NEW EXTRACTING AGENTS FOR METAL IONS

H.N.Al-Jallo, S.S.Ahmed and F.I.Saleh

Chemistry Dept., Nuclear Research Center

Tuwaitha, Baghdad, IRAQ.

Recently, hydroxamic acids of the general formula RCONHOH (R have the neo-type structure) (I) were used as a convenient extracting agents for analytical and industrial purposes and mainly for actinides and fission products (1,2).

As (I) are not easily available, the present work deals with the synthesis and properties of a number of N-substituted hydroxamic acids (II and III) from commercially available carboxylic acids. The study of the above properties include solubility behaviours, thermal and chemical stabilities as well their extraction behaviours toward uranyl ions. The results of N-substitution showed to improve the above properties, it increases and reduces the solubilities in organic and aqueous phases respectively and increases the thermal and chemical stabilities. Moreover, the results showed that the above properties could be improved by increasing the number of methylene groups as in (II) specially when $R_1=CH_3$. In addition, the above properties were also improved by di-ortho substitution as in (IIIa) or p-substituted long chain alkyl group (IIIb).

Quantitative extraction of UO_2^{2+} with II will be discussed. The overall results obtained for II and III are parallel to those reported for (I).

$C_6H_5.(CH_2)_nCON(R_1)OH$ (II)

n = 3 or 4

$2\text{-}R_2,4\text{-}R_4,6\text{-}R_3.C_6H_2CON(R_1)OH$ (III)

a, $R_2=R_3=CH_3$ b, $R_2=R_3=H, R_4=n\text{-}C_8H_{17}$

[$R_1=H, CH_3$ or C_6H_{11}]

REFERENCES

(1) G.M.GASPARINI AND E.POLIDORI, J.CHEM. AND ENG. DATA, 21, 504 (1976).

(2) G.M.GASPARINI AND A.BRIGNOCCHI, CNEN, RT/CHI (78) 4 (1978).

SCHIFF BASE OF 2-AMINO-3-AMINOMETHYL-4-METHOXYMETHYL--6-METHYLPYRIDINE WITH SALICYLIC ALDEHYDE AS A PROMISING EXTRACTANT FOR COPPER

Z. Cimerman, A. Deljac, and Z. Štefanac

Faculty of Science, University of Zagreb

Strossmayerov trg 14, 41000 Zagreb, Yugoslavia

Complex formation with 2-amino-3-N-(2-hydroxybenzylidene) aminomethyl-4-methoxymethyl-6-methylpyridine is shown to be a promising basis for the separation of copper(II) from zinc(II) and cadmium(II) by extraction into organic phase and for a sensitive spectrophotometric copper determination.

A critical parameter is the acidity of the aqueous phase. At pH < 5 the Ligand molecule is degraded to the protonated diamine and salicylic aldehyde which is withheld in the organic phase. In the range 5<pH<7 the complex is present in the organic and in the aqueous phase. The pH > 7 promotes the complex formation and the extraction with chloroform.

The composition of the complex species present in the aqueous phase has not been determined because of its considerable unstability. A copper to ligand ratio of 1:3 has been found in chloroform solution by Job's continuous variation method at pH 9.8 and 5.0.

The method described by W. Likussar and D.F. Boltz[1] has been applied and log K = 14.52 at pH 9.8 and log K = 9.04 at pH 5.0 have been determined.

The efficiency of copper extraction has been calculated in percents on the basis of the results obtained by copper determinations in the aqueous phase using atomic absorption and VIS spectrophotometric methods[2]. The extraction efficiency of about 80% at pH > 7 of the aqueous phase and 1:3 metal to Ligand ratio amounts to 97% with a tenfold excess of the Ligand.

A high sensitivity of the succeeding copper determination is ensured by the effective log $\varepsilon = 1.2 \times 10^4$ value of the complex at 364 nm.

The herewith introduced ligand forms also complexes with Co(II) and Ni(II) but the selectivity for copper with regard to zinc or cadmium allows a quantitative extraction even in the presence of a hundredfold excess.

REFERENCES

[1] Likussar, W. and Boltz, D.F., Anal. Chem.1971, 43, 1265.

[2] Iwamoto, T., Bull. Chem. Soc. Japan 1961, 34, 605.

THE USE OF 4-THIOBENZOYL 2,4-DIHYDRO 5-METHYL 2-PHENYL 3H-PYRAZOL-3-ONE (SBMPP) AND THIOBENZOYL TRIFLUOROACETONE (SBTA) AS CHELATING EXTRACTANTS

G.N.RAO AND V.S.CHOUHAN
Chemistry Department
INDIAN INSTITUTE OF TECHNOLOGY
NEW DELHI, INDIA

The reagents 4-thiobenzoyl 2,4-dihydro 5-methyl 2-phenyl 3H-pyrazol-3-one (SBMPP), and thiobenzoyltrifluoroacetone (SBTA) were prepared from BMPP and BTA respectively,following a method similar to that employed by Berg and Reed[1] for the synthesis of thioderivatives of β-diketones. Since heavy metals show a preference to coordinate to sulphur as compared to oxygen, such compounds appear to be very promising as selective reagents. It has been proved that thiocompounds are more efficient due to their lower pK_a values as compared to their present compounds[2].

Solvent extraction of ^{60}cobalt, ^{65}zinc and $^{152+154}$europium from aqueous acetate buffers into benzene containing SBMPP and SBTA has been investigated comprehensively. Stoichiometry of the extracted species corresponded to 1:2 (metal:ligand) with Co(II) and Zn(II) and 1:3 with Eu(III). Extraction constant values (Table-1) showed that the thioligands, SBMPP and SBTA are more efficient in the extraction of Co(II) and Zn(II) as compared to BMPP and BTA respectively, whereas the reverse is the case in the extraction of Eu(III)[3].

Synergistic enhancement of extraction has been observed in these systems with auxiliary ligands like pyridine, γ-picoline, quinoline, tri-n-octylphosphine oxide (TOPO), tri-n-butylphosphate (TBP), bipyridyl and ortho-phenanthroline. In general γ-picoline exhibited more enhancement in the extraction than pyridine and quinoline. Also TOPO is better synergistic agent than TBP.Ortho-phenanthroline and bipyridyl exhibit considerable enhancement as compared to other auxiliary ligands.

Table-1 Extraction constant (log K_{ex}) values for SBMPP, SBTA BMPP and BTA systems

	BMPP	SBMPP	BTA	SBTA
Co(II)	-7.25	-3.08	-8.72	-4.88
Zn(II)	-5.80	-2.68	-7.88	-5.92
Eu(III)	-3.96	-7.08	-9.90	-11.34

REFERENCES

1. E.W.Berg and K.P.Reed, Anal. Chim.Acta, 36, 372 (1966)
2. J.P.Shukla, V.K.Manchand and M.S.Subramaniam, J.Electroanal. Chem., 50, 253 (1974)
3. V.S.Chouhan and G.N.Rao,J.Radioanal.Chem.,52, 199 (1979)

Mass transfer
Session 2

Co-chairmen : C. Hanson (University of Bradford, Bradford, U.K.)
R. Jottrand (University of Bruxelles, Belgium)

2A

80-18 Mass transfer during droplet formation in liquids.
V. Zimmermann, W. Halwachs and K. Schügerl, Universität Hannover, Germany.

80-194 Mass transfer coefficients in D_1 (2-ethyl hexyl) phosphoric acid for cobalt and nickel.
J.A. Golding and V.N. Salch, University of Ottawa, Canada.

80-220 About the influence of soluble absorption layers on the mass transfer between liquid phases controlled by transport processes.
W. Nitsch and L. Navazio, Technischen Universität München, Germany.

80-121 Phase transfer and micellar catalysis in metallurgical liquid-liquid extraction systems.
K. Osseo-Asare and M.E. Keeney, Pennsylvania State University, University Park, Pennsylvania, U.S.A.

80-16 Extraction with chemical reaction : sulphonation of toluene.
P.R.L. Grosjean and H. Sawistowski, Imperial College of Science and Technology, London, U.K.

80-118 Kinetics and mechanism of extraction of copper by hydroxyoximes under quiescent and turbulent mixing.
M. Cox, C.G. Hirons and D.S. Flett, The Hatfield Polytechnic and Warren Spring Laboratory, Stevenage, U.K.

2B

80-17 Mass and heat transfer in partially miscible liquid-liquid extraction systems using radioactive emission of tracers and image analysis technology.
F.J. Aguirre, S.H. Chiang and G.E. Klinzing, University of Pittsburg, U.S.A.

80-12 Solvent refining of lubricating oil with furfural and furfural-cyclohexa-none in electric field.
Ding Jian-Chun, Xu Jun and Fan Wei-Min, Shangai Institute of Chemical Technology, China.

80-79 Stirred cell study of copper extraction kinetics.
R.E. Molnar and J.H.E. Jeffes, Imperial College, London, England.

80-196 Extraction of copper (II) by hydroxyoxines in an electric field.
P.J. Bailes and I. Wade, University of Bradford, U.K.

80-209 The determination of mass-transfer coefficients and interphase surface during extraction of uranium by tri-N-butylphosphate in centrifugal field.
M.F. Pushlenkov, G.I. Kuznetsov, N.N. Shchepetil'nikov and A.T. Filyanin, V.G. Khlopin Radium Institute, Leningrad, U.S.S.R.

80-225 Short cut of calculation procedure for countercurrent extractions.
J.A.M. Spaninks and S. Bruin, Agricultural University of the Netherlands, De Dreyen, 12, The Netherlands.

MASS TRANSFER DURING DROPLET FORMATION IN LIQUIDS

V. Zimmermann, W. Halwachs, and
K. Schügerl
Institut für Technische Chemie der
Universität Hannover
Hannover, W-Germany

ABSTRACT

Mass transfer during the droplet formation was measured employing a modified liquid scintillation technique with a time resolution of 0.01 sec. Mass transfer is considerably enhanced by the liquid circulation within the droplet if the main mass transfer resistance is located within the droplet. The instantaneous mass transfer coefficient passes a maximum as a function of the droplet formation time within the first 0.5 sec. This maximum seems to coincide with the maximum droplet circulation rate. The erroneous statements of the droplet formation models which disregard this circulation are illustrated by several examples.

The aim of the investigations presented here was to measure the mass transfer during the droplet formation (in the time range 0.01 to 1 sec) by employing a very precise optical method with high time resolution without disturbing the droplet formation and the mass transfer by solute concentration measurement.

1. MASS BALANCE OF THE NON-STATIONARY MASS TRANSFER

To the correct description of the mass transfer the variations of solute mole numbers within the developing droplet, of the molar flow rate from the hypodermic needle and of the molar flow rate due to mass transfer through the interface must be considered (figure 1):

$$\frac{d(C_1V_1)}{dt} = C_{10}\frac{dV_1}{dt} - \beta_{1f,t}A(C_1H-C_2) \qquad (1)$$

Eq.(1) yields the relationship (2) for the overall mass transfer coefficient $\beta_{1f,t}$:

$$\beta_{1f,t} = \frac{(C_{10}-C_1)(dV_1/dt)-V_1(dC_1/dt)}{A(t)(C_1H-C_2)} \qquad (2)$$

Due to the differential quotient in eq.(2) $\beta_{1f,t}$ is an instantaneous (differential) overall mass transfer coefficient. Since the volume of the continuous phase, V_2, in comparison with the droplet volume V_1 can be considered as infinitely large, i.e.

$$\lim_{V_2\to\infty} C_2 = \lim_{V_2\to\infty} \frac{n_2}{V_2} = 0$$

eq.(2) can be reduced to

$$\beta_{1f,t} = \frac{(C_{10}-C_1)(dV_1/dt)-V_1(dC_1/dt)}{A(t)C_1H} \qquad (3)$$

At dC_1/dt $\beta_{1f,t}$ has its maximum.

To calculate the developing droplet surface area a growing sphere with the radius r was assumed. Its center M is shifted along the nozzle axis during the droplet formation (figure 2). The surface area is calculated employing the relationship for the spherical segment surface area:

$$A = \pi(s^2+h^2) \qquad (4)$$

It can be shown that for the heights of the spherical segment h_k and of the spherical segment complement h_{kk} the following relationships hold:

$$h_k = r-(r^2-s^2)^{1/2} \qquad (5a)$$

$$h_{kk} = r+(r^2-s^2)^{1/2} \qquad (5b)$$

Eqs.(4) and (5) yield the surface areas of the spherical segment A_k and spherical segment complement A_{kk}:

$$A_k = \pi[2r^2-2r(r^2-s^2)^{1/2}] \qquad (6a)$$

$$A_{kk} = \pi[2r^2+2r(r^2-s^2)^{1/2}] \qquad (6b)$$

$A = A_k$ for $h \leq r$ and

$A = A_{kk}$ for $h \geq r$

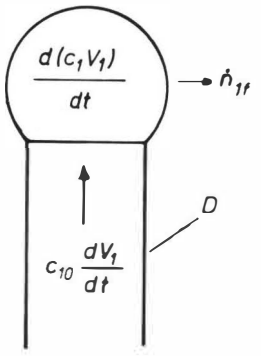

FIG. 1
Mass balance during the droplet formation. D = nozzle

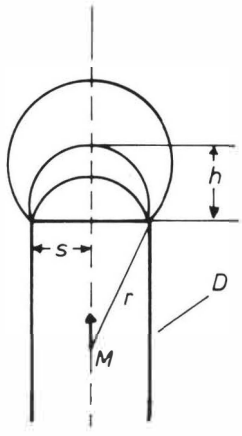

FIG. 2
Spherical segment method for the droplet formation. D = nozzle

2. PRINCIPLE OF THE MEASURING TECHNIQUE

The determination of the dissolved solute concentration was carried out optically without touching the developing droplet by employing a modified liquid scintillation technique, which has already been described [1]. Therefore this technique should only be considered shortly.

The solvent (toluene, n-butylacetate) contains polar solute and apolar scintillator molecules. The solvent or the solute is labelled by tritium or C-14 atoms. The emitted ß rays excite the solvent molecules which transfer the excitation energy by collisions to the scintillator molecules. The latter emit light. In the presence of polar solute molecules this energy exchange process is perturbed and a larger part of the excitation energy converted into heat than in their absence (quenching). There is a unequivocal relationship between the light emission reduction and the solute concentration in the solvent. In the present case the solute was labelled by C-14 and the concentration was calculated by the counting rate and not by means of the quench effect. After correction due to the quench by dividing count rate by count efficiency at the concentration in question the light emission is proportional to the solute concentration. The relationship between light emission and solute concentration has to be evaluated by calibration measurements.

3. EXPERIMENTAL SETUP

The single droplets were formed at the tip of stainless steel nozzles 0.5 to 2.0 mm in inner diameter. By means of a thin teflon tubing the droplet forming liquid is fed by a dosimat (with variable feeding rates) into the hypodermic needle (nozzle). By means of electronic timers the droplet formation rate and time can be controlled exactly. Thus the droplets with well reproducible volumes could be formed (for details see [2]).

For counting rate measurements two photomultipliers in coincidence circuit, a three-channel liquid scintillation-spectrometer (Tricarb 3003 of Packard Instruments) and a multi-channel analyser were employed. By means of additional electronics the time resolution of the data acquisition system was reduced to 1 msec. However, for the measurements discussed here it was sufficient to store the concentration data in each 10 msecs.

4. RESULTS

The location of the main mass transfer resistance in liquid/liquid systems can vary according to the solute partition coefficient, H, and its diffusivities in the two phases.

According to Schmidt-Traub [3] the product $H(D_1/D_2)^{1/2}$ is suitable to estimate the location of main mass transfer resistance.

For $H(D_1/D_2)^{1/2} < 0.03$ the main resistance is within the droplet phase, i.e. the resistance within the continuous phase can be neglected.

For $H(D_1/D_2)^{1/2} > 30$ the resistance is within the continuous phase (the resistance within the droplet phase can be neglected) and

for $0.03 < H(D_1/D_2)^{1/2} < 30$ the resistances of both phases must be considered.

For acetone in water/n-butylacetate this product is nearly constant and has the unit value. For acetic acid in water/toluene it increases from 10^{-2} (at a concentration of 1 mg/cm^3) to 1 (at 500 mg/cm^3). Below 1.8 mg/cm^3 only the resistance within the droplet must be considered.

For propionic acid in water/toluene this product increases from 10^{-1} (at 0.1 mg/cm^3) to about 1 (at 10^2 mg/cm^3), therefore the mass transfer resistances within both of the phases have to be considered. However, at low concentrations the resistance within the droplet phase dominates.

5. INFLUENCE OF THE DROPLET FORMATION RATE ON THE MASS TRANSFER

Typical results are shown in figure 3. Here the solute concentration within the droplet is plotted as a function of the

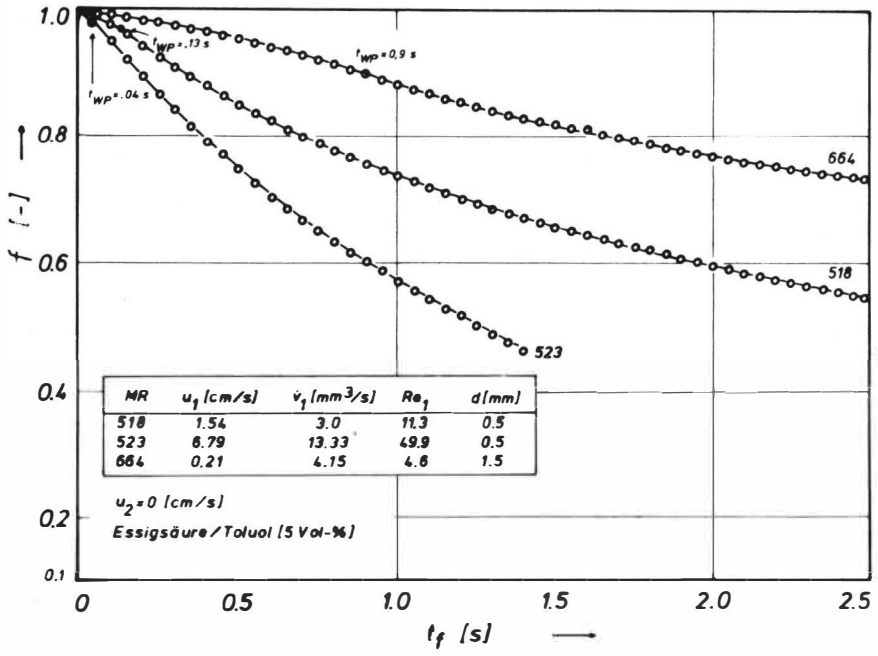

FIG. 3
Relative solute concentration f within the droplet as a function of the droplet formation time t_f during the droplet formation. Acetic acid-toluene-water. Initial concentration: 5 % per volume acetic acid in toluene. t_{wp} = inversion point

droplet formation time for different droplet formation rates. The high acetic acid mass transfer rate in run MR 523 (figure 3) is obvious. Up to 1.4 s 46.5 % of the initial solute amount has been transferred from the droplet into the water phase. This is due to the partition coefficient, shifted to the water phase and dominating mass transfer resistance in the droplet phase. Therefore the droplet formation rate strongly influences the mass transfer rate. The more the resistance is located in the continuous phase, the less is the influence of the droplet formation rate on the mass transfer rate.

It is important to point out that all concentration vs. time curves show an inflexion point. (In figure 3 these points are marked.)

6. INSTANTANEOUS MASS TRANSFER COEFFICIENT

By means of the employed liquid scintillation technique true differential measurements allow to calculate the instantaneous mass transfer coefficients according to eq.(3).

In figure 4 some instantaneous mass transfer coefficients, $\beta_{1f,t}$, are plotted as a function of the droplet formation time,

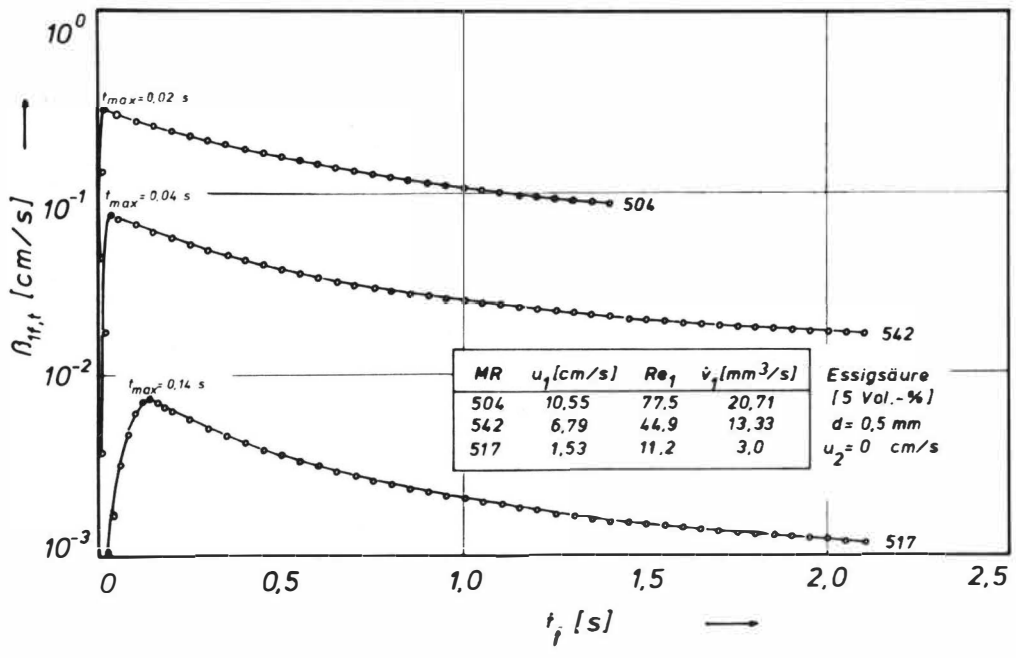

FIG. 4
Instantaneous mass transfer coefficient $\beta_{1f,t}$ as a function of the droplet formation time t_f. Acetic acid. Initial concentration: 5 % per volume solute in toluene.

t_f, at different droplet formation rates. All of these curves pass a maximum. The location of this $\beta_{1f,t}$ maximum shifts with increasing droplet formation rates to shorter times, t_f. A comparison of different systems indicates that at the same droplet formation rate the $\beta_{1f,t}$ maximum occurs at the same time.

Increasing the droplet formation rate from 1.53 cm/s to 6.79 cm/s $\beta_{1f,t}$ maximum significantly increases by one order of magnitude (figure 4). At higher droplet formation rates this influence of formation rate on $\beta_{1f,t}$ maximum is slighter.

Based on the experimental results of the present paper the following statements can be made with regard to the inflexion point and/or the maximum of $\beta_{1f,t}$:

- the location of the inflexion point does not depend on the chemical properties of the components (figure 5),
- at constant liquid velocity in the nozzle, u_1, the increase of the nozzle diameter causes a shift of the inflexion point to larger t_f [2],
- the location of the inflexion point shifts to smaller t_f if u_1 is increased (figure 4)
- the location of the inflexion point shifts to smaller t_f if the continuous phase flow rate is increased (figure 6).

One can conclude from these facts that the location of the inflexion point is controlled by geometrical and fluiddynamical

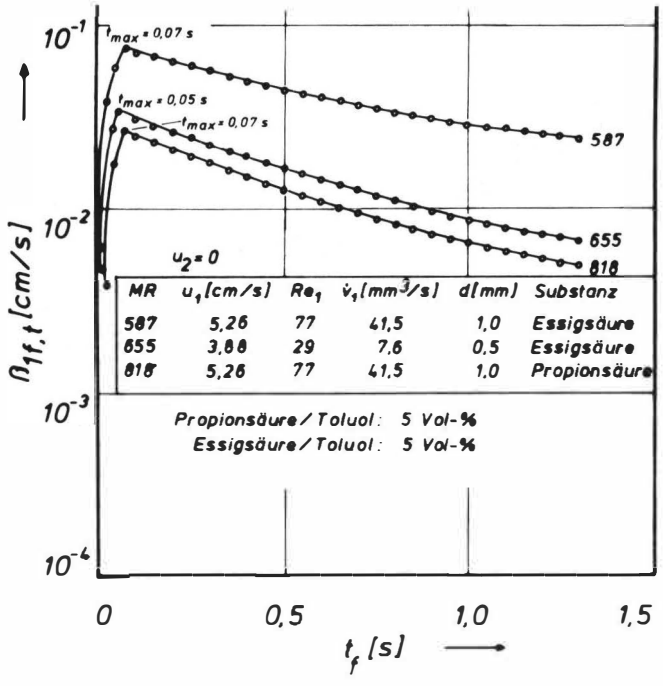

FIG. 5
Instantaneous mass transfer coefficient, $\beta_{1f,t}$, as a function of the droplet formation time, t_f. Comparison of acetic (MR 587 and 655) and propionic (MR 818) acids. Initial concentration: 5 % per volume solute in solvent.

parameters alone and not influenced by the chemical properties of the system.

In all of the investigated systems the inflexion point and/or the maximum of $\beta_{1f,t}$ was attained at the developing droplet segment height which is slightly larger than the nozzle radius. The height of $\beta_{1f,t}$ maximum considerably depends on the chemical properties of the system (figure 7). Employing acetic acid (main resistence is in the droplet phase) the highest $\beta_{1f,t}$ maxima are attained. With nearly equal mass transfer resistences in both the phases (acetone, propionic acid) the $\beta_{1f,t}$ maximum is lower (figure 7).

7. COMPARISON OF THE RESULTS WITH LITERATURE DATA

Plotting the extraction degree as a function of the square root of the droplet formation time no linear relationship was found. This is true for all investigated systems without exception [2]. This result is in sharp contradiction to all known droplet formation models [4]. This deviation between theory and practice is due to the erroneous assumption of the models, especially on the postulation that the mass transfer is a pure

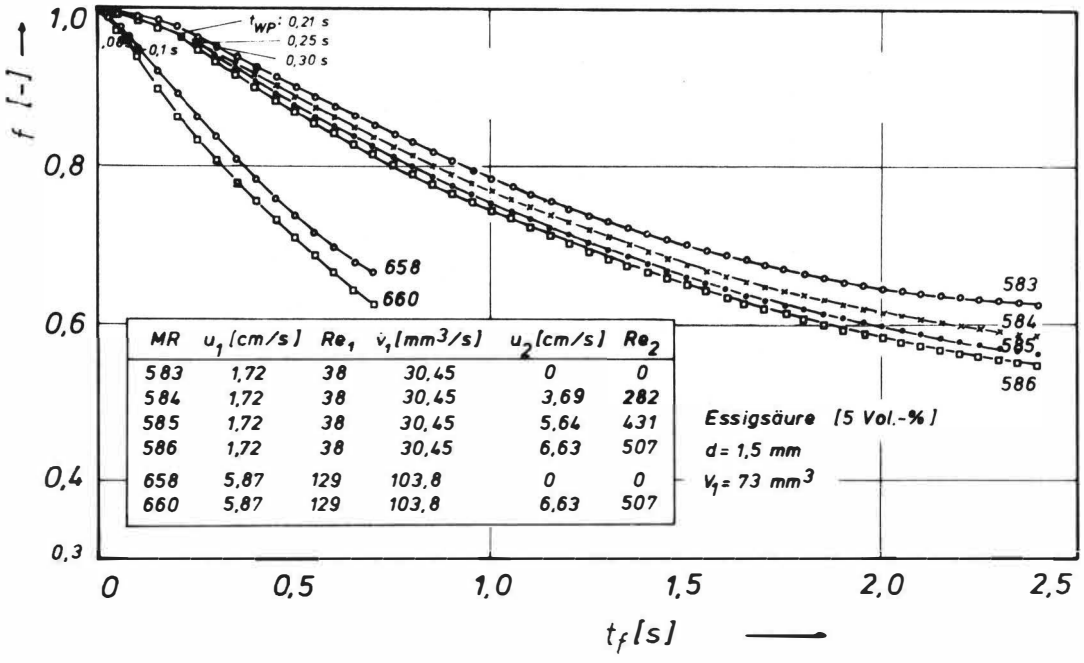

FIG. 6
Influence of the continuous phase flow on the $f(t_f)$ function. Acetic acid I. Initial concentration: 5 % per volume solute in toluene.

diffusion process. The large discrepancy between theory and practice can be illustrated by the comparison of the exchanged substrate masses which were measured and calculated by the models.

For the acetic-acid-toluene-water-system under the conditions which were employed in the present paper the calculated and measured exchange solute masses deviate by a factor of 1000. This illustrates the extremely large influence of the droplet circulation and interfacial turbulence on the mass transfer. The diffusion model leads to several erroneous statements:

- Acetone and propionic acid solutes should be extracted faster due to their higher diffusivities than acetic acid. This statement is disproved by the experiments.
- According to the diffusion model several important parameters like nozzle diameter, solute partition coefficient, droplet size, viscosity, droplet formation rate, do not influence the mass transfer coefficient. Even at different droplet formation rates the concentration vs. time functions are identical according to the diffusion model. These statements are disproved by the experiments as well.
- The models of Losev-Zheleznyak [5] and Skelland-Minhas [6] consider the geometrical parameters as nozzle and droplet diameters indeed. However, the droplet formation rate effect and the influence of the location of the main mass transfer re-

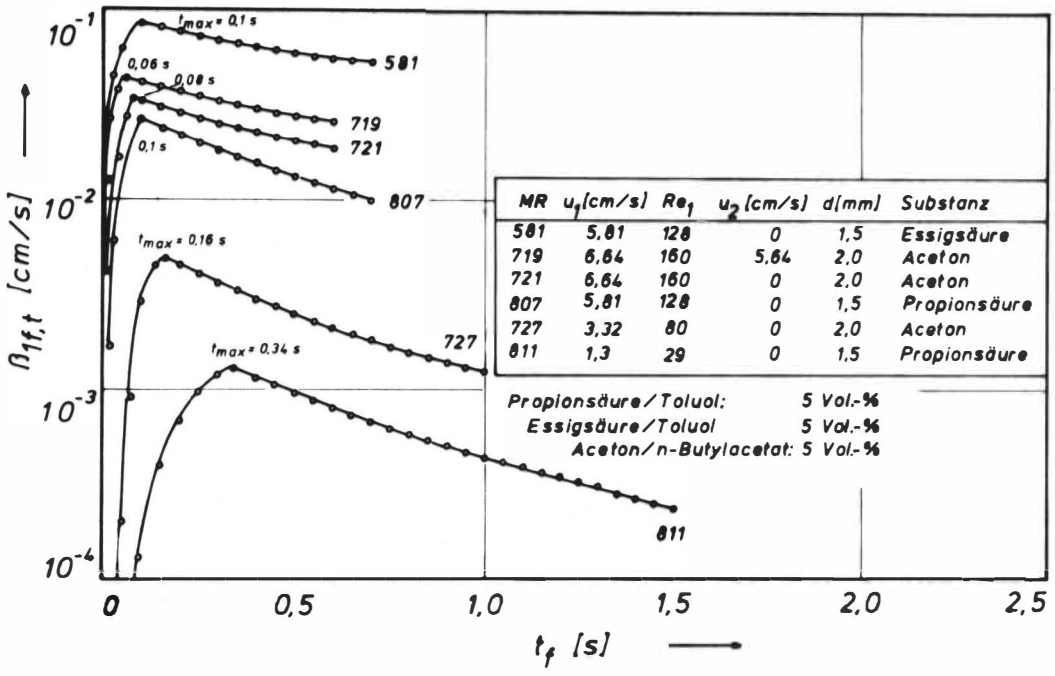

FIG. 7
Comparison of different chemical systems. Acetic (MR 581) and propionic (MR 807, 811) acids in toluene and acetone (MR 719, 721) in n-butylacetate. Initial concentration: 5 % per volume solute in solvent.

sistance are not taken into account by them. Thus - in contrast to the experimental results - they again predict that the acetic acid extraction rate is the slowest.
- All of the models assume that the mass transfer coefficients have their highest value at t = 0, which is disproved by the measurements.
- Furthermore, it should be pointed out that no model considers the complete mass balance (eq.(1)), which makes the theoretical statements of these models questionable.

8. SYMBOLS

A	surface area	cm^2
C	concentration	$mmol/cm^3$
D	diffusivity of the solute	cm^2/s
d_1	droplet diameter	cm
d	nozzle diameter	cm

$f = \frac{C_1}{C_{10}}$

$H = (\frac{C_2}{C_1})_{equil}$ solute partition coefficient

h	spherical segment height	cm
n	molar solute flow	mmol/s
R	droplet radius	cm
r	radius of curvature of the forming droplet	cm
s	nozzle radius	cm
t	time, t=0 start of droplet formation	s
u	liquid velocity	cm/s
V	volume	cm^3
$\dot{V}$	volumetric flow rate	cm^3/s
ß	mass transfer coefficient	cm/s
ν	liquid kinematic viscosity	cm^2/s

Re $= \frac{u\ d}{\nu}$ Reynolds number

INDICES AND ABBREVIATIONS

f	during the droplet formation
t	instantaneous value
wP	at the inflexion point
O	at the time t = 0
1	with regard to the droplet phase
2	with regard to the continuous phase
MR	run

REFERENCES

1. R. Streicher, K. Schügerl
   Chem. Eng. Sci. 32, 23 (1977)

2. V. Zimmermann, Dissertation Universität Hannover 1979

3. H. Schmidt-Traub
   Instationärer Stofftransport an festen Partikeln, Tropfen und Blasen. DFG-Forschungsbericht Br 260/30 (1973)

4. C. Hanson
   Neuere Fortschritte der Flüssig-Flüssig-Extraktion
   Verlag Sauerländer Aarau/Frankfurt (1979)

5. B.D. Losev, A.S. Zheleznyak
   Theoret. Osn. Khim. Tekn. 10, 670 (1974)

6. A.H.P. Skelland, S.S. Minhas
   A.I.Ch.E. Journal 17, 1317 (1971)

MASS TRANSFER COEFFICIENTS IN D_1(2-ETHYL HEXYL) PHOSPHORIC ACID FOR COBALT AND NICKEL

J.A. Golding & V.N. Saleh*

Chemical Engineering Department
University of Ottawa

Ottawa, Canada. K1N 9B4

ABSTRACT

Mass transfer coefficient values ($\bar{K}_{org}$) have been determined for extraction in di(2ethyl-hexyl) phosphoric acid (10% D2EHPA in kerosene) using a modified Lewis cell. Three contacting regions were studied; co-extraction, scrubbing and stripping and runs were carried out at stirrer Reynolds numbers ranging from 1000 to 3000.

$\bar{K}_{org}$ values varied in value from 0.9×10^{-3} to 1.4×10^{-2} cm/s for co-extraction and scrubbing and depended on the direction of mass transfer, organic phase loading and stirrer Reynolds number. $\bar{K}_{org}$ values for stripping were found to be lower than those observed in the other contacting regions and were not greatly affected by change in Reynolds number.

INTRODUCTION

Di(2-ethyl hexyl) phosphoric acid (D2EHPA) has been used for the extraction and separation of cobalt and nickel from aqueous sulphate solutions (1-3). Three distinct contacting steps are required. In the first an aqueous solution containing both metals is extracted using a solution of D2EHPA in kerosene with tri-butyl phosphate added as a phase modifier. The equilibrium in this stage is such that the loaded solvent contains both cobalt and nickel. In the second stage the loaded solvent is scrubbed with an aqueous cobalt solution where the equilibrium is displaced so that nickel is transferred from the organic to the aqueous phase. Finally, in the third stage the scrubbed solvent is stripped with aqueous sulphuric or nitric acid solutions to produce a concentrated cobalt solution. The stripped organic phase is pre-equilibrated before being recycled. Little work, however, has been carried out to determine mass transfer characteristics for this system (4-6). Brisk and McManamey[4] measured mass transfer coefficients in a stirred equilibrium cell by means of an "equilibrium extraction" technique using radio active isotopes. D2EHPA concentrations were varied from 0.1 to 0.5 g.mol. per litre. The authors reported

*Energy, Mines & Resources, 555 Booth St., Ottawa, Canada.

the presence of an interfacial resistance dependent on both organic phase concentration and pH. Golding and Lee[5] determined average $\bar{K}_{org}$ values for cobalt and nickel in a pulsed sieve plate extraction column, mass transfer coefficient values were found to be dependent on pulse amplitude and region. An effect of organic phase loading on $\bar{K}_{org}$ values was found during co-extraction. In a previous study, Golding et al[6] obtained binary equilibrium data and determined mass transfer coefficients for cobalt and nickel in 10% D2EHPA. Contacting region and Reynolds number were found to be the major factors influencing $\bar{K}_{org}$ values. This investigation was undertaken to extend this work to a more complete study of the variables influencing mass transfer in the different contacting regions i.e., co-extraction scrubbing and stripping. To minimize the effect metal concentration on organic phase physical characteristics a 10% solution of D2EHPA in kerosene (Shell Sol Lx154) with 5% tri-butyl phosphate was again used. All concentrations were on a volume/volume basis.

EXPERIMENTAL

The apparatus used was a modified Lewis Cell[7] and the operating conditions studied are given in Table (1).

Contacting region	Stirrer Reynolds Number, n $D^2\rho/\mu$		Cell Volume, ml		Inlet Conditions		
					Metal Concentration g/l		pH
	Aqueous Phase	Organic Phase	Aqueous Phase	Organic Phase	Aqueous Phase	Organic Phase	
Co-Extraction	1500 1500 3000	1000 2000 1000	1730	1010	nickel 4.9 cobalt 1.97-2.03	0.0	3.8-4.0
Scrubbing	1500 1500 3000	1000 2000 1000	1730	1010	nickel 0.0 cobalt 14.8-15.0	nickel 3.6-4.5 cobalt 1.7-2.4	5.4-5.6
Stripping	*1500 1500 3000	1000 2000 1000	1085	1735	0.0	nickel 0.38-0.46 cobalt 6.0-7.45	

*Aqueous solutions of H_2SO_4(10%) used as the strip liquor

Table (1) Operating and Inlet Conditions

Operating procedures were as follows. The stirrer speeds were set to give the desired aqueous phase and organic phase Reynolds numbers. The aqueous phase was then introduced into the lower compartment until the aqueous phase level was at the mid point of the annular space. The upper compartment was then filled with the organic phase. Care was taken when adding the organic phase to minimize any disturbance at the interface. The stirrers were then started and zero time recorded. Samples were taken from each phase at pre-determined time intervals and the metal concentration analyzed by means of an atomic absorption spectrophotometer. In the co-extraction runs, organic phase analysis was carried out by extracting the metals with acid. In the stripping and scrubbing runs the high cobalt concentrations in the organic phase precluded this method and the organic phase was analysed directly. Full details of the apparatus and procedures are given in Reference(14). A further two runs were carried on the extraction of acetic acid into benzene and into kerosene so that the value of mass transfer coefficients for these systems could be compared to values found for cobalt and nickel in D2EHPA.

THEORETICAL

The mass transfer rate for extraction into the organic phase is given by the following differential equation:

$$V_{org}\, d\, C_{org}/_{dt} = K_{org}\, A\, (C_{org}^{*} - C_{org}) \qquad \ldots\ldots\ldots\ldots (1)$$

Although K_{org} does vary, it can be considered constant over a time interval ΔT and equation (1) can be rearranged to give:

$$\int_{C_t}^{C_t + \Delta t} \frac{d\, C_{org}}{C_{org}^{*} - C_{org}} = \bar{K}_{org}\, A\, \Delta t / V_{org}$$

where $\bar{K}_{org}$ is the integral mean value over the time period Δt. When the equilibrium concentration C_{org} is constant K_{org} can be evaluated from the plot of $\ln(C^{*}_{org} - C_{org})$ versus t. However, when C^{*}_{org} varies as was the case for the majority of these runs $\bar{K}_{org}$ has to be evaluated by numerical integration. A first order algorithm was found to be sufficiently accurate in the investigation.

RESULTS

Runs were carried out to obtain data for co-extraction, scrubbing and stripping, see Table (1). A computer programme was used to fit experimental data, equilibrium data and to calculate $\bar{K}_{org}$ values (i) either numerically or from the $\ln(C^{*}_{org} - C_{org})$ data. Typical data obtained from the computer

print-out is given in Table (2).

```
N I C K E L

E X T R A C T I O N:  RE-ORGANIC = 1000     RE-AQUEOUS = 1500

TIME              AQ                ORG                    ORG EQU
 0                 4.8996           -.093813                3.73336
1/C*-C            AREA              ARE-K.00               LOG(C*-C)
 .26129            .150947           2.77699E-3              1.34212
ORG MED .17333    C*-C 3.82717      SLP-K.00-2.77032E-3
* * * * * * * * * * * * * * * * * * * * * * * * * * * * * * * * * * * *
TIME              AQ                ORG                    ORG EQU
 30                4.60342           .440473                3.73262
1/C*-C            AREA              ARE-K.00               LOG(C*-C)
 .303753           .159355           2.93167E-3              1.19154
ORG MED .681983                     C*-C 3.29214           SLP-K.00-2.92384E-3
* * * * * * * * * * * * * * * * * * * * * * * * * * * * * * * * * * * *
TIME              AQ                ORG                    ORG EQU
 60                4.34223           .923492                3.78188
1/C*-C            AREA              ARE-K.00               LOG(C*-C)
 .356076           .167728           3.08571E-3              1.03261
ORG MED 1.13937                     C*-C 2.80839           SLP-K.00-3.07639E-3
* * * * * * * * * * * * * * * * * * * * * * * * * * * * * * * * * * * *
TIME              AQ                ORG                    ORG EQU
 90                4.11603           1.35524                3.73117
1/C*-C            AREA              ARE-K.00               LOG(C*-C)
 .420889           .175442           3.22761E-3              .865387
ORG MED 1.54549                     C*-C 2.37592           SLP-K.00-3.21693E-3
* * * * * * * * * * * * * * * * * * * * * * * * * * * * * * * * * * * *
TIME              AQ                ORG                    ORG EQU
 120               3.92483           1.73573                3.7305
1/C*-C            AREA              ARE-K.00               LOG(C*-C)
.50131             .181385           3.33695E-3              .690526
ORG MED 1.90034                     C*-C 1.99477           SLP-K.00-3.32481E-3
* * * * * * * * * * * * * * * * * * * * * * * * * * * * * * * * * * * *
TIME              AQ                ORG                    ORG EQU
 150               3.76862           2.06494                3.72991
1/C*-C            AREA              ARE-K.00               LOG(C*-C)
 .600614           .183705           3.37964E-3              .509801
ORG MED 2.20392                     C*-C 1.66496           SLP-K.00-3.36684E-3
* * * * * * * * * * * * * * * * * * * * * * * * * * * * * * * * * * * *
TIME              AQ                ORG                    ORG EQU
 180               3.6474            2.3429                 3.72941
1/C*-C            AREA              ARE-K.00               LOG(C*-C)
 .721233           .179498           3.30224E-3              .326792
ORG MED 2.45624                     C*C 1.38651            SLP-K.00-3.29008E-3
* * * * * * * * * * * * * * * * * * * * * * * * * * * * * * * * * * * *
TIME              AQ                ORG                    ORG EQU
 210               3.56118           2.56958                3.72904
1/C*-C            AREA              ARE-K.00               LOG(C*-C)
 .862471           .164801           3.03186E-3              .147955
ORG MED 2.65729                     C*-C 1.15946           SLP-K.00-3.02228E-3
* * * * * * * * * * * * * * * * * * * * * * * * * * * * * * * * * * * *
TIME              AQ                ORG                    ORG EQU
 240               3.50995           2.745                  3.72881
1/C*-C            AREA              ARE-K.00               LOG(C*-C)
 1.01646           .135311           2.48934E-3             -1.63255E-2
ORG MED 2.80707                     C*-C .983809           SLP-K.00-2.48329E-3
* * * * * * * * * * * * * * * * * * * * * * * * * * * * * * * * * * * *
NOTATION
TIME = Minutes
AQ = Aqueous Concentration (g/l)
ORG = Organic Concentration (g/l),C
ORG EQU = Organic Equilibrium Concentration (g/l),C*
AREA = Area from graphical integration of  (dc/(C-C*)
ARE-K.00 = Mass Transfer Coefficient, (cm/sec), using graphical integration
ORG MED = Organic Medium Concentration
SLP-K.00 = Mass Transfer Coefficient, cm/sec, evaluated from a plot of
           ln(C*-C) vs t
```

Table (2) Computer Print-out for Nickel-Co-extraction

CO-EXTRACTION. Overall mass transfer coefficients for co-extraction were found for cobalt to lay in the 1.20×10^{-3} to 2.5×10^{-3} cm s^{-1} range. They were observed to depend on Reynolds number and on organic phase metal concentration. Thus $\bar{K}_{org}$ values for both metals increased with increase in Reynolds number in either the organic and aqueous phases, see Figure (1). It can also be seen from Figure (1) that $\bar{K}_{org}$ values for cobalt increased with increase in metal concentration in the organic phase. Similar results were obtained for nickel with $\bar{K}_{org}$ values for nickel being higher than those observed for cobalt.

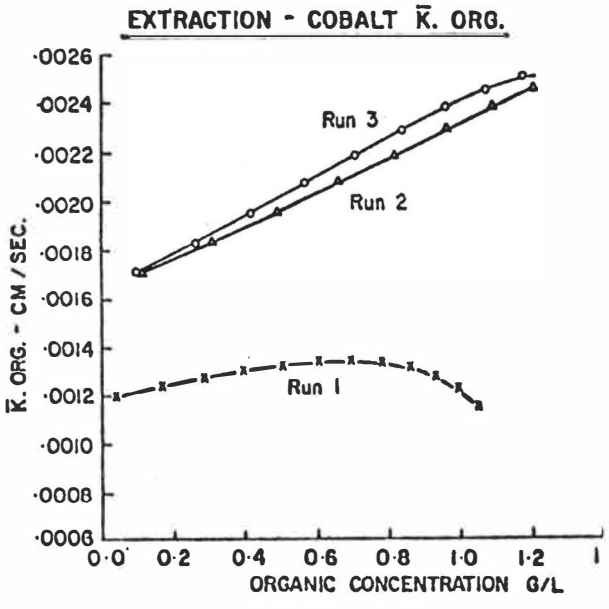

FIG. (1) Overall Mass Transfer Coefficient for Cobalt - Co-extraction

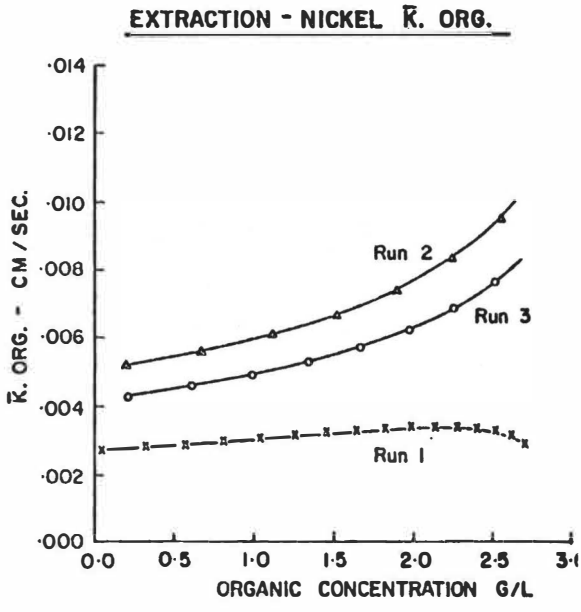

FIG. (2) Overall Mass Transfer Coefficients for Nickel - Co-extraction

Legend

x-x Re_{aq} = 1,500 ΔΔ Re_{aq} = 1,500 o-o Re_{aq} = 3,000

R_{org} = 1,000 Re_{org} = 2,000 Re_{org} =1,000

SCRUBBING. In this contacting region $\bar{K}_{org}$ values were of the same order of magnitude being in the 0.5×10^{-3}-7.5×10^{-3} cm s^{-1} range for cobalt and the 0.5×10^{-3} to 5.0×10^{-3} cm s^{-1} range for nickel. These latter values were lower than was observed for extraction of nickel indicating an effect of the direction of mass transfer on the value the mass transfer coefficient. Increase in Reynolds number in either phase again resulted in an increase in $\bar{K}_{org}$ values for both metals, see Figure (3).

An effect metal concentration in the organic phase was noted when the agitation in the organic phase was raised, $\bar{K}_{org}$ values increasing with an increase in the metal concentrations in the organic phase for cobalt. However for nickel $\bar{K}_{org}$ values decreased with increase in organic phase composition.

STRIPPING. In this contacting region C* values for stripping were approximately equal to zero and $\bar{K}_{org}$ values could be obtained from plots of ln(C*-C) versus the contacting time. $\bar{K}_{org}$ values were considerably lower than the values found for co-extraction and scrubbing; the values for cobalt lay in the 2.46×10^{-4} to 3.0×10^{-4} cm s^{-1} range while for nickel values varied from 2.15×10^{-4} to 2.55×10^{-4} cm s^{-1}. The $\bar{K}_{org}$ values in this contacting region were not dependent on the metal concentration in the aqueous and there was only a slight increase in K_{org} values with increase in Reynolds number.

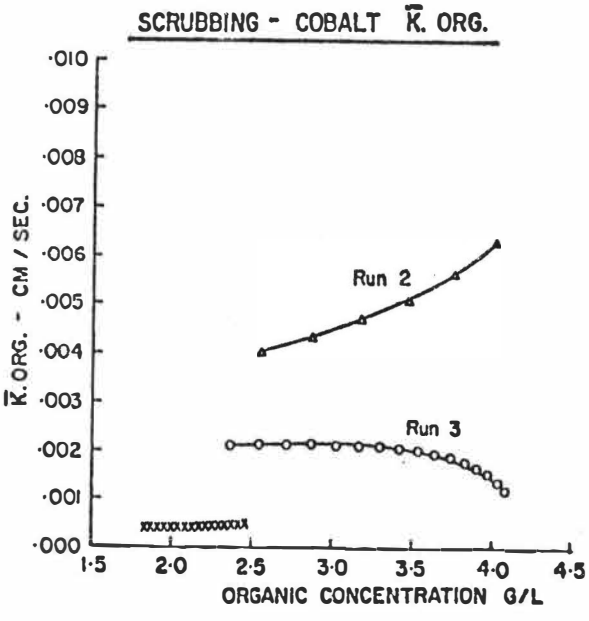

FIG. (3) Overall Mass Transfer Coefficients for Cobalt-Scrubbing

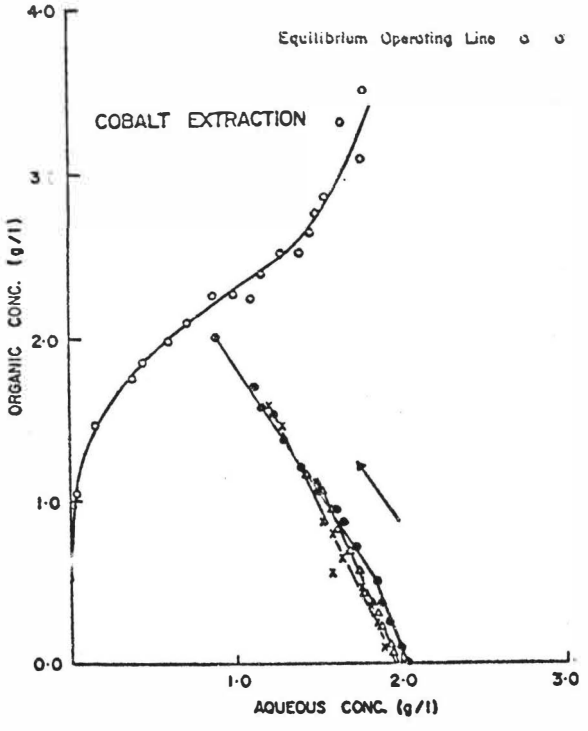

FIG. (4) Operating and Equilibrium Lines for Cobalt Co-extraction

Legend

x-x Re_{aq} = 1,500 Re_{org} = 1,000

Δ-Δ Re_{aq} = 1,500 Re_{org} = 2,000

o-o Re_{aq} = 3,000 Re_{org} = 1,000

Δ-Δ Re_{aq} = 1,500 Re_{org} =1,000

o-o Re_{aq} = 1,500 Re_{org} = 2,000

x-x Re_{aq} = 3,000 Re_{org} = 1,000

DISCUSSION

The results indicated that mass transfer coefficient values depended not only on Reynolds number and organic phase loading but also the contacting region. Thus in co-extraction and scrubbing, K_{org} values were affected by change in either the aqueous or organic phase Reynolds number indicating that there was resistance to mass transfer in both phases (8). In addition, the results suggested that the mass transfer rate was diffusion controlled (11). The values of K_{org} obtained in these contacting regions are the same order of magnitude as values found for the extraction of acetic acid into benzene or kerosene when integral average K_{org} values were 3.31×10^{-3} cm s^{-1} and 2.33×10^{-3} cm s^{-1} respectively: aqueous phase Reynolds number 1,000 organic phase Reynolds number 1,500. This was again indicative of a diffusion controlled mass transfer process.

The variation of $\bar{K}_{org}$ values with organic phase loading in these regions was, however, inconsistent firstly with the two-film theory (8) and secondly with the report that metal polymers are formed in D2EHPA (9-11). The data indicated that during co-extraction $\bar{K}_{org}$ values increased with increase in metal loading. However, from the equilibrium line and operating line data figures (4) and (5) the slope of the equilibrium line, m, would have increased slightly as the run progressed which should have resulted in a small decrease in $\bar{K}_{org}$ values. Polymer formation would also be favoured by increased metal loading and a decrease in $\bar{K}_{org}$ values should have been observed. In scrubbing the total metal concentration was approximately the same throughout the run so that any polymer formation would be constant. Also there was very little variation if any in the slope of the equilibrium line Figure (5). The $\bar{K}_{org}$ values then would have been expected to be independent of the individual metal concentration in this contacting region as was observed in a pulsed sieve tray column (5). However, when the organic phase Reynolds number was increased $\bar{K}_{org}$ values increased with increase in the individual metal concentration for cobalt but for nickel an opposite effect was observed.

The major reason for these inconsistencies is considered to be due to errors in the value of the equilibrium concentration C*. The C* values shown in Figure (3-5) are "operating" equilibrium lines and are the locus of the points on the true equilibrium isotherms which are dependent on the individual metal concentration in both phases and the pH. These lines were obtained by shake-out-extraction carried out at varying phase ratio, r. It is considered, therefore, that runs on this system be carried out in under steady state contacting conditions (11). Under these conditions C* could be estimated much more accurately while eliminating the errors found at the end of unsteady state data when concentration changes are small, see Table (2).

In the stripping region, mass transfer would be expected to be organic phase controlled, Figure (7). Thus as would be expected $\bar{K}_{org}$ values were independent of organic phase loading

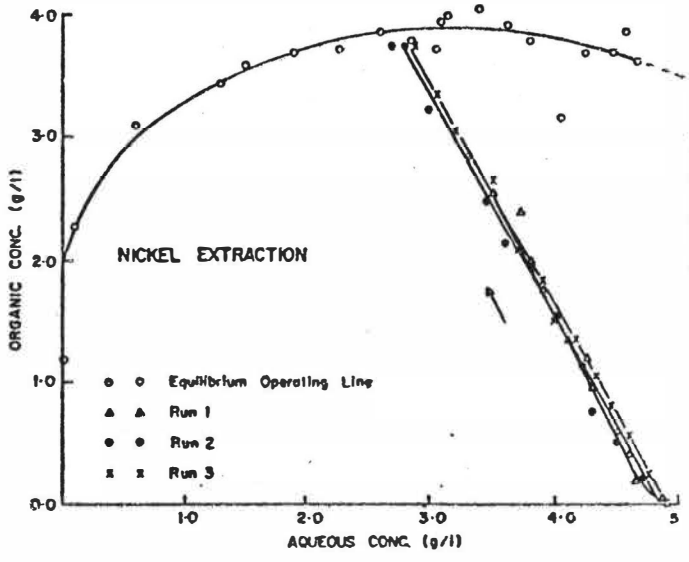

FIG. (5) Operating and Equilibrium Lines for Nickel-Co-extraction

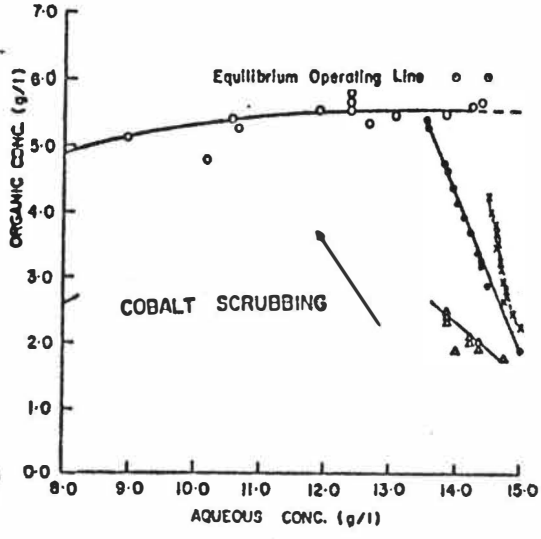

FIG. (6) Operating and Equilibrium Line for Cobalt-Scrubbing

Legend

Δ-Δ $Re_{aq} = 1,500$ $Re_{org} = 1,000$ o-o $Re_{aq} = 1,500$ $Re_{org} = 2,000$

x-x $Re_{aq} = 3,000$ $Re_{org} = 1,000$

but only varied slightly with increase in organic phase Reynolds number. This in contrast with the results obtained in the other contacting region. This could be a result of resistance due to chemical reaction or perhaps of an interfacial resistance as suggested by Murdoch & Pratt (13) and further work is required to determine the controlling kinetic region in stripping.

CONCLUSIONS

The results show that for the cobalt-nickel-di(2 ethyl hexyl) phosphoric acid system mass transfer coefficient values are dependent on the contacting region. In co-extraction and scrubbing, mass transfer is considered to be a diffusion controlled process, although further work is required to determine the controlling resistance. In addition, the effect of metal up-take in the organic phase on K_{org} values has to be more fully investigated particularly at higher D2EHPA concentrations.

FIG. (7) Operating Line for Cobalt-Stripping

Legend:
- ▲-▲ Re_{aq} = 1,500
- ▼-▼ Re_{org} = 1,000
- ●-● Re_{aq} = 1,500; Re_{org} = 2,000
- x-x Re_{aq} = 3,000; Re_{org} = 1,000
- o-o Re_{aq} = 1,500; Re_{org} = 1,500

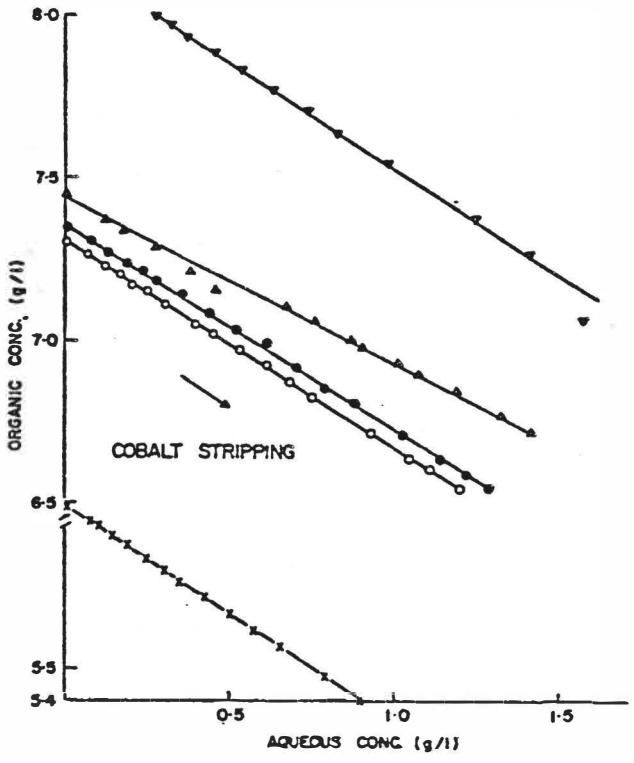

In the stripping region, mass transfer rates can be expected to be much slower than in extraction and scrubbing. However, further study is required to determine the kinetic region controlling mass transfer in this region.

NOMENCLATURE

A	interfacial or contacting area, cm^2
C_{org}	organic phase concentration, g ℓ^{-1}
C^*_{org}	organic phase equilibrium concentration g ℓ^{-1}
D	impeller diameter, m
$\bar{K}_{org}$	overall organic phase mass transfer coefficient, cm s^{-1}
$\bar{\bar{K}}_{org}$	integral average overall organic phase
m	slope of the equilibrium line
n	stirrer speed, s^{-1}
r	volumetric ratio of organic phase to aqueous phase
t	contacting time, s
V	cell volume, ml

GREEK LETTERS

μ	absolute viscosity, kg m^{-1} s^{-1}
ρ	density, kg m^{-3}

REFERENCES

1) RITCEY, G.M., and ASHBROOK, A.W., "Separation of Nickel and Cobalt in Ammoniacal Solutions by Liquid-Liquid Extraction", Trans. Inst. of Mining and Metallurgy, (1969), C 78, No. 751, 57 U.S. Patent (1969) 3, 438, 768, April.

2) RITCEY, G.M., ASHBROOK, A.W. and LUCAS, B.H., "Development of a Solvent Extraction Process for the Separation of Cobalt from Nickel", C.I.M. Bulletin (1975) 68, 111.

3) RITCEY, G.M. and ASHBROOK, A.W., "Separation of Cobalt and Nickel by Liquid-Liquid Extraction from Acid Solutions", U.S. Patent 3, 399, 055, Aug. (1968).

4) BRISK, M.L. and McMANAMEY, W.J., "Extraction of Metals from Sulphate Solutions by Alkyl Phosphoric Acids II, J. Appl. Chem. (1969) 19, 109.

5) GOLDING, J.A. and LEE, J., "Recovery and Separation of Cobalt and Nickel in a Pulsed Sieve-Plate Extraction Column" A.I.Ch.E. 87th Annual Meeting, Boston (1979).

(6) GOLDING, J.A., FOUDA, S.A. and SALEH, V.N., "Equilibrium and Mass Transfer for the Separation of Nickel and Cobalt in di(2-Ethyl Hexyl)Phosphoric Acid", Proc. Int. Solvent Extraction Conference ISEC-74, CIM Special Vol. 21 (1979).

7) LEWIS, J.B., "The Mechanism of Mass Transfer of Solutes Across Liquid-Liquid Interfaces", Part I, Chem. Eng. Science (1954) 3, 248.

8) LEWIS, W.K. and WHITMAN, W.G., "Principles of Gas Absorption", Ind. and Eng. Chem. (1924) 16, 1215.

9) MADIGAN, D.C., "The Extraction of Certain Cations from Aqueous Solution with Di-(2-Ethyl Hexyl) Orthophosphate" Austr. J. of Chem. (1960) 13, 58.

10) BAES, C.F. and BAKER, H.T. "The Extraction of Iron III from Acid Perchlorate Solutions in Di-(2-Ethyl Hexyl) Phosphoric Acid in n-Octane" J. Phys. Chem. (1960) 64, 89.

11) BARNES, J.E., SETCHFIELD, J.H. and WILLIAMS, G.O.R., "Solvent Extraction Unit Di(2-Ethyl Hexyl) Phosphoric Acid A Correlation between Selectivity and the Structure of the Complex", J. Inorg. Nucl. Chem., (1976) 38, 1065.

12) LEVENSPIEL, O. and GODFREY, J.H., "A Gradientless Contactor for Experimental Study of Interphase Mass Transfer with/ without Chemical Reaction", Chem. Eng. Sci., (1974) 29, 1723.

13) MURDOCH, R. and PRATT, H.R.C., "Extraction of Uranyl Nitrate in a Wetted Wall Column", Trans. Inst. Chem. Engrs. (1953) 31, 307.

(14) SALEH, V.N., "Mass Transfer Coefficients in the Extraction and Recovery of Cobalt and Nickel", M.A. Sc. Thesis, University of Ottawa (1980).

ABOUT THE INFLUENCE OF SOLUBLE ADSORPTION LAYERS ON THE MASS TRANSFER BETWEEN LIQUID PHASES CONTROLLED BY TRANSPORT PROCESSES.

W. Nitsch and L. Navazio*

Institut für Technische Chemie der
Technischen Universität München

D-8046, Garching, Lichtenbergstr. 4
W-Germany

ABSTRACT. The hydrodynamic effect of soluble adsorbates (sodium alkyl sulfonates) was studied by measurements of the acetone transfer between liquid phases in a stirring cell. Related to the state of rigid behaviour of the interface, a mechanism is proposed based on the kinetics of adsorption and desorption. By estimation of the rate of adsorption and the increase of transfer rates near the critical micelle concentration, it was possible to calculate the surface pressure gradient and to verify the kinetic approach.

INTRODUCTION.

In the past many experimental studies have shown the influence of surface active substances on the rate of mass transfer between fluid phases (1). Two explanations are possible. The so-called hydrodynamic theory is related to the effect of gradients in surface tension on the boundary layer flow (2). The other possible explanation is the blocking of the interface (sieve effect) (3,4), or a catalytic interaction of the adsorbed molecules with the interfacial reaction (5, 6, 7). In general, it is not easy to distinguish between these mechanisms.

Three years ago, we published our results about the transfer of zinc ions out of water into dithizon-loaded CCl_4 in a stirring cell with (8) and without surface active substances (9). It was possible to show that the influence of stirring speed on the mass flux allowed the discrimination between both mechanisms. In the case that interfacial reactions are rate-determining, the flux is independent of the stirring speed with and without adsorption layers; the blocking and/or catalytic mechanism is the kind of action. Otherwise, if transport processes are rate-determining (a linear relationship between

*Excerpt of Thesis, L. Navazio, TU München 1979.

flux and stirring speed), the fingerprint of the hydrodynamic action of surface layers is to be observed.

Because sufficiently systematic studies related to the influence of soluble monolayers on mass transfer are not available, we started research work in order to understand the characteristic dependence between transfer rate, forced convection and surface concentration.

In a horizontal interface the hydrodynamic action of a compressed surface layer on boundary layer flow comes from the flow induced gradient of surface tension produced by unequal distribution of adsorbed molecules. The mechanical equilibrium

$$\tau_x = \frac{d\Pi}{dx} \qquad (1)$$

is established by the local shear stress τ_x and the corresponding local gradient of surface pressure with

$$\Delta\Pi = \int_{x=0}^{x=R} \tau_x \, dx \qquad (2)$$

as the integral expression for the pressure difference in the compressed monolayer. Until now measurements of flow profiles sufficiently near the fluid interface are as unknown as measurements of surface pressure gradients in the stressed layer.

With a simplifying assumption about the fluid dynamic in stirring cells, Davies (10) has proposed a model related to the action of insoluble monolayers and turbulent flow at the interface. For laminar flow in stirring cells, a treatment is given (11) which is also related to insoluble molecules. This project aims at the action of soluble monolayers in order to understand the characteristic hydrodynamic fingerprint.

EXPERIMENTAL

The cell employed for the investigation is already described elsewhere (12); only the stirrer applied in this work is much less effective in comparison with our prototype. The schematic illustration in FIG. 1 shows the direction of flow

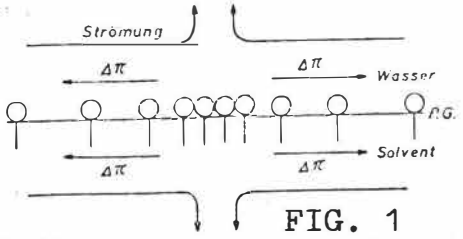

FIG. 1

Direction of flow, pressure gradient and compression of monolayer (schematic).

produced by baffle and stirrer. The stirring speed ratio is always constant (n_s/n_w = 0,79) in order to get a linear connection between stirring speed and transfer rate (13).

The applied highly purified water came from a quarz bidistiller. CCl_4 was distilled and subsequently purified over aluminium oxide. The sodium alkyl sulfates are products of pA-quality (Merck Company). The tensides were recrystallized out of absolute ethanol until the minimum of interfacial tension near the cmc disappeared (14). This finding in connection with standard values of cmc and γ_{cmc} is our criterion for sufficiently clean tensides.

The surface concentration Γ_e is evaluated from measurements of surface tension with the Gibbs equation

$$\Gamma_e = - \frac{RT}{2} \frac{d\gamma}{d\ln c} \qquad (3)$$

or calculated by the Küster equation

$$\Gamma_e = K\, c^{2/3} \qquad (4)$$

with a value for K from approximation of the Gouy-equation as proposed in (17).

The mass transfer of acetone out of water (c = 0,5 g/l) into CCl_4 was selected as the basic test system. Time-dependent concentrations are measured photometrically in the solvent phase (λ = 290 nm). The effects of adsorbate are expressed with the overall mass transfer coefficient $\beta_{o,s}$ calculated by

$$\beta_{o,s} = - \frac{2{,}3\ VH}{F(H+1)} \frac{d \log \left(\frac{c_{w,o}}{H+1} - c_{s,t} \right)}{dt} \qquad (5)$$

The plot of $\log \left(\frac{c_{w,o}}{H+1} - c_{s,t} \right)$ over the time is always a linear one.

RESULTS.

FIG. 2 shows the characteristic connection between mass-transfer coefficients, tenside concentration and stirring speed as an example for all the applied sodium alkyl sulfates (sodiumdecyl-, -dodecyl-, -hexadecylsulfate).

The upper border line (FIG. 2) is related to the "clean system", characterized by time independent mass transfer coefficients. The method for proving clean interfaces has already been published elsewhere (12).

The lower border line (FIG. 2) is related to the state of a rigid interface: the pressure gradient is sufficient to produce (as the maximum hydrodynamic action) a flow profile

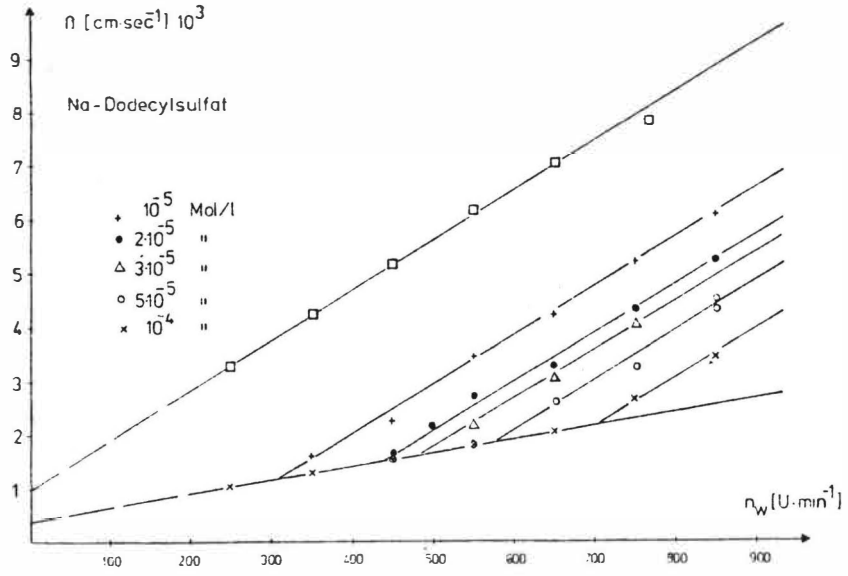

FIG. 2
The effect of stirring speed on the overall coefficient for different sodium dodecylsulfate concentrations in the water.

analogous to the profile of solid/fluid interfaces (see FIG.3). This interpretation was proved experimentally. With heat transfer between liquid phases, the depression of the heat transfer coefficient with adsorbates down to the rigid region is equal to the depression produced by a copper blade between the liquid phases (5). Besides, in the rigid region produced by adsorbates, there is no momentum flux between the stirred liquids (16).

FIG. 3
Schematic representation of boundary flow for a solid/liquid (a) and a fluid (b) interface.

For the following kinetic model, the fact is important that the range of rigid behaviour (expressed with the so-called critical stirring number n_k) is to be attached to the tenside concentration. Therefore, different alkyl sulfate layers with the same rigid range are in the same mechanical state and therefore comparable. FIG. 4 shows this comparison. To produce the same rigid range n_k, the requisite surface concentration Γ_e decreases with increasing length of the alkyl chain. Because the alkyl sulfates have the same compression isotherms, the

different effects of the same surface concentration (the equilibrium value) must be caused by the kinetics of adsorption and desorption of the water soluble layer. In the following, a simplified model is proposed related to the corresponding state of different adsorbates at the same n_k.

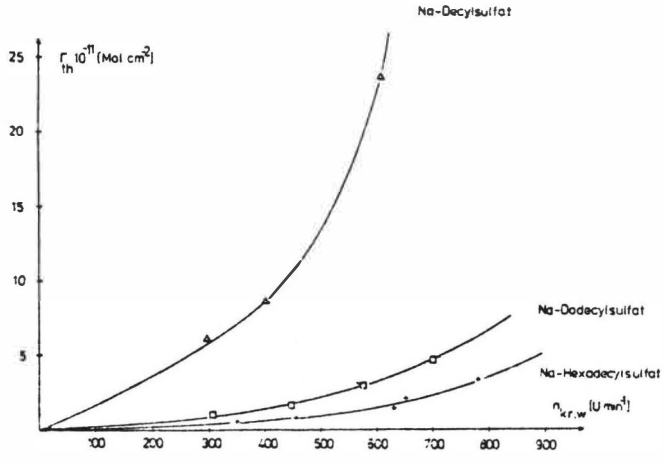

FIG. 4
Surface concentration $\overline{\Gamma}_e$ (equilibrium value) necessary to produce n_k (rigid region^e) for different tensides.

KINETICS OF ADSORPTION.

Recognizable density schlieren show a laminar flow near the interface and, corresponding to the direction of this flow (see FIG. 1), it is assumed that on the periphery of the circular interface there is a continuous surface renewal with a surface production of $dF/dt = Uw^*$. The flow velocity w^* idealized in the position $x = 0$ is parallel and neighbouring to the interface.

In the case that equilibrium of adsorption is established instantenously at the new interface produced at $x = 0$, the net transport of molecules $\dot{n}_a$ to the interface should follow

$$\dot{n}_a = \overline{\Gamma}_e \; Uw^* \qquad (6)$$

With the equation

$$n = 2 \, (Dt/\pi)^{1/2} \, c(N_1/1000) \qquad (7)$$

for the diffusion to the interface (17), it is possible to estimate the time t_e for equilibration. In TABLE 1 this calculated time together with a corrected time value t'_e is tabulated. The correction (factor 4) is necessary with respect to desorption which is neglected in equation (7).

TABLE 1

Equilibrium position x for $w^* = 0{,}1$ cm/s at $n_k = 450$.

	c_{450} mol/l	Γ_e mol/cm^2 10^{11}	$t_e' = 4t_e$ s	x cm
c_{10}	$1{,}58\ 10^{-3}$	11,69	$2{,}86\ 10^{-3}$	$2{,}86\ 10^{-4}$
c_{12}	$2{,}3\ 10^{-5}$	1,74	$3{,}0\ 10^{-1}$	$3{,}0\ 10^{-2}$
c_{16}	$5\ 10^{-7}$	0,84	148	14,8

The path of the surface elements to reach the equilibrium value Γ_e is dependent on w^*. Because of the low values of w^*, which are to be assumed corresponding to the rigid interface (see TABLE 1), the equilibrium position should be very near to x = 0 for sodium decyl- and sodium dodecyl sulfates in the relevant concentrations to realize $n_k = 450$. Therefore, for these two surfactants it may be allowed to operate with established equilibrium of adsorption at x = 0, corresponding to equation (6). Moreover, this means that at x = 0 there is a surface pressure corresponding to the bulk phase concentration. For sodium hexadecyl sulfate an analogous conclusion is uncertain because of the low concentration level necessary to produce $n_k = 450$.

PRESSURE GRADIENT.

Corresponding to equation (2), for each rigid range n_k there is a necessary gradient of interfacial pressure. This gradient is to be estimated on the basis of the steep increase of transfer rate near the cmc as shown in FIG. 5. This increase of transfer rate near the cmc comes from the fast micellation which destroys the diffusion barrier of desorption (18). The important fact is the very beginning of the $\beta_{0,5}$-increase at $c' <$ cmc. This means that for the bulk concentration c' in the position of maximal compression at x = r, the cmc is reached near the interface. Therefore, the pressure gradient for the investigated rigid range at $n_k = 450$ is to be estimated with $\bar{\pi}_{cmc}$ at x = r and $\bar{\pi}_{c',e}$ at x = 0. In TABLE 2 the experimental results for different alkyl sulfates investigated with respect to the cmc-effect are summarized. The resulting $\Delta\bar{\pi}$ values are comparable to the pressure difference estimated in (11) from flow field measurements.

KINETICS OF DESORPTION.

In the case of equilibrium near x = 0 desorption occurs at the whole interface. Corresponding to the increase of

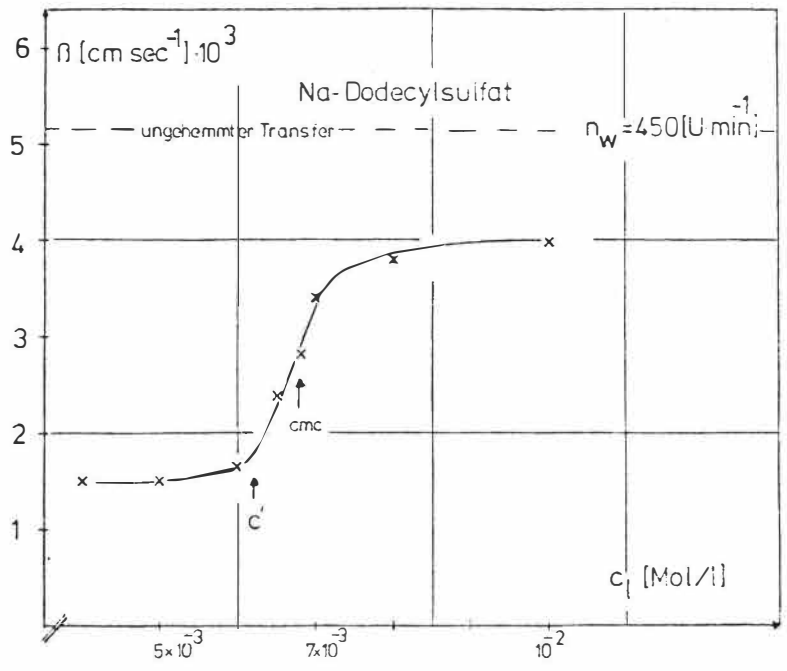

FIG. 5
The increase of $\beta_{o,s}$ near the cmc.

compression with x, there is also an increase of $\overline{\Pi}_x$ and of the concentration c^*_x in equilibrium with $\overline{\Gamma}_x$.

Because of the circular shape of the interface, the entire rate of desorption is to be treated as the sum of the rates related to concentric ring shaped plains dF. Corresponding to diffusive desorption, equation

$$\dot{dn}_d = \beta \, dF \, (c^*_x - c) \qquad (8)$$

should be an appropriate expression. The value of the transport coefficient β is to be calculated from the individual transport coefficient of the acetone transfer at n_k = 450 (β=1,38 10^{-3} cm/s)

TABLE 2
Data for Estimation of the pressure gradient $\Delta\overline{\Pi}$ at n_k = 450

	c' mol/l	$\overline{\Pi}_{c'}$ mN/m	cmc mol/l	$\overline{\Pi}_{cmc}$ mN/m	$\Delta\overline{\Pi}$ mN/m
c_{10}	2,5 10^{-2}	34,05	3,2 10^{-2}	36,35	2,3
c_{12}	6,1 10^{-3}	36,2	6,8 10^{-3}	37,7	1,5
					$\overline{\Delta\Pi}$ = 1,9

corrected with respect to the influence of diffusion coefficient with the expression of the penetration theory (20).

Assuming a linear increase of surface pressure from x = 0 to x = r with the pressure differences in TABLE 2 and the equilibrium value π_e^* at x = 0, it is possible to calculate the increase of c_x^* with x, if the concentration dependence of π from measurements of surface tension is known.

With the course of c^* with x, distributed over 8 annular plains of equal width, the desorption rates for these annular surface parts are calculated with equation 8. Summing up these values one obtains the whole desorption rate listed in TABLE 3.

TABLE 3
Estimation of the boundary flow velocity w^* at n_k = 450 on the basis of equations 6, 8 and 9.

	c mol/l	Γ_e mol/cm^2 10^{11}	$\dot{n}_d$ mol/s	w^* cm/s
c_{10}	$1{,}58\ 10^{-3}$	11,69	$11{,}4\ 10^{-9}$	4,12
c_{12}	$2{,}5\ 10^{-5}$	1,74	$1{,}3\ 10^{-9}$	3,1

STATIONARY STATE.

In the stationary state of the flow compressed adsorption layer from the kinetic point of view, the expression

$$\dot{n}_a = \dot{n}_d \qquad (9)$$

must hold. With equation 9 it is possible to calculate values of w^* which are summarized in TABLE 3. These values are to be compared with the bulk flow w which is known to be 13 cm/s in the annular space of the stirring cell (21).

The result, that the calculated values for w^* are reasonable and, moreover, that the condition for a solid/liquid profile $w^* \ll w$ seems to be fulfilled, shows the justification of the applied kinetic model.

In spite of several assumptions in the above model, we are publishing our approach in order to stimulate further investigations into the influence of soluble monolayers on transfer rates, which is very important for experimental work with respect to mass transfer kinetics.

ACKNOWLEDGEMENT.

This investigation was supported by The Deutsche Forschungsgemeinschaft within the framework of Sonderforschungsbereich 153.

REFERENCES

(1) J.T. Davies, Turbulence Phenomena, Academic Press, New York, 1972.
(2) V.G. Levich, Physicochemical hydrodynamics. New York, Prentice Hall Inc., 1962.
(3) C.T. De Jonge-Vleugel and B.H. Bijsterbosch, Proc. VI. Intern. Congr. Surface active Subst. (1973), 2, 469.
(4) K.P. Lindland and S.G. Terjesen, Chem. Engng. Sci. (1956) 5,1.
(5) H.P. Ring, G.L. Bertrand and D.F. Sears, Biophys. J. (1966), 6, 813.
(6) J.H. Schulman, Ann. New York Acad. Sci. (1966) 137, 860.
(7) V.P. Shanbag, Biochem. Biophys. Acta (1973) 320,517.
(8) W. Nitsch and K. Roth, Coll. Polym. Sci. (1978), 256,1182.
(9) W. Nitsch and B. Kruis, J. inorg. nucl. Chem. (1978), 40 857.
(10) J.T. Davies, Proc. R. Soc. London (1966) A290, 515.
(11) B.J.R. Scholtens, S. Bruin and B.H. Bijsterbosch, Chem. Engng. Sci. (1979) 34, 661.
(12) W. Nitsch, M. Raab and R. Wiedholz, Chem.-Ing.-Tech., (1973) 16, 1026.
(13) W. Nitsch and J.G. Kähni, Chem.-Ing.-Tech., (1979), 9,890.
(14) E. Hutchinson, Trans. New York Acad. Sci. (1949) 11, 226.
(15) W. Nitsch, M. Raab and P. Kniep, Proc. VI. Intern. Congr. Surface active Subst. (1973) 2, 147.
(16) W. Nitsch and K.D. Heck, Wärme- und Stoffübertragung (1976) 9, 53.
(17) J.T. Davies and E.K. Rideal, Interfacial phenomena. New York, Academic Press 1963.
(18) W. Nitsch and G. Weber, Chem.-Ing.-Tech., (1976) 8, 715.
(19) W. Nitsch, M. Raab and R. Wiedholz, Chem.-Ing.-Tech., (1973) 45, 1026.
(20) R. Higbie, Trans. Amer. Inst. Chem. Engrs., (1935) 31, 365.
(21) K.D. Heck, Thesis, Technische Universität München (1974).

SYMBOLS USED.

c mol/l	bulk concentration	V cm^3	volume of solv.phase
c* mol/l	interfacial conc. water phase	w cm/s	flow velocity
		w* cm/s	flow velocity at x=0
D cm^2/s	diffusion coeff.	x	radial coordinate (be gins in the periphery)
F cm^2	interfacial area	$\beta_{o,s}$ cm/s	overall mass transfer coefficient
H	distr.coeff. c_w/c_s		
N_L	Loschmidt'sche No.		
n 1/min	stirring number	σ dyn/cm	interfacial tension
$\dot{n}_a$ mol/s	rate of adsorpt.	Γ mol/cm^2	surface concentration
$\dot{n}_d$ mol/s	rate of desorpt.	π dyn/cm	interfacial pressure
U cm	periphery of the interface	τ dyn/cm^2	shear stress

INDICES

e - equilibr.; w - water; s - solvent; t - time; o - initial

PHASE TRANSFER AND MICELLAR CATALYSIS IN HYDROMETALLURGICAL LIQUID-LIQUID EXTRACTION SYSTEMS

K. Osseo-Asare and M. E. Keeney
Metallurgy Section, Department of Materials Science and Engineering
The Pennsylvania State University
University Park, PA 16802, USA

ABSTRACT

A discussion is presented of the factors which contribute to phase transfer catalysis (PTC) and reversed micellar catalysis (RMC) in hydrometallurgical liquid-liquid extraction systems. It is shown that the ability of an extractant to act as a phase transfer catalyst is dependent on its reactivity, interfacial activity and aqueous solubility. It is demonstrated that the potential for effective utilization of RMC in liquid-liquid extraction systems depends primarily upon the ability of micelles to solubilize both extractant molecules and metal ions, and stabilize H_2O-extractant ligand exchange reactions. A discussion is presented of catalysis and inhibition in micellar and non-micellar systems involving LIX63, HDNNS, DEHPA, lauric acid, and Aliquat 336.

INTRODUCTION

The advent of the commercial hydroxyoxime- and hydroxyquinoline-based reagents has stimulated research into the synergic potential of mixtures of these chelating reagents with each other (1-8) as well as with other types of extractants such as phosphoric, carboxylic, and sulfonic acids (9-32). For many of the systems, the presence of mixed ligand complexes has been reported, and several authors have attributed the observed synergic effects to solvation mechanisms (13,15,21,22). The importance of solvation effects in synergism has been well documented in the literature (33). There are now indications, however, that other mechanisms such as phase transfer catalysis (1-8, 16, 17) and micellar catalysis (23-32) may also be operating.

Phase transfer catalysis (PTC) is based on the fact that two species located respectively in two immiscible solvents can only react with great difficulty (if at all) if neither reactant is soluble in its opposite solvent (34,35). The role of a phase transfer catalyst is to transport one of the reactants across the interface into the opposite bulk phase, where the desired reaction can take place at much higher rates than previously attainable. It is interesting to note that much of the PTC work in the literature has used Aliquat 336, a quaternary ammonium reagent (Henkel Corp.) which is also used as a metallurgical solvent extraction reagent. In addition to PTC, it is necessary to consider interfacial chemical phenomena within the organic phase proper. At sufficiently high concentrations, the salts of some organic acids, as well as the water-wet organic solutions of the acids themselves, form aggregates or micelles. These micelles have polar cores which can

solubilize considerable quantities of water and there is much interest in the use of micelles as models for the study of enzymatic reactions (36).

In this paper a review of selected literature on PTC and RMC is presented with emphasis on those aspects which are relevant to metal separation processes in liquid-liquid systems. In addition, new data are presented on the physiochemical phenomena underlying inhibition, PTC and RMC in mixed extractant systems involving LIX63, HDNNS, DEHPA, lauric acid and Aliquat 336.

EXTRACTANT SOLUBILITY AND INTERFACIAL ACTIVITY

When an extractant HR is placed in a liquid-liquid extraction system, it may distribute itself among several different locations and assume several degrees of molecular aggregation. Thus, HR may (1) exist in the bulk organic phase as monomers or aggregates solvated by diluent molecules, (2) adsorb at the liquid/liquid interface, (3) dissolve into the aqueous phase, or (4) form monomeric or polymeric complexes with metal ions (these complexes in turn distribute between the organic and aqueous phases).

The successful commercial utilization of the hydroxyoxime-based reagents derived partly from their organic solubility made possible by the presence of alkyl groups. This enhanced organic solubility has been so impressive that there has been a tendency to simply dismiss the aqueous solubility as negligible. It is now known that there is some aqueous solubility and for example, Foakes et al (37) have determined the solubilities of LIX63 and anti-LIX65N to be 15.5 and 1.0 μmol dm^{-3} respectively. Whether the solubility of a given extractant is significant or not would depend on the particular process relative to which solubility is being considered.

To various degrees, solvent extraction reagents possess some interfacial activity and populate the liquid-liquid interface (2,25-28,38-45). The interfacial activity is related to the presence of hydrophobic and hydrophilic groups in the same molecule. The hydrophobicity is contributed by the hydrocarbon radicals while the polar functional groups such as -COOH, -OH, =O, $-SO_3H$, and -POOH are responsible for the hydrophilic nature. At the organic/aqueous interface, these molecules orient themselves with the hydrophilic groups directed towards the aqueous phase and the organic substituents directed towards the organic phase. Thus the interfacial activity is demonstrated by interfacial tension lowering as shown schematically in Figure 1 for purified LIX63, HDNNS, DEHPA, and lauric acid.

Of the extractants represented in Figure 1, the most interfacially active is HDNNS which at concentrations as low as 10^{-5} mol dm^{-3} is capable of lowering the hexane/aqueous interfacial tension from 50 mN/m to 8 mN/m. HDNNS exhibits the characteristics of a classical surfactant. There is an abrupt change in the interfacial tension curve at $5x10^{-5}$ mol dm^{-3} which represents the critical micelle concentration (CMC). At the CMC, HDNNS is present in the bulk organic phase primarily as micelles - aggregates consisting of several molecules with the polar groups turned inwards away from the organic solvent. The micellization of HDNNS and its salts has been the subject of several studies in the literature (42,46-49). Kaufman and Singleterry (46) found that micelles were present in benzene at sulfonate salt concentrations as low as 10^{-6} mol dm^{-3}, and aggregation numbers ranging from 6 to 14 metal-sulfonate monomers per micelle were determined (47). The micellization of

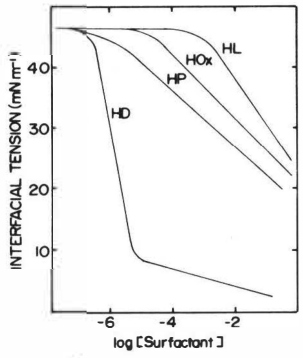

FIG. 1. Interfacial tension isotherms at the hexane/water interface for purified reagents (mol dm^{-3}): HDNNS (HD); DEHPA (HP); LIX63 (HOx) and lauric acid (HL). Aqueous conditions: 0.5 mol dm^{-3} KNO_3,pH=2.5. (25°C)

carboxylate salts has also been reported (50-52). Although the other extractants shown in Figure 1 do not exhibit a critical micelle concentration, they, nevertheless, do undergo some aggregation as a result of hydrogen bonding (51). Aggregation numbers as high as 4 have been reported for LIX63 in iso-octane (8).

PHASE TRANSFER CATALYSIS

As far as liquid-liquid extraction of metals is concerned, what is observed when two extractants are used together would depend on the interactions of all the factors discussed above. For example, the two extractants will compete for adsorption sites at the organic/aqueous interface. The more interfacially active of the two will populate the interface at the expense of the other. If the two extractants associate, it is possible for the more surface active species to be removed from the interface.

Let us consider the simple case of two extractants HR and HL (ignoring bulk phase aggregation and HR-HL interactions) and focus on three effects: interfacial activity, aqueous solubility, and the nature of the extracted complex. Several possibilities may be envisaged as outlined in Figure 2. In system 1, none of the extractants exhibits any significant interfacial activity. However, HR is more soluble than HL, and is also responsible for metal complexation. Thus addition of HL would not be expected to have any effect on metal extraction. Similarly, no PTC would be observed with systems 3 and 5. In system 2, the extracted complex is MeL_2 even though HR has a greater aqueous solubility than HL. In this case, phase transfer catalysis can account for the extraction of an MeL_2 complex as shown in Figure 2a. System 4 in which HR is the more interfacially active of the two extractants, can give rise to enhanced extraction if the rate limiting step occurs at the organic/aqueous interface. The neutral complex MeR_2 may be formed at the organic/aqueous interface, and subsequently transferred into the bulk organic phase where ligand exchange occurs, forming MeL_2 and regenerating HR for further reaction. This is illustrated in Figure 2b.

The ligand exchange reaction may occur completely at the organic/aqueous interface (Figure 2c) or it may be preceded by interfacial mixed complex information (Figures 2d and 2e). When extractant HR is the more soluble as

SYSTEM	INTERFACIAL ACTIVITY	AQUEOUS SOLUBILITY	EXTRACTED COMPLEX
1	--	HR	MeR_2
2	--	HR	MeL_2
3	HR	--	MeR_2
4	HR	--	MeL_2
5	HR	HR	MeR_2
6	HR	HR	MeL_2
7	HR	HL	MeR_2
8	HR	HL	MeL_2

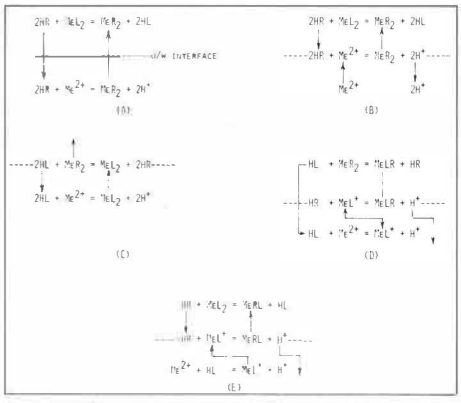

FIG. 2. Schematic representation of phase transfer catalytic systems involving mixed liquid-liquid extractants (HR;HL).

well as the more interfacially active of the two extractants, PTC can take place to yield a complex MeL_2 (System 6) through either one or both of the mechanisms illustrated in Figures 2a and 2b. It is also possible for HR to possess the greater interfacial activity and yet give slow extraction rates in the absence of HL. In this case, if the aqueous phase reactivity of HL is greater than that of HR, it would be possible to observe enhanced kinetics in the mixed extractant System 7 as demonstrated in Figure 2c; mixed complex formation is also possible (see Figure 2d). System 8 represents the case where a complex MeL_2 is formed even though the second extractant HR is more surface active. Under these circumstances, enhanced extraction may be due to increased rate of interfacial reaction involving HR alone (Figure 2b) or mixed complex formation (Figure 2e).

Several of the mechanisms that have been proposed (1-8) to explain the catalytic effect of LIX63 (HL) on copper extraction by LIX65N (HR) can be treated in terms of the phase transfer models outlined in Figures 2a-e. As an example, the mechanism proposed by Fleming (6) may be cited. This investigator presents interfacial tension results which indicate that LIX63 is excluded from the liquid-liquid interface in LIX63-LIX65N mixtures. It is then argued that the aqueous solubility of CuL^+ exceeds that of CuR^+ and that the aqueous phase reaction to form the 1:1 copper-ligand complex proceeds much more rapidly for LIX63 than for LIX65N. The rate-limiting step is proposed to be an interfacial reaction (Figure 2d). Although Fleming does not provide any experimental data to substantiate his claim that CuL^+ is more soluble and forms faster than CuR^+, there is some merit in his hypothesis. As Foakes et al have shown (37), LIX63 is more water-soluble than LIX65N. In addition Van der Zeeuw and Kok (7) have pointed out that when LIX63 chelates copper, a five-membered ring is formed, whereas a six-membered ring is formed in the case of LIX65N; the accelerating capacity of LIX63 may be due to the greater ease of forming a five membered ring compared with a six membered ring.

Metal extraction with mixtures of chelating reagents and organic acid mixtures may proceed via mechanisms such as those given in Figures 2a to 2e depending on the relative importance of aqueous phase and interfacial reactions. The effect of lauric acid concentration on interfacial tension and copper extraction with HOx-lauric acid mixtures is shown in Figure 3a. The experimental techniques are discussed in detail elsewhere (26-28). It can be seen that, at constant HOx concentration, enhanced extraction occurs only

as the interfacial tension begins to decrease, i.e. as lauric acid begins to adsorb at the liquid-liquid interface. The ability of minute amounts of HDNNS (up to 0.01 mol dm^{-3}) to increase metal extraction rates with LIX reagents and Kelex 100 (20,22) may be attributed to a similar mechanism. It must be noted that the reaction steps shown in Figures 2a to 2e may be further complicated by mixed complex formation.

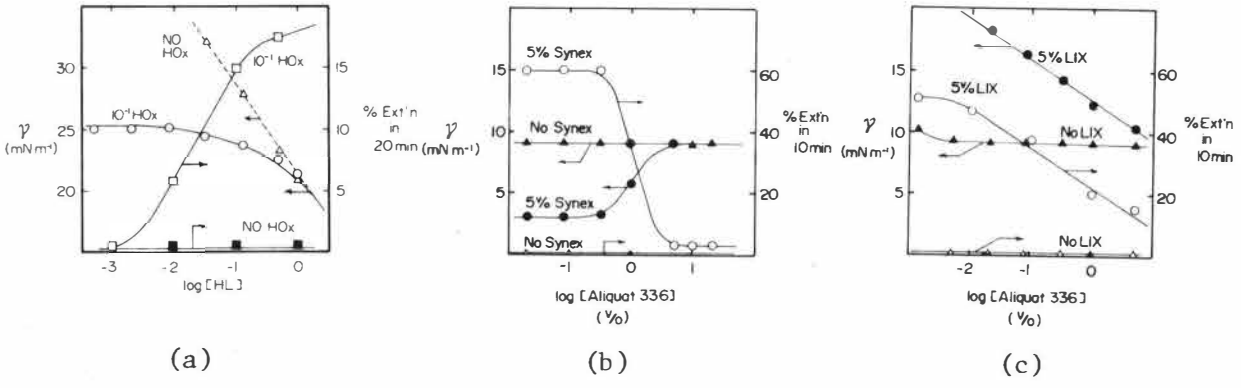

(a) (b) (c)

FIG. 3a-c. Comparison of interfacial tension and nickel extraction at 25°C for systems (a) HL/HOx M; (b) Synex/Aliquat 336; and (c) LIX63/Aliquat 336. Diluent:hexane. Initial aqueous conditions: (a) 0.5M KNO_3, $5x10^{-3}$M $NiNO_3$, pH 2.5; (b,c) 0.5M NH_4OH, 0.5M NH_4NO_3, $5x10^{-3}$M $NiNO_3$. O/A=1. Synex 1040:40% HDNNS in heptane (King Ind.).

Preferential population of the interface by one extractant in a mixed extractant system can also have adverse effects on metal extraction. The effects of Aliquat 336 on the interfacial tensions and the rate of nickel extraction with HDDNS are shown in Figure 3b. For the individual extractants, Aliquat 336 has no extraction capability for Ni in ammoniacal solution while HDDNS extracts quite well. However, in the mixed extractant system, extraction occurs only in those regions where Aliquat 336 has been displaced from the interface by the sulfonic acid (i.e. HDDNS preferentially populating the interface). Aliquat 336, being cationic, has a strong inhibiting effect on nickel extraction in regions where it is preferentially populating the interface. Similar results are found for the Aliquat 336/LIX63 extraction system as shown in Figure 3c.

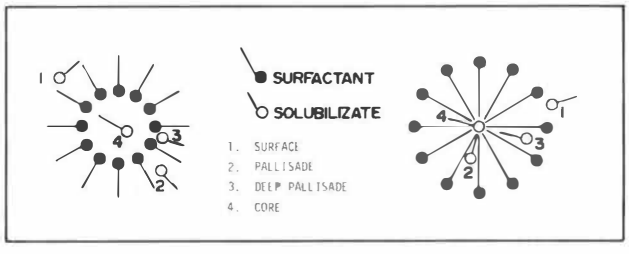

FIG. 4. Possible solubilizate locations in a micelle.

MICELLAR CATALYSIS

In the discussion above, the effects of extractant aggregation were not considered. The presence of aggregation affects metal extraction. Thus, the fractional orders observed in extraction rate studies with LIX reagents have been attributed by some investigators to organic phase aggregation of the extractant molecules (6,8). When reversed micelles are present, even more drastic effects may be observed. Reaction products as well as reaction rates may be profoundly affected when species which have been solubilized by micelles undergo chemical reactions (36). Figure 4 illustrates the possible locations of a solubilizate in a micellar environment. The micelle core, site 4, is hydrophobic for aqueous phase micelles and hydrophilic (may involve trapped water pools) for reversed organic phase micelles.

Cho and Morawetz (54) studied the effect of aqueous phase micelles of sodium dodecyl sulfate (SDS) on the aquation of $Co(NH_3)_5Cl^{2+}$ induced by Hg^{2+}. As SDS concentration was increased, a sudden increase in reaction rate was observed in the neighborhood of the CMC. Further SDS addition beyond the CMC resulted in a rate decrease. The rate increase was interpreted in terms of an increase in the effective concentration of Hg^{2+} and $Co(NH_3)_5Cl^{2+}$ at the anionic micelle surface as a result of electrostatic attraction. The rate decrease at high SDS concentrations was attributed to a decrease in the reactant concentration per micelle as the number of micelles increased.

The effect of aqueous SDS micelles on a reaction involving Ni^{2+}, Mn^{2+}, and a hydrophobic organic ligand, pyridine-2-azo-p-dimethylaniline (PADA) has been investigated by James and Robinson (55), and Holzwarth et al (56). In the presence of SDS, the cations are attracted to the anionic micelle/water interface. PADA, being hydrophobic, is solubilized within the hydrophobic micelle core. In both the micellar and non-micellar systems, the rate-limiting step was determined to be the ligand exchange reaction. The activation energy for the reaction was found to be the same in the micellar and non-micellar systems. It was therefore concluded that the main effect of the micelles was not in the enhancement of the ligand-water exchange but rather in the creation of a concentrative effect. The ability of micelles to solubilize and therefore localize reacting species leads to an increase in the effective concentration of the reactants, thereby increasing reaction rates. Similar results have been reported by Diekmann and Frahn (57,58) who used sodium decylsulfate instead of SDS. Using electrical double layer theory, these authors demonstrate that the electrostatic interaction between the anionic polar heads and Ni^{2+} dramatically enhances the local Ni^{2+} concentration at the micelle surface.

The aquation of tris(oxalato)chromate(III) anion, $Cr(C_2O_4)_3^{3-}$ to cis-$Cr(C_2O_4)_2(H_2O)_2^-$ has been investigated by O'Connor et al (59,60) in the presence of water solubilized by alkylammonium carboxylates in benzene. It was found that the rate of the aquation reaction in the micellar system was greater than the aqueous phase value by a factor of 5×10^6. The rate enhancement in the micellar system was attributed to (1) hydrogen bonding between the oxygen atoms of the oxalate ligands, and the ammonium ion of the micelle, (2) the ability of the ammonium ion to deprotonate and donate a proton to the hydrogen-bonded oxalate ligand and (3) an apparent increase in water activity in the micellar polar environment. A similar explanation has been given for the enhanced rate of the trans-cis isomerization of bis (oxalato)diaquochromate (III) anion in micellar alkylammonium carboxylate solution in benzene (61).

Robinson and Steytler (62) investigated the reaction of nickel (II) with murexide in water pools contained in Aerosol OT micelles in heptane. The rate of complex formation was found to be controlled by the rate of water exchange. In the micellar region there was a slight decrease in water exchange rate, which was attributed to the adsorption of Ni^{2+} at the anionic AOT surface. The presence of reaction inhibition was also observed by Fisher et al (63) when the Ni^{2+}-Mur^{-} reaction was studied in aqueous SDS micellar solutions. The binding of Ni^{2+} to the anionic polar heads reduced its effective bulk concentration and thereby, reduced the reaction yield.

Van Dalen and coworkers (29-32) have examined the role of HDNNS micelles in the extraction of various trivalent metal ions. In mixed HDNNS/DEHPA extractant systems, unexpected enhanced metal extractions were found. The authors observed that water is released from the HDNNS micelle as DEHPA is added to the organic phase. Using various techniques (vapor pressure osmometry, IR, interfacial tension), they concluded that DEHPA is solubilized in the aqueous micelle core, replacing water molecules originally solubilized. They attributed the enhanced extraction of trivalent metal ions to the cosolubilization of the metal ions and the DEHPA in the micellar core (i.e. site 4 in Figure 4).

Osseo-Asare, et al. (25-28) have examined the mixed LIX63/HDNNS extractant system and have also shown that water is released from the HDNNS micelle upon addition of LIX63. However, this effect has been attributed to micelle destruction (and subsequent release of solubilized H_2O) as a result of preferential association of the oxime and the sulfonic acid in the bulk organic phase. Micelle destruction is demonstrated in Figure 5 which shows that the CMC shifts to a higher HDNNS concentration in the presence of LIX63. The oxime-sulfonate interaction has been further confirmed by infrared spectroscopy (26).

The interfacial tension data of van Dalen, et al. (29-32) have been replotted and included in Figure 5. The isotherm shows a shifting of the CMC to higher HDNNS concentration as the concentration of DEHPA is increased, analogous to the results for LIX63/HDNNS. However, on the basis of infrared spectra, van Dalen et al. have suggested that there is no interaction between the phosphoric and sulfonic acids. In the absence of any interaction between the extractant species, it is difficult to explain the shifting in the interfacial tension isotherms as shown in Figure 5. Further work is necessary to explain the observed shifts.

Enhanced extraction of Ni^{2+} has been observed in the LIX63/HDNNS system (23-28) and this has been attributed to a micellar catalytic mechanism (26-28). It has been proposed that the function of the HDNNS micelle is to concentrate the reactants and increase their mutual accessibility. The heteropolar nature of the oxime results in LIX63 being drawn into the polar region of the HDNNS micelle. However, given the relatively low aqueous solubility of LIX63, it is more likely that the oxime is solubilized in the palisade region (site 3, Figure 4) rather than in the aqueous core.

CONCLUSION

The major factors contributing to phase transfer catalysis and reversed micellar catalysis have been discussed with emphasis on their relationship to hydrometallurgical liquid-liquid extraction systems. The ability of charged

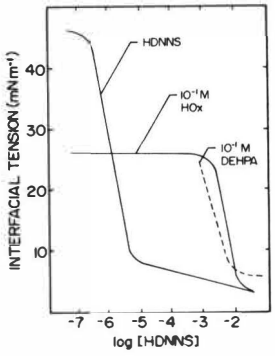

FIG. 5. Effect of HOx and DEHPA on the interfacial tension vs log HDNNS isotherm at the hexane/water interfaces. (After refs. 26 and 32).

interfaces to promote or inhibit extraction has been demonstrated. It has been shown that for an extractant to function as a phase transfer catalyst it must (1) preferentially adsorb at the aqueous/organic interface, (2) have greater solubility in the aqueous phase, or (3) have a greater reactivity. The potential for effective utilization of reversed micellar catalysis in hydrometallurgical systems has been shown to be dependent upon (1) a metal-extractant concentrative effect due to solubilization of the reactant species in the reversed micelle and (2) the ability of the micelle to promote the H_2O-extractant ligand exchange reactions. With appropriate selection of extractants and extraction conditions, it seems likely that PTC or RMC could be used to advantage in hydrometallurgical liquid-liquid extraction systems.

ACKNOWLEDGEMENTS

This work was supported by the National Science Foundation.

REFERENCES

1. D. S. Flett, D. N. Okuhara and D. R. Spink, J. Inorg. Nucl. Chem., 1973, 35, 2471
2. D. S. Flett, Acct. Chem. Res., 1977, 10, 99.
3. A. W. Ashbrook, Coord. Chem. Rev., 1975, 16, 285.
4. R. L. Atwood, D. N. Thatcher and J. D. Miller, Met. Trans. B., 1975, 6B, 465.
5. R. J. Whewell, M. A. Hughes and C. Hanson, J. Inorg. Nucl. Chem., 1976, 38, 2071.
6. C. A. Fleming, South African NIM, 1976, Rept. No. 1973.
7. A. J. Van der Zeeuw, and R. Kok, paper no. 1c, ISEC 77.
8. L. Hummelstedt, T. Tammi, E. Paatero, H. Andrésen and J. Karjaluoto, Proc. 4th Int. Congr. Scand. Chem. Eng. Copenhagen, 1977, 123.
9. E. G. Joe, G. M. Ritcey and A. W. Ashbrook, J. Metals, 1966, 18, 18.
10. G. M. Ritcey and B. H. Lucas, Can. Metall. Quart., 1971, 10, 223.
11. D. S. Flett and S. Titmuss, J. Inorg. Nucl. Chem., 1969, 31, 2612.
12. D. S. Flett and D. W. West, ISEC 71, 214.
13. M. Cox and D. S. Flett, ISEC 71, 204.

14. D. S. Flett and D. W. West, Trans IMM, 1973, 82, C107.
15. D. S. Flett, M. Cox and J. D. Heels, ISEC 74, 2559.
16. D. S. Flett, M. Cox, and J. D. Heels, J. Inorg. Nucl. Chem, 1975, 37, 2533.
17. D. S. Flett, M. Cox and J. D. Heels, J. Inorg. Nucl. Chem., 1975, 37, 2197.
18. V. I. Lakshmanan and G. J. Lawson, J. Inorg. Nucl. Chem., 1973, 35, 4285.
19. V. I. Lakshmanan, G. J. Lawson and J. L. Tomliens, J. Inorg. Nucl. Chem., 1975, 37, 2181.
20. R. H. Moore and J. A. Partridge, Battelle Northwest Laboratories, 1972, Rept. No. BNWL-SA-4476.
21. B. G. Nyman and L. Hummelstedt, ISEC 74, 669.
22. L. Hummelstedt, H.-E. Sund, J. Karjaluoto, L.-O. Berts and B. G. Nyman, ISEC 74, 829.
23. S. O. Fekete, G. A. Meyer and G. R. Wicker, 1977, paper no. A77-95, AIME.
24. L. V. Gallacher, 1977, U.S. Patent 4,018,865.
25. K. Osseo-Asare, H. Leaver and J. Laferty, 1978, paper no. 78-B-61, AIME.
26. K. Osseo-Asare and M. E. Keeney, Met. Trans. B., 1980, 11B, 63.
27. K. Osseo-Asare and M. E. Keeney, Separat. Sci. and Technol., 1980, (in press).
28. M. E. Keeney, M. S. Thesis, The Pennsylvania State University, 1979.
29. A. van Dalen, K. W. Gerritsma and J. Wijkstra, ISEC 71, 1096.
30. A. van Dalen, K. W. Gerritsma and J. Wijkstra, J. Colloid Interface Sci., 1974, 48, 127.
31. A. van Dalen, J. Wijkstra and K. W. Gerritsma, J. Inorg. Nucl. Chem., 1978, 40, 875.
32. A. van Dalen, RCN-141, Petten, The Netherlands, Reactor Centrum Nederland, 1971.
33. H. M. N. H. Irving, in Solvent Extraction Chemistry, D. Dryssen, J. O. Liljenzin and J. Rydberg. Eds., North-Holland, Amsterdam, 1967, 91.
34. C. M. Starks, J. Amer. Chem. Soc., 1971, 93, 195.
35. W. P. Weber and G. W. Gokel, Phase Transfer Catalysis in Organic Synthesis, Springer-Verlag, New York, (1977).
36. J. H. Fendler and E. J. Fendler, Catalysis in Micellar and Macromolecular Systems, Academic Press, New York, (1975).
37. H. J. Foakes, J. S. Preston and R. J. Whewell, Anal. Chim. Acta, 1978, 97, 349.
38. M. Cox and D. S. Flett, paper no. 5a, ISEC 77.
39. G. Scibona, P. R. Danesi, A. Conte and B. Scuppa, J. Colloid Interface Sci., 1971, 35, 631.
40. G. F. Vandergrift and E. P. Horwitz, J. Inorg. Nucl. Chem., 1977, 39, 1425.
41. E. C. Hunt, J. Colloid Interface Sci., 1969, 29, 105.
42. R. Chiarizia, P. R. Danesi, G. D'Alessandro and B. Scuppa, J. Inorg. Nucl. Chem., 1976, 38, 1367.
43. T. A. B. Al-Diwan, M. A. Hughes and R. J. Whewell, J. Inorg. Nucl. Chem., 1977, 39, 1419.
44. E. S. P. de Ortiz, J. Appl. Chem. Biotechnol., 1978, 28, 149.
45. S. J. Lyle and D. B. Smith, J. Colloid Interface Sci., 1977, 61, 405.
46. S. Kaufman and C. R. Singleterry, J. Colloid Sci., 1955, 10, 139.
47. S. Kaufman and C. R. Singleterry, J. Colloid Sci., 1957, 12, 465.
48. D. F. Morris, J. Colloid Interface Sci., 1975, 51, 52.
49. A. van Dalen, K. W. Gerritsma and J. Wijkstra, J. Colloid Interface Sci., 1974, 48, 122.
50. N. Pilpel, Chem. Revs., 1963, 63, 221.
51. A. S. Kertes, Surf. and Colloid Sci., 1976, 8, 193.

52. F. M. Fowkes, in K. Shinoda, Ed., Solvent Properties of Surfactant Solutions, Marcel Dekker, New York, 1967, 165.
53. A. Kitahara, K. Watanabe, K. Kon-No and T. Ishikawa, J. Colloid Interface Sci., 1969, 29, 48.
54. J.-R Cho and H. Morawetz, J. Amer. Chem. Soc., 1972, 94, 375.
55. A. D. James and B. H. Robinson, J. C. S. Faraday I, 1978, 74, 10.
56. J. Holzwarth, W. Knoche and B. H. Robinson, Ber. Bunsenges. Phys. Chem., 1978, 82, 1001.
57. S. Diekmann and J. Frahm, Ber. Bunsenges. Phys. Chem., 1978, 82, 1013.
58. S. Diekmann and J. Frahm, J. C. S. Faraday I, 1979, 75, 2199.
59. C. J. O'Connor, E. J. Fendler and J. H. Fendler, J. Amer. Chem. Soc., 1973, 95, 600.
60. C. J. O'Connor, E. J. Fendler and J. H. Fendler, J. C. S. Dalton, 1974, 625.
61. C. J. O'Connor, E. J. Fendler and J. H. Fendler, J. Amer. Chem. Soc., 1974, 96, 370.
62. B. H. Robinson, D. C. Steytler and R. D. Tack, J. C. S. Faraday I, 1979, 75, 481.
63. M. Fisher, W. Knoche, B. H. Robinson and J. H. M. Wedderburn, J. C. S. Faraday I, 1979, 75, 119.

EXTRACTION WITH CHEMICAL REACTION: SULPHONATION OF TOLUENE

P.R.L. Grosjean and H. Sawistowski

Department of Chemical Engineering,
Imperial College of Science and Technology

London SW7, England

ABSTRACT

Investigation was conducted on sulphonation of toluene in a stirred cell which was provided with a clearly defined interface. The employed range of concentration of sulphuric acid was from 68 to 84% by weight and a threefold variation in stirring speed was used. An attempt was made to explain the results in terms of mass transfer accompanied by first-order chemical reaction. This was successful up to a concentration of sulphuric acid of about 75%. Higher concentrations resulted in unexpected and sharp increases in transfer rates which were independent of the rate of stirring. It is postulated that these increases are the result of an interfacial reaction which becomes superimposed on the transfer mechanism in consequence of change in interfacial properties of the system.

SYMBOLS USED

C	concentration
D	diffusivity
Ha	Hatta number
K	mass transfer coefficient
k	reaction rate constant
ℓ	film thickness
M	molar mass
m	parameter in eqns. 8 and 9
N	molar flux
N_A	Avogadro number
n	surface concentration
R	universal gas constant
r	rate of reaction
S	interfacial area
T	temperature
t	time
V	molar volume
v	phase volume
w	mass fraction of sulphuric acid
z	distance from interface (normal direction)
β	parameter in eqns. 8 and 9
Γ	surface excess concentration
γ	activity coefficient
μ	viscosity
σ	interfacial and surface tension
ϕ	association factor

Superscripts

b	bulk
o	absence of reaction (physical extraction)
s	surface
*	equilibrium

Subscripts

i	interface
S	sulphuric acid
T	toluene
TSA	toluene sulphonic acid
W	water
2	phase 2 (acid)

INTRODUCTION

Most of the existing work on mass transfer with chemical reaction in liquid-liquid systems was reviewed by Hanson et al. (1, 2). The work on aromatic nitration is of particular relevance to the present study since it is often assumed that a certain analogy exists between this process and aromatic sulphonation. Since it was shown by Hanson that several assumptions concerning aromatic nitration are of doubtful validity and arise out of misinterpretation of experimental results, it was felt that similar conclusions may apply to sulphonation. Since most previous work was conducted in stirred dispersions, the misinterpretation was ascribed to the effect of various parameters on the interfacial area and not solely on the mass transfer coefficient. It was therefore important to use an apparatus with a geometrically well-defined interface and thus be able to isolate and evaluate the effect of phenomena other than variation in interfacial area.

Models of mass transfer accompanied by chemical reaction have already been described extensively in literature (3, 4). Although they were originally developed for absorption, there is no reason why they should not be applied to liquid-liquid systems, provided secondary phenomena, such as the Marangoni effect, are taken into account. It is mainly this reason which makes experimental verification of the models difficult (5, 6, 7).

Previous work (8) on liquid-liquid mass transfer accompanied by a neutralization reaction (transfer of propionic acid from toluene into aqueous solution of sodium hydroxide) provided a qualitative assessment of the secondary effects. It also confirmed that, provided these are taken into account, the film model of mass transfer is applicable to extraction with instantaneous chemical reaction. It is now proposed to extend the work to cover extraction with pseudo first-order reaction. Sulphonation of toluene was chosen as an example on account of availability of kinetic data and the information it may supply on aromatic nitration and sulphonation in agitated dispersions.

EXPERIMENTAL

The main requirements of the equipment was the presence of a smooth interface of known geometry and a uniform concentration in the turbulent bulk of each phase. Such conditions were satisfied by the stirred cell described by Austin and Sawistowski (9, 10) which was a modification of an earlier stirred cell developed by Lewis (11). It was decided to employ the Austin cell in this work but modify it by dispensing with the subsidiary, manually-operated, stirred cell of variable volume, which was used for controlling the position of the interface. In order to minimise the resulting error, each run was stopped if the interface moved vertically by more than 3 mm. This permitted runs to be carried out lasting at least 100 to 200 min.

Experiments were performed at 25^{o}C and stirring speeds of 100, 200 and 300 rev/min. Since contradictory statements were made by Austin (9) and Lewis (11) concerning the influence of direction of stirring in the two phases, this effect was fully investigated (12). No significant difference between co-rotating and counter-rotating configurations was observed and the latter was adopted.

The solvents employed were toluene (phase 1) and aqueous sulphuric acid (phase 2). Toluene is slightly soluble in the acid phase (29) and it is generally accepted that this is the phase in which the sulphonation reaction takes place. The product of the reaction is toluene sulphonic acid (subsequently referred to as TSA) which is retained in the acid phase and can be easily analysed spectrophotometrically. The method developed by Saunders

(13) was found suitable for this purpose and the Hitachi-Perkin-Elmer 139 UV-Spectrophotometer was employed.

An experiment was started by filling the cell with known volumes of aqueous sulphuric acid and toluene. The stirring speed was then adjusted to its desired value. The problem was complicated by the fact that the chemical reaction begins immediately on contacting the phases. Zero time was therefore arbitrary and since, in addition, disturbances created by filling cannot be avoided the experimental concentration-time profiles (Fig. 1) do not pass through the origin.

Results were obtained by periodic withdrawal of 3 ml samples from the acid phase. Its absorbance was quickly measured at 256 nm and the sample returned to the cell. Experiments were performed at 25°C at stirring speeds of 100, 200 and 300 rpm and various initial concentrations of sulphuric acid in the range from 68 to 83 per cent by weight. Higher concentrations were not employed as they produced discoloration of the acid phase.

PROPERTIES OF THE SYSTEM

Since the reaction takes place in the acid phase, it is the properties of this phase, i.e. of the aqueous sulphuric acid solution, which need to be considered. The variation of density and viscosity with concentration of sulphuric acid is well established (14) and it can be assumed that both these properties are unaffected by the small content of toluene and TSA. The viscosity relation is not a simple function of concentration but it remains monotonic up to a concentration of 85 per cent by weight.

The diffusion coefficient of toluene in aqueous sulphuric acid, D_{T2} (cm^2/s) was estimated from viscosity data using the Wilke-Chang equation in the form proposed by Perkins and Geankoplis (15)

$$D_{T2} = 7.4 \times 10^{-8} (M\phi)^{0.5} \, T/\mu_2 \, V_T^{0.6} \qquad (1)$$

where V_T (cm^3/mol) is the molar volume of toluene at its normal boiling point, μ_2 (cP) is the viscosity of the acid phase, T (K) is the temperature and $M\phi$ is defined by the relation:

$$M\phi = x_W \, \phi_W \, M_W + x_S \, \phi_S \, M_S \qquad (2)$$

In this equation x, ϕ, M denote mole fraction, association factor and molar mass respectively and the subscripts W and S refer to water and sulphuric acid respectively.

This method was already employed by Cox and Strachan (16-18) in their work on two-phase nitration of toluene and chlorobenzene. They found that by taking $\phi_S = 2.0$ and $\phi_W = 2.6$ there was good agreement between calculated and experimental values. If, therefore, w_2 is used as mass fraction of sulphuric acid in water, equations 1 and 2 reduce to

$$D_{T2} = 53.37 \times 10^{-7} \left[\frac{2.6 - 0.6 \, w_2}{1 - 0.826 \, w_2} \right]^{\frac{1}{2}} \mu_2^{-1} \qquad (3)$$

at 25°C. The equation is valid only for high acid concentrations, i.e. for the conditions employed in the experiments.

The solubility of toluene in sulphuric acid solutions has already been presented in (29) and it will be taken to represent the equilibrium

interfacial concentration C_T^*.

The kinetics of toluene sulphonation was studied in detail by Cerfontain et al. (19-24). It was found that the reaction was pseudo first-order with respect to toluene so that the rate of consumption of toluene was given by

$$r_T = k_1 C_T \tag{4}$$

A general review of the kinetic work was presented by Saunders (13) who assessed the available experimental evidence and presented them in the form of the rate constant k_1 at 25°C as

$$\ln k_1 = - 64.32 + 67.50 w_2 \tag{5}$$

THEORY

The mathematical statement of the problem is given by the conservation equation of the solute (toluene) in an element of the film

$$\frac{\partial C_{T2}}{\partial t} = D_{T2} \frac{\partial^2 C_{T2}}{\partial z^2} - k_1 C_{T2} \tag{6}$$

with the following initial and boundary conditions

(i) $t = 0, C_{T2} = 0$; (ii) $z = 0, C_{T2} = C_{T2}^*$; (iii) $z > \ell, C_{T2} = C_{T2}^b = f(t)$

where ℓ is the film thickness and condition (iii) is represented by

$$v_2 \frac{\partial C_{T2}^b}{\partial t} = - S D_{T2} \left(\frac{\partial C_{T2}}{\partial z} \right)_{z=\ell} - k_1 v_2 C_{T2}^b \tag{7}$$

In eqn. 7 v_2 is the volume of the acid phase (290 cm^3), S is the interfacial area (30.25 cm^2) and C_{T2}^b is the concentration of toluene in the perfectly stirred bulk of the lower phase.

An approximate solution of eqn. 6 was adopted by assuming pseudo-stationary conditions in the film, i.e. that the conditions can be represented by a sequence of steady-state events. For each of the sequences a steady-state solution can be obtained which gives

$$C_{T2}^b = \frac{m}{m+k_1} \frac{C_{T2}^*}{\cosh \beta} \left\{ 1 - \exp \left[-(m+k_1) t \right] \right\} \tag{8}$$

and

$$N_{Ti} = - D_{T2} (dC_{T2}/dz)_{z=0}$$

$$= K_2^o \, Ha \, C_{T2}^* \left\{ 1 - \frac{1 - \exp \left[-(m+k_1) t \right]}{(1+k_1/m) \cosh^2 \beta} \right\} \tag{9}$$

$$\beta = (k_1 D_{T2})^{\frac{1}{2}}/K_2^o; \quad Ha = \beta/\tanh \beta; \quad m = K_2^o \, Ha \, S/v_2.$$

Equations 8 and 9 contain K_2^o, the mass transfer coefficient of toluene into the acid solution in the absence of chemical reaction. This coefficient was determined from existing correlations and checked experimentally on the test system toluene-propionic acid-water both for physical extraction and with sodium hydroxide present in the water phase (8).

The relevant correlations existing in literature were those of Austin (10) and of Davies (25). Austin's correlation was established using an almost identical cell to that employed in the present work. However, the work was performed on partially miscible binary systems, i.e. systems of low interfacial tension, and the correlation was found not to apply to the test system employed. Better results were obtained with Davies' correlation since it includes interfacial tension as a parameter. Its validity was confirmed by the work on extraction with instantaneous chemical reaction.

It is known from theory (3, 4) that the value of β is indicative of the regime of mass transfer with simultaneous chemical reaction. For $\beta > 3$ the reaction is regarded as fast and for $\beta < 0.2$ as slow. The estimation of β will therefore throw some light on the extraction process and may lead to simplifications in the theoretical treatment. For $w_2 = 0.7$, $k_1 = 3.86 \times 10^{-8}$ s^{-1}, $k_2^o = 1.3 \times 10^{-4}$ cm/s at 200 rev/min and $D_{T2} = 1.5 \times 10^{-6}$ cm^2/s. Consequently, $\beta = 1.85 \times 10^{-3}$. For $w_2 = 0.8$, β was found to be equal to 0.077. Hence, over the range of operation the reaction could be considered as slow, i.e. it was confined to the bulk and did not affect diffusion across the film.

On substitution of values into eqns. 8 and 9 it was found that the time dependent term in these equations could be neglected. For the extreme case of a contact time of 2 hours its omission introduced an error of 6% at 100 rev/min, 10% at 200 rev/min and 13% at 300 rev/min. These errors are of the same order of magnitude as the experimental errors and probably smaller than those involved in the estimation of mass transfer coefficients. Consequently, the toluene flux at the interface could be written as

$$N_{Ti} = K_2^o \, C_{T2}^* \tag{10}$$

and, incorporating the stoichiometry of the reaction into the material balance, as

$$N_{Ti} = \frac{1}{M_{TSA}} \frac{v_2}{S} \frac{dC_{TSA}}{dt} = 5.634 \times 10^{-5} \frac{dC_{TSA}}{dt} \tag{11}$$

where N_{Ti} is expressed in $mol/cm^2 s$, C_{TSA} in kg/m^3 and t in s.

RESULTS AND DISCUSSION

Experimental results were obtained by measuring variations in concentration of TSA with time (Fig. 1). In order to calculate the slope of the line, data were computed using a least square curve fitting technique. The toluene flux was subsequently calculated from eqn. 11 and the experimental mass transfer coefficient determined as

$$K_T = N_{Ti}/C_{T2}^* \tag{12}$$

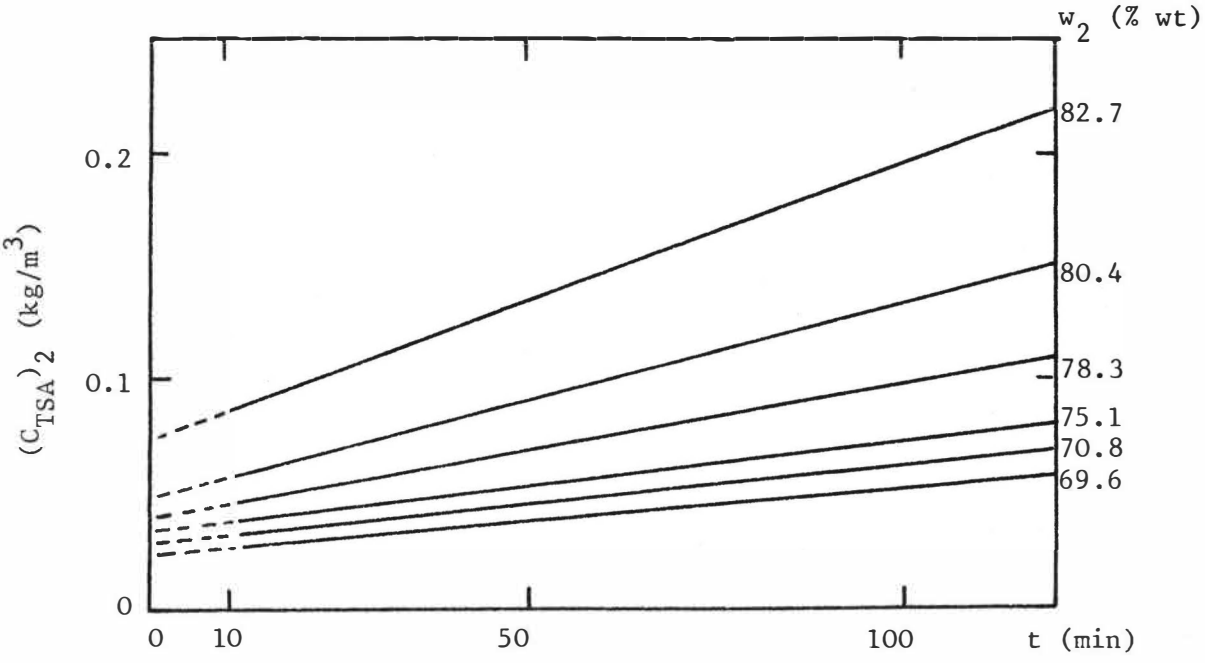

FIG. 1
Experimental concentration profiles of TSA for different sulphuric acid strengths (% by wt) at 25°C. Stirring speed: 100 rpm.

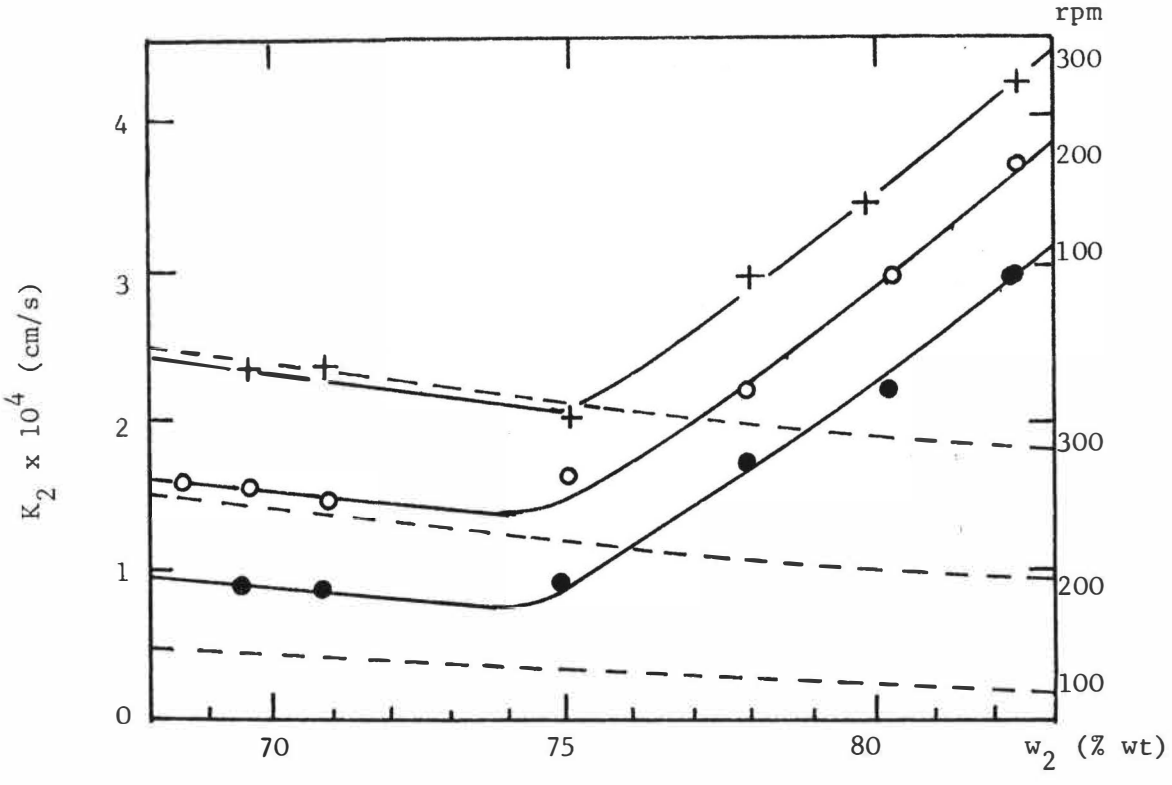

FIG. 2
H_2SO_4 concentration at various stirring speeds (—— experimental, --- predicted).

and plotted in Fig 2, where predicted values are presented by broken lines. It can be seen that the curves consist of two parts:

(a) The section under about 74.5% by weight of H_2SO_4 where there is reasonably good agreement between experimental and predicted results. This applies particularly to the trend of the results and the operation at 300 rev/min. The increased deviation at lower speeds is not surprising since the validity of Davies' correlation decreases with decreasing stirring speed.

(b) The section above 74.5% characterised by a sudden unpredicted increase in mass transfer coefficients. This increase cannot be ascribed to a change from a slow to a fast reaction regime, as such a change should take place at values greater than 82% by weight of H_2SO_4. Nor, as shown by the viscosity variation, can it be ascribed to any unexpected changes in bulk properties, as these do not occur below 84% by weight.

It has, however, been found that the surface tension σ_2 of aqueous H_2SO_4 increases with w_2, reaches a maximum at 49% for 25°C and then decreases (14). There is an appreciable increase in its rate of change beyond 75%. Since the two phases react when brought into contact, it is difficult to obtain stable experimental results for the interfacial tension σ. However, results are reported by Davies and Rideal (26) for the system benzene/aqueous H_2SO_4 which indicate that Antonoff's rule can be applied to this system provided an additional constant of around 10 mN/m is subtracted. The estimation of σ for the system under consideration was conducted using the relation

$$\sigma = \sigma_o + \sigma_2 - \sigma_w = \sigma_2 - 36 \qquad (13)$$

where σ_w is the surface tension of pure water and σ_o the interfacial tension of the system toluene/water. It has subsequently been established experimentally (27) that results obtained from eqn. 13 are reasonably correct. This means that the interfacial tension of the system toluene/aqueous H_2SO_4 decreases steeply beyond 75% solution. In other words, there will be a large excess of H_2SO_4 molecules present in the interface which indicates the possible occurrence of an interfacial reaction.

In order to check this hypothesis the results of Fig. 2 have been replotted in terms of the molar flux in Fig. 3. The flux given by eqn. 10 has also been recalculated with the values of the constant in Davies' correlation adjusted for K_2^o in the left-hand section of Fig. 2 to agree with experimental results. The difference was also plotted in Fig. 3 and is represented by the broken line. It confirms the hypothesis of an interfacial reaction by being independent of the stirring speed. Hence, it is suggested that

$$N_{Ti} = K_2^o C_T^* + r_{Ti} \qquad (14)$$

where r_{Ti} is the rate of the interfacial reaction per unit surface area.

Further development of the hypothesis of an interfacial reaction is highly speculative by assuming that pseudo-equilibrium conditions exist at the interface and thus ensure the applicability of Gibbs' equation. Starting from classical thermodynamic considerations (28) it can be shown that Γ_S, the surface excess concentration of sulphuric acid, can be obtained from

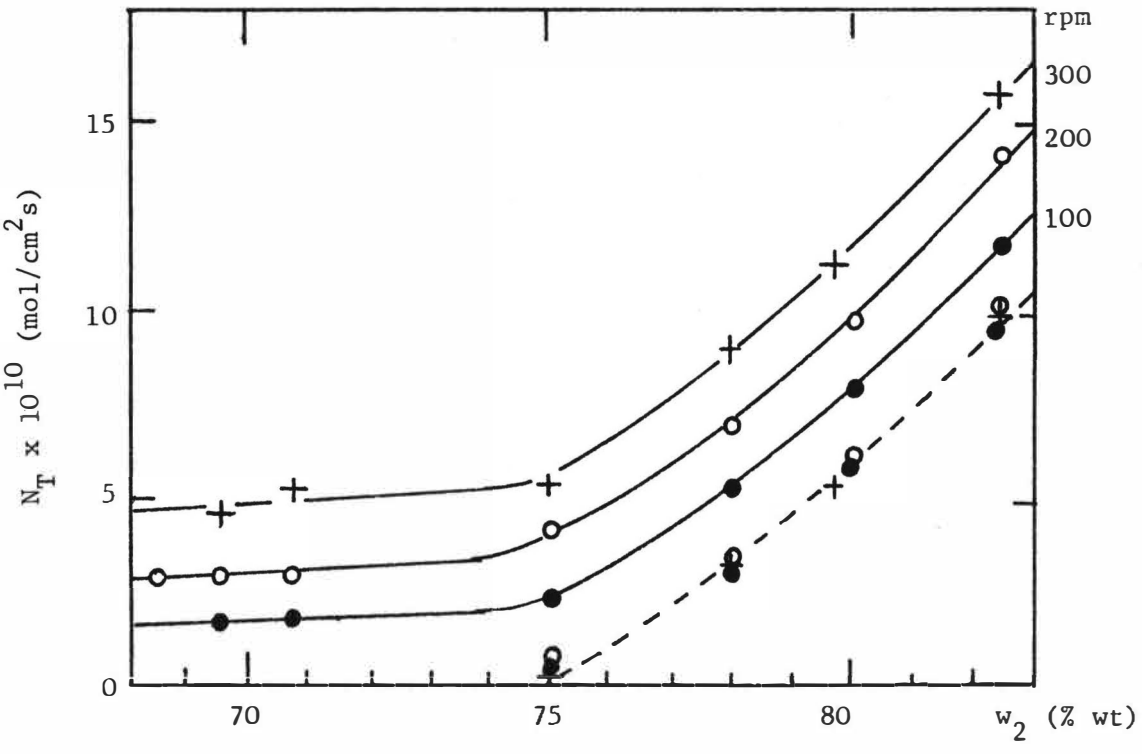

FIG. 3
Mass transfer flux as a function of H_2SO_4 concentration for various stirring speeds(--- interfacial reaction rate).

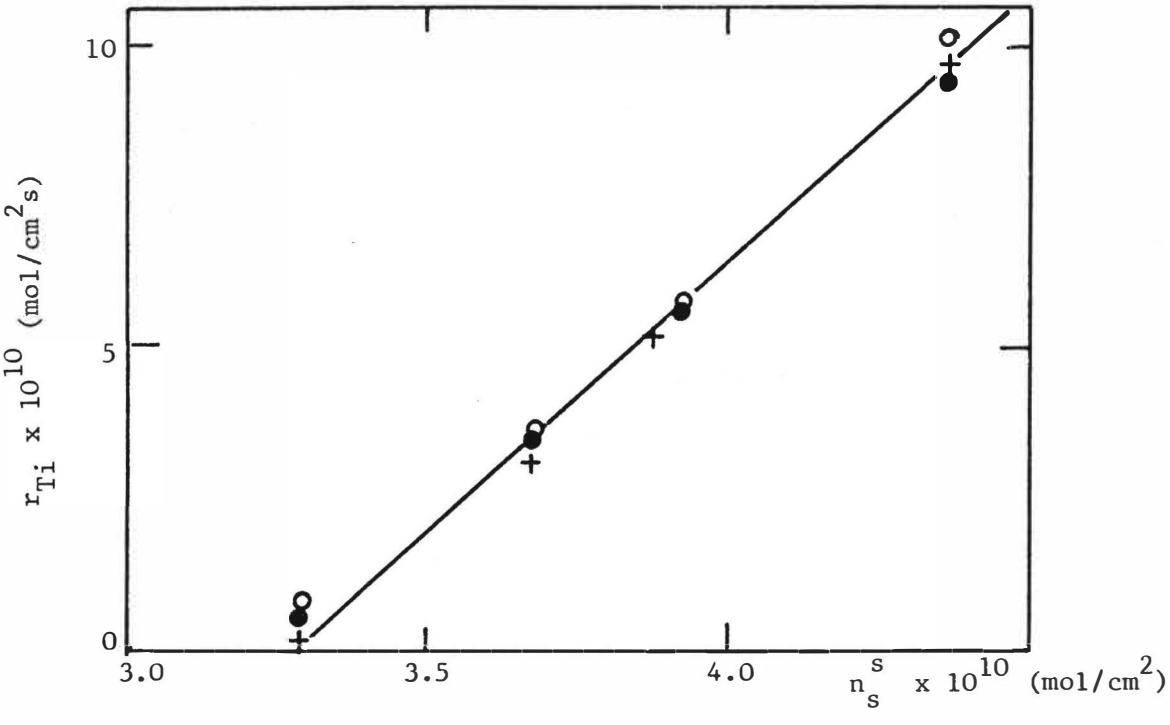

FIG. 4
Interfacial reaction rate as function of surface concentration of sulphuric acid.

the equation

$$-\frac{d\sigma}{dx_S} = \Gamma_S \frac{RT}{w_W}\left[\frac{1}{x_S} + \frac{d \ln \gamma_S}{dx_S}\right] \quad (15)$$

where R is the universal gas constant, w_W the mass fraction of water in phase 2 and Γ_S the activity coefficient of H_2SO_4 in that phase. The relation $\gamma_S = f(x_S)$ is given by Giauque (29) so that Γ_S could be calculated. This was added to the calculated bulk contribution of H_2SO_4 obtained as $x_S(N_A/V_S)^{2/3}/N_A$ to give n_S^s, the molar surface concentration of sulphuric acid.

The interfacial reaction will possess different reaction kinetics than the surface reaction. It can no longer be regarded as pseudo-first order with respect to toluene since sulphuric acid is no longer present in excess. In fact, the reverse is true so that

$$r_{Ti} = k_2^s \, n_T^s \, n_S^s = k_1^s \, n_S^s \quad (16)$$

The experimentally determined value of r_{Ti} is plotted against n_S^s in Fig. 4 and does, in fact, produce a straight line. In spite of the simplicity of the considerations, it forms additional evidence to support the hypothesis of an interfacial reaction.

CONCLUSIONS

The rate of sulphonation of toluene can be predicted on the basis of the film model of diffusion accompanied by simultaneous first-order chemical reaction up to sulphuric acid concentrations of 75% by weight. In this concentration range it follows the pattern of a slow reaction occurring principally in the bulk of the acid phase. There is, however, a large increase in reaction rate, i.e. also in the toluene flux, above 75% which is independent of the rate of stirring. It is proposed that this increase is produced by the appearance of a significant contribution of an interfacial reaction resulting from changes in the interfacial behaviour of the system.

REFERENCES

(1) Hanson, C., Recent Advances in Liquid-Liquid Extraction, Pergamon Press, London, 1971.
(2) Hanson, C., Hughes, M.A. and Marsland, J.G., Proc. Int. Solvent Extraction Conf., Soc. Chem. Ind., London, 1974.
(3) Astarita, G., Mass Transfer with Chemical Reaction, Elsevier, Amsterdam, 1967.
(4) Danckwerts, P.V., Gas-Liquid Reactions, McGraw-Hill, New York, 1970.
(5) Cho, D.H. and Ranz, W.E., Chem. Eng. Prog. Symp. Series No. 72, 1967, 63, 37.
(6) Bakker, C.A.P., Fentenev Van Vlissingen, F.H. and Beek, W.J., Chem. Engng. Sci., 1967, 22, 1349.
(7) Sawant, S.B. and Ramachandran, P.A., Summaries of Indian Inst. of Chem. Engrs., Silver Jubilee Meeting, 1972, p.69.
(8) Grosjean, P.R.L. and Sawistowski, H., Trans. Instn. Chem. Engrs., 1980, 58, 59.
(9) Austin, L.J., Ph.D. thesis, Univ. of London, 1966.
(10) Austin, L.J. and Sawistowski, H., I. Chem. E. Symp. Series, London, 1967, 26, 3.
(11) Lewis, J.B., Chem. Engng. Sci., 1954, 3, 248.
(12) Grosjean, P.R.L., Ph.D. thesis, Univ. of London, 1976.
(13) Saunders, A., Ph.D. thesis, Univ. of London, 1971.
(14) International Critical Tables, McGraw-Hill, New York, 1963.
(15) Perkins, L.R. and Geankoplis, C.J., Chem. Engng. Sci., 1969, 24, 1035.
(16) Cox, P.R. and Strachan, A.N., Chem. Engng. Sci., 1971, 26, 1013.
(17) Cox, P.R. and Strachan, A.N., Chem. Engng. Jl., 1972, 4, 253.
(18) Cox, P.R. and Strachan, A.N., Proc. Int. Solvent Extraction Conf., Soc. Chem. Ind., London, 1974.
(19) Cerfontain, H., Mechanistic Aspects in Aromatic Sulphonation and Desulphonation, Interscience, New York, 1968.
(20) Cerfontain, H., Duin, G.J. and Vollbracht, L., C. Anal. Chem., 1963, 35, 1005.
(21) Cerfontain, H., Kaandorp, A.W. and Sixma, F.L.J., Rec. Trav. Chim. Pays-Bas, 1963, 82, 113.
(22) Cerfontain, H., Sixma, F.L.J. and Vollbracht, L., Rec. Trav. Chim. Pays-Bas, 1964, 83, 226.
(23) Cerfontain, H., Sixma, F.L.J. and Vollbracht, L., Rec. Trav. Chim. Pays-Bas, 1964, 83, 226.
(24) Cerfontain, H., Vollbracht, L. and Sixma, F.L.J., Rec. Trav. Chim. Pays-Bas, 1961, 80, 11.
(25) Davies, J.T., Turbulence Phenomena, Academic Press, New York, 1972.
(26) Davies, J.T. and Rideal, E.K., Interfacial Phenomena, Academic Press, New York, 1961.
(27) Peker, S., private communication, 1979.
(28) Adamson, A.W., Physical Chemistry of Surfaces, Interscience, New York, 1967.
(29) Cerfontain, H. and Telder, A., Rec. Trav. Chim. Pays-Bas, 1965, 84, 545.

KINETICS AND MECHANISM OF EXTRACTION OF COPPER BY HYDROXYOXIMES UNDER QUIESCENT AND TURBULENT MIXING

M Cox and C G Hirons School of Natural Sciences, The Hatfield Polytechnic, Hatfield, Hertfordshire, UK
D S Flett, Warren Spring Laboratory, Stevenage, Hertfordshire, UK

The kinetics of extraction of copper with a pure synthesised reagent, 2-hydroxy-5-t-octylacetophenone oxime have been studied in both a quiescent interface stirred cell and AKUFVE equipment. The diluents used were n-heptane and toluene. Interfacial and bulk properties of the reagent have also been measured in these diluents. The results have been interpreted using a model incorporating both chemical reaction at the liquid-liquid interface and diffusion, and it was noted that diffusional processes were important even under turbulent mixing when rapid metal extraction occurs. A mechanism has been proposed for the metal extraction involving as the rate determining step reaction of an interfacial complex with a second reagent molecule.

Since the commercial availability of hydroxyoxime reagents in the mid-1960's, the kinetics of extraction of metals, in particular copper, with these reagents have been the subject of a number of investigations. Three basic systems have been used: rising or falling drops; quiescent interface cells; and fully dispersed systems. Results of these studies have been explained in terms of a number of possible rate limiting steps, within certain well defined boundary conditions. At one extreme, the reaction may be diffusion controlled under all conditions, and the rate of extraction is then dependant upon the interfacial area and concentration of the slowest diffusing species. At the other extreme, the reaction may be chemically controlled, in which case the rate of extraction is dependant upon the site of the chemical reaction.

Recent homogeneous phase studies (1) of the rate of formation of copper hydroxyoximes have shown the rate to be independant of pH, and the rate controlling step to be the addition of unionised hydroxyoxime to form a 1:1 complex. Heterogeneous studies on the other hand (2) have generally shown the rate to be dependant on pH, and while all have been first order with regard to copper, reaction orders for extractant and pH have varied considerably. Clearly there is a difference in the chemical rate controlling step between the homogeneous and heterogeneous reactions, and most authors have concluded that the heterogeneous rate involves chemical reactions at the aqueous/organic interface.

Footnote: present address (CGH) Johnson Matthey Chemicals Ltd. Royston, Hertfordshire

Thus the kinetics of solvent extraction with hydroxyoximes are clearly complex involving mass transfer with chemical reaction in this heterogeneous system. Generally the type of rate equation describing the initial rate of extraction in such systems is of the form:

$$\text{rate} = \frac{k[Cu^{2+}]^{l}[RH]^{m}}{[H^{+}]^{n}} \qquad (1)$$

(where the symbols used here and in other equations are defined in the notation list). Values of l, m, and n in the literature have varied from zero through fractional orders to values of one and greater.

At ISEC77 a model was proposed (3) in which both chemical and mass transfer parameters were incorporated, and it was concluded that 'discrepancies in the reaction order are directly attributable to the neglect of the mass transfer contributions in the development of the various reaction mechanisms'. At that stage, it was not possible to fully evaluate the model in terms of available results because of the imprecise nature of the hydrodynamic conditions used, however, the general trend of published results appeared to give reasonable agreement. Also the use of commercial reagents, maybe containing significant amounts of surface active impurities, could affect the results obtained.

This paper presents results of the kinetic data for the copper/ hydroxyoxime system to test the applicability of this model in both a quiescent interface stirred cell, and in a fully dispersed, AKUFVE, system. The stirred cell was preferred to the single drop technique because greater control over interfacial area was possible and surface renewal of the interface could be controlled by rate of stirring.

EXPERIMENTAL

The quiescent interface cell consisted of a glass vessel of 180 cm^3 capacity for each phase fitted with high density polythene stirrers mounted on concentric titanium shafts with a polythene interfacial baffle to eliminate vortexing. This baffle gave an interfacial area of 82 cm^2. The stirrers were connected to the same stirrer motor and were normally driven contrarotatory. The kinetic data were obtained under conditions far removed from chemical equilibrium by taking samples from both phases at defined times and analysing for copper. The overall time for a single run varied between 30 minutes and 4 hours.

The kinetic data using the AKUFVE were obtained using a relaxation technique (4). Here the system equilibrium is disturbed by, for example, addition of tracer radioactive copper and the return to equilibrium followed by counting techniques. As there is a significant contribution from the back reaction influencing the rate of extraction the appropriate kinetic equations must be used.

The study used a synthetic reagent, 2-hydroxy-5-t-octylacetophenone oxime (HOAO), synthesised and purified in these laboratories so as to avoid the problems of impurities mentioned above. Diluents used were n-heptane (IP spec) and toluene (AR). The aqueous phase was 0.1M sodium nitrate with pH adjustments using nitric acid or sodium hydroxide, all being AR grade. Measurements were made at 25°C.

RESULTS

In all cases the rate of extraction was found to be first order with

respect to copper concentration as in previous studies (2). A typical set of results for the stirred cell experiments on the variation of rate of extraction with pH and reagent concentration is shown in figures 1 and 2 for the system HOAO/heptane. Common features of this data are that the reaction orders, i.e. the slopes of rate vs pH and rate vs reagent concentration, varied from values of unity or approaching unity at low pH and low oxime concentration, i.e. low extraction rate, to approximately zero at high pH and high oxime concentration, i.e. high extraction rate. As found by others (5) on changing the diluent from heptane to toluene the extraction rate decreased by about a factor of 10 at high rates of extraction, and a factor of 2 at low rates of extraction, at the same concentration of HOAO in each diluent.

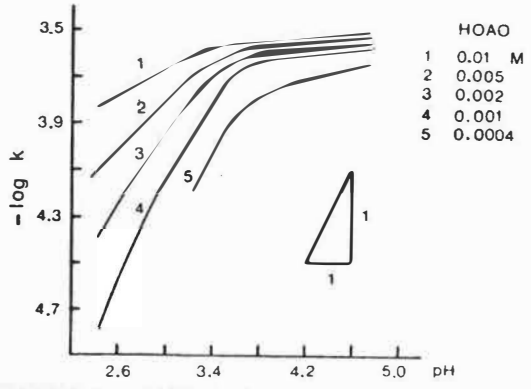

FIGURE 1 HOAO in heptane (stirred cell) rate vs pH

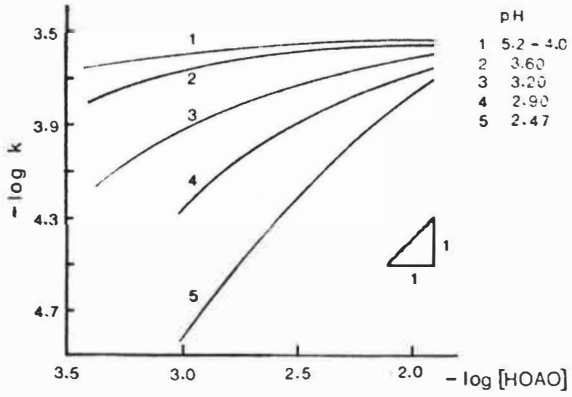

FIGURE 2 HOAO in heptane (stirred cell) rate vs log [HOAO]

Data from studies with the AKUFVE showed similar variations to those from the stirred cell, but because of the high turbulence in this apparatus the extraction rate using heptane as diluent was too high for accurate measurement so the majority of the results shown in figures 3 and 4 typifying this equipment relate to toluene as diluent.

One of the factors which influence the rate of diffusion controlled interfacial reactions is the stirring rate, or rate of surface renewal. Data on the effect on the observed copper extraction rate were obtained for HOAO/heptane at pH 3.6, fast kinetic region, and pH 2.9, slow kinetic region, using the stirred cell. At the higher pH a linear dependance of extraction rate on stirring speed was found while at the lower pH only a small increase in the rate was observed.

As well as these kinetic studies, measurements were also made on the interfacial tension and aggregation behaviour of the compound in both diluents. Interfacial tension results, figure 5, were obtained using the Wilhemy plate method and indicate interfacial saturation in heptane at concentrations $> 10^{-3}$M and in toluene at > 0.04M. Information on the state of aggregation of the hydroxyoxime has been obtained by vapour phase osmometry, table 1. The results show that the reagent is essentially monomeric throughout the range of organic phase concentrations of interest.

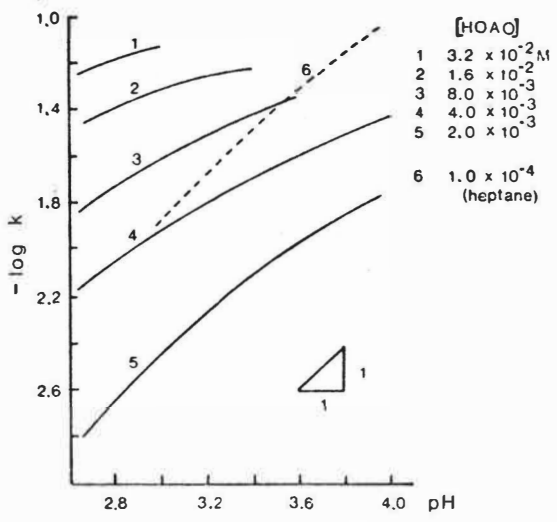

FIGURE 3 HOAO in toluene (AKUFVE) rate vs pH

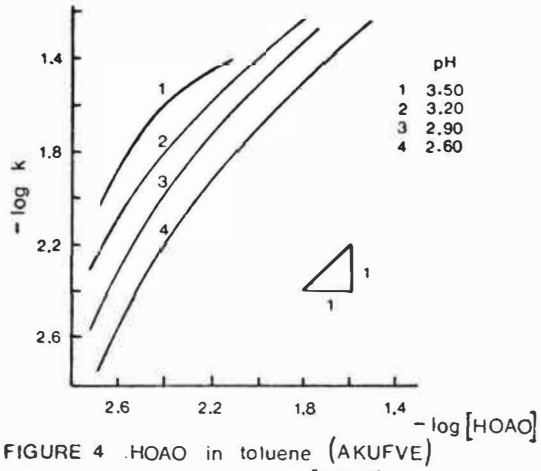

FIGURE 4 HOAO in toluene (AKUFVE) rate vs log [HOAO]

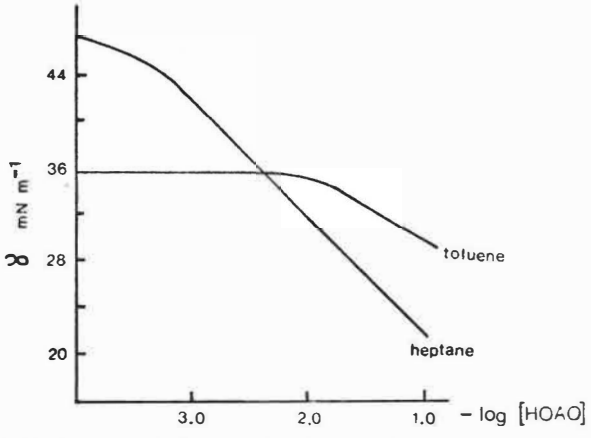

FIGURE 5 Interfacial tension of HOAO

Oxime concentration (mole dm^{-3})	Mean aggregation number n-heptane	toluene
10^{-1}	-	1.0
10^{-2}	1.07	-
5×10^{-3}	1.01	1.0

Table 1 Aggregation of HOAO in heptane and toluene at 37°C.

DISCUSSION

GENERAL CONSIDERATIONS

Using the model previously described (3) curves have been computed using the experimental data from the stirred cell which yield plots similar to those predicted but displaced by a common factor in each case. An example is shown in figure 6. The shape however, is different from that predicted by Ortiz et al (3) for the stirred cell and more nearly resembles those computed for the falling drop conditions. Thus it would appear that the selected value of the ratio of the interfacial rate constant to the mass transfer coefficient of copper was incorrect in the previous study, i.e. the value selected for the stirred cell conditions was ten times the actual value as shown by the present data. Further evidence that the variation in degree of turbulence as indicated by the value of the selected ratio may have been in error, particularly in relation to the relative positions on the scale for the stirred cell and the falling drop, has been given by Whewell (6).

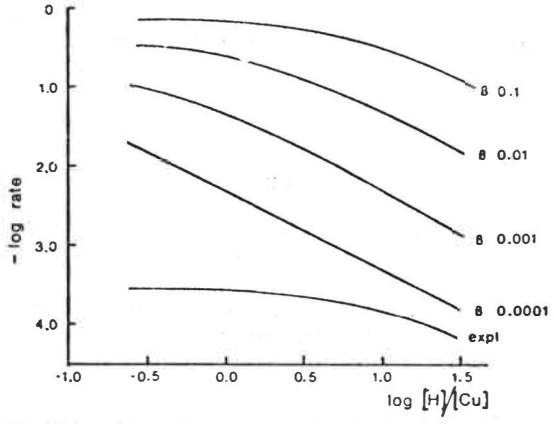

FIGURE 6 Computed curves compared with stirred cell results. [HOAO]/[Cu] = 50

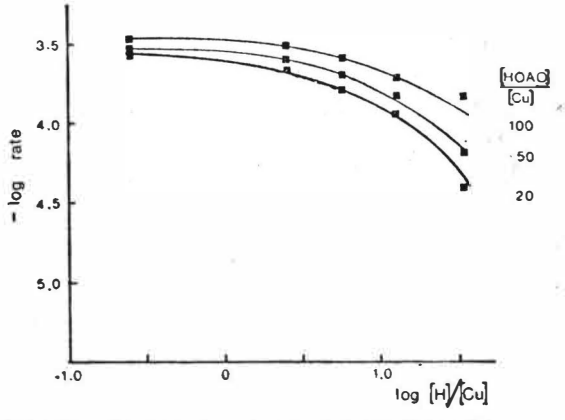

FIGURE 7 Adjusted computed curves compared with experimental points

KINETIC MODEL

The earlier study (3) assumed that l, m, and n in equation 1 had a value of unity. However, based on Pratt's work (1) and the observations by the majority of workers that, for heterogeneous reactions, the rate of extraction is dependant on the hydrogen ion concentration, in these systems the chemical rate controlling step must involve the addition of the second ligand at the interface. Thus it would seem that l=n=1, but m might be expected to have a value of 2. Use of the latter values in the model as originally described produced computed curves that in no way resembled the experimental data. Therefore in order to reconcile this problem and to obtain a better fit between observation and prediction it is necessary to reconsider the basis for development of the model.

The kinetic sequence given before (3,4) can be modified to encompass species adsorbed at the interface and species adjacent to the interface as described by Komasawa et al (7) thus accounting for differences in interfacial activity, i.e.

$$\overline{RH} \rightleftharpoons RH_{int} \rightleftharpoons RH_{ad} \qquad (2)$$

$$Cu^{2+}_{int} + RH_{ad} \rightleftharpoons CuR^{+}_{ad} + H^{+}_{int} \qquad (3)$$

$$CuR^{+}_{ad} + RH_{int} \rightleftharpoons CuR_{2,int} + H^{+}_{int} \qquad (4)$$

$$CuR_{2,int} \rightleftharpoons \overline{CuR_2} \qquad (5)$$

where subscript "ad" identifies adsorbed species and "int" identifies species adjacent to the interface and bars denote bulk phase concentrations, (for simplicity solvating water molecules have been omitted). The concentrations of the species adsorbed on or adjacent to the interface and the bulk phase concentrations are related by the appropriate physical chemical relationships, i.e.the appropriate adsorption isotherm for adsorbed species and diffusional relationships for the species adjacent to but not adsorbed on the interface.

If reaction (4) is rate controlling, as suggested by previous workers, then reaction (3) will be at equilibrium, i.e.:

$$K = [CuR^{+}_{ad}][H^{+}_{int}][Cu^{2+}_{int}]^{-1}[RH_{ad}]^{-1} \qquad (6)$$

thus $$\text{rate} = k_f K[Cu^{2+}_{int}][RH_{ad}][RH_{int}][H^{+}_{int}]^{-1} \qquad (7)$$

Under experimental conditions where the interface is saturated by RH, then $[RH_{ad}] \gg [CuR^{+}_{ad}]$ and both $[RH_{ad}]$ and $[RH_{int}]$ may be considered constant for a particular value of $[\overline{RH}]$, as also concluded by Komasawa et al (7). Thus the rate of extraction will be determined solely by the rate of disappearance of $[CuR^{+}_{ad}]$.

$$\text{rate} = k'_f[CuR^{+}_{ad}] \qquad (8)$$

or substituting for $[CuR^{+}_{ad}]$:

$$[CuR^{+}_{ad}] = K[Cu^{2+}_{int}][RH_{ad}][H^{+}_{int}]^{-1} \qquad (9)$$

therefore $$\text{rate} = k'_f K[Cu^{2+}_{int}][RH_{ad}][H^{+}_{int}]^{-1} \qquad (10)$$

relating these interfacial concentrations to the appropriate bulk phase concentrations as referred to above, the observed rate approximates to:

$$\text{rate} = K''[\overline{Cu}^{2+}][\overline{RH}][\overline{H}^{+}]^{-1} \qquad (11)$$

Thus it is possible to reconcile the observed rate dependencies of the reacting species with the model as originally proposed.

REVISED NUMERICAL ANALYSIS

Based on the above arguments it is possible to repeat the numerical analysis of Ortiz et al (3) varying the ratio of the interfacial reaction rate constant, to mass transfer coefficient for copper (β), the diffusivity ratios using data from Hughes and Middlebrook (8), and the value for K'' in equation (10). For calculation purposes K'' was regarded as being mainly derived from

the mass action constant for reaction (3) although it also contains elements of the dimerisation constant of the reagent, activity coefficients of the species involved, the rate coefficient for reaction (4), and the constant of the appropriate adsorption isotherm.

A best fit was obtained as shown in figure 7 for values of 0.15 for the reaction rate constant to mass transfer coefficient ratio (β) and 4.0×10^{-4} for $\underline{K}''$ under stirred cell conditions.

Because of the kinetic technique employed when using the AKUFVE it is not possible to treat the data there from using the model described above. However it is clear from the shape of the curves given in figure 3 that even in such a turbulent regime, diffusion can still be an important factor of the overall kinetic behaviour in situations close to equilibrium. An interesting feature of the data in figure 4 is the departure from linearity of the dependency, 1st order, of log k_f on log [RH] at low extractant concentrations. Here the value of the exponent in the kinetic expression increases beyond unity at a bulk phase concentration lower than 4×10^{-3}M, which corresponds to the value at which the interfacial tension of the HOAO solution in toluene begins to change with increasing bulk concentration, figure 5. This would seem to reinforce the assumption made earlier that under conditions of interfacial saturation the reation rate has an apparent zero order with respect to the interfacial concentration of the extractant. Finally under the condition of total or near saturation of the interface used in this study and the low value found for the ratio of the interfacial rate constant to mass transfer coefficient from the stirred cell data, it seems logical to conclude, in agreement with Hughes and Middlebrook (8), that the slow diffusion process relates to the removal of the copper complex from the interface into the bulk organic phase.

NOTATION

k_f	reaction rate constant
k_f'	reaction rate coefficient
$\underline{K}$	mass action equilibrium coefficient
$\underline{K}'$,$\underline{K}''$	lumped coefficients
l,m,n	reaction order exponents
β	ratio of interfacial reaction rate constant to mass transfer coefficient of copper
[ ]	concentration of species enclosed
subscripts:	
ad	species adsorbed at interface
int	species adjacent to the interface
superscript:	
——	bulk phase species

REFERENCES

1. Pratt J M and Tilley R I Hydrometallurgy 5, 29-45, (1979)
2. Flett D S AIME Meeting, New Orleans, Feb 1979
3. Perez de Ortiz E S, Cox M and Flett D S CIM Spec. Vol. 21, 198-203, (1979)
4. Flett D S, Okurara D N and Spink D R J. inorg. nucl. Chem. 35, 2471-2487, (1973)
5. Van der Zeeuw A J and Kok R CIM Spec. Vol. 21, 210-218, (1979)
6. Whewell R J, Hughes M A and Hanson C CIM Spec. Vol. 21, 185-192, (1979)
7. Komasawa I, Otake T and Muraoka T J. Chem. Eng. Japan 13, 204-208, (1980)
8. Hughes M A and Middlebrook P D Int. J. Min. Process. 5, 229-240, (1978)

MASS AND HEAT TRANSFER IN PARTIALLY MISCIBLE LIQUID-LIQUID EXTRACTION SYSTEMS USING RADIOACTIVE EMISSION OF TRACERS AND IMAGE ANALYSIS TECHNOLOGY

F. J. AGUIRRE
S. H. CHIANG
G. E. KLINZING

University of Pittsburgh

Pittsburgh, PA 15261 U.S.A.

The mass transfer that takes place when two partially miscible liquids are placed in contact is indeed of interest industrially with its importance in the field of liquid-liquid extraction. Interfacial activity generated in some industrial systems can greatly enhance the mass transfer in a unit.(2,3)

Since the processes of both mass and heat transfer appear to be taking place simultaneously (1) an effort has been made to measure and model them by use of radioactive tracer and microthermocouples coupled with image analysis technology and a computer software development package for analysis.

A teflon cell for the contacting of the two phases at a planar interface has been employed. This cell has two cylindrical wells of fluid and each cell half rotates such that the two wells can be contacted by appropriate rotation thus giving a good undisturbed interface for study. In the sides of the wall of the fluid wells, fiber optic probes (200 μm in diameter) and microthermocouples are inserted together. A radioactive tagged species (transferring in a partially miscible system) continuously gives off beta radiation which is captured by a scintillator counter at various stages of time in the mass transfer process. The light signals caused by the radioactive decay is fed to the AMP solid state image sensor which changes the light energy generated to electrical current. This current is further changed to a voltage and discreetized and stored on a computer for analysis by generated software.

In addition to the simultaneous heat and mass transfer determinations, a series of experimental measurements have been conducted to determine the "pure" heat transfer effect. For these measurements a fine nichrome mesh placed exactly at the interface is used to provide a constant heat flux at this point. The results are used to separate (or decouple) the interactions resulted from simultaneous heat and mass transfer in the same or similar systems. Experiments for "pure" heat transfer were conducted with pure water, isobutanol, ethylacetate and saturated solutions of water/isobutanol and water/ethylacetate. Considering that only part of the heat input is absorbed by the bottom phase the shapes of the temperature profiles are in agreement with the theory if pure conduction in a cylinder with constant heat flux at the boundary is assumed.

REFERENCES

1. Austin, L. J., Sawistowski, H., Solvent Extraction (eds. J. G. Gregory, B. Evans, P. C. Weston) pp. 840-851, Proc. Int. Solvent Extraction Conf. (1971)
2. Ying, W. E., Sawistowski, H., Solvent Extraction (eds. J. G. Gregory, B. Evans, P. C. Weston) p. 840, Proc. Int. Solvent Conf. 1971, Soc. of Chem. Ind. London (1971).
3. Perez de Ortiz, E. S., Sawistowski, H., CES, 28, 205 (1973).

SOLVENT REFINING OF LUBRICATING OIL WITH FURFURAL AND FURFURAL-CYCLOHEXANONE IN ELECTRIC FIELD

DING JIAN-CHUN, XU JUN
and FAN WEI-MIN

Shanghai Institute of Chemical Technology

Shanghai 201107, CHINA

This article describes a process in which furfural and furfural-cyclohexanone mixture of 3:1 volume ratio are used to refine lubricating oil. Experimental measurements of interfacial tension, density of surface charges of droplet and performance of "electrorefining" contactor are carried out in D.C. electric field for both solvent systems.

The refining process is studied in an experimental "electrorefining" contactor at various conditions for both solvents and two kinds of oil with different properties. Some of the experimental results are shown in the following Table. It is recognized that the increase in refining efficiency due to the presence of electric field is obvious and the requirement of electric energy is relatively low. When the potential gradient is raised to 950 v/cm, the variation in efficiency of refining due to change in solvent or temperature becomes undetectable for oil-II, perhaps owing to severe axial mixing existing between the electrodes. From the Table, it seems that the mixed solvent gives better results than furfural alone in the "electrorefining".

TABLE Experimental Data of "Electrorefining"

Solvent	Oil/Solvt vol.ratio	Oil 1/h	Temp. °C	voltage per cm	Δn_D^{50}	R.E.*	Energy Req't V.H./M^3
	oil-I μ^{50} = 19.44 (C.P.), n_D^{50} = 1.4803						
Furfural	0.5	0.36	50	760	0.0023	3.8	5.3
			60		0.0028	3.5	15.8
Mixed Solvt	0.5	0.36	50	680	0.0048	4.2	47.2
				760	0.0049	4.4	73.9
	Oil-II μ^{50} = 11.42 (C.P.), n_D^{50} = 1.4782						
Furfural	0.5	0.36	50	950	0.0028	2.2	5.3
			60		0.0045	3.8	73.9
Mixed Solvt	0.5	0.36	50	950	0.0045	3.8	42.2
			60		0.0044	3.8	47.5

Δn_D^{50} = (n_D^{50} Base Oil) - (n_D^{50} Raffinate)

*Relative Effectiveness = Δn_D^{50} (with elec. field/Δn_D^{50}(without elec. field)

STIRRED CELL STUDY OF COPPER EXTRACTION KINETICS

R. E. Molnar , J. H. E. Jeffes

Imperial College
Royal School of Mines

London, England

The extraction of copper from sulphate solutions using Kelex 100 (manufactured and supplied by Ashland Chemical) which had been purified by vacuum distillation, has been studied in a baffled stirred cell. The 300 ml bulk phases could be kept homogeneous while the inter-phase contact was effected across a quiescent 30.5 cm^2 interface. No organic phase modifiers were employed and the ionic strength was not controlled. Sulphuric acid was used to alter the pH.

The extraction rate was found to be independent of stirring speed over a 200 rpm range. This, together with comparative evidence of the dependence of extraction rate on the square root of stirring speed in a mass transfer controlled system studied in the same cell, was taken to indicate that a chemical reaction was controlling the extraction process. An activation energy for the initial extraction rate of about 8 kcal/mol also pointed towards chemical reaction control with due consideration for the precise meaning of the value that had been calculated. The linear dependence of the extraction rate on the interfacial area indicated that the chemical process was interfacial.

The rate controlling mechanism was studied by varying the organic Kelex and aqueous copper and hydrogen ion concentrations and observing the effect on the extraction rate. The results were consistent with a mechanism where the rate controlling steps were the two successive addition reactions whereby unionized Kelex, adsorbed at the interface, reacted with hydrated cupric ions in the aqueous phase. The significant contribution of reactions between ionized Kelex and copper and of single step additions was ruled out based on the evidence from the present experiments and the literature. The hypothesis that one of the two addition steps was primarily responsible for the observed rate, and so was much slower than the other step, was also discounted from the examination of the experimental results.

A rate equation was derived taking into account the forward and reverse rates of the two additions, and eliminating the intermediate concentration using the steady state assumptions. Under the experimental conditions employed, where the ratio of Kelex to hydrogen ion concentrations was large enough, and there was negligible back extraction, the rate equation simplified to a function where the rate was linearly dependent on the product of the bulk aqueous copper and organic Kelex concentrations. This model was found, both in the differential and integrated forms, successfully to represent the results. Deviations from the model could be qualitatively explained in terms of the assumptions made in relating interfacial concentrations (from interfacial reactions) to bulk values, and also in terms of the limitations imposed by the experimental range considered so that the effects of some factors such as the hydrogen ion concentration could not be precisely determined

EXTRACTION OF COPPER (II) BY HYDROXYOXIMES IN AN ELECTRIC FIELD

P.J. Bailes and I. Wade

Schools of Chemical Engineering,
University of Bradford

Bradford, West Yorkshire BD7 1DP, UK

The extraction of copper from acidified sulphate media by 20% LIX 64N in Escaid 100 in the presence of an electrostatic field was studied using a single droplet apparatus. A parallel plate electrode geometry was used with the drops being formed at the upper electrode and collected at the lower electrode. The inter-electrode region was filled with the highly insulating organic solvent. The discrete drops carried a free charge of the same polarity as the upper plate which could be positive or negative with respect to the lower earthed electrode.

The nature of the experiments ensured that the organic phase remained substantially unloaded and that relatively small quantities of copper were transferred. The extraction performance and droplet size were recorded for nominal field strengths up to 2 kV/cm.

A reduction in droplet size was observed with increasing field strength, and can be explained by considering the forces on the forming droplet. Measurements of the overall rate at which copper was transferred at different voltages revealed that charged droplets of the same size have different extraction rates depending on the sign of the voltage applied to the upper plate.

LIX 64N contains both active and inactive isomers of an aromatic hydroxyoxime (LIX 65N), a small percentage of an aliphatic hydroxyoxime (LIX 63) which acts as a catalyst, impurities and a kerosene make-up. These components may be influenced by the electric field to a different degree and this may account for the differences in extraction performance.

Experiments were conducted at $\pm$ 1 kV/cm for five hydroxyoxime extractants of different composition. The positive:negative extraction performance ratios showed that the polarity of the applied potential only had a significant effect on mass transfer in mixtures of LIX 65N and LIX 63.

Samples of organic phase were removed from near the upper electrode and subsequent infra-red analysis showed no significant deviation from the bulk composition. This was true for LIX 64N, LIX 65N + LIX 63 and loaded LIX 64N. It was concluded that no physical concentration of components was taking place at the upper electrode.

It seems probable that charging of the aqueous-organic interface influences the role which LIX 63 plays in the overall extraction mechanism.

THE DETERMINATION OF MASS-TRANSFER COEFFICIENTS AND INTERPHASE SURFACE DURING EXTRACTION OF URANIUM BY TRI-N-BUTYLPHOSPHATE IN CENTRIFUGAL FIELD.

M.F. Pushkenkov, G.I. Kuznetsov,
N.N. Shchepetil'nikov, A.T. Filyanin

V.G. Khlopin Radium Institute

Leningrad, USSR.

The centrifugal extractor under consideration was similar to that referred in the work /1/. As the extraction process of uranyl nitrate and nitric acid by TBP diluted in the mixture of saturated hydrocarbons occurs mainly in diffusion region /1, 2/, the volume coefficients of mass-transfer depend largely on phase mixing intensity. The values of the volume coefficients of mass-transfer depend also to a large degree on TBP concentration similarly to the distribution factors of uranyl nitrate. The tests with non-diluted TBP have shown that the efficiency of uranium extraction is near to 1 at 2500 rpm and contact time 0.3 sec and therefore the determination of mass-transfer coefficients involves methodical difficulties.

A knowledge of interphase surface enables to use the data on extraction kinetics for the other apparatus or for the comparison with the results obtained in the cell with fixed interphase surface /3/. To determine the emulsion drop size in centrifugal apparatus, we used two methods, namely the hardening of drops of dispersed phase (paraffin) and the sedimentation of drops. It should be noted that the properties of melted paraffin approximate those ot saturated paraffin mixture widely used as TBP diluent. For the systems nitric acid - paraffin (60°C) and uranyl nitrate - paraffin, the tangent of the curves representing the dependence of the interface surface on the rotation rate of the centrifugal apparatus was 0.67-0.76 in logarithmic coordinates. At 20°C, the sedimentation method yields a straight line with a slope of 0.8 ; this value is in good agreement with the results obtained by hardening method. The results obtained by sedimentation method using decane as dispersed phase coincide with those for saturated hydrocarbons. The mass-transfer coefficients of nitric acid, uranyl nitrate at low concentration of the latter are close to each other with regard to interphase surface. The mass-transfer coefficients of uranyl nitrate at the concentration of 0.5 M calculated also with regard to interphase surface are lower because the increase in system viscosity and the reduction in drop size lead to the weakening of circulation in drops and of their interaction.

REFERENCES

1. M.F. Pushlenkov, N.N. Shchepetil'nikov etc. ISEC-74, 1, 493.
2. N.N. Shchepetil'nikov etc. Radiokhimiya, 1972, 14, 3, 344.
3. M.F. Pushlenkov, N.S. Tikhonov, N.N. Shchepetil'nikov, ISEC-77, 2, 648.

SHORT CUT CALCULATION PROCEDURES FOR COUNTERCURRENT EXTRACTORS

J.A.M. Spaninks and S. Bruin

Department of Process Engineering,
Agricultural University of the Netherlands,
De Dreyen 12,
6703BC Wageningen, The Netherlands.

Mass transfer rates in extraction calculations are often described with a constant transfer coefficient, the overall value k_{od} being defined by $Sh_{od}=2\ R\ k_{od}/D = -2\ R\ (dx/dr)_i/(x_a-x^*)$, where x is the dispersed phase concentration; $x^*=m\ c$ refers to the concentration in equilibrium with the local continuous phase concentration c; o,a and i refer to initial, average and interface respectively. It can be shown that Sh_{od}, which is essentially time dependent for rigid particles, reaches an asymptotic value $Sh_{od,a}$ for long contact times. Spaninks calculated asymptotic Sh-numbers for co- and countercurrent extraction of particles with simple geometry, e.g. Fig 1 for slabs.

For short contact times the extraction flux can be obtained from the penetration solution. Using this solution to calculate x_a and x^* shows that with increasing time Sh_{od} exhibits a -unrealistic- minimum, which is close to the asymptotic $Sh_{od,a}$ value. The minimum is located close to $Fo=D\ t/R^2 \sim 0.21$ for slabs, almost independent of the Biot-number $Bi=m\ k_c\ R/D$ and the extraction factor Λ, the ratio of flow rates of continuous and dispersed phase multiplied by m; the same holds for cocurrent extraction. The dimensionless dispersed phase concentration at this transition point $W_t=(x_o-x_{a,t})/(x_o-x_o^*)$ is shown in Fig 2. It is interesting to note that at this point $E_t=(x_o-x_{a,t})/(x_o-x_i)$ is always close to 0.5, the value calculated by Schoeber for mass transfer in slabs with a constant surface concentration.

The total extraction time can be estimated by combining the penetration solution for contact times up to Fo=0.21 and the asymptotic value of Sh_{od}.

REFERENCES

Spaninks J., 1979, Ph.D. Thesis, Agric. Univ., Wageningen, The Netherlands.
Schoeber W., 1976, Ph.D. Thesis, Univ. Technol., Eindhoven, The Netherlands.

FIG 1

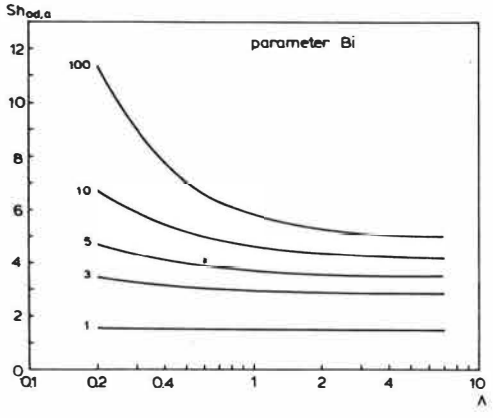

FIG 2

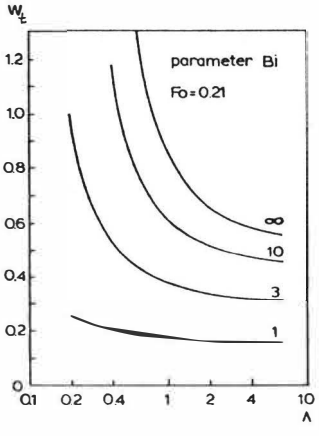

Dispersion
Session 3

Co-chairmen : H. Sawistowski (Imperial College, London, U.K.)
G. L'Homme (University of Liège, Belgium)

3A

80-19 Measurement of droplet coalescence rates in a packed extraction column using a novel colorimetric technique.
J.A. Hamilton and H.R.C. Pratt, University of Melbourne, Parkville, Victoria, Australia.

80-25 Techniques for determination of the dispersed phase hold-up in pulsed columns used in a nuclear fuel reprocessing plant.
A.F. Cermak, Allied-General Nuclear Services, Barnwell, South Carolina, U.S.A.

80-23 Microemulsion formation in the organic phase of some important extractants and its effects on the extraction mechanism.
Wu Chin-Kwang, Kao Hung-Cheng, Chen Tien, Li Seng-Chung, King Tien-Chu and Hsu Kwang-Hsien, Peking University, Peking, China.

80-24 Studies of the stability of haze generated in the aqueous phase on contact with hydroyoximes.
M.A. Hughes and P.D. Middlebrook, University of Bradford, Bradford, U.K. and N.C.C.M., R & D, Kitwe, Zambia.

80-39 Fluid dynamics of centrifugal extractors.
M. Stölting, Technische Universität München, München, Germany.

3B

80-231 Drop size distributions in a sieved plate pulsed column. Influence of break-up mechanism.
S. Pakdee Patrakorn, G. Muratet and G. Casamatta, Institut du Génie Chimique, Toulouse, France.

MEASUREMENT OF DROPLET COALESCENCE RATES IN A PACKED EXTRACTION COLUMN USING A NOVEL COLORIMETRIC TECHNIQUE

J.A. Hamilton and H.R.C. Pratt

Dept. of Chemical Engineering,
University of Melbourne.
Parkville, Victoria, 3052, Australia.

ABSTRACT

A novel technique is described for determining droplet coalescence rates in liquid extraction columns. This involves passing equal volumes of size-equilibrated droplets containing nickel di (ethyl xanthate) and dithizone, of yellow and green colour respectively, into the contactor. Coalescence of yellow and green droplets leads to the formation of red ones, the proportions of which can be determined as a function of droplet size from colour photographs. Experimental data are presented for the system methyl isobutyl ketone-water in a 76 mm diameter column packed with 12.5 mm Raschig rings. These show that coalescence is a relatively fast process, with typically 80% of red droplets present in the size ranges around the mean after 30 cm of packing under conditions giving 10% holdup of dispersed phase.

1.0 INTRODUCTION

1.1 General

It is now well established that the performance of most types of liquid extraction column is adversely affected by axial dispersion of one or both phases. In the case of the continuous phase this is due mainly to backmixing, in the form of a cocurrent circulatory flow set up by the droplet motion (1,2). In some types of mechanically agitated column backflow of dispersed phase droplets can be observed, although with other types, e.g. the packed column, there is little or no evidence of this. Satisfactory theoretical models covering backmixing in one or both phases are now available (3,4,5).

As first pointed out by Olney (6), another form of axial dispersion, in the forward direction, can also occur in the dispersed phase; this is a result of the differing velocities, and hence residence times, of the various droplet sizes present. Thus, each size has its own characteristic H.T.U., and provided there is no coalescence and re-dispersion the smaller droplets approach equilibrium more quickly than the larger ones, leading to a reduced performance. Olney (6) formulated the mass transfer equations on this basis for a differential contactor, but did not solve them. Rod (7) later gave a solution for a simplified model in which it was assumed that the dispersion consisted of two sizes of droplet only.

Chartres and Korchinsky (8), in a computer study using both experimental and theoretical droplet size dispersions, confirmed that the performance

for polydispersed systems is considerably lower than for monosized dispersions of the same Sauter mean droplet diameter, d_{32}. They also showed, as expected, that the effect of size dispersion is reduced progressively by an increasing coalescence rate, due to the tendency to equalise the dispersed phase concentration laterally. Other theoretical models, of stagewise type, have been studied (9,10) and shown to give similar results.

It is apparent that, while the theory of mass transfer in polydispersed systems is now reasonably well developed, this is of little relevance to the practical design and operation of extraction columns in the absence of experimental values of coalescence rates. The aim of the present work, therefore, was to develop a method of measurement of such rates, and to apply this in the first instance to packed columns.

1.2 Previous Work

The only aspect of coalescence rate which has received extensive study is that between droplets and a plane interface, where the rate is determined by the time required for drainage prior to rupture of the layer of trapped continuous phase (11). A similar mechanism has also been proposed for inter-drop coalescence (12,13,11).

Some attempts have been made to measure inter-droplet coalescence rates in batch agitated mixers using chemically reacting systems. Thus, a reagent solution is dispersed in the continuous phase and a further quantity of dispersed phase containing the other reagent is added suddenly. The coalescence frequency is obtained from measurements of the extent of reaction with time using a simple model which assumes, *inter alia*, that coalescence takes place between equi-sized droplets. Madden and Damerell (14) employed the reaction between iodine and sodium thiosulphate for this purpose, while Shiloh *et al* (15) used ferric chloride and sodium ferrocyanide, following the rate of formation of Prussian Blue by light absorption.

Coalescence rates have also been determined in continuous flow mixers. Thus Groothuis and Zuiderweg (16) introduced two separate dispersed phase streams, both benzene-carbon tetrachloride mixtures, of densities 1.030 and 0.990 into a single stage mixer-settler; since coalescence of two such equal sized droplets gives one of density 1.010, the non-coalesced low density droplets separated at the top of the settler, permitting their volume to be measured. Verhoff *et al* (17) introduced two streams of dyed droplets into a mixer and withdrew samples of the dispersion; these were stabilized by surfactant addition, permitting droplet sizes and colour to be determined.

Theoretical models of droplet breakdown and coalescence in dispersed systems have been proposed by Valentas *et al* (18) and by Bajpai *et al* (19). These are based on droplet population balance equations, together with assumed forms for the coalescence and breakdown probabilities. Bajpai *et al* concluded from the agreement between their experimental and predicted size distributions that their model was realistic.

Few studies of droplet coalescence and breakdown in packed columns have been reported. In an early photographic study Lewis *et al* (20,21) found that a constant equilibrium size distribution of droplets was obtained at the packing exit irrespective of the inlet size. However, the approach to the equilibrium value of d_{32} was slower with relatively small inlet droplets, indicating that the coalescence rate is lower for the smaller sizes. Ramshaw and Thornton (22) measured the rate of breakdown of relatively large droplets

in a packing and found that the equilibrium value of d_{32} was approached exponentially with packing height. Komasawa *et al* (23) proposed a collision model which assumed that coalescence occurred between freely moving and trapped droplets in the packing. They also determined coalescence rates from measurements of the extent of the oxidation-reduction reaction between two streams of aqueous droplets containing respectively ferric chloride and stannous chloride dispersed in kerosene in a 40 mm diam column packed with 6 mm polythene Raschig rings. This packing size is certainly less than the "critical size" for their system (20,24) and would lead to excessive coalescence rates (20).

1.3 Basis of Present Method

In the present method two equal streams of dispersed phase were used, each containing a differently coloured reagent which gave droplets of a third colour on coalescence. Hence using colour photography the sizes and colour of individual droplets could be recorded, allowing coalescence rates to be determined. Organic-soluble reagents were required for this purpose to enable conventional hydrophilic constructional materials to be used for the column.

In preliminary experiments with 5.0 cm diam. column using the second of the methods described below, promising results were obtained using dispersed phase streams of toluene coloured blue and yellow by means of Waxoline dyes, giving green droplets on coalescence (25). In a search for more effective additives, the possibility was considered of using diphenyl thiocarbazone (dithizone), the well known analytical reagent for lead, which forms a dark green solution in solvent, turning red with lead. However, no suitable organic-soluble lead compound could be found, but Winter (26) suggested the use of nickel di(ethyl xanthate), which gives a pale yellow solution, forming a similar red colour with dithizone.

Two experimental techniques were devised using this system, viz (i), two separate streams of mono-sized droplets were formed, allowed to mingle, photographed, and then passed through a variable length of packing and re-photographed; and (ii), the two streams of coloured droplets were first size-equilibrated by passage through a length of packing divided longitudinally by means of partitions, after which they were allowed to mingle and treated as before. After preliminary tests the first method was abandoned since it was not found practicable to produce satisfactory mono-sized dispersions over the range of flow rates required. Further work was therfore confined to the second method, as described below.

2.0 EXPERIMENTAL

2.1 Equipment

The column assembly was constructed from standard borosilicate glass sections with buttress joints (see Fig. 1). The lower (i.e. size equilibration) section was a 1.0 m length of 72.45 mm i.d. precision bore tube divided into quadrants by means of longitudinal 20 s.w.g. S.S. partitions; the coalescence and interface sections were 0.3 and 0.5 m lengths respectively of 76 mm nominal bore tube. The photographic cells comprised 18 s.w.g. S.S. bodies with tapered ends and parallel sections 165 mm wide by 25 mm deep, fitted with 130 x 160 mm laminated safety glass windows. Millimetre scales were attached to the front and back windows, and the former were provided with 25 mm square grids. Both the equilibration and coalescence sections of the column were packed with 12.5 mm x 2 mm thick Raschig rings, the height in the latter section being varied from 5 to 30 cm.

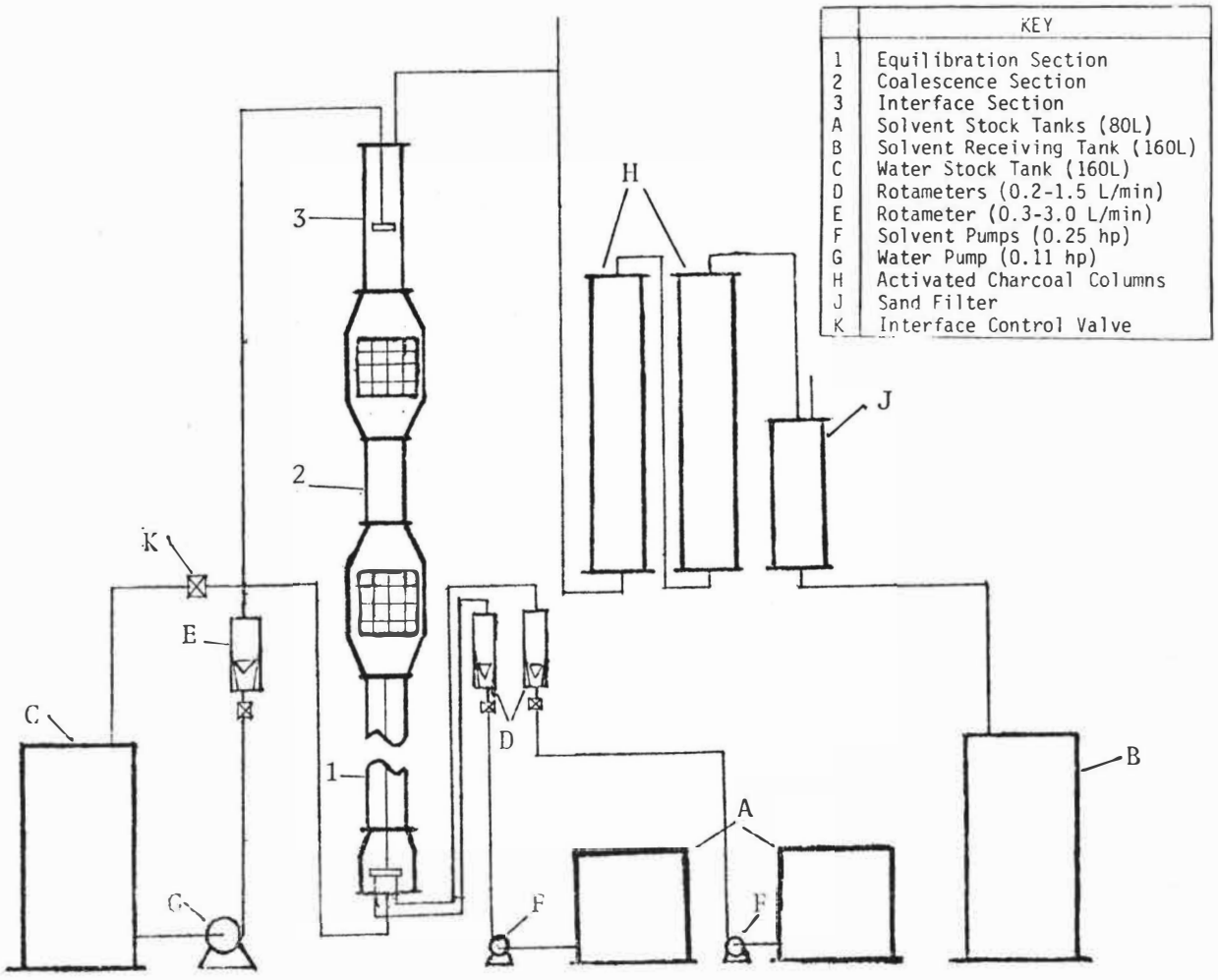

(a) General Arrangement

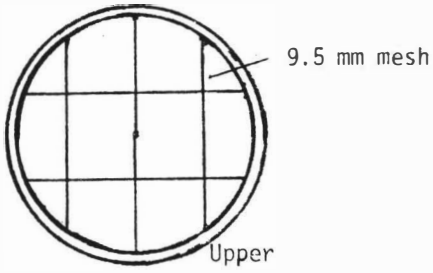

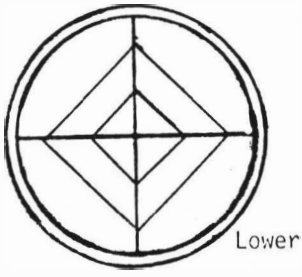

(b) Details of Packing Supports

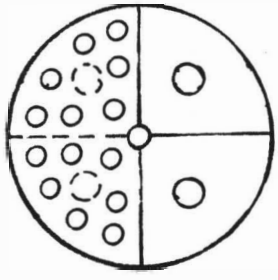

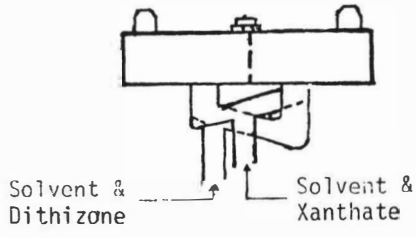

(c) Details of Solvent Distributor

FIG 1: Details of Equipment

The dispersed phase distributor was 75 mm diam. and was divided into four compartments each fitted with seven 4.5 mm nozzles from which the droplets passed into the corresponding quadrant of the equilibration section. Opposite pairs of compartments were coupled via rotameters and needle valves to separate solvent stock tanks. The distributor was located within a glass expansion piece of 100 mm base diameter. Outgoing mixed solvent was stripped of colour reagents by passage through two 1 m lengths of 100 mm bore tube packed with activated charcoal, followed by a filter bed of sand.

The general arrangement of the remainder of the equipment is shown in Fig. 1. The pipework was mostly of 12.5 mm o.d. tube connected by compression type fittings. Stainless steel was used throughout for tanks, pipework, etc., to avoid unwanted colour reactions between dithizone and corrosion products.

2.2 Materials

Commercial grade methyl isobutyl ketone (M.I.B.K.) was used as dispersed phase, with deionized water as continuous phase. Both were presaturated before use by repeated recirculation through the column. The activated charcoal was I.C.I. "Darco" grade of nominal size 4 x 12 mm.

The diphenyl thiocarbazone was obtained from laboratory suppliers. The nickel di(ethyl xanthate) was prepared by adding 2 moles of potassium ethyl xanthate to 1 mole of nickel chloride dissolved in water, filtering off the brown precipitate and recrystallizing from hot ethanol.

The reagents were added to the solvent tanks in concentrations of 0.1 g/l for the xanthate and 0.05 g/l for the dithizone. The latter was added to the solvent immediately before a run, in view of its instability.

2.3 Procedure

The two solvent streams and the water were admitted to the column at the predetermined flow rates and the interface position was stabilised above the upper window by adjustment of the water outlet valve. Two photographs were taken of the lower and 4-5 of the upper window on Kodak Ektachrome 35 mm A.S.A. 160 Professional Colour Slide Film using a camera with a 50 mm lens and a 1/250 sec exposure time. Illumination was provided by means of 500 watt Photoflood lights arranged to reflect from opaque white screens behind each window.

The resulting colour slides were projected on to a screen using a suitable magnification as determined by the scales on the windows. Grid areas were selected at random and all droplets within these, numbering at least 150 per slide, were counted and their colour and size of minor and major axes recorded; the effective diameters were then calculated as $\sqrt[3]{d_1^2 d_2}$. Taking the smallest size as 0.712 mm diameter, they were classified into 9 ranges with sizes based on intervals of $\sqrt[3]{2}$, i.e. so that the mean droplet volume of any given size is twice that of the size below. The results were used to compute the Sauter mean diameter, d_{32}, and the frequency distributions of all droplets and of red droplets.

3.0 RESULTS

Three series of runs were carried out using a single aqueous phase flow rate with three values of the total dispersed phase flow, corresponding to estimated holdup values (24) of 4.8, 10.6 and 17.0 respectively. In each series four or five packing heights were used, from 5.0 to 30.0 cm inclusive

In all cases the degree of coalescence below the packing, i.e. in the lower window, was found to be negligible.

Considerable scatter of the data was apparent when assessing the fraction of coalesced (i.e. red) droplets within each size range, especially at the smaller packing heights. The data were therefore fitted by means of an $\ell 1$ norm (i.e. least linear deviation) regression analysis to the following generalised expression for the rate of an n-th order reaction.

$$1 - f_{r,j} = \frac{1}{(1 + Ah)^n} \qquad (1)$$

where $f_{r,j}$ is the fraction of red droplets of size j and h is the packing height. The resulting values of the constants n and A corresponded to the "best fit", from which smoothed curves were calculated using eq. (1). In the course of this work it was observed that a better fit was obtained by reducing the actual packing height by 2.5 cm; this suggests that the first two courses of packing were ineffective in promoting droplet coalescence, presumably due to orientation produced by the packing support.

A summary of the coordinates of the smoothed coalescence curves for the three series of runs is given in Table 1. The experimental data for selected droplet sizes are compared with the smoothed curves for Series 2 in Fig. 2, and a comparison of the smoothed curves for the three series of runs is shown in Fig. 3. Histograms of the overall size distribution are shown in Fig. 4 and the cumulative size distributions are compared with the theoretical Mugele-Evans distribution (27) in Fig. 5. Finally, values of d_{32}, the Sauter mean droplet diameter, computed from the experimental data are compared with the values predicted from the Gayler-Pratt correlation (eq. 9 of ref. 21) in Table 2.

4.0 DISCUSSION

In assessing the present results it is important to note that the true coalescence rates are twice those given by the initial slopes of the curves in Figs. 1 and 2, i.e. at (h-2.5) = 0, since only coalescences between different coloured droplets are observed. In consequence, at a height for which $f_{r,j} = 0.50$, the number of coalescences of droplets of size j is somewhat greater than the total number of that size entering the packing, due to the additional incidence of coalescences involving red droplets.

Before commencing the present experimental programme, consideration was given to the possibility that the results would be invalidated by surface tension gradient (i.e. Marangoni) effects. For this reason careful measurements were made of the interfacial tensions of the mutually saturated solvent -water and reagent solution-water systems, both before and after reaction, using a du Noüy balance, but no differences could be detected. In any case, it is to be expected that interfacial tension gradients would not influence the time required for coalescence to start once two droplets came together, since this is determined by the time required for drainage of the trapped layer of continuous phase. However, once film rupture occurred such effects could conceivably enhance the rate at which the contents of the two droplets would mix, but this would if anything be of advantage in the present method.

Using data of the present type, a mathematical model can be developed for the droplet coalescence/breakdown process in terms of the appropriate rate constants. For this purpose, using the $\sqrt[3]{2}$ size distribution series, population balances are written for each size, noting that the number of

TABLE 1: Summary of Fraction Red Droplets as a Function of Packing Height, Smoothed Using Eqn. 1 (h' = (h - 2.5) cm)

j	DIAM (mm)	Series 1: 4.8% Holdup Fraction Red						Series 2: 10.6% Holdup Fraction Red				
		% No SIZE	HEIGHT, h' (cm)					% No SIZE	HEIGHT, h' (cm)			
			5	10	15	20	30		5	10	15	30
1	0.712	7.4	.157	.206	.235	.255	.284	5.6	.259	.374	.444	.558
2	0.897	7.7	.156	.205	.234	.254	.283	7.5	.248	.385	.474	.622
3	1.130	10.2	.198	.248	.276	.296	.323	8.9	.359	.492	.566	.677
4	1.424	15.0	.261	.445	.578	.674	.800	9.0	.446	.645	.751	.885
5	1.794	16.6	.274	.376	.436	.477	.531	10.2	.514	.646	.713	.803
6	2.260	16.4	.202	.297	.357	.399	.458	13.3	.464	.621	.702	.812
7	2.847	14.3	.306	.508	.644	.738	.851	19.5	.534	.762	.869	.970
8	3.587	9.9	.606	.684	.808	.878	.946	17.4	.722	.862	.915	.966
9	4.520	2.5	.571	.600	.616	.627	.642	8.6	.928	.941	.948	.958

TABLE 1: Continued

j	DIAM (mm)	Series 3: 17.0% Holdup Fraction Red				
		% No SIZE	HEIGHT, h' (cm)			
			5	10	15	30
1	0.712	5.6	.553	.712	.788	.881
2	0.897	7.9	.479	.616	.686	.783
3	1.130	9.0	.601	.718	.774	.847
4	1.424	9.2	.525	.643	.702	.785
5	1.794	13.0	.485	.715	.833	.957
6	2.260	14.7	.522	.738	.843	.952
7	2.847	20.4	.664	.817	.880	.946
8	3.587	13.7	.752	.895	.944	.984
9	4.520	6.5	.940	.976	.986	.995

TABLE 2: Comparison of Experimental and Calculated Sauter Mean Diameters

Hold up	Sauter Mean, d_{32} (cm)	
	Expt.	Predicted
4.8	2.899	2.64
10.6	3.489	2.79
17.0	3.319	2.87

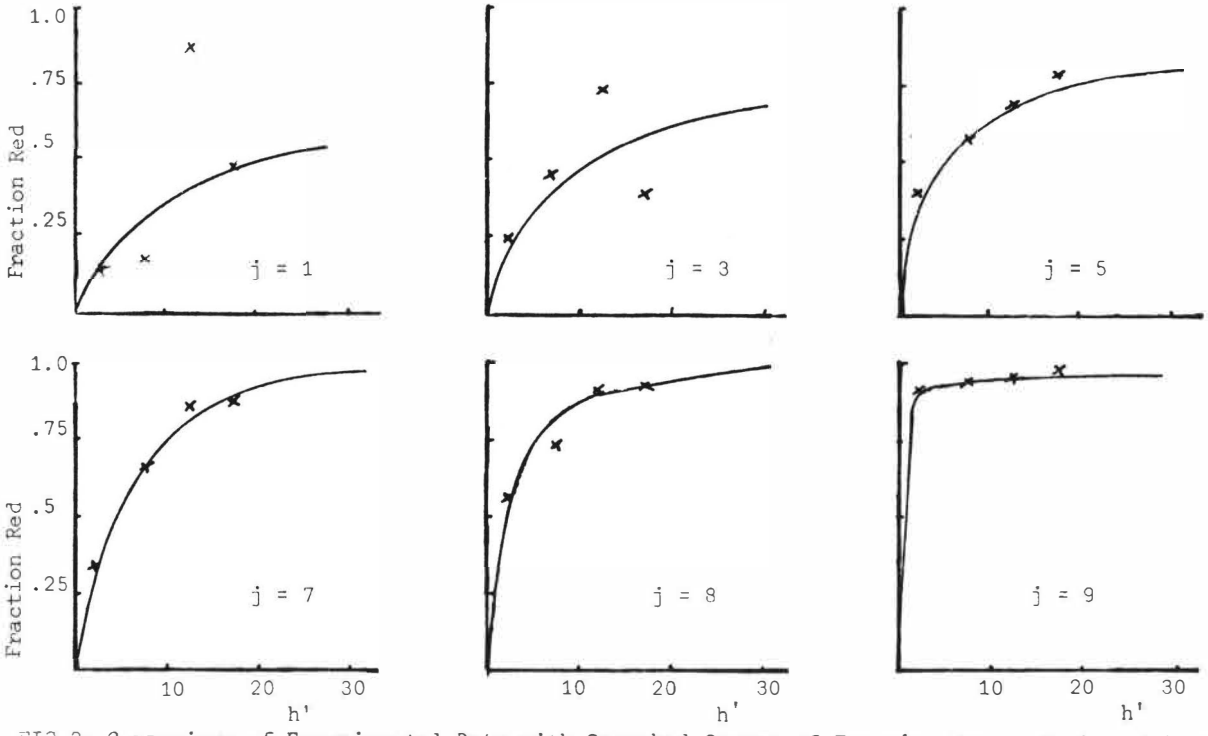

FIG 2: Comparison of Experimental Data with Smoothed Curves of Fraction Red vs Packed Height for Series 2 (h' = (h - 2.5) cm)

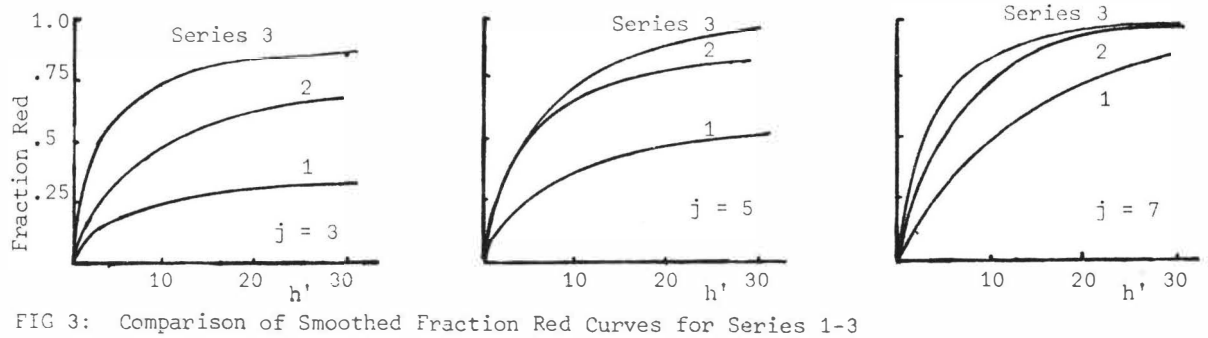

FIG 3: Comparison of Smoothed Fraction Red Curves for Series 1-3

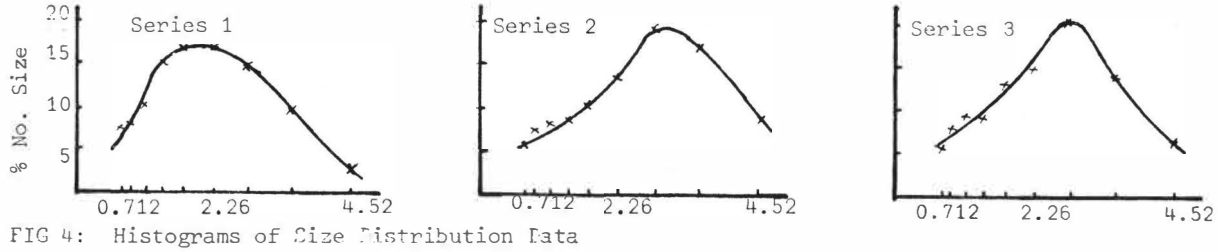

FIG 4: Histograms of Size Distribution Data

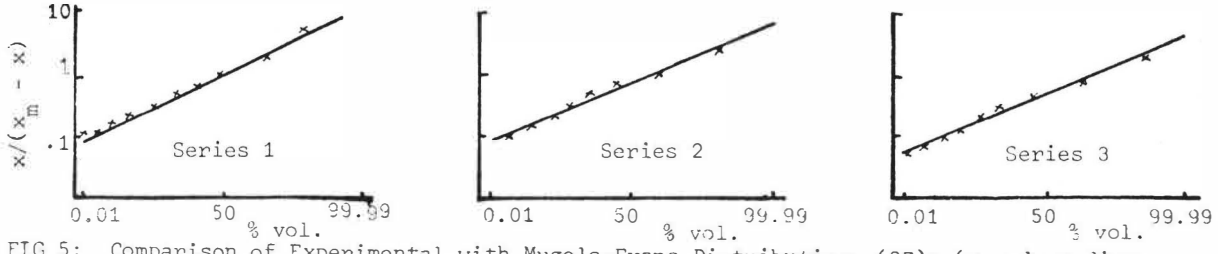

FIG 5: Comparison of Experimental with Mugele-Evans Distributions (27); (x = drop diam., x_m = max. drop diam.)

droplets within a given size range is decreased by coalescence to the size above and breakdown to size below, and increased by breakdown from above and coalescence from below. The effect of the flow rates can be accommodated in terms of holdup, while the rates for a given size j can be expressed in terms of a second order coalescence rate constant, k_j, and a first order breakdown constant K_j, with the driving force expressed as the number concentration of size j. Assuming n size ranges, two sets of n simultaneous equations result, one set defining the steady state population balance and the other the rate of formation of red droplets; these can be expressed as two n x n simultaneous matrix equations which can be solved for the rate constants. The development of such a model will form the subject of a further communication.

5.0 ACKNOWLEDGEMENT

Thanks are due to Dr. G. Winter (26) for advice on suitable reagents for our purpose.

REFERENCES

(1) Wijffels, J.-B. and K. Rietema, Trans. Inst. Chem. Eng. 50, 224, 233 (1972).

(2) Anderson, W.J. and H.R.C. Pratt, Chem. Eng. Sci. 33, 995 (1978).

(3) Sleicher, C.A., A.I.Ch.E. Jnl. 5, 145 (1959); 6, 529 (1960).

(4) Miyauchi, T., U.S. Atomic Energy Commission Rpt. U.C.R.L. 3911 (1957); T. Miyauchi and T. Vermeulen, I.E.C. Fundam. 2, 113 (1963).

(5) Vermeulen, T., J.S. Moon, A. Hennico and T. Miyauchi, Chem. Eng. Prog. 62, 95 (1966).

(6) Olney, R.B., A.I.Ch.E. Jnl. 10, 827 (1964).

(7) Rod, V., Brit. Chem. Eng. 11, 483 (1966).

(8) Charters, R.H. and W.J. Korchinsky, Trans. Inst. Chem. Eng. 53, 247 (1975).

(9) Rod, V. and T. Misek, Proc. Internat. Solv. Extn. Conf. 1971 (ISEC 71), Vol. 1, 738.

(10) Korchinsky, W.J. and S. Azimzadeh-Khatyloo, Chem. Eng. Sci. 31, 871 (1976).

(11) Jeffries, G.V. and G.A. Davies, "Recent Advances in Liquid-Liquid Extraction" (Ed. C. Hanson), Chap. 14, p. 495, (Pergamon Press, 1971).

(12) Derjaguin, B.V. and A.S. Titijerskaya, Disc. Farad. Soc. 18, 27 (1954).

(13) Marrucci, G., Chem. Eng. Sci. 24, 975 (1969).

(14) Madden, A.J. and G.L. Damerell, A.I.Ch.E. Jnl. 8, 233 (1962).

(15) Shiloh, K., S. Siderman and W. Resnick, Can. Jnl. Chem. Eng. 51, 542 (1973).

(16) Groothuis, H. and F.J. Zuiderweg, Chem. Eng. Sci. 19, 63 (1964).

(17) Verhoff, F.H., S.L. Ross and R.L. Curl, I.E.C. Fundam. 16, 371 (1977); 17, 101 (1978).

(18) Valentas, K.J., O. Bilous and N.R. Amundson, I.E.C. Fundam. 5, 271 (1966); K.J. Valentas and N.R. Amundson, *ibid*, 533.

(19) Bajpai, R.K., D. Ramakrishna and A. Prokop, Chem. Eng. Sci. 31, 913 (1976).

(20) Lewis, J.B., I. Jones and H.R.C. Pratt, Trans. Inst. Chem. Eng., 29, 126 (1951).

(21) Gayler, R. and H.R.C. Pratt, Trans. Inst. Chem. Eng. 31, 69 (1953).

(22) Ramshaw, C. and J.D. Thornton, I.Chem.E. Symposium Series No. 26, "Liquid-Liquid Extraction", p. 80 (1967).

(23) Komasawa, I., E. Kunugita and T. Otake, Kagaku Kogaku (Abridged Edn.) 4, 288 (1966); 5, 125 (1967); I. Komasawa, S. Hisatani, E. Kunugita and T. Otake, *ibid*, 4, 363 (1966).

(24) Gayler, R., N.W. Roberts and H.R.C. Pratt, Trans. Inst. Chem. Eng. 31, 57 (1953).

(25) Bierwirth, P. and B. McCurry, Final Year Project Rpt., Dept. of Chem. Eng., Univ. of Melbourne (1976).

(26) Winter, G., Private Communication (Univ. of Melbourne, Dept. of Chemistry), 1977.

(27) Mugele, R. and H.D. Evans, Ind. Eng. Chem. 53, 1317 (1951).

TECHNIQUES FOR DETERMINATION OF THE DISPERSED PHASE HOLD-UP IN PULSED COLUMNS USED IN A NUCLEAR FUEL REPROCESSING PLANT

Dr. Anthony F. Cermak
Allied-General Nuclear Services
Post Office Box 847
Barnwell, South Carolina 29812
United States

ABSTRACT

The knowledge of liquid phase hold-up in contactors is essential for determination of materials inventory in a nuclear fuel reprocessing plant. Equations have been developed expressing the dispersed phase hold-up in a pulsed column as a function of column dimensions and liquid density as measured by a weight recorder. Tests performed on a 5-cm diameter column with the binary system 30 v/o TBP - 0.1M HNO_3 verified the acceptability of this method, and have proven the significant effect of the pulse velocity, difference in linear phase velocities, and flow rate ratio on dispersed phase hold-up.

INTRODUCTION

A pulse column operates efficiently in the emulsion zone, sometimes called the dispersion zone, which starts roughly 40% below flooding and ends at flooding. The highest efficiency is just below the upper flooding curve. This is caused in part by the dispersed phase hold-up (X_d) which increases rapidly with an increase in the pulse velocity at a constant flow. Several authors (Ref. 1 to 4) tried to express hold-up changes in the emulsion zone in relation to different hydrodynamic variables. The effect of the total liquid linear velocity ($U_t = U_d + U_c$) on hold-up was very small in comparison with other variables, such as pulse frequency (f), pulse amplitude (A_o), and ratio of the dispersed phase to continuous phase velocity (U_d/U_c). However, all data in the above references, which apply to pulsed columns provided with simple sieve plates, did not correlate well with experimental data[5,6] obtained from columns with nozzle plates (used at AGNS).

DISPERSED PHASE HOLD-UP

Determination of the dispersed phase hold-up in contactors is essential for uranium and plutonium accountability (inventory) in the separation facilities of a nuclear fuel reprocessing plant, such as the Allied-General Nuclear Services plant at Barnwell, South Carolina. The AGNS contactors

are pulsed columns, except the centrifugal contactor used for uranium and plutonium coextraction in the first process cycle. The dispersed phase hold-up (X_d) in the column working section can be determined through hydrodynamic tests on pilot-scale, as well as on plant size pulsed columns by use of a calibrated weight recorder attached to the column. At AGNS, techniques have been developed to define the dispersed phase hold-up (X_d) in pulsed columns, i.e., to determine the effect of main operating parameters on the X_d value. The hold-up is given by the ratio of the dispersed phase volume in the column working section to the total volume of the column working section. The techniques can be described as follows:

(a) Single process columns: (Figures 1 and 2)

Taking into account data shown for the column in Figures 1(a) and 1(b) and the (columns) liquid density ρ^x determined by the calibrated weight recorder, the average dispersed phase hold-up in the column working section can be expressed as

$$X_d = \frac{H_o \cdot (\rho_c - \rho^x) - h_1(\rho_c - \rho_d)}{[h_3 + h_2 (D_c/D_S)^2] \cdot (\rho_c - \rho_d)} \qquad \text{.....(1)}$$

The equation which applies to the column in Figures 2(a) and 2(b), has the form

$$X_d = \frac{H_o(\rho_c - \rho^x)}{[h_3 + h_2 (D_c/D_S)^2] \cdot (\rho_c - \rho_d)} \qquad \text{.....(2)}$$

(b) Dual process columns: (Figure 3)

From data in Figures 3(a) and 3(b), the dispersed phase hold-up in the working section of the column part, ending with the disengaging section with interface control, can be calculated from the equation

$$X_d = \frac{H^* \cdot (\rho^x - \rho_c) - h_1(\rho_d - \rho_c)}{[h_3 + h_2 (D_c/D_S)^2] \cdot (\rho_d - \rho_c)} \qquad \text{.....(3)}$$

The X_d value in the other column part can be determined from the equation

$$X_d = \frac{H \cdot (\rho^x - \rho_c)}{h_4(\rho_d - \rho_c)} \qquad \text{.....(4)}$$

Densities ρ_c and ρ_d are mean values determined from density profiles along the column, e.g., measured on a pilot-scale unit.

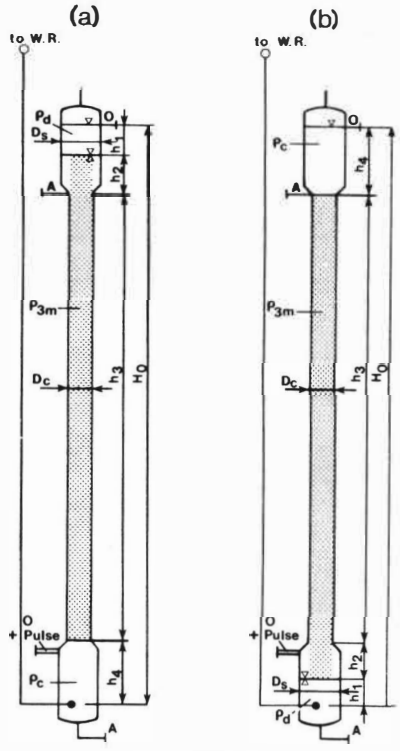

FIGURE 1
Single Process Columns
(a) Aqueous Continuous Process
(b) Organic Continuous Process

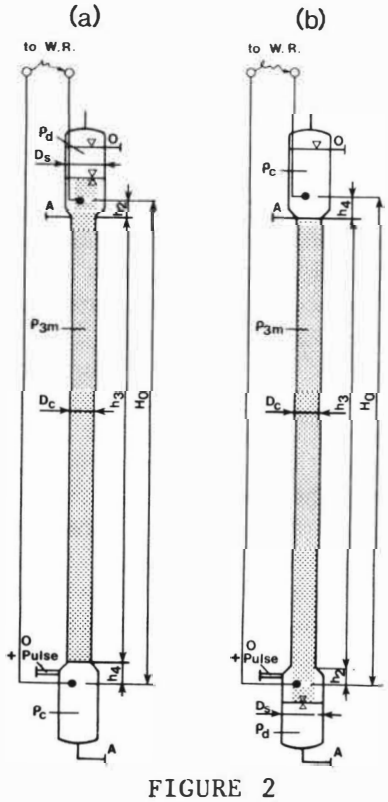

FIGURE 2
Single Process Columns
(a) Aqueous Continuous Process
(b) Organic Continuous Process

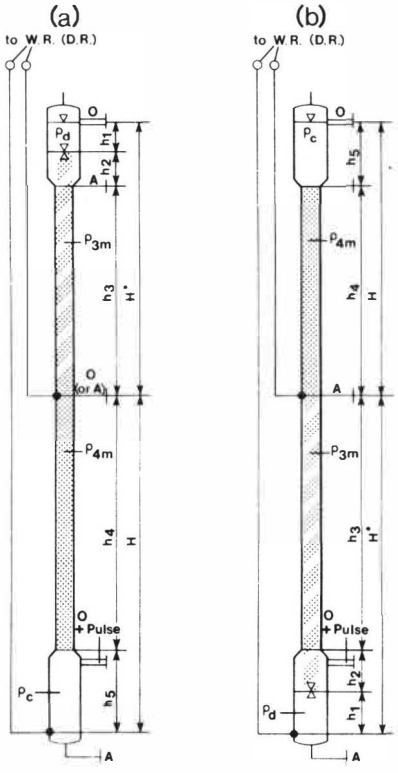

FIGURE 3
Dual Process Columns

(a) Aqueous Continuous Process
(b) Organic Continuous Process

EXPERIMENTAL

The AGNS techniques for determination of X_d in single process columns were tested and demonstrated on a 50 mm diameter glass pulsed column at the General Atomic Company Laboratories. The arrangement shown in Figures 1(a) and 2(b) was tested. The column, about 8.5 meters tall, was provided with stainless steel nozzle plates (23% free surface area) at a plate spacing of 50 mm. Nozzles, 4 mm in diameter, were turned upwards during tests with the aqueous phase continuous and turned downwards during tests with the organic phase continuous. A direct bellows type pulser with a continuous pulse frequency control was used for liquid pulsation. The column was equipped with a purge air interface control device and calibrated weight recorder for determination of the liquid density in the column (ρ^x). The liquid system consisted of 30% tributyl phosphate in normal paraffin diluent (organic phase) and 0.1 M nitric acid (aqueous phase).

Tests were performed at about fifty different (set) flow conditions, at room temperature and a constant pulse amplitude of A_o = 2.2 cm. The flow rate ratio was tested within a range of O/A = 0.1 to 10. For each set flow condition, the pulse frequency was increased stepwise from about f = 50 cycles per minute up to flooding.

Weight recorder data were evaluated and density (ρ^x) values were determined. Equations (1) and (2) were used for evaluation of the dispersed phase hold-up (X_d). Resultant data are shown in Figure 4. As

indicated in this figure, the dispersed phase hold-up is affected by both the flow ratio (O/A) and product of pulse frequency and pulse amplitude ($f \cdot A_o$). The effect of total liquid phase linear velocity U_t on X_d, at a flow ratio of O/A = 1, is negligible in comparison to the effect of both the above variables. At a given pulse velocity, $f \cdot A_o$, the higher (or the lower) was the flow rate ratio (O/A) value than one, the higher was the effect of the total liquid velocity U_t on the dispersed phase hold-up. This observation was made in all cases regardless of which phase was continuous.

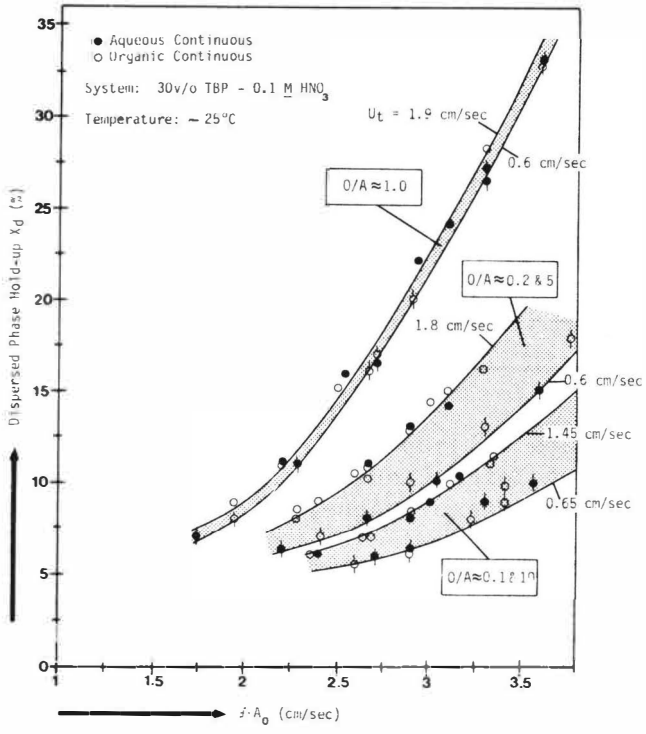

FIGURE 4
Dispersed Phase Hold-up (X_d) Versus Pulse Velocity ($f \cdot A_o$) at Different Total Liquid Velocities (U_t) and Flow Ratios (Organic/Aqueous) in the Columns

RESULTS

Experimental data were mathematically analyzed and correlated. By plotting X_d against $2fA_o + |\Delta U|$ values in Figure 5, curves were obtained at each tested flow rate ratio. The expression $2fA_o + |\Delta U|$ in this graph can be taken as twice the higher of two possible pulse velocities in the column. Theoretically, only at a flow ratio of O/A = 1, the pulse amplitude at upstroke equals the pulse amplitude at downstroke. At a ratio of O/A $\neq$ 1, the upstroke amplitude will be different from that at the downstroke. Consequently, the upstroke pulse velocity will be different than the downstroke pulse velocity.

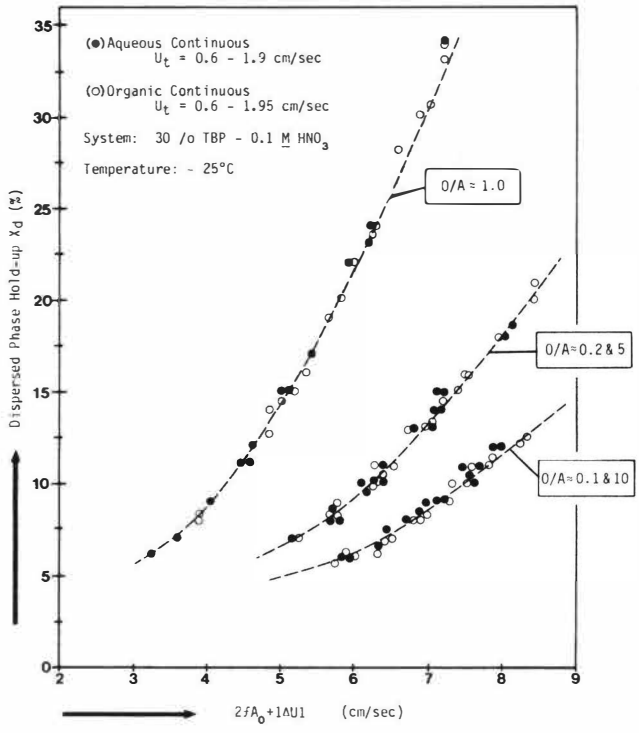

FIGURE 5
Dispersed Phase Hold-up (X_d) Versus $2fA_o + |\Delta U|$ Values at Different Total Liquid Velocities (U_t) and Flow Ratios (Organic/Aqueous) in the Columns

Based on all data, an empirical equation was derived defining the effect of tested variables during the experimental work, including the liquid linear velocities difference, on the dispersed phase hold-up. The equation has the form

$$X_d \approx 0.3(2fA_o + |\Delta U|)^{2.4} \cdot (U_d/U_c + U_c/U_d - 1)^{-0.6} \quad \ldots\ldots\ldots (5)$$

where

X_d = dispersed phase hold-up (%),

f = pulse frequency (1/sec),

A_o = pulse amplitude (cm),

U_d = dispersed phase linear velocity (cm/sec),

U_c = continuous phase linear velocity (cm/sec)

$|\Delta U| = |U_c - U_d|$; absolute value of the difference between the liquid linear velocities (cm/sec).

Figure 6 shows the relationship between the dispersed phase hold-up (X_d) and the function $(2fA_o + |\Delta U|)^{2.4} \cdot (U_d/U_c + U_c/U_d - 1)^{-0.6}$.

For each flow condition, tests were made at several pulse velocities up to flooding. The flooding curves determined for the liquid system 30 v/o TBP - 0.1 M HNO_3 (at room temperature) are shown in Figure 7. The curve corresponding to continuous organic phase operation lies approximately 25 to 35% above the curve for continuous aqueous phase operation. From equation 5 and flooding data, empirical equations were derived for evaluation of the dispersed phase hold-up at flooding. The equation for the aqueous phase continuous has the form:

$$(X_d)_{flood} \approx 0.926\ [5.5 - (U_t - 0.62|\Delta U|)]^{2.4} \cdot (U_d/U_c + U_c/U_d - 1)^{-0.6} \qquad .....(6)$$

For operation with the organic phase continuous, the hold-up at flooding can be evaluated from the equation:

$$(X_d)_{flood} \approx 0.649[6.8 - (U_t - 0.72|\Delta U|)]^{2.4} \cdot (U_d/U_c + U_c/U_d - 1)^{-0.6} \qquad .....(7)$$

Equations 6 and 7 are expressed graphically in Figures 8 and 9, respectively. The equations apply to the system tested at room temperature and within the experimental range.

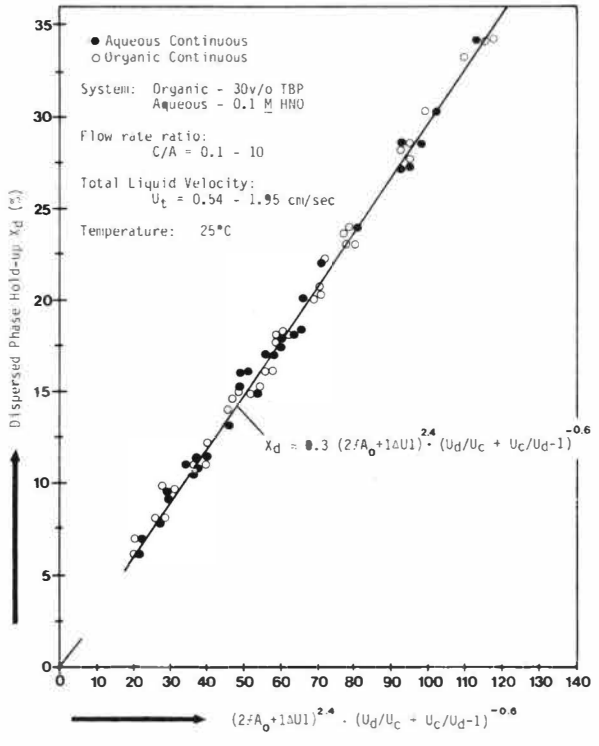

FIGURE 6
Dispersed Phase Hold-up (X_d) Versus Functions
$(2fA_o + |\Delta U|)^{2.4} \cdot (U_d/U_c + U_c/U_d - 1)^{-0.6}$

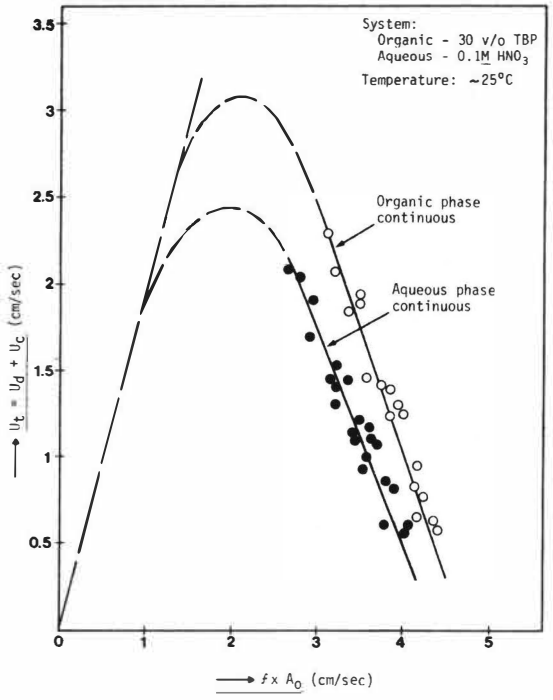

FIGURE 7
Pulsed Column Flooding Curves

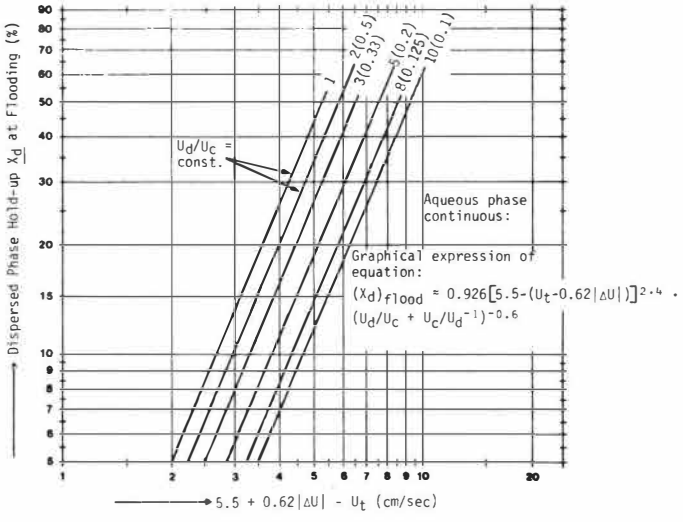

FIGURE 8
Dispersed Phase Hold-up (X_d) at Flooding Versus Liquid Velocity Function (5.5 + 0.62|ΔU| - U_t) at Different Flow Ratios (U_d/U_c)

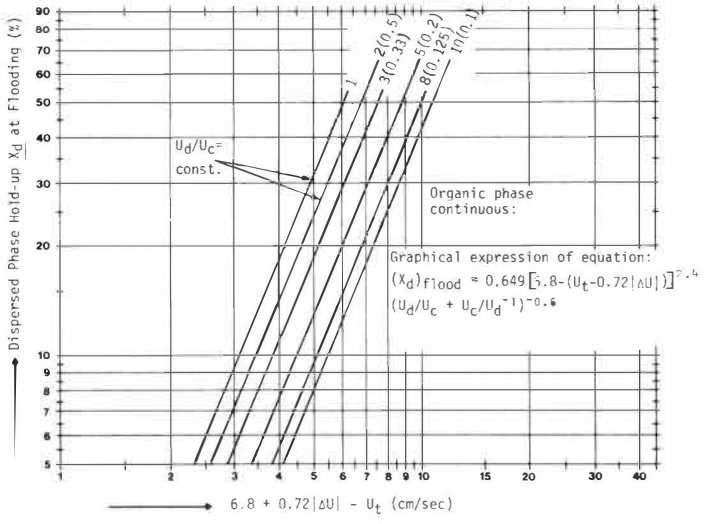

FIGURE 9
Dispersed Phase Hold-up (X_d) at Flooding Versus Liquid Velocity Function (6.8 + 0.72|ΔU| - U_t) at Different Flow Ratios (U_d/U_c)

DISCUSSION

In a nuclear fuel reprocessing plant, a reliable inventory of plutonium and other fissile materials is required. Accountability of solutes (U, Pu, HNO_3) in pulsed columns used in a reprocessing plant can be made readily by use of the described techniques. At different plate geometries and arrangements, different liquid systems and process temperatures, different dispersed phase hold-up values are expected than predicted by equation 5; however, techniques for X_d determination will be always the same. Accountability of the solute in question is performed by (a) determining column liquid density ρ^x from weight recorder data, (b) calculating X_d from equations (1) - (4), and (c) determining the concentration and density profile along the column either experimentally on a pilot-scale column, or analytically using a suitable computer program. From concentration profile data and the X_d value the solute inventory in the column can be determined.

REFERENCES

1. Cermak, A. F., and Spaunburgh, R. G., "Development of Columns for Continuous Process (U Reduction)," Allied Chemical report (1972) (unpublished).

2. Sato, T., et al, Kagaku Kogaku, 27, 583 (1963).

3. Eguchi, W., et al, Kagaku Kogaku, 23, 146 (1959).

4. Misek, T., Col. Cz. Chem. Comm., 29, 1755 (1964).

5. Cermak, A. F., "Two-Inch Diameter Pulsed Column Hydraulic Tests," AGNS report (1974) (unpublished).

6. Cermak, A. F., "Two-Inch Diameter Pulsed Column Dispersed Phase Hold-up Tests," AGNS report (1975) (unpublished).

MICROEMULSION FORMATION IN THE ORGANIC PHASE OF SOME IMPORTANT EXTRACTANTS AND ITS EFFECTS ON THE EXTRACTION MECHANISM

Wu Chin-kwang, Kao Hung-cheng, Chen Tien, Li Seng-chung, King Tien-chu and Hsu Kwang-hsien
Dept. of Chemistry, Peking University Peking, People's Republic of China

ABSTRACT: Through the investigation of several typical extractant systems commonly used in hydrometallurgy and nuclear industry, we have suggested and proved that the saponification of extractants such as naphthenic acid, D2EHPA, ect., is a process of the formation of a microemulsion of water in oil type, and the extraction of rare earths or divalent metal ions by the saponified extractant is a process of the destruction of the w/o emulsion, thus emphasizing the importance of the role of water in the extraction process and providing a new approach to the study of extraction mechanisms.

Introduction

During the last three decades, solvent extraction of inorganic compounds has become an extensively investigated field, from both theoretical and practical points of view. But the importance of the role of water in the extraction process has not been much studied and many phenomena observed remain unexplained. For example, in the course of investigation of naphthenic acid-sec. octyl alcohol-kerosine system as an extractant for the separation of very pure yttrium from other rare earths, we have found when aqueous NH_4OH solution was added to the extractant, the volume of the organic phase could increase up to 50% and yet remained clear and transparent in appearance. After the extraction of a rare earth, the water contained in the organic phase will return back to the aqueous phase causing a big change in phase volumes.

In order to explain the above-mentioned phenomena, we have investigated the naphthenic acid and other acid extractants in detail and found that the saponification is a process of the formation of a w/o microemulsion, and the extraction of a rare earth or divalent metal ion is a process of destruction of the microemulsion.

Experimental

1. Instruments

(1) Unicam SP100 IR Spectrometer, 670-8850 cm^{-1}, wave numbers were calibrated with a polystyrene thin film and CH_3Cl.

(2) DDS-11A Type Conductometer, made by the Second Analytical Instruments, Inc., Shanghai.

(3) JANETZKI VAC-60 Type Ultracentrifuge, max. speed 60000 r.p.m.

2. Reagents

Naphthenic acid was bought from Shanghai Tung-Feng Chemical Works, treated with urea to remove the straight chain hydrocarbons and then redistilled to collect the fraction from 150 °C to 210 °C under a reduced presure of 3-5 mm Hg. The average molecular weight was determined to be 254.2. Secondary octyl alcohol (BDH) and D2EHPA (Peking Chemical Works) were used as such. Kerosine was treated by conc. H_2SO_4 and redistilled. Other chemicals used were reagents of A.R. grade.

Results and Discussions

I. The Naphthenic Acid (22%)-Sec. Octyl Alcohol (18%) Kerosine (60%)-System

1. Conductance Measurements

10 ml of the naphthenic acid extratant (0.81 M) was titrated with 10.7 N NH_4OH and the conductance was measured during the titration as shown in Fig.1. The regions of turbid and clear transparent solutions were also shown in the figure.

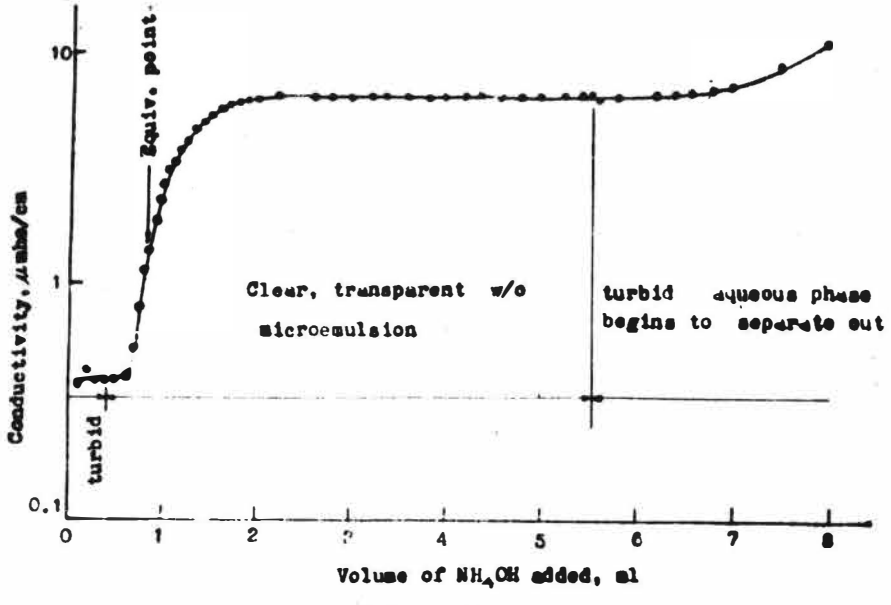

Fig. 1

Change of conductivity during the titration of 10 ml naphthenic acid with NH_4OH

2. Extraction equilibria between the naphthenic acid extractant and aqueous alkali hydroxide solution.

10 ml of aqueous alkali hydroxide solutions (KOH, NaOH, LiOH or NH_4OH) of different initial concentrations were added to 10 ml naphthenic acid extractant in a calibrated and stoppered tube agitated in a thermostat for 20 minutes. The % increase of organic phase volumes (as shown in Fig. 2), the alkali concentrations of both phases, the conductance and the water content (as measured by the near IR method using 1.4$\mu$and 1.9μ overtones) and the IR spectra of the organic phase were determined.

The presence of free water in tne organic phase was clearly seen from the 1650 cm^{-1}peak, which is the bending frequency of H_2O molecule. When heavy D_2O was used to dissolve the alkali hydroxide in place of H_2O, the 1650 cm^{-1}peak disappeared and 1200$cm^{-1}$and 2490 cm^{-1}peak of D_2O were observed as shown in Fig. 3.

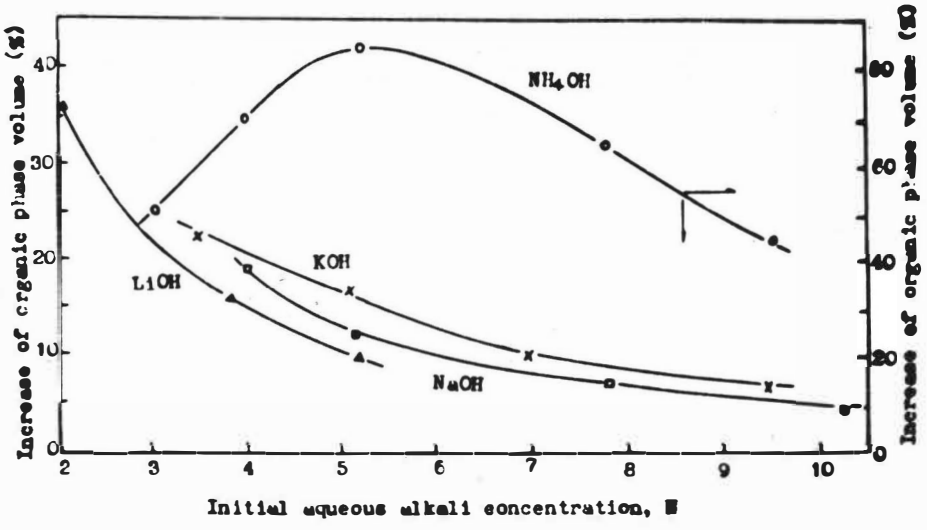

Fig. 2
Effect of initial alkali conc. on the increase of organic phase volume after equliibrium

3. The Structure of the Saponified Extractant

According to the above-mentioned experiments, the water contents in the organic phase in equilibrium with the concentrated alkali hydroxide solutions may be as high as 20% (in case of KOH, NaOH and LiOH) or 50% (NH_4OH), and yet remained very clear and transparent in appearance. This apparently clear and transparent "solution" could not be a true molecular solution of water in the organic sovlvent because the solubility of water in the organic solvent is usually small and could not reach as high as 20% or 50%. The light scattering phenomenon observed showed that it is a dispersed system of water in oil type. Xylenol orange is a water soluble indicator , insoluble in the unsaponified naphthenic acid, but very soluble after saponification with NH_4OH or NaOH, showing a brilliant rosy color. This

may be reasonable explained that xylenol is solubly in the small water drops dispersed in the continuous organic phase.

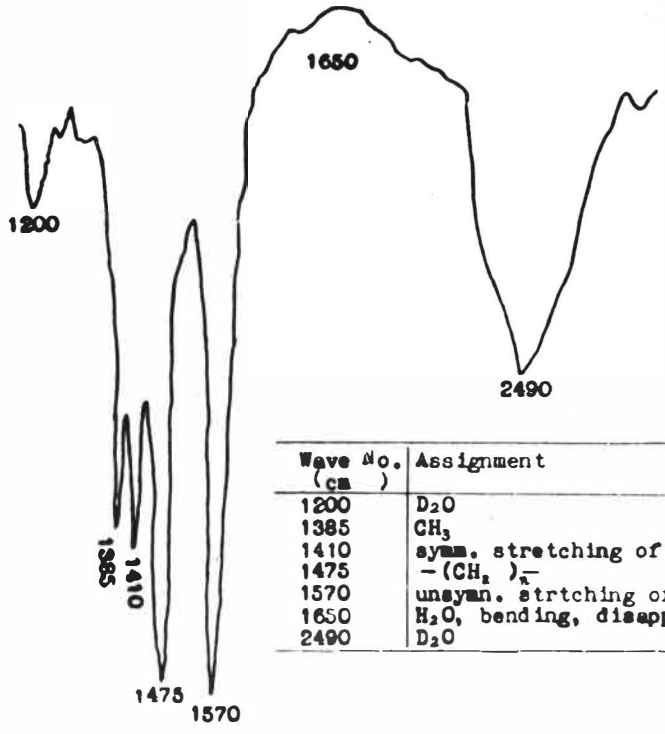

Wave No. (cm^{-1})	Assignment
1200	D_2O
1385	CH_3
1410	asym. stretching of COO^-
1475	$-(CH_2)_n-$
1570	unasym. strtching of COO^-
1650	H_2O, bending, disappeard
2490	D_2O

Fig.3
IR spectra of the org. phase. of the extraction system Naphthenic acid-ROH-Kerosine-NaOH (5N) D_2O

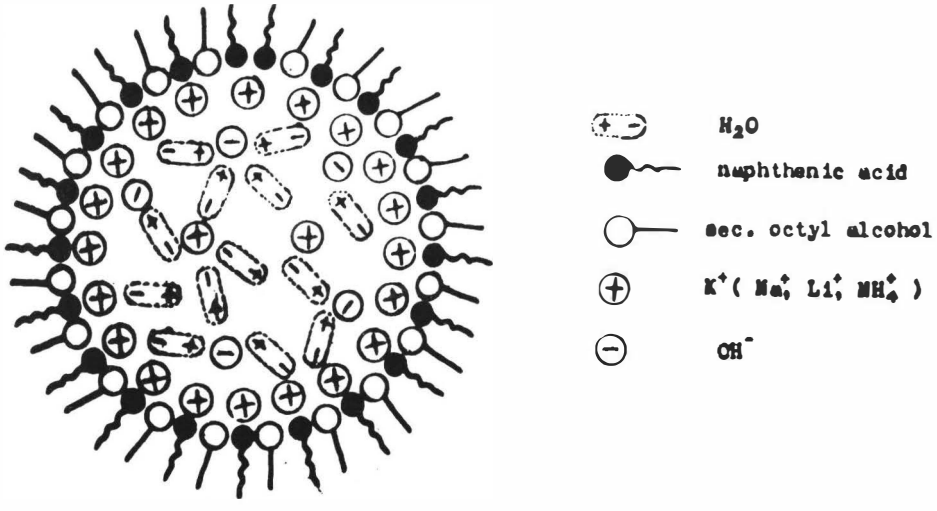

Fig.4
Model of a dispersed aqueous droplet in the microemulsion of the saponified naphthenic acid extractant

On the other hand,,the saponified extractant "solution" could not be an ordinary liquid-liquid dispersion system or emulsion in the usual sense. Because, firstly, the usual macro-emulsion is turbid instead of being transparent. Secondly, we could not observe the dyed droplets when xylenol was added to

the saponified extractant and viewed with a microscope of high magnifying power (1600x). The resolving power of the microscope is about 2000Å-3000Å, so that the size of the droplets should be less than 2000Å. Thirdly, the saponified extractant "solution" was supercentrifuged (42000 r.p.m. corresponding to 140000 G) for 5 minutes at 0 °C, and no separation of any aqueous phase was observed. This shows that the "solution" is not an ordinary macro dispersion system, but is a very stable "microemulsion".

Recently, microemulsion formation was reported[1-3] in the long-chain fatty acid salt-long chain alcohol-saturated hydrocarbon-water-electrolyte system under suitable conditions, where the size of the dispersed water droplets is less than a quarter of the average wave length of the visible light (5600Å), so that the light would not be reflected and the microemulsion looks transparent. When our saponified extractant is compared with the reported microemulsion system in Table 1 the similarity is obvious.

Table 1 Comparision of the Saponified Naphthenic Acid Extractant with a Typical Microemulsion System

Composition of the Extractant	Composition of the Typical Microemulsion System
1. Naphthenic acid NH_4OH (or KOH, NaOH, LiOH)	1. Potassium Salt of oleic acid
2. Secondary octyl alcohol	2. normal hexyl alcohol
3. Kerosine	3. normal hexane
4. the aqueous solution	4. water

In Table 1 we see that four ingredients are indispensable in order to form such a microemulsion, namely, water (the aqueous solution), oil (kerosine), an ionic surfactant (the alkaline soap of naphthenic acid) and a long-chain alcohol acting as a co-surfactant. In the unsaponified naphthenic acid , there is no ionic surfactant so that microemulsion cannot be formed. The long-chain alcohol is also an indispensable ingredient. If we use iso-propyl alcohol instead of sec-octyl alcohol, microemulsion could not be formed during the saponification of the naphthenic acid extractant. The excess alkaline solution exists in the micro droplets dispersed in the organic phase.

Fig. 4 is a sketch of the suggested structure of the micro droplet, where the naphthenate ions and the long-chain alcohol molecules are arranged on the surface of the micro droplet with their long-chain hydrocarbon tails pointing into the continuous organic phase. The counter cations NH_4^+ (or K^+, Na^+, Li^+) are arranged on the inner surface to balance the negative charge of naphthenate anions. Within the surface of the droplet there is the aqueous phase containing excess NH_4OH (or KOH, NaOH, LiOH).

4. Mechanism of Extraction of Rare Earth by Naphthenic Acid

Mikhlin[4] studied the mechanism of extraction of Nd^{+++} by naphthenic acid and concluded that the extraction reactions

may be expressed by

$$Nd^{+++} + 3\ H_2A_2 + nH_2O = NdA_3 \cdot 3HA \cdot nH_2O \quad (1)$$

$$2\ NdA_3 \cdot 3HA \cdot nH_2O = (NdA_3 \cdot 3HA \cdot nH_2O)_2 \quad (2)$$

Korpusov[5] studied the extraction of La^{+++} by naphthenic acid with formation of $(LaA \cdot 3HA \cdot nH_2O)_2$. They determined the molar ratio of the rare earth ion (M^{+++}) to the naphthenate anion (A^-) to be 1:6 in the extracted species from the slope of the plot of $pH_{1/2}$ vs. log (H_2A_2). But we found the extracted species by analyzing the composition of the saturated organic phase to be $MA_3 \cdot nH_2O$ where n=1 for Pr^{+++}, Ho^{+++}, Eu^{+++}, Tb^{+++} and n=0 for La^{+++}, Ce^{+++}, Nd^{+++}, Sm^{+++}, Gd^{+++}, Dy^{+++}, Er^{+++}, Tm^{+++}, Yb^{+++}, Lu^{+++} and Y^{+++}. The reason for these discrepancies will be discussed below.

Mikhlin and Korpusov assumed that the naphthenic acid existed as dimers H_2A_2, and the extraction was assumed to be

$$M^{n+}_{(aq)} + \frac{m}{2} H_2A_{2(o)} = MA \cdot (m-n)HA_{(o)} + nH^+_{(aq)} \quad (3)$$

$$K = \frac{[MA_n(m-n)HA]_o [H^+]^n}{[M^{n+}][H_2A_2]^{m/2}} = D[H^+]^n / [H_2A_2]^{m/2} \quad (4)$$

$$\log D = \log K + (m/2)\log[H_2A_2]_o + n\,pH \quad (5)$$

$$\left[\frac{\partial \log D}{\partial\, pH}\right]_{(H_2A_2)_o} = n\ , \qquad A = \frac{d\ pH_{1/2}}{d\ \log[H_2A_2]_o} = -\frac{m}{2n} \quad (6)$$

where $pH_{1/2}$ is the pH value at D=1. They found the slopes by experiments to be n=3, A=-1=-m/2n thus obtaining m=6.

Although the naphthenic acid in inert solvent does exist in dimer form H_2A_2, it will partially convert to a monomer complex HA·ROH upon the addition of octyl alcohol. After saponification, the 1728 cm^{-1} peak characteristic of the dimer disappears completely therefore we assume

$$M^{n+}_{(aq)} + m\ HA_{(o)} = MA_n(m-n)HA_{(o)} + nH^+_{(aq)} \quad (7)$$

instead of (3). From (8) we obtain

$$A = \frac{d\ pH_{1/2}}{d\ \log[HA]_o} = \frac{d\ pH_{1/2}}{d\ \log 2[H_2A_2]_o} = \frac{m}{n} \quad (8)$$

If we use the same experimental data as Mikhlin's, i.e. n=3, A=-1, we would obtain m=3, consistent with our results.

Therefore the determination of m from the experimental slope A is unreliable. In fact, the extraction mechanism is far more complex. It involves an ion exchange in the water/oil interface of the microemulsion:

$$3\ NH_4^+A^-_{(o)} + M^{+++}_{(aq)} = MA_{3(o)} + 3\ NH_4^+{}_{(aq)} \quad (9)$$

From the IR spectra of the organic phase after extraction of rare earth, we found the 1410 cm^{-1} peak characteristic of the symmetrical stretching frequency of $RCOO^-$ almost disappears. It means. that ionic naphthenate $RCOO^-NH_4^+$ has been converted to the rare earth chelate causing the destruction of the microemulsion and forcing the water in the micro droplets back to the aqueous phase, as may be seen from the disappearance of the 1650 cm^{-1} (H_2O bending frequency) in the IR spectra of the organic phase.

5. Extraction of Some Divalent Metal Ions

(1) The extracted species for Ni^{++}, Zn^{++} and Cu^{++} were found to be MA_2 containing less water than the detection limit by the near IR method (<0.02%).

For Mn^{++}, Cd^{++}, Pb^{++} the extracted species roughly correspond to $MA_2 \cdot H_2O$.

(2) Under the condition of saturation of extraction of Ca^{++} or Mg^{++} the organic phase contains about 1% H_2O and this dispersed system is very sensitive to temperature. Water will begin to separate out and organic phase becomes turbid when the temperature is raised above 30 °C. When the temperature is lowered, the organic phase becomes clear again so that the process is reversible.

II. The D2EHPA (1M)-Sec. Octyl Alcohol or TBP(15%) -Kerosine System

Acidic organophosphorus compounds such as D2EHPA form one of the most important types of organic extractants. The unsaponified acids usually exist in dimer form, (H_2A_2), in most organic diluents. They extract metals by a cation exchange reaction as follows :

$$M^{n+} + n\ H_2A_2 = M(HA_2)_n + n\ H^+ \qquad (10)$$

The hydrogen ion liberated during the reaction will prohibit further extraction of metals. In order to increase the loading capacity, we have saponified both acidic hydrogens of the dimer (H_2A_2) with NH_4OH or NaOH and have succeeded to extract some divalent metals with this 100% saponified extractant to form extracted species of the composition MA_2 instead of $M(HA_2)_2$, without formation of any gelatinous matter in the organic phase, thus doubling the loading capacity of the extractant. We found also that the saponification is a complicated process accompained with the formation of microemulsion as in the naphthenic acid extractant.

1. Microemulsion formation during the saponification

The evidences of formation of microemulsion may be summarized as follows : (1) Strong Tyndall effect was observed in the saponified D2EHPA so it is a dispersion system with particle size > 100 Å (2) The dispersed water droplets could not be observed in a microscope whose resolving power is about 2000 Å (3) The saponified D2EHPA was supercentrifuged

at 140000 G for 5 minutes at 0 °C, and no separation of any aqueous phase was observed. (4) Here the ionic surfactant forming the microemulsion is the alkali or ammonium salt of D2EHPA, while the long chain alcohol or TBP serves as cosurfactant.

In Fig. 5 the phase volume change were plotted against the equivalent of alkali added per equivalent D2EHPA. Regions of microemulsion and ordinary emulsion were also indicated in the figure. For example, in the case of titration with 7.5 N NaOH, the organic phase was turbid before 60% neutralization. From 60% to 100% neutralization, a very clear microemulsion was obtained. After that, turbid aqueous phase began to separate out, while the organic phase remained clear and transparent.

In Fig. 6 the changes of conductivity and viscosoty were plotted against the equivalents of NaOH added per equivalent of D2EHPA. It may be seen that both the conductivity and the viscosity increase with the water content in the microemulsion, reaching maximum at the equivalence point. After equivalence point, turbid aqueous phase begins to separate out, the water content of the organic phase decrease (see Fig. 5) and the conductivity and viscosity decrease also (see Fig. 6).

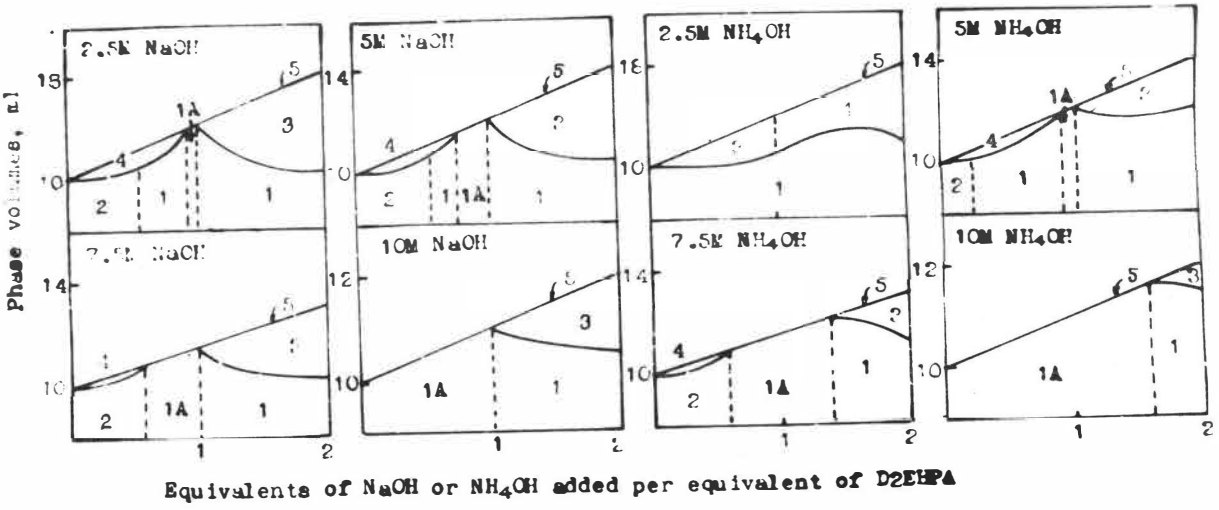

Fig. 5

Microemulsion formation during the saponification of 10 ml. of 1 M D2EHPA-sec. octyl alcohol (18%)-kerosine with NaOH or NH_4OH of different concentrations at 18 °C

Key to numbers in figures

1. Organic phase : w/o microemulsion clear and transparent
1A. Single organic phase : w/o microemulsion clear and transparent
2. Organic phase : ordinary w/o emulsion turbid
3. Aqueous phase : o/w emulsion turbid
4. Aqueous phase : NaOH or NH_4OH solution clear
5. Total volume of organic and aqueous phase

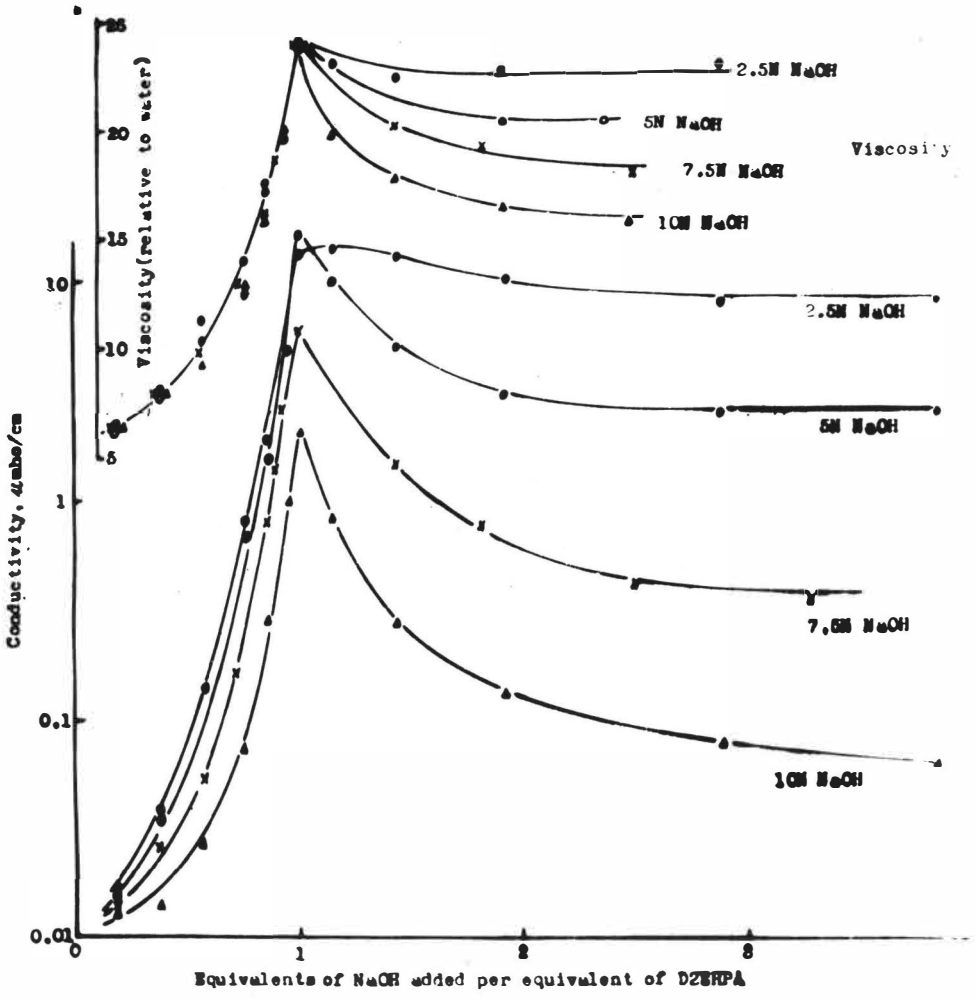

Fig. 6
Change of viscosity and conductivity of the organic phase during the titration of 1M D2EHPA-sec. octyl alcohol (18%)-kerosine with NaoH of different concentrations at 18°C

2. Extraction of metal ions

The microemulsion of the saponified D2EHPA is a good extractant for most cations. Usually the extraction is accompanied with the formation of a metal chelate, thus destroying the microemulsion due to the absence of ionic surfactant and forcing the water back to the aqueous phase, leaving very little, if any water in the organic phase (less than the limit of detection by the IR method, namely ⟨o.o2%).

III. Quarternary Ammonium Nitrate-Octyl Alcohol-Kerosine System

A quarternary ammonium nitrate (such as Aliquot 336)-octyl alcohol-kerosine system can take up a few% of water when in equilibrium with aqueous salt solution and form a

microemulsion. The amount of water taken-up by the organic phase decreases as the concentration of the salt (e.g. NH_4NO_3) in the aqueous phase increases. The extraction of rare earth ions is also accompanied by the destruction of the microemulsion in the organic phase.

Further investigation on the physico-chemical properties accompanying the formation and destruction of microemulsion and their effects on the mechanism of extraction will be reported later.

REFERENCE

(1). S. Friberg and I. Burasczensk, Progress in Colloid and Polymer Science, 63, 1 (1978).
(2). K.L. Mittal, Micellization, Solubilization and Microemulsions (plenum press), (1977).
(3). D.O. Shak and R.M. Hamlin Jr., Science, 171,483 (1971).
(4). E.V. Mikhlin, Zh. Neog. Khim.,17(2)492(1972).
(5). G.V. Korpusov, Radiokhimiya, 17,356(1975).

STUDIES OF THE STABILITY OF HAZE GENERATED IN THE AQUEOUS PHASE ON CONTACT WITH HYDROXYOXIMES

M.A. HUGHES and P.D. MIDDLEBROOK*

Schools of Chemical Engineering,
University of Bradford,
Bradford, U.K.

& *N.C.C.M., R & D, Kitwe, Zambia.

ABSTRACT

Factors affecting the stability of haze are discussed. Practical work is described where haze is in the systems LIX 65N/toluene, ESCAID 100, and LIX 64N/ESCAID 100 contacted with acidic aqueous phases containing metal ions. The droplet size is in the region 1 to 20 μm. It is the diluent which dictates haze stability. The haze is least stable in low ionic strengths and at pH 3 to 6. Acid increases the stability. Stokesien creaming accounts for rate of haze removal of droplets $d > 2$ μm, drops with $d < 1$ μm coarsen by diffusion.

1. INTRODUCTION

The loss of expensive extractant is of special economic importance in the case of commercial plant operating liquid-liquid extraction processes for the recovery of copper from acid leach liquor by hydroxyoximes. Losses as low as 4-15 ppm have been quoted (1). Operating plant may run in steady state at ca 30 ppm (2) or go as high as 200-300 ppm. At start-up, or when solids break through, the losses may be ca 1000 ppm. Other workers (3,4) have considered the mechanisms of solvent loss.

Impingements of a drop at an interface yield secondary small drops (5) and in the case of LIX reagents for copper extraction this process has been filmed; in this way small drops can be formed in the settler. Other workers (6) consider that small drops are mainly formed in the mixer compartment through shearing processes and these drops are carried through the settler with consequential solvent loss. It is these drops which are the main cause of haze conditions accompanying the commercial operation of mixer-settlers.

Systems involving true surfactant type extractants are particularly prone to severe haze production, examples being when 1) tertiary amines are used to extract tungsten, and 2) Na-D2EHPA is used to extract cobalt and nickel. LIX type reagents are not true surfactants at low pH.

The haze which we have measured with hydroxyoximes in the absence of copper is in the size range 1 to 20 μm diameter. It is this range which is of importance in the following calculations.

2. POSSIBLE REASONS FOR INSTABILITY

One would expect that those factors which affect the rate of creaming of oil in water emulsions would also influence the stability of oil in water dispersions, e.g. haze. But hold-up in emulsions might typically be 40 oil: 60 water, whereas haze exists at say 200 ppm organic or approximately 0.02 oil: 99.98 water.

The haze exhibits a thermodynamic instability, there is a tendency towards minimum free energy through loss of interfacial area; the process is one of creaming followed by coalescence or just coalescence alone. The reason for any observed stability is a kinetic one dependent upon either collision processes or diffusion of material from small droplets to larger ones, both leading to loss of interfacial area.

Collision kinetics can be dependent upon one, or combinations of, the following:

(a) direct impingement of the growing drops;
(b) impingement resulting from Stokes migration whereby the droplet velocity is a function of its radius;
(c) impingement resulting from Brownian motion;
(d) impingement resulting from velocity gradients within the host-fluid flow field, and
(e) impingement resulting from temperature gradient induced variation of interfacial area (the Marangoni effect).

Effect (e) is absent in the experimental study reported here because equilibrium is established before haze is generated. Effect (a) is probably negligible. Of course, a collision, having taken place, must be "effective". Films at the interface may then prevent, or aid, coalescence.

DROP RIPENING BY DIFFUSION

Small droplets of an organic phase in an aqueous continuum are more soluble than large droplets of the same phase (7). Solvent diffuses from small to large droplets. The following equations apply (8) for the rate of coarsening by diffusion when two different size droplets A and B are present.

$$\frac{dr_A}{dt} = \frac{D\, c_\infty\, K}{\rho\, r_A^2} \left[\frac{n_B (r_B - r_A)}{n_A\, r_A - n_B\, r_B} \right] \qquad (1)$$

$$\frac{dr_B}{dt} = \frac{D\, c_\infty\, K}{\rho\, r_B^2} \left[\frac{n_A (r_B - r_A)}{n_A\, r_A + n_B\, r_B} \right] \qquad (2)$$

where r_A, r_B are the radii of particles and n_A, n_B are number concentrations, D is the molecular diffusion coefficient of the droplet phase in the host fluid, c_∞ is the solubility of an infinitely large drop. K is given by $K = 2\, \gamma_i\, M/\rho\, R\, T$, where γ_i is the interfacial tension, M is the molecular

weight of the drop phase and ρ is the density of the drop phase.

Now in an equal number mixture of two different size droplets of radii 0.5 and 1.0 μm with a solubility of 3×10^{-8} kg dm^{-3} (0.03 ppm), γ_i = 0.1 mNm^{-1}, then integration of Equations (1) and (2) shows that there will be only a 10% change in the radius of small drops in one year, but with radii 0.05 and 0.10 μm the corresponding change is 1000 times faster. The stability is seen to be dependent on the cube of the radius.

Since: $$c_\infty = (\rho^2 t' R T)/(2 D t \gamma_i M) \quad (3)$$

where Higuchi and Misra (8) define t' as:

$$t' = (D c_\infty K T)/\rho \quad (4)$$

Then using $t' = 4 \times 10^{-14}$ secs (± 10% change in size (7)), ρ = 1, γ_i = 16 mNm^{-1} (8), (the latter being typical of hydroxyoximes in aliphatic hydrocarbons in the absence of copper and at pH 2) and $D = 5 \times 10^{-6}$ cm^2 sec^{-1}, then $c_\infty = 7.2 \times 10^{-6}$ kg dm^{-3} or 7.2 ppm. This is an upper limit but suggests that solvent droplets of solubility about 10 ppm and of < ca 1-0.5 μm radii grow markedly through a diffusion mechanism. The solubility of most LIX type reagents is rather lower than this (9), e.g. $1 - 5 \times 10^{-6}$ kg dm^{-3}. Of more importance is the solubility of the kerosene type components; hexane at 9.4×10^{-3} kg dm^{-3}, dodecane at 8.0×10^{-6} kg dm^{-3} and toluene at 5.4×10^{-1} kg dm^{-3} are examples (10). Thus according to the diffusion theory, all other things being equal, then the most soluble diluents (or extractants) should give the most unstable haze if this mechanism is operating. Reduction in viscosity of the host phase, increase in temperature and interfacial tension aids clearance of haze through droplet diffusion processes. If surfactants are present they generally reduce γ_i so increasing haze stability, they may, however, also increase the solubility of the droplet which then offsets the effect of reduced γ_i.

STOKESIAN CREAMING

The droplets may obey a Stokes law for creaming velocity which can only be applied to droplets below a certain size where, d_{st} is the upper critical diameter and:

$$d_{st} = (3.6\eta^2)/((\rho_d - \rho_h)\rho_h g) \quad (5), \quad u_{st} = ((\rho_d - \rho_h) g d^2)/(18\eta) \quad (6)$$

in which η = absolute viscosity (0.001 Nsm^{-2}), ρ_d is density of the dispersed phase taken as 900 kg m^{-3}, ρ_h is density of host phase taken as 1000 kg m^{-3}, and g is 9.81 m s^{-2}, whence d_{st} = 156 μm. The droplets we have observed in haze are well below this diameter mostly in the region d < 50 μm. The Stokesian velocity, u_{st}, is given by Equation (6) and can be used without corrections for discontinuity of the fluid.

INFLUENCE OF BROWNIAN MOTION

Brownian motion will hinder creaming through gravitational flow if the droplets are small enough. The size of the random motion imparted to the droplets can be calculated (11) from:

$$\bar{x}^2 = (4 R T t)/(3 \pi^2 \eta N d) \quad (7)$$

where $\bar{x}$ is the statistical average displacement in a given direction in time t, R is the gas constant, N is Avogadro's number. It can be seen, Table 1, that Brownian motion markedly affects the smallest droplets, e.g. d < 1.0 μm. However, these are also the droplets which grow rapidly through diffusion processes.

TABLE 1

Droplet Diameter μm	Displacement in 1.0 Second (μm) at 300K	
	Via Gravitation (Eq. 6)	Via Brownian Movement (Eq. 7)
0.01	5.45×10^{-6}	7.47
0.1	5.45×10^{-4}	2.36
1	5.45×10^{-2}	0.74
10	5.45	0.24
20	21.8	0.167

The coalescence effect via Brownian motion can be calculated in another way. Taking an initially uniform size distribution then it can be shown (12) that:

$$N_t = N_o(1 + t/\tau_B)^{-1} \quad (8)$$

N_t and N_o are the concentration of droplets at time t, and τ_B is the characteristic time and is given by:

$$\tau_B = (3\eta)/(4k\ T\ N_o) \quad (9) \quad , \quad N_o = (3f)/(4\pi\ \bar{r}_o^3) \quad (10)$$

in which η is the viscosity of the continuous media and k is Boltzmanns constant and $\bar{r}_o$ is the initial mean radius.

The volume fraction, f, of droplets is related to N_o through the mean initial radius $\bar{r}_o$ by Equation (10). Using $f = 2 \times 10^{-4}$ then we obtain the following, at 300K with water as the host phase and solvent dispersed at $\bar{r}_o = 1$ μm, $N_o \sim 5 \times 10^{13}\ m^{-3}$, $\tau_B \simeq 4 \times 10^{3}$ s or at $\bar{r}_o = 10$ μm, $N_o \simeq 5 \times 10^{10}\ m^{-3}$, $\tau_B \sim 4 \times 10^{6}$ s (see also Table 2). These times are rather long, indicating that the Brownian motion coalescence for droplets > 2 μm diameter is not very effective. This is also demonstrated in the next section.

COMPARISON OF BROWNIAN MOTION INDUCED COALESCENCE WITH DIFFUSION GROWTH

It can be shown for growth by diffusion control alone (13) that:

$$N_t = N_o(1 + t/\tau_D)^{-1} \quad (11)$$

applies if the size distribution at t_o is of asymptotic form. In Equation (11) the characteristic time, τ_D, is given by:

$$\tau_D = (9k\ T\ \bar{r}_o^3)/(8\gamma_i\ V_m^2\ C_\infty\ D) \quad (12)$$

where V_m is the molar volume of the droplet phase. Taking for solvent drops (LIX in kerosene), $\gamma_i = 16\ mNm^{-1}$, $C_\infty = 8 \times 10^{-6}\ kgdm^{-3}$ (dodecane), $D \equiv 5 \times 10^{-6}\ cm^2\ sec^{-1}$ and V_m for dodecane (by the Le Bas method) $3 \times 10^{-17}\ m^3$, then τ_D at various initial radii can be calculated, Table 2.

TABLE 2

Characteristic Time τ_D in Secs. for Growth of Droplets by Diffusion Mechanism and τ_B for Brownian Coalescence

Initial Droplet Diameter	τ_D (Eq. 12) Secs.	τ_B (Eq. 9) Secs.
0.01	6.7	4.7×10^{-4}
0.1	6.7×10^{3}	4.7×10^{-1}
1	6.7×10^{6}	4.7×10^{1}
10	6.7×10^{9}	4.7×10^{5}
20	5.4×10^{10}	3×10^{9}

The characteristic times for Ostwald ripening are much larger than for the Brownian effect so the former is an unlikely mechanism here. Also the results in Table 2 show that the diffusion effect is only important with the very smallest drops agreeing with previous calculations and the Brownian motion becomes unimportant for drops of $\geq$ 2 μm diameter.

VELOCITY GRADIENT EFFECTS

In a closed system the velocity gradients generated during mixing disappear rapidly (however, it is not certain if thermally induced velocity gradients are still present in the experiments which we carried out).

According to Lindborg and Torsell (14) the average velocity gradient, $|\overline{\text{grad } V}|$ is:

$$|\overline{\text{grad } V}| = 5\ V/\ell + V^{3/2}/\vartheta^{1/2}\ \ell^{1/2} \qquad (13)$$

in which ϑ = kinematic viscosity of continuous phase, V = macroscopic flow velocity in the continuous phase, ℓ = a characteristic length.

For the vessel used in the present study $\ell \equiv$ diameter = 15 cm, ϑ for water at 300K $\simeq$ 0.001 $m^2\ sec^{-1}$ and V is taken as the average velocity of the primary break over the last 10% of the process = 3×10^{-3} cm sec^{-1} (typical of the primary break curve measured in one of our settling tests), then $|\overline{\text{grad } V}| = 1.8 \times 10^{-3}\ sec^{-1}$. Now suppose two droplets, each of diameter 1 μm, are separated by 2 μm from their centres then the relative velocity along the separation direction is $2 \times 1.8 \times 10^{-3} = 3.6 \times 10^{-3}$ μm sec^{-1} the displacement of one droplet in 1 sec is of course 1.8×10^{-3} μm which is much less than the Brownian movement reported in Table 1.

Velocity gradient induced collisions of haze droplets in closed systems seems to be of small importance in these studies. It may be of more importance in commercial settlers where V may equal ca 3 cm sec^{-1} then the displacement in 1 second is 1.8 μm.

EFFECTIVE COLLISIONS

The collision must be effective for coalescence. Two main features of the drop surface are now important. It is known that in the case of solids dispersed in water, primary coagulation takes place when the zeta potential, ζ, approaches zero (15). In hydroxyoxime systems the value of ζ is partly

dependent on the absorption of extractant or other molecules at the interface and their degree of ionisation. Also the physically observable films at interfaces (16,17) may be viscous or visco-elastic and they may prevent the thinning of the interfacial film. Amphipathic chemicals adsorbed in molecular films at the interface exert their effect by a combination of viscous and mechanical properties, this layer allows the drop to deform on approach of a second drop so aiding the formation of the lens prior to drainage and coalescence. Of course, films also interfere with diffusion mechanisms for droplet growth.

3. EXPERIMENTAL

Commercial chemicals used in the work, e.g. LIX 65N (Henkel Ltd.), P5000 (Acorga Ltd.), SME529 (Shell Chemicals Co.), were "purified" by several aqueous washes. Purified chemicals were also prepared through chemical routes such as copper complex isolation and then regeneration of the oxime with acid. The diluents were either A.R. Toluene (BDH) Ltd., which was further purified by passing through a column of silica gel and then alumina, or the commercial kerosene ESCAID 100. Other chemicals were of BDH Analar grade.

The contacting vessel was a glass cylinder, ht. 30 cm, diam. 15 cm, with four vertical baffles of 12 mm width. A cruciform stainless steel impeller was used, vanes 5 mm long and 10 mm deep. Experiments were conducted at 23-25^{o}C and N_2 gas was introduced over the mixture to prevent oxidation. The apparatus was thoroughly cleaned between each experiment. A standard procedure was followed using one litre of each phase. The impeller was immersed into the centre of the aqueous phase before start-up to ensure organic dispersion. Pre-equilibrated phases were used. A constant speed of 500 rpm was chosen which was low enough to avoid observable air ingestion. Each mix was of fifteen minutes duration.

At the end of an experiment samples were prepared for the following techniques.

TECHNIQUES EMPLOYED

Microscopic examination was carried out after a sample had been left to cream for various times. A Baker particle sizing microscope with British Standard particle sizing graticule (18) was used. Droplets down to d = 1 μm could be seen clearly. Entrainment levels were measured either by the infra red technique using Arklone P as extractant and described elsewhere (19), or by a copper complexation technique originally described by Ashbrook (20). The primary break velocities of the mix were also taken directly from the mixing vessel using a fixed scale and height or depth of dispersion were plotted against time. The zeta potential, ζ, was calculated from electrophoretic mobilities measured with the aid of a Rank Bros. electrophoresis apparatus using the thin walled cylindrical cell at 25 $\pm$ 2^{o}C.

RESULTS

LIX 65N in Toluene

LIX 65N in toluene at 18.7 vol% was contacted with the following aqueous phases in separate experiments. (Salt and/or acid conc. at 10^{-3} mol dm^{-3}.) (A) distilled water only; (B) $Al_2(SO_4)_3$ + H_2SO_4; (C) H_2SO_4; (D) $MgSO_4$ +

H_2SO_4; (E) $MgSO_4$; (F) Na_2SO_4; (G) $Na_2SO_4 + H_2SO_4$. Basic properties of the haze dispersion are given in Table 3.

TABLE 3

Properties of the Haze Dispersions with 18.7 Vol% LIX65N/Toluene

Aqueous	A H_2O	B Al^{3+}/H^+	C H^+	D Mg^{++}/H^+	E Mg^{++}	F Na^+	G Na^+/H^+
Ionic Strength m mol dm^{-3}	-	16	1	5	4	3	4
pH	4.9	2.8	2.8	3.5	6	6	2.8
ζ, mv	-17	+24	+7	+5	-37	-26	+20
Average Entrainment in mg dm^{-3}	130	1250	1110	1600	150	1000	2500
d_{av} (μm)	3	17	13	20	4	10.5	23
Primary Break Rate $cm\ sec^{-1}$	5.5	1.2	0.8	0.7	4.2	0.8	0.8

The photomicrograph direct measurements of droplet diameter demonstrated that haze droplets were mostly in the range 1 to 20 μm. The entrainment values are a linear function of d_{av} but they do not appear to correlate with other parameters. The ζ values follow the pH of the host phase (comparison is possible where the ionic strengths are about equal). This feature is probably reflected in the protonation or degree of ionisation of the extractant held at the interface. Indeed in other experiments reported elsewhere (21) we find that the ζ potential of the drop becomes more -ve as pH is increased, giving a sigmoidal shaped curve of ζ versus pH.

There is no general correlation between primary break times and other features although experience shows that the primary emulsion is often more stable in low ionic strength conditions and would appear to be more stable at high pH (and therefore the most -ve ζ value). Just the opposite occurs with haze stability as measured by the number of droplets in arbitrary volume, see Figure 1. For now the least stable haze is that found with the least acidic solutions. If ζ potential is considered alone then one would expect those haze systems with $\zeta \rightarrow 0$ to coalesce the most readily, this is not the case. Ionic strength is important and in the absence of salts the haze degenerates rapidly. Again, this observation is the opposite to that found with primary emulsions. These observations point to coalescence being the least important in the creaming process.

If the experiments with aluminium salts are attempted at pH > 3 then hydrolysis occurs and networks of hydrated aluminium oxide coat the haze droplets, the haze is now some 100 x more stable than for the corresponding experiment at low pH. The same effect has been found with soluble silica in the pH range 3 to 7.

ESCAID 100

Apparently, haze results with ESCAID alone, Figure 1. In other experiments we have noticed that ESCAID is unstable to u-v light and also forms a definite visible "skin" at the interface when contacted with strong sulphuric

acid (e.g. 180 g dm^{-3}) over a long period.

FIG.1

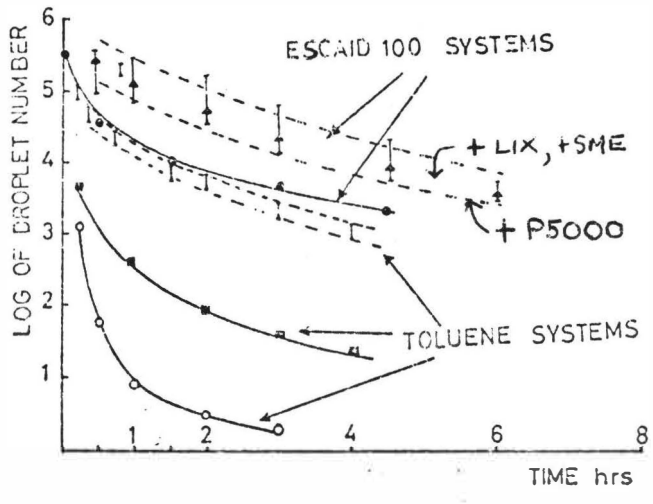

FIG. 1: Log of droplet number in arbitrary volume versus time; ▲ ESCAID 100 in H_2SO_4, ● LIX 64N/ESCAID 100 in Mg^{++}/H^+, ■ LIX 65N/toluene in H_2SO_4, o LIX 65N/toluene in water.

LIX 64N in ESCAID 100

LIX 64N at 20 vol% in ESCAID was contacted with the aqueous phases previously described for the LIX 65N work, see Figure 1. The ESCAID hazes are more stable than those for toluene. They show similarity with those for ESCAID alone suggesting that the diluent plays a dominant role in haze stability.

The frequency/size graphs for this organic system contacted with H^+/Mg^{++} were prepared from aqueous samples taken at various times, see Figure 2. The size dispersion in the haze is seen to be bimodal. We note that in emulsion formation bimodal distributions are sometimes observed (21). Also, Lindborg and Torsell found experimentally that an initial unimodal distribution of droplet diameters generated a bimodal one.

The mean particle diameter on a volume basis from Figure 2 is roughly constant with time at 5 μm. If Stokesien creaming is assumed the maximum diameter d_{st} above which all droplets have creamed can be calculated at various times and then compared with the maximum diameter observed in the sizing experiments, see Figure 3. The reasonable fit over the latter period of the experiment reinforces the previous view that Stokesien creaming is the main mechanism for the clearance of the haze for droplets > 2 μm diameter. Brownian motion affects droplets of about 1 μm diameter.

FIG. 2

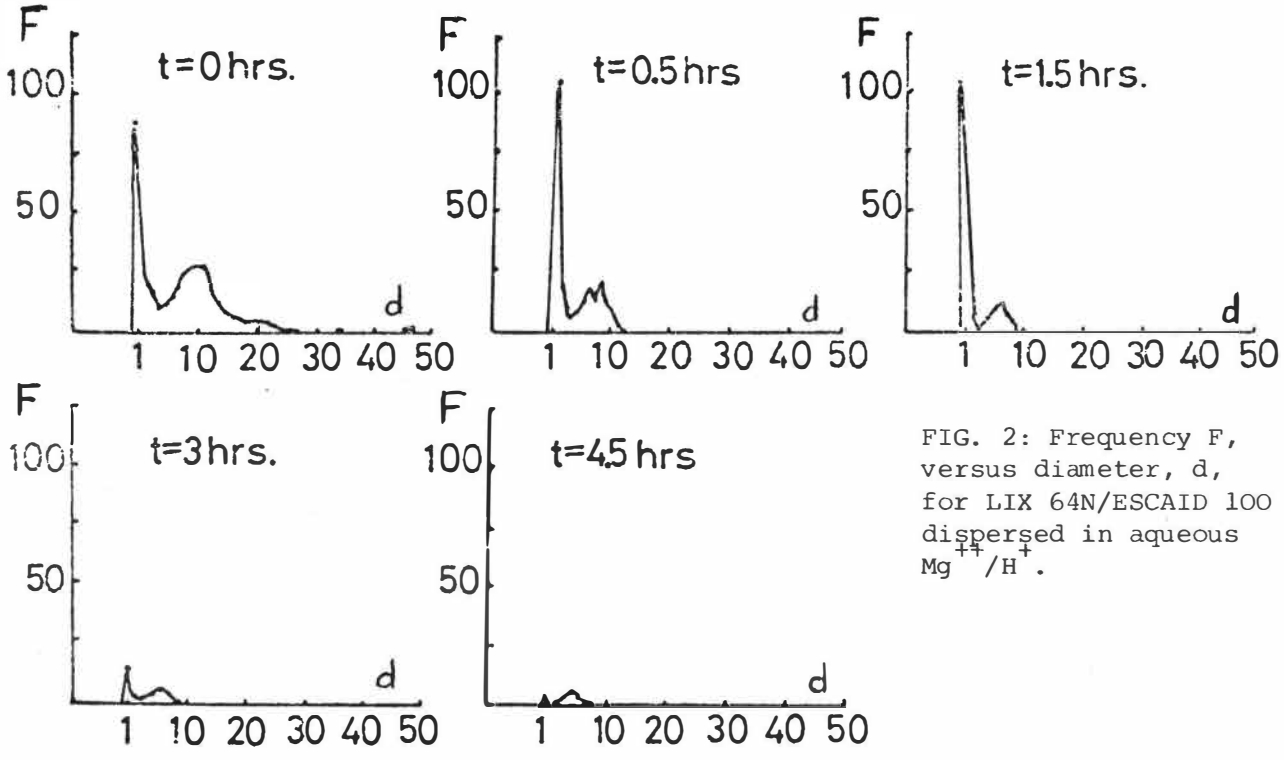

FIG. 2: Frequency F, versus diameter, d, for LIX 64N/ESCAID 100 dispersed in aqueous Mg^{++}/H^{+}.

FIG. 3

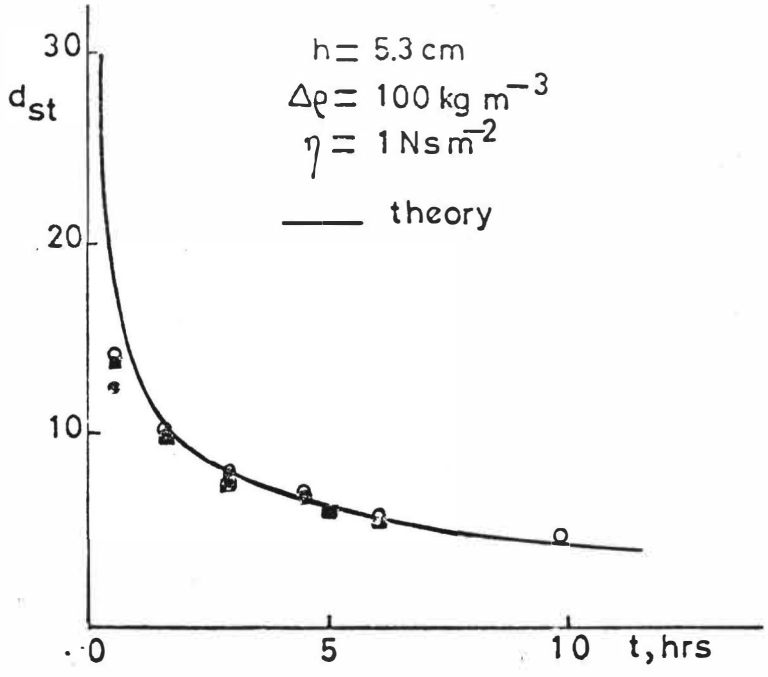

FIG. 3: Maximum diameter, d_{st}, left at time, t, after Stokesien settling; O, □, ● for LIX 64N/ESCAID 100 dispersed in H_2SO_4, Mg^{++}/H^{+} and Na^{+}/H^{+} aqueous respectively.

REFERENCES

1. A.W. Ashbrook, Canadian Mines Branch Information Circular, IC284.

2. G. Rossiter, A.I.M.E., Hydromet. Division, Spring Meeting, Arizona, 1976.

3. C. Hanson, M.A. Hughes, paper presented at A.I.M.E. Annual Meeting, Las Vegas, Feb. 1980.

4. R.J. Whewell, M.A. Hughes, H. Foakes, Hydrometallurgy, 1980, in press.

5. G.E. Charles, S.G. Mason, J. Colloid Science, 1960, 15, 105.

6. J.C. Godfrey et al, A.I.Chem.E. Symp. Series, 1978, Vol. 74, No. 173, 127.

7. W.I. Higuchi, J. Misra, J. Pharm. Sci., 1962, 51, 459.

8. T.A.B. Al-Diwan, M.A. Hughes, R.J. Whewell, J.I.N.C., 1977, 39, 1419.

9. R.J. Whewell, M.A. Hughes, C. Hanson, Proc. ISEC '77, publ. C.I.M., Special Volume 21, 1980, 185.

10. C. McAuliffe, J. Phys. Chem., 1966, 70, 1267.

11. E.D. Washburn, Phys. Rev., 1921, 17, 374.

12. E.M. Baroody, J. Appl. Phys., 1967, 38, 4893.

13. A.J. Markworth, Metallography, 1970, 3, 197.

14. U. Lindborg, K. Torssell, Trans. Met. Soc. A.I.M.E., 1968, 242, 94.

15. "Solid-Liquid Separation", Ed. L. Svarovsky, publ. Butterworths, 1977, p 68.

16. M.A. Hughes, Hydrometallurgy, 1978, 3, 85.

17. G.A. Yagodin, V.V. Tarasov, Tr-Mezhdunar, Kong. Poverkhn-Akt Veshchestvam, 7th 1976, (Publ. 1978), 2(I), 410.

18. "Particle Size Measurement", T. Allen, publ. Chapman and Hall, 1974.

19. P.D. Middlebrook, Ph.D. Thesis, Bradford University, U.K., 1980.

20. A.W. Ashbrook, Anal. Chim. Acta., 1972, 58, 115.

21. "Theory and Practice of Emulsion Technology", Ed. A.L. Smith, publ. Acad. Press, 1976, p 336.

FLUID DYNAMICS OF CENTRIFUGAL EXTRACTORS

M.Stölting
Lehrstuhl A für Verfahrenstechnik
Technische Universität München
Arcisstr. 21
8000 München 2
Western Germany

ABSTRACT

Centrifugal extractors of the Podbielniak-type are investigated covering flooding-point-diagrams and the influence of fluiddynamics on mass transfer.The flooding-point-diagram exists of three limits,two of them are calculated by the investigation of the location of the principle interface.The third limit is given by a theoretical and experimental investigation of the formation and trajectories of single drops in a rotating fluid.The results are independent of the extractor type.Optimum working conditions were found at maximum speed of rotation,combined throughput of about 80% of the flooding limit and a location of the principle interface according to system properties between 20% and 80% of maximum backpressure.

INTRODUCTION

Centrifugal extractors are commonly used in systems,which have a low density difference,a strong tendency to emulsify or a short contact time requirement,in any case the high throughput, small hold-up and small space requirement is advantegeous. One of the best known centrifugal extractors is of the Podbielniak type,a cutaway of which is shown in figure 1 /1/. Both phases are fed through the shaft,the light phase enters the extractor at the periphery,the heavy at the center and they pass countercurrently through a contacting zone,which exists for example of several perforated cylinders,other mixing elements are possible.In this zone both phases are thoroughly mixed and separated several times to give optimum mass transfer.Both phases are dispersed and continuous,depending on radial displacement and the location of the principle interface.In a subsequent calming zone both phases are cleared and leave the extractor through the shaft.Details of various constructions and several applications in the chemical and pharmaceutical industry are found in literature /2 to 5/.Some integral data exist on fluiddynamic behaviour and mass transfer,but for a reasonable calculation an exact investigation of the fluid movement inside the extractor is neccessary.As a first step,the volumes of single drops,which are formed at a nozzle in a centrifugal

field and the motion of these drops in an extractor model without internal fittings were investigated /6/,the results applied to industrial equipment and tested in a Podbielniak A1 pilot extractor.

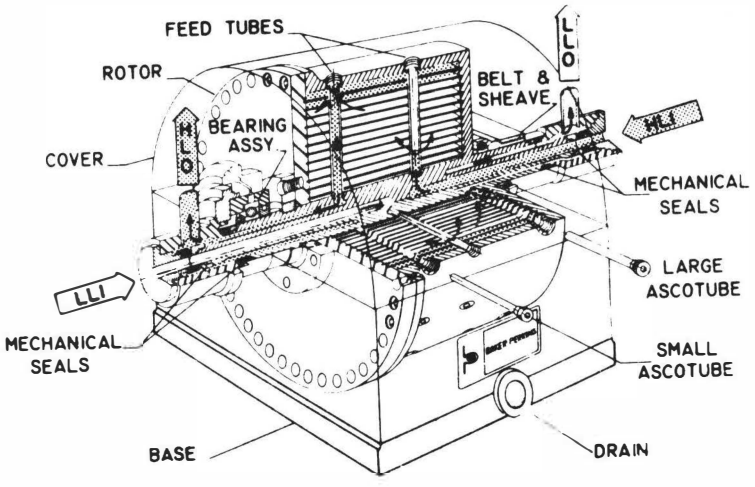

FIG. 1
Cutaway of a Podbielniak centrifugal extractor

EXPERIMENTAL PROCEDURE AND SIGNIFICANCE

Figure 2 shows a cross section of the extractor model we used for single drop measurements.It consists of a cylindrical chamber,60 cm in diameter,rotating around a vertical axis.The feed of the heavy and light phases is through the shaft.Starting experiments,the model was filled with the light phase,which was the continuous one;the heavy,disperse phase enters through a variable nozzle system near the center and is driven to the periphery by centrifugal force,there it leaves through a special outlet tube.Drop formation and trajectories were filmed with a Hycam high speed camera,the films gave informations on drop volumes,radial and acimutal displacement and velocities.Details of experimental procedure are given elsewhere /7/.

The results of this experiments were used to test the theoretical considerations given below,their application to industrial equipment was tested in a Podbielniak A1 extractor for the system Toluene-(Acetone-)water with and without mass transfer.The flowsheet is given in figure 3.Additional data from literature were tested too,the parameter variation is given below.

$$0{,}5 = \dot{V}_d/\dot{V}_c = 2$$

$$19 \leq \sigma \leq 39 \qquad 10^{-3}\ N/m$$
$$0{,}59 \leq \eta_c \leq 2 \qquad 10^{-3}\ Pas$$
$$\eta_d \leq 1 \qquad 10^{-3}\ Pas$$
$$0{,}131 \leq \Delta\rho \leq 0{,}2 \qquad g/cm^3$$

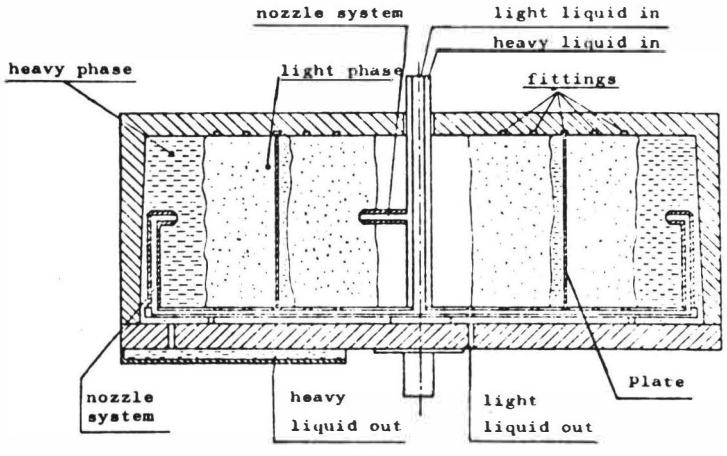

FIG. 2
Cross section of the model

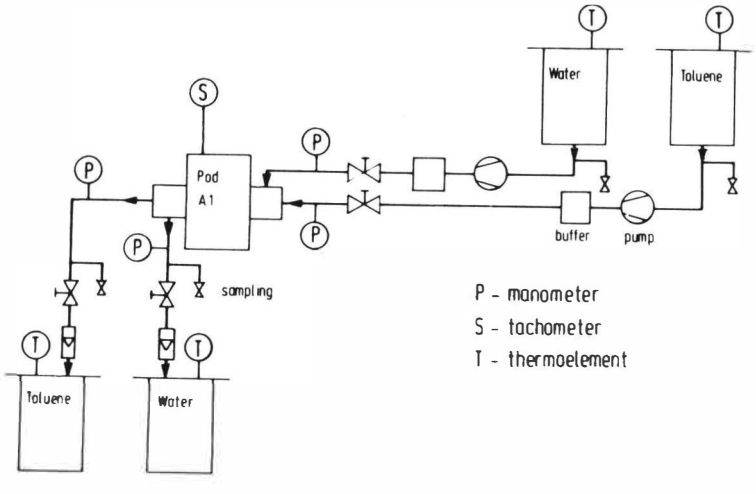

FIG. 3
Flow sheet of Pod A1 tests

A typical result of this measurements is given in figure 4,here the number of theoretical plates,calculated by the McCabe-Thiele diagram is given against backpressure $\overline{p_{llo}} = p_{llo} - p_{hlo}$ for three different speeds of rotation and five different throughputs.

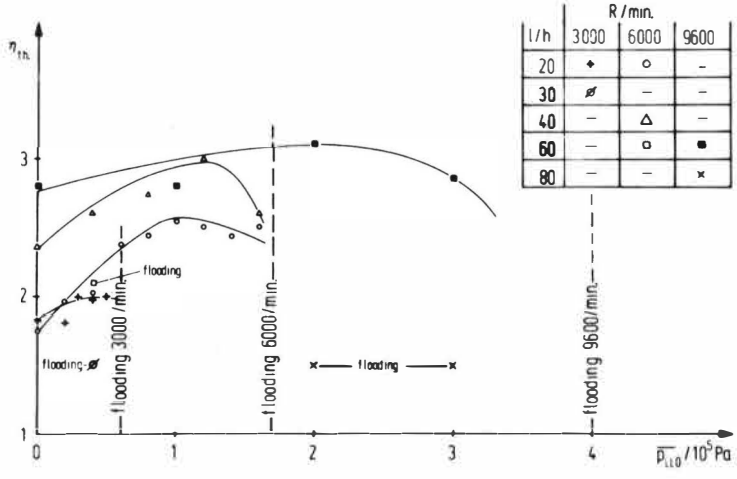

FIG. 4
Number of theoretical plates depending on backpressure,speed and throughput for a Pod A1,system Toluene-Acetone-water.

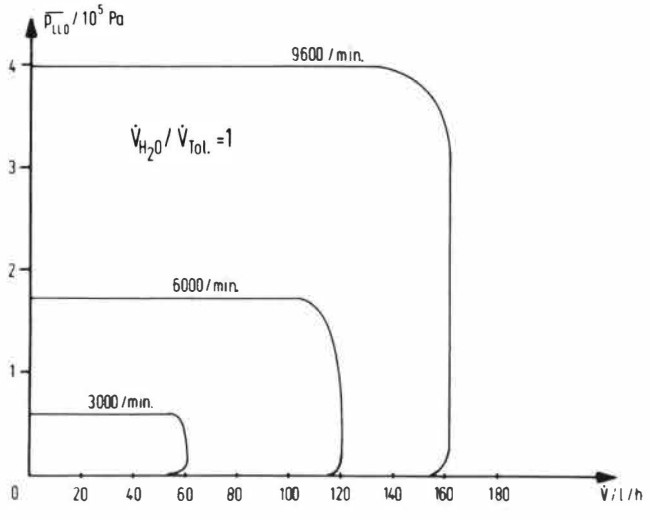

FIG. 5
Flooding point diagram for the measurements given in FIG. 4.

The feed ratio was 1:1 in all cases.Fig.5 gives the corresponding flooding point diagram.Some conclusions can be drawn from this:

1) n_{th} increases with increasing speed
2) there is an optimum n_{th} with increasing throughput
3) there is an optimum backpressure
4) with increasing speed maximum throughput increases

These results of our own are supported by literature /4,5,8,9/, some rules of thumb can be given from that for operating conditions of a centrifugal extractor :

1) run highest speed
2) optimum combined throughput is about 80% maximum throughput
3) optimum backpressure must be tested for each system,it should be between 20% and 80% of maximum backpressure.

Some further reasons for this and the calculation procedure is given below.

THEORY

The flooding point diagram exists of three different limits,as shown in figure 5.Two of them,the maximum and minimum backpressure can be calculated from a simple pressure balance /3,7/, the result is

$$\overline{p_{llo}} = \omega^2 r_I^2 \Delta\rho/2$$

where r_I is the location of the principle interface,where both phases are separated.Flooding occurs,if the principle interface comes to the llo-tube or the hlo-tube respectively,that means,we can calculate these limits by

1) $r_I = r_o$ (llo-tube location)
$$\overline{p_{llo}} = \omega^2 r_o^2 \Delta\rho/2 \qquad (1)$$

2) $r_I = r_3$ (hlo-tube location)
$$\overline{p_{llo}} = \omega^2 r_3^2 \Delta\rho/2 \qquad (2)$$

In any case the principle interface is not a sharp one,drops must coalesce and a dispersion layer of a certain thickness depending on system properties and operation conditions will occur.Therefore a security limit of about 20% maximum backpressure should not be exeeded.If flooding occurs and backpressure can not be changed,then a change in speed will help.For flooding in the hlo-tube increased speed will help,for flooding

in the llo-tube decreased speed will force the principle interface back into the contacting zone.

The third flooding limit can not be given that easy,here we must know,what happens inside the extractor.Starting from observations of single drops described before,we can calculate the trajectory of a drop by solving the equation of motion,which is given by two coupled differential equations of second order /6/

$$m\ddot{r} = mr(\omega - \dot{\varphi})^2 - \omega^2 r V_p \rho_c - C_r \dot{r}$$
$$mr\ddot{\varphi} = -2m\dot{r}(\omega - \dot{\varphi}) - C_\varphi r\dot{\varphi} \qquad (3)$$

For the calculation of flooding points only the radial movement is interesting,here a solution is given by

$$r(t) = r_1 \exp(\lambda t) \qquad (4)$$

where r_1 is the starting point of a single drop,here the hli-tube location and λ is given by

$$\lambda = -\frac{C}{2m} + \sqrt{\frac{C^2}{4m^2} + \omega^2(1 - \rho_c/\rho_d)} \qquad (5)$$

The given solution (4) and (5) is only a good approximation,including some physical reasonable assumptions /7/.The drag in equation (5) is given by

$$\frac{C}{2m} = \frac{9}{d_p^2} \frac{w_\infty \eta_c}{\rho_d w_{rel}} \qquad (6)$$

In countercurrent flow flooding occurs at

$$u_d/\varepsilon = u_c/(1-\varepsilon)$$

that means

$$\lambda r/\varepsilon = \dot{V}_{c,max}/(2\pi rb(1-\varepsilon))$$

From this it follows,that flooding occurs at the minimum possible radius,the radius of the hli-tube,that means

$$\dot{V}_{c,max} = 2\pi r_{hli}^2 b(1-\varepsilon)\lambda/\varepsilon \qquad (7)$$

The hold up ε and the velocity ratio w_∞ / w_{rel} consider the fact, that in industrial equipment swarms of drops exist,which influence one another.This terms can be calculated from system properties and flow ratio,as Pilhofer has shown /11/.For flooding conditions we get

$\dot{V}_c/\dot{V}_d = 1$	$w_{rel}/w_\infty = 0,5$	$\varepsilon = 0,3$
$\dot{V}_c/\dot{V}_d = 2$	$w_{rel}/w_\infty = 0,45$	$\varepsilon = 0,35$
$\dot{V}_c/\dot{V}_d = 0,5$	$w_{rel}/w_\infty = 0,55$	$\varepsilon = 0,25$

for the feed ratios we have tested nearly independent of system properties.

Drop formation in centrifugal extractors is by atomization as Todd /1/ has shown,he found experimentally a typical drop size of below 30 μ .Recalculation of flooding point diagrams from literature and our own led us to the empirical equation /10/

$$d_p/\mu = \frac{423}{\sqrt{\omega/(1/s)}} \quad \frac{\dot{V}_d+\dot{V}_c}{\dot{V}_d} \qquad (8)$$

for drop size at flooding.Recalculating the system Todd has used we get a drop size of 26,7 μ in good agreement with the experimental value.Now we are able to calculate the third flooding limit,using equations (4) to (8).Using equations (1) and (2) additionally,we can calculate the total flooding point diagram. Typical examples are given in figures 6 and 7.The solid lines are measured ones,the dotted lines are calculated by this theory the agreement is sufficiently well,more examples are given elsewhere /10/.The drop size in industrial equipment is not unique, equation (8) gives the diameter of a medium drop,that means, there is a distribution in drop size.Therefore there is no sharp limit in maximum throughput,coming near to this value more and more drops will go with the continuous phase and thereby deteriorate the equipment efficiency.Typical measurements of this behaviour are given in figure 4,points x and □ .As can be seen from the corresponding figure 5 these probs were taken near maximum throughput.Again as a rule of thumb the extractor should be run at 80% of maximum throughput,because mass transfer and throughput are optimal near this point.

SUMMARY

Measurements of mass transfer in a Pod A1 pilot extractor with the system Toluene-(Acetone-)water with and without mass transfer led to a discussion of the influence of fluiddynamics on efficiency of a centrifugal extractor.A reasonable understanding

of the fluiddynamics of a centrifugal extractor starts with

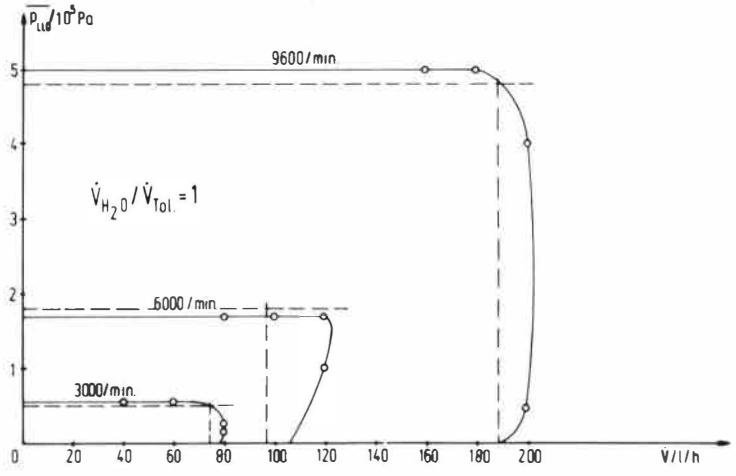

FIG. 6
Flooding point diagram for a Pod A1 pilot extractor for the system Toluene-water.Solid lines - measured,dotted lines - calculated by this theory.

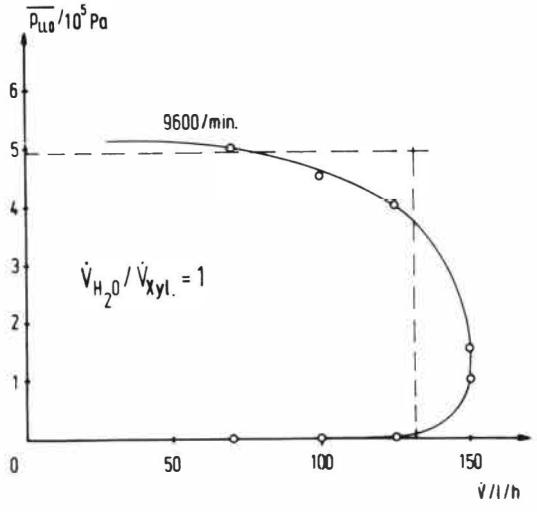

FIG. 7
Flooding point diagram for a Pod A1 pilot extractor for the system Xylene-water.Solid lines - measured,dotted lines - calculated by this theory /9/.

the investigation of the behaviour of single drops.By that flooding point diagrams can be calculated from equations (1) and (2) by a simple pressure balance and the set of equations (4) to (8).Optimum conditions for operation can be given by rules of thumb.

NOTATION

b	rotor width	cm
C	Constant	-
m	mass	g
n_{th}	number of theoretical plates	-
p	pressure	Pa
r	radius	cm
t	time	s
u	superficial velocity	cm/s
V	volume	cm^3
$\dot{V}$	throughput	cm^3/s
ε	hold up	-
η	viscosity	Pas
ρ	density	g/cm^3
σ	interfacial tension	N/m
ω	speed	1/s

Indices

c	continuous
d	disperse
hli	heavy liquid in
hlo	heavy liquid out
I	principle Interface
lli	light liquid in
llo	light liquid out
max	maximum
p	particle
rel	relative
O-3	special locations
∞	single particle for $t \longrightarrow \infty$

REFERENCES

/1/	D.B.Todd G.R.Davies	Proceedings ISEC 1977
/2/	D.B.Todd G.R.Davies	Filtration & Separation Nov/Dec 1973,663

/3/	F.M.Jacobsen G.H.Beyer	AIChE J 2(1956)3,283
/4/	N.Barson G.H.Beyer	Chem Engng Progr 49(1953)5,245
/5/	D.B.Todd	GVC/AIChE Joint Meeting,München 1974,Vol.II,D 4-4
/6/	M.Stölting E.Blaß	Ger Chem Engng 2(1979)1,14
/7/	M.Stölting	Diss TU München 1979
/8/	D.W.Anderson E.F.Lau	Chem Engng Progr 51(1955)11,507
/9/	J.Schröter Bayer AG	private comm.
/10/	M.Stölting	AIChE Joint Meeting Philadelphia 1980
/11/	Th.Pilhofer	Ger Chem Engng 2(1979)4,200

ACKNOWLEDGMENT

The author wishes to acknowledge the generous financial assistance of the "Deutsche Forschungsgemeinschaft ".

DROP SIZE DISTRIBUTIONS IN A SIEVED PLATE PULSED COLUMN
INFLUENCE OF BREAK-UP MECHANISM

PAKDEE PATRAKORN S.,MURATET G.,CASAMATTA G.

INSTITUT DU GENIE CHIMIQUE

Chemin de la Loge

31078 TOULOUSE CEDEX

FRANCE

Extensive studies have been carried out in our laboratory upon perforated plate pulsed columns. Experimental results have been interpreted by deriving the equation of the MIYAUCHI model.

Some revealing discrepancies are pointed out between theory and experiments. The main reason is that the dispersed phase cannot be regarded as a whole being submitted to overall back mixing, but it does actually consist of drops of different diameters, each of them having it's own velocity and undergoing rupture and coalescence.

Therefore we propose a new mathematical model taking in account foward mixing due to drop size distribution and, rupture and coalescence.

In this paper the mathematical equations are derived. The experimental results involved to validate our model having been carried out in the field of low hold-ups, the described equations do not contain coalescence terms. The following is assumed :

- the classical piston-diffusion model is adapted for the continuous phase flow

- each drop shows a relative velocity towards the continuous phase and undergoes the same back mixing as the continuous phase

- the relative velocity of drops is derived from the terminal velocity of unique drops in the actual flowing conditions.

Numerical solution of the continuous equations of the dispersed phase flow has been achieved by deriving a discrete model. The chosen technique, i.e., counter-current stages with back flow model, affords a second order approach of the continuous equations.

Hydrodynamic diffusivities have been assumed to be equal to the formerly obtained values. The relative velocities and a simple rupture model have been fitted to experimental data. Accuracy between theory and experimental results has been checked by comparing hold-up profiles and drop size distribution profiles.

A satisfactory agreement is pointed out and the validity of the model is claimed.

Equipment
Session 4

Co-chairmen : J.B. Scuffham (Power Gas Corp., Teeside, U.K.)
P. Groteaers (Extraction De Smet, Antwerpen, Belgium)

4A

80-21 Mixing index as a performance indicator of pump-mix type mixers on continuous flow systems.
J. Roberts and J. McGee, University of Newcastle, New South Wales, Australia.

80-26 Logical pump design for pump mix mixer-settlers.
E. Barnea, D. Meyer and S. Wahrmann, IMI Institute for Research and Development, Haïfa, Israël.

80-31 Copper extraction with a sulzer in-line mixer using Acorga reagent P5100.
M.J. Slater, J.C. Godfrey, A. Temple, N.P. Wynn and M. Zabelka, University of Bradford, Bradford, U.K. and Sulzer Bros. Ltd., Winterthur, Switzerland.

80-34 The settler with laminar corrugated filling.
J.M. Josa and A. Moral, Junta de Energia Nuclear, Madrid, Spain.

80-36 Advances in the design of unpulsed sieve-plate extraction columns.
Th. Pilhofer, Technical University Munich, Munich, Germany.

80-35 Theoretical and experimental study of transient start-up behavior of pulsed sieve-plate extraction columns.
E. Blass and H. Zimmermann, Technische Universität München, München, Germany.

4B

80-28 The reciprocating plate extraction column as a cocurrent mixer.
A.E. Karr, Chem-Pro Equipment Corp., Fairfield, New Jersey, U.S.A.

80-30 Hydrodynamic studies in a reciprocating plate column.
N.V. Ramarao, N.S. Srinivas and B.G.V. Varma, Indian Institute of Technology, Madras, India.

80-148 The QVF-stirred-cell-extractor - Idea and special aspects of calculation.
J. Postl and R. Marr, Institut für Grundlagen der Verfahrenstechnik, TU Graz, Austria.

80-213 Mixer-settler-column, a new stagewise contactor.
U. Bühlmann, Kühni Ltd., Allschwill, Switzerland.

80-229 A new type of agitated liquid-liquid extraction colum with enhanced coalescence plates.
L. Steiner and S. Hartland, Swiss Federal Institute of Technology (ETH), Zürich, Switzerland.

20-207 A centrifugal extractor for fast and slow mass transfer processes.
G.I. Kuznetsov, S.M. Belyakov, L.I. Shklyar and A.A. Pushkov, State Committee for Atomic Energy, Moscow, U.S.S.R.

MIXING INDEX AS A PERFORMANCE INDICATOR OF PUMP-MIX TYPE MIXERS ON CONTINUOUS FLOW SYSTEMS

John Roberts and Jennifer McGee
Department of Chemical Engineering
The University of Newcastle
New South Wales, 2308
Australia

ABSTRACT

Optimisation of mixer performance is constrained by the need to avoid carryover of fine non-settling droplets when operating at the relatively high impeller speeds required to achieve mass transfer rates and reduce phase inversion phenomena. Disperse phase hold-up is a measure of the degree of phase mixing actually taking place in continuous flow mixers, and as such, it is an important process variable.

A correlation procedure is described for determining disperse phase hold-up and an associated mixing index. For single stage laboratory and pilot pump-mix units operating with acidified copper sulphate/kerosene, it was found that the mixing index was much greater for aqueous continuous than organic continuous operation. An added turbine up the shaft considerably improved mixing index for organic continuous operation.

INTRODUCTION

The disperse phase holdup in the mixer is defined as the volume fraction ϕ_D of the total liquid in the vessel which is disperse, under operating conditions.

Whereas, in the case of batch operations, ϕ_D will be the same as the volume fraction of dispersed liquid in the continuous flow mixers, ϕ_D will only approach this fraction under conditions of vigorous agitation.

A mixing index or degree of "mixedness", I_m has been defined (1) as

$$\phi_D = I_m \frac{Q_D}{Q_D + Q_C} \quad \text{or} \quad I_m \frac{v_D}{v_D + v_C} \tag{1}$$

where Q = volumetric flow rate through the mixer
v = net velocity through the mixer
subscripts C = continuous phase
D = disperse phase

For aqueous continuous systems, I_m ranges between 0 and 1.0 with ϕ_D going between 0 and 0.5, while for organic continuous systems, I_m ranges between 2 and 1.0 with ϕ_D going between 1 and 0.5.

Only a few investigations of this parameter have been reported for baffled mixer-continuous flow units (1,2). More recent publications have considered the ambivalence region and phase inversion, both important aspects of the overall performance of commercial mixers (3,4), but not the same phenomena as reported here.

At any set O/A ratio and flow rates, $\phi_D \propto I_m$ for eqn (1), and I_m is

dependent upon agitator power per unit volume or $N^3D_i^2$, and phase properties.

where D_i = impeller diameter (m)
N = impeller rotation (rps)

Importance of Mixer Holdup

(a) Power Required or $N^3D_i^2$

With increasing equipment and electricity costs, it is important to be able to accurately calculate agitator power requirements in commercial sized units. The physical properties of mixture density and viscosity are needed for continuous flow (not batch mix) systems (2), that is

$$\bar{\rho} = \rho_C (1-\phi_D) + \rho_D\phi_D \tag{2}$$

$$\bar{\mu} = \mu_C \left(1 + 1.5 \frac{\mu_D\phi_D}{\mu_C+\mu_D}\right) \tag{3}$$

where ρ = density
μ = viscosity

(b) Disperse Phase Residence Time

The reaction-extraction residence time is a necessary design criterion and is defined as the average retention time of the disperse phase,

$$\theta_D = \phi_D \cdot \frac{V}{Q_D} \tag{4}$$

where V = mixer volume.

(c) Phase Segregation

Phase segregation or stratification in small or large mixer units can be a problem at power inputs as low as 0.15 Kw/m^3(5), which means that the mixer is not being utilised to its full extent and inferring that the mixing index or "mixedness" is low.

(d) Sauter Mean Droplet Diameter and Surface Area

The volume surface mean droplet size can now be determined from direct field measurements (6). It has been observed that Sauter mean diameter $\bar{d}_{SM}$, increases with phase holdup (4,7). By definition the specific surface area (a) is:-

$$a = \frac{6\phi_D}{\bar{d}_{SM}} \tag{5}$$

and this parameter also increases with phase holdup (8).

(e) Mass Transfer

Both mean droplet size and specific surface area are the principle controlling variables for extraction efficiency and mass transfer between phases. The droplets generated in the mixer must be small, thereby providing large surface area via eqn (5). However, the low end of the droplet size spectrum cannot be too tiny, yielding droplets which will pass through the settler as gross entrainment.

In a given mixer-settler the extraction efficiency can also be significantly affected by varying which phase is continuous. The effect of phase

continuity, direction of mass transfer on droplet size and degree of "mixedness" in the mixer are important interdependent parameters (3).

(f) Droplet Coalescence

If there is lack of sufficient turbulence throughout the mixer, coalescence of droplets will occur, resulting in partial stratification and possible alteration of phase continuity.

Droplet coalescence rate increases markedly with increase in phase holdup (8). While this phenomenon would be beneficial to the settler, it may require improved "mixedness" in the mixer unit to obtain the maximum achievable mass transfer parameters noted previously. To minimise stratification, implying final droplet coalescence, complete turnover of the mixer contents is required. This allows the two phases to have multiple passes through the impeller sphere of influence continually recreating a spectrum of droplet sizes.

CORRELATING PROCEDURE

For mixing Index, I_m as a function of power per unit volume or $N^3D_i^2$ and mixer-impeller-baffles geometry the fraction unmixed $(1-I_m)$ is considered to be the dependent variable in one of the original publications (2).

$$\text{Assume} \quad \log(1 - I_m) = A - B.N^3D_i^2 \tag{6}$$

for a particular system geometry, with A being a mixer unit geometry constant and B being a function of the two-phase physical chemistry properties and phase velocities through the mixer. The dominant properties are density difference and interfacial tension for these aqueous organic mixtures. For constant flow rate through the mixer

$$B \propto 1/(\delta\Delta\rho^{4/3})^{0.49} \tag{7}$$

where δ = interfacial tension, 13.85 to 38.^ dynes/cm

$\Delta\rho$ = density difference, 180 to 532 Kg/m^3

and A = 0, i.e. as $N^3D_i^2 \to 0, (1-I_m) \to 1.0$

$\therefore \log(1 - I_m) \to 0$

Equation (6) becomes $\log(1-I_m) = - B.N^3D_i^2$

$$\text{or } I_m = 1 - \exp(-B.N^3D_i^2) \tag{8}$$

Figure 1 shows the predicted results superimposed on the original curves of Reference (2), with excellent agreement.

Using this procedure, two similar pump-mix continuous flow systems were evaluated.

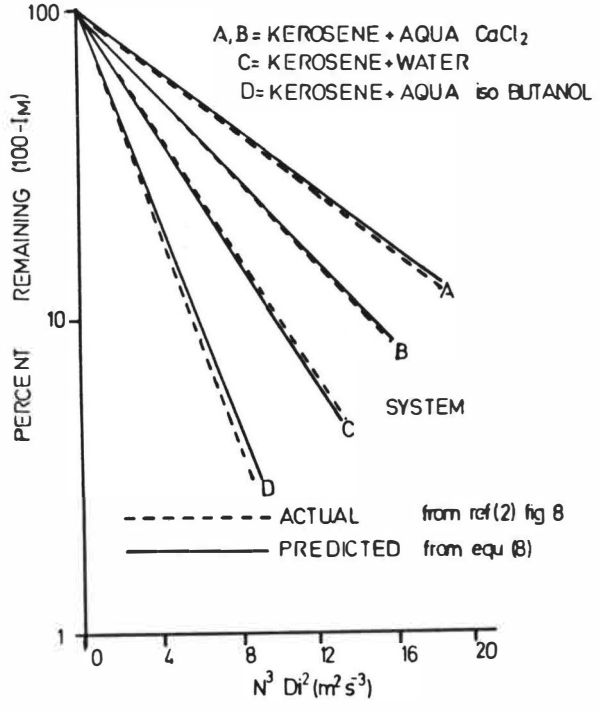

FIG. 1
Proposed Mixing Index Correlation

EXPERIMENTAL DETAILS AND RESULTS

The two pump-mix continuous flow systems used were a single-stage laboratory-scale unit, and a larger pilot unit, of near equivalent geometry. Both units and their operation have been previously described (9,10).

Shut-down phase hold-ups were determined for the range of operating conditions given in the table below. For steady-state operation, the units were run for $^1/_2$ to $^3/_4$ hour, before instantaneous shut-down and isolation of the flow control valves.

Variable	Laboratory Unit	Pilot Unit
Mixer Diameter (m) (D_T)	0.265	0.800
Impeller Diameter (m) (D_i)	0.150	0.380
Power Input N^3D^2 (m^2s^{-3})	2.8 - 17	3.5 - 25
Total Phases Flow ($m^3/m^2.min$)	0.05 - 0.3	0.2 (constant)
Temperature (°C)	27 - 28	15 - 25
Flow Ratios	1:1, 1:2, 1:3 either phase dispersed	
Aqueous Phase	Copper sulphate Solution at pH 1.5, 760 ppm Cu^{2+}	
Organic Phase	Escaid 110	

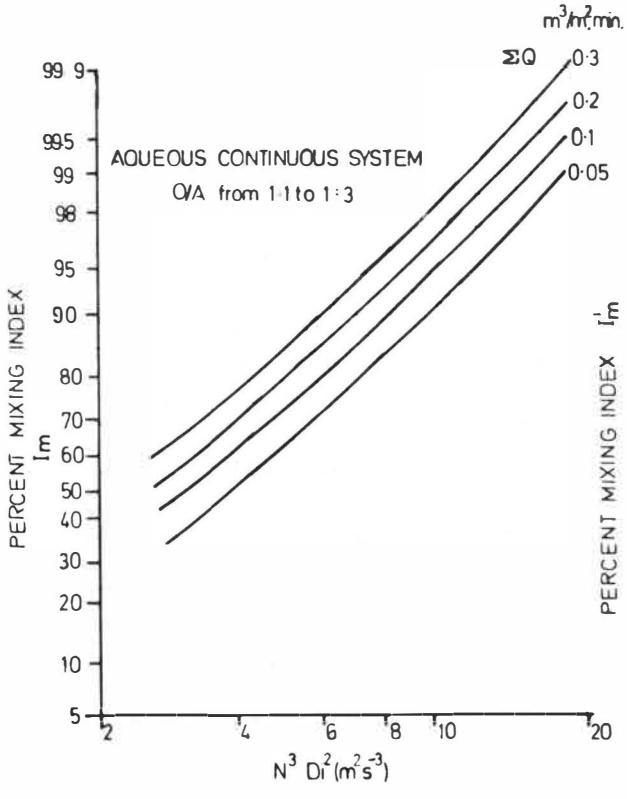

FIG. 2
Aqueous Continuous Correlation
Laboratory Unit

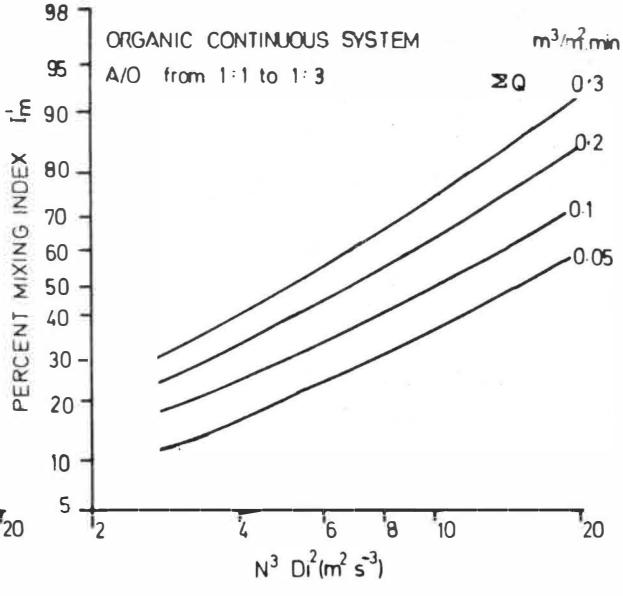

FIG. 3
Organic Continuous Correlation
Laboratory Unit

The equation used to satisfactorily correlate the data was

Aqueous Continuous: $\ell n\ (1 - I_m) = A - C.\ N^3D_i^2$ (9)

Organic Continuous: $\ell n\ (I_m - 1) = A - C.N^3D_i^2$ (10)

noting that as $N^3D_i^2 \to 0$, $I_m \to 2$, then $(I_m - 1) \to 1$ where $I'_m = I_m - 1$

and as $N^3D_i^2 \to \infty$, $I_m \to 1$, then $(I_m - 1) \to 0$

in conjunction with eqn (1) for known Q_C, Q_D and ϕ_D;

where C = function total flow rate (aqueous + organic phases) assumed to be of form $C = m\ (\Sigma Q)^n$, with m,n being equipment coefficients. Figures 2,3 show the spread of data with fitted correlations for aqueous continuous and organic continuous systems, for the range of conditions given.

The correlating equations proposed are:-

Aqueous Continuous

$I_m = 100\ (1-1.400\ \exp(-\ 0.653\ (\Sigma Q)^{0.276}.N^3D_i^2))$ percent

correlation coefficient r = 0.998 N = 23 data

$r_{critical} = 0.509$ @ 95% confidence level

Probable error in $I_m = \pm$ 1.2 percent

Organic Continuous

$I_m = 100\ (1 + \exp\ (-0.263\ (\Sigma Q)^{0.558}.\ N^3D_i^2))$ percent

correlation coefficient r = 0.74 N = 14 data

$r_{critical} = 0.532$ @ 95% confidence level

Probable error in $I_m = \pm$ 15 percent.

It is interesting to note that for either phase dispersed, the mixing index is independent of phase ratio, but dependent only on total phases flow rate and $N^3D_i^2$ or power per unit volume.

Laboratory Unit

Effect of Second Impeller on Shaft

An added investigation was the effect of a Rushton type flat-bladed turbine mounted at various relative positions up the shaft from the pump-mix impeller. Figure 4 shows the general trend at constant $N^3D_i^2$. At the 2/3 shaft position, air ingestion and extra turbulence could not be tolerated in a practical situation. However, the improvement in mixing index is considerable for the organic continuous system.

Figure 5 indicates the improvement obtained with increase in $N^3D_i^2$, for the organic continuous condition for the case of added turbine half-way up the shaft. Im comparing Figures 2,5 it can be seen that there is little improvement in mixing index for the aqueous continuous system. The type of upper turbine seems to be important, in as much as flat blades give better performance than an angled blade turbine, the trend improving with position up the shaft as shown in Figure 4.

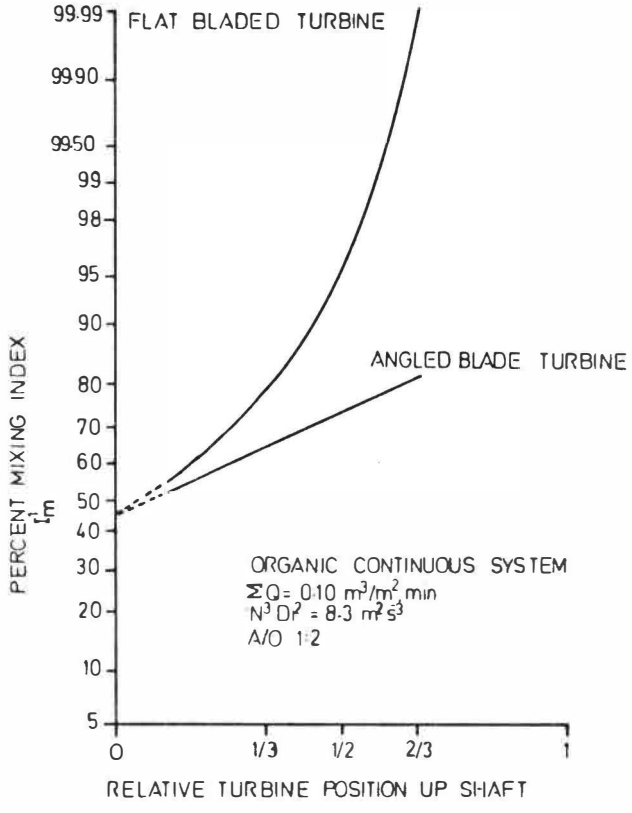

FIG. 4
Effect of Added Turbine-Lab. Unit

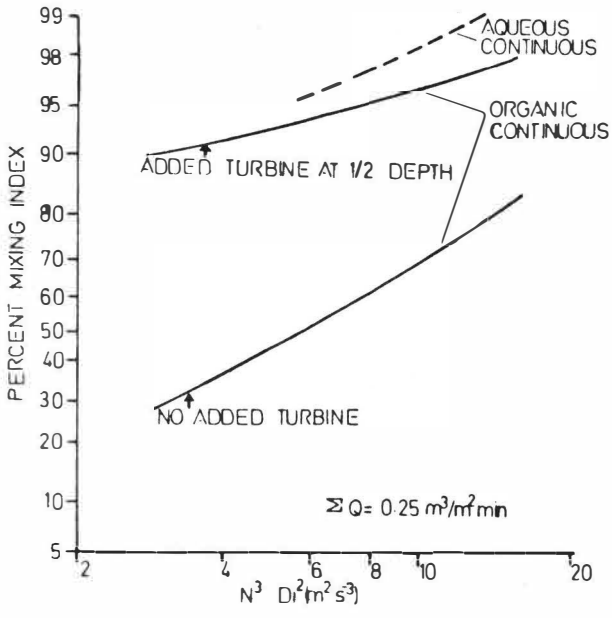

FIG. 5
Comparison of Turbine Addition
Laboratory Unit

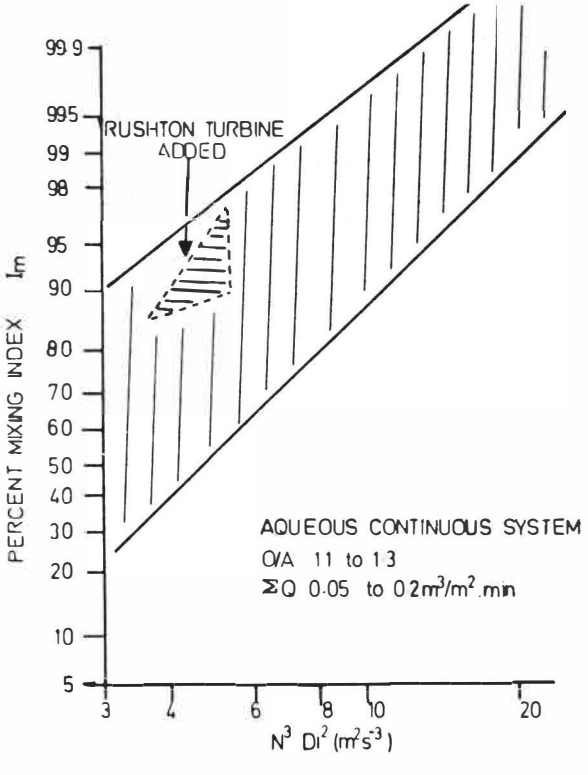

FIG. 6
Aqueous Continuous Correlation
Pilot Plant

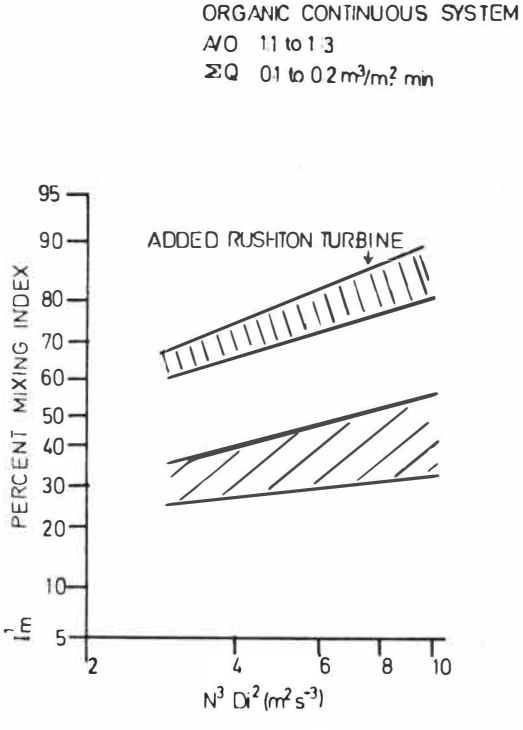

FIG. 7
Organic Continuous Correlation
Pilot Plant

Pilot Mixer Unit

An added investigation was the effect of (a) impeller clearance from the inlet-base plate, (b) a Rushton turbine impeller mounted half way up the shaft from the pump-mix impeller.

Figures 6,7 show the spread of data for both aqueous and organic phase continuous systems. The scatter is considerable compared to the better controlled conditions of the laboratory unit. However, for either phase dispersed, the laboratory mixer and larger pilot unit have similar performance relative to $N^3D_i^2$.

As the impeller clearance is increased, shown in Figures 8,9, the mixing index improves for either system; more so for the organic continuous runs at higher $N^3D_i^2$. This general finding has been qualitatively reported in investigations with Power Gas type mixers. (5)

The addition of a Rushton turbine to the midsection of the shaft does not alter performance in the aqueous continuous system.

For the organic continuous runs, however, it is quite clear that there is a considerable improvement in "mixedness" or mixing index. The addition of the extra turbine evidently widens the "sphere of influence" of the mixing zone for which the mixing index I_m is a simple direct measure of this effect.

DISCUSSION

In generally comparing the aqueous and organic continuous systems,with varying $N^3D_i^2$, it can be seen that the aqueous continuous has a much higher mixing index or better "mixedness" than the organic continuous system, for the same total flow rate and $N^3D_i^2$. This could partly explain why an organic continuous dispersion in the settler is very much smaller in volume. For

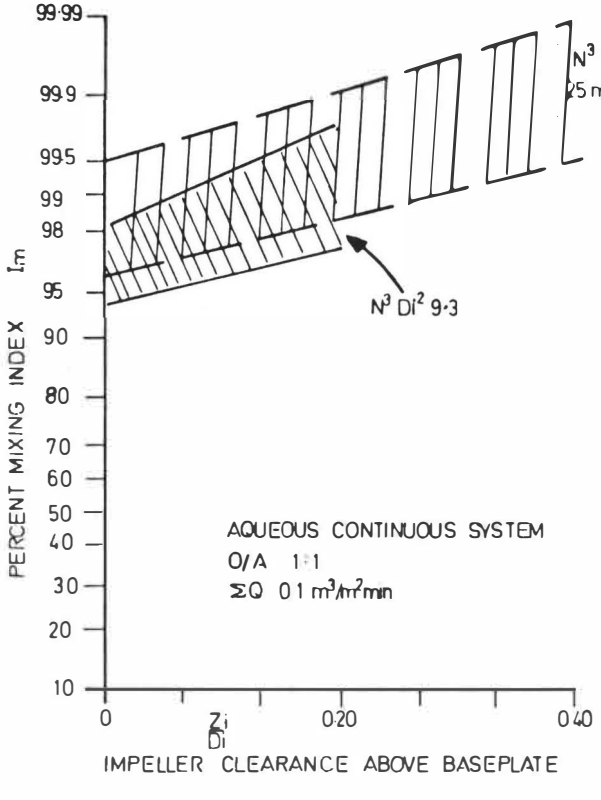

FIG. 8
Impeller Clearance-Aqueous Cont.
Pilot Unit

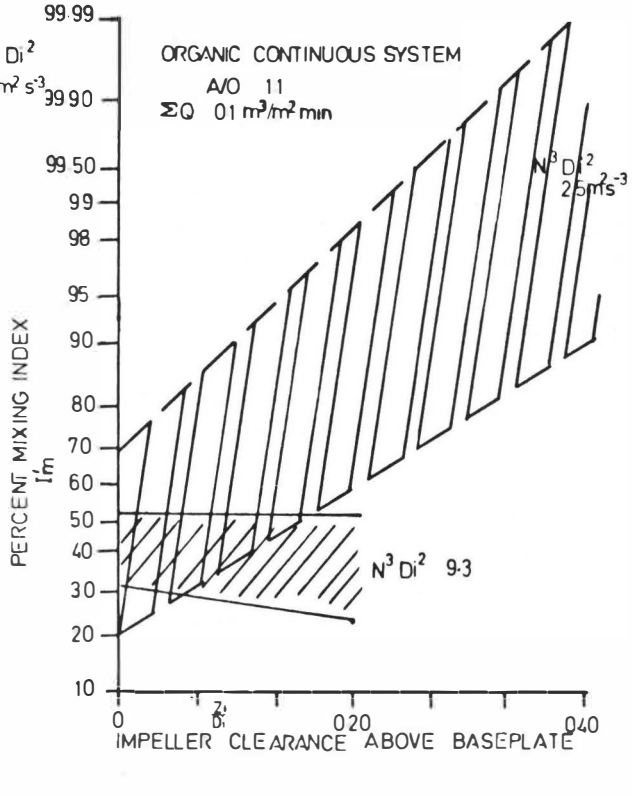

FIG. 9
Impeller Clearance-Organic Cont.
Pilot Unit

Begin here example, see Figures 2,3, at $N^3D_i^2$ 5.6 m^2s^{-3} and ΣQ = 0.2 $m^3/m^2.min$,

I_m = 87 percent in the aqueous continuous

and I'_m = 45 percent in the organic continuous system.

This could be inferred to mean that 13 percent of the dispersion had already coalesced in the aqueous continuous system, but 55 percent had coalesced in the organic continuous mixer unit prior to flowing through the picket fence into the settler.

The other important comparison is in attempting to achieve the same mixing index for both systems. Again, using the same example as before, $N^3D_i^2$ = 5.6 m^2 s^{-3} aqueous continuous, I_m = 87 percent; the organic continuous system would need to run at $N^3D_i^2 \sim 19$ or greater than three times the power requirement of the former.

By adding a Rushton turbine to the shaft, the needed $N^3D_i^2 \sim 11$ or about twice the power required as before.

The final consideration is the effect of improvement of "mixedness" on stage efficiency and mass transfer rate. For a fixed D_i/D_T, mass transfer calculations have provided the following table

INFLUENCE OF MIXING INDEX

Parameter	Maximum Mixing Index (I_m) 0.75	0.90	0.95
Stage Efficiency %	87.9	88.9	89.3
Mass Transfer Rate N, $kg/m^3.min.$	11.9	13.3	13.7
Total Operating Cost, \$/min	0.0493	0.0488	0.0487

For $\frac{D_i}{D_T}$ = 0.40; D_T = 1.0 m; $N^3D_i^2$ = 5 m^2s^{-3}

Stage efficiencies are marginally improved and operating costs are slightly lower; however the mass transfer rate is considerable enhanced. Thus improving the "mixedness" gives more profitable metal extraction at lower overall running cost.

CONCLUSIONS

Mixer holdup is an important parameter in extraction economics for determining or understanding:

(i) disperse phase residence time
(ii) phase segregation
(iii) Sauter mean droplet diameter and specific surface area
(iv) mass transfer rate
(v) droplet coalescence.

(a) Disperse phase holdup for either phase dispersed can be adequately correlated by eqn (1)

$$\phi_D = I_m \cdot \frac{Q_D}{Q_D + Q_C}$$

with I_m termed the mixing index.

(b) The mixing index is independent of flow ratios, but is dependent on $N^3D_i^2$ and system properties.

(c) Mixing index is well correlated by

$$I_m = 1 - \exp(A - B.N^3D_i^2) \text{ for aqueous continuous}$$

and $$I_m = 1 + \exp(A - C.N^3D_i^2) \text{ for organic continuous systems.}$$

(d) For constant system liquid properties, coefficients B, C in (c) above are correlated by

$$B \text{ or } C = m\ (\Sigma Q)^n$$

with m,n being equipment coefficients.

(e) With constant flow rate in one continuous flow mixer assembly but varying liquid phase properties

$$B \text{ or } C \propto 1/(\delta\Delta\rho^{4/3})^{0.49}$$

providing a near perfect correlation.

(f) For a pump mix assembly at constant flow rates and $N^3D_i^2$ the mixing index is much greater for an aqueous rather than organic continuous system.

(g) At higher $N^3D_i^2$, for either phase dispersed, a wide clearance between baseplate and impeller improves mixing index.

(h) A flat-bladed turbine about midsection on the shaft considerably improves mixing index for organic continuous conditions with otherwise constant conditions.

REFERENCES

1. Treybal R.E., "Estimation of the Stage Efficiency in Mixer-settler Extractors", A.I.Ch.E.J. 4, 202-7 (1958)

2. Treybal R.E., "Stirred Tanks and Mixers for Liquid Extraction" I.E.C. 53, 597-606 (1961)

3. Lott J.B., Warwick G.I. and Scuffham J.B., "Design of Large Scale Mixer-settlers", Trans. A.I.M.E. 252, 27-35 (1972)

4. Rowden G.A. et al, "Considerations of Ambivalence Range and Phase Inversion.....", I.Chem.E.Symp.Series No.42, 17.1-17 (1974)

5. Orjans J.R., et al "The Design of Mixer-settlers for the Zambian Copper Industry", I.S.E.C.(1977) 60, p58-9.

6. Godfrey J.C., Grilc V., "Drop-Size and drop size distribution...." Mixing Conference, Cambridge Univ. U.K. (March 1977), 28 pages

7. Van Heuven J.W. and Beek W.J., "Power Input, Drop Size for Liquid-Liquid Dispersions", I.S.E.C. (1971), Paper 51, p12-23.

8. Luhning R.W., and Sawistowski H., "Phase Inversion in Stirred liquid-liquid Systems",I.S.E.C.(1971), Paper 136, p51-65

9. Roberts J. et al "Improving the Performance of Gravity Settlers with Vertical Baffles and Picket Fences", I.S.E.C.(1977) 8e pp418

10. Lewis I.E.,"Design of Mixer-Settlers to achieve low Entrainment Losses and Reduce Capital Costs",I.S.E.C.(1977) 7a, pp325.

ACKNOWLEDGEMENT

To Conzinc Riotinto Australia for use of their pilot unit on site.

LOGICAL PUMP DESIGN FOR PUMP MIX MIXER-SETTLERS

E. Barnea, D.Meyer, S. Wahrmann

I.M.I. Institute for Research & Development,

Haifa, Israel

ABSTRACT

A logical method of pump-mix design has been developed, based on rearrangement of the classical parameters into dimensionless groups. The design method permits experimental investigation of parameters on a suitably small scale, and selection of the optimum parameter assembly for a particular application.

1. INTRODUCTION

The design of mixing and pumping equipment has been based on practical considerations, including:

- mass transfer considerations, namely a close approach to equilibrium narrow residence time distribution, high turndown ratio, low response time.
- effect on phase separation, including maximum droplet size on a narrow drop size distribution.

IMI has devoted much effort to the development of high throughput contacting equipment based on the concept of hydraulic independence between mixer and settler and between adjacent units.
Two types of pumping equipment have been evolved - the axial pump and the turbine pump; these have been described previously (1,2).
The conflicting demands on a pump-mix unit, which may be summarized as generation of sufficient surface for efficient mass transfer without impairing phase separation, necessitate the formulation of a logical, empirically based design procedure supported by the generation of the necessary experimental data. In this paper the principles for design, and scale-up and the experimental set-up are described.

2. THE PUMP MIX UNITS

The basic concept for mixer design is absolute hydraulic independence

between mixer and settler and between adjacent units, in order to eliminate backmixing and to prevent backflow on plant shut-down. The design must also take limitations of materials of construction into account as one or both of the fluids handled may require special materials in order to ensure integrity of equipment.
The contradictory demands (1) have led IMI to develop two design solutions namely:

- the axial pump mix unit
- the turbine pump mix unit

In both axial and turbine pumps, the mixing and pumping effects are obtained from a single drive unit. The shapes of rotating parts have not been designed to generate flow lines of minimum turbulence; However, considering the absolute velocity along the blades, the relatively small sacrifice in efficiency is an acceptable price to pay for the ease of fabrication. Cavitation is not a problem at the speeds normally encountered.

2.1. The Axial Pump Mix

This consists of an axial flow impeller housed in a draft tube, equipped with straightening vanes located upstream and downstream of the impeller (FIG.1).Mechanical considerations fix the diameter

FIGURE 1

THE AXIAL PUMP MIXER

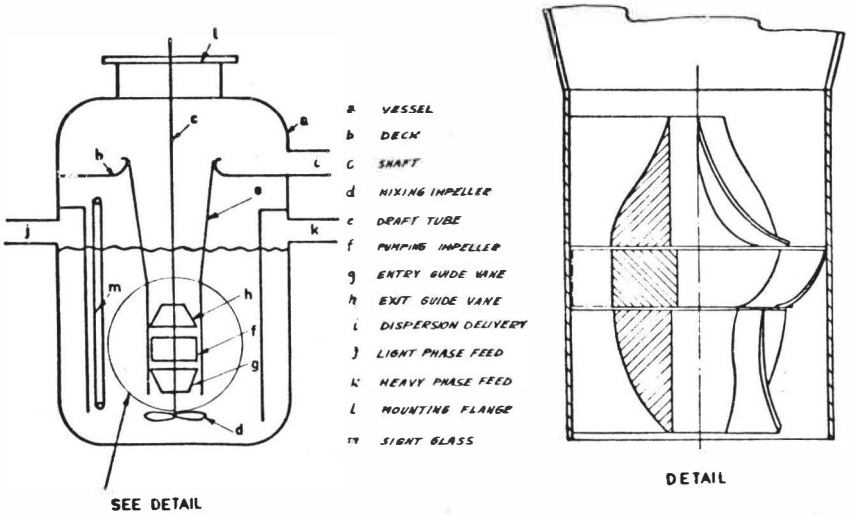

of pumping and mixing impeller while mass transfer and phase separation determine the speed range. The design solution shows acceptable mechanical efficiency at low speeds. The unit is designed for easy removal for maintenance of the rotating assembly. The surfaces of both impeller and guide vanes have simple curvatures and the clearance between the impeller vanes and the draft tube is small. The axial unit is characterised by a small high shear mixing zone and relatively large recoalescence zone.
The unit thus provides an ideal solution where mass transfer is easy and phase separation is relatively insensitive to mixing parameters and dispersion type.
Its main advantages are simplicity, low cost and insensitivity to operating conditions. Limitations are liability to breakage when constructed in synthetic materials if solid material is present, broad residence time distribution, a need for accurate balancing and an upper size and capacity limit.

FIGURE 2
THE TURBINE MIXER

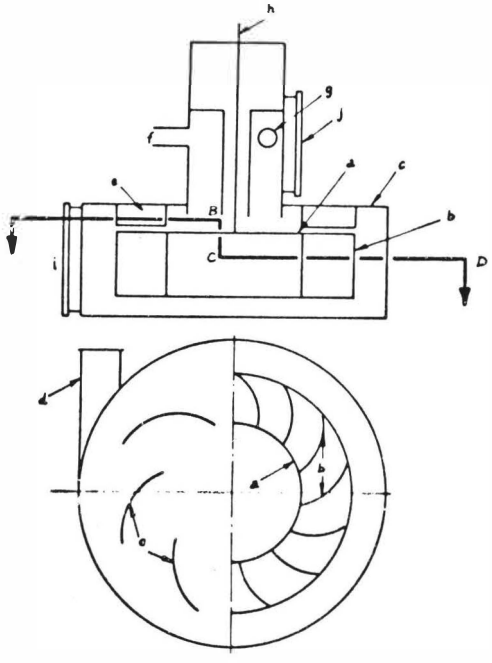

SECTION ABCD

a TURBINE
b TURBINE BLADES
c MIXING COMPARTENT
d TANGENTIAL DISPERSION DELIVERY
e STATOR BLADES
f LIGHT PHASE ENTRY
g HEAVY PHASE ENTRY
h SHAFT
i SIGHT GLASS
j SIGHT GLASS

2.2. The Turbine Pump Mix

This consists of a curved blade turbine of large diameter relative to the vessel (FIG.2). It is equipped with a stator which forces a recirculation within the pump, which is many times the nett throughput.The unit features high mass transfer efficiency ensuring maximum exploitation of the mixer volume and by an intensive coalescence-redispersion cycle induced by recirculation. Narrow clearances are avoided, reducing the sensitivity of the presence of solids. Low speeds of rotation are employed for sensitive liquid-liquid systems and for production of large drop size with a narrow size distribution. The turbine pump is designed for large throughputs, efficiency of mass transfer and optimal dispersion control.

3. EXPERIMENTAL SET-UP

An experimental set-up for testing both units is shown in FIG.3.
Prototypes are tested under varying conditions of flow, heat and rotational speed. Absorbed power is also measured. Data obtained are displayed on the classical head vs throughput, power vs throughput curves, and are converted for use in the design correlations.

The unit has been designed for pumping impellers of 100-150 mm (axial pump) and up to 450 mm diameter (turbine pump). It permits throughputs of 0-40 m^3/hr, heads of 0-100 cm and rotational speeds up to 1000 rpm. Sizing of the test unit was defined as a compromise between minimizing scale-up factors and avoiding excessive test equipment size.

FIG. 3
EXPERIMENTAL SET UP FOR PUMP TESTING

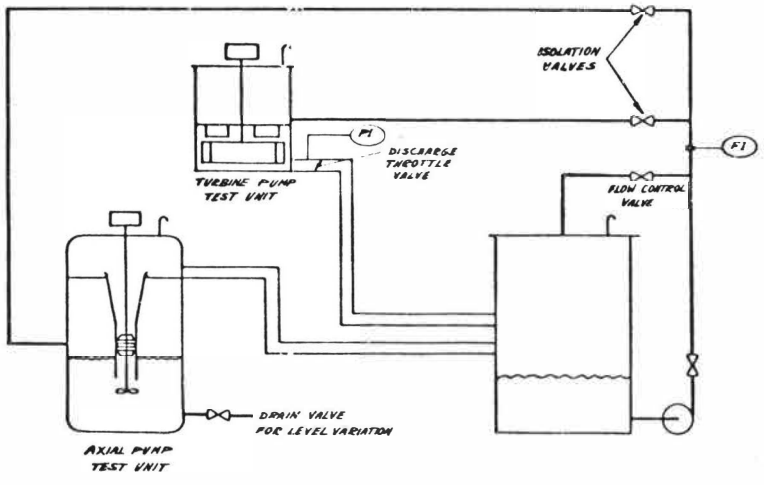

For special cases, or where a design may fall close to the boundaries of the data base of the design correlations, a full scale prototype may be built.

4. DESIGN BASIS

4.1. Principles for Design Procedure

The pump, fully geometrically described, (data base for identification) is tested in the prototype test unit. The performance of rotary pumps depends upon a number of dimensional parameters, all of which are closely interconnected. Unfortunately the classical description of pump characteristics i.e. head developed against flow and power absorbed against flow at varying speeds does not yield more than an intuitive picture of the effect of design parameters on performance, and scale-up based on these characteristics is also intuitive to a great extent.
Analysis of results show that the classical proportionalities i.e. $Q\alpha\ N$, $H\ \alpha N^2$, and $P\ \alpha N^3$ apply. Dimensional analysis shows that the following relationships can be derived:

$$Q\ \alpha\ ND^3$$
$$gH\ \alpha\ N^2D^2$$
$$P\ \alpha\ N^3D^5$$

If full geometrical similitude is assumed, the pump characteristics can now be described as two dimensionless spaces which can be defined as plots of $gHN^{-2}D^{-2}$ against $QN^{-1}D^{-3}$ and ρQHP^{-1} against $QN^{-1}D^{-3}$. These dimensionless characteristics have been plotted for both axial and turbine pumps of different sizes (FIGS. 4,5,6)

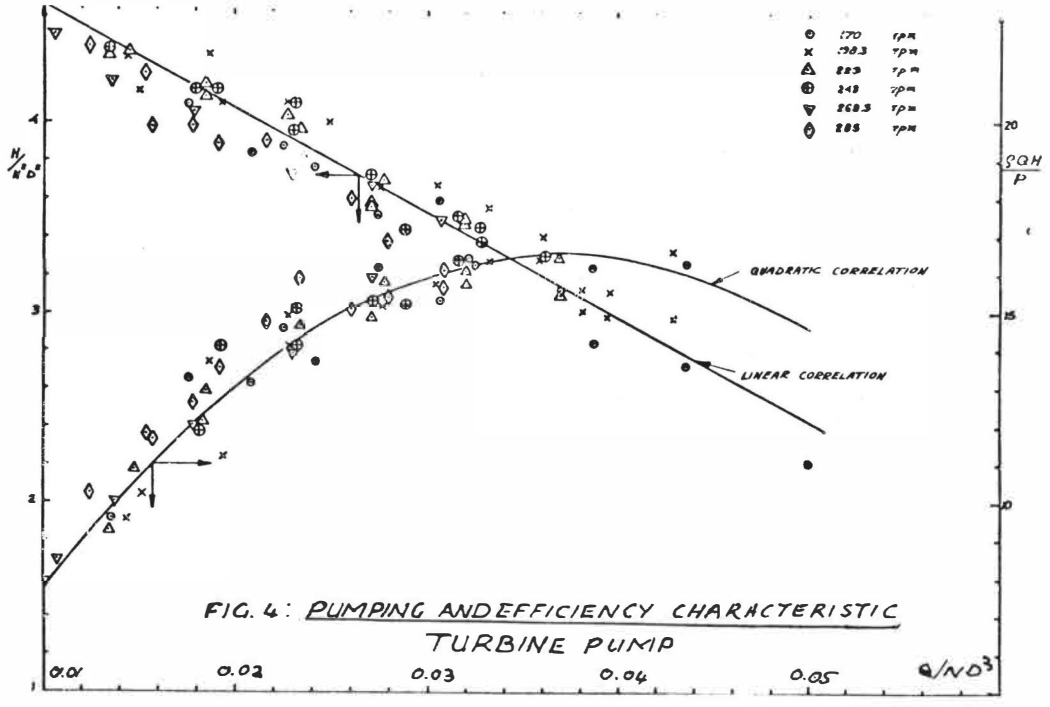

FIG. 4: PUMPING AND EFFICIENCY CHARACTERISTIC
TURBINE PUMP

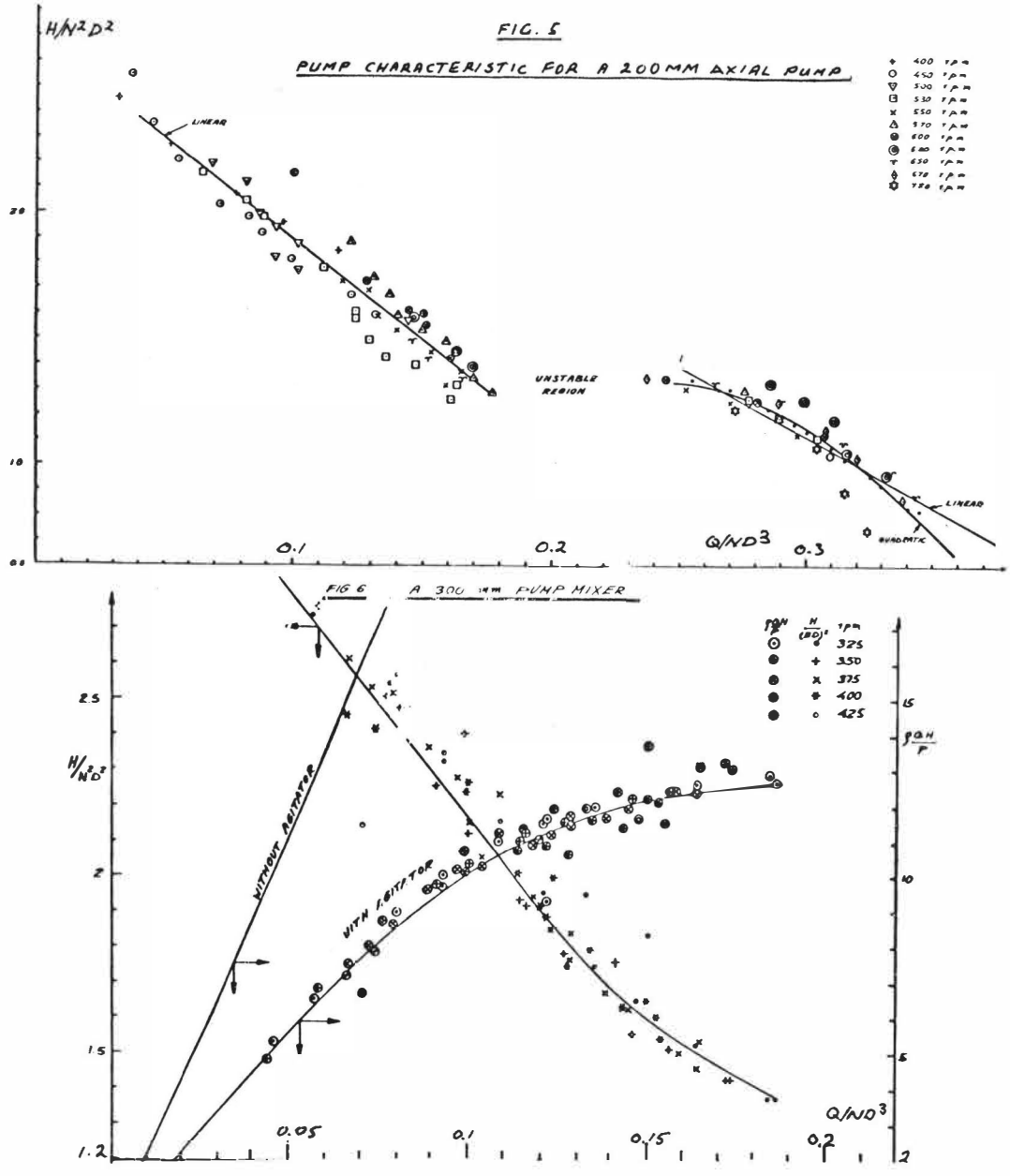

Analysis of experimental data shows that the use of such plots is valid for a large range of rotational speeds.

4.2. Analysis of Results

For the turbine pump, FIG.4 indicates that there is a moderate dependence of pumping efficiency and head developed on the pump throughput which permits using fixed speed pumps. The apparent low efficiencies are a result of the high recirculation rates required for mass transfer.

For the axial pump mix, FIG.5 shows two regions of sharp dependence of head on throughput with an instable region between them. Operation in this region is avoided. The influence of an upthrust mixer impeller on the pumping efficiency is also evident from the characteristics drawn in FIG.6.

4.3. Application of the Design Procedure

The application of the procedure described above can now be formulated. The use of the non-dimensional analysis permits derivation of mathematical expressions for the characteristics. Polynominal fits have generally been shown to be sufficient. The use of mathematical correlations allows easy use of optimization algorithms.

It has been found that highly significant statistical expressions are obtained for each case and the mathematical expression can confidently be used for scale-up and optimization.

The procedure is used for several purposes.

4.3.1. Determination of the optimal impeller configuration. A systematic study of different mixer geometries can now be carried out using the test unit with various impellers. Valuable information then be found in order, for each application, to determine the optimal impeller configuration. In FIGS. 7 and 8 the influence of various parameters for a turbine pump such as number of blades, angle of attack, stator, etc., are shown.

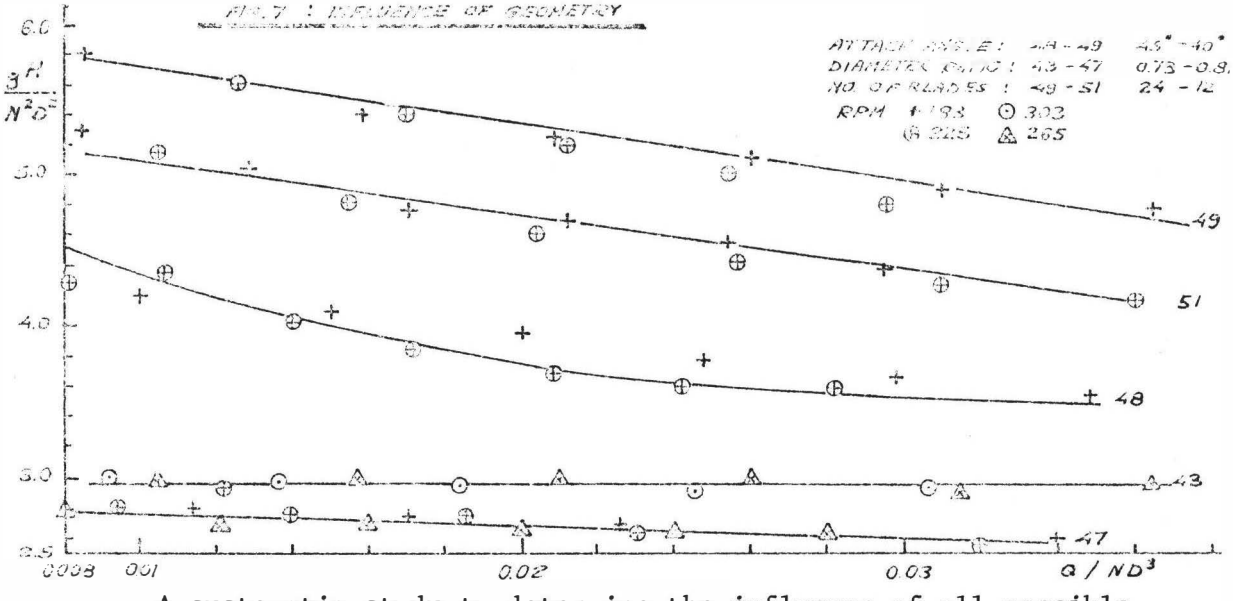

A systematic study to determine the influence of all possible parameters is being undertaken.

4.3.2. It is clear that the scale-up of a pump using the dimensionless characteristics will only apply for cases with full geometrical similitude. Several applications have been noted:

a) Determine the operating point of a turbine with given head, throughput and residence time.
This problem is obvious as throughput and residence time define the diameter and only the operating speed has to be found.
The efficiency of the pump is then given.

b) For a given throughput and head find the optimal mixer. The problem is then to maximize the efficiency and determine the feasible diameter and speed. Such a problem should also contain constraints on optimal operation for mass transfer which complicates the solution.

A mathemathical approach (optimisation) is here advantageous. Determine the operating conditions of a mixer for given throughput and head.

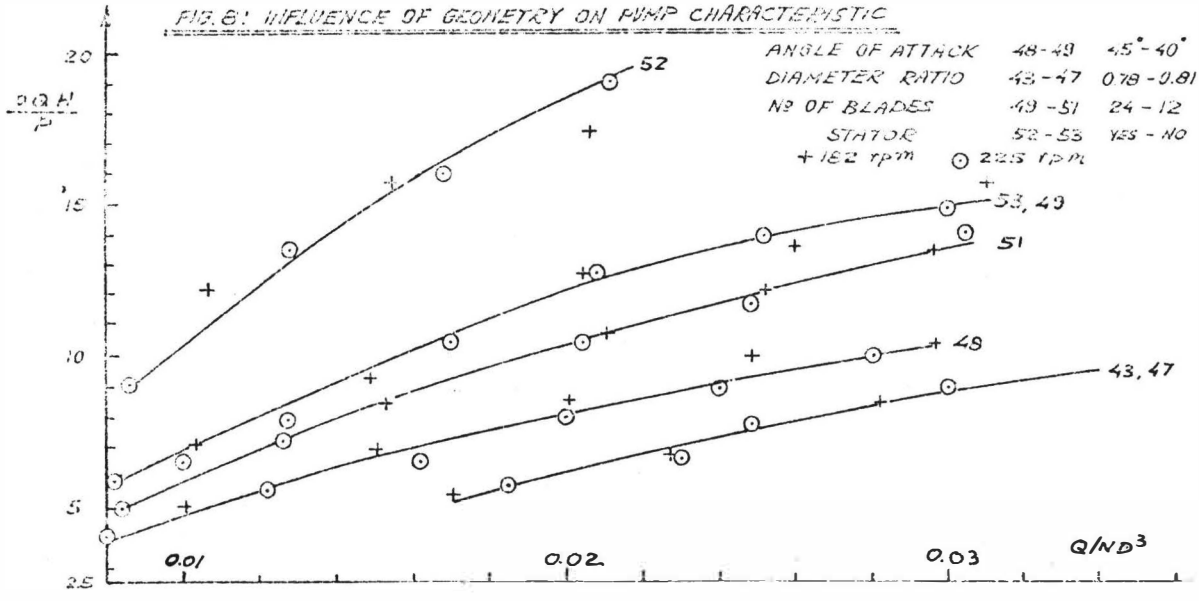

Nomenclature

Q = volumetric fluid flow
N = rotational speed
D = impeller diameter
H = pumping head
P = power absorbed
g = gravitational acceleration
ρ = fluid density

All quantities are expressed in dimensionally consistent units.

REFERENCES

1. J. Mizrahi, E. Barnea and D.Meyer. Proceedings ISEC 1974.

2. IMI Staff Report. Proceedings ISEC 71 Paper 94.

COPPER EXTRACTION WITH A SULZER IN-LINE MIXER USING ACORGA REAGENT P5100

J.C.Godfrey, M.J.Slater, A.Temple,
Schools of Chemical Engineering,
University of Bradford,
W. Yorks, BD7 1DP
U.K.

N.P. Wynn,
M. Zabelka,
Sulzer Bros.Ltd.
CH 8401
Winterthur,
Switzerland.

ABSTRACT

A study has been made of the extraction of copper from acid solutions using a Sulzer static mixer and the extractant P5100. Rate of extraction was measured as a function of velocity and residence time. Phase inversion, settler and entrainment characteristics were also studied. Extraction performance was compared with predictions for a continuous stirred tank on the basis of power consumption and residence time. The Sulzer mixer offers considerable advantages under extraction conditions of practical interest.

INTRODUCTION

For many years large scale mixer-settlers have been used in hydrometallurgical applications. The most widely used mixer design is the pump-mix type in which compromise is necessary between pumping and mixing requirements. One aspect of mixer performance where improvement has been sought is in extraction rate. This can be obtained by using longer residence times or more agitation. Problems have also been experienced with phase stability and high entrainment levels in large equipment.

Because of these disadvantages attention has been paid to the use of in-line mixers containing fixed mixing elements as an alternative to the agitated tank. The plug flow characteristic of the in-line mixer is theoretically superior to the fully backmixed agitated tank for a homogeneous process and if this is also the case for heterogeneous systems the size of an in-line mixer should be smaller than an agitated tank for the same duty.

In an agitated tank there is ample opportunity for coalescence and redispersion of the dispersed phase, thought to be a desirable process for mass transfer. In an in-line mixer energy distribution is more uniform and the opportunity for coalescence and redispersion seems less. Claims have been made for better coalescence characteristics for the dispersion from in-line mixers because of an assumed narrow drop size distribution. The evidence for these claims is not strong.

Although pump-mix equipment has been in use for a long time and the design principles are well established there is little quantitative design information available. For the in-line mixer the topic of pressure loss is well understood and there have been several drop size studies. Data have been presented for empty pipes (1), the Kenics mixer (2,3) and the Sulzer mixer (4). Streiff reports a correlation for drop size in the Sulzer mixer:

$$\frac{d_{sm}}{d_h} = We_h^{0.5} \; Re_h^{-0.15} \qquad (1)$$

and uses the Rosin-Rammler-Sperling equation to describe drop size distribution. Middleman (2) has also studied drop size distribution for the Kenics mixer. The influence of hold-up on drop size, in contrast to agitated tanks, has been reported to be slight(2,3). Tunison and Chapman(3) have studied copper extraction using the Kenics mixer and the extractant Kelex 100 in xylene. They discuss the problems encountered in using drop size in the interpretation of rate measurements. Merchuk, Shai and Wolf(5) have also studied extraction using both Koch (under licences from Sulzer) and Kenics in-line mixers using the extractant LIX64N in an unspecified kerosene. They compare the extraction performance and energy requirements of the in-line mixers with packed tube, empty tube and continuous agitated tank data.

In the present paper an experimental study has been made of extraction in terms of concentration and time, phase inversion and settler characteristics. Measurements have been made over a range of velocities and flow ratios and comparisons made with the performance of an agitated tank including the consideration of energy requirements.

EQUIPMENT

Stainless steel Sulzer mixing elements (type 4Y) were used in glass tubes of 22mm diameter in lengths of 0.5m, 1.0m and 1.5m. A range of diameters were used for the inner inlet tube, see figure 1, so that equal inlet velocities for the two liquid phases could be obtained at flow ratios of 1/1, 3/1 and 4/1 (O/A)

FIG.1
INLET ARRANGEMENT

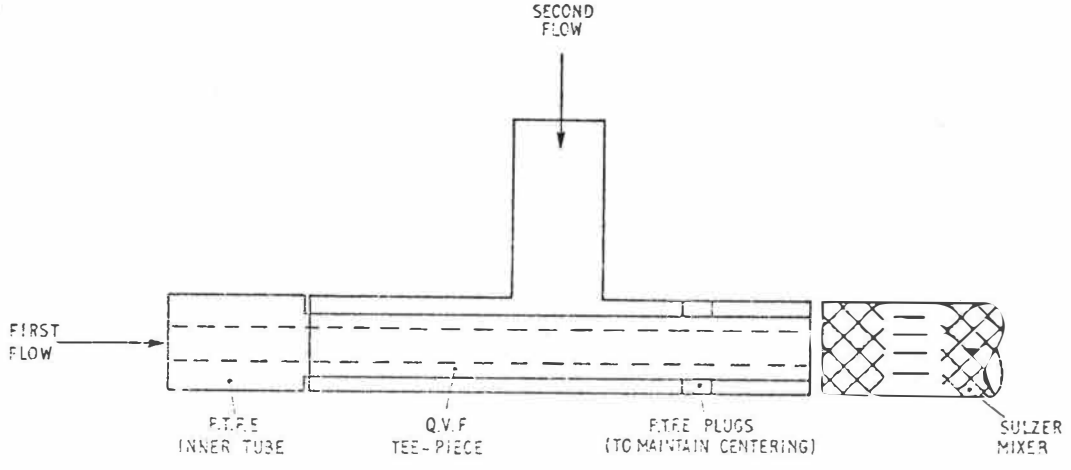

A rectangular perspex settler was used to separate the dispersion. The 300ℓ feed tanks were medium density polyethylene and the centrifugal pumps had glass filled polypropylene impellers and housing with magnetically coupled ceramic spindles. Fittings and pipework were in stainless steel with some Viton tubing and PTFE valve diaphrams and seals.

PHASE STABILITY

In the agitated tanks used in mixer-settler equipment it is possible to operate with either aqueous or organic phase dispersed over a wide range of flow ratios. It is likely that the extent of this ambivalent region may be affected by equipment size, equipment design, mass transfer, degree of turbulence and materials of construction but as yet the subject is not well documented. However, since mass transfer rates, settler coalescence characteristics and entrainment levels can be affected by which phase is dispersed, some understanding of phase stability is required.

An aqueous stream of $2kg/m^3$ H_2SO_4 in de-ionized water (no copper) was introduced to the mixer through a centrally located inlet tube, Fig.1. The organic stream (no copper) of 10% by volume P5100 (Acorga) in the kerosene diluent Escaid 100 (Exxon) was introduced into the annulus around the aqueous phase inlet tube. Each test was commenced at a flow ratio of A/O=1/1 and at a maximum flow rate available. This starting condition always produced an organic drop dispersion. The organic flow rate was then slowly increased and the aqueous flow rate simultaneously decreased, keeping the total flow constant, until inversion occurred to give an aqueous drop dispersion. The process was then reversed until once again the organic phase became dispersed. The total flow was then reduced and the experimental procedure repeated. Because these experiments by necessity covered a range of flow ratios it was not possible to maintain equal velocities in the two liquids. To assess the effect of relative inlet velocities the inlet pipe diameter was changed and the experiments repeated.

Early in the experimental programme it was found that aqueous dispersed conditions were being favoured progressively as the equipment and liquids aged. No difference in interfacial tension (0.015 to 0.016 N/m) was found between fresh and aged liquids. As a further check the equipment was treated with a Decon 90 solution and then washed with water to remove any organic surface contaminants; the effect on performance was negligible. Reproducible results were only obtained after the test liquids had been passed through the mixer several times. Changes in the diameter of the central inlet tube had no significant effect over a wide range of velocity ratio. In one experiment the inlet conditions were reversed (organic phase in the central tube) and it was notable that this condition favoured the aqueous dispersed behaviour.This behaviour was also favoured by increasing the mixer length from 0.5m to 1.5m.

A plot of phase stability characteristics is given in Figure 2 showing an upper region where the organic phase is always dispersed and a lower region where the aqueous phase is always dispersed. Unlike the agitated tank there is no true ambivalence region but only a narrow band where both types of dispersion are formed. In this mode of operation slugs of opposite phase continuity travel consecutively along the tube. This is an ill-defined operating condition likely to lead to the generation of very small drops which may be entrained from the settler.

FIG. 2

SULZER STATIC MIXER;PHASE STABILITY
1.5m MIXER LENGTH,ENTRY TUBE
AREA RATIO 1.0, NO MASS TRANSFER

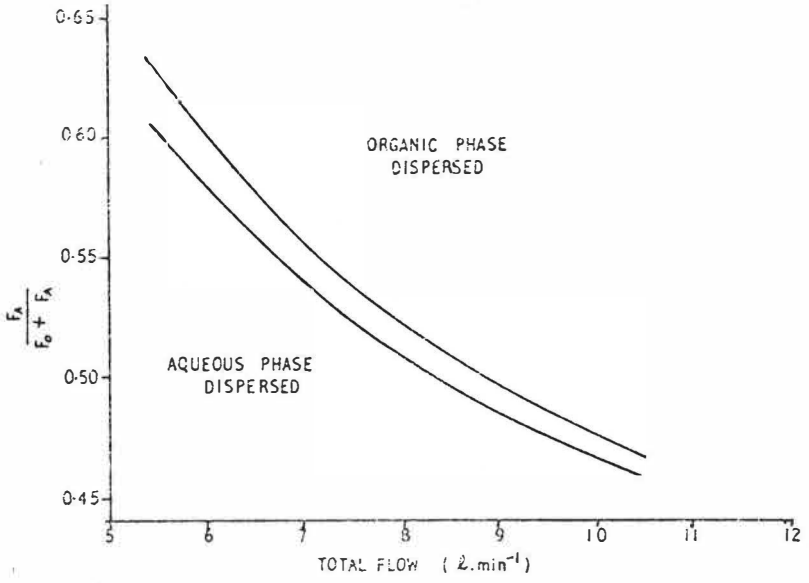

Away from this region flow ratio and throughput determine which phase will be dispersed in contrast to the agitated tank where start-up procedure determines which phase will be dispersed in the ambivalent region.

During mass transfer experiments (described in detail below) with an aqueous phase containing 3kg/m^3 Cu and 2kg/m^3 H_2SO_4 fed through the centre tube it was this phase that was dispersed in all cases. The flow ratio was varied from A/O = 0.82/1 to A/O = 1.22/1 with velocities up to 0.50m/s in a mixer 1.0m long. With an aqueous phase containing 5.12kg/m^3 Cu and 2kg/m^3 H_2SO_4 the phase dispersed, although steady in any one experiment, changed in an irregular manner from experiment to experiment. The flow ratio was A/O = 1/1 with a velocity of 0.59m/s.

There are few data available on phase inversion in in-line mixers and nothing which is directly comparable with the present work. Tunison and Chapman (3), using Kelex 100 in xylene for the extraction of copper, found that the Kenics mixer always gave organic drop dispersions over a wide range of flow ratios for velocities up to 0.19 m/s. Similarly Merchuk et. al. (5) using LIX64N in kerosene obtained organic drop dispersions in Kenics and Sulzer type mixing equipment. In both studies the predominance of organic drop dispersions and aqueous continuity is likely to be the combined influence of wetting properties and small equipment.

SETTLER PERFORMANCE

Measurements were made of dispersion band depth as a function of through put of dispersed phase per unit horizontal settler area for mixer velocities of 0.307 m/s and 0.504 m/s at a flow ratio of A/O = 1/1. Dispersion band depth was varied by changing the settler area. The aqueous and organic streams used contained copper but had been previously equilibrated so no mass transfer occurred during the tests. However, these measurements proved

time consuming and a procedure was adopted where samples were taken at the mixer exit in a measuring cylinder (2ℓ) and the data obtained used to estimate continuous settler performance (6).

FIG. 3
COALESCENCE DATA

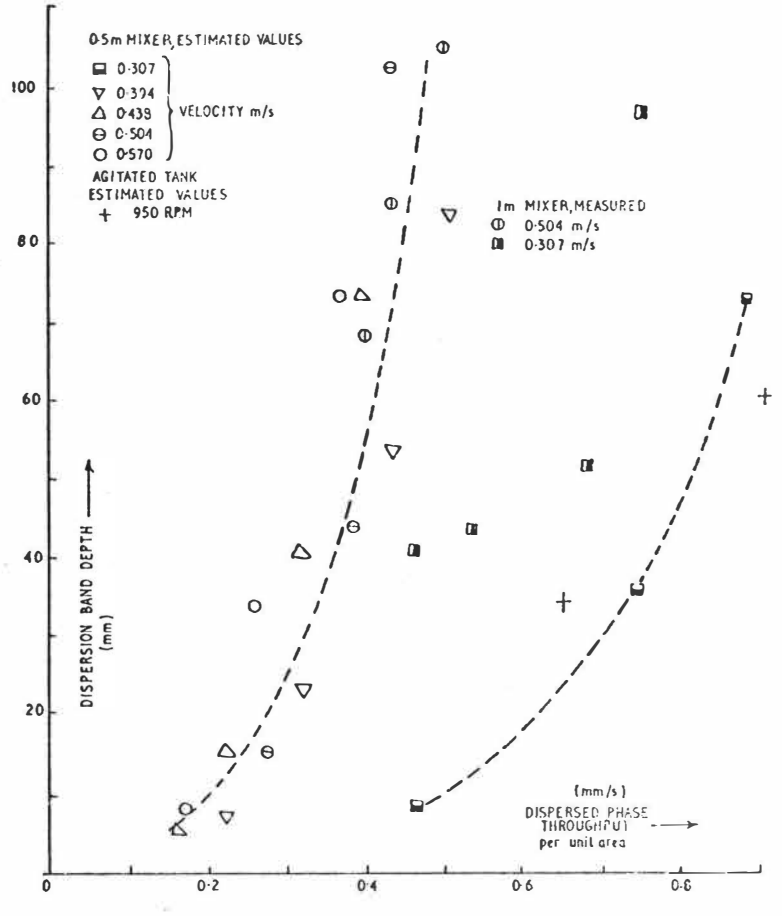

In the velocity range 0.394 m/s to 0.570 m/s the agreement between measured and predicted data is good with little influence of velocity (Fig.3). At 0.307 m/s, the dispersion bands were much thinner with more scatter and less agreement with predicted values. Mixer length did not affect performance.

Batch tests were conducted with the agitated tank used for extraction studies (950 rpm, P/v = 2 kW/m^3). Predictions from these data fall near the predictions for the Sulzer mixer at 0.307 m/s.

ENTRAINMENT

In the operation of large scale settlers high levels of entrainment are sometimes encountered and it has been demonstrated that the level of energy input is an important factor (7). Thus a possible limit on operating velocity with static mixers may be set by excessive entrainment. In this work a study has been made of entrainment of the organic phase in the aqueous under conditions where the aqueous phase was dispersed. Equilibrated liquids were used at a flow ratio of A/O = 1/1 at velocities of 0.504 m/s and 0.705 m/s.

Samples of dispersion were collected according to a previously established procedure (6). The sampling procedure must also be consistent with respect to the age of the sample since larger entrained drops are lost progressively. The levels of entrainment recorded were low, 12 ppm at the lower velocity and in the range 14 to 30 ppm at the higher velocity. In the settler both phases were visually clear.

MASS TRANSFER

With slower mass transfer processes, as can be the case with copper extraction, a degree of success has been achieved in predicting approach to equilibrium in a continuously operated tank from batch studies at the same scale using simple reactor theory. For the present in-line mixer programme approach to equilibrium was studied as a function of velocity and residence time. Short lengths of mixer tube were used and repeated passes employed to give a range of residence times. The data were processed to give the relationship between concentration, C, and its rate of change with time, dC/dt, which avoids some end effect problems.

In all experiments the aqueous phase was introduced through the central feed tube with the area ratio of the two inlet regions at 1.0. Tube lengths of 0.5 m and 1.0 m were used and contact times per pass ranged from 0.846 s to 3.54 s. Samples of dispersion were collected at the tube exit and, since the aqueous phase was always dispersed, an electrostatic field was used to accelerate coalescence. Without the use of electrostatic field the long coalescence times cause problems due to the continuing mass transfer during phase separation.

Since steady state operation is established within one minute at any particular operating condition several velocities could be used in any one run with the same feed streams. The products could be used as the feeds for the next run, once again collecting data for a range of velocities. This procedure produces discontinuities in the concentration versus residence time plot but the data may be satisfactorily processed by determining dC_A/dt as a function of C_A. A value of dC_A/dt can be estimated from the inlet and outlet concentrations and contact time for each pass:

$$\frac{C_{A\ in} - C_{A\ out}}{\Delta t} = \frac{\Delta C_A}{\Delta t} \simeq \frac{dC_A}{dt} \qquad (2)$$

The corresponding concentration value, C_A, is also estimated from the average of inlet and outlet concentrations. The equilibrium data are described by the equation:

$$\frac{C_o}{5.25 - C_o} = 35\,\frac{C_A}{3 - C_A} \qquad (3)$$

The effect of velocity was studied at a flow ratio of A/O = 1/1; the results are presented in terms of $F_A \Delta C_A/\Delta t$ as a function of C_A in Figure 4, where a comparison of the total rate of copper mass transfer for various velocities can be made. In all cases total mass transfer rate increased with throughput. Similarly, the value of $\Delta C_A/\Delta t$ is increased and high total mass transfer rates are not obtained at the expense of reduced approach to equilibrium. A similar relationship was observed between extraction rate and velocity by Merchuk et al (5). Figure 4 also includes data obtained with an aqueous feed stream containing 5 kg/m^3 Cu, 2 Kg/m^3 H_2SO_4 when the extraction rate is much lower, indicating that the rate is at least partly chemically

controlled. It may be important to note that there are variations in copper concentration in the feed streams used by Merchuk et al (5) in the comparison of various mixer types. Because of the differences in copper concentration and equipment size it is difficult to make any direct comparisons between the results of Merchuk or Tunison and the present work.

FIG.4
EFFECT OF VELOCITY ON EXTRACTION

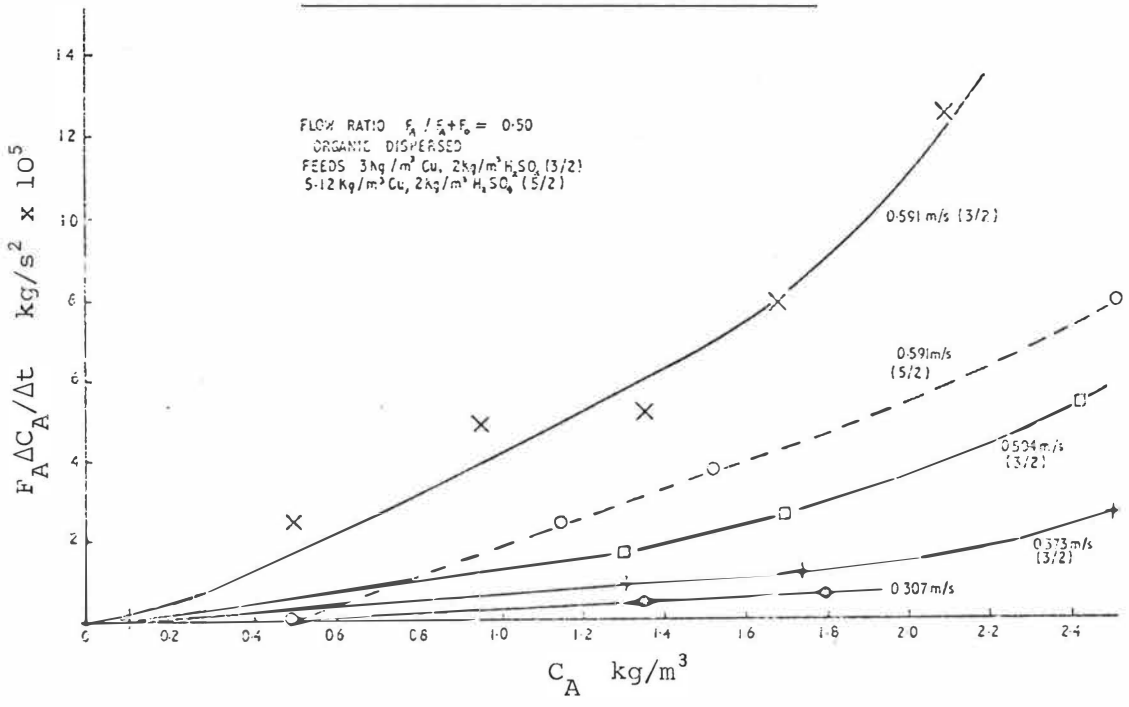

COMPARISON OF MASS TRANSFER IN THE SULZER IN-LINE MIXER AND AN AGITATED TANK

Batch agitated tank extraction tests were conducted using 3 kg/m^3 Cu and 2 Kg/m^3 H_2SO_4 with 10% P5100 in Escaid 100. A square cross section tank 150 mm x 150 mm with two vertical side baffles was used with a liquid depth of 150 mm. A six blade Rushton turbine of 51 mm diameter was run at 950 rpm. Aqueous and organic dispersed conditions gave similar results.

TABLE 1
BATCH STIRRED TANK RESULTS AT A/O = 1/1

	C_A kg/m^3	1 - E	t,s
P5100; 23.7°C,	1.08	0.340	11
960 rpm	0.55	0.158	20
	0.30	0.072	30
Aqueous dispersed	0.19	0.034	45

Data processing was conducted in the same manner as used for the Sulzer mixer with $\Delta C_A/\Delta t$ being determined as a function of C_A. Estimates of continuous mixer performance, assuming the same mixer size and impeller speed, were determined from the relationship:

$$C_{A\ in} - C_{A\ out} = \theta \left[\frac{\Delta C_A}{\Delta \theta}\right]_{C_{A\ out}} \qquad (4)$$

The approach to equilibrium (E) may be calculated as a function of residence time θ.

$$E = \frac{C_{A\ in} - C_{A\ out}}{C_{A\ in} - C_{Ae}} \qquad (5)$$

A comparison of the Sulzer and agitated tank mixers was then made on the basis of the energy requirements per unit volume of dispersion at values of E of 0.6 and 0.9. It was necessary to extrapolate the Sulzer mixer data for the calculation at E = 0.9, interpolating between the lowest data point and $F_A \Delta C_A / \Delta t = 0$ at $C_A = C_{Ae} = 0.09$ kg/m^3. The contact times were then calculated graphically:

$$t = \int_{C_{A\ in}}^{C_{A\ out}} \frac{1}{\frac{\Delta C_A}{\Delta t}}\, dC_A \qquad (6)$$

The corresponding energy requirements were determined (4):

$$p = \frac{f_h \rho_c L V^2}{2 d_h} \qquad (7)$$

The energy requirements for the agitated tank (8) were calculated using Po = 5.0 (Table 2). At E = 0.6 the Sulzer mixer at 0.307 m/s offers a marginal reduction (-18%) in residence time for a marginal increase (+26%) in energy requirement; at 0.504 m/s there is a substantial reduction in residence time (-73%) for a substantial increase in power (+86%). At E = 0.9 the predicted advantages of the Sulzer mixer are more obvious: a reduction in residence time (-55%) and a reduction in energy requirement (-28%) at 0.307 m/s; and a large reduction in residence time (-83%) for a small increase in energy requirement (+17%) at 0.504 m/s.

TABLE 2
RESIDENCE TIME AND ENERGY REQUIREMENTS

	E = 0.6		E = 0.9	
	Residence time s	Energy per unit volume kJ/m^3	Residence time s	Energy per unit volume kJ/m^3
Mixer 960 rpm	17	34	114	226
Sulzer 0.307 m/s	14	43	52	162
Sulzer 0.504 m/s	4.6	63	19	264

The preceding discussion refers to the solvent extraction of copper from acid systems but the plug flow characteristics of the Sulzer static mixer also offer a particular advantage if a separation can be made on a kinetic basis. In the Caron Process for nickel extraction from lateritic ores an ammoniacal leach solution containing nickel and copper is generated from which copper can be extracted by hydroxyoximes. A process using two continuous flow countercurrent mixer-settler stages has been able to reduce aqueous phase copper concentration to 30 ppm. However, batch agitated tank tests at the same phase ratio have shown that, while a concentration of less that 5 ppm can be obtained after short contact times of the order of 15 seconds, at longer contact times the copper taken up by the organic phase is displaced by Ni giving aqueous phase copper concentrations higher than 80 ppm. In separations of this type the narrow residence time distribution characteristics of the Sulzer mixer are preferable to the broader distribution of a continuously operated agitated tank. Sulzer are currently designing a solvent extraction plant for the above process.

CONCLUSIONS

The Sulzer in-line mixer was shown to have suitable characteristics for the extraction of copper from acid solutions using the reagent P5100. The mixer has phase inversion characteristics which differ from those of the continuous stirred tank in that there is no ambivalent region. The aqueous dispersed and organic dispersed regions are instead separated by a narrow region in which double dispersions are generated. Mass transfer causes a shift in this region and during tests some influence of ageing of liquids or equipment was observed. Settler studies gave dispersion band characteristics which, above a certain limit, were not influenced by energy input. Settler performance was similar to that for conventional laboratory mixers using similar power input per unit volume. Entrainment of organic in aqueous for aqueous dispersed conditions was low, similar to the best results obtainable in conventional equipment. Mass transfer rate increased significantly with velocity in spite of the reduced residence time in the fixed mixer length. The mass transfer capacity compared very favourably with continuous agitated tank performance estimated from batch tests. For a stage efficiency of 90% it is predicted that the Sulzer mixer requires only one-sixth the residence time required for a continuously operated tank with similar energy requirements. Thus the theoretical advantages of plug flow mixing appear to have been achieved without serious penalties in settler behaviour. In addition, the narrow residence time distribution of the Sulzer mixer offers advantages for separations which can be effected on a kinetic basis and benefit from a precise contact time.

ACKNOWLEDGEMENTS

The work carried out at the University of Bradford was financed by Sulzer Bros.Ltd., Switzerland.

NOMENCLATURE

C	concentration of copper	kg/m^3
D	mixer diameter	m
D_h	hydraulic diameter	m
d	drop diameter	m
E	fractional approach to equilibrium	-
F	flow rate	m^3/s
f	friction factor	-
L	calculated mixer length for specific extraction	m
P	power consumption	W
Po	power number	-
p	pressure	N/m^2
Re_h	Reynolds number $(\frac{\rho_c V D_h}{\mu_c})$	-
t	residence time in Sulzer mixer	s
V	velocity in Sulzer mixer	m/s
v	volume	m^3

We_h	Weber number $(\frac{\rho_c v^2 D_h}{\gamma})$	-
γ	interfacial tension	N/m
μ	viscosity	Ns/m^2
θ	residence time in agitaged tank	s
ρ	density	kg/m^3

Subscripts

A	aqueous phase	in	inlet
c	continuous phase	out	outlet
e	equilibrium	O	organic phase
h	hydraulic diameter basis	sm	Sauter mean

REFERENCES

1. Kubie, J. and Gardner, G.C., Chem.Eng.Sci., 32, 195 (1977).
2. Middleman, S., Ind.Eng.Chem.Proc.Des.Dev., 13 (1), 78 (1974).
3. Tunison, M.E. and Chapman, T.W., A.I.Ch.E. Symposium Series, 74, 112 (1978).
4. Streiff, F., Sulzer Technical Review, 59 (3), 108 (1977).
5. Merchuk, J.C., Shai, R. and Wolf, D., Ind.Eng.Chem.Proc.Des.Dev., 19 (1), 91 (1980).
6. Godfrey, J.C., Chang-Kakoti, D.K., Slater, M.J. and Tharmalingam, S., Proceedings ISEC '77, 2, 406 (1979).
7. Godfrey, J.C., Slater, M.J. and Tharmalingam, S., A.I.Ch.E. Symposium Series, 74 (173), 127-133 (1978).
8. Grilc, V., PhD Thesis, University of Bradford (1976).

THE SETTLER WITH LAMINAR CORRUGATED FILLING

J.M. Josa and A. Moral

Junta de Energía Nuclear

Madrid, Spain

Experimental work has been conducted in bench scale and in two continuous mixers-settlers with a view to get information on coalescence action of sloped tubes and plates, and on area requirements. Three uranium extraction systems, Amex, D2T and Purex have been studied. The data allow to compare the behaviour of these systems. A very effective, simple, and cheap internal corrugated filling has been developed. The settlers with it are smaller than a conventional unit. Entrainment losses have been also reduced. Design criteria and data for industrial settlers are given.

INTRODUCTION

The mixer-settler is the most current equipment for the liquid-liquid extraction in the hydrometallurgical operations. It has the advantage of a direct scale-up, besides its construction and operation is easy, and normally, few theorical steps are needed to obtain an efficient operation in the most important applications (Cu, U, etc.). Although it is necessary to remark some inconvenients: the high space requirement, the high investment, and above all the great inventory of valuable liquids, as the organic phase or as the own metal present.

A mixer-settler step is composed by a mixer and a settler. The first gets the dispersion of one phase in the other, in order to obtain the material transfer and to reach the equilibrium. The settler has to separate the dispersion in their phases, organic and aqueous, and to avoid the entrainments of either phase in the other. In the settler we can distinguish three zones: the dispersion band, where the coalescence of the dispersed drops is carried out, the clear organic zone in which the aqueous entrainment is avoided, and the clear aqueous zone where is possible the separation of the last organic droplets.

The working conditions of the mixer effect the good performance of the settler, its size requirements and the entrainments. It is usual to work with organic continuous dispersions in order to avoid the entrainments of

organic phase, and also use of lowest unit power (1) compatible with the necessities of material transfer. There is also a trend towards the feeding of bigger dispersion drops into the settler (2).

The settler is dimensioned based on the area requirements, in order to avoid entrainments. In the copper industry is very normal a dispersion specific flow of 2 gal.min^{-1}.ft^{-2} (82 l.min^{-1}.m^{-2}). As a matter of fact the active zone is the dispersion band and the emulsion retained therein. The dispersion band thickness (ΔH) is related with the specific flow (Q/A) by the formala $\Delta H = K\,(Q/A)^n$.

For the settler design there are two tendencies, one of them (3,4) tries the work with simple equipments and a thin dispersion band, and the other one (5,6,7) works with a depth band and especially with accesories (laminar packages, chemineys, baffles, etc.) to increase the coalescence area and to improve the evacuation of the separated phases. This last tendency produces most compact equipments, with small inventory, although sometimes the equipment is more expensive and difficult to maintain due to the sophistication introduced in it (8). Actually, it is necessary to remark the importance of this working line which worries a lot engineers, and to which we adhere too. For several years we are trying to handle together the aspects of simplicity, efficiency, and cost in the gravitational settler design.

Table 1. Separation time (sec.) in batch studies.

A Emulsion Thickness mm	B Emul. type	C Mixing gradient	D Tube form	E Size ø mm	F, EXTRACTION SYSTEM											
					F1 = AMEX				F2 = D2T				F3 = PUREX			
					θ, TUBE ANGLE WITH HORIZONTAL (*)											
					θ1	θ2	θ3	θ4	θ1	θ2	θ3	θ4	θ1	θ2	θ3	θ4
A1 = 275	B1-Wo	C1-0,0	D1-SQ	20	290	180	170	130	320	210	200	200	270	170	140	120
				40	270	180	170	140	420	270	270	250	260	170	150	140
			D2-CL	20	230	150	140	120	440	270	230	200	210	140	130	100
				40	210	160	150	130	270	200	170	150	190	130	120	110
		C2-0,5	D1-SQ	20	370	190	180	150	260	170	150	120	230	170	140	130
				40	220	160	150	130	200	170	150	120	220	150	130	120
			D2-CL	20	180	140	130	120	330	210	170	140	180	120	110	100
				40	210	150	130	120	270	140	120	110	190	130	110	90
	B2-Ow	C1-0,0	D1-SQ	20	240	150	130	100	230	170	160	150	100	70	60	60
				40	200	160	120	110	110	80	70	60	90	70	60	50
			D2-CL	20	160	80	70	60	240	150	130	110	90	60	50	40
				40	150	120	100	90	150	110	90	80	130	90	80	70
		C2-0,5	D1-SQ	20	110	80	70	50	160	100	90	80	110	80	80	70
				40	170	130	110	90	210	120	100	90	110	70	60	50
			D2-CL	20	140	80	70	70	270	150	120	100	90	50	40	30
				40	160	110	100	80	180	120	100	90	130	90	80	70
A2 = 560	B1-Wo	C1-0,0	D1-SQ	20	490	290	230	180	410	170	150	130	520	270	230	200
				40	480	310	270	210	420	190	180	170	280	130	120	100
			D2-CL	20	430	280	230	190	560	330	280	250	230	170	160	160
				40	410	200	170	170	560	370	310	270	450	290	250	210
		C2-0,5	D1-SQ	20	430	250	220	180	270	100	100	90	460	260	240	120
				40	430	270	230	200	390	150	140	120	220	110	100	160
			D2-CL	20	420	260	240	210	570	430	360	290	200	120	120	200
				40	230	100	90	80	780	480	320	310	350	210	180	100
	B2-Ow	C1-0,0	D1-SQ	20	190	110	100	80	190	140	120	110	200	120	100	80
				40	210	160	140	110	180	140	120	110	190	100	70	60
			D2-CL	20	230	130	110	90	380	240	210	170	160	90	80	70
				40	150	80	70	60	410	210	170	140	200	100	90	80
		C2-0,5	D1-SQ	20	190	110	90	70	240	130	110	90	190	110	90	80
				40	260	150	140	110	220	130	120	110	180	120	100	90
			D2-CL	20	230	130	110	100	490	230	160	120	180	90	80	70
				40	130	90	70	60	320	160	140	120	200	110	90	70

(*) $\theta 1 = 90^{\circ}$; $\theta 2 = 56^{\circ}30'$; $\theta 3 = 45^{\circ}30'$; $\theta 4 = 31^{\circ}45'$

In this communication are presented the results obtained from the three uranium systems :

a) Amex : terciary amine + decanol, kerosene, solution of sulfuric acid.

b) D2T : D2EHPA + TOPO, kerosene, phosphoric acid.

c) Purex : TBP, kerosene, solution of nitric acid.

Some of these tests have been carried out in a continuous circuit and others in bench scale. The results permit the design of settlers compact, effective, stable, with easy construction and low cost.

BATCH STUDIES

With these studies, we have tried to resolve the influence of the decantor device (vertical or sloped), and moreover, to compare three systems used in the uranium industry so that the experience can be extended from one to another.

The experimental device is a mixer where the emulsion is produced. In the mixer the organic and aqueous components, at 20 ± 2 °C, are introduced and they are mixed for a minute. The agitation is stopped and inmediatelly the emulsion falls down to the settler tube through the bottom of the mixer. The tube is placed vertically or sloped depending on the test. The decantor tube has a graduated scale to read the interface positions at different times, until the total phase separation is obtained.

The following variables and levels have been considered,

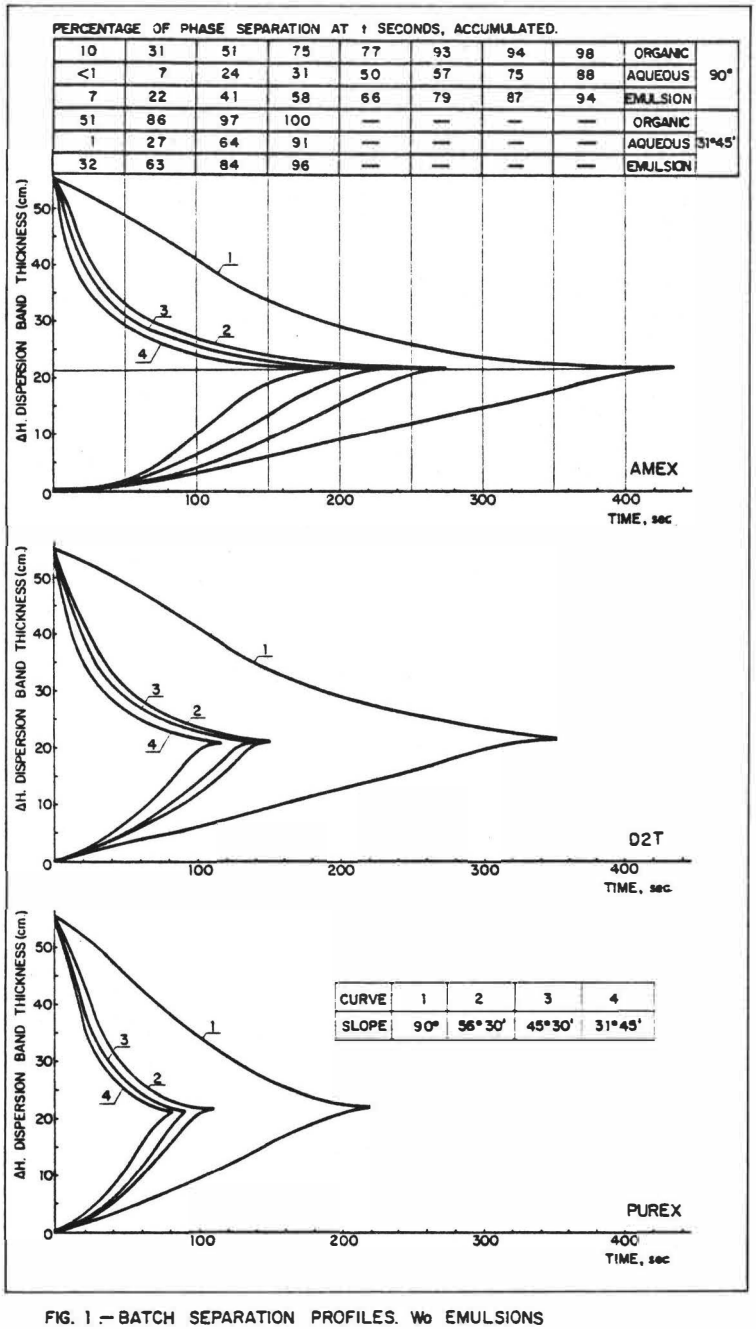

FIG. 1 — BATCH SEPARATION PROFILES. Wo EMULSIONS

Table 2. Significant effects for the batch separation time.

Source of variance	Mean Squares (a)	Degrees of freedom	Effect sec	Probability point
F, Extraction system, between Amex and D2T				
A, Between emulsion thickness	1,81 (5)	1	75,3	0,001
B, Between emul. type	4,03 (5)	1	-112,0	0,001
C, Between gradient	1,12 (4)	1	- 18,7	0,1
D, Between tube form	1,71 (4)	1	23,1	0,05
F, Between extr. system	7,42 (4)	1	48,1	0,001
G, Between slope	8,06 (5)	1	-159,0	0,001
Interaction AB	3,31 (4)	1	- 32,2	0,005
Interaction AD	4,21 (4)	1	36,3	0,001
Interaction DE	1,12 (4)	1	- 18,8	0,1
Interaction DF	1,14 (5)	1	59,7	0,001
Interaction AG	6,85 (4)	1	- 46,3	0,001
Interaction BG	4,80 (4)	1	38,8	0,001
Interaction FG	1,32 (4)	1	- 20,3	0,05
Residual (3-7) = Exp. error	3,25 (3)	99		
F, Extraction system, between Amex and Purex				
A, Between emulsion thickness	1,30 (5)	1	63,7	0,001
B, Between emul. type	3,50 (5)	1	-104,0	0,001
C, Between gradient	8,13 (3)	1	- 15,9	0,05
D, Between tube form	2,21 (4)	1	- 26,2	0,005
F, Between extr. system	3,25 (4)	1	- 31,9	0,001
G, Between slope	5,02 (5)	1	-125,0	0,001
Interaction AB	2,76 (4)	1	- 29,4	0,001
Interaction BD	7,20 (3)	1	15,0	0,1
Interaction BE	6,90 (3)	1	14,7	0,1
Interaction DE	5,51 (3)	1	13,1	0,1
Interaction AG	4,06 (4)	1	- 35,6	0,001
Interaction BG	3,85 (4)	1	34,7	0,001
Interaction DG	6,61 (3)	1	14,4	0,1
Interaction FG	5,51 (3)	1	13,1	0,1
Residual (3-7) = Exp. error	2,00 (3)	99		

(a)(i) 10 exponential

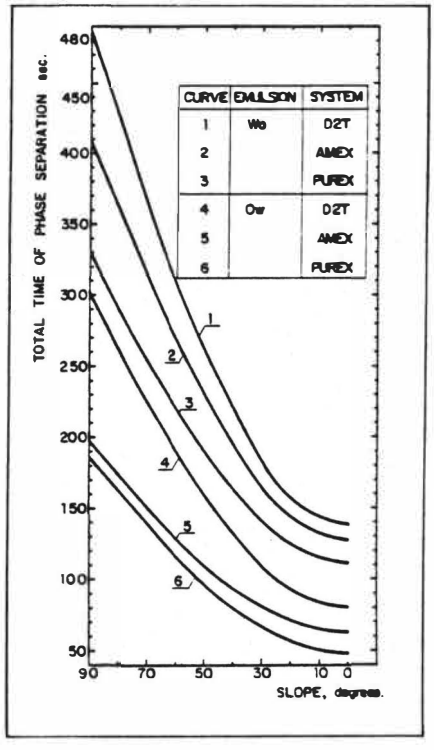

FIG.2.-TIME OF PHASE SEPARATION IN BATCH TESTS.

A,	emulsion thickness, or tube length, mm	275 and 560
B,	emulsion type	Wo and Ow
C,	mixing gradient, V/V (actually 60, 50 and 40 % of org. phase)	0 and 0,5
D,	tube form (and material)	square (plexiglas) and cylindrical (glass)
E,	tube diameter or side, mm	20 and 40
F,	extraction system	Amex, D2T, Purex
G,	tube angle with the horizontal	90°, 56°30', 45°30', 31°45'

In the Figure 1 are shown three series of typical decantation profiles for each tested system. The Table 1 compiles the total time of phase separation.

The development of data can be done by the analysis of variance of a factorial $2 \times 2 \times 2 \times 2 \times 3 \times 4$. Anyway, it has been preferred to do it in base to a factorial of 2^7 only, that is, with two levels for each variable. In the Table 2 the significant results for the comparison of the vertical tube (90°) and sloped (31°45') are indicated. The effects measure the change from the lower level to the higher. The mean value for the Amex-D2T system is 212 seconds, while for the Amex-Purex system is 172 seconds. From Table 2 it can be observed that,

The variance deduced of the residual is relatively high, between $2{,}00 \times 10^3$ and $3{,}25 \times 10^3$.

There is no influence of the tube diameter that contains the emulsion.

The factor which has most influence upon the reduction of the decantation time (-159 and -126 sec) is the slope of the settler tube.

Afterwards, the effect (-112 and -104 sec) of the change from a Wo dispersion to an Ow dispersion follows it. Anyway the interaction BG shows that a fraction of that improvement is lost in the sloped system.

The thickness of the emulsion to be separated has also influence. It is interesting to point out nevertheless, the relatively high value (-46,3 and -35,6 sec) of its interaction (AG) with the slope, which indicates that the greatest time needed by the greatest thickness is partially compensated by the slope.

The tube form, square or cylindrical, (in which the material, organic or inorganic, is also implicated), is statistically significant but its sign is different depending on the system Amex-D2T or Amex-Purex.

The volume gradient (0,5) of the organic phase in the emulsion system is also significant, but in a very low value (-18,7 and -15,9 sec). It is lower than 10 % of the mean value.

The three extraction systems Amex, D2T and Purex, behave statistically in a different way. The easier is the Purex one, then (+ 31,9 sec) is the Amex one, and finally (+ 48,1 sec) the D2T one.

The angle of the settler tube has a big influence, and therefore we have tried to correlate the average separation time (y, sec) with the cosine value (X) of the angle referred to the horizontal. A good correlation was found, and it permits us to extrapolate for angles lower than the ones tested. The regressions for the different extraction systems are :

Amex,	(Wo)	$y = 411-284\ X$	(Ow)	$y = 198-135\ X$
D2T,	(Wo)	$y = 486-348\ X$	(Ow)	$y = 301-220\ X$
Purex,	(Wo)	$y = 330-218\ X$	(Ow)	$y = 186-137\ X$

Figure 2 represents the average time (sec) against the angle of the settler tube. The curves obtained are similar to a parabolic branch where the apex (0°) would be in the lowest point. The tangent to the curve is rather constant over 30°. Afterwards between 20° and 10° it decreases a lot. In short, it seems that the best slope, from the point of view of coalescence, would be comprised between 10° and 20°. It is also necessary to take into account the evacuation of the separated phases.

Table 3. Aqueous specific flow ($l.min^{-1}\ m^{-2}$) in continuous tests.

A Emulsion type	B Plate gap mm	C Settler length mm	D Plate width mm	E, SYSTEM E1 - AMEX F, DISPERSION BAND THICKNESS, cm F1-30	E1 - AMEX F2-50	E1 - AMEX F3-70	E2 - D2T F1-30	E2 - D2T F2-50	E2 - D2T F3-70
A1-Wo	B1-40	C1-500	D1-75	47	71	81	66	83	90
			D2-150	46	70	81	65	84	92
		C2-2000	D1-75	78	96	106	72	84	97
			D2-150	80	94	107	70	85	100
	B2-60	C1-500	D1-75	48	67	77	46	72	80
			D2-150	47	65	78	44	68	79
		C2-2000	D1-75	55	75	81	62	78	87
			D2-150	53	73	79	60	76	83
A2-Ow	B1-40	C1-500	D1-75	68	83	100	75	97	106
			D2-150	71	95	110	74	95	107
		C2-2000	D1-75	77	92	104	56	79	91
			D2-150	85	114	130	51	80	91
	B2-60	C1-500	D1-75	68	81	91	74	96	100
			D2-150	70	80	94	75	94	98
		C2-2000	D1-75	70	83	99	58	69	74
			D2-150	69	86	104	54	55	75

The coalescence and decantation profiles provide additional information on

the behaviour of each system and situation. So, it is possible to evaluate the separated fraction of each component for different intermediate times - (Figure 1), and consecuently the volume for the emulsion. So for instance, with the Amex system, organic continuous dispersion with 60 % of organic in it and $\alpha = 90^{o}$, the emulsion volume is represented by 930 and while it is 320 for $\alpha = 31^{o}45'$. This ratio 2,81 is better than the total separation time ratio 2,5. The profiles give also an indication of the quality of the final phases, so, while the aqueous continuous dispersions have a shorter total separation time their coalescence front is not clear and they give phases with entrainments of the other phase.

CONTINUOUS TESTS

The tests were carried out in two circuits composed by a mixer (tm = 0,43/1,80 min), a settler, a security decantor (240 l, and $S_T = 2,5\ m^2$), two intermediate storages, for the organic and the aqueous phases, two pumps and a flowmeter for each phase. The phase ratio fed was 60 % of organic phase for the organic continuous dispersion (Wo), and 40 % of organic phase - for the aqueous continuous dispersion (Ow). In the mixer the nature of emulsion was checked with two conductivity sensors, one at the upper part and the other at the lower part. The phase ratio was also checked by sampling. The settler was the element which defined each circuit; its dimensions - L x W x H were : 50 x 20 x 130 cm and 2000 x 20 x 130 cm. The criteria of superficial similarity were maintained but not the one of L/H.

A rather pessimistic information could result from the small settler. This information could be similar to the behaviour of the fraction nearest to the feed entrance in an industrial settler. The settler was made in plexiglas in order to observe on the dispersion band and the clear phases behaviour. The settler was studied empty and with the different accesories - which are quoted below. The Bellinghan's factor in the mixer through the whole experiments was 78 for the small unit and 32 and 13,5 for the big one.

Table 4. Significant effects for the aqueous specific flow in continuous tests.

Source of variance	Mean Squares (*)	Degrees of freedom	Effect (**)	Probability point
Thickness of dispersion band between 30 and 50 cm				
A, B. emulsion type	1,34 (3)	1	9,15	0,001
B, B. laminar gap	1,51 (3)	1	- 9,72	0,001
C, B. settler length	1,13 (2)	1	2,66	0,01
F, B. thickness of band	5,31 (3)	1	18,20	0,001
Interaction AB	1,29 (2)	1	2,84	0,1
Interaction AC	1,61 (3)	1	-10,00	0,001
Interaction BC	2,29 (2)	1	- 3,78	0,05
Interaction AE	3,85 (2)	1	- 4,91	0,005
Interaction CE	1,65 (3)	1	-10,20	0,001
Residual (3-6) = Exp. error	3,46 (1)	42		
Thickness of dispersion band between 50 and 70 cm				
A, B. emulsion type	1,55 (3)	1	9,84	0,001
B, B. laminar gap	2,49 (3)	1	-12,50	0,001
E, B. extraction system	1,65 (2)	1	- 3,22	0,05
F, B. thickness of band	1,95 (3)	1	11,00	0,001
Interaction AC	1,08 (3)	1	- 8,22	0,001
Interaction BC	3,47 (2)	1	- 4,66	0,005
Interaction AD	8,79 (1)	1	2,34	0,1
Interaction BD	1,53 (2)	1	- 3,10	0,05
Interaction AE	4,78 (2)	1	- 5,47	0,001
Interaction CE	1,77 (3)	1	-10,50	0,001
Interaction DE	1,41 (2)	1	- 2,97	0,05
Residual (3-6) = Exp. error	3,01 (1)	42		

(*)(1) 10 exponential (**) $l.min^{-1}.m^{-2}$

We have studied the following factors : the entrance of the emulsion into the settler to reduce its kinetic energy; the use of the empty settler without any accesory; - the use of picket fences with different gap (W/9 and W/6), also the picket fence with its upper part - either free or covered with a wall, to avoid the reverse flow; the use of a baffle covering half of the height; the introduction of a laminar package either transversal or parallel to the dispersion flow; - the angle of the plates with the horizontal (10^{o}, 20^{o} and especially 15^{o}); the profile of the plates - (plane or corrugated); the plate material (FRP, plexiglas, stainless steel, or mixed plates FRP + stainless steel and stainless steel + FRP); the percentage of the settler covered by the package (40 and

Table 5. Relationship between dispersion band thickness and specific flow.

Settler length cm	Extraction system	Emulsion type	Accesory and its geometry	Plate gap mm	Probability point	Y = K X^n (c) K	n
500 (a)	AMEX	Wo	Free	-	0,01	5,27 (7) (d)	4,05
			Baffle	-	0,02	2,16 (5)	2,98
			Picket fence (w/9)	-	0,05	9,00 (16)	7,84
			Corrugated plate, FRP	40	0,01	1,98 (4)	2,41
			Plane plate, FRP/stainless steel	40	0,001	5,05 (4)	2,18
			Plane plate, stainless steel	40	0,05	1,07 (3)	2,13
			Plane plate, FRP	40	0,05	1,37 (4)	2,53
		Ow	Free	-	0,01	2,80 (11)	6,11
			Baffle	-	0,001	8,53 (11)	5,83
			Picket fence (w/9)	-	0,02	1,43 (11)	6,41
			Corrugated plate, FRP	40	0,001	2,99 (4)	2,44
			Plane plate, FRP/stainless steel	40	0,01	4,85 (3)	1,87
			Plane plate, stainless steel	40	0,01	0,04 (0)	1,49
			Plane plate, FRP	40	0,01	0,01 (0)	1,75
	D2T	Wo	Baffle	-	0,001	1,86 (8)	4,54
			Corrugated plate, FRP	40	0,01	1,36 (4)	2,42
			Castle corrugated plate, FRP	40	0,01	1,46 (4)	2,90
			Plane plate, FRP/stainless steel	40	0,01	3,53 (5)	2,77
		Ow	Corrugated plate, FRP	40	0,01	1,10 (3)	2,12
			Castle corrugated plate, FRP	40	0,01	7,25 (5)	2,72
			Plane plate, FRP/stainless steel	40	0,001	2,43 (3)	2,03
2.000 (b)	AMEX	Wo	Baffle	-	0,01	1,45 (10)	5,31
			Corrugated plate, FRP	20	0,001	2,89 (5)	2,63
			Corrugated plate, FRP	40	0,01	7,14 (7)	3,30
			Corrugated plate, FRP	60	0,01	1,51 (6)	3,34
			Corrugated plate, FRP	80	0,01	8,10 (7)	3,45
		Ow	Baffle	-	0,10	5,04 (4)	2,49
			Corrugated plate, FRP	20	0,02	6,30 (4)	2,16
			Corrugated plate, FRP	40	0,01	3,07 (3)	1,85
			Corrugated plate, FRP	60	0,01	4,75 (3)	1,86
			Corrugated plate, FRP	80	0,001	2,39 (4)	2,52
	D2T	Wo	Baffle	-	0,01	4,43 (10)	5,03
			Corrugated plate, FRP	20	0,01	1,14 (3)	1,89
			Corrugated plate, FRP	40	0,01	7,75 (5)	2,49
			Corrugated plate, FRP	60	0,01	3,04 (5)	2,75
			Corrugated plate, FRP	80	0,01	5,00 (11)	5,34
		Ow	Corrugated plate, FRP	20	0,001	0,08 (0)	1,29
			Corrugated plate, FRP	40	0,01	9,56 (4)	2,23
			Corrugated plate, FRP	60	0,01	0,02 (0)	1,65
			Corrugated plate, FRP	80	0,01	8,37 (7)	3,84

(a) width plate 2 x 75 mm, (b) width plate 1 x 150 in both cases 40 % of settler covered, (c) Y, dispersion band thickness (cm) and X, dispersion specific flow $Lmin^{-1}m^{-2}$ (d) (-i) 10 exponential.

80); the position of the package in the settler (near to the dispersion entrance, at the middle, and at the end of its length). The working temperature was 23 ± 1 °C, although we tested high temperatures (35 and 42 °C) for the D2T system. Our main interest was the study of corrugated plates (λ = 18 mm) disposed in parallel to the flow, with a slope equal to 15°, a 40 % of settler covered with the package and placed at the middle of the settler. We have tested the following variables and levels.

A,	the emulsion type	Wo and Ow
	(including a 60 and a 40 % of org. phase)	
B,	the plate gap, mm	(20), 40, 60 and (80)
C,	the settler length, mm	50 and 2000
	(including a L/H = 0,43 and 1,74)	
D,	the plate width, mm	2 x 75 and 1 x 150
	(including one or two org. chimneys)	
E,	the extraction system	Amex and D2T
F,	the dispersion band thickness, cm	30, 50 and 70

We took account of the answers : The dispersion band thickness for increasing flows; the total decantation area (settler plus package) covered by the dispersion band; the entrainment of either phase in the other; the phase ratio in different positions and depths of the dispersion band;

electrical conductance in the dispersion band; and the flow profiles in the security zones and in the dispersion band. The continuous tests were very informative, both in respect to qualitative magnitudes, or tendencies, and also to quantitative values.

Firstly we analyse the aqueous specific flow (Table 3) vs the dispersion band thickness and the other factors of the factorial design. According to the statistically development (Table 4) result :

The internal variance of the tests for 84 degrees of freedom is 32,38.

The dispersion band thickness was the greatest effect; 18,2 (for the change of 30 to 50 cm) and 11,0 (for the change of 50 to 70 cm). It is necessary to indicate that the mean value for 30-50 cm is 72,7 $l.min^{-1}.m^{-2}$, and 87,5 $l.min^{-1}.m^{-2}$ for 50 - 70 cm.

The plate gap has a rather considerable response (-9,72 and -12,50) when it is increased from 40 to 60 mm.

The change from the Wo emulsion to Ow improves the settler capacity (9,15 and 9,84 $l.min^{-1}.m^{-2}$).

The size of the settler has only effect upon thin bands (2,66). By the contrary the extraction system from Amex to D2T in not statistically significant for thin bands but it is for depth bands, -3,22 $l.min^{-1}.m^{-2}$. Actually, there also exists the interaction CE (-10,20/-10,50) between the size of the settler and the system.

The interaction AC (-10,00/-8,22) between the emulsion type and the size of the settler has an appreciable value. This interaction indicates that when we change to the D2T system we lose a part of the improvement obtained in the change to the Ow emulsion.

It is interesting to point out that the plate width (2 x 75 vs, 1 x 150 mm) has no effect, although several of its interactions have some value. It seems that it is possible to work with plates that will be set up in a cheaper device.

As a complement to this sistematic study, in Table 5 is presented the relationship between the thickness (cm) of the dispersion band ΔH and the dispersion specific flow (Q/A, $l.min^{-1}.m^{-2}$). We checked that the correlation,

$$\Delta H = K \ (Q/A)^n$$

was statistically significant at the significance levels of the 0,1 and higher of 0,001. Anyway, the values of the constants were very different from some cases to others. The value of K was comprised between 1×10^{-2} and 9×10^{-16}, and the value of n was between 1,29 and 7,84. The regresion formulas permit to rebuild the capacity curves, but their direct analysis is complex because of the changes in the value of K.

The significance of the exponent is very clear since it gives a measure of the system sensibility to overloads. The smaller, the less sensible will be the system to overloads. Without entering into discussion of the different cases, we consider suitable to point out the high values of the

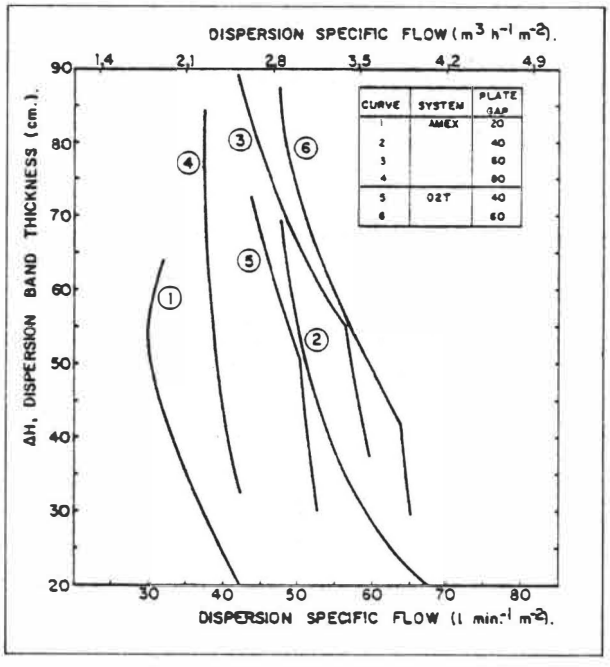

FIG. 3 - CURVES OF CORRECTED DISPERSION SPECIFIC FLOW ($Q_D \cdot S_T^{-1}$). RESULTS WITH Wo, T = 23 °C, $N^3 D^2 = 13,5$.

exponents for the simple systems - (empty, fences, or baffle) and the low values (between 1,29 and 3,3) for the filled systems, especially with corrugated plates of FRP such as the ones used in the construction of covers.

Some other aspects to quote are : the possibility of a safety handling aqueous continuous emulsions, which had given unclear phases in batch tests. With simple - settlers the organic entrainment - with these emulsion types were very high (5 $l.m^{-3}$), but using corrugated plates they decreased to figures like 500 $ml.m^{-3}$. In systems with continuous organic phase the entrainments were as small as 15 $ml.m^{-3}$ using settlers with plates and a 100 $ml.m^{-3}$ for settlers with only baffle.

We payed some attention to the internal flows in the settler and we observed that with the filling of corrugated plates the waves upon the boundary dispersion band-organic are lessened, the bigger thickness of the emulsion band the lower the waves. Also the organic phase rises vertically and it flows along the boundary organic-air. We did not note significant recirculations in the safety zones.

SUMMARY AND CONCLUSION

In summary we can conclude that it is possible to obtain simple, compact and efficient settlers by filling the conventional prismatic settlers with polyester (FRP) corrugated plates. This material is cheap, available anywhere and easy to handle.

The increase in the throughput depends on filling proportion. But it seems it is not suitable to surpass a 40 % of coverage of settler section. Actually the differential efficiency of each new surface decrease. In the Figure 3 there is the dispersion specific flow referred to the whole surface (or corrected specific flow) vs the dispersion band thickness.

As a matter of fact the optimum size of the settler and the amount of filling is a compromise between the cost of the empty settler, the cost of the filling and the inventories in it, plus other factors such as space requirement, fire risks, etc.

Finally we want to give some typical figures about costs. A conventional settler in FRP and 60 m^2 in size, could cost about US $ 38.500. The plates in the settler have a cost in the order of US $ 14 m^{-2}. For an application such as the recovery of the uranium from 2.000 $m^3.d^{-1}$ of wet phosphoric - acid, the total investment for a system of four settlers assembled and ready to operate and including its inventories, would be about US $ 310.000 using filling, against US $ 950.000 using conventional settlers.

REFERENCES

1. Bellinghan, A.T., Proc. The Ans. I.M.M. (198) 85, 1961.

2. Barnea, E. and Mizrahi, J., In Proc. ISEC '77, CIM Special Volume 21, Montreal 1979, 374.

3. Agers, D.W. and Dement, E.R. International Symposium Solvent Extraction Metallurgy Processes. Antwerp, 4-5, May 1972.

4. Lott, J.B., Warwick, G.T., and Scuffham, J.B. Trans. AIME (SEM) 252, 1972.

5. Mizrahi, J. and Barnea, E., Israeli Patent 30304, 30 July 1968.

6. Martin Stönner, H. and Wohler, F., Paper 14 to the Symposium of Hydrometallurgy-University of Manchester (2-4 April 1975). The I. Chem. E. Symposium Series No. 42. London.

7. Lewis, I.E., In Proc. ISEC '77, CIM Special Volume 21. Montreal 1979, 325.

8. Finney, S.A., In Proc. ISEC '77, CIM Special Volume 21, Montreal 1979, 574.

9. Moral, A., Gasós, P. and Josa, J.M., Ingeniería Química 10 (116) 55, 1978.

10. Moral, A. and Josa. J.M. Paper to the 2nd International Congress on Phosphorus Compounds, Boston, USA, 20-25 April 1980.

ADVANCES IN THE DESIGN OF UNPULSED SIEVE-PLATE EXTRACTION COLUMNS

Th. Pilhofer

Lehrstuhl A Verfahrenstechnik
Technical University Munich

Munich, Fed. Rep. Germany

ABSTRACT

The operating range of unpulsed sieve-plate columns is determined by 4 different limiting phenomena. For further explanation, recent results of the investigation of the minimum load of the dispersed phase to achieve operation of all holes and of the adjustment of the height of the coalesced layer depending on operating parameters are described. Additionally, it is shown how the operating range changes with plate geometry and how the plate geometry is chosen. Finally, the calculation of the plate efficiency is reported. It may be essentially simplified if the load of the dispersed phase varies within a certain region only.

Unpulsed sieve-plate columns (SEC) in a form applied to-day are well-known since a long time (1). Their special advantage is the subdivision of the column volume in several stages. As a consequence of this construction and of the well-aimed flow control of both phases, the effect of axial dispersion is restricted to one stage. This is a considerable advantage with respect to column design because scale-up problems are largely cancelled.

Nevertheless, after many publications till 1955 the interest in SEC has remarkably weakened. This may be a consequence of several investigations from which low mass transfer rates have been reported. Yet, to the authors opinion it must be differentiated whether these effects are specific for SEC or if they are caused by other facts, e.g. wrong operating conditions. In the following, results of own investigations of the fluiddynamics and of the mass transfer are reported. They have been carried out in order to improve the knowledge of the function of a SEC. By that means, it has become possible to define the operating region more precisely and to develop on that basis a simple model for the calculation of the stage efficiency.

DETERMINATION OF THE OPERATING RANGE

The operating range is determined by different requirements which are met by appropriate choice of the phase throughputs. These requirements are (2):

1) No flooding of the two-phase system
2) Minimum flow of the dispersed phase to achieve operation of all holes of a plate
3) Ensuring a minimum head of the coalesced layer before a plate
4) Maximum height of the coalesced layer equal to the length of the continuous phase downcomer of a plate.

The determination of these different limits of the operating range requires a thorough insight in the function of a column. Improved equations for the determination of the flooding conditions have been presented (3). In the following, some aspects of the drop formation at a sieve plate and of the adjustment of the coalesced layer are treated.

Opposite to a widespread opinion(4), the laws of the drop formation at a single orifice cannot transferred unrestrictedly to a sieve plate. As a consequence of the dependence of the orifice pressure drop on the throughput, each hole needs a certain minimum throughput in order to come into operation (5). This throughput is equal to the throughput at the transition point of a single orifice to the formation of a jet (6).

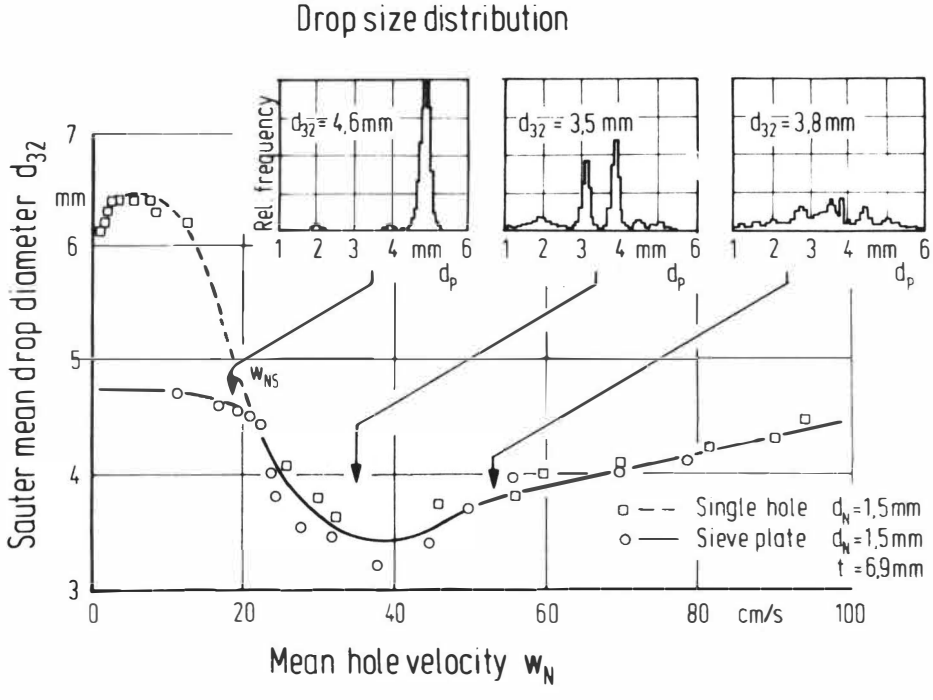

FIG.1
Relation between the mean drop diameter and the mean hole velocity for the system toluene in water(7)

Consequently, as can be seen from Figure 1, drop sizes at single orifices resp. at sieve plates only agree if the mean throughput of the dispersed phase exceeds the value w_{NS} which corresponds to the transition point to the jetting region. Up to this limit the mean drop size remains nearly constant, then decreases, passes through a minimum before again increasing.The drop size minimum appears at a roughly double value of the velocity w_{NS}. Additional drop size distribution measurements revealed that from the mean throughput w_{NS} up to the throughput according

to the drop size minimum, very narrow size distributions can be expected.

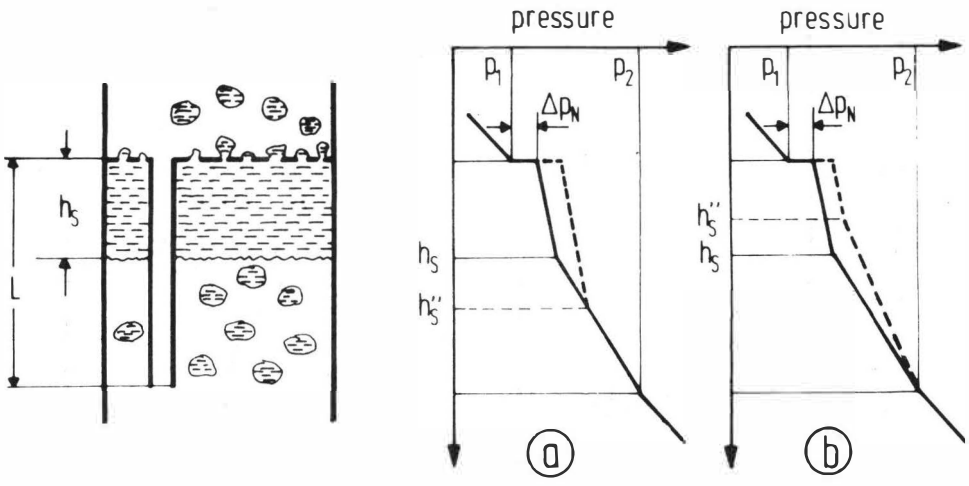

FIG.2
Adjustment of the height of the coalesced layer according to the operating conditions(comments in the text)

The height of the coalesced layer results from the condition that the difference of the static pressure between the upper edge of the sieve plate and the level of the downcomer exit must be the same along the downcomer and along the two-phase mixture. If one assumes a constant pressure difference, the change of the pressure along the two-phase mixture results in a height of the coalesced layer as represented in Figure 2a. Usual calculation procedures (8) suppose that the holdup of the dispersed phase is vanishingly small. Thus, an increase of the plate pressure drop Δp_N causes a rise of the height h_S (dashed lines in Figure 2a). On the other hand, Mewes and Kunkel (9) demonstrated that an increase of the dispersed phase throughput may also result in a decrease of the height h_S. This appears if as a consequence of the increase of the holdup a much steeper ascent of the static pressure in the region of the two-phase mixture is present (Figure 2b). This possibility must be considered because the function of the column requires a certain minimum height of the coalesced layer in order to warrant the hydraulic sealing of one stage against the neighbour stages.

INFLUENCE OF THE PLATE GEOMETRY ON THE OPERATING RANGE

The operating range of a column may be influenced by the plate geometry parameters like hole diameter, fractional free area of holes and downcomer as well as the length of the downcomer. The hole diameters mainly influence the size of the produced drops and thus the flooding conditions of the two-phase system (10). By the fractional areas of holes and downcomers the adjacent pressure drops and the limits of the operating regions as a consequence of the minimum and maximum height of the coalesced layer are influenced. Additionally, the fractional area of the

holes determines the minimum throughput of the dispersed phase to achieve operation of all holes.

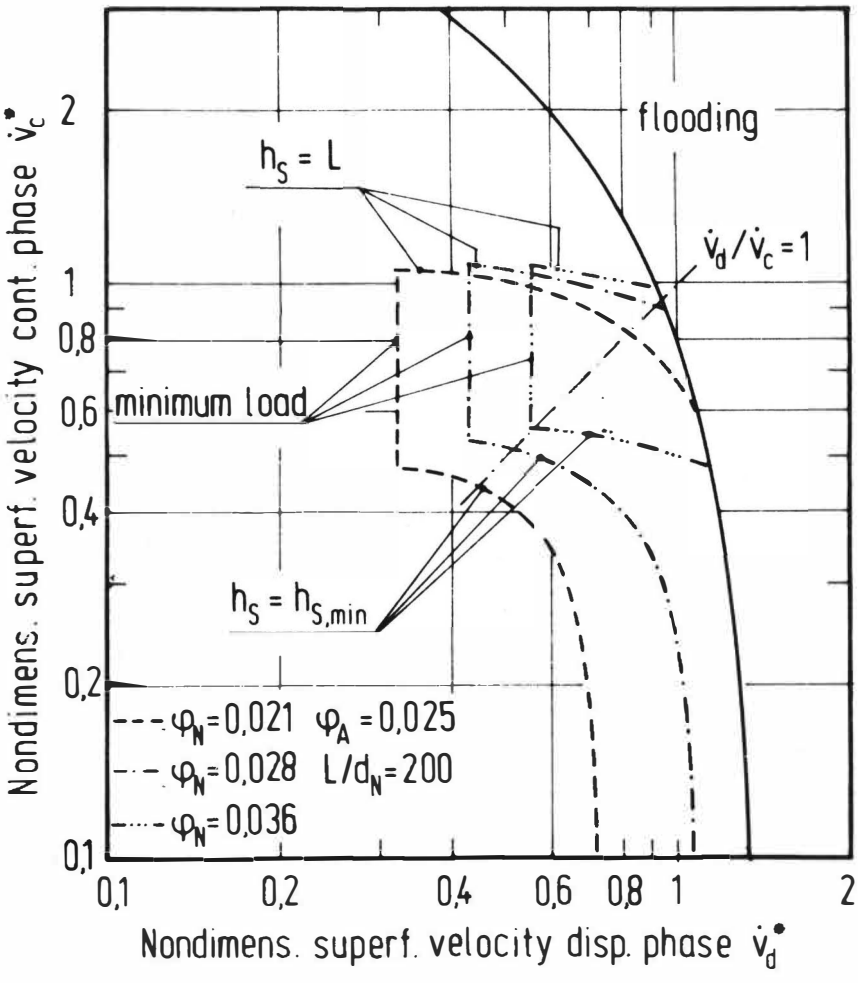

FIG.3
Influence of the fractional free area of the holes on the operating range of a column

The Figures 3 to 5 are valid for one system which is characterized by the following data: $K'_{Fc} = 2{,}6 \cdot 10^{10}$, $K'_{Fd} = 4{,}6 \cdot 10^{10}$, $\eta_c/\eta_d = 1{,}03$, Ar= 70200, $h_{S,min} = 0{,}1$. In Figure 3 the influence of the fractional free area of the holes on the operating range is represented. It may be seen that at constant throughput of the continuous phase a certain height of coalesced layer requires a higher dispersed phase throughput at greater fractional areas. The minimum load of the dispersed phase is also greater and uniform drop size distributions are reached at higher throughputs, at higher values of the holdup and thus at higher interfacial areas.

An increase of the fractional area of the downcomer results in a displacement of the operating range in the region of the minimum load of the dispersed phase (Figure 4): Because of the lower pressure drop of the downcomer, generally higher throughputs are necessary to get an operating point within the admissible range.

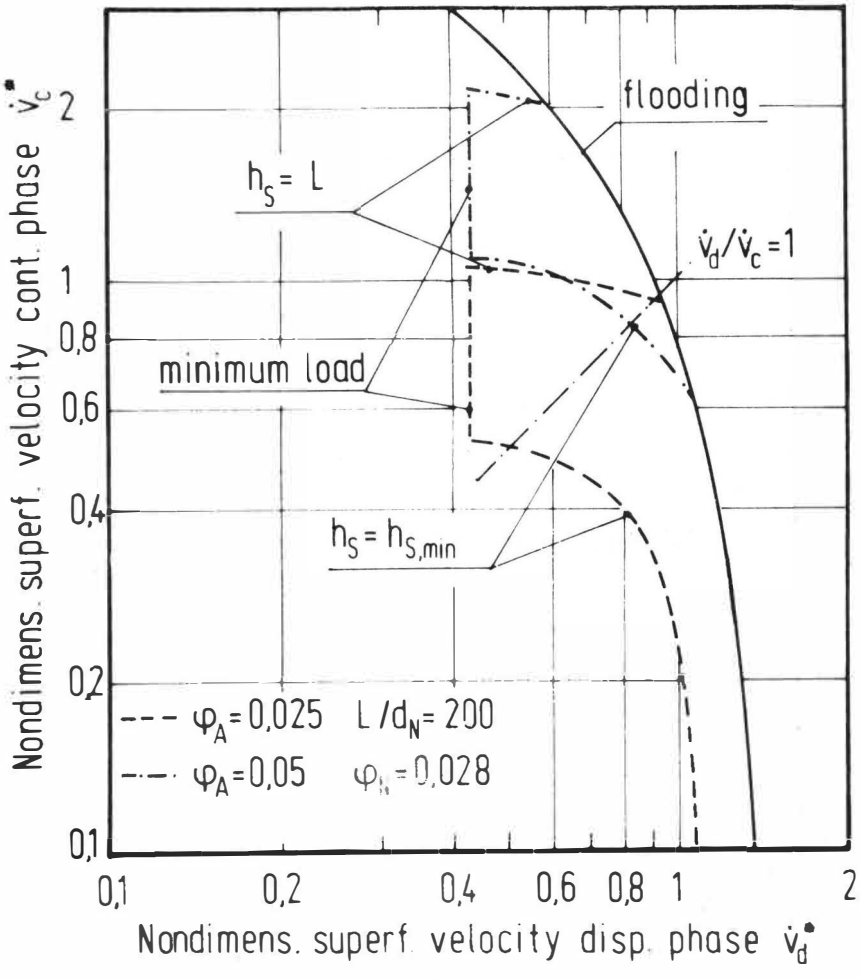

FIG.4
Influence of the fractional area of the downcomers on the operating range of a column

The length of the downcomers mainly influences the upper limit resulting from the height of the coalesced layer(2).

The selection of the operating point is carried out as follows: For given system properties and given phase ratio a hole diameter is presumed. Thus, the minimum drop diameter according to Figure 1 and the flooding conditions can be calculated. The operating point is then fixed to 80% of the throughputs at flooding.

The choice of the plate geometry which determines the operating range takes place as follows: The throughput of the dispersed phase at the operating point is to be equal to the throughput at the drop size minimum. Thus, the minimum load of the dispersed phase for operation of all holes and the fractional area of the holes can be calculated. In the next step, the fractional free area of the downcomer is determined with the request that the limit for the minimum height of the dispersed layer meets the intersection of the minimum load line and of the line of constant phase ratio. This request enables a large operation range when reducing the throughput at constant phase ratio. In the last step, the originally presumed ratio L/d_N is

set so that at the operating point a certain throughput augmentation is possible without leaving the operating range. As L/d_N influences also other limits, a recalculation of the whole procedure may be necessary.

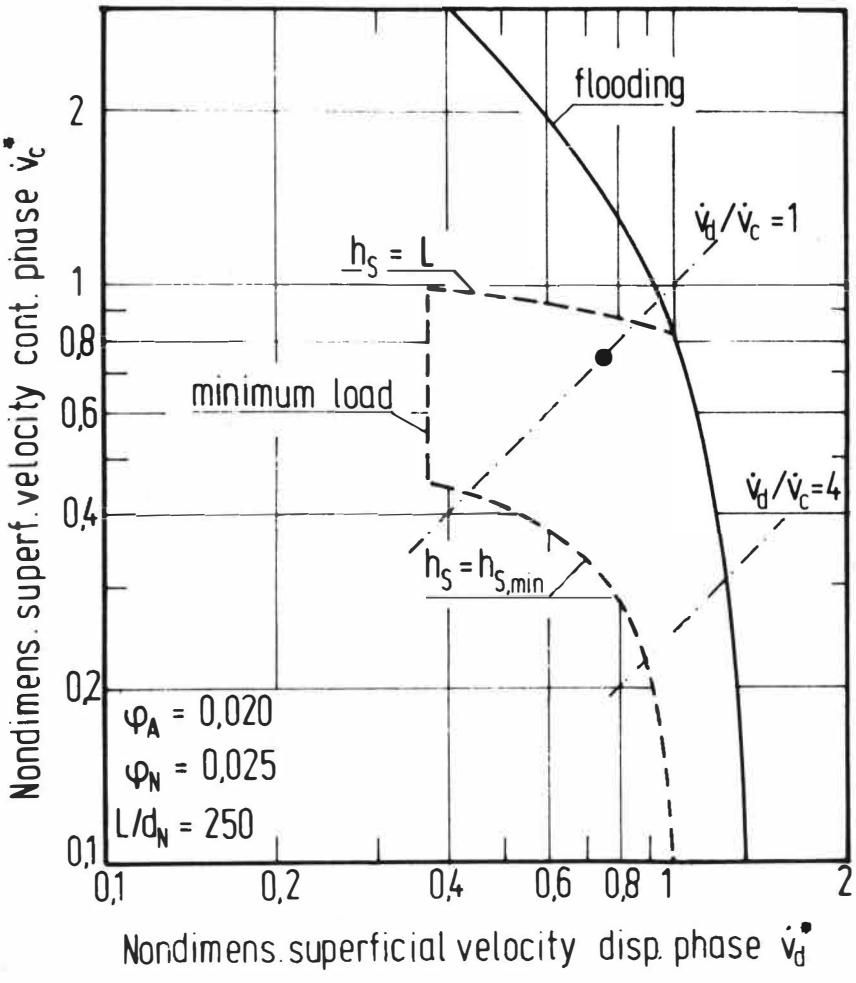

FIG.5
Choice of the operating point and the operating region for a phase ratio of 1

As an example, the operating point and the resulting operating range from the above procedure are plotted in Figure 5 for a phase ratio of 1. As may be also seen, for greater phase ratios than 1 it is difficult to fulfill all aforementioned requirements. High throughputs of the dispersed phase result in relative high fractional areas of the holes. As a consequence of this, a large operating range can only be installed if the fractional area of the downcomer is reduced considerably. However, if from the point of view of the column operation a determination of the coalesced layer not by the downcomer pressure drop but by the holes pressure drop is preferred, the large operating range must be reduced in favor of the aforementioned requirement.

STAGE EFFICIENCIES

The operation of the column within the range of the production of very narrow drop size distributions makes it possible to develop a very simple calculation procedure for the stage efficiency(10). The formation of very narrow drop size distributions justifies the assumption that the dispersed phase moves in plug flow. On the other side, no great mistake seems to be made if the continuous phase is considered as perfectly mixed. Thus, the stage efficiency is equal to the point efficiency of one drop in the swarm. For the stage efficiency then holds:

$$E_0 = E_P = 1 - (1-E_{PF}) \cdot (1-E_{PM}) \cdot (1-E_{PC}) \qquad (1)$$

The point efficiency of drop coalescence, E_{PC}, can be neglected according to literature data. Own investigations (10) revealed that the term E_{PF} is much lower during drop formation by jet disintegration than by periodic drop formation. Thus, the plate efficiency is mainly affected by the point efficiency of the drop motion, E_{PM}, whereas the fraction of the drop formation can be assumed constant as 0,05.

The point efficiency E_{PM} can be calculated as follows:

$$E_{PM} = 1 - \exp\left\{-\frac{6 \cdot \tau \cdot k}{d_P}\right\} \qquad (2)$$

with the mean residence time of a drop in the swarm:

$$\tau = \frac{(h_n - h_S)\,\varepsilon_d}{\dot{v}_d} \qquad (3)$$

By use of equation (1) and assuming E_{PF} as constant 0,05, one gets:

$$E_0 = 0{,}05 + 0{,}95 \cdot \exp\left\{-\frac{6 \cdot \tau \cdot k}{d_P}\right\} \qquad (4)$$

In the case of prevailing resistance to mass transfer on the side of the dispersed phase, the overall coefficient k may be substituted by the individual coefficient k_d. Here the equation of Handlos and Baron (11) has proven reliable:

$$k_d = \frac{0{,}00375 \cdot w_R}{1 + \eta_d/\eta_c} \qquad (5)$$

By use of this model, it was possible to get good agreement between experimental and theoretical values not only for the own investigations (10) but also for the results of other authors (Skelland and Conger (12), Pyle, Colburn and Duffey(13)).

REFERENCES

(1) Harrington, P.J., U.S. Patent 1943822 (1943)

(2) Mewes, D., Pilhofer, Th.,Ger. Chem. Eng. 2(1979),69

(3) Pilhofer, Th.,Ger. Chem. Eng. 2(1979),200

(4) Skelland, A.H.P., Conger, W.L., Ind. Eng. Chem. Proc. Des. Dev. 12(1973), 448

(5) Goedl, R., Ph.D. Diss. Techn. Univ. Munich, 1977

(6) Ruff, K., Pilhofer, Th., Mersmann, A., Int. Chem. Eng. 18 (1978), 395

(7) Miller, H.D., Pilhofer, Th., Chem. Ing. Techn. 48 (1976), 1069

(8) Major, C.J., Hertzog, R.R., Chem. Eng. Prog. 51(1955), 17

(9) Mewes, D., Kunkel, W., Ger. Chem. Eng.1(1978), 111

(10) Schulz,L., Pilhofer, Th., Verfahrenstechnik 13(1979), 361

(11) Handlos, A.E., Baron, T., AIChE J. 3(1957), 127

(12) Skelland, A.H.P., Shah, V., Ind. Eng. Chem. Proc. Des. Dev. 14 (1975(, 379

(13) Pyle, C., Colburn, A.P., Duffey, H.R., Ind. Eng. Chem. 42 (1950), 1042

NOTATION

d_N	mm	hole diameter
d_P	mm	particle diameter
d_{32}	mm	sauter mean diameter
E_0	--	plate efficiency
E_P	--	point efficiency
E_{PF}	--	point efficiency drop formation
E_{PM}	--	point efficiency drop motion
E_{PC}	--	point efficiency drop coalescence
g	m/s^2	gravitational acceleration
h_n	m	plate distance
h_S	m	height of coalesced layer
k	m/s	overall mass transfer coefficient
k_d	m/s	individual mass transfer coefficient disp.ph.
L	m	length of the downcomer
p	N/m^2	pressure
Δp_N	N/m^2	pressure drop sieve plate
t	mm	hole pitch
$\dot{V}_c$	m/s	superficial velocity continuous phase
v_d	m/s	superficial velocity dispersed phase
w_N	m/s	mean velocity dispersed phase in a hole
w_{NS}	m/s	velocity dispersed phase at transition to jetting region
w_R	m/s	relative velocity
ε_d	---	holdup dispersed phase
η_c	kg/ms	dynamic viscosity continuous phase
η_d	kg/ms	dynamic viscosity dispersed phase
ν_c	m^2/s_3	kinematic viscosity continuous phase
ρ_c	kg/m_3	density continuous phase
ρ_d	kg/m^3	density dispersed phase

$\Delta\rho$	kg/m^3	density difference
σ	N/m	interfacial tension
τ	s	resindence time of a drop during drop motion
φ_A	---	fractional free area of the downcomer
φ_N	---	fractional free area of the holes

dimensionless parameters:

$$Ar = \frac{\Delta\rho}{\rho_c} \cdot \frac{d_P^3 \cdot g}{\nu_c^2}$$ Archimedesnumber

$$K'_{Fc} = \frac{\rho_c}{\Delta\rho} \cdot \frac{\rho_c \cdot \sigma^3}{\eta_c^4 \cdot g}$$ Fluidnumber continuous phase

$$K'_{Fd} = \frac{\rho_d}{\Delta\rho} \cdot \frac{\rho_d \cdot \sigma^3}{\eta_d^4 \cdot g}$$ Fluidnumber dispersed phase

$$v_c^* = \dot{v}_c \cdot \frac{\rho_c}{(\Delta\rho \cdot \nu_c \cdot g)^{1/3}}$$ dimensionless superficial velocity continous phase

$$v_d^* = \dot{v}_d \cdot \frac{\rho_c}{(\Delta\rho \cdot \nu_c \cdot g)^{1/3}}$$ dimensionless superficial velocity dispersed phase

THEORETICAL AND EXPERIMENTAL STUDY OF TRANSIENT START-UP BEHAVIOR OF PULSED SIEVE PLATE EXTRACTION COLUMN

H. Zimmermann, E. Blaß
Lehrstuhl A für Verfahrenstechnik
Technische Universität München
Arcisstr. 21
D-8000 München 2

From the plurality of column types for liquid-liquid extraction the pulsed sieve plate extraction column was chosen for this investigation, which is known as a simple and reliable apparatus.

For this type of column the transient start-up behavior was experimentally tested for two various systems as a function of operating and design parameters.

For the unsteady state of the extractor a mathematical model was developed which fundamental structure and the obtained results were presented.
From the experimental and theoretical results a suitable control strategy was developed.

INTRODUCTION

Liquid-liquid extraction is an energy saving separation process for solutions, application of which is increasing rapidly in the process industry.

As is well known, the extraction process is a very slow process, so that, depending on the column type, column size and applied systems, it may last hours till a steady state concentration profile is reached in the extractor.

For the reliable operating of an extractor, information is needed not only of the steady state operating parameters but also of the dynamics especially of the start-up behavior of such a column.

Start-up behavior means the change of concentration per unit time of the phases which left the apparatus, till after a certain time - the so-called start-up time - a steady state concentration profile is reached.

Previous investigations to the start-up behavior are mostly of theoretical type, they are restricted to the description of an extraction process with the aid of mathematical models.

The results of such investigations may be used to develop control strategies for the start-up with regard to reduce start-up times.

EXPERIMENTAL

The start-up behavior was tested in a pilot plant pulsed sieve plate extraction column with the two systems MIBK (methyl isobutyl keton)-acetic acid-water and toluene-acetone-water. These two systems belong to the recommended systems for liquid liquid extraction /1/ studies and they differ in the most significant physical property for two-phase liquid systems- interfacial tension.
Both systems show interfacial turbulence, the system MIBK-acetic acid-water by the direction of mass transfer from the organic to the aqueous phase, the system toluene-acetone-water by the direction of mass transfer from the aqueous to the organic phase. A fact which may lead to higher separating efficiency.

In all investigations the organic phase was the dispersed phase and mass transfer took place from the dispersed organic to the continuous water phase.

Table 1 shows the geometrical dimensions of the pulse column, the physical properties of the two systems and the chosen feed concentrations and phase ratios.

SYSTEMS

	σ	$\Delta\varrho$	η
	10^{-3} kg/s	kg/m^{-3}	10^{-3} kg/m·s
MIBK-acetic acid-water	9,04	196	0,58
toluene-acetone-water	35,40	131	0,59

feed-concentration , phase ratio

	c_{Ra} / vol %	$\alpha = \dot{v}_c / \dot{v}_d$
MIBK-acetic acid-water	15	0,3 ÷ 0,7
toluene-acetone-water	10	0,3 ÷ 0,7

DIMENSIONS

diameter	: D_c = 4,7 cm
plate spacing	: H_p = 5 ÷ 15 cm
hole diameter	: d_L = 0,2 cm
free area	: 21,6 %
high of column (without disengaging chamber)	: H_c = 100 ÷ 200 cm

Table 1:
Systems and dimensions

In all experiments the pulse amplitude was constant (a= 8 mm) and only pulse frequency was varied.

The solvent was introduced always unloaded into the apparatus.

For each experiment the two phases were mutually saturated. Figure 1 shows the experimental procedure to the dynamic investigations of start-up.

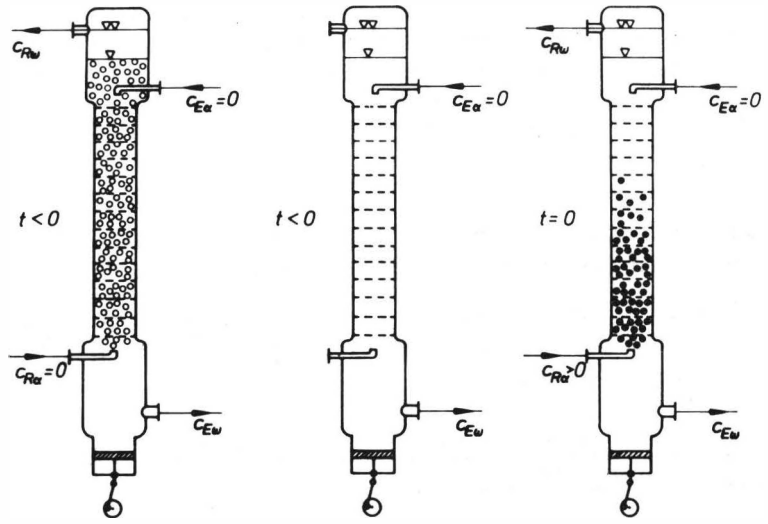

Fig. 1: Schematic description of start-up

t < 0

First the extractor is filled with the unloaded saturated continuous phase (water) to the height of the interface level and the aqueous flow rate is set up to the chosen value.
To create a defined beginning (concentration of the raffinate phase = 0) unloaded dispersed phase is then fed into the column till a coherent layer of dispersed phase at the interface is developed. Then the flow rate of the organic phase is set to zero.

t = 0

At time zero the flow rate of the organic phase (solute concentration > 0) is started at the chosen specific rate.
This corresponds to the usual start-up strategy for industrial plants.

t > 0

The raffinate and extract concentration were determined as a function of time by taking periodic samples (5 min) which were analyzed by titration.

EXPERIMENTAL RESULTS

The transient start-up behavior and the start-up time were determined as a function of operating variables - flow rate of the continuous phase $\dot{v}_c$, phase ratio α, pulse frequency f- and design parameters - plate spacing H_p, column heigth H_c.

Change of variables:

flow rate of cont. phase $\dot{v}_c$	:	0,14 ÷ 0,46	cm/s
phase ratio α	:	0,29 ÷ 0,70	
pulse frequency f	:	60 ÷ 150	1/min
plate spacing H_p	:	5,10,15	cm
column height H_c	:	100, 200	cm

To explain the course of curves an additional information is needed about the separating efficiency in the column. This efficiency was estimated by the "Height of a theoretical plate"

$$HETS = \frac{H_c}{n_{th}} \qquad (1)$$

in which several effects on mass transfer a summarized and which proved itself in industrial design praxis.

The solution follows the assumption of linear equilibrium line and linear load line, which comes true for both systems in the measured concentration limits.

Start-up behavior as a function of the superficial velocity of the continuous phase

Figure 2 shows the start-up behavior of both systems as a function of the superficial velocity of the continuous phase for the raffinate concentration (normalized between 0 and 1), which is plotted against time.
In all investigations phase ratio was constant, only the superficial velocity was varied.

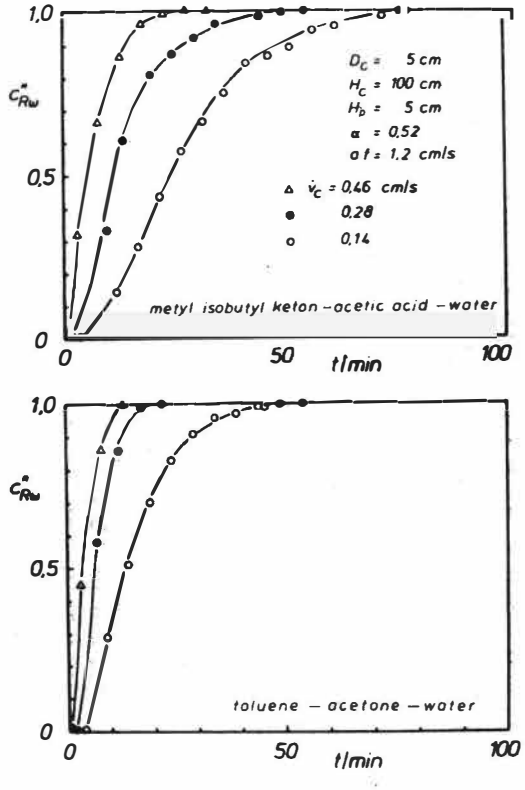

Fig. 2: Start-up behavior as a function of $\dot{v}_c$

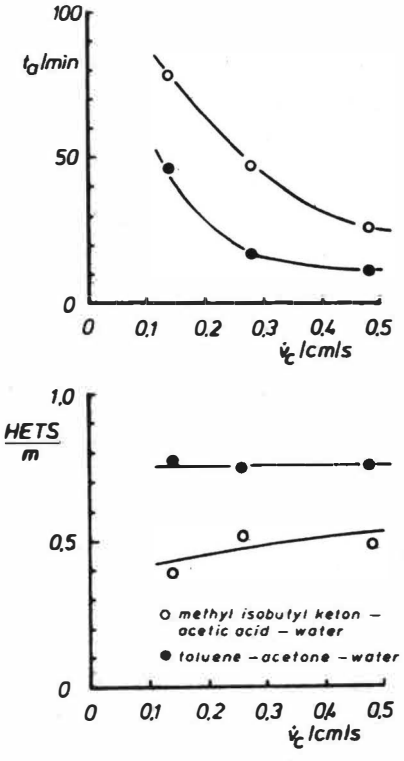

Fig. 3: Start-up time and HETS as a function of v_c

An increase of the superficial velocity of the cont.Phase means simultaneously an increase of the superficial velocity of the dispersed phase and therefore a decrease of the residence time of the dispersed phase. The smaller the residence time the faster steady state conditions will be reached. This result is to be current for both systems.
The start-up times of the system toluene-aceton-water are remarkably shorter (fig.3), a fact which can be explained by the essential lower separating efficiency of this system. A smaller separating efficiency means a decrease of solute concentration difference between feed and raffinate and therefore smaller start-up times.
The start-up times for the system MIBK-acetic-acid vary between 78 and 26 minutes, for the system toluene-acetone-water between 46 and 11 minutes.
The values for HETS show, that backmixing does not occur in the system toluene-acetone-water. There is no change of the HETS with increasing superficial velocity of the continuous phase, in contrast to the system MIBK-acetic acid-water, showing an increase of the HETS, which may be explained by the effect of backmixing.

Start-up behavior as a function of phase ratio

An increase of the phase ratio α by constant superficial velocity of the continuous phase, means a decrease of the superficial velocity of the dispersed phase and an increase of residence time of dispersed phase.
Otherwise a decrease of the phase ratio is connected with a decrease of the separating efficiency. Smaller concentration differences between feed and raffinate effects a shortening of start-up times (fig. 4 and fig. 5).

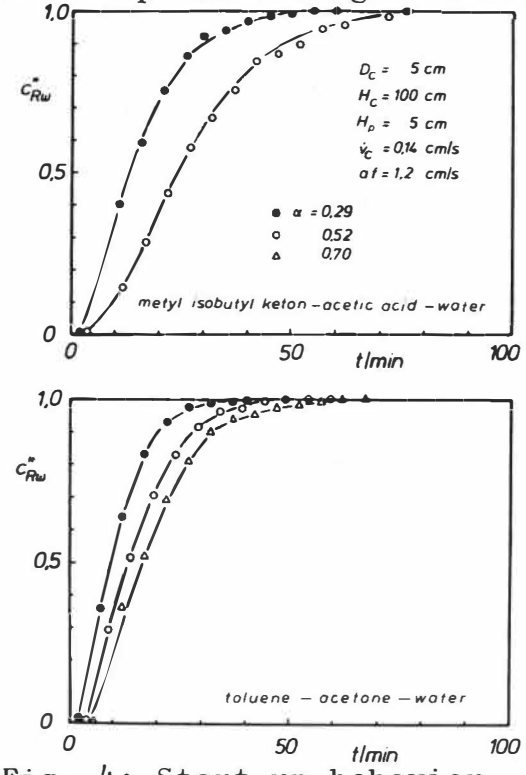

Fig. 4: Start-up behavior as a function of α

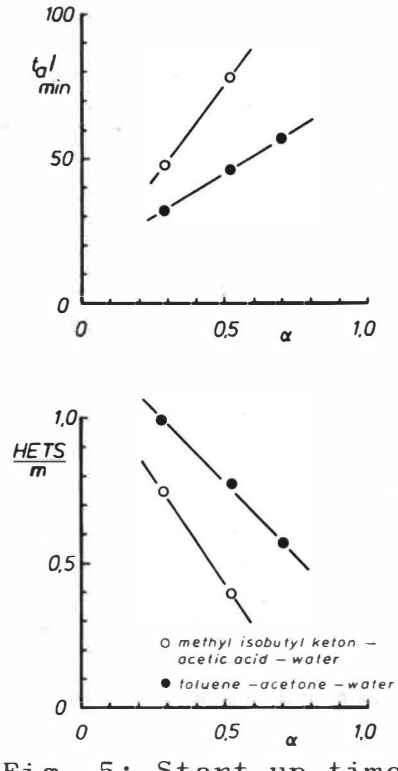

Fig. 5: Start-up times and HETS as a function of α

Start-up behavior as a function of pulse frequency f

For both systems no reliable dependence of pulse frequency was found (fig.6 and fig.7).
With increasing pulse frequency, a decrease of the drop diameter, an increase of the specific mass transfer area and an increase of the separating efficiency are to be expected.
In opposite to these facts backmixing increases with increasing pulse frequency.
It seems that backmixing effects do not exist, perhaps based on the small plate spacing.

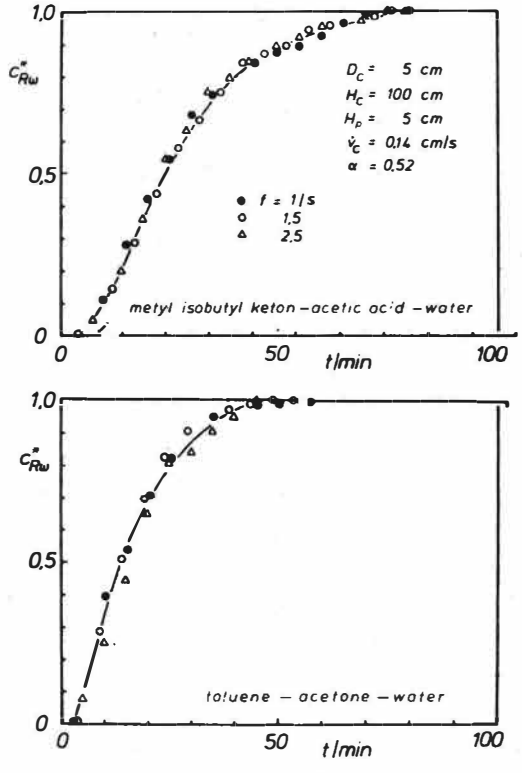

Fig. 6: Start-up behavior as a function of f

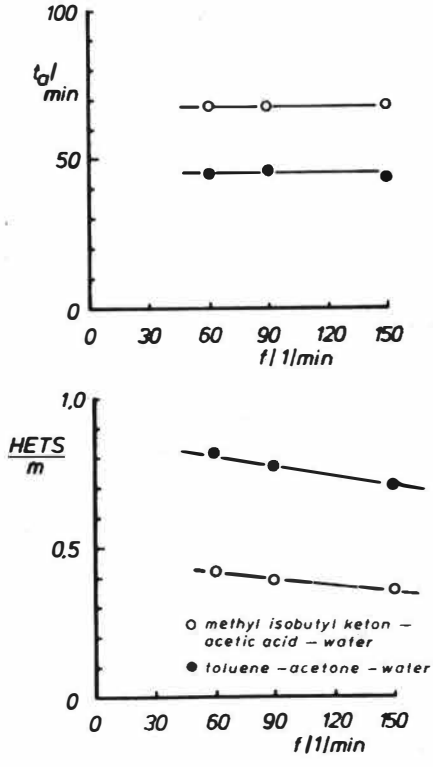

Fig. 7: Start-up time and HETS as a function of f

Start-up behavior as a function of plate spacing

As for the system MIBK-Acetic acid-water the start-up behavior and the start-up time show a small dependence on plate spacing, the start-up behavior for the system toluene-acetone-water is independent of plate spacing (fig.8 and fig.9).

In both systems an increase of the HETS values, that means a decrease in separating efficiency is investigated, whereas the dependence for the system MIBK-Acetic acid-water is essentially greater. A fact which can be reduced to the increasing backmixing and the decreasing fractional volume-holdup of the dispersed phase.

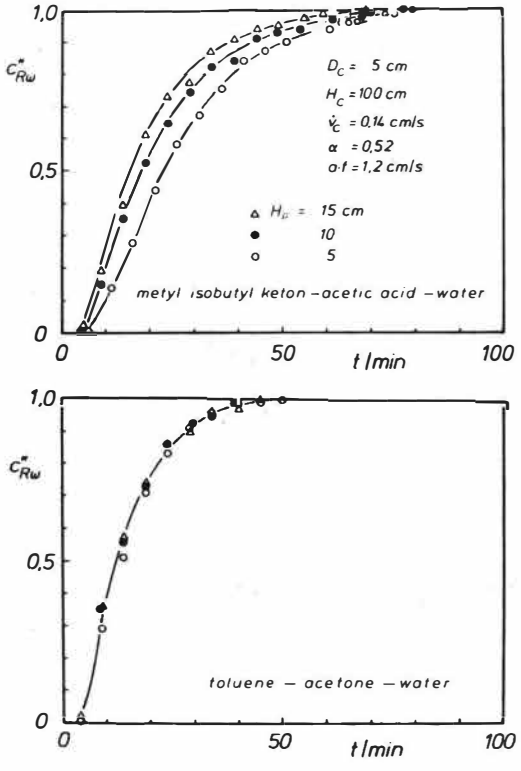

Fig. 8: Start-up behavior as a function of H_p

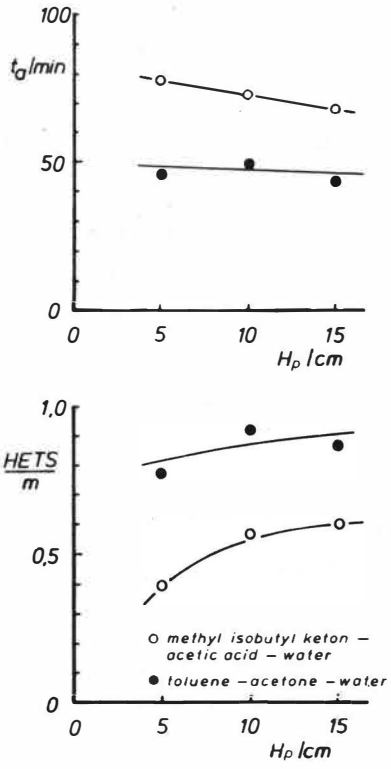

Fig. 9: Start-up time and HETS as a function of H_p

Start-up behavior as a function of column height

Because of the increasing residence time of the dispersed phase and the higher separating efficiency, start-up times are essentially longer. Doubling of column height effects a doubling of start-up time.

MATHEMATICAL MODEL

To simulate the experimental transient curves a mathematical model developed by Bauermann and Blaß /2/ was modified. The mathematical description based on the backflow model, which was introduced first by Sleicher /3/.
The column comprises N complete mixed stages, identical with the plate separation distance, arranged in series with backmixing taking place between the stages in addition to the net flows of the organic and aqueous feed.
Unsteady-state material balance was formed over a plate separation section of the column (fig.10). The results were partially differential equations which were reduced to a large set of ordinary differential equations. The differential equations were solved on a digital computer.

Comparison of experimental and predicted results

Fig.11 shows the comparison of experimental and predicted results for the system MIBK-acetic acid-water for change in phase ratio and pulse frequency.
By change in phase ratio agreement between predicted and experimental results is given.

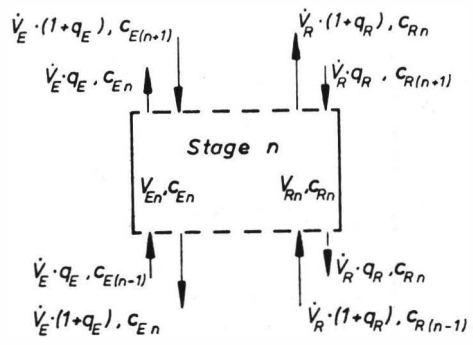

$$\frac{\partial c_{Rn}}{\partial t}[\varepsilon_R + kE_v(1-\varepsilon_R)] =$$

$$c_{R(n-1)}\frac{\dot{v}_R}{H_P}[(1+q_R)+\alpha kE_v\cdot q_E]$$

$$- c_{Rn}\frac{\dot{v}_R}{H_P}[(1+2q_R)+\alpha kE_v\cdot(1+2q_E)+\frac{\partial \varepsilon_R}{\partial t}(1-kE_v)\frac{H_P}{\dot{v}_R}]$$

$$+ c_{R(n+1)}\frac{\dot{v}_R}{H_P}[\ q_R\ +\alpha kE_v\cdot(1+q_E)]$$

Fig.10: Unsteady-state material balance

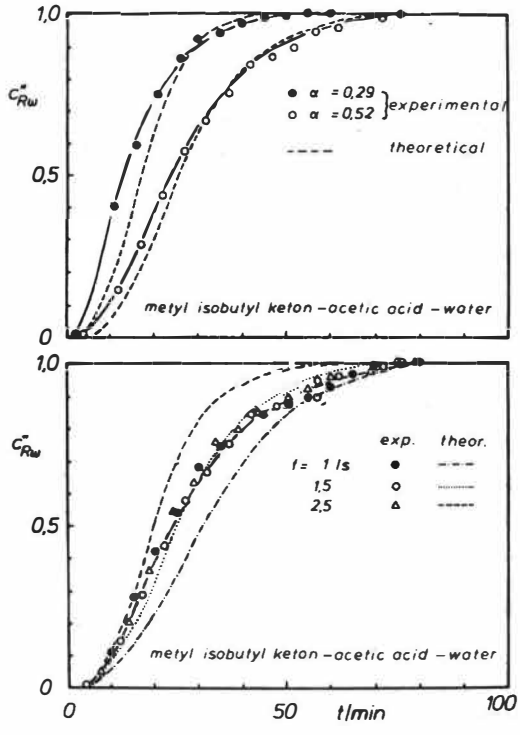

Fig.11: Comparison of exper. and theoretical results

There is no agreement by change of pulse frequency. The theoretical curves show a remarkable dependence of pulse frequency. This deviation is caused by the use of empirical correlations for hold-up and backmixing coefficients /4/ in the mathematical model, which show a great dependence on pulse frequency. The magnitude of error is ± 40 % by predicting the start-up time and ± 25 % by predicting the steady state concentration profile for all invetigations.

DEVELOPMENT OF A START-UP CONTROL STRATEGY

Fig.12 shows schematically a possibility to reduce start-up times. Plotted is the raffinate concentration versus time t. $C_{R\omega soll}$ is the aspired value of the raffinate concentration. The lower curve shows the normally employed start-up strategy, that means the flow rate of feed and solvent are set up immediately to their desired values ($\dot{v}_c$ and $\dot{v}_d > 0$).

If the flow rate of the solvent (continuous phase) is set up to zero from the beginning, the flow rate of the feed (dispersed phase) to its desired value, the continuous phase will be saturated with the solvent. This is a procedure, which is in the beginning remarkably faster. After saturating the raffinate concentration has the same value as the feed concentration ($\dot{v}_c = 0$, $\dot{v}_d > 0$).

If the flow rate of the continuous phase is followed up at time $t = t_1$ the dashed concentration curve results.

The upper picture of figure 13 shows experimental results of the controlled and uncontrolled (dashed curve) transient start-up behavior of the pulse column. The lower picture shows the variation of flow rate of the continuous phase during start-up.

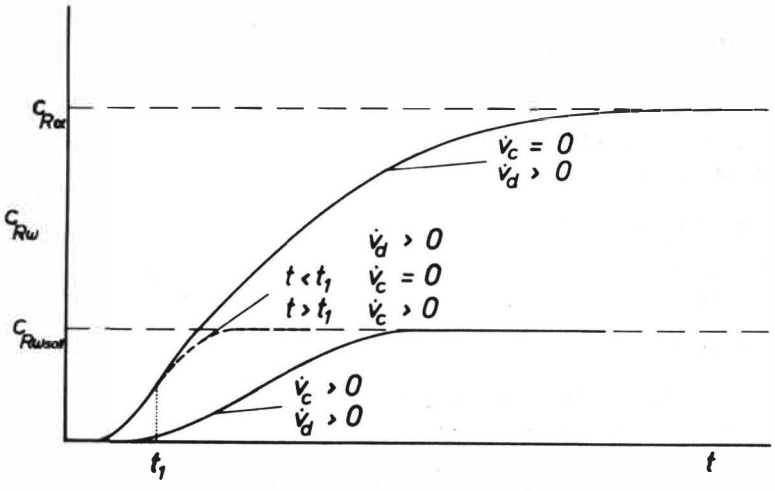

Fig.12:
Development of control strategy for start-up

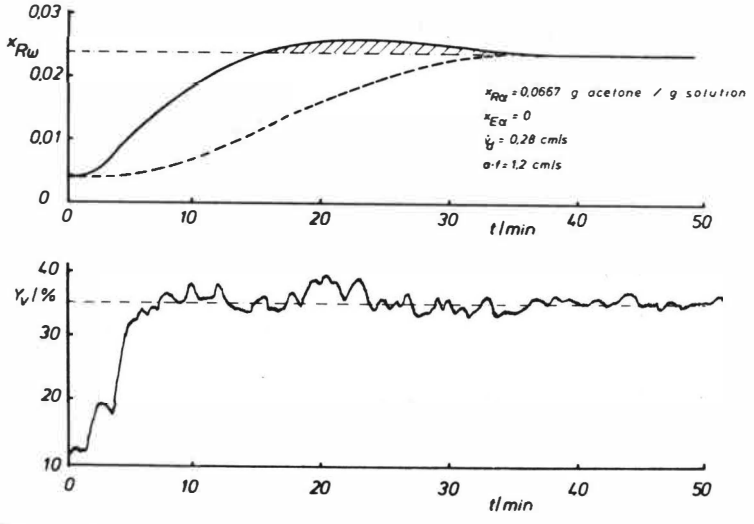

Fig.13:
Controlled and uncontrolled start-up behavior

(Y_v describes the nonlinear characteristic of the mechanically operated valve for the continuous phase)
The desired value of the raffinate concentration is indicated by the dot-dash line.
Apart from a small exceeding of the raffinate concentration above its desired value, steady-state conditions may be reached in half of the normally needed time.

CONCLUSIONS

The transient start-up behavior of a laboratory pulsed sieve plate extraction column was experimentally and theoretically investigated. From the results a control strategy for the start-up behavior was developed and experimentally tested, which reducedthe time to reach steady-state to the half of normally needed time.
All investigations were made for the individual apparatus - here "Pulsed Sieve Plate Extractor". In reality an extraction apparatus is always fitted in a plant which includes reaction or distillation processes. Therefore further investigations had to be made, testing this strategy in complete plants.

NOMENCLATURE

a	pulse amplitude
c	volume concentration
c^+ (...)	equilibrium concentration to (...)
c^*	normalized concentration
D_c	column diameter
E_v	separating efficiency
f	pulse frequency
H_c	column height
H_p	plate spacing
HETS	height of a theoretical plate
k	distribution constant
n	number
n_{th}	number of theoretical stages
q	backmixing coefficient
t	time
t_a	start-up time
$\dot{v}$	superficial velocity
V	volume
x	mass concentration
Y_v	valve characteristic
σ	interfacial tension
ϱ	density
η	viscosity
α	phase ratio
ε	holdup of the dispersed phase

Indices

R	raffinat
E	extract
c	continuous
d	dispersed
α	inlet
ω	outlet

REFERENCES

/1/Misek, T. Recommended systems for liquid extraction studies
Int.Chem.Engrs.,165-171 Railway Terrace, Rugby Warwickshire cv21 3 HQ, England

/2/Bauermann, H.-D. Simulation und mathematische Modellierung der Dynamik gepulster Gegenstromextraktoren
KfK-PDV Bericht 112(1977)

/3/Sleicher, C.A. Axial mixing and extraction efficiency of mixer settlers
AIChE-J. 5(1959)2, 145/149

/4/ Marr, R. Moser, F. Vermischungseffekte in Flüssig-Flüssig Extraktionskolonnen
Chem.Ing.Techn. 50(1978)2, 90/100

THE RECIPROCATING PLATE EXTRACTION COLUMN AS A COCURRENT MIXER

Andrew E. Karr

Chem-Pro Equipment Corp.

Fairfield, New Jersey 07006, U.S.A.

A plug flow mixer in a mixer-settler extraction system is inherently more efficient than a conventional mixer. In the present work data were obtained in short sections of the Karr Reciprocating Plate Extraction Column (RPEC)[1],[2],[3] employed as a cocurrent mixer. The column employed was 25mm in diameter. Plate spacing was 50mm. Plate stack heights of 0.61, 0.91 and 1.22m were studied. With the system o-xylene-acetic acid-water, stage efficiencies close to 100% were achieved at a total flow rate of 220 $m^3/hr.(m^2)$ when 0.91m of plate stack operating at an agitation intensity of 1270 cm/min. was employed. Agitation intensity is the product of stroke length and RPM. At a total flow of 2010 $m^3/hr.(m^2)$ the stage efficiency was 96.7% at an agitation intensity of 1778 cm/min.

The data on this system showed:

1. The lower the throughput the higher the efficiency for a given intensity of agitation
2. The greater the agitation intensity the greater the efficiency
3. The longer the plate stack the higher the efficiency.

Systems of commercial interest have been tested for clients in essentially the same equipment. With these systems somewhat lower degrees of agitation intensity were required to achieve a close approach to 100% stage efficiency at throughputs up to (2032 $m^3/hr.(m^2)$). However, for these systems, unlike the o-xylene-acetic acid-water system, it was possible to overmix, which resulted in excessive settling times. For example, with a system consisting of an amine and an aliphatic diluent extracting a compound from an aqueous solution, the following results were obtained:

Agitation Intensity cm./Minute	Stage Efficiency %	Settling Time, Minutes
1016	97	2
1524	99	10+

The above typical results indicate the need to optimize the agitation intensity which is readily achieved in the RPEC.

The flexibility, plug flow and isotropic turbulence in the RPEC permits one to minimize settler volume and, therefore, minimize investment.

REFERENCES

(1) Karr, A. E., AIChE J., 5, 446 (1959)
(2) Karr, A. E. and T. C. Lo, "Proc. Int'l. Solvent Extraction Conf.", 1, 299 (1971)
(3) Karr, A. E. and T. C. Lo, Chem. Eng. Prog. 72, 68 (1976)

HYDRODYNAMIC STUDIES IN A RECIPROCATING PLATE COLUMN

N.V.Ramarao, N.S.Srinivas & Y.B.G.VARMA

Indian Institute of Technology

Madras-600 036 ; India

The two-phase frictional pressure drop, ΔP_{TP} and the dispersed-phase holdup, ε were measured for countercurrent gas-liquid and liquid-liquid flow in a reciprocating plate column. The experimental range of investigation was:-column diameter, D:9.2-15.3 cm; perforation diameter, d_o:0.3-0.9 cm; free area, f:0.1-0.3; plate spacing, p:2.0-5.6 cm; amplitude, A:1.4-6.4 cm; frequency, :0.8-4 Hz; superficial velocity of heavy phase, U_c:0.1-3.72 and of light phase, U_d:0.004-5.1 cm/s. The system exhibited three distinct types of phase dispersion, Viz. mixing-settling, emulsion and an unstable region preceeding flooding as a function of throughput rates, agitation speed and column geometry.

Fig.1 presents typical variation of ΔP_{TP} for the gas-liquid system with increasing region corresponding to mixing-settling and emulsion; in comparison, ΔP_{TP} increases slowly for the liquid-liquid system followed by a sharp increase indicative of flooding. ΔP_{TP} decreases in gas-liquid system, but increases in liquid-liquid system with increase in dispersed-phase velocity. An increase in heavy phase throughput increases ΔP_{TP} substantially in either of the system. ΔP_{TP} increases with increase in plate spacing, but decreases with free area of the plate. An increase in d_o increases ΔP_{TP} till d_o=0.65, beyond which ΔP_{TP} decreases. Fig.2 presents the variation in ε with the falling region corresponding to mixing-settling. ε is strongly influenced by the dispersed-phase throughput and is less affected by the continuous phase flow rate. ε is relatively insensitive to the variation in plate spacing and free area.

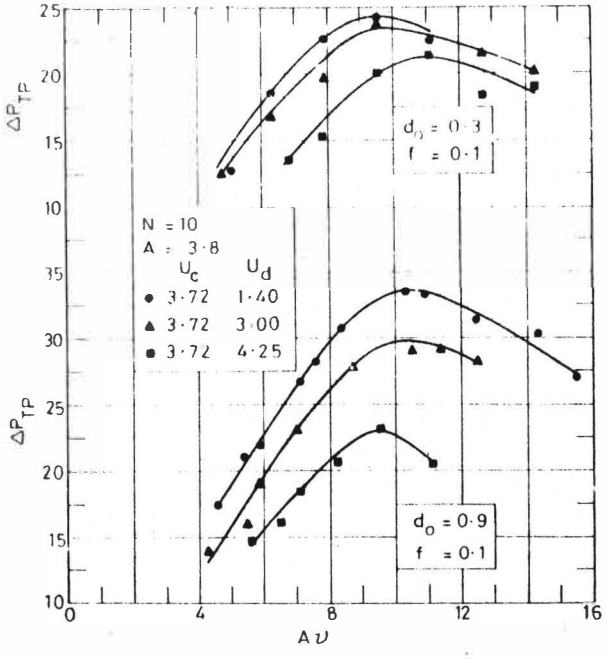

FIG. 1. VARIATION OF TWO-PHASE FRICTIONAL PRESSURE DROP WITH OPERATING CONDITIONS

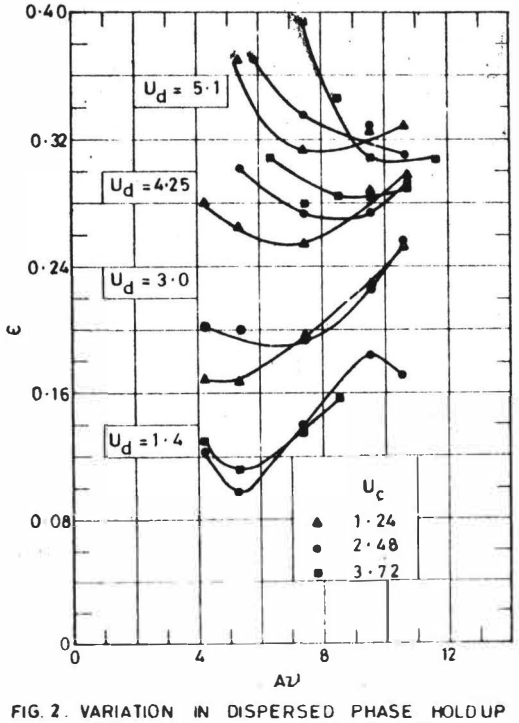

FIG. 2. VARIATION IN DISPERSED PHASE HOLDUP WITH AGITATION AND FLOW RATE OF THE PHASES (d_o = 0·5, A = 6·35, N = 10)

THE RECIPROCATING PLATE EXTRACTION COLUMN AS A COCURRENT MIXER

Andrew E. Karr

Chem-Pro Equipment Corp.

Fairfield, New Jersey 07006, U.S.A.

A plug flow mixer in a mixer-settler extraction system is inherently more efficient than a conventional mixer. In the present work data were obtained in short sections of the Karr Reciprocating Plate Extraction Column (RPEC)[1],[2],[3] employed as a cocurrent mixer. The column employed was 25mm in diameter. Plate spacing was 50mm. Plate stack heights of 0.61, 0.91 and 1.22m were studied. With the system o-xylene-acetic acid-water, stage efficiencies close to 100% were achieved at a total flow rate of 220 $m^3/hr.(m^2)$ when 0.91m of plate stack operating at an agitation intensity of 1270 cm/min. was employed. Agitation intensity is the product of stroke length and RPM. At a total flow of 2010 $m^3/hr.(m^2)$ the stage efficiency was 96.7% at an agitation intensity of 1778 cm/min.

The data on this system showed:

1. The lower the throughput the higher the efficiency for a given intensity of agitation
2. The greater the agitation intensity the greater the efficiency
3. The longer the plate stack the higher the efficiency.

Systems of commercial interest have been tested for clients in essentially the same equipment. With these systems somewhat lower degrees of agitation intensity were required to achieve a close approach to 100% stage efficiency at throughputs up to (2032 $m^3/hr.(m^2)$). However, for these systems, unlike the o-xylene-acetic acid-water system, it was possible to overmix, which resulted in excessive settling times. For example, with a system consisting of an amine and an aliphatic diluent extracting a compound from an aqueous solution, the following results were obtained:

Agitation Intensity cm./Minute	Stage Efficiency %	Settling Time, Minutes
1016	97	2
1524	99	10+

The above typical results indicate the need to optimize the agitation intensity which is readily achieved in the RPEC.

The flexibility, plug flow and isotropic turbulence in the RPEC permits one to minimize settler volume and, therefore, minimize investment.

REFERENCES

(1) Karr, A. E., AIChE J., 5, 446 (1959)
(2) Karr, A. E. and T. C. Lo, "Proc. Int'l. Solvent Extraction Conf.", 1, 299 (1971)
(3) Karr, A. E. and T. C. Lo, Chem. Eng. Prog. 72, 68 (1976)

HYDRODYNAMIC STUDIES IN A RECIPROCATING PLATE COLUMN

N.V.Ramarao, N.S.Srinivas & Y.B.G.VARMA

Indian Institute of Technology

Madras-600 036 ; India

The two-phase frictional pressure drop, ΔP_{TP} and the dispersed-phase holdup, ε were measured for countercurrent gas-liquid and liquid-liquid flow in a reciprocating plate column. The experimental range of investigation was:-column diameter, D: 9.2-15.3 cm; perforation diameter, d_o: 0.3-0.9 cm; free area, f: 0.1-0.3; plate spacing, p: 2.0-5.6 cm; amplitude, A: 1.4-6.4 cm; frequency, : 0.8-4 Hz; superficial velocity of heavy phase, U_c: 0.1-3.72 and of light phase, U_d: 0.004-5.1 cm/s. The system exhibited three distinct types of phase dispersion, Viz. mixing-settling, emulsion and an unstable region preceeding flooding as a function of throughput rates, agitation speed and column geometry.

Fig.1 presents typical variation of ΔP_{TP} for the gas-liquid system with increasing region corresponding to mixing-settling and emulsion; in comparison, ΔP_{TP} increases slowly for the liquid-liquid system followed by a sharp increase indicative of flooding. ΔP_{TP} decreases in gas-liquid system, but increases in liquid-liquid system with increase in dispersed-phase velocity. An increase in heavy phase throughput increases ΔP_{TP} substantially in either of the system. ΔP_{TP} increases with increase in plate spacing, but decreases with free area of the plate. An increase in d_o increases ΔP_{TP} till d_o=0.65, beyond which ΔP_{TP} decreases. Fig.2 presents the variation in ε with the falling region corresponding to mixing-settling. ε is strongly influenced by the dispersed-phase throughput and is less affected by the continuous phase flow rate. ε is relatively insensitive to the variation in plate spacing and free area.

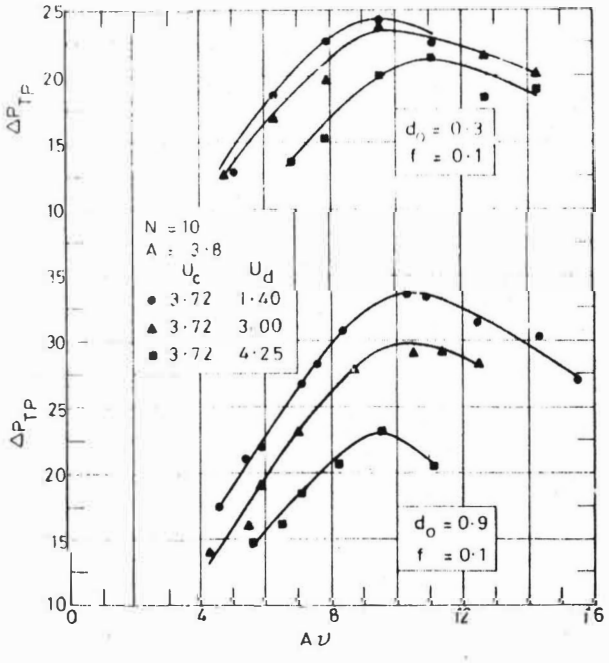

FIG. 1. VARIATION OF TWO-PHASE FRICTIONAL PRESSURE DROP WITH OPERATING CONDITIONS.

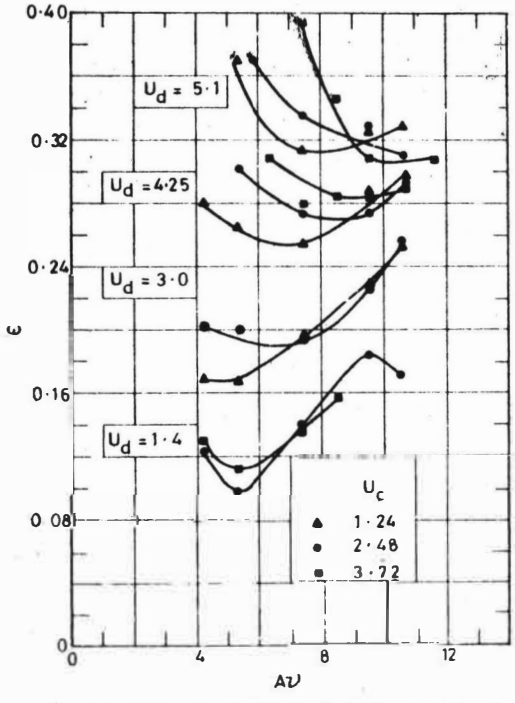

FIG. 2. VARIATION IN DISPERSED PHASE HOLDUP WITH AGITATION AND FLOW RATE OF THE PHASES (d_o = 0·5, A = 6·35; N = 10)

THE QVF-STIRRED-CELL-EXTRACTOR — IDEA AND SPECIAL ASPECTS OF CALCULATION

Dipl.-Ing. J. Postl
Prof. Dr.-Ing. R. Marr

Institut für Grundlagen der
Verfahrenstechnik, TU Graz
Kopernikusgasse 24, A-8010 Graz

Austria

The new Quickfit-stirred-cell-extractor is an extraction column with rotating installations, such as RDC, ARD, Oldshue-Rushton or the KÜHNI-Column. An impeller with four flat blades disperses one phase. The separating baffles are endowed with meander-shaped weirs at the border of the central ring-shaped openings (Fig. 1). These weirs favour the separation of the phases and canalize the two counter-current streams, as can be seen schematically in Fig.2. The heavy (here: continuous) phase flows through the openings in the upper part of the weirs to the free stator-area and along the adjacent weir-blade downwards. The light phase coalesces behind the weirs and reaches the higher situated cell in an analogue way.Therefore reduced axial mixing

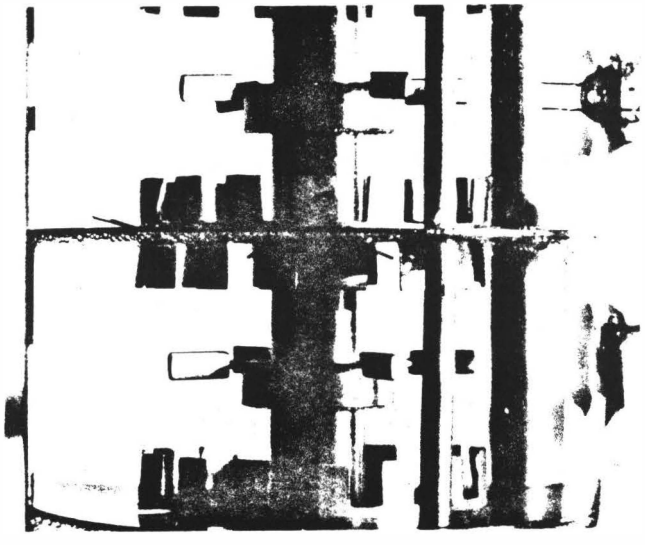

Fig. 1

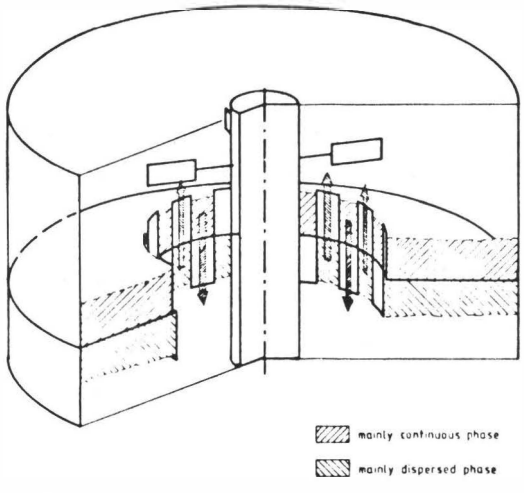

Fig. 2

as well as higher flow-rates may be expected.

At first the limiting flow-rates and the Hold-Up values have been measured altering the working parameters rotor-speed and ratio of the phases. The maximal flow-rate of both phases was about 25 m^3/m^2h (system water/toluene, free stator-area 20%).

The drop-size-distributions were also investigated dependant on rotor-speed and Hold-Up. The new installations favour small drop-size-spectra. The distributions have been described by a modified Muggle&Evans-distribution and the Sauter-diameter have been calculated. A general valid correlation cannot be given because of the great influence of the direction of mass-transfer on drop-size.

Based on a hydrodynamical model the following equation has has been developed for the calculation of the effective phase-velocities [1,2] :

$$\frac{v_c}{\varphi(x_d)} + \frac{v_d}{x_d}\left[1 + 0{,}640\,\frac{x_d^{2/3}}{\varphi(x_d)}\right] = u_s.C \qquad (1)$$

$$\varphi(x_d) = 1 - 0{,}959\,x_d^{2/3}$$

$$C = 0{,}31$$

The column-diameter may be designed with the help of this equation.

The axial mixing of each phase was measured according to the unsteady tracer-method and was evaluated using the dispersion-model.

For the continuous phase the results of these experiments, i.e. the Bodenstein- (or Peclet-) Numbers, have been correlated by an equation derived from the theory of isotropic turbulence.

$$\frac{1}{Bo_{c,m}} = H_Z\left[0{,}280 + 0{,}187\,\left(\frac{D_S}{D_C}\right)^2\left(\frac{D_C}{H_Z}\right)^{0{,}33}\frac{Re_r^{0{,}8}}{Re_c}\right] \qquad (2)$$

$$Bo_{c,m} = \frac{\bar{v}_c}{D_{ax,c}}$$

$$Re_r = \frac{D_R^2\,r}{\nu_c}$$

$$Re_c = \frac{D_C\,\bar{v}_c}{\nu_c}$$

Another equation has been correlated for the description of the axial mixing of the dispersed phase :

$$\frac{1}{Bo_{d,m}} = H_Z\left[0{,}229 + 245{,}3\,Re_d^{-1}\right] \qquad (3)$$

$$Bo_{d,m} = \frac{\bar{v}_d}{D_{ax,d}}$$

$$Re_d = \frac{D_C\,\bar{v}_d}{\nu_c}$$

At last mass-transfer experiments were taken through, measuring all important parameters : Hold-Up, axial-mixing-parameters of both phases, drop-size-distribution, concentration of both phases at inlet and outlet as well as at four further positions of the column. Concentration profiles were calculated theoretically, using the dispersion-model (The mass-transfer-coefficients were ascertained by available correlations for single drops, and were used related to the actual distribution of drop-sizes). The good agreement with the measured profiles confirms the applicability of the dispersion-model.

Thus the design of the column-height with the help of the dispersion-model seems to be successfully.

REFERENCES :

[1] Marr, R. et al.: Chem.-Ing.-Techn. 46(1974)5,207
[2] Postl, J. : Dissertation, TU Graz (in edition)

NOMENCLATURE :

Bo	-	Bodenstein- (Peclet-)Number (related to 1 Meter)
C	-	Constant
D	m	Diameter
D_{ax}	m^2/s	Dispersion-coefficient
H	m	Height
r	1/s	rotor-speed
Re	-	Reynolds-Number
u_S	-	rising-velocity of a single drop with the Sauter-diameter(in resting continuous phase)
v	m/s	phase-velocity (related to the column-diameter)
$\bar{v}$	m/s	effective phase-velocity
x_d	%	Hold-Up of the dispersed phase
ν	kgm/s	viscosity

Indices :

C	Column
c	continuous phase
d	dispersed phase
R	Rotor
S	Stator
Z	Cell

MIXER-SETTLER-COLUMN, A NEW STAGEWISE CONTACTOR

U. Bühlmann

Kühni Ltd

CH-4123 Allschwil (Switzerland)

As its name implies, the mixer-settler-column belongs to the classification of stagewise liquid-liquid contactors, but its construction is clearly that of a column.

Each stage of the column is divided into two sections. The two phases are intimately mixed in the mixing zone and then completely separated again in the following settling zone. Countercurrent flow is achieved by the action of gravity alone. The clear dispersed phase flows into the next stage via a hydraulic seal and the continuous phase is conducted along a separate path through the settling zone in order to avoid disturbing the settling operation. Settling aids are installed in the settling compartments to promote coalescence of the dispersed phase.

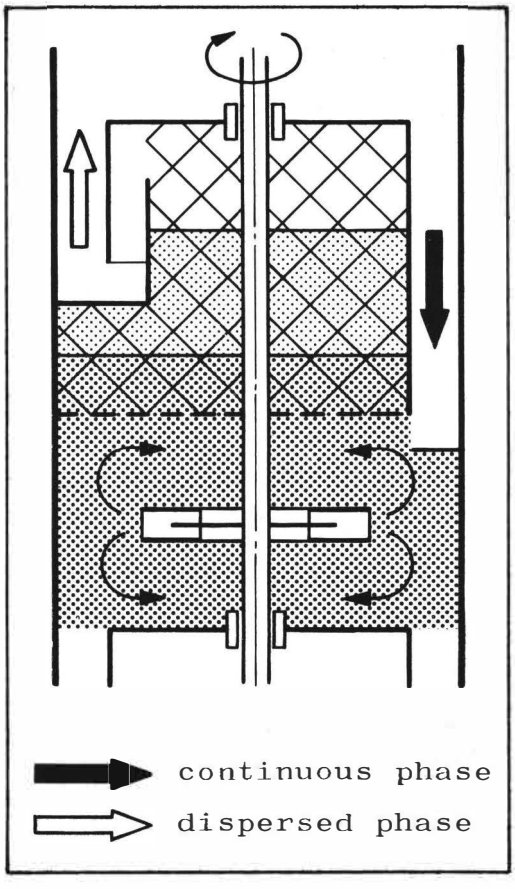

The general characteristics and advantages of the mixer-settler-column may be summarized as follows:

- Zero backmixing between the stages and therefore high stage efficiency
- Complete separation of the mixing and phase transport processes
- No necessity for phase recirculation even at extreme phase ratios
- The possibility to allow for long residence times in the mixing zone
- Low floor space requirements

The main application for the new contactor is likely to be in processes with extreme phase ratios and for liquid-liquid systems, which are difficult to separate, or which are subject to emulsification. A further example would be extraction combined with chemical reaction, where a particular residence time for each stage is required. Especial interest is therefore expected in the metals extraction field, where the first industrial tests have been performed using a pilot scale column.

A NEW TYPE OF AGITATED LIQUID/LIQUID EXTRACTION COLUMN WITH ENHANCED COALESCENCE PLATES

Ladislav Steiner, S.Hartland

Swiss Federal Institute of Technology (ETH)
Department of Industrial & Engineering Chemistry
Zürich, Switzerland

To improve the loading capacity and efficiency of agitated liquid/liquid extractors a new plate has been designed for the separation of mixing cells (Fig.1). It consists of vertical or slightly inclined elements arranged in a lattice,or concentric cylinders and ribs(Fig.2). The Plate elements are made of materials preferably wetted by the disperse phase so that drop coalescence is greatly enhanced. The plate free area is extremely high,up to 90%,so that the resistance of the plate to the axial flows of the phases is very small. However,due to its height and arrangement of its elements it hinders all other types of flow, especially the radial and tangential components.When working,the plate free volume is filled with the dispersed phase,leaving only the space necessary for the flow of the continuous phase.In this way a plate with variable free area has been developed which adjusts its operation to existing conditions. The plate possesses the following advantages over other types: (a) Wide operating range:Because of the variable plate free area the column is not sensitive to flooding and works well with high phase throughputs.It also works well in the region of low throughputs as the plates are then partially blocked by the dispersed phase.Phase ratios of 1:20 and 20:1 have been experimentally used. (b) Insensitivity to impurities:If there are solid contaminants in the feeds they can pass through the column due to the extremely large free areas of the plates. (c) High efficiency: The repeated coalescence in the plates and redispersion by the stirrers considerably enhances the mass transfer rate. In a prototype column of 80 mm diameter over 6 theoretical stages/meter with a load of 30 m^3/m^2h have been reached (Toluene(d),Acetone,Water (c).

The column provides an attractive alternative to solve large-scale extraction production problems when extreme phase ratios are necessary.

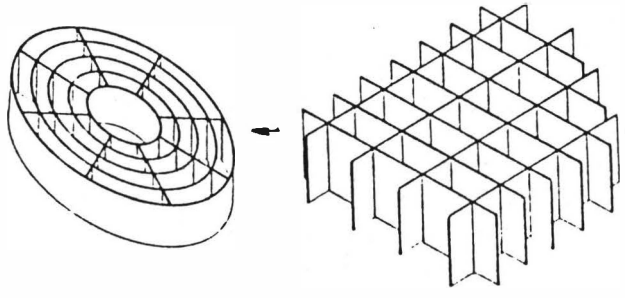

Fig.2 Different Plate Constructions

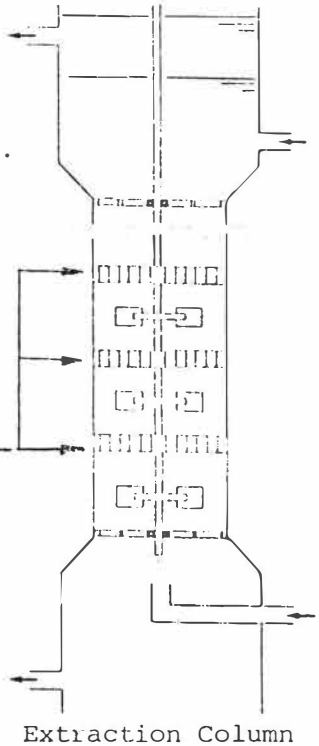

Fig.1 Extraction Column

A CENTRIFUGAL EXTRACTOR FOR FAST AND SLOW MASS TRANSFER PROCESSES.

G.I. Kuznetsov, S.M. Belyakov,
L.I. Shklyar, A.A. Pushkov

State Committee for Atomic Energy, Moscow, USSR

Centrifugal extractor has been devised for processes with both fast and slow rates of mass transfer*. The extractor is furnished with a set of interchangeable stirrers and mixing chambers of the volume from 0.4 x $10^{-3}m^3$ to 21.2 x $10^{-3}m^3$, this allowing for changing the time of phases contact in the mixing chamber from 1s to 53s with no change in throughput capacity.

The technical data of the extractor: throughput -0.4x$10^{-3}m^3/s$ at phase entrainment does not exeed 0.02%, diameter of rotor - 0.125 m, operating volume of separating chamber - 0.9x$10^{-3}m^3$, overall dimension including electric motor -0.31m x x 0.31m x 0.85m.

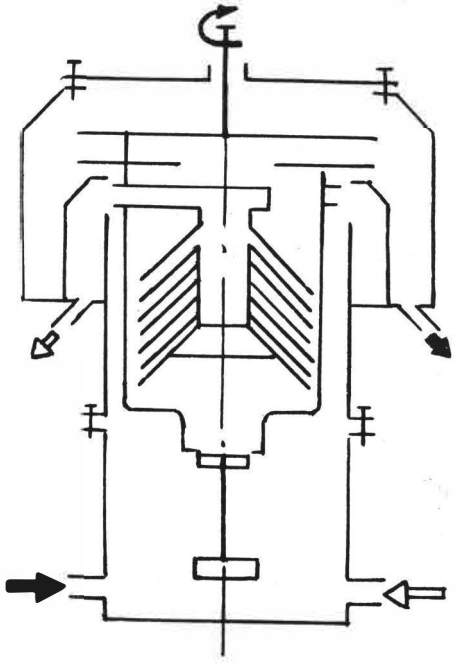

Principle of operation of the extractor is shown here on figure.

The extractor stably operates in any ratio of flow rates of feed and solvent solutions as well as in the range of their density ratio from 0.6 to 0.98.

The efficiency of mass transfer on system: 1.1 M TBP in aliphatic hydrocarbons - 0.1 M $UO_2(NO_3)_2$ in 2M HNO_3 depends on the contact time in the mixing chamber and at 3.6s is over 95%.

In the system 0.1M HDEHP in aliphatic hydrocarbons - 0.05M UO_2SO_4 in 0.5M H_2SO_4 the rate of mass transfer is likely to be limited by a slow stage of chemical reaction and the 95% efficiency is attained over 50-60s.

Irrespective of the method of obtaining the time of phases contact (by changing the flow rate of solutions or by varying the mixing chamber volume) the efficiency of mass transfer is governed by the contact time only.

* REFERENCES:
G.I. Kuznetsov, A.A. Pushkov, V.A. Elin, S.M. Belyakov, V.A. Komarov, V.P. Pashkov, A.A. Tolmachev, L.I. Shklyar. USSR Certificate of Authorship No 548291, 1975.

Modelling
Session 5

Co-chairmen : A.L. Mills (Exp. Reactor, Daunreay, U.K.)
B. Kalitventzeff (University of Liège, Belgium)

5A

80-41 A model for reciprocating plate extraction columns.
M.M. Hafez, M.H.I. Baird and I. Nirdosh, Imperial Oil Ltd., Sarnia, and McMaster University, Hamilton, Canada.

80-233 A fundamental approach to the design and optimization of industrial solvent extraction plants.
J.E. Sepulveda and J.D. Miller, University of Utah, Salt Lake City, Utah, U.S.A.

80-176 Modelling of countercurrent flow liquid-liquid extraction columns.
W.J. Korchinsky and J.J.C. Cruz-Pinto, University of Manchester, U.K. and Universidade do Minho, Braga, Portugal.

80-37 A dynamic model of solvent extraction mixer-settler stage based on predicted flow patterns.
F. Medina Gomez and W.L. Wilkinson, University of Bradford, Bradford, U.K.

80-42 A model for the co-extraction kinetics of uranium, plutonium and nitric acid.
G. Petrich, Institut für Heisse Chemie, Kernforschungszentrum, Karlsruhe, Germany.

80-134 Mathematical modelling as an R&D tool in solvent extraction.
S. Wahrmann and J.E. GAI, IMI, Institute for Research and Development, Haifa, Israel.

80-142 The use of Letagrop computer program for the analysis of solvent extraction data.
D. H. Liem, Royal Institute of Technology (KTH), Stockholm, Sweden.

80-38 The kinetics of copper (II) extraction from sulphuric acid solutions by LIX 64N : a mathematical modelling approach.
C.J. Valdes, W.C. Cooper and D.W. Bacon, Queen's University, Kingston, Ontario, Canada.

5B

80-13 Comparing scale-up methods for solvent extraction mixers.
J. Roberts, University of Newcastle, New South Wales, Australia.

80-29 Model of dispersion band in a centrifugal contactor.
R.A. Lenoard, G.J. Bernstein, R.H. Pelto and A.A. Ziegler, Argone National Laboratory, Illinois, U.S.A.

80-40 Experimental and theoretical investigation of film flow on a tilted plate as the basis of a settler design.
E. Blass and D. Rautenberg, Technical University, München, Germany.

80-143 The dispersion model : concentration profils in and design of rotating disc contactors.
B. Wolschner and R. Marr, Institut für Grundlagen der Verfahrenstechnik, TU Graz, Austria.

80-172 Batch and continuous pilot plant studies, leading to full-scale mixer design for continuous countercurrent extraction.
J.Y. Oldshue, Mixing Technology, Mixing Equipement Company, Div. of General Signal, Rochester, New York, U.S.A.

80-198 Modeling of breakage and coalescence in a mixing tank.
H. Sovová and J. Procházka, Institute of Chemical Process, Acad. of Sc., Prague, Czechoslovakia.

80-215 Dynamic behaviour of mixer-settlers. Applicability of the orthogonal collocation method.
G. Aly, Dept. of Chemical Engineering, Lund, Sweden.

A MODEL FOR RECIPROCATING PLATE EXTRACTION COLUMNS

M.M. Hafez,
Imperial Oil Ltd., Sarnia, Canada, N7T 1M7

M.H.I. Baird and I. Nirdosh,
McMaster University, Hamilton, Canada, L8S 4L7

ABSTRACT

A design model is presented based on several fundamental studies of hydrodynamics and mass transfer in reciprocating plate columns of the type introduced by Karr (1959). For a given system, flow rates and plate configuration, the diameter at which flooding occurs can be calculated. If the required degree of extraction is known, the height of the plate stack can also be calculated. The model has been compared with published data.

In solvent extraction as in other areas of chemical engineering interest, great advances have been made in the past 25 years towards an understanding of basic principles. The mass transfer process itself is better understood, and there has also been considerable work in droplet breakup and coalescence and the hydrodynamic behaviour (mixing, flooding, etc.) of liquid-liquid systems in countercurrent flow. This progress was typified by the papers in sessions 4, 9, 12, 25 and 29 at ISEC 77(1). However there have been relatively few attempts to synthesise the results of the basic studies in the different areas so as to simulate, from first principles, the overall performance of a piece of equipment. One such attempt was made a few years ago by Korchinsky (2) who took available results on drop size, holdup etc. as the basis for design models for several different types of contactor. The advantages of a soundly based design or simulation model for equipment performance are obvious. Such a model allows designs to be carried out with confidence for systems which have not previously been handled in the equipment under consideration, and there is a reduction in the number and cost of pilot-scale tests. A good model can also allow the effects of changes in design methodology to be examined by calculation.

In this work, basic correlations and theory are combined to model the reciprocating plate extraction column. This type of column was introduced by Karr (3) in 1959 and many descriptions are available (3-9). It uses reciprocating perforated plates which are characterised by a relatively large hole size (12-14 mm) compared to those in

conventional pulsed plate columns. The fractional open area o is also comparatively large, in the order of 60%. These characteristics permit a relatively high throughput per unit area, coupled with ease of plate removal and cleaning. The columns are widely used industrially, particularly in the U.S.A., in sizes up to 1.0 m. Experimental data on the scale-up of columns up to 0.914 m diameter have been published (4). There have also been several studies of various hydrodynamic aspects of this type of column, namely flooding (5,6), droplet size and holdup (7), power consumption (8) and axial mixing (6,9). The results of these studies have been incorporated into the model described here.

CONSTRUCTION OF THE MODEL

The information flow diagram for the model is given in Figure 1. The central box contains information which is assumed to be available to the designer (e.g. system properties) or which he can specify (e.g. amplitude and frequency of plate oscillation). The objective of the model is to calculate the column diameter D for a given throughput, and the height of plates required for a given degree of extraction.

The first calculation is that of the power dissipation per unit volume, ψ. This calculation uses the quasi-steady friction concept proposed originally by Jealous and Johnson (10) for pulsed columns. The equation was confirmed (8) for reciprocating plate columns at normal amplitude and frequencies as:

$$\psi = \left(\frac{2\pi^2}{3}\right) \cdot \rho \left[\frac{1 - o^2}{C^2 o^2}\right] (Af)^3/h \qquad (1)$$

The specific power ψ is important in determining the Sauter mean droplet diameter d_{32}. The Kolmogoroff isotropic turbulence model, extended by Hinze (11), was applied (7) to reciprocating plate columns to give:

$$d_{32} = 0.36 \frac{\gamma^{0.6}}{\rho^{0.2} \psi^{0.4}} \qquad (2)$$

The coefficient 0.36 is empirical but dimensionless and the above equation is restricted to fairly well-agitated systems with $Af > 3$ cm/s.

The operating column diameter D must exceed the diameter D_F at which the column would flood for a given throughput. The model calculates D_F as follows. First, the dispersed phase holdup at flooding, ϕ_F, is estimated from the ratio of flow rates by Thornton's (12) equation.

$$\phi = \frac{(L^2 + 8L)^{1/2} - 3L}{4(1 - L)} \qquad (3)$$

This value is substituted in the equation developed by Hafez et al (6) for the "slip velocity" at the flooding point.

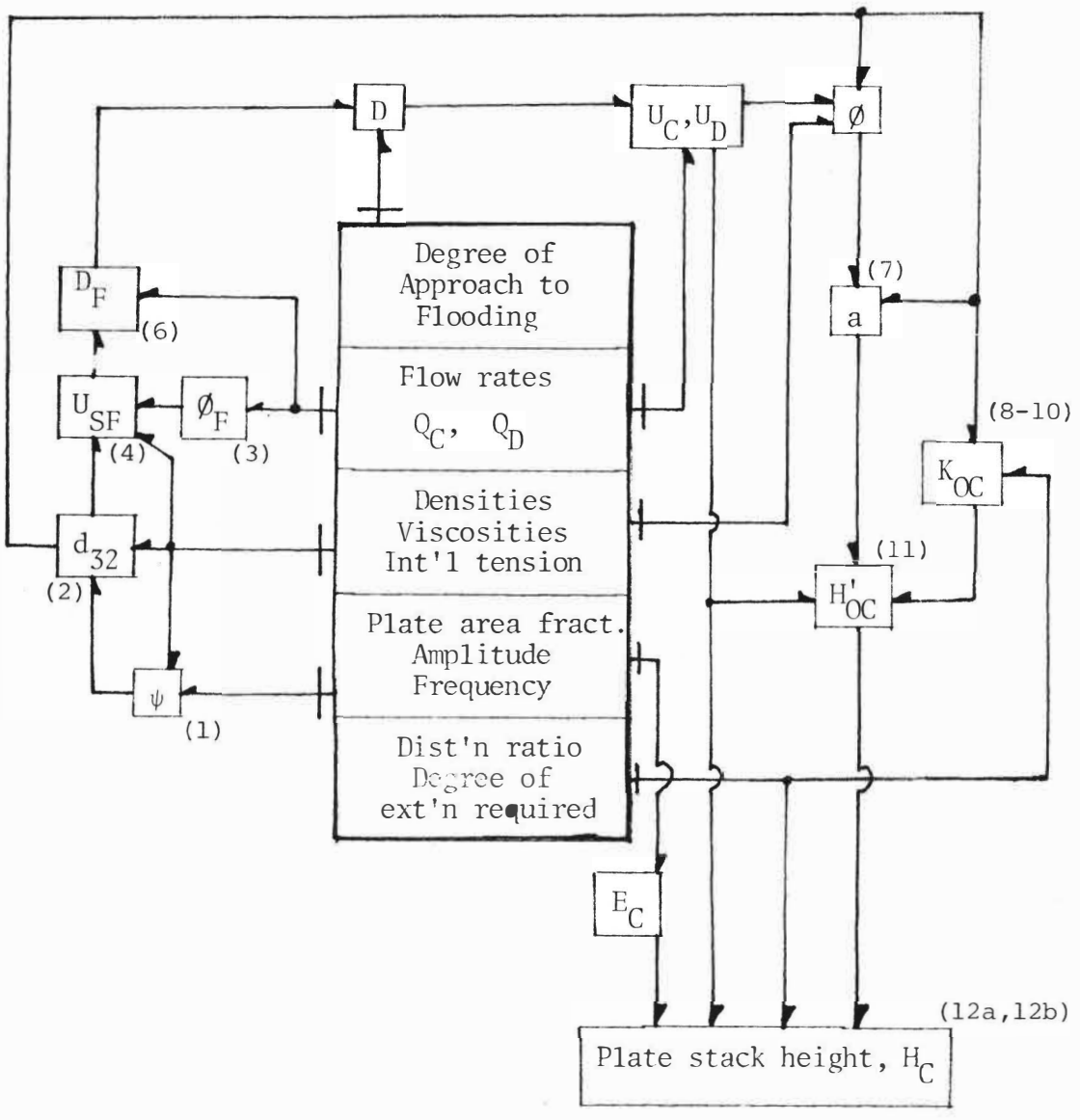

FIG. 1 Information flow diagram for model. The bracketed numbers refer to equations.

$$U_{SF} = \left(\frac{\phi_F}{1-\phi_F}\right) U_{CF} + U_{DF} = K \left(\frac{g^2 \Delta\rho^2}{\rho_c \mu_c}\right)^{1/3} d_{32} \left(\frac{(1-\phi_F)^3}{K \phi_F^{1/2}}\right)^{2/3} \qquad (4)$$

The dimensionless constant K was found to have a value of 0.01166 for non-circulating droplet systems. Since the flow rate ratio L is already specified, the value of U_{SF} from equation (4) permits calculation of either U_{CF} or U_{DF}. For example, since $U_{DF} = L\, U_{CF}$, it can be seen that

$$U_{SF} = U_{CF}\left[\frac{\phi_F}{1-\phi_F} + L\right] \qquad (5)$$

Hence the column diameter at flooding is found, given Q_C the continuous phase flow rate.

$$D_F = \left(\frac{4\,Q_c}{\pi U_{CF}}\right)^{1/2} = \left[\frac{4Q_c}{\pi U_{SF}}\left(\frac{\phi_F}{1-\phi_F} + 1\right)\right]^{1/2} \qquad (6)$$

At this juncture, the designer must decide how close to the flooding point the column will normally be operated. For example, if the column is to be operated at 80% of flooding velocity, the column diameter D is calculated to exceed D_F by a factor of $(0.8)^{-1/2} = 1.118$. Once D has been established, the operating superficial velocities U_C and U_D are calculated. Then the operating holdup ϕ is calculated from an equation similar to eq. (4) except that the subscripts "F" are removed. It may be noted that this calculation is not explicit; an iteration is used to obtain ϕ. The evaluation of the holdup, with the previously calculated Sauter mean diameter, leads to the specific interfacial area by the well-known relationship

$$a = 6\phi/d_{32} \qquad (7)$$

The overall mass transfer coefficient K_C is expressed on the basis of the continuous phase and is related to the individual film coefficients assuming equilibrium at the interface:

$$K_C = [1/k_C + 1/mk_D]^{-1} \qquad (8)$$

No direct measurements have been made of mass transfer coefficients in reciprocating plate columns or indeed in most other types of equipment; however, reliable correlations are available on the basis of laboratory experiments with some theoretical justification. For the continuous phase (13),

$$Sh_c = 0.83\, Re_c^{\,0.5}\, Sc_c^{\,0.5} \qquad (9)$$

For the dispersed phase (14)

$$k_D = \frac{2\pi^2}{3} \cdot \frac{\mathcal{D}}{d_{32}} \qquad (10)$$

These correlations (13,14) are applicable to rigid (i.e. non-circulating) droplets, as it is believed that in most of the systems investigated the drops were behaving in this manner. The value of K_C obtained from eqs. (8)-(10) was combined with that of $\underline{a}$ from eq. (7) to give the "true" height of a transfer unit:

$$H'_{OC} = \frac{U_C}{K_C a} \qquad (11)$$

If the columns operated in plug flow, H'_{OC} would also be the effective height of a transfer unit, but in practice axial mixing effects cause the effective H.T.U. to exceed the true value. The effect of axial mixing may be found by calculating the dimensionless

concentration profile in each phase by solving the steady state differential material balance equations:

$$\frac{d^2X}{dZ^2} - P_C B \frac{dX}{dZ} - N_{OC} P_C B (X - X^*) = 0 \qquad (12a)$$

$$\frac{d^2Y}{dZ^2} - P_D B \frac{dY}{dZ} - F N_{OC} B P_C (X - X^*) = 0 \qquad (12b)$$

Pratt (15) has recently developed an easily applicable procedure for solving these equations for the plate stack height H_C, given the values of the Peclet numbers and the dimensionless concentrations X and Y at each end of the column. The continuous phase Peclet numbers can be obtained using available axial dispersion data (6,9); no data exists on the mixing in the dispersed phase, so various assumptions have been necessary as discussed later in this paper.

TESTING OF MODEL FOR COLUMN DIAMETER AT FLOODING.

The calculations indicated in Figure 1 and equations (1) to (6) were carried out for column conditions and systems corresponding to published flooding studies (4, 6, 16). The parameters are given in Table 1; continuous phase flow Q_C and agitation levels are with one exception those corresponding to the actual flooding conditions (4, 6, 16), while the flow ratio (dispersed/continuous) was the design variable in this case.

Table 1. Experimental conditions corresponding to data points on flooding shown in Figure 2.

	Hafez et al (6)	Karr & Lo (16)		Karr & Lo (4)
Cont.phase	Water	MIBK		Water
Disp. phase	kerosene	water		Xylene
Intl. tension γ(mN/m)	20	9		32
Plate characteristics				
Open area fract. σ	0.58	0.61	0.61	0.61
Spacing h (cm)	5	2.5	2.5	5.0
Stroke A (cm)	2.50	1.27	1.27	2.54
Frequency f (s^{-1})	2.3	5.6	6.2	3.6
Cont.phase flow (mL s^{-1}) ($Q_D = Q_C$ and L is variable in Fig.2)	150	15.5	1.42	2965
Symbol in Fig.2	O	□	▽	△
Actual col. diam. (cm)	15.2	7.62	2.54	91.4

Figure 2 shows that the computed curves of D_F versus L pass close to the majority of experimental points which correspond to the column diameters actually studied (4, 6, 16). The exception is the large 91.4 cm column (4) but this column was not actually flooded, merely operating close to the flood point. The computation indicates that if the column had been 80 cm in diameter rather than 91.4 cm, it would have flooded at the given flow and agitation level.

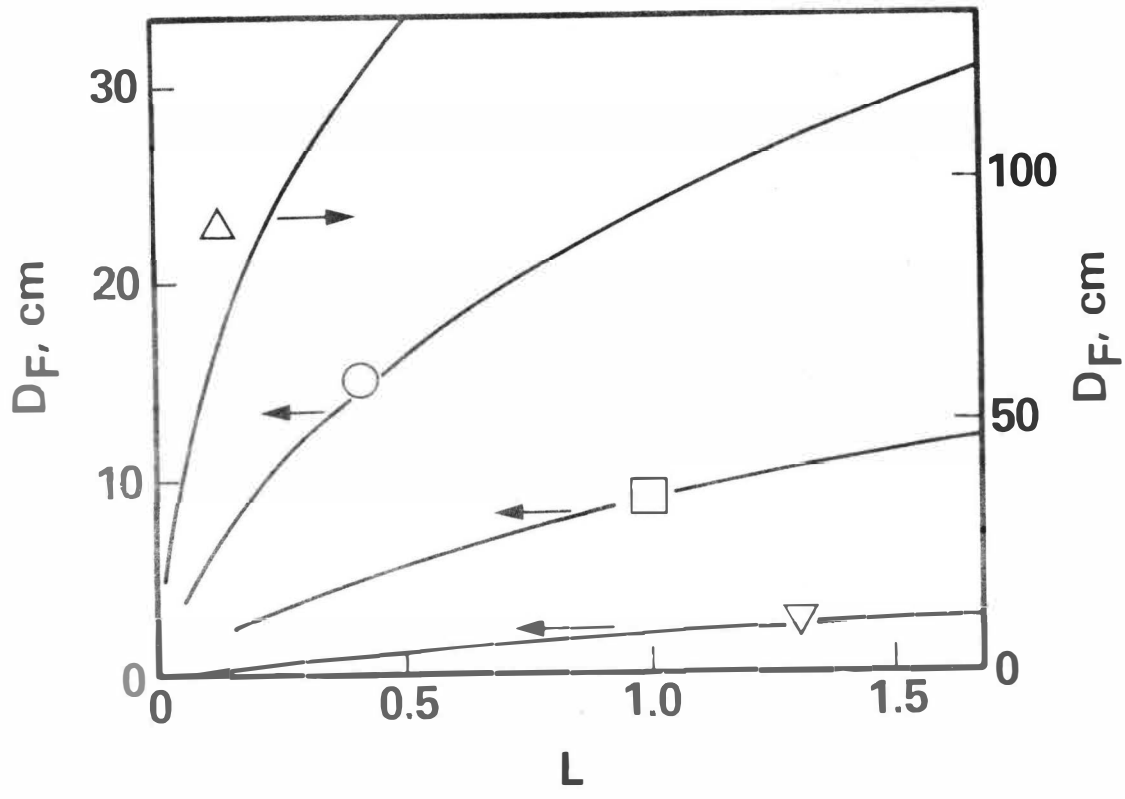

FIG.2 Computed values of D_F as a function of flow ratio L for conditions noted in Table 1. Continuous lines are computed and the single data points refer to actual values of column diameter and L.

TESTING OF MODEL FOR HEIGHT OF PLATE STACK

Tests on the transfer of acetic acid from kerosene (dispersed) to water (continuous) have been carried out in the 15 cm column described previously (6) by the present authors. The plate stack height was 2.05 m and extraction rates were controlled mainly by the kerosene-phase resistance because of the high distribution coefficient of acetic acid (water/kerosene). The kerosene raffinate was carefully analysed for remaining acid, and the degrees of extraction X and Y at input and output of each phase were thereby determined. Note was also made of the flow rate of each phase, agitation rate, and column parameters, e.g. plate spacing, etc.

In calculating the plate stack height according to the scheme shown in Figure 1, it was necessary to have data on the axial dispersion coefficients in each phase (see eqs. (12a) and (12b)). Continuous-phase data for the column were available from a previous investigation (6), but no data on dispersed-phase axial dispersion are available. Therefore it was assumed either that: (i) $E_D = E_C$, or (ii) $E_D = 0.5\ E_C$, or (iii) $E_D = 0$ (i.e. plug flow in dispersed phase).

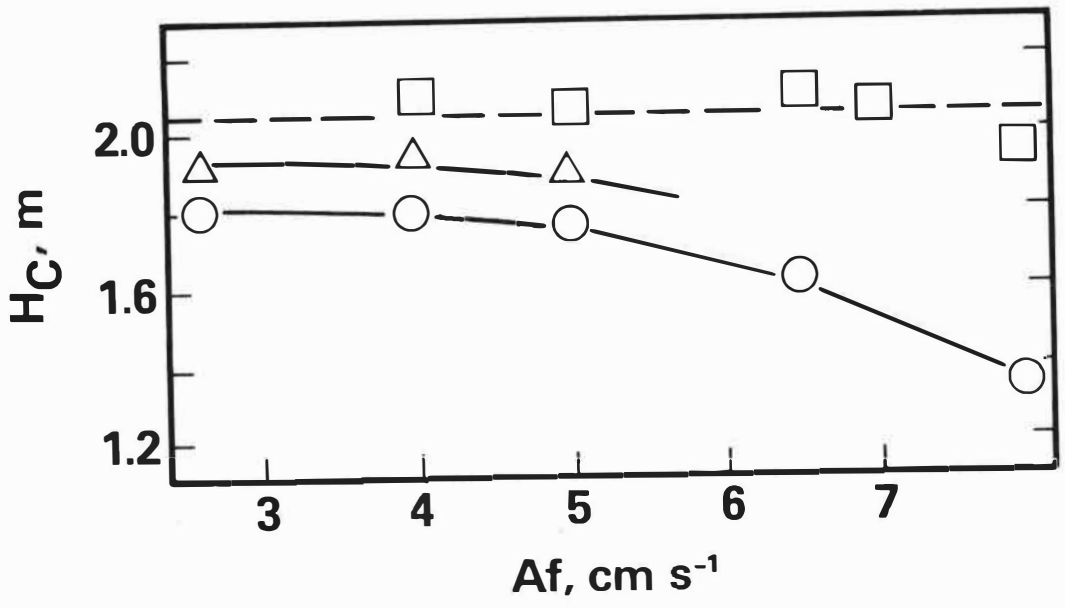

FIG.3 Computed values of plate stack height in 15 cm diameter column (L=0.26)

□ $E_D = E_C$ Δ $E_D = 0.5\ E_C$ o $E_D = 0$

--- actual plate stack height = 2.05 m.

Calculations of plate stack height were made from the experimental X, Y, Af, etc. under each of these assumptions, and are shown as points in Fig. 3. It is apparent that assumption (i) gives the best agreement with the given plate stack height, while assumption (iii) is reasonable only at agitation levels near the lower bound of applicability of the model (Af ≈ 3 cm/s). The intermediate assumption (ii) gives an intermediate result as might be expected. Assumption (iii) of plug flow in the dispersed phase tends to overestimate the column effectiveness, i.e. to underestimate the plate stack height, because of the effect of dispersed phase axial mixing. This effect appears to increase strongly with agitation. Although no data exist for E_D in Karr reciprocating plate columns, data from large pulsed columns (17) show that $E_D \approx E_c$ at high levels of agitation. Similar behaviour in reciprocating plate columns seems to be indicated by the success of assumption (i).

A difficulty in the treatment of large-scale columns lies in the lack of firm data on E_c and E_D. There is much evidence however that axial mixing increases with column diameter due to circulation effects, and that consequently the height of a transfer unit (or H.E.T.S.) increases with scale-up. Karr and Lo (4) have found that for reciprocating plate columns the H.T.U. increases with the 0.38 power of diameter. Data (4) on the transfer of acetic acid between o-xylene and water in a 0.914 mm column were used to obtain the values of E_c (assumed equal to E_D) which would give an estimate of stack height equal to the actual height of 6.0 m. This necessitated a trial-and-error computation repeatedly using the scheme shown in Figure 1. The resulting values of

E_c plotted as a function of Af, parallel those from the small column (6) and the ratio of values is close to the (ratio of column diameters)$^{0.38}$! This is coincidental as there is no general justification for a proportionality between H.T.U. and axial dispersion coefficient.

However, the effect of assuming E_D=0 for the same value of E_C is even more striking than in the case of the 15 cm column (Fig. 3). The dispersed phase plug flow assumption can lead to an underestimate of plate stack height by over 50% in the case of the 91.4 cm column.

Additional computations have been carried out, but space limitations prevent their inclusion. It is believed that the main usefulness of this model will be found in designing for "difficult extractions", e.g. systems of high viscosity and/or low interfacial tension. Sometimes, the interfacial tension can change significantly between the top and bottom of a column (see for instance ref. 18) and localised flooding could occur where γ is a minimum. The model could be adopted to calculate the optimum variation of plate spacing so that the calculated D_F is constant at all points in the column. This would ensure that all sections of the column are being utilised to their full capacity. The main difficulty in applying the model is the relative lack of axial dispersion data, particularly for large columns. However the inversion of the model in a trial-and-error procedure allows calculation of E_C from mass transfer data assuming $E_C = E_D$. This suggests the possibility of obtaining some pilot-scale data for "simple" mass transfer systems, calculating E_C from these data, and applying the resulting E_C values to calculation of a "difficult" mass transfer under the same hydrodynamic conditions. The present calculations have indicated that the assumption that $E_D = E_C$ is reasonable.

Acknowledgments. This work was largely supported by a grant from the Natural Sciences and Engineering Research Council of Canada. The authors are also grateful to Dr. A.E. Karr for many helpful discussions.

NOTATION

a	specific area
A	stroke (= twice amplitude)
B	ratio H_c/d_{32}
C	discharge coefficient
d_{32}	Sauter mean droplet diameter
D	column diameter
$\mathcal{D}$	molecular diffusivity
E	axial dispersion coefficient
f	frequency
F	extraction factor
g	acceleration due to gravity
h	interplate spacing
H_c	plate stack height
H_T	true height of transfer unit (plug flow)
k	mass transfer coefficient in one phase
K	dimensionless constant (only in eq. (4))
	overall mass transfer coefficient elsewhere

L	flow ratio Q_D/Q_C
m	distribution ratio
N	number of transfer units
P	volume flow rate
Sh	Sherwood number
Re	Reynolds number
Sc	Schmidt number
U	superficial velocity
X	dimensionless concentration, continuous phase, defined in ref. 15
Y	dimensionless concentration, dispersed phase, defined in ref. 15
Z	dimensionless height from bottom of plate stack (0<Z<1)

Greek letters

γ	interfacial tension
$\Delta\rho$	density difference
μ	viscosity
ρ	density
$\bar{\rho}$	dispersion density
σ	fractional open area of plates
ψ	power dissipation per unit volume
ϕ	dispersed phase holdup

Subscripts

C	continuous phase
D	dispersed phase
F	flooding
O	overall
S	slip value

REFERENCES

(1) Proceedings of International Solvent Extraction Conference (ISEC 77), Toronto, 1977. (Canadian Institute of Mining and Metallurgy, Montreal, 1979)
(2) Korchinsky, W.J., Can. J. Chem. Eng. 52, 468 (1974).
(3) Karr, A.E., A.I.Ch.E.J. 5, 446 (1959).
(4) Karr, A.E. and Lo, T.C., Chem. Eng. Progr. 72 (11), 68(1976).
(5) Baird, M.H.I., McGinnis, R.G. and Tan, G.C., Proc. Intl. Solvent Extn. Conf. (ISEC 71), The Hague, 1971, p.251 (Society of Chemical Industry, London, 1971).
(6) Hafez, M.M., Baird, M.H.I. and Nirdosh, I., Can. J. Chem. Eng. 57, 150 (1979).
(7) Baird, M.H.I. and Lane, S.J., Chem. Eng. Sci. 28, 947(1973)
(8) Hafez, M.M. and Baird, M.H.I., Trans. Inst. Chem. Engrs. (London), 56, 229 (1978).
(9) Kim, S.D. and Baird, M.H.I., Can. J. Chem. Eng. 54, 81 (1976).
(10) Jealous A.C. and Johnson, H.F., Ind. Eng. Chem. 47, 1159 (1955).
(11) Hinze, J.O., A.I.Ch.E.J. 1, 289 (1955).
(12) Thornton, J.D., Chem. Eng. Sci. 5, 201 (1956).
(13) Heertjes, P.M., Holve, W.A. and Talsma, H., Chem. Eng. Sci. 3, 122 (1954).
(14) Treybal, R.E., Liquid Extraction, 2nd. Edition, p.186 (McGraw Hill, New York, 1963).
(15) Pratt, H.R.C., Industr. Eng. Chem. Proc. Des. Dev. 14, 74 (1975).
(16) Karr, A.E. and Lo, T.C., Proc. Intl. Solvent Extr. Conf. (ISEC 71), The Hague, 1971, p.299 (Soc. Chem. Ind., London, 1971).
(17) Kharpacheva, S.M., et al., Zh. Prikl. Khim., 47, 806 (1974) [Engl. trans. J. Apl. Chem. USSR., 47, 821 (1974)].
(18) Sharma, R.N. and Baird, M.H.I., Can. J. Chem. Eng. 56, 310 (1978).

A FUNDAMENTAL APPROACH TO THE DESIGN AND OPTIMIZATION OF INDUSTRIAL SOLVENT EXTRACTION PLANTS

J.E. Sepulveda and J.D. Miller
Department of Metallurgy and
Metallurgical Engineering
University of Utah
Salt Lake City, Utah 84112
U.S.A.

ABSTRACT

The design, optimization and control of continuous flow countercurrent solvent extraction circuits is generally accomplished by an equilibrium stage analysis. The formulation of a quantitative, time dependent description of these circuits incorporates information regarding the intrinsic reaction kinetics of the system into a population balance model involving the droplet size distribution. Importantly, simulations show that for simple, first order reversible reaction kinetics maximum selectivity is achieved at intermediate retention times before the system is allowed to reach equilibrium. Preliminary model verification for the UO_2/D2EHPA has encouraged the further development of this research program.

INTRODUCTION

Solvent extraction technology, originally adopted for the recovery of uranium and plutonium from fission products, is rapidly becoming a conventional processing strategy for the production of other important metals such as copper, nickel, cobalt, beryllium, tungsten, vanadium and rare earths. At present, solvent extraction techniques are being employed on a worldwide basis, for the recovery, purification and concentration of nearly 25,000 tons of uranium and 200,000 tons of copper per year.

Nevertheless, the wide implementation of solvent extraction technology in the mineral industry by no means implies that the actual processing plants have been efficiently designed or fully optimized. In most applications, the selection and sizing of the equipment, in particular the phase contactor, has been based on expensive, time-consuming scale-up techniques without much consideration of the now available information on the process fundamentals.

In view of the above considerations, the need for an improved approach to the design -- as well as the optimization and control -- of solvent extraction operations can not be overemphasized. It is the main purpose of our ongoing research program to develop simple, but realistic, mathematical models of multistage mixer-settler units, the most widely used type of phase contactor, based on recent advances in the characterization of heterogeneous reaction kinetics for continuous, multicomponent liquid/liquid

extraction systems.

BASIC MODEL STRUCTURE

An appropriate mathematical model for the design and optimization of solvent extraction operations should be capable of:

1. Describing the steady state response of multistage systems; not necessarily operated at equilibrium conditions.
2. Considering variations in the dispersed phase drop size distribution and hence, incorporating the interfacial area in the calculations.
3. Quantifying the degree of separation between two or more components for any specified set of conditions.

The mathematical formulations to be described are intended to comply with each one of these requisites. By consideration of both the forward and backward reaction kinetics, it is possible to characterize systems far from equilibrium as well as those operated near equilibrium conditions. In addition, a population balance model has been developed to describe the drop size distribution of the dispersed phase in continuous well-mixed phase contactors. The overall model then arises as a combination of both sources of information -- intrinsic reaction kinetics and droplet size distribution -- via mass continuity expressions for each of the extractable components in the mixer. The mathematical framework used in the formulation of the general model and its application to the design of actual solvent extraction plants is schematically represented in Figure 1.

By way of example, a two component, countercurrent system was considered as depicted in Figure 2. For an acidic extractant, the two overall extraction reactions can be generally described as:

$$A^{+n} + n\tilde{RH} \leftrightarrows \tilde{R_n A} + nH^{+} \qquad (1)$$

$$B^{+m} + m\tilde{RH} \leftrightarrows \tilde{R_m B} + mH^{+} \qquad (2)$$

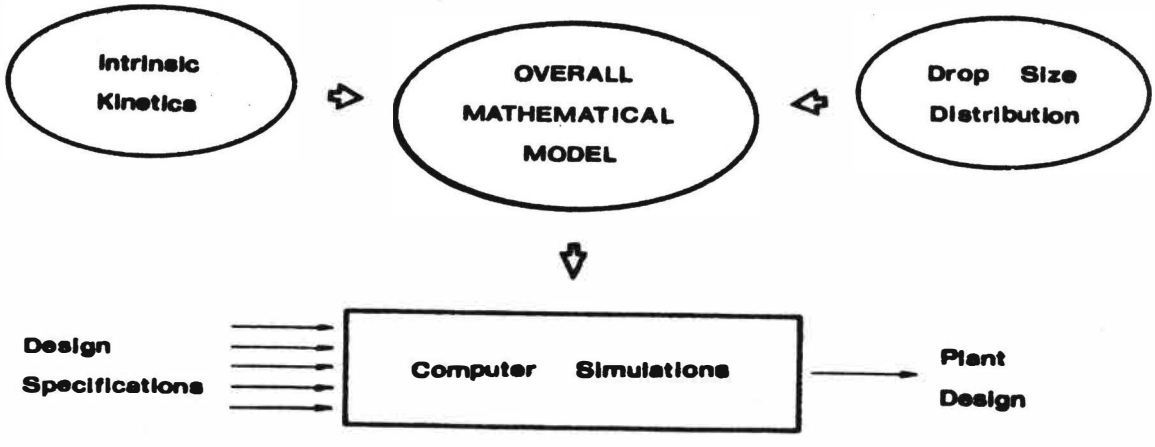

FIG. 1

Schematic representation of the overall mathematical model framework and its application to the design of actual plant operations.

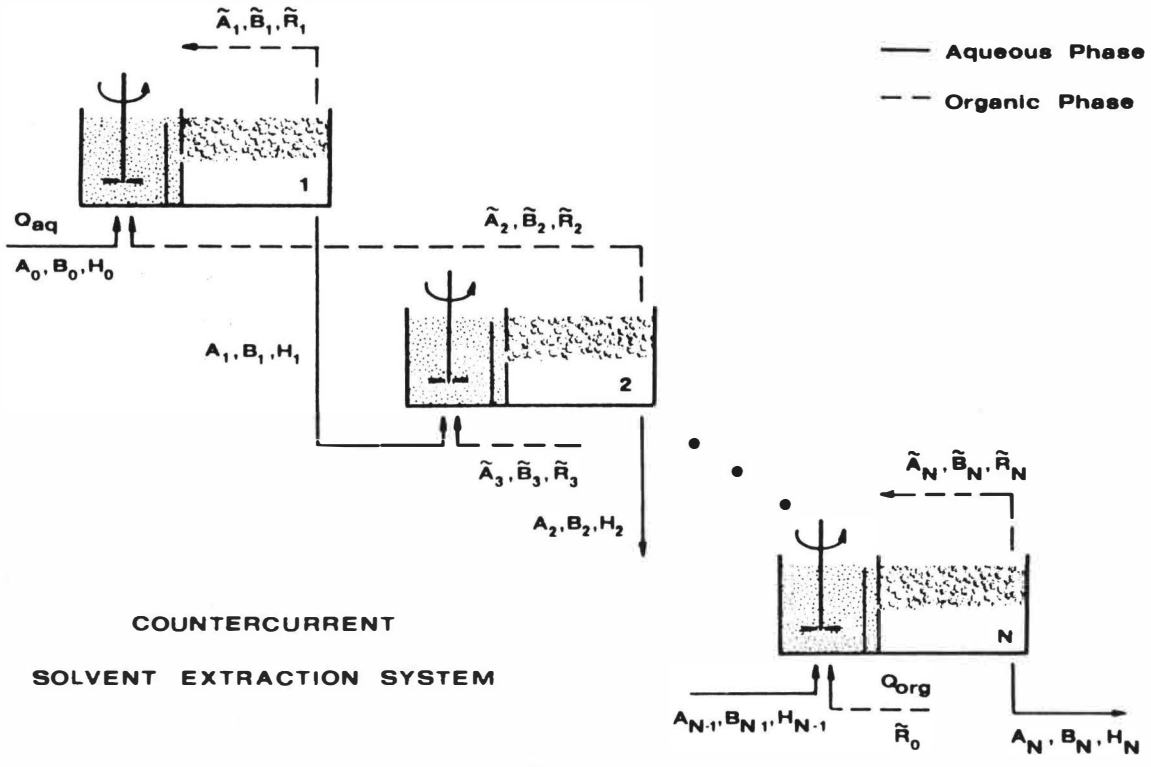

FIG 2.

Schematic representation of a countercurrent solvent extraction system.

where A^{+n} and B^{+m} are the extractable species and the symbol (~) denotes the organic phase. It is desired to describe the overall extraction of each component as a function of the mean residence time in the system. In this context, at each stage k in the system (k = 1,2,..,N), the following mass continuity expression for component A must be satisfied at any time:

$$\begin{bmatrix}\text{Rate of Accumulation}\\ \text{of A in the}\\ \text{Aqueous Phase}\end{bmatrix}_k = \begin{bmatrix}\text{Rate of Input}\\ \text{of A into the}\\ \text{Aqueous Phase}\end{bmatrix}_k - \begin{bmatrix}\text{Rate of Output}\\ \text{of A from the}\\ \text{Aqueous Phase}\end{bmatrix}_k$$

$$- \begin{bmatrix}\text{Rate of Transfer}\\ \text{of A into the}\\ \text{Organic Phase}\end{bmatrix}_k \qquad (3)$$

and similarly for component B.

Appropriate mathematical representation of the two continuity equations and consideration of first-order, reversible intrinsic reaction kinetics, leads to the following expressions:

$$A_k = A_k^{IN} - \left(\frac{\phi+1}{\phi}\right) k_f^A \bar{a}_k \tau_k \left(\tilde{R}_k A_k - \frac{1}{K_A} H_k \tilde{A}_k\right) \qquad (4)$$

$$B_k = B_k^{IN} - \left(\frac{\phi+1}{\phi}\right) k_f^B \bar{a}_k \tau_k \left(\tilde{R}_k B_k - \frac{1}{K_B} H_K \tilde{B}_K\right) \quad (5)$$

where:

$\phi = V_{aq}/V_{org} = Q_{aq}/Q_{org}$ = phase ratio

τ_k = mean residence time in the k^{th} vessel, k = 1,2,..,N

K_A, K_B = equilibrium constants of the rate controlling steps in the extraction of A and B, respectively.

k_f^A, k_f^B = rate constants for the forward reactions.

and the integral factor:

$$\bar{a}_k = \int_o^\infty a(v)\bar{n}_k f_o^{(k)}(v)dv, \quad (6)$$

where:

a(v) = interfacial area of a drop of size v

$\bar{n}_k$ = total number of drops per unit volume of vessel in the kth stage.

$f_o^{(k)}(v)$ = number drop size distribution density function in the kth vessel.

The term, $\bar{a}_k$ corresponds to the specific interfacial area, i.e. the total area, per unit volume of vessel, available for extraction. The fact that this term can be factored out as the specific interfacial area is characteristic of chemical reaction rate controlled processes and may not be the case when other reaction steps are rate controlling.

The last step in the formulation is to relate the organic phase concentrations of extractable species, $\tilde{A}_k$ and $\tilde{B}_k$, the free extractant concentration in the organic phase, $\tilde{R}_k$, and the hydrogen concentration in the aqueous phase, H_k, in terms of the aqueous concentrations, A_k and B_k, and inlet conditions. This can be accomplished through a set of mass balance and mass action expressions.

The complexity of the resulting system of equations makes the use of a computer a practical necessity. Fortunately, these equations can be expressed in terms of a reduced number of dimensionless variables and parameters; therefore, minimizing the total computational effort involved in numerical simulations.

For non-dimensionalization purposes, the inlet aqueous phase concentrations (A_o and B_o, see Figure 2) were selected as characteristic concentrations; while the batch time required for 50% extraction of A (when the back reaction kinetics are unimportant and the extractant is supplied in the exact stoichiometric amount for complete extraction), was taken as the characteristic time:

$$t_k^{50} = \frac{1}{n(\phi+1)k_f^A \bar{a}_k A_o} \quad (7)$$

COMPUTER SIMULATIONS

A Fortran V program was written for the numerical evaluation of the dimensionless model equations. Typical simulation results for a monocomponent singlestage system are presented in Figure 3 which shows the effect of the apparent equilibrium constant of the rate controlling step, K_A, on the overall fraction extracted as a function of the mean residence time. As expected, $\tilde{A}_1^*$ reaches higher levels for any given mean residence time as K_A increases. Interestingly enough, the simulations presented in Figure 3 indicate that at low extraction levels, away from equilibrium conditions, the overall rate of extraction is independent of the equilibrium constant value; hence, not significantly affected by the back reaction kinetics. On the other hand, as the mean residence time increases, the overall fraction extracted approaches different equilibrium values depending on the apparent equilibrium constant value, K_A. This characteristic feature of solvent

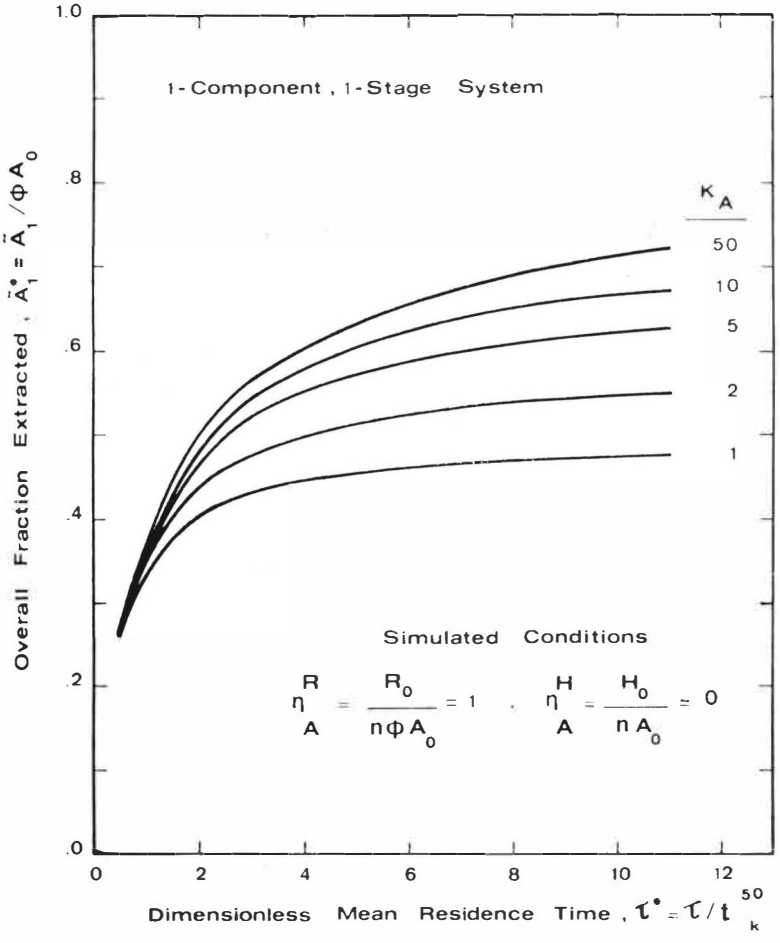

FIG. 3

Effect of K_A on the overall fraction extracted.

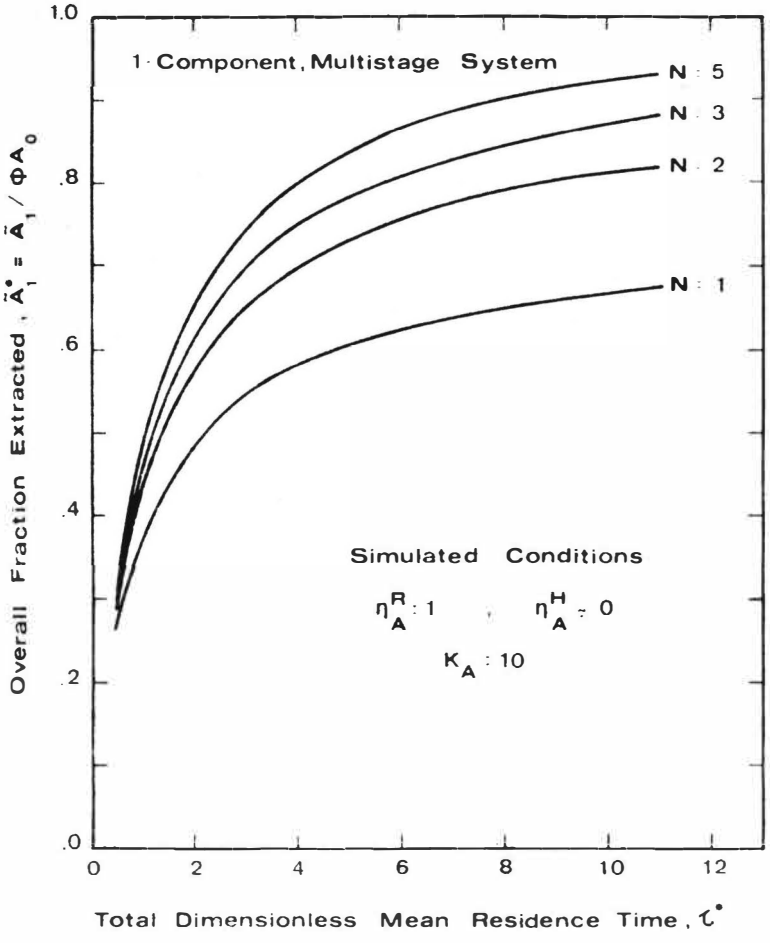

FIG. 4

Effect of the number of stages on the overall fraction extracted with "equal-size" mixers: $\tau_1^* = \tau_2^* = \ldots = \tau_N^* = \tau^*/N$.

extraction systems could simply not be described by the type of rate expressions proposed by other investigators (1-4) since the significant contribution of the back reaction kinetics to the overall rate of extraction, near equilibrium conditions, is not acknowledged.

The simulated responses presented in Figure 4, for a monocomponent system, clearly verify the predicated assumption that multistage, countercurrent systems are significantly more efficient than singlestage systems, for any specified total mean residence time, τ^*. Even more significant from a design standpoint, is the fact that the total mean residence time required to achieve a specified extraction level may be several times larger -- if at all finite -- for a singlestage system than it is for an equivalent countercurrent system, operated under similar conditions.

Finally, the capability of the model to predict the overall fraction extracted of two or more competitive species in solution is illustrated in Figure 5, by consideration of a two-component, multistage system. This is one of the most striking observations resulting from the current modeling effort. The quality of the separation, quantified in this case by the

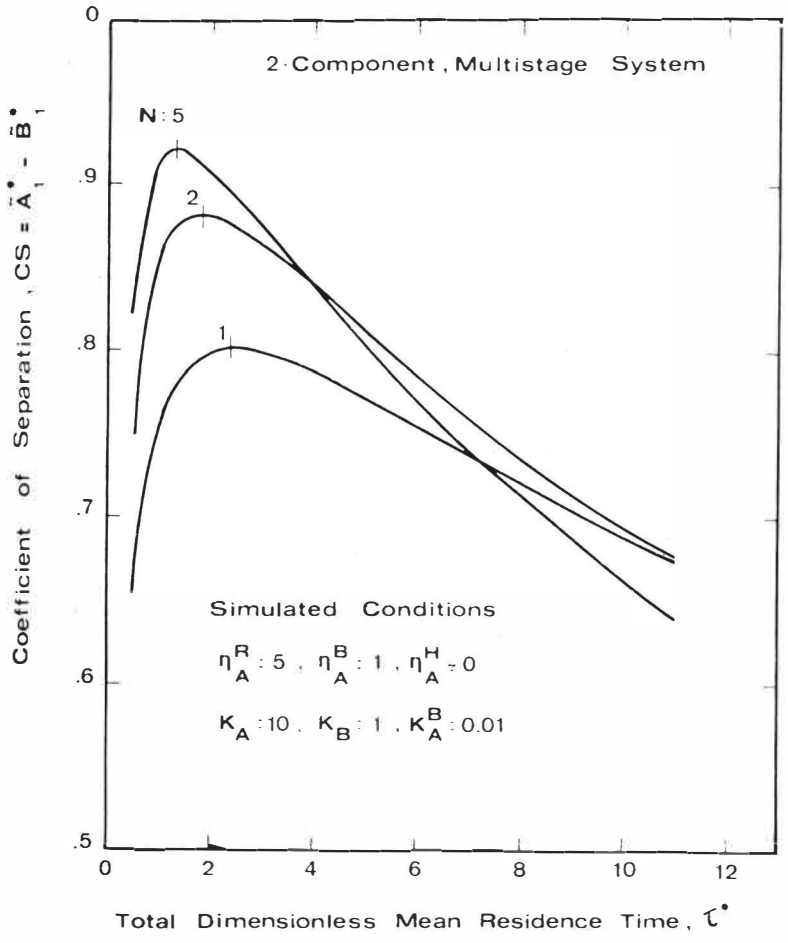

FIG. 5

Effect of the number of stages on the coefficient of separation for a particular two-component, multistage system with "equal-size" mixers.

coefficient of separation (CS = $\tilde{A}_1^* - \tilde{B}_1^*$), goes through a maximun as the mean residence time increases, indicating that optimun selectivity is not necessarily achieved at equilibrium conditions. Furthermore, multistage systems are shown to be significantly more selective than singlestage systems.

Other simulation results could not be accomodated due to space restrictions imposed by the publisher. As expected, many of the conclusions arising from them are intuitively obvious and apparent from a conventional *equilibrium stage analysis*. For instance, it is well known that extraction will be enhanced by a higher extractant concentration and/or a larger equilibrium constant value. However, the *kinetic* nature of our model makes it possible to describe other effects -- such as the influence of the mean residence time on the quality of the separation -- in a quantitative fashion.

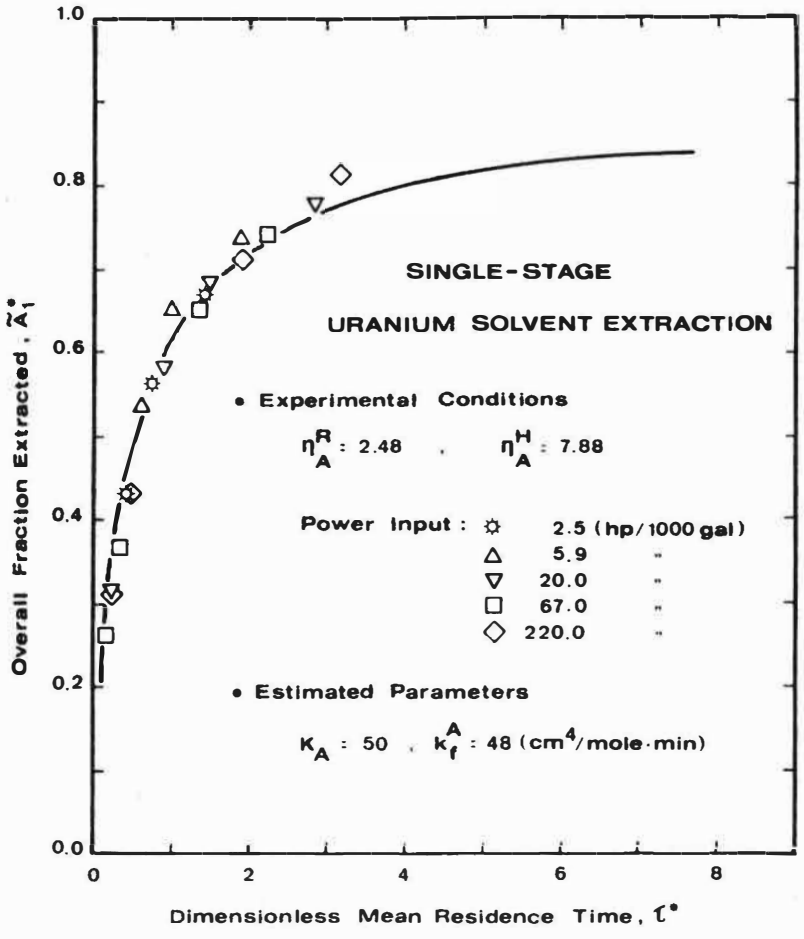

FIG. 6

Comparison of experimental and model-predicted overall fractions extracted, as it applies to the singlestage, continuous uranium solvent extraction in the Dapex Process. Experimental data from Reference 5.

PRELIMINARY MODEL VERIFICATION

The validity of the above statements is obviously dependent on whether or not the model is capable of describing the behavior of actual solvent extraction operations with a reasonable degree of accuracy. In this regard, the independent study of Ryon et. al. (5) on the Dapex uranium solvent extraction process serves well as a preliminary verification of the appropriateness of the current approach.

The overall extraction reaction can be written as:

$$UO_2^{+2} + 2\tilde{RH} \leftrightarrows \tilde{R_2UO_2} + 2H^+ \qquad (8)$$

where RH space represents the extractant D2EHPA. Based on their experimental observations, Ryon et. al. (5) postulated a first order rate expression of the form:

$$-r^A(v) = a(v)\ [k_f'\ A\ -\ k_b'\ \tilde{A}] \qquad (9)$$

which in this analysis was modified to include a first order effect of the free extractant and hydrogen concentrations:

$$-r^A(v) = a(v)\ [k_f^A \tilde{RA} - k_b^A H\tilde{A}] \qquad (10)$$

Based on the work of Rodger and Trice with geometrically similar mixing vessels, Ryon and coworkers were able to estimate the available interfacial area as a function of the specific power input. For our analysis, the apparent equilibrium constant, K_A, was estimated from the extraction isotherm and the rate constant k_f^A from continuous data by non-linear regression.

A comparison of experimental and predicted values is presented in Figure 6. These data correspond to a nominal one-gallon mixer with flow-rates from 0.2 to 5.0 gpm. Specific power input to the mixer varied by two orders of magnitude. Considering the experimental error involved in Ryon's sampling and analytical techniques and the idealized nature of our interpretation, the agreement between experimental and predicted values appears to be just excellent.

Other experimental systems, as well as the application of the model to their design and optimization, are currently under study at the University of Utah. The limitations of the conventional equilibrium stage design procedure and the need for an improved kinetic description of continuous flow systems are evident from these simulation studies.

REFERENCES

1. Flett, D.S., Okuhara, D.N. and D.R. Spink, "Solvent Extraction of Copper by Hydroxyoximes," J. of Inorg. Nucl. Chem., Vol. 35, p. 2471, 1973.

2. Flett, D.S. Hartlage, J.A., Spink, D.R. and D.N. Okuhara, "The Extraction of Copper by an Alkylated 8-hydroxy Quinoline," J. of Inorg. Nucl. Chem., Vol. 37, p. 1067, 1975.

3. Flett, D.S., "Chemical Kinetics and Mechanisms in Solvent Extraction of Copper Chelates," Accounts of Chemical Research, Vol. 10, p. 99, 1977.

4. Whewell, R.J., Hughes, M.A. and C. Hanson, "The Kinetics of Solvent Extraction of Copper (II) with Lix Reagents -- I", J. of Inorg. Nucl. Chem., Vol. 37, p. 2303, 1975.

5. Ryon, A.D., Daley, F.L. and R.S. Lowrie, "Design and Scale-up of Mixer-Settlers for the Dapex Solvent Extraction Process," Oak Ridge National Laboratory, Report ORNL-2951, October 5, 1960.

ACKNOWLEDGEMENTS

Financial support from the National Science Foundation, Grant No. ENG-7826302 and the Engineering Experiment Station, University of Utah has contributed significantly to the success of this research program.

MODELLING OF COUNTERCURRENT FLOW LIQUID-LIQUID EXTRACTION COLUMNS

W.J. Korchinsky* and J.J.C. Cruz-Pinto†

*University of Manchester Institute of Science and Technology, Manchester, England.

†Universidade do Minho, Braga, Portugal.

ABSTRACT

The objective of this work is to determine whether, with carefully obtained data, including drop size distribution, and accurately solved model equations, extraction column performance can be predicted accurately. Applying the Handlos-Baron drop model to the column model equations with drop size distribution influence included, gave reasonable (± 20%) prediction of the number of transfer units. Further analysis of the data indicates that rates of mass transfer (predicted by the Handlos-Baron drop model with the Calderbank Moo-Young continuous phase coefficient) and axial mixing (predicted by Misek) are overestimated.

INTRODUCTION

Recent work has established that modelling of mass transfer processes in extraction columns by dispersion or backmixing models has not given satisfactory results. The dispersed phase behaviour particularly has not been adequately modelled. It has been made apparent by Rod (1), Misek (2), Olney (3), and Korchinsky and co-workers (4,5,6,7), that a model (before it can satisfactorily predict column performance), must take into account the polydispersed nature of the dispersed phase, or the distribution of drop sizes, which exists.

Experimental evidence of the strong influence of drop size has been obtained by Chartres and Korchinsky (8), and direct experimental verification of the influence of drop size distribution has been made by the authors (7). Theoretical models developed by Chartres (5), and by Azimzadeh-Khatayloo (4) predicted large effects of size distribution on column performance. These models utilized single drop model predictions for the mass transfer coefficients, with the rigid drop (9) and turbulent circulating drop model (of Handlos and Baron (10)) used. These single drop model predictions, however, were only approximate predictions of the model equations as several assumptions normally made in the solutions of the single drop model equations are unrealistic when applied to extraction column conditions.

Further work was therefore desirable in order to improve the theoretical model predictions and to attempt experimental verification of the model.

THEORETICAL MODELLING

Model equations, and computer-programmed solutions, developed by Chartres served as the starting point for this study. The model assumed that drops of different diameters moved through the continuous phase at different velocities but only in the forward direction. The continuous phase was modelled by plug flow with axial dispersion. Column design or performance prediction required the calculation or measurement of the following parameters:

a) Drop size distribution.

b) Drop velocity distribution and dispersed phase hold-up.

c) Mass transfer coefficients - drop side.

- continuous phase.

d) Axial dispersion coefficients - continuous phase.

- Drop size distribution

These are highly dependent on the distributor, agitator type and speed, and direction of mass transfer, and will depend also on flow rates, physical properties, etc. They must be measured to obtain accurate predictions of column performance. They were measured photographically in this study.

- Drop velocity distribution and dispersed phase hold-up

Although it would be highly desirable to have measured values of drop velocities, which will undoubtedly be highly dependent on drop size, such measurements have not been made so some approximation is necessary. Hence it is assumed that the drop velocities relative to the continuous phase are proportional to the single drop terminal velocity predicted by Misek's (11) or Hu-Kintner (12) relationships, depending on the drop Reynolds number. The proportionality constant is then determined from the dispersed phase hold-ups, preferably experimental values (see Appendix).

- Mass transfer coefficients

The measurement of drop-size dependent mass transfer coefficients in an operating extraction column would require techniques not yet demonstrated. For the time being it seems more logical to assume a model for the drop behaviour, predict drop-side and continuous phase mass transfer coefficients, or the equivalent overall mass transfer coefficient, and then compare predicted and experimental column performance to determine the applicability of the assumed drop behaviour.

Two models of drop behaviour have been investigated in detail - the rigid drop and the Handlos-Baron turbulent circulating drop. The previous approaches to the determination of mass transfer coefficients for these single drop models have required making assumptions which are not really

valid for the countercurrent flow situation. In particular, a constant continuous phase concentration has been assumed. This assumption, and others normally made, have been eliminated (19) and the resulting single drop, and column, model equations (see Appendix) have been solved using advanced numerical techniques to obtain predictions of column performance.

Although in the numerical solution of the drop and column model equations we no longer obtain drop-side or overall mass transfer coefficients, but get concentration changes directly, values of the continuous phase mass transfer coefficient are required. Again there is a lack of data for the extraction column situation so that some estimate is required from previous work on single drops, or on agitated systems. For this study the relationships of Calderbank and Moo-Young (13) and of Linton and Sutherland (14) were used in rigid drop predictions, and those of Calderbank and Moo-Young and of Garner and Tayeban (15) were used in the Handlos-Baron drop predictions, for the agitated section of the column.

A small settling zone normally is present above the agitated section of any extraction column. The theoretical model used here included this. Prediction of the continuous phase mass transfer coefficient for this zone was by another equation developed by Calderbank and Moo-Young (13).

- Axial dispersion coefficients, continuous phase

A considerable amount of work has been done in this area with correlations of experimental data available for a number of columns. The correlation of Misek (16) seemed most broadly based of those available for the Rotating Disk Contactor so was used in this study. For the settling zone the correlation of Vermeulen (17) was used. Measurement of these coefficients at the same time as the remaining measurements are made should be possible from concentration profiles (18). Although this was beyond the scope of this study, a limited number of concentration profiles was obtained and used to check on the accuracy of prediction of these profiles by the model equations.

EXPERIMENTAL

A Rotating Disc Contactor, diameter 22 cm, height 147 cm, was used in this study. Experimental measurements were made of

- drop size distributions at several levels in the column
- dispersed phase hold-up
- extraction efficiencies
- continuous phase profile concentrations (in some cases)

Now as the model equations have certain limitations, great care was taken in the experimental programme to keep within these limitations. Low solute concentrations were used to maintain constant flow conditions. Perhaps more importantly, low flows and correctly-sized distributor plates provided drop size distributions which were nearly uniform over the height of the column. There were slight reductions in drop size in some runs due to drop break-up, but with the low dispersed phase hold-up levels, and

TABLE 1

Results

Run No.	h_C (cm)	w_C (g/s)	w_D (g/s)	n (1/5)	ϕ	d_{32} (cm)	m	E_{OC}	N_{OCP} Exp.	N_{OCP} Predicted
1	4.5	25.8	44.3	4.0	0.050	0.386	0.852	0.765	2.24	1.94
2		25.8	44.3	5.0	0.074	0.260	0.764	0.816	3.03	2.06
3		20.0	26.5	4.0	0.038	0.259	0.720	0.627	1.75	2.05
4		20.0	29.7	4.0	0.044	0.186	0.725	0.686	2.03	2.71
5		29.5	43.9	4.0	0.098	0.188	0.604	0.687	2.52	3.53
6		20.0	29.7	4.0	0.057	0.190	0.584	0.700	2.89	2.89
7		29.5	43.9	4.0	0.092	0.178	0.691	0.754	2.94	3.31
8		28.5	39.0	5.1	0.105	0.165	0.755	0.791	3.57	4.28
9		28.5	39.0	5.1	0.093	0.165	0.746	0.778	3.38	3.76
10		20.0	26.5	5.1	0.057	0.161	0.765	0.763	3.15	3.19
11	7.2	20.0	29.7	4.9	0.039	0.176	0.804	0.730	2.24	2.63
12		29.5	43.9	4.9	0.055	0.172	0.755	0.730	2.37	2.82
13		20.0	29.7	4.9	0.042	0.174	0.736	0.706	2.19	2.61
14		39.0	53.1	4.9	0.070	0.175	0.774	0.706	2.27	2.84
15		20.0	29.7	4.9	0.058	0.120	0.765	0.814	3.52	3.35
16		20.0	29.7	5.8	0.069	0.117	0.770	0.815	3.51	3.35

particular conditions used in these test runs, coalescence was avoided.

RESULTS

Experimental conditions, and results obtained, are summarized in Table 1. These runs covered a range of flows, disc speeds, and three different distributor plates, which gave a range of drop sizes. Some drop break-up occurred when the largest drops were introduced (Runs 1 - 3) with significant reductions in drop sizes through the column. In the vast majority of runs (Nos. 4 - 16), however, little or no drop breakup occurred, with drop sizes remaining constant through the column.

Mass transfer results are best examined in terms of the 'plug flow number of transfer units', N_{OCP}, in this case based on the continuous phase concentrations. Experimental values, as well as those predicted by the most accurate combination of single drop model (the Handlos-Baron model) and continuous phase mass transfer coefficient (by Calderbank and Moo-Young), are given in Table 1. These N_{OCP} values are also compared in Figure 1.

Measured continuous phase concentration profiles are illustrated in Figures 2 - 5. On these figures are also plotted predicted profiles for the Handlos-Baron drop model and

A) as predicted k_C and E_C values, and

B) adjusted k_C and/or E_C values.

All theoretical profiles are obtained by fixing the exit (at z=0) continuous phase concentration at the experimental value, hence calculating the concentrations toward, and including, the inlet concentration.

To improve the agreement between predicted and experimental concentration profiles changes could be made in

1) the single-drop model (e.g. Handlos-Baron),

2) the continuous phase mass transfer coefficient, k_C,

and/or 3) the continuous phase axial mixing coefficient, E_C.

In this study the values of k_C and E_C are varied, retaining the Handlos-Baron model. Profiles are again predicted from the experimental exit concentration, but now the parameters are varied to obtain accurate prediction of the concentration profiles AND the experimental inlet concentration - and thus the correct, experimental, value for N_{OCP}.

DISCUSSION OF RESULTS

A comparison of experimental, and model-predicted, number of transfer units, N_{OCP} (see Fig. 1), shows that experimental values were closely predicted by the Handlos-Baron drop model, when the Calderbank and Moo-Young continuous phase mass transfer coefficient and Misek axial mixing coefficient were utilized.

Predicted values of N_{OCP} average about 10% higher than experimental

values, and range from 70 to 140% of experimental values. Other combinations of drop model, e.g. rigid drop, and k_C and E_C correlations did not give nearly as accurate predictions of N_{OCP}.

Does this mean that extraction column performance is therefore now accurately predictable? Or is it by chance that these results have been obtained? The comparison of experimental and theoretically predicted continuous phase acetone concentrations may give some clues to the answers to these questions.

For the six runs for which profiles were measured, predicted values of N_{OCP} ranged from values which were 5% below experimental values (in Runs 15, 16) to one which was 33% above the experimental value (in Run 4). Only in one run, Run 11, did the predicted profile closely follow the experimental profile, though the predicted N_{OCP} value was higher by 17% because the inlet concentration was not accurately predicted.

What are the reasons for the differences between experimental and predicted results? Assuming the general model is applicable, differences in concentrations may be due to errors in either the mass transfer predictions or the axial mixing predictions.

Adjustment of the continuous phase mass transfer, and the axial mixing, coefficients in order to improve the prediction accuracy gave the following results:

1) In 5 out of 6 runs, values of mass transfer and axial mixing coefficients had to be reduced below the values calculated by the original correlations, indicating that rates of mass transfer and axial mixing were originally over-estimated. This is true when N_{OCP} is originally over-estimated, as in Runs 3, 4 and 11, and when N_{OCP} is under-estimated, as in Runs 15 and 16, because the concentration profiles indicate an over-estimate of the axial mixing influence for the same runs. Reduction of the axial mixing coefficient then requires a reduction in k_C if the experimental N_{OCP} is to be accurately predicted. In the sixth run (Run 6) N_{OCP} is accurately predicted, and concentration profiles, too, are reasonably well predicted (Fig. 3) with no adjustment of parameters. If anything, the extent of axial mixing in this run seems under-estimated, so increases in k_C and E_C are necessary if predicted results are to improve. But the effect on the predicted profiles of such simultaneous changes are slight, for quite large changes in k_C and E_C (see Fig. 3).

2. In 3 of the 6 runs (Runs 11, 15 and 16), those with RDC internals modified to give larger compartment heights, the reduction in the axial mixing coefficients required was much greater, indicating that the influence of the compartment height is not accurately predicted by Misek's correlation.

The adjusted parameters used in generating the "improved" concentration profiles will not be the only combination of parameters which will produce the same results. As four parameters may be varied, i.e. k_C and E_C in both agitated and settling zones, these four parameters cannot be uniquely determined from the limited data obtained. However, they do give an indication

of the possible sources of error in the prediction method. The evidence here indicates that, although the original prediction method was quite good, significant errors in mass transfer and axial mixing rates have been compensating. It must be stressed that mass transfer rates, adjusted here by varying k_C, may in fact be wrongly predicted due to the inapplicability of the Handlos-Baron model to some or all of the drops. Perhaps the rigid drop model applies to the smaller drops. This possibility will be explored in further studies.

CONCLUSIONS

1. Though the data are limited, the proposed single drop, and extraction column, model equations, with the appropriate data, give accurate prediction of extraction column performance.

2. Comparison of experimental with theoretically-predicted concentrations indicates that adjustments to the predicted mass transfer, and axial mixing, coefficients are required to improve model predictions.

REFERENCES

1. Rod, Br. Ch. Eng., 1966, 11(6), 483.

2. Misek, T., Coll. Czech. Chem. Comm., 1968, 33, 2855.

3. Olney, R.B., A.I.Ch.E. J.,1964, 10 (6), 827.

4. Korchinsky, W.J. and Azimzadeh-Khatayloo, S., Ch. Eng. Sci., 1976, 31, 871.

5. Chartres, R.H. and Korchinsky, W.J., Trans. I. Chem. E.,1975, 53, 247.

6. Korchinsky, W.J. and Cruz-Pinto, J.J.C., Ch. Eng. Sci. 1979, 34, 551.

7. Cruz-Pinto, J.J.C. and Korchinsky, W.J., Ch. Eng. Sci., accepted for publication.

8. Chartres, R., and Korchinsky, W.J., Trans. I. Ch. E., 1978, 56, 91.

9. Newman, A.B., Trans. I. Ch. E.,1931, 27, 310.

10. Handlos, A.E. and Baron, T., A.I.Ch.E. J., 1957, 3, 127.

11. Misek, T., Coll. Czech. Chem. Comm., 1967, 32, 4018.

12. Hu, S. and Kintner, R.C., A.I.Ch.E. J., 1955, 1, 42.

13. Calderbank, F.H. and Moo-Young, M.B., Ch. Eng. Sci. 1961, 16, 39.

14. Linton, M., and Sutherland, K.L., Ch. Eng. Sci. 1960, 12, 214.

15. Garner, F.H. and Tayeban, M., An. R. Soc. Esp. Fis. Quim. 1960, 56B, 479.

16. Misek, T., Coll. Czech. Chem. Comm. 1975, 40, 1686.

17. Vermeulen, T., Moon, J.S., Hennico, A and Miyauchi, T., Chem. Eng., Prog., 1966, 62 (9), 95.

18. Jeyakumar, T., M.Sc. Dissertation, The Victoria University of Manchester, 1977.

19. Cruz-Pinto, J.J.C., Ph.D. Thesis, The Victoria University of Manchester, 1979.

NOTATION

C = constant of proportionality

d_i = drop diameter, ith fraction

d_{32} = Sauter-mean drop diameter ($\Sigma n_i d_i^3 / \sum_i n_i d_i^2$)

D_{AD} = solute molecular diffusivity in the dispersed phase

E_C = axial dispersion coefficient, continuous phase

E_{OC} = extraction efficiency, continuous phase basis

f_i = volume fraction of dispersed phase, drop diameter d_i

h_C = RDC compartment height

k_C = mass transfer coefficient, continuous phase

m = solute distribution coefficient, y^*/x

n = RDC disc speed

N_{OCP} = plug flow number of transfer units, continuous phase basis

r = radial coordinate

r' = reduced radial coordinate ($2r/d$)

V_C = superficial velocity, continuous phase

$V_{d,i}$ = drop vertical velocity

V_D = superficial velocity, dispersed phase

$V_{s,i}$ = drop slip velocity

$V_{t,i}$ = single drop terminal velocity, drop diameter, d_i

W_C, W_D = mass flow rates, continuous and dispersed phases

x = weight fraction solute, continuous phase

y_i = dispersed phase solute weight fraction, ith fraction

y = weight fraction solute, variable within drop

y^* = weight fraction solute, equilibrium with continuous phase

z = column vertical position

Greek Symbols

μ_C, μ_D = viscosity, continuous and dispersed phases

ρ_C, ρ_D = density, continuous and dispersed phases

ξ = reduced radial coordinate, $4r/d$

ξ' = $1 - \xi$

ϕ = fraction dispersed phase hold-up

APPENDIX

Drop Velocity Equations

$$V_{d,i} = C\, V_{t,i}(1 - \phi) - \frac{V_C}{1 - \phi} = V_{s,i} - \frac{V_C}{1 - \phi}$$

$$C = \left[V_D/\phi + V_C/(1 - \phi)\right] \Big/ \sum_i f_i\, V_{t,i}(1 - \phi)$$

$$V_D = \sum_i f_i\, V_{d,i}\, \phi$$

Mass Transfer Equations

Drops - A. Rigid

$$\frac{\partial^2 y}{\partial r'^2} + \frac{2}{r'}\,\frac{\partial y}{\partial r'} - \frac{V_{d,i}\, d_i^2}{4\, D_{AD}}\,\frac{\partial y}{\partial z} = 0$$

B. Handlos-Baron Turbulent-Circulating

$$\frac{\partial y}{\partial z} = \frac{V_{s,i}}{128\, d_i\, V_{d,i}(1 + \mu_D/\mu_C)(1 - \xi')}\,\frac{\partial}{\partial \xi'}\left[(1 - 5\xi' + 10\xi'^2 - 6\xi'^3)\,\frac{\partial y}{\partial \xi'}\right]$$

Column $$\rho_c\, E_c\, \frac{d^2x}{dz^2} + V_c \rho_c\, \frac{dx}{dz} = \sum_i f_i\, V_{d,i}\, \rho_D\, \phi\, \frac{dy_i}{dz}$$

FIG.1

Predicted v Experimental N_{OCP}

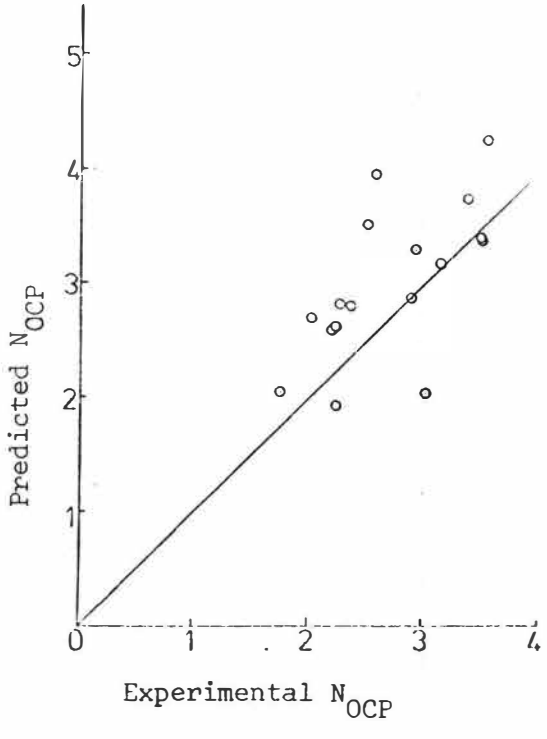

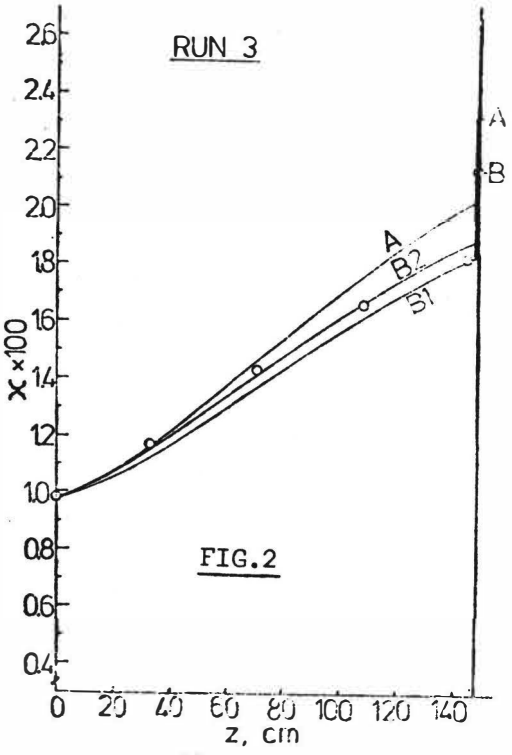

FIG.2

O Experimental

A Predicted Profiles

B 'Adjusted' Parameter Profiles

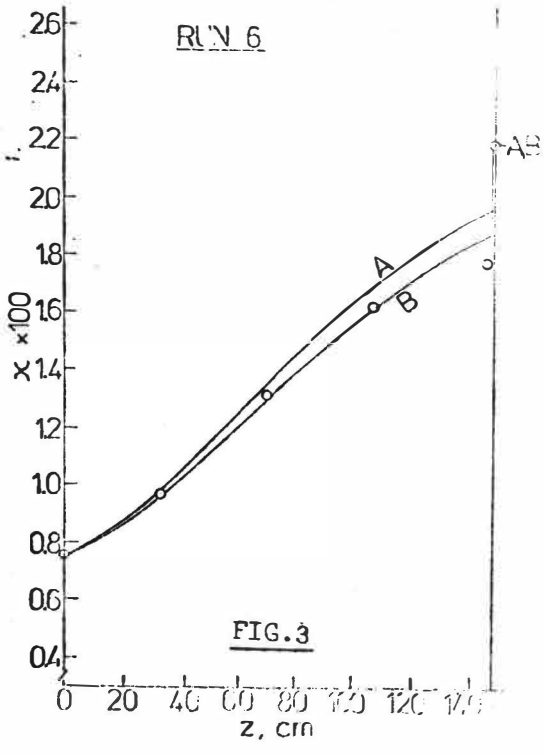

FIG.3

Parameter adjustments

Fig.No.	Run No.	Curve	Mixing - Zone - Settling			
			k_C	E_C	k_C	E_C
2	3	B1	x0.7	-	-	-
2	3	B2	x0.6	x0.6	-	x0.6
3	6	B	x2.4	x1.7	-	-
4	11	B	x0.5	x0.4	x0.3	x0.4
5	16	B	x0.4	x0.4	x0.4	-

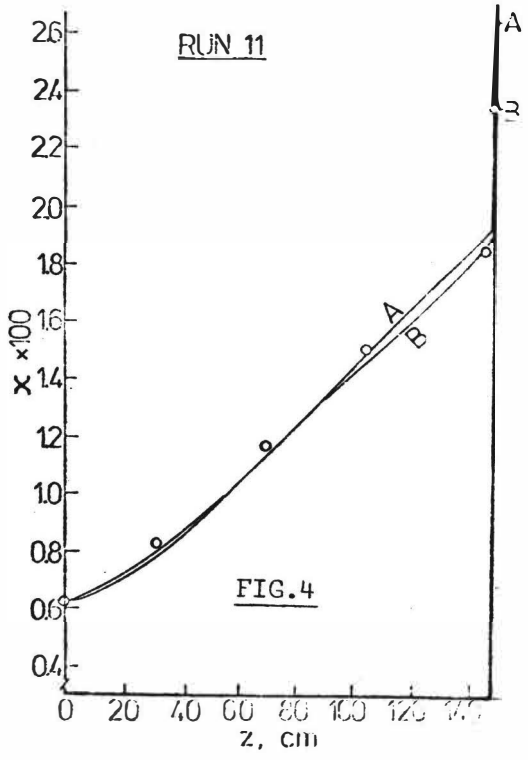

FIG.4

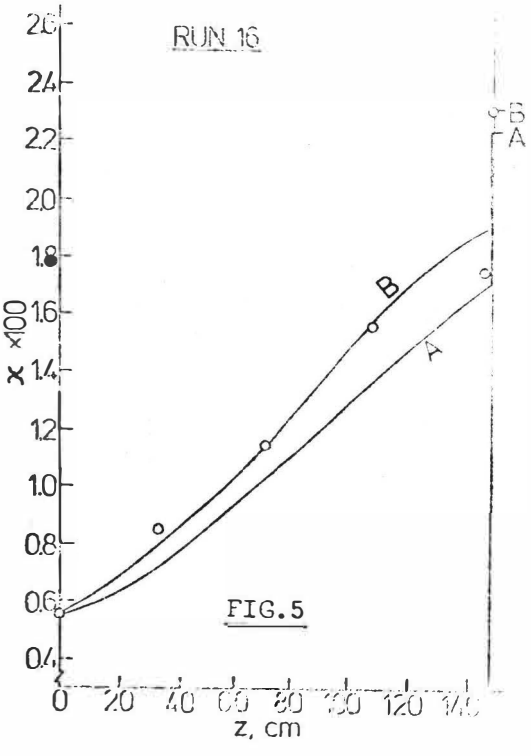

FIG.5

A DYNAMIC MODEL OF A SOLVENT EXTRACTION MIXER-SETTLER STAGE BASED ON PREDICTED FLOW PATTERNS.

F. Medina Gomez and W. L. Wilkinson*

Schools of Chemical Engineering, University of Bradford, Bradford, West Yorkshire, BD7 1DP, U.K.

* present address British Nuclear Fuels Ltd. Risley, U.K.

ABSTRACT

A mathematical model which describes the dynamic behaviour of a single stage mixer-settler unit has been developed. The mixer has been described in terms of instantaneous mass balances and holdup relationships and equilibrium is not assumed. The emulsion band has been divided into elements of uniform phase composition and the flow patterns in the continuous phase in the settler have been predicted to obtain the residence times in flow channels defined by streamlines. Typical results demonstrating the effect of the main variables and mass transfer relationships on the open loop response are presented. A comparison with experimental data shows good agreement for both single and multicomponent transfer.

INTRODUCTION

Mathematical models which are capable of describing the dynamic behaviour of processes are useful to predict the open loop response of controlled variables to uncontrolled disturbances, start-up and shut-down behaviour, and also as a basis for the design of automatic control systems. However, in spite of many years of operating and design experience, the dynamic behaviour of mixer-settlers is still not well understood. Whereas the dynamic behaviour of the mixer can be described quite easily, the settler presents a more difficult problem. Empirical approaches have been adopted in the past which are not useful in design.

The objective of this work was to develop a model based on a prediction of the flow patterns in the emulsion band and the two liquid phases in the settler instead of using arbitrary assumptions about the characteristics of the settler. This description of the process dynamics also involves the hydrodynamic characteristics of the mixer, as well as its hydraulic interactions with the settler and a novel approach, which relaxes the assumption that equilibrium is necessarily achieved, is presented.

REVIEW OF PREVIOUS WORK

Extensive literature surveys on the dynamic behaviour and control of mixer-settlers have been presented elsewhere (7, 8), so only the literature dealing with hydrodynamic modelling of the settler will be considered here. The simplest approach to modelling the settler has been to assume that the two phases are in plug flow and that the settler concentration response is

the same as that leaving the mixer but delayed by the time required to pass through the appropriate phase in the settler. However, there is considerable evidence of appreciable mixing in the settler. Beetner, Frey and Bautista (1) found experimental evidence of plug flow in the organic phase in the settler and partial mixing in the aqueous phase and derived a simulation technique (2) in which the settler's volume was divided into different regions with either plug flow or perfect mixing, according to the region.

Chester (4) made an analysis into the hydrodynamic behaviour of a multistage mixer-settler, extending static considerations for the unit to include recycle flows and a flooding profile for normal operation. He derived linearised transfer functions to simulate single and multistage units. Probably the most thorough investigation on flow patterns in the settler is to be found in the parallel studies by Rouyer (9) who explained the mixing phenomena in the settler and obtained experimental results for upward steps in aqueous feed concentrations, and Demarthe (5) who investigated the flow patterns in the settler by applying both upward and downward concentration steps and described the existence of an associated flow rate, which was a measure of convection in the settler.

The need to consider settler hydrodynamics in design was recognised by Drown and Thompson (6) who observed that settlers could be characterised by three distinct regions, viz., the entrance, the emulsion band and the exit region. They found that velocity distributions varied considerably from plug flow and that the emulsion band was capable of absorbing momentum from both bulk phases, causing a deceleration of the emulsion band and enhancing the dynamic coalescence rates.

From the above review it is seen that the different types of representation of settler hydrodynamics are somewhat arbitrary. A more fundamental approach is therefore needed.

Consider a conventional box mixer-settler. The length of the emulsion wedge increases as the flow rate increases until, with a throughput corresponding to a correct sizing of the settler, the height of the emulsion band becomes uniform. Since the rate of coalescence in the emulsion band is a function of its height, once this becomes uniform it is reasonable to assume that the rate of coalescence will also be uniform over the whole area of the settler. In other words, the liquid flux from the emulsion band into both continuous phases will be uniform. On this basis the flow patterns in the two phases can be predicted, and this is the aim of the present work.

DEVELOPMENT OF THE MATHEMATICAL MODEL

The Mixer. With good mixing it is reasonable to assume that the ratio of the two phase holdup volumes is in direct proportion to the inlet aqueous and organic volumetric flow rates, L_F and V_F respectively. Thus, the aqueous outlet flow, L_m, will be given by

$$L_m = \frac{(L_F + V_F)\, H_L}{H_L + H_V} \qquad (1)$$

where H_L and H_V are the aqueous and solvent holdups respectively. Variations in H_L will be given by

$$\frac{d H_L}{dt} = L_F - L_m \qquad (2)$$

Similar expressions can be derived for the organic phase. A solute balance on the aqueous phase gives

$$\frac{d}{dt}(H_L X_i^m) = L_F X_i^F - L_m X_i^m - Q_i \quad (3)$$

where X_i^F and X_i^m are the aqueous concentrations of component i in the feed to the mixer and the outlet from the mixer respectively. Q_i, the amount of solute i transferred from the aqueous to the solvent phase is given by

$$Q_i = K_i^x (X_i^m - X_i^*) \quad (4)$$

where K_i^x is a mass transfer coefficient and X_i^* is the concentration in the aqueous phase which would be in equilibrium with Y_i^m. Substituting Eqn.(2) in (3) and rearranging gives

$$\frac{d X_i^m}{dt} = \frac{L_F (X_i^F - X_i^m) - Q_i}{H_L} \quad (5)$$

Similarly, for the organic concentration of i, Y_i, it follows that

$$\frac{d Y_i^m}{dt} = \frac{V_F (Y_i^F - Y_i^m) + Q_i}{H_V} \quad (6)$$

Most previous work has assumed an equilibrium relationship to express Y_i^m as a function of X_i^m. However, equilibrium is not always achieved in the mixer and it is possible to determine experimentally the rate of mass transfer.

Single Component Transfer. For the system under consideration a pseudo equilibrium relationship of the form $Y^m = a_1 + a_2 X^m$ was developed, where a_1 and a_2 are constants. Such a relationship actually measures the fractional approach to equilibrium and substituting its derivative in Eqn. (6) and adding (5) to the equation thus obtained, Q_i is cancelled giving finally

$$(H_L + a_2 H_V)\frac{dX^m}{dt} = L_F X^F + V_F Y^F - L_m X^m - V_m Y^m - L_F X^m - V_F Y^m + (H_L X^m + H_V Y^m)\left(\frac{V_F + L_F}{H_L + H_V}\right) \quad (7)$$

Multicomponent Transfer. Assuming equilibrium relationships of the form

$$\left(\frac{Y_i}{X_i}\right)^* = \phi (X_j^m, Y_j^m) \quad (8)$$

where j = 1, 2, ..., number of components, (7), K_i^x can be calculated by substituting Eqn. (4) in (5) and integrating numerically using experimental values of X_i^m and Y_i^m.

The Emulsion Band. The band, Fig. 1, is divided into N finite difference elements so that the composition of each phase in each element is assumed to be uniform. Consider the nth element. Since there is a constant flux of both phases from the emulsion band, the flows displacing the solute along the band are

$$\text{Aqueous phase in } L_{n-1} = (N + 1 - n) L_m/N \quad (9)$$

Aqueous phase out $L_n = (N - n)\, L_m/N$ (10)

If the flows across an element boundary are at the means of the concentration of the adjacent elements for both phases, then the concentrations of aqueous entering the elements are

$$X_{n-1} = \frac{1}{2} (X_{n-1} + X_n) \quad (11)$$

The variation in the height of the emulsion band, l_e, is given by

$$A_s \frac{d\, l_e}{dt} = L_m + V_m - N (L^1 + V^1) \quad (12)$$

where A_s is the base area of the settler and L^1 and V^1 are the aqueous and solvent fluxes from each element of the emulsion band respectively. Since l_e is not usually dependent on V^1 if the aqueous phase is dispersed (and vice versa), then $V_m = NV^1$ and Eqn. (12) reduces to

$$A_s \frac{d\, l_e}{dt} = L_m - NL^1 \quad (13)$$

The band height, l_e, is a function of L^1 and under conditions of constant impeller speed and temperature a relationship of the form

$$L^1 = k_e\, l_e^{\alpha} \quad (14)$$

fitted the experimental observations very closely for a given phase ratio and total throughput. The index α was about 0.5. The change in the aqueous holdup, h_L, is

$$\frac{d\, h_L}{dt} = \frac{L_m}{N} - L^1 \quad (15)$$

and a solute balance in the aqueous phase for element n of the emulsion band gives

$$h_L \frac{d\, X_n}{dt} = \frac{L_m}{2N} \left[(N + 1 - n)\, X_{n-1} - X_n - (N - n)\, X_{n+1} \right] \quad (16)$$

Expressions equivalent to Eqns. (9)(10)(11) and (16) can be derived for the organic phase, thus presenting the dynamic behaviour of the emulsion band.

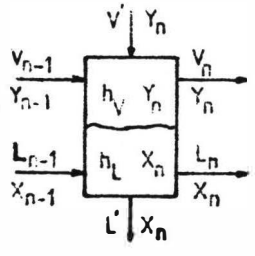

FIG. 1

Section n of the emulsion band

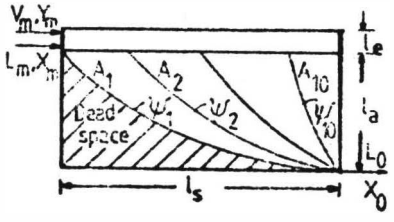

FIG. 2

Streamlines in the aqueous phase in the settler predicted by Eqn.17

The Continuous Phases. The flow field in the two continuous phases may be solved using the potential flow equation:

$$\frac{\partial^2\psi}{\partial x^2} + \frac{\partial^2\psi}{\partial y^2} = 0 \qquad (17)$$

where ψ is the stream function and x and y represent the Cartesian coordinates. The flow situation in the aqueous phase is presented in Fig. 2 where the length of the settler is l_s, the height of the aqueous phase l_a, and the areas between the streamlines A_1, A_2, etc. are relative to the total area of the settler and thus independent of its geometry. The length of the settler was divided into N equal sections. Eqn. (17) was solved numerically for different values of N using Liebman's method for a rectangular mesh grid and N = 10 proved to be sufficient for the problem. Values of the flow areas A_1 to A_{10} were then calculated by numerical integration and the dead space obtained by linear interpolation of the areas.

However, previous studies (7),(6) had already indicated the importance of the horizontal component of velocity in the emulsion band which is not accounted for in Eqn. (17). Therefore, two alternative expressions, the vorticity transport equation

$$\frac{\partial}{\partial t}(\nabla^2\psi) + \frac{\partial(\psi, \nabla^2\psi)}{\partial(x,y)} = \nu\,\nabla^4\psi \qquad (18)$$

where the second term is the Jacobian and ν the kinematic viscosity, and the biharmonic equation

$$\nabla^4\psi = 0 \qquad (19)$$

were used, incorporating as a boundary condition a simplified, normalized, linear horizontal component of velocity. The flow situation thus predicted is represented in Fig. 3 and the different flow areas, A_k, relative to the total area, A_T, in Fig. 4.

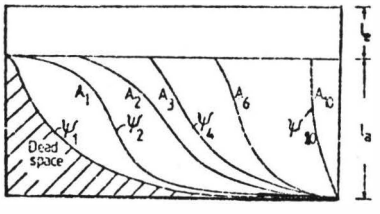

FIG. 3

Streamlines in the aqueous phase in the settler predicted by Eqn. 18

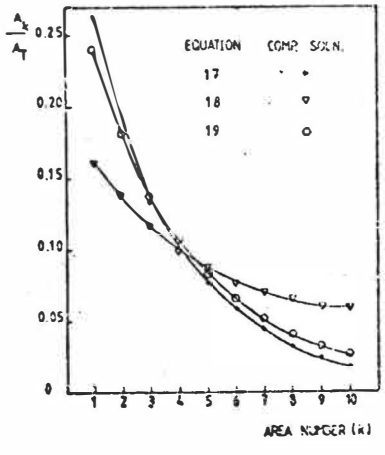

FIG. 4

Flow areas obtained by Solving Eqns. 17, 18 and 19

The residence time in each flow channel, τ_n, can be found from

$$\tau_n = \frac{A_n W}{F} \qquad (20)$$

where W is the width of the settler and $F = L^l$ or V^l according to the phase to be considered.

The solution of the system of simultaneous equations representing mixer, emulsion band and continuous phases was carried out numerically in the time domain, to avoid the linearisation implied by analytical solutions.

EXPERIMENTAL EQUIPMENT AND PROCEDURE

The experimental equipment consisted of two single stage, perspex mixer-settler units and the necessary tanks, piping, pumps and instrumentation to operate the units as a continuous extraction/stripping system. A flow diagram of the equipment is shown in Fig. 5. The extraction unit operated at room temperature while the stripping unit operated at 50°C. Full details of the equipment are available elsewhere (7). The experimental programme was devised to investigate the open loop response of the unit to step disturbances in the aqueous feed concentration and the aqueous and organic feed flows. Initially the transfer of a single solute was considered, the chemical system being water/nitric acid/ 20% v/v tri-n-butyl phosphate (TBP) in kerosene. The work was then extended to the multicomponent system water/nitric acid/uranyl nitrate/20% TBP. The equipment was allowed to reach an initial steady state before introducing a step change.

The dynamic concentration response was measured by taking simultaneous samples, at regular intervals, of the two phases and the aqueous phase in the mixed phase port and of the aqueous outlet from the settler. The dynamic response of the aqueous outlet flow was measured with a rotameter. Measurements were also made of l_e and l_a with respect to time.

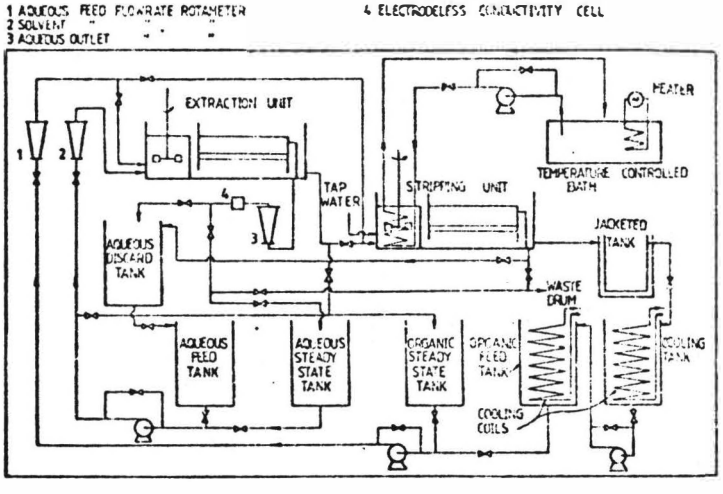

FIG. 5

Flow diagram of the experimental equipment

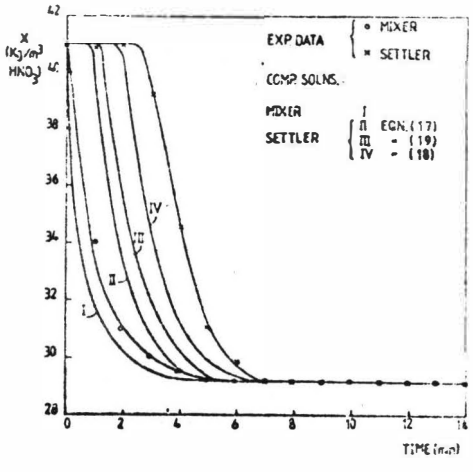

FIG. 6

Effect of flow areas on downward step acid concentration response

EXPERIMENTAL RESULTS AND DISCUSSION

Six runs representative of the experimental programme are summarised in Table 1.

TABLE 1. Experimental Programme

FIG. No.	L_F (l/min)		V_F (l/min)		X_H^m	X_H^F	Y_H^m	Y_H^F	X_U^m	X_U^F	Y_U^m	Y_U^F	l_e	l_a
	STEADY STATE	STEP CHANGE	STEADY STATE	STEP CHANGE	FIGS. 6 - 9 : Kg/m^3 FIGS. 10 - 11 : gmole/l								cm	
6	2.4		4.5		41.02	33.02	4.26	10^{-4}					3.0	6.0
7	2.4		4.5	5.0	33.02		4.71	10^{-4}					2.2	6.3
8	3.4		3.8		23.16	33.55	1.28	10^{-4}					3.0	6.0
9	3.4	1.95	3.8		30.63		2.62	10^{-4}					3.2	5.9
10	3.0		3.0		2.247	2.025	0.19	10^{-4}	0.1014	0.337	0.126	10^{-3}	2.8	6.6
11	3.0		3.0		1.971	1.964	0.44	10^{-4}	0.21	0.176	0.152	10^{-3}	2.0	5.0

Superscript m refers to concentrations in the mixed pnase port at the initial steady state, wnile F refers to feed concentrations at zero time, i.e. the step perturbation in the aqueous feed and the solute concentration in the regenerated solvent feed. Subscripts U and H denote uranium and nitric acid respectively. The values of l_e and l_a correspond to the final steady state. The flow rate perturbations were introduced under conditions of no mass transfer.

Figs. 6 to 11 show the experimental data compared with the computed solutions. The agreement is generally good and, in all cases, the simulated response is faster than its experimental counterpart. An examination of the reliability of the experimental results and the mathematical shortcomings of the computer simulation is therefore indicated. To illustrate the latter, the effect on the theoretical predictions of the flow areas in the settler and the approach to equilibrium in the mixer will be shown. Three different sets of areas (Fig. 4) were used to simulate the run presented in Fig. 6. The application of a horizontal component of velocity, Curves III and IV, improves the prediction of the settler's response by introducing a hydrodynamic lag absent in II. Furthermore, IV, obtained using the areas given by the solution to the vorticity transport equation (18) predicts more accurately the behaviour of the settler than III, which uses the areas obtained from the biharmonic equation (19). Curves I and II in Fig. 8 were obtained using experimentally determined pseudo equilibrium relationships. Curves III and IV were obtained using the actual linear equilibrium relationships, derived experimentally in a manner similar to that described in (3) and they predict a final steady state involving a higher aqueous nitric acid concentration than is found experimentally. This is not surprising since the pseudo equilibrium relationships were tailored to the experimental results, but it indicates clearly that equilibrium is not necessarily achieved in the mixer and that the introduction of a mass transfer term would be perhaps a better approach.

The response of the multicomponent runs, Figs. 10 and 11, exhibits the same behaviour pattern of the single component response. Fig. 9 shows the dramatic effect of the mass transfer coefficient on the mixer's response.

If K_i^x is chosen to be sufficiently small, Curve III, it can reverse the trend and make the experimental response faster than the computed one, while if it is large, as in I, the predicted response can be too fast. The best fit, II, was obtained with the experimentally determined K_U^x and K_H^x, which reflects again the validity of such an approach.

Figs. 7 and 9 illustrate the dynamic response of the aqueous outlet flow rate L_o. l_e was the determining factor and the start-up point for the

computed result was slightly different from the experimental one, due to the nature of Eqn. (14). Fig. 9 exhibits an unusual pattern which was predicted by the model. As the solvent phase holdup increases, so does the aqueous flow rate, simply because the aqueous holdup decreases. Once the decrease in aqueous flow rate reaches the settler's outlet, the throughput starts decreasing until it reaches steady state.

Another determining factor on the accuracy of the simulated response was the use of a Runge-Kutta-Merson method not specifically designed to solve stiff systems of equations. The large time constant of the settler, compared with that of the mixer, may require smaller integration step sizes and therefore dominate the overall speed of solution.

Regarding the reliability of the experimental results, there are inevitably errors in the sampling technique since sampling had to take place over a very short period of time. Most of the concentration change in the mixer, for both phases, took place before the first sample was taken due to the very short residence time. The sampling for the settler was more reliable since it was recorded continuously on an electrodeless conductivity monitor. It served as a check on the mixer's response, as in Fig. 10, where a minimum in the nitric acid concentration, undetected by the sampling of the mixer, was recorded for the settler. The analysis of samples was reliable and so was the overall performance of the aqueous outlet rotameter. Fig. 12 shows a typical pattern for the dynamic behaviour of the emulsion band. The predicted response was faster than the experimental one, but since the values of k_e and α were determined empirically, it could be due to the fitting of the experimental observations to the power curve. l_e was not strictly constant throughout the length of the settler, diminishing very slightly with increased distance from the mixed phase port at lower throughputs. This can be explained in terms of the overall coalescence rate being faster than the horizontal component of velocity of the emulsion band.

CONCLUSIONS

The work has shown that a useful dynamic model of a mixer-settler can be developed based on a prediction of the flow behaviour in the settler. This approach is superior to those which are based on arbitrary assumptions.

REFERENCES

1. Beetner, G. A., Frey, L. A., and Bautista, R. G., Proc. 2nd Int. Symp. on Hydrometallurgy, 1973, 906-19.

2. Beetner, G. A., Frey, L. A., and Bautista, R. G., Trans. Soc. Mining Engrs., AIME, 1973, 254, 349-53.

3. Burns, P. E., and Hanson, C., J. Appl. Chem., 1964, 14, 117-21.

4. Chester, M. W., PhD Thesis, University of Southampton, 1970.

5. Demarthe, J. M., C.E.N., Commis. En At., CEA-R-4350, 1973.

6. Drown, D. C., and Thompson, W. J., I.&.E.C., Process Des. Dev., 1977, 16, 197-206.

7. Medina Gomez, F., M.Sc. Dissertation, University of Bradford, 1978.

8. Medina Gomez, F., and Wilkinson, W. L., To be published, Chem.Eng.Sci.

9. Rouyer, H., C.E.N., Commis. En. At., CEA-R-4189, 1972.

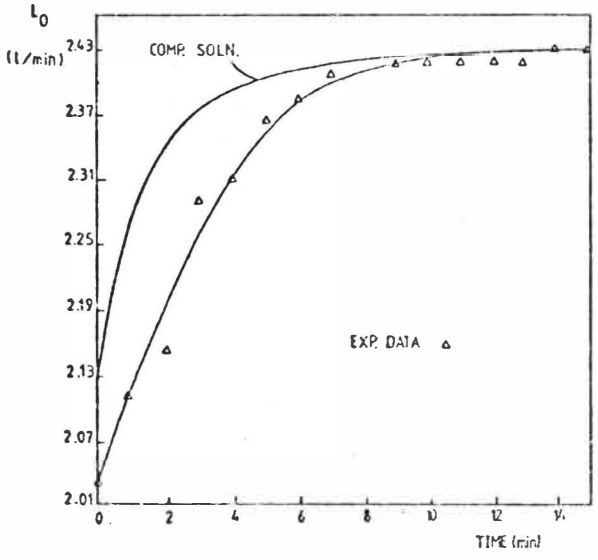

FIG. 7

Example of upward step solvent flow rate response

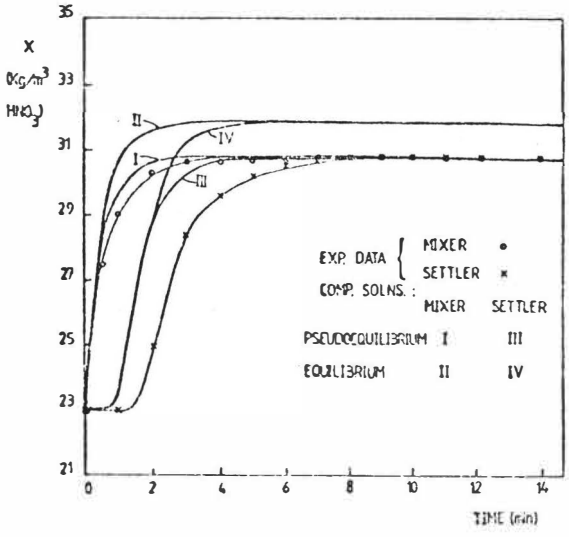

FIG. 8

Effect of approacn to equilibrium on upward step acid concentration response

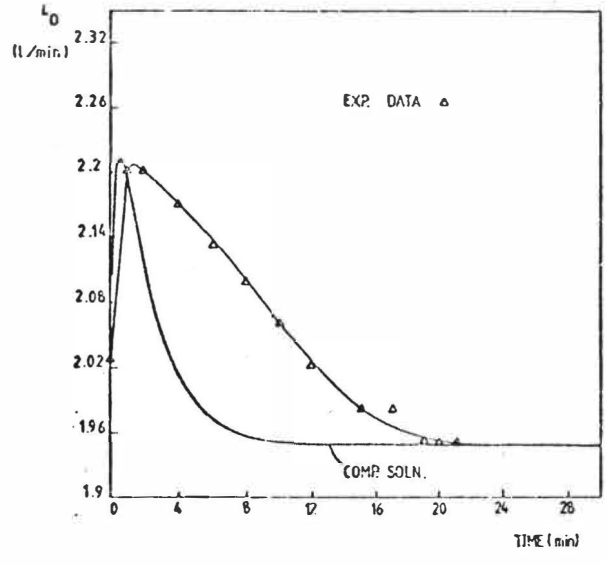

FIG. 9

Effect of downward step aqueous flow rate response

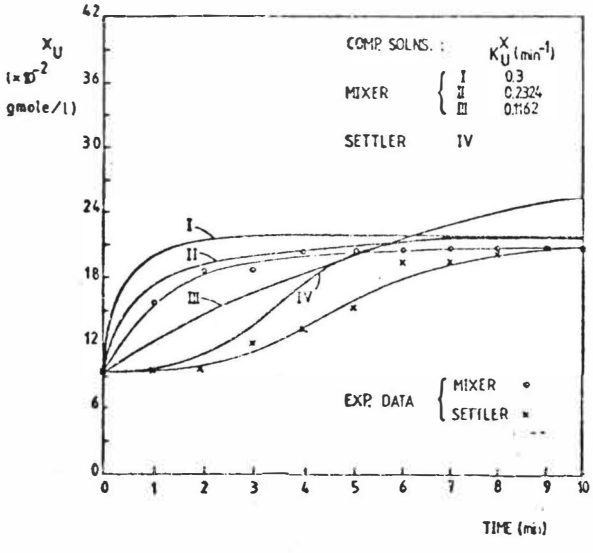

FIG. 10

Effect of the mass transfer coefficient on upward step U concentration response

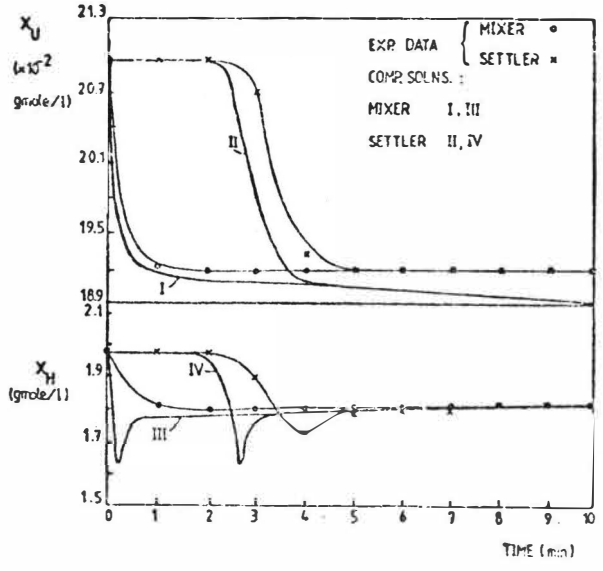

FIG. 11

Example of downward step U and acid concentration response

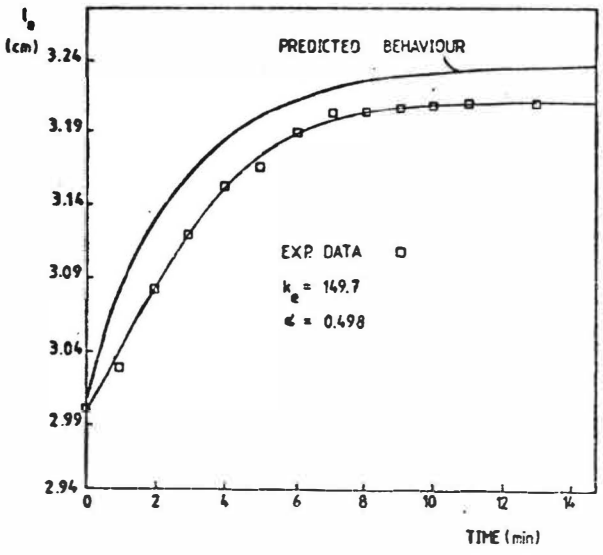

FIG. 12

Example of the dynamic behaviour of the emulsion band

NOTATION

a_1, a_2	pseudo equilibrium relationship constants
$A_n = A_k$	flow area of the nth flow channel
A_s	base area of settler
A_T	total cross sectional area of settler
h	holdup in the emulsion band
H	holdup in the mixer
k_e	power curve constant (Eqn. 14)
l_e^a	height of the aqueous phase in the settler
	height of the emulsion band
K^x	mass transfer coefficient from aqueous to solvent phase
L_1	aqueous phase flow rate
L	aqueous flux from the emulsion band
N	number of sections in emulsion band
Q	rate of mass transfer
t	time
V_1	solvent
V	solvent flux from the emulsion band
W	width of settler
X	aqueous concentration
Y	organic concentration
ψ	stream function
α	power curve index (Eqn. 14)
τ	residence time

Subscripts and Superscripts

*	equilibrium	F	feed to the mixer
A	nitric acid	i	component
L	aqueous phase	m	outlet from the mixer
n	section in settler	U	uranium
V	solvent phase		

ACKNOWLEDGEMENT

The contribution of J. Retamales towards the provision of experimental data is gratefully acknowledged.

A MODEL FOR THE CO-EXTRACTION KINETICS OF URANIUM, PLUTONIUM AND NITRIC ACID

G. Petrich
Institut für Heisse Chemie
Kernforschungszentrum
D-7500 Karlsruhe, W-Germany

ABSTRACT A model is presented for the mass transfer kinetics of uranium, plutonium and nitric acid in the system uranyl nitrate-plutonium(IV)nitrate, nitric acid, sodium nitrate/TBP. The model describes experimental data previously measured by Finsterwalder /1/ for transfer from a continuous phase into a rising/falling drop phase at macro concentrations of U and Pu. It was found that all data are well fitted by a mass transfer rate which depends only on the gradient of the equilibrium concentration curve of the transfering species. The nitric acid extraction rate is additionally enhanced by the co-extraction of uranium.

INTRODUCTION

A valuable tool in the design and safety analysis of the Purex process for the separation and purification of uranium and plutonium from fission products is the computer simulation of the various extractor types employed.

Simulation of the coextraction of uranium, plutonium and nitric acid in mixer-settlers is in a good state, because comparatively long residence times in the stages and the stagewise cocurrency of the phases allow a more or less complete chemical equilibrium of the interacting solutes between the phases to be obtained /2/. Hence, the central problem is a good model of the distribution equilibria and a practical way to describe non-ideal flow patterns in the mixer-settler.

This is not true for the simulation of pulsed sieve plate columns. Apart from the description of hydraulics, a model for the solute transfer kinetics is needed. A method frequently found in literature to calculate concentration profiles in pulsed columns is by intersecting the length of the column in a number of stages and to assume that a HTU-dependent percentage of chemical equilibrium is reached. This may lead to rather poor results. The reason is that for all heights within a column, the phase concentrations are far from chemical equilibrium and that all solutes have different and generally concentration dependent time constants for transfer between the phases.

Previous attempts to predict transfer time constants for the Purex-system at macro concentrations of U and Pu from either reaction kinetics at the phase interface or from transport processes have not yet to our knowledge led to a model that could be used in computer simulation. We have therefore tried a more empirical approach to model the kinetics of simultaneous uranium, plutonium and nitric acid transfer.

The model had to fulfill the following requirements:

R1: Description of experimental data measured by the rising/falling drop method. Stationary and drop phase are an aqueous and an organic TBP/kerosine phase resp. or vice versa. $UO_2(NO_3)_2$ ranged from 0 to 0,8 M aqueous and from 0 to 0,21 M organic. The $Pu(NO_3)_4$ ranged from 0 to 0,1 M aqueous and 0 to 0,14 M organic. HNO_3 ranged from 0,01 to 3 M aqueous and from 0 to 0,32 M organic. TBP concentrations were 5,10 and 20 weight percent in dodecane. Additional measurements existed for 3 M $NaNO_3$ in the aqueous phase. Almost all of the more than 1000 data points have been taken at ambient temperature.

R2: Keeping in mind that the model should be used for the simulation of a pulsed column its structure should be as simple as possible. The introduction of hypothetical interface concentrations should be avoided to minimize core memory and computer time needed for simulation. Interface concentrations will in addition greatly extend the range of time constants in the model and thus lead to a stiff system of equations which is difficult to integrate numerically.

R3: For sufficiently long contact times the model has to produce the correct equilibrium concentrations as predicted from the distribution model used in mixer-settler simulation. It is not enough to model the initial transfer rates from the linear part of the mass-transfer versus time curves.

R4: In the different separation and purification cycles of the Purex process both aqueous and organic phases are used as the dispersed phase. A common model for the extraction rates is thus desirable.

R5: Mass transfer rates for U, Pu and HNO_3 are, like distribution equilibria, known not to be constants with respect to varying concentrations. While distribution equilibria are readily measured and are tabulated /3/ and are precisely described in mathematical models, the measurement of reaction rates encompasses many problems and is very time consuming. If it is at all possible, it is thus preferable to model the transfer kinetics solely on the basis of equilibrium relations to allow for extrapolation.

KINETIC DATA

The experimental conditions under which the experiments have been conducted are described in detail in /1/. The kinetic data for the forward and reverse extraction were measured by /1/, by letting initially unloaded drops rise or fall through the loaded continuous phase. Only 3 runs were performed for the reverse reaction of HNO_3 in the rising drop mode. Following a procedure developed by Nitsch /4/, drop concentrations were measured for each run at 4 different column lengths each with 4 different throughputs. To eliminate mass transfer during drop formation and coalescence the data was

$$\beta'_{theo} = (0{,}0047 \pm 0{,}0004)\,(dy/dx)^{0{,}57 \pm 0{,}13}$$

which is within the error limits of (2).

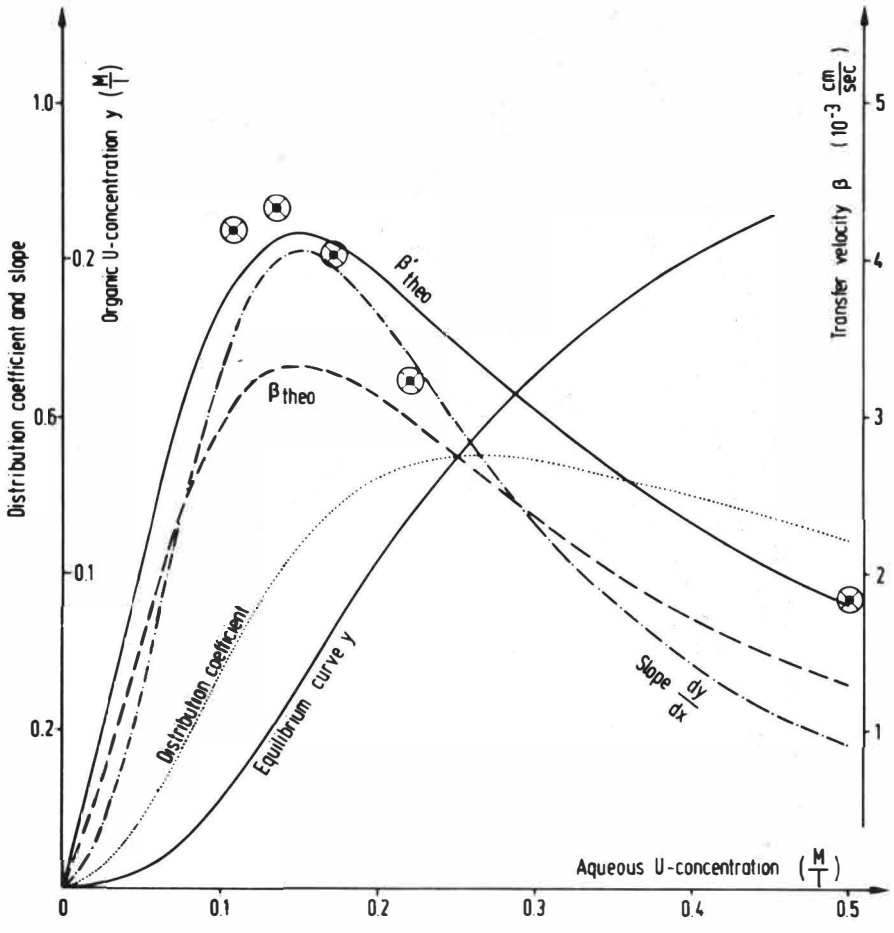

FIG. 2

Back extraction of uranium in 20 w% TBP into 0,01 n HNO_3 drop

Quite in contrast to uranium and plutonium the aqueous to organic nitric acid transfer as a function of time follows relation (1) only if no or very little uranium is present. With increasing uranium the rate of HNO_3 extraction increases considerably, even at aqueous uranium concentrations as low as 0,008 M. At U-concentrations of more than about 0,01 M the extracted HNO_3 overshoots its equilibrium value within the short measuring time of less than 4 sec and its rate of transfer increases further up to U-concentrations of at least 0,3 M. At U-concentrations of more than about 0,08 M, the extracted HNO_3 reaches a maximum within the measuring time and then decreases again until it finally reaches its equilibrium value (data symbols in FIG. 3).

These findings were up to now the main obstacle in setting up a model based on stoichiometry relations such as quoted above. Instead a term proportional to the rate of uranium transfer had to be added to equ. (1) to adjust the transfer rate of nitric acid:

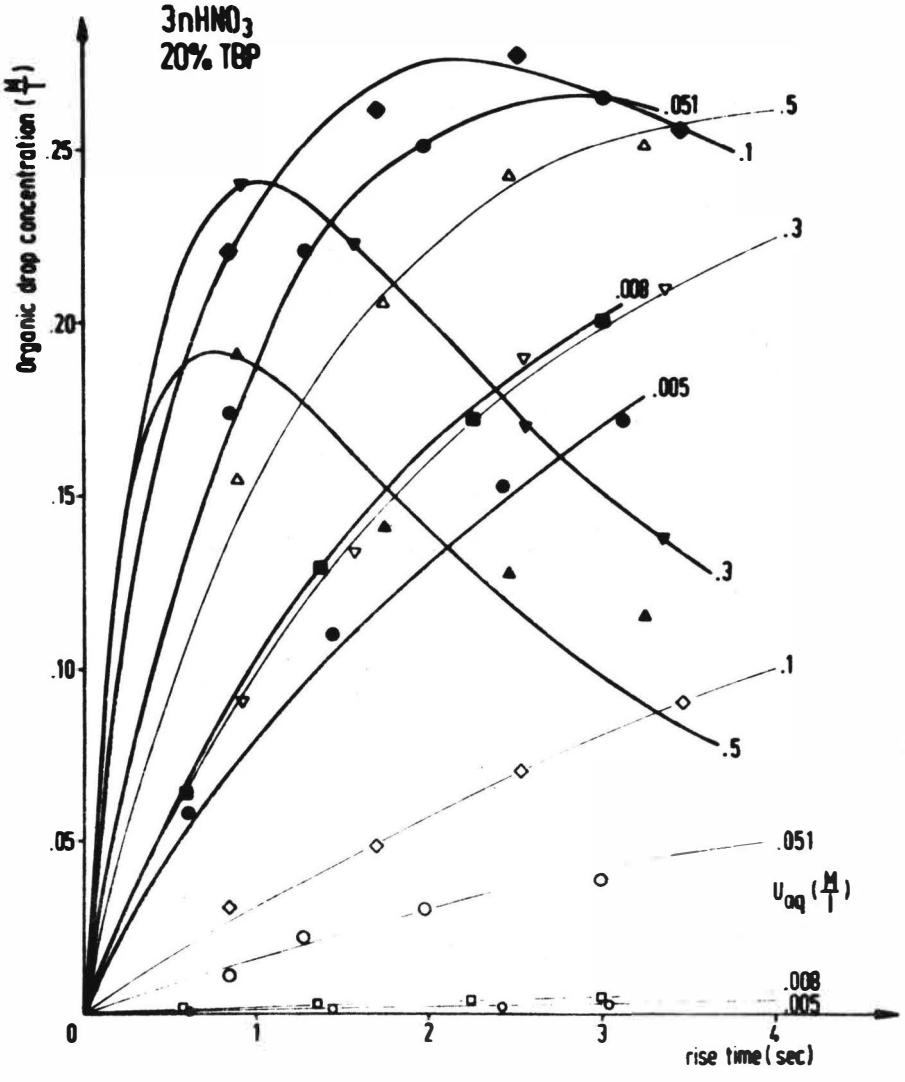

FIG. 3

Uranium (empty symbols, light curves) and nitric acid (filled symbols, heavy curves) transfer

$$dc_h/dt = A\beta_h(c_{h,inf} - c_h) + \lambda dc_u/dt \qquad (3)$$

The subscripts h and u stand for HNO_3 and U resp. Curves in FIG. 3 are best fits to equ. (3). While the values obtained for β_u by a simultaneous fit of U and HNO_3 transfer via equ. (1) and (3) are only insignificantly different from a sole fit of U to equ. (1), the values obtained for β_h are somewhat higher than expected from relation (2).

Using β_h as calculated from (2), values for the proportionality constant λ are derived as shown in FIG. 4. Further work is required here since it is not known whether equ. (3) also holds for the reverse reaction or for aqueous drops. Furthermore the concentration dependence of λ does not meet requirement R5 above.

DISCUSSION

So far, all our results for the mass transfer rates of U, Pu and HNO_3

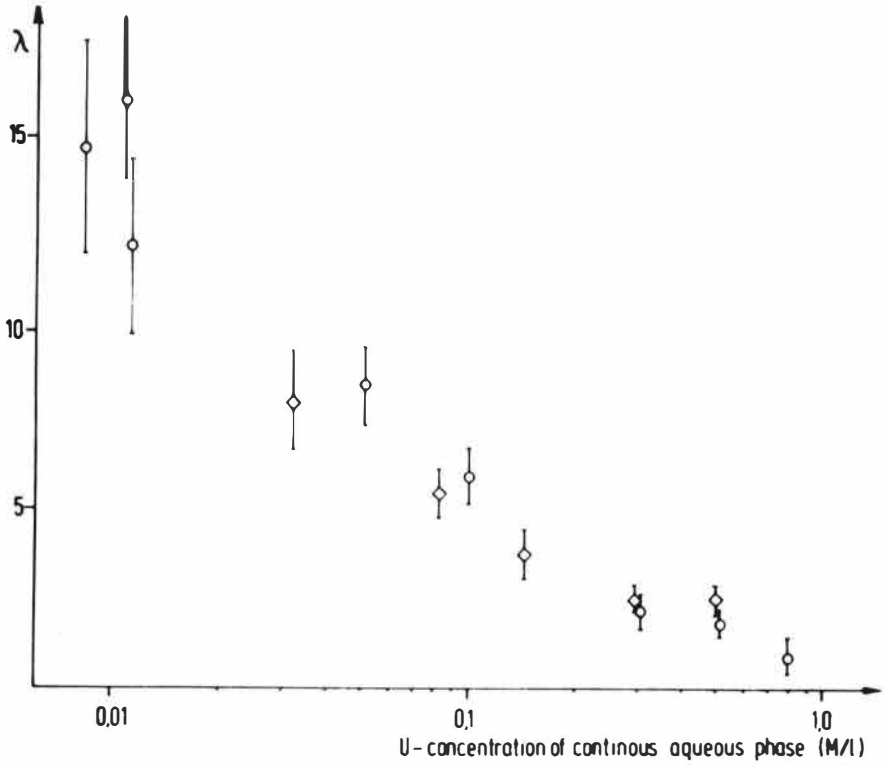

FIG. 4

Enhancement factor λ for nitric acid transfer from 3 n HNO_3 into 20 w% (circles) and 10 w% (diamonds) TBP-drops by the presence of uranium

are consistent with the use of the equilibrium curve slope as an interpolation variable, at least with transfer into the drop phase. A physical interpretation of this slope is the sensitivity of one phase to small concentration changes in the other phase.

For transfer out of the drop into the continuous phase we have only 3 ß-values available for the reverse reaction of HNO_3, marked as ◎ in FIG. 1. The 3 points fit well in our correlation if we use dc_{aq}/dc_{org} as an abscissa value in FIG. 1 instead of dc_{org}/dc_{aq} used for the reverse reaction data with transfer from the continuous organic phase into the aqueous drop phase. This implicates that within the frame of our correlation dc_{cont}/dc_{drop} has to be employed as the rate determining quantity.

Here lies the major source of uncertainty in our procedure since no further experiments for U and Pu transfer from the drop into the continuous phase are available from /1/, the basis of our data. A literature search has had only limited success: although published transfer rates are within the range of our data, a precise comparison is almost impossible. This is due to the following reasons:

Experimental methods different from the rising/falling drop scheme lead to transfer rates which depend on experimental conditions such as stirrer speeds, centrifuge rotation speed or flow rates. In addition, the surface area per unit volume A is not always known and sometimes there are doubts as to which phase is continuous and which is dispersed. Since we aim at the numerical simulation of pulsed columns which requires the absolute magnitude of transfer between continuous and drop phase the published data is of a

rather qualitative nature for our purposes.

Published transfer rates as calculated from rising/falling drop experiments do not always quote all the variables required for a quantitative comparison with our correlation: metal and nitric acid concentrations of aqueous and organic phase, TBP-concentration, direction of transfer, indication which phase is continuous and which is drop phase. In addition the equilibrium curves are not known to us for all cases.

Farbu et al. /5/ measured forward and reverse reaction rates for organic drops with a 0,99 M $NaNO_3$ / 0,01 M HNO_3 solution as the continuous aqueous phase and TBP drop concentrations ranging from 0,02 M to 0,4 M. Uranium was present only in trace amounts. While $ß_u$ at 0,4 M TBP (14 w%) fits very well in our correlation, the rates at the lowest TBP-concentrations are considerably over-estimated by the correlation. Although the rates of /5/ for the reverse reaction increase with increasing slope dc_{aq}/dc_{org} the change in transfer rates is not pronounced enough to significantly corroborate the choice of dc_{cont}/dc_{drop} as an interpolation variable for all modes of uranium mass transfer.

In two recent publications Horner et al. /7,8/ claim that the rate of aqueous to organic transfer of macro amounts of uranium was the same for the falling drop and the rising drop modes. A value $ß_u = 7,3 \pm 2,5 \times 10^{-3}$ cm/sec is quoted for the forward reaction from 3,5 M HNO_3 into 30 % TBP, averaged from experiments with a Kenics mixer, a Lewis cell and rising/falling drop tests. In a graphical presentation of ß-values in /7/ not enough information is given to make a further comparison.

Much of the previous work on transfer rates in the Purex system nas been conducted with the nature of the transfer process in mind. Both diffusion and chemistry controlled processes have been deduced as well as combinations of the two possibilities. This paper cannot solve this problem but it is hard to conceive that diffusion control should be dominant in rising/falling drop experiments when the correlation shown in FIG. 1 is viewed.

CONCLUSION

A model for the mass transfer rates of uranium, plutonium and nitric acid in the Purex system has been given which

- is consistent with experimental data over wide concentration ranges
- is easy to integrate
- fulfills the equilibrium relations for sufficiently long contact times
- works for aqueous and organic dispersed phases
- depends solely on equilibrium relations.

The last point is not completely satisfied due to the introduction of a uranium-rate dependent term in the nitric acid transfer rate equation with a concentration dependent constant of proportionality.

The model requires further validation for mass transfer out of the drop phase.

While it is not claimed that the present model is the only one which can be developed to describe the system, it does serve to make computer

simulation of continuous extractors in the Purex process such as pulsed columns a practical tool.

ACKNOWLEDGMENT

Grateful acknowledgment is made to Prof. F. Baumgärtner and to Dr. L. Finsterwalder for permission to use their experimental data.

REFERENCES

/1a/ Finsterwalder L., Ph.D. thesis, Technische Universität München (1968)
/1b/ Baumgärtner F., Finsterwalder L., J. Phys. Chem. 74, 108 (1970)
/2/ Petrich G., Berliner A., KfK-Nachrichten 3/1979, p. 64 ff.
/3/ Petrich G., Kolarik Z., KfK 2536 (1977)
/4/ Nitsch W., Dechema Monograph. 55 (1965)
/5/ Farbu L., McKay H.A.C., Wain A.G., Proc. ISEC'74 (Lyon), p. 2427
/6/ Heertjes P.M., de Nie L.H., in C. Hanson ed., Recent Advances in Liquid-Liquid Extraction, Pergamon Press, Oxford (1971), p. 367
/7/ Horner D.E., Mailen J.C., Scott T.C., Thiel S.W., Yates R.G., ORNL/TM-6786 (1979)
/8/ Horner D.E., Mailen J.C., Trans.Am.Nucl.Soc., 27, 484 (1977)

MATHEMATICAL MODELLING AS AN R & D TOOL IN SOLVENT EXTRACTION

S. Wahrmann, J.E. Gai

I.M.I. Institute for Research & Development.

Haifa, Israel

ABSTRACT

The easy accessibility of computers makes it worthwhile to revise methods of constructing material balance flowsheets especially for processes involving the extraction of significant amounts of more than one component. The new approach would consist of the careful planning and execution of a series of partition tests which would then be subject to computer aided analysis. The advantages of the new approach are clearly shown by some simple examples and IMI experience is described showing how the new approach is rapidly gaining ground.

Research at IMI on solvent extraction, started some 25 years ago, has resulted in the development and industrial implementation of several novel processes. These processes related to multicomponent, interacting systems which defied the mathematical or graphical analysis so readily applicable to systems in which a single component is transferred.

About five years ago, work started on the first computer simulation of a steady state model, and since then, computer use for R & D purposes has been steadily expanded. What follows can be considered as a summary of our experience with this useful tool, the emphasis being on the approach and methods used to arrive at material balance flowsheets (configuration, flowrates, concentrations and number of stages).

Prior to the use of electronic computers, the technique developed at IMI usually included the following stages :

a) In order to overcome the complexity of multicomponent systems, the "limiting conditions" concept was developed, according to which equilibrium conditions in a multistage battery can be obtained by contacting a small quantity of solvent with a quantity of aqueous phase large enough so that the resulting transfer would not materially alter the aqueous phase composition. The results of this test were then used to calculate a material balance using a number of simplifying assumption, which established terminal conditions while disregarding possible internal interactions.

b) Cross-current batch tests in the relevant battery. These results were used to estimate the number of stages required in the battery.

c) Batchwise experimental simulation of countercurrent operation. At this point the preceding estimates were confirmed or amended, and ideally a final material balance was obtained.

d) Continuous countercurrent operation in bench-scale equipment and/or in a pilot plant.

As already stated, some notable successes were achieved with this approach, but is has certain limitations, particularly in the later stages. The results of the cross-current tests are not usually likely to expose special physico-chemical interactions in the system (e.g. the chloride-bromide interaction in the IMI $MgCl_2$ - $MgBr_2$ Process, which gave rise to rather striking results, described in Ref. 1).
Batchwise simulation of countercurrent operation can be a laborious operation, the number of variations which can be tested is usually limited, and complete simulation of an integrated flowsheet with more than say,two batteries is difficult. Continuous operation is always necessary in the later stages for final flowsheet verification as well as for other purposes (e.g. long-term effects, testing of equipment, etc.) and it sometimes may not be amenable to testing of variations. Pilot plant operation will certainly be prohibitively expensive if the evaluation of all the different operating parameters is intended rather than verification of the final process configuration.

Computer simulation can alleviate these limitations, but it requires adjusting to a different approach which will typically contain the following sequence of operations :

a) Accumulation of a data base derived from a planned set of partition tests. No hard and fast rules can be given for planning the set except to note that time devoted to analysis of the system, and to careful planning and execution, is well spent. The ranges of concentrations, and of combinations of components, to be tested should be significantly broader than those to be expected in the process. This is where temperature effects should be studied, particularly if the process is expected to be operated at ambient temperatures with no control of this parameter.

b) Derivation of correlations to represent the distribution data, including the effects of interaction between the components. Although correlations are not absolutely essential for modelling (interpolation methods can be used instead), they are convenient and save computer time during execution of the program. Very often they also have the important advantage of providing insight and better understanding of the chemistry involved. Here, already, the computer permits easy testing of many forms of regression equations which previously were wellnigh impossible to perform. When the form of the regression equation is not known in advance, it is particularly convenient to work interactively on a computer, using a language which employs an interpreter (e.g. BASIC or APL).

c) Computer simulation for study of parameters and of different configurations, and for optimization. Ideally, these simulations should also be coupled to an economic evaluation program so that also the economic optimum, and not only the technical one, is obtained, but at IMI we have not yet reached this level of sophistication. The simulations may sometimes lead to the need for extending the data base if compositions are predicted which are outside of the range previously studied.

d) Continuous experimental operation for verification, but this will now usually be performed only on the optimized flowsheet.

A more or less standard approach to the calculation algorithm has been adopted at IMI which is similar to that previously described (1) except that improvements have been introduced in the convergence procedures. The previously described search procedure is now normally used only to bring the interations sufficiently close to the solution so that thereafter convergence can be reliably accelerated by use of more sophisticated procedures. For programmers working in FORTRAN, we can recommend subroutines available from HARWELL (2). In particularly difficult cases it has been found efficient to begin calculations with only one stage per battery, where convergence is easy, and then add on one stage at a time until the desired number is reached. After solving for the addition of the second stage, an extrapolation procedure is used to provide the initial estimates when the next stage is added on. Since no convergence procedure is as efficient as are good initial estimates, this procedure sometimes saves time and effort as well as automatically providing the effects of number of stages.

In some cases, where complete phase separation is difficult, and where large concentration changes are involved, provision has also been made for calculating the effect of entrainment of one phase in the other. Assuming the degree of entrainment given, insertion into the "function" to be solved is easy, requiring only the appropriate material balance equations. However, depending on the form of the regression equations developed and on which phase is entrained in the other, the complexity of the convergence problems can sometimes be doubled.

Implementation of the new approach has been gradual, since it was necessary to first prove that reliable results could be obtained. The first test case was the previously reported comparison with pilot plant data for the IMI $MgCl_2$ - $MgBr_2$ Process (1). At the time the general attitude to such a model was one of slight doubt but that it was worth the try. Work was commenced while the particular variation being considered was still being developed. In a lighter vein it may be mentioned that someone asked who would come up first with a satisfactory process, the experimenters or the computers. The regular process developers won that race because they were experienced and the modeller was not, but the results of the model were considered as being more than good enough to pursue the subject.

Courage and persuasive ability are required to request the large budgets required for full process development on the basis of a series of partition tests, bypassing the cumbersome procedure of process definition in the laboratory. However, the demonstrated efficacy and reliability of the computer model has resulted in an increasing willingness to devote

budgetary resources to peripheral, but vital aspects of process development at an early stage.

Attention was then focused on the IMI Standard Phosphoric Acid Process (3) in which IMI has a continuing interest. In this process phosphate rock is attacked with hydrochloric acid and the phosphoric acid is recovered from the dissolution liquor (containing H^+, Ca^{++}, Cl^-, phosphate and impurities) and purified in an integrated, four-battery, solvent extraction circuit, the solvent being pentanol.

The simulation results were tested by comparison with two plants operating the process, although with some differences between them in their operating conditions. Some of the main difficulties experienced in developing this model was that the correlations were developed from existing data which had accumulated over the years. These had resulted from process development work, but had certainly never been planned to serve as a data base. The result was that four difficulties were encountered: a) The data were concentrated around the operating concentration profiles and consequently the data base was not always sufficiently broad. b) The data were not evenly balanced over the concentration ranges studied so that uneven weight was sometimes given to different portions of the regression equations. c) Because of different sources of information, different operating conditions, etc., the data were not always consistent and the first correlations derived did not (and could not) have the desired accuracy of fit. d) The data available were not always complete, since one or more components were often not analysed. In addition, some ambiguity exists since chemical analysis expresses components as ionic concentration, while material balance requires allocation of ionic species to compounds and analysis of minor components is often required in order to achieve a correct allocation of a key major component.

The former three problems were solved as best as possible by selection of the data to give consistent and balanced sets. Despite these difficulties, a sufficiently quantitative model was developed and gave good agreement with the results of one of the plants. The model was used to test suggested improvements which were afterwards implemented. In the case of the second plant agreement was not quite so good and it was concluded that equilibrium was not being attained in the mixers, a fact which was afterwards substantiated by plant personnel. This indicates the additional use of steady state models for troubleshooting purposes.

The effort expended on this model found its most fruitful rewards in connection with a third plant now being constructed, in two different directions. One of them was in the determination of an optimum material balance for the particular dissolution liquor expected. As an example of the agreement obtained between calculated results (performed first) and a continuous bench scale run is shown. The sequence of operation was as follows :

a) "Limiting conditions" test and flowsheet calculation
b) Parametric study using the computer process model
c) Continuous pilot plant verification

The results are illustrated below :

Flowsheet	Alcohols per 100 P_2O_5	HCl per 100 P_2O_5	Extract P_2O_5	Composition HCl	Residual P_2O_5 in raffinate
Calculated	1258	117	55	49	
Simulated Optimum	1242	94	55	37	2.7
Continuous Operating Data	1436	82	51	32	2.3

It should be mentioned that for operating reasons the bench unit was run with more solvent and less HCl resulting in the same residual. Obviously this resulted in a more diluted extract.

The other reward was experienced during training of the senior technical personnel of the plant (for whom this project constituted their first encounter with a solvent extraction process). The use of the model played an important part in the training program and greatly facilitated understanding the complexity of the various interactions involved. The best proof of the appreciation of the model is the fact that the client wishes to have the model available during the commisioning period .

With increasing confidence in the method, it has been implemented for other processes to a greater or lesser extent along the lines indicated above, sometimes more so and sometimes less so. It is not superfluous to add that even with computer assistance, there is no substitute for ingenuity and basic understanding of a process in order to decide which combinations to test. Intuition is also useful but simulations have sometimes revealed significant differences between intuition and fact which might have taken much longer to discover by the other approach.

An example of a case where intuition was proved wrong was in a process for recovering a particular component, designated here as A, from a multicomponent aqueous feedstock. The solvent utilized was capable of extracting two components, A and B, initially present in the feedstock.

The initial concentration of A was significantly lower than that of B, but selectivity ratios were in the range of 7 to 17 in favour of the former. Both the total loading of extracted solutes in the solvent, and the selectivity toward A, increased with increasing total solute concentration in the aqueous phase. From preliminary partition tests it was concluded that a simple three-battery flowsheet would suffice (see fig. 1). The three important performance criteria of the process were the degree of recovery (minimum 70%), the purity (minimum ratio of A/B being 30/1), and the concentration of the product.

Intuitively it was expected that optimum performance should be obtained with the smallest ratio of solvent to aqueous feed which would satisfy the minimum requirements of recovery and purity. Since the total

concentration of solutes (expressed in equivalents) drops continuously in the scrubbing battery, in the direction of the solvent flow , it is natural to expect that the minimum ratio would provide maximum concentration of product. At the minimum ratio it was established that a 5 - 4 - 6 (extraction - scrubbing - stripping) stage combination was necessary. However, during a parameter study using the computer model, to test the sensitivity of operation to flow ratios, it was discovered that a 50% increase in solvent flowrate (compared to the minimum possible) would provide a purer product and/or a more concentrated one, with two stage less, i.e. with a 4 - 4 - 5 stage combination. Although perhaps not immediately obvious, the explanation turns out to be relatively simple.

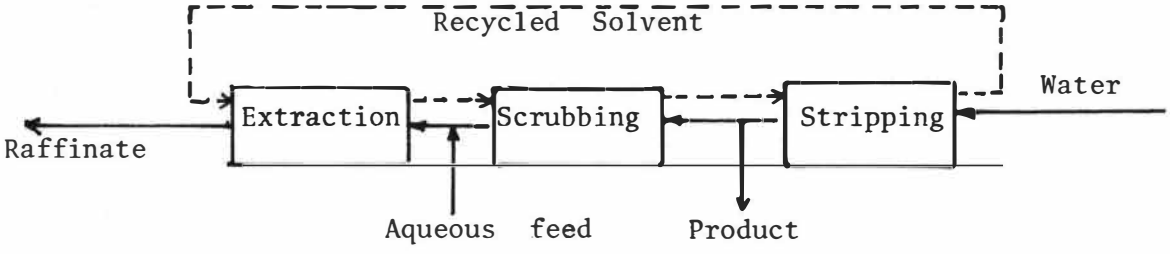

Fig. 1: Schematic Flowsheet for Recovery of A from a Multicomponent feed

It is quite evident that increasing the solvent flowrate tends to increase the recovery, at the expense of obtaining a more dilute extract. Instead of increasing the recovery, one stage of the stripping battery is eliminated, using a slightly lower water to solvent ratio. One effect is that the recycled solvent is returned to extraction with a higher residual A content, and another is to obtain A in the aqueous phase exiting from stripping at a slightly higher concentration than would be obtained for more complete stripping. Equally important is that a larger percentage of this latter aqueous phase is refluxed to the scrubbing battery because, despite the slight decrease in wash water to solvent ratio, the ratio of wash water to feedstock has increased, while the absolute quantity of the product does not change much. The increased reflux ratio improves the performance of the scrubbing battery, gives a purer product, and the overall cooperative effect of increased internal A recycles also yields a more concentrated product.

Although everything appears perfectly logical after seeing the results, it is unlikely that they would have been otherwise forecast, whereas to reach them experimentally would probably have required a fortuitous error. Testing of the sensitivity to flow ratios also indicated that results would be quite sensitive to the reflux ratio and appropriate conclusions were reached concerning how this parameter should be controlled.

It takes quite some courage, and also persuasive ability to go from a series of partition tests to a relatively large continuous unit via calculations only. In practice , we still do not always do it that way, partly because of lack of conviction on the part of the process developers but also because of the needs associated with the other aspects of developing a process. However, the new approach is steadily gaining ground.

Acknowledgement

The authors are grateful to the IMI Management for allowing publication of this paper and to Mr. D. Meyer for his useful suggestions.

REFERENCES

1. "Modelling of the IMI $MgBr_2$ $MgCl_2$ Process" - J.E. Gai
Proceeding ISEC 1977, Toronto Canada.

2. "Harwell Subroutine Library. A Catalogue of Subroutines"
Computer Science and Systems Division.

3. AERE Harwell Oxfordshire.
IMI Staff Report : Proc. Intern. Solvent Extraction Conference.
ISEC 71, Vol. 2, p. 1356. Society of Chem. Industry, London (1971).

THE USE OF LETAGROP COMPUTER PROGRAM FOR THE ANALYSIS OF SOLVENT EXTRACTION DATA.

D. HAY LIEM
Department of Inorganic Chemistry
Royal Institute of Technology (KTH)

S-100 44 Stockholm 70
Sweden

THE LETAGROP VERSION FOR ANALYSIS OF LIQUID-LIQUID DISTRIBUTION DATA, CALLED DISTR, IS DISCUSSED AND ITS APPLICATION TO SEVERAL TYPES OF DISTRIBUTION DATA GIVEN. THE DISTR PROGRAM CAN BE USED TO TREAT A FOUR-COMPONENT SYSTEM CONTAINING SPECIES OF THE FORM $A_pB_qC_rL_s$. BOTH SOLVENT EXTRACTION AND TWO-PHASES TITRATION DATA CAN BE USED.

Solvent extraction has been established as an effective and valuable technique for the study of chemical equilibria in both aqueous and organic phases. From liquid-liquid distribution data one can draw conclusions on the chemical species formed in the two-phase system and calculate the equilibrium constant for the formation of these species. Graphical analysis of extraction data, e.g. slope analysis, can effectively be used for the determination of the main species formed. However, graphical methods are less applicable for making detailed analysis in more complicated systems, e.g. in a four component system where several species may be formed in the same extent. The use of a high-speed computer as a supplement to graphical methods has been shown to be a valuable method for the detailed analysis of chemical equilibrium data. Computer analysis of data enables us in an objective way to determine the model which out of different possible models gives the best description to the chemical system studied. The LETAGROP program developed by Sillén and coworkers(1) is a powerful computer program for the analysis of chemical equilibrium data. The program has successfully been applied for the analysis of chemical equilibrium data, such as potentiometric titration(2), calorimetric(3), osmometric(4), NMR(5) and liquid-liquid distribution data(6). LETAGROP is a general minimizing program which consists of a main part common to all types of problem and a special part (PUTS, UBBE) which is specific for the type of data to be treated. The use of LETAGROP for treatment of a specific type of problem thus only requires the definition of the problem in the special part of the program, e.g. in which form the data are to be given and the type of error-square sum to be minimized.

In the LETAGROP program the error-square sum U which is minimized is

generally defined by (1):

$$U = \sum_{1}^{Np} w_i (y_{calc} - y_{exp})^2 \qquad (1)$$

In (1) Np represents the number of experimental points, w_i a weight-factor, y_{exp} a known measured quantity, e.g. the measured EMF of a cell in a potentiometric titration or the distribution ratio D in solvent extraction, and y_{calc} is a quantity which may be calculated from a derived functional relationship $y_{calc} = f(k_i, a_j)$, i = 1,2,... M; j = 1,2,... N, where k_i is a set of constants, e.g. equilibrium constants, and a_j are quantities known or derivable from the primary experimental data, e.g. total concentration of the reaction components. The LETAGROP version for liquid-liquid distribution data is called DISTR(6), which has successfully been applied to the treatment of several solvent extraction systems (7-18). The program can be used to treat a four-component system containing species of the form $A_pB_qC_rL_s$, where usually A = H^+, B the component for which the distribution between the two phases is studied, while C and L represent ligands which may form complexes with e.g. A or B. With this LETAGROP-DISTR program the computer is ordered to calculate the set of values of the constant K_1, K_2, ...K_n for the formation of the species $A_pB_qC_rL_s$ in the aqueous phase and in the organic phase which minimize e.g. the error-square sum $U = \sum_{1}^{Np} (\log D_{calc} - \log D_{exp})^2$. Recently the DISTR program has been extended and can now be used to treat two-phase potentiometric titration data(19). The description of the DISTR program has been given elsewhere(6,19) and in the following discussion the reader is referred to these publications for more detailed informations. The present paper aims primarily to discuss the application of DISTR-program on different types of liquid-liquid distribution data.

SOME CONCEPTS AND SYMBOLS IN THE LETAGROP-DISTR PROGRAM

Input data: In the LETAGROP calculations the input data consist of three parts. The first part is a general information of procedures for the computer which are specific for the type of the computer, e.g. time limit of calculation, number of lines to be printed, required memory space of computer, customer's account number, specification that DISTR is to be made available for use etc. This part is different from one machine to the other but the user will usually be assisted by the operator of the machine or by the operation manuals. The second part of input data consists of instructions to the computer to select the required type of program in DISTR which accept a given set of primary data. This is effected using the control number Rurik = 9, followed by a number indicating the type of primary data set available. The instruction 9, 2, on a card, e.g., implies that the set of primary data available for the analysis is loga, Btot, Ctot, Ltot, I_0, I_1, i.e. log[H^+], total concentration of the component B, C and L, the number of counts of B in the aqueous phase per time unit and volume unit (=I_0), and the number of counts of B in the organic phase (=I_1). The set of data which follow are preceded by the control number Rurik = 6 with the necessary information regarding the data, e.g. number of series of data (=Ns), number of constants common to all points (Nag), number of constants common to each series of data (=Nas), specification of these constants ag_1, ag_2 ... ag_N and as_1, as_2 ... as_N. The third part consists of instructions on what chemical model is to be assumed and how the analysis is to be performed. This "day order" will vary in the search of the best model for the system. An example

of day order is given in ref.(6), Table 2 and the following numerical illustrations. Several types of day order will be discussed in this paper.

Control numbers Rurik: The LETAGROP program is run by means of a set of control numbers called Rurik, which may have the values 1, 2, ... 20. A given value of Rurik corresponds to a specified instruction in the program (cf. Ref.1). In the present form of DISTR program Rurik = 19 and 20 are not available, since no group parameters ks are given.

Reaction components: Three or four reaction components A, B, C, and L may be used in DISTR to build a given chemical system by assuming the formation of complexes $A_pB_qC_rL_s$ in the aqueous and organic phases. A given complex is characterized by the set of numbers(p,q,r,s,0) or (p,q,r,s,1), in which the last number 0 or 1 indicates whether the complex is formed in the aqueous phase or in the organic phase. The formation constant of a given complex $A_pB_qC_rL_s$ corresponds to the equilibrium constant for reaction (2):

$$pA + qB + rC + sL \rightleftarrows A_pB_qC_rL_s \qquad (2)$$

$$K = [A_pB_qC_rL_t][A]^{-p}[B]^{-q}[C]^{-r}[L]^{-s} \qquad (3)$$

The status of the chosen reaction components, i.e. whether in the aqueous or in the organic phase,is given by ascribing a value of 1 for the formation constant and the set of numbers for species identification, e.g. for B = Zn^{2+} (aq):(0,1,0,0,0), which means p=0, q=1, r=0, s=0 and fas(=phase)=0 (=aqueous phase), and for C = HDEHP (org): (0,0,1,0,1). In the program A usually represents H^+(aq) and need not be identified in the same way as for other reaction components. The coefficients p,q,r, and s may assume both positive and negative values, e.g. $Zn(OH)^+$(aq) is identified by (-1,1,0,0,0),(p=-1, q=1, r=0, s=0 and fas=0) with the formation according to (4):

$$Zn^{2+}(aq) + H_2O \rightleftarrows Zn(OH)^+(aq) + H^+(aq) \qquad (4)$$

Types of primary data: The type of primary data is identified in the program by the control number, Rurik =9, typ, in which typ may have values 1,2,3,4, 5,6,7,8. The following types of distribution data may be used:

Typ	log a	B_{tot}	C_{tot}	L_{tot}	I_0	I_1	D_{exp}	V(O/A)	λ	I_{exp}
1	x	x	x		x	x			(x)	
2	x	x	x	x	x	x			(x)	
3	x	x	x				x	x		
4	x	x	x	x			x	x		
5	x	x	x		x	x		x	(x)	
6	x	x	x	x	x	x		x	(x)	
7	x	x	x					x		x
8	x	x	x	x				x		x

The cross-marked quantities are the primary data given as ap, i.e. the data are given for each point. The correction factor λ may be used if the distribution ratio D must be corrected due to different absorption (in β counting) or quenching (in liquid scintillation counting) in the two liquid phases. In the program, we may choose λ as ap quantity or as ag, i.e. a constant common to all points. I_0, I_1 = radioactivity of a tracer isotope of the reaction component B in e.g. cpm/volume unit. Instead of radioactivity we may of course use concentration units for I_0 and I_1, e.g. if B is analyzed by a

titration or atomic absorption spectroscopic method. V(O/A) = phase ratio organic/aqueous; I_{exp} = proton excess over chosen levels. log a = log$[H^+]$; B_{tot}, C_{tot}, L_{tot} = initial total concentration referred to the aqueous phase, e.g. $B_{tot} = N_B/V_{aq}$, where N_B is total moles of B and V_{aq} represents the volume of the aqueous phase. Usually loga is log$[H^+]$ but may also represent other ionic species, e.g. Cl^-, with known free concentration.

Types of error-square sum minimized: In the program the choice of the error-square sum U to be minimized is effected using the control number Rurik = 18, val, where val can have the values 1, 2 or 3. In the day order if there is no specific requirement of the error-square sum to be minimized is given, using the above Rurik = 18, val is automatically ascribed the value of 1 and the error-square sum corresponding to it is minimized. The following types of error-square sum may be minimized for different values of typ, i.e. type of primary data.

Error-square sum minimized, U

val	typ = 1 - 6	typ = 7,8
1	$\sum_{1}^{Np} (\log D_{calc} - \log D_{exp})^2$	$\sum_{1}^{Np} (\log I_{calc} - \log I_{exp})^2$
2	$\sum_{1}^{Np} (D_{exp} D_{calc}^{-1} - 1)^2$	$\sum_{1}^{Np} (I_{exp} I_{calc}^{-1} - 1)^2$
3	$\sum_{1}^{Np} (D_{calc} D_{exp}^{-1} - 1)^2$	$\sum_{1}^{Np} (I_{calc} I_{exp}^{-1} - 1)^2$

D is distribution ratio; I proton excess and Np number of points. In the program D_{calc} and I_{calc} correspond to D_{Ber} and I_{Ber}.

In the present form of DISTR program the weight-factor w = 1, i.e. we assume that the experiment has been carried out in such a way as to give data of comparable accuracy. This assumption seems in most cases to be justifiable since minimizing different types of error-square sum given above, which implies giving other weight-factors to the data, is found to give the same result of calculations (cf. Ref. 12-15).

Calculation of D_{calc} or I_{calc}: During the calculations D_{calc} or I_{calc} (typ = 7 or 8) must be evaluated for each point from given values of primary data and equilibrium constants β_i. From the mass balance equations for B, C, L, the values of log a and the set of equilibrium constants β_i for the formation of the species $(A_{p_i}B_{q_i}C_{r_i}L_{s_i})$ in the aqueous and organic phase, for i=1 to Nk(=number of complexes), we can calculate [B], [C], [L] D_{calc} (or I_{calc}) (cf. Ref. 6, 19).

COMMENTS ON THE USE OF LETAGROP

The availability of a computer program for data analysis, such as LETAGROP, implies a powerful tool in chemical equilibrium analysis. The obvious advantage of data treatment using high-speed computers is the possibility to make an objective comparison of the different reasonable chemical models which may fit the experimental data. Usually this type of model searching can be carried out effectively in a minimum of time with

the LETAGROP program. For a successful use of LETAGROP, however, some requirements have to be met. First of all the quality of the data to be treated is of fundamental value. Both the accuracy and the relevance of the data are important for finding the correct chemical model of the system. These points are of course also valid for graphical analysis of data. To be able to determine the equilibrium constant within reasonable accuracy of a given complex requires the availability of data in the range where the species of interest are formed in measurable quantity. Neglect of this plain principle will give rise to problems and cost computer time. Another point of interest is that one has to check whether there are any data present with unaccountable big errors compared with the rest of the data, either caused by real experimental error or other errors. The presence of these "bad" data may spoil the whole analysis since the U value will now mainly be determined by the error-square sum of these points, and a change of chemical model will usually be of no effect in decreasing the value of U_{min}. Errors of data of this type may easily be detected if the computer analysis is preceded by a graphical analysis of the data whenever this is possible. The additional use of graphical analysis is also valuable in the search of the main species which are predominant in the system studied (cf. Ref. 13,16). Finally the proper use of day order is of great importance e.g. the order of the data to be included in the analysis, using Rurik=11, or which equilibrium constants are to be varied. This type of skill usually can be mastered by the average chemist after a short period of practice.

CASE STUDIES

The LETAGROP-DISTR program has been applied to the analysis of several solvent extraction systems. A brief description of some of these cases will be given below. The reader is referred to the references for a more detailed information.

1. Chemical system: Dibutylphosphate (HDBP)-tributylphosphate(TBP)-hexane/ 0.10 M H_2SO_4 (cf. Ref. 7)

   Primary data:

   loga = log[H^+] = -0.923 was kept constant during the experiment. The value was calculated assuming $K_a = [H^+][SO_4^{2-}]/[HSO_4^-] = 2.894 \times 10^{-2}$ M.

   $B_{tot} = [HDBP]_{tot}$ was varied during the experiment and given for each point;
   $C_{tot} = [TBP]_{tot}$ was varied in some sets and kept constant in other sets of experiment and given for each point;

   $I_0 (=I_{aq})$ and $I_1 (=I_{org})$ = β-activity of P-32 labelled HDBP in the aqueous and organic phase in cpm for equal volumes of samples and given for each point. The phase ratio V(O/A)=1 was kept constant and given for each serie of data ($as_1 = 1$). The correction factor $\lambda (=ag_1)$ was assumed to be constant.

   Description of the system: We assume the formation of the species $(H^+)_p (HA)_q (C)_r$ in both phases (HA=HDBP; C=TBP). The different HDBP-TBP species found to give the "best" description to the system, i.e. the lowest U_{min}, may be represented as (p,q,r,fas), where fas=0 for aqueous and fas=1 for organic phase: HA(aq)=(0,1,0,0), A^-(aq)=(-1,1,0,0), HA(org)=(0,1,0,1), H_2A_2(org)=(0,2,0,1), HAC(org)=(0,1,1,1), HAC_2(org)=(0,1,2,1), H_2A_2C(org)=(0,2,1,1), H_4A_4(org)=(0,4,0,1).

   The data consist of a 3 component system and may be analyzed using typ=1. The main species HA(aq), A^-(aq), HA(org), H_2A_2(org) and HAC(org) found from graphical analysis were used as a starting model.

2. Chemical system: U(VI)-0.10 M H_2SO_4/HDBP-TOPO-hexane (cf. Ref. 8)

Primary data:

loga = log[H^+] = -0.923 was kept constant during the experiment.

B_{tot} = $[U(VI)]_{tot}$ ≈ 9×10^{-6} M was practically constant during the experiment and given for each point. Formation of only mononuclear U(VI) species were assumed.

C_{tot} = $[HDBP]_{tot}$ was varied during the experiment and given for each point.

L_{tot} = $[TOPO]_{tot}$ was given for each point.

$I_0(=I_{aq})$ and $I_1(=I_{org})$ = α-activity of U-233 in the aqueous and organic phases in cpm for equal volumes of samples are given for each point. The phase ratio V(O/A)=1 was kept constant and given for each serie of data.

Description of the system: The system is described by the reaction components H^+, UO_2^{2+}(aq), HDBP(=HA)(aq) and TOPO(=L)(org) and the formation of the species $(H^+)_p(UO_2^{2+})_q(HA)_r(L)_s$ in the two phases.

The following HDBP-TOPO species are known from previous studies (cf.Ref.7) $(H^+)_p(UO_2^{2+})_{q=0}(HA)_r(L)_s$ = (p,0,r,s,fas), where fas=0 for aqueous and 1 for organic phase: HA(aq)=(0,0,1,0,0), A^-(aq)=(-1,0,1,0,0), HA(org)=(0,0,1,0,1), H_2A_2(org)=(0,0,2,0,1), H_4A_4(org)=(0,0,4,0,1), HAL(org)=(0,0,1,1,1), H_2A_2L(org)=(0,0,2,1,1). The analysis of the data shows that the "best" description of the chemical system is given by assuming the formation of the following U(VI)-HDBP-TOPO species:

$UO_2A_2(HA)_2$(org)=(-2,1,4,0,1), UO_2A_2L(org)=(-2,1,2,1,1), $UO_2A_2L_2$(org)=(-2,1,2,2,1), $UO_2SO_4L_2$(org)=(0,1,0,1,1). The system can be described by four components and the data analyzed using DISTR typ=2.

3. Chemical system: Hf(IV)-1 M H_2SO_4/HDEHP-TOA-toluene (cf. Ref. 11)

Primary data: log a = log[H^+] = 0.0319 was kept constant and given to each point; B_{tot}=$[Hf(IV)]_{tot}$ ≤ 0.723×10^{-7} M was given for each point, and the formation of only mononuclear Hf(IV) species were assumed.

C_{tot} = $[HDEHP]_{tot}$ was varied and given for each point.

L_{tot} = $[TOA]_{tot}$ was varied and given for each point.

$I_0(=I_{aq})$ and $I_1(=I_{org})$ = γ-activity of Hf-181, 175 in the aqueous and organic phase, cpm for equal volumes of samples, and given for each point. The phase ratio V(O/A) = 1 was kept constant and given for each serie of data.

Description of the system: The chemical system is described using the reaction components H^+(aq), Hf^{4+}(aq), HDEHP(=HA)(aq), TOA (=L)(org) and assuming the formation of the species $(H^+)_p(Hf^{4+})_q(HA)_r(L)_s$ in the two phases. The equilibrium constant for the formation of HDEHP-TOA species in 1.0 M H_2SO_4/toluene two phases system has been determined previously (cf. Ref.9). The best model to describe the chemical system is by assuming the formation of the following species (p,q,r,s,fas): HA(aq)=(0,0,1,0,0), A^-(aq)=(-1,0,1,0,0), H_2A_2(aq)=(0,0,2,0,0), H_2A_2(org)=(0,0,2,0,1), HA(org)=(0,0,1,0,1), (LH)(HSO_4)(org)=(2,0,0,1,1), $(LH)_2SO_4$(org)=(2,0,0,2,1), HfA_4(HA)(org)=(-4,1,5,0,1), $HfA_4(HA)_2$(org)=(-4,1,6,0,1), $(LH)_2Hf(SO_4)_3$(org)=(2,1,0,2,1), $(LH)_2Hf(SO_4)_2A_2$(org)=(0,1,2,2,1). The data may be analyzed by DISTR, typ=2, since the system can be described by four reaction components. The value of [HSO_4^-] may be assumed to be

constant throughout the experiment.

4. Chemical system: MeHg(II) distribution between o-xylene/1.0 M (Na,H) (Cl, NO_3, PO_4) (cf. Ref. 13)

Primary data:

loga = log[H^+]= was varied and given for each point.
B_{tot} =[MeHg(II)]$_{tot}$ was varied and given for each point.
C_{tot} = [Cl^-]$_{tot}$ was kept constant and given for each point.
L_{tot} = [P(V)]$_{tot}$ was varied and given for each point.
$I_0(=I_{aq})$ and $I_1(=I_{org})$ = γ-activity of MeHg-203 in the aqueous and organic phase, cpm for equal volumes of samples, and given for each point. The phase ratio V(O/A) = 1 was kept constant and given for each serie of data.

Description of the system: The chemical system may be described by using as reaction components H^+(aq), $MeHg^+$(aq), Cl^-(aq) and $H_2PO_4^-$(aq) and assuming the formation of the species $(H^+)_p(MeHg^+)_q(Cl^-)_r(H_2PO_4^-)_s$ in the two-phase system. In a previous work (cf. Ref. 12) the equilibrium constants for the formation of the species MeHgCl(aq) and MeHgCl(org) have been determined. Computer analysis of the data indicates that the data may satisfactorily be described by assuming the formation of the following species with equilibrium constants given in Ref. 13:

$MeHg^+$(aq)=(0,1,0,0,0), MeHgCl(aq)=(0,1,1,0,0), MeHgCl(org)=(0,1,1,0,1), MeHgOH(aq)=(-1,1,0,0,0), $MeHgHPO_4^-$(aq)=(-1,1,0,1,0). We have a four component system and the data may be analyzed using typ=2. Minimizing the error-square sum U using val = 1,2 or 3 gave practically the same values for the equilibrium constants. From graphical analysis the formation of MeHgOH and $MeHgHPO_4^-$ were indicated, but the use of computer analysis has made it possible to show that the model found seems to be the best out of other chemical models tried.

5. Chemical system: 3-nitrophenol-CH_2Cl_2/Tetrabutylammoniumsulphate Two-phases titration with NaOH solution (cf. Ref. 20).

Primary data:

loga = log[H^+] = was varied during the experiment and given for each point;
B_{tot} = [TBA^+]$_{tot}$ was given for each point; (TBA^+=tetrabutylammonium ions)
C_{tot} = [HX]$_{tot}$ was given for each point (HX=3-nitrophenol).
I_{exp} = [HX]$_{tot}$ - [OH^-]$_{tot}$, proton excess over H_2O, X^- and TBA^+ as zero levels. I_{exp} and the phase ratio V(O/A) were given for each point.

Description of the system: The two-phase potentiometric titration was carried out by starting with given values of $B_{tot}(=[TBA^+]_{tot})$ and $C_{tot}(=[HX]_{tot})$, phase ratio V(O/A). Known volumes of standard NaOH solution are added to the two-phase system and the pH of the aqueous solution determined potentiometrically. The chemical system may be described by assuming the reaction components H^+(aq), TBA^+(aq), X^-(aq) and the formation of the species $(H^+)_p(TBA^+)_q(X^-)_r$ in both phases. In a previous experiment the equilibrium constant for the formation of HX(aq) and HX(org) have been determined by two-phase titration with B_{tot}=0. In the LETAGROP calculation the values of their equilibrium constant may thus be kept constant. We assumed the following species to be formed in the two-phase system:

$HX(aq)=(1,0,1,0)$, $X^-(aq)=(0,0,1,0)$, $HX(org)=(1,0,1,1)$, $TBA^+(aq)=(0,1,0,0)$, $TBAX(org)=(0,1,1,1)$, $TBAX(HX)(org)=(1,1,2,1)$ and $TBAX(HX)_2(org)=(2,1,3,1)$.

Minimizing the error-square sum $U = \sum_1^{10} (\log(I_{calc}/I_{exp}))^2$, the lowest $U_{min}=0.039$, $\sigma(y)=0.018$, was found assuming the formation of TBAX(org) and TBAX(HX)(org). The value of U may be compared with the values found for other models: Model(U_{min},$\sigma(y)$): TBAX(3.426,0.506); TBAX(HX)(0.078,0.093); TBAX+$TBAX(HX)_2$ (0.070, 0.093); TBAX(HX) + $TBAX(HX)_2$(0.308,-), TBAX + TBAX(HX) + $TBAX(HX)_2$ (0.0775, 0.033).

Out of the different models tried, the "best" model to describe the chemical system is the assumption of the following species with the equilibrium constants:

	log K
$H^+ + X^-(aq) \rightleftarrows HX(aq)$	+8.25
$H^+ + X^-(aq) \rightleftarrows HX(org)$	9.05
$TBA^+(aq) + X^-(aq) \rightleftarrows TBAX(org)$	2.03±0.25(3σ)
$H^+ + TBA^+(aq) + 2X^-(aq) \rightleftarrows TBAX(HX)(org)$	15.59(log(K+3σ) = 15.90)

6. In Table 1 the results found from an analysis by the LETAGROP-DISTR program and those by graphical methods are compared for some solvent extraction systems. The results show us that the conclusions found from graphical analysis usually agree with the computer analysis regarding the main species, but may differ substantially in the detailed analysis of the other species.

We may conclude from the given illustrations that the DISTR program is a valuable tool for the analysis of liquid-liquid distribution data. Effective use of the program requires good quality of data and chemical understanding of the problem.

Acknowledgements. This work has been financially supported by the Swedish Natural Science Research (NFR) and the Swedish Board for Technical Development (STU).

Table 1. Equilibrium constant logβ for the formation of extractable species in various two-phase systems.

Two-phase system	Equilibrium reaction	Letagrop analysis[a]	Graphical analysis	Ref.
Eu(III)-0.1 M HNO_3/HDBP-hexane	$Eu^{3+} + 6HA(aq) \rightleftarrows \overline{EuA_3(HA)_3} + 3H^+$	10.65±0.15	10.66	21,23
Am(III)-0.1 M HNO_3/HDBP-CCl_4	$Am^{3+} + 6HA(aq) \rightleftarrows \overline{AmA_3(HA)_3} + 3H^+$	12.19±0.08	12.33	-"-
Eu(III)-0.10 M HNO_3/HDBP-isopropylether	$Eu^{3+} + 6HA(aq) \rightleftarrows \overline{EuA_3(HA)_3} + 3H^+$	β=0,max.10.44	11.94	-"-
	$Eu^{3+} + 5HA(aq) \rightleftarrows \overline{EuA_3(HA)_2} + 3H^+$	8.83±0.10	-	
Th(IV)-1 M (Na,H)ClO_4/HDBP-$CHCl_3$	$Th^{4+} + ClO_4^- + 5HA(aq) + \rightleftarrows \overline{ThClO_4A_3(HA)_2} + 3H^+$			
Th(IV)-1 M (Na,H)NO_3/HDBP-hexol	$Th^{4+} + 4NO_3^- \rightleftarrows \overline{Th(NO_3)_4}$	-2.03±0.08	-2.0	-"-
	$Th^{4+} + 3NO_3^- + HA(aq) \rightleftarrows \overline{Th(NO_3)_3A} + 3H^+$	2.01,max.2.29	-	
	$Th^{4+} + 2NO_3^- + 2HA(aq) \rightleftarrows \overline{Th(NO_3)_2A_2} + 2H^+$	6.09±0.22	6.6	
	$Th^{4+} + NO_3^- + 4HA(aq) \rightleftarrows \overline{ThNO_3A_3(HA)} + 3H^+$	12.96±0.07	13.4	

[a] Minimizing the error-square sum $U = \sum_{1}^{Np} (\log D_{calc} - \log D_{exp})^2$. The limits given correspond approximately to $\log(\beta \pm 3\sigma(\beta))$ and if $\sigma(\beta) > 0.2$, the maximum value $\log(\beta + 3\sigma(\beta))$ is given.

REFERENCES

1. Sillén, L.G. Acta Chem. Scand. 10 (1962) 159; Ingri, N. and Sillén, L.G. Acta Chem. Scand. 16 (1962) 173; Sillén, L.G. Acta Chem. Scand. 18 (1964) 1085; Ingri, N. and Sillén, L.G. Arkiv Kemi 23 (1964) 97; Sillén, L.G. and Warnqvist, B. Arkiv Kemi 31 (1969) 315; Arkiv Kemi 31 (1969) 341; Arnek, R. Sillén, L.G. and Wahlberg, O. Arkiv Kemi 31 (1969) 353.
2. Brauner, P., Sillén, L.G. and Whiteker, R. Arkiv Kemi 31 (1969)365.
3. Arnek, R. Arkiv Kemi 32 (1970) 81.
4. Warnqvist, B. Chem. Scripta 1 (1971) 49.
5. Warnqvist, B. and Högfeldt, E. Chem. Scripta 7 (1975) 196.
6. Liem, D.H. Acta Chem. Scand. 25 (1971) 1521.
7. Liem, D.H. Acta Chem. Scand. 22 (1968) 753.
8. Liem, D.H. Acta Chem. Scand. 22 (1968) 773.
9. Liem, D.H. Acta Chem. Scand. 26 (1972) 191.
10. Liem, D.H. and Sinegribova, O. Acta Chem. Scand. 25 (1971) 277.
11. Liem, D.H. and Sinegribova, O. Acta Chem. Scand. 25 (1971) 301.
12. Budevsky, O., Ingman, F. and Liem, D.H. Acta Chem. Scand. 27 (1973)1277.
13. Ingman, F. and Liem, D.H. Acta Chem. Scand. A 28 (1974) 947.
14. Aguilar, M. and Liem, D.H. Acta Chem. Scand. A 30 (1976) 313.
15. Jawaid, M., Ingman, F., Liem, D.H. and Wallin, T. Acta Chem. Scand. A 32 (1978) 7.
16. Liem, D.H. and Zangen, M. Proc. Int. Conf. Solvent Extraction Chem. (ISEC 77) 1977, Toronto, Canada.
17. Alegret, S., Aguilar, M. and Liem, D.H. Proc. Int. Conf. Solvent Extraction Chem. (ISEC 77) 1977, Toronto, Canada.
18. Alegret, S. and Liem, D.H. Unpublished.
19. Liem, D.H. and Ekelund, R. Acta Chem. Scand. A 33 (1979) 481.
20. Johansson, P-A, Acta Pharm. Suec. 14 (1977) 345.
21. Dyrssen, D. and Liem, D.H. Acta Chem. Scand. 14 (1960) 1100.
22. Dyrssen, D. and Liem, D.H. Acta Chem. Scand. 18 (1964) 224.
23. Liem, D.H. Inaugural Dissertation, Royal Institute of Technology, Stockholm 1971.

THE KINETICS OF COPPER(II) EXTRACTION FROM SULPHURIC ACID SOLUTIONS BY LIX 64N: A MATHEMATICAL MODELLING APPROACH

C.J. Valdes*, W.C. Cooper*, and D.W. Bacon**

Queen's University
*Department of Metallurgical Engineering
**Department of Chemical Engineering
Kingston, Ontario, CANADA K7L 3N6

ABSTRACT

A statistical modelling study of the kinetics of copper extraction in the system LIX 64N, Escaid 100/copper sulphate, sulphuric acid, has shown that the kinetics are quite complex and can involve both chemical reaction and mass transfer. The rate determining chemical step appears to incorporate dimerised LIX 65N molecules with the possible formation of intermediate copper-extractant complexes.

The confidence intervals for the estimates of the parameters in the rate expression suggest that the fitted model cannot be considered as the only and ultimate representation of the kinetic data. There are indications that a number of competing reactions are occurring and that these reactions are dependent on the relative abundance of the different complex species which are present especially in the organic phase.

INTRODUCTION

No agreement exists among researchers in the field of solvent extraction regarding the kinetics and the mechanism of copper extraction by hydroxyoximes. This is particularly true for the copper(II)-LIX 64N system, which has been the subject of extensive investigation. Thus, despite the widespread application of LIX 64N in commercial operations, controversy in the elucidation of the kinetics and mechanism of the extraction of copper by this extractant continues.

This situation arises for two main reasons. First, difficulties exist in making direct comparison of published experimental data because of the variety of techniques and apparatus used in the measurement of reaction rates. Such techniques include: (1) agitation experiments carried out either by simple shake-out tests or by means of the AKUFVE apparatus[1-4]; (2) mass transfer experiments characterised by a quiescent interface without stirring in the bulk of the phases, such as with the single drop technique [5-7]; and (3) stirred mass transfer cell experiments, involving the use of apparatus such as the Lewis Cell[8-10] which attempt to maintain a known and measurable interfacial area.

Secondly, the systems selected for the study and evaluation of the kinetics of copper extraction have been different for each investigation. Studies of the kinetics of copper extraction by LIX 64N from both acidic sulphate[11-14] and nitrate[15,16] solutions have been reported. In addition, differences can be expected to arise as a result of the choice of diluent,

which has been shown to exert an effect upon the rate of the reaction[17].

The data generated from the application of the aforementioned techniques are often inconclusive, or even contradictory, in elucidating the physical processes or chemical steps which determine the rate of copper extraction. However, each of these techniques offers advantages in the evaluation of specific aspects of the reaction mechanism.

Despite the apparent complexity of the mechanism of copper extraction by hydroxyoximes[18], the existing data on the kinetics of the copper-LIX 64N system indicate that the rate of copper extraction may be limited by: (1) the rate of the chemical reaction, thought to take place either at the aqueous/organic interface[11,12,15], or in an aqueous reaction zone adjacent to the interface[19,20]; (2) mass transfer in the organic phase, possibly involving the diffusion of the copper-LIX 65N complex away from the interfacial zone[16]; and (3) mass transfer with chemical reaction[14]. In a given situation, and depending upon the choice of experimental conditions, any one of these processes may be rate-controlling.

In view of the apparent complexity of the copper(II)-LIX 64N extraction process and the shortcomings of the experimental procedures employed to date especially vis-a-vis the process as carried out in industrial practice, it was considered worthwhile to study the kinetics of extraction using a statistical modelling approach. This approach incorporated an incomplete three-level factorial experimental design and was based on simple shake flask extractions. The results of this study form the basis of the present paper.

EXPERIMENTAL

A stock solution comprising 15% by volume LIX 64N (General Mills Inc., Lot No. 5G19275) in Escaid 100 was prepared and purified by contact with an aqueous phase containing 5 g dm^{-3} copper, followed by stripping with 10% by volume sulphuric acid, and distilled water washing to remove residual acid and any remaining water-soluble impurities[21]. The concentration of active oxime in this purified solution, the anti-isomer of LIX 65N, was determined by Barkley's method[22] which consisted of the potentiometric titration of the solution with 0.1M tetrabutylammonium hydroxide. Typical analyses of 15% by volume LIX 64N gave a concentration of 0.17M LIX 65N anti-isomer.

Reagent-grade copper sulphate was used in the preparation of a stock solution containing 15 g dm^{-3} copper. Its copper concentration was confirmed by atomic absorption spectrophotometry. Reagent-grade sulphuric acid was added to aqueous phase solutions as required. The concentration of reagent-grade sulphuric acid was determined by dilution and titration with standardised sodium hydroxide solution.

Copper extraction rates were derived by contacting equal volumes of aqueous and organic solutions of known compositions at 22°C. Intense mechanical agitation was provided in separatory funnels. The aqueous raffinate from each test was analysed for copper by atomic absorption spectrophotometry. The rate of the reaction was estimated from each analysis.

RESULTS

To explore the full region of operating conditions as efficiently as possible, 27 experiments were carried out using an incomplete three-level factorial design[23]. The results are shown in Table 1.

TABLE 1

RATES OF COPPER EXTRACTION FROM SULPHURIC ACID SOLUTIONS BY LIX 64N IN ESCAID 100 DILUENT

Run No.	x_1 LIX 65N concn. (mole l^{-1})	x_2 Copper concn. (mole l^{-1})	x_3 H_2SO_4 concn. (mole l^{-1})	x_4 Reaction Time (min.)	Calculated Copper Chelate concn. (mole l^{-1})	Calculated Rate of Copper Extraction (mole l^{-1} min^{-1})
1	0.054	0.079	0.102	1.5	0.0069	0.0046
2	0.162	0.079	0.102	1.5	0.0191	0.0127
3	0.054	0.236	0.102	1.5	0.0012	0.0008
4	0.162	0.236	0.102	1.5	0.0327	0.0218
5	0.108	0.158	0.051	0.5	0.0170	0.0339
6	0.108	0.158	0.153	0.5	0.0074	0.0148
7	0.108	0.158	0.051	2.5	0.0340	0.0136
8	0.108	0.158	0.153	2.5	0.0193	0.0077
9	0.108	0.158	0.102	1.5	0.0207	0.0138
10	0.054	0.158	0.102	0.5	0.0017	0.0034
11	0.162	0.158	0.102	0.5	0.0144	0.0288
12	0.054	0.158	0.102	2.5	0.0138	0.0055
13	0.162	0.158	0.102	2.5	0.0378	0.0148
14	0.108	0.079	0.051	1.5	0.0201	0.0134
15	0.108	0.236	0.051	1.5	0.0281	0.0187
16	0.108	0.079	0.153	1.5	0.0075	0.0050
17	0.108	0.236	0.153	1.5	0.0387	0.0258
18	0.108	0.158	0.102	1.5	0.0203	0.0135
19	0.054	0.158	0.051	1.5	0.0155	0.0103
20	0.162	0.158	0.051	1.5	0.0393	0.0262
21	0.054	0.158	0.153	1.5	0.0092	0.0061
22	0.162	0.158	0.153	1.5	0.0234	0.0156
23	0.108	0.079	0.102	0.5	0.0066	0.0132
24	0.108	0.236	0.102	0.5	0.0114	0.0228
25	0.108	0.079	0.102	2.5	0.0190	0.0076
26	0.108	0.236	0.102	2.5	0.0285	0.0114
27	0.108	0.158	0.102	1.5	0.0156	0.0104

The initial model

An initial analysis of the results showed that the following kinetic model could be considered to represent the experimental data.

$$r = \frac{k_1 [\text{LIX 65N}]^{a1} [Cu^{2+}]^{a2}}{[H_2SO_4]^{a3} [CuR_2]^{a4}} + k_2 [CuR_2]^{a5} \qquad (1)$$

where r denotes the reaction rate of the copper extraction and is independent of interfacial area, k_1 and k_2 are reaction rate constants, and the coefficients a_i, i = 1,..., 5, denote the reaction rate dependencies of the reacting species.

This model was not acceptable since valid estimates of the parameters in the model could not be obtained by minimising the function

$$\sum_{i=1}^{n} (r_i - \hat{r}_i)^2 \qquad (2)$$

where r_i denotes the observed reaction rate for experiment i, $\hat{r}_i$ denotes the predicted reaction rate for experiment i using model (1) and n denotes the total number of experiments. The estimation problem using criterion (2) arises because values of the variable $[CuR_2]$, the concentration of copper chelate, must be treated as known when in fact they are measured and have associated random errors. In addition, the variance of the reaction rate r changes as operating conditions change instead of remaining constant as is

assumed for ordinary least squares estimation. Violation of these assumptions can have serious effects on the values and precision of the parameter estimates[24].

Because the measured response variable was in fact $\Delta[Cu^{2+}]$, the change in aqueous copper concentration, rather than r, model (1) was reformulated and fitted to the data by minimizing the function

$$\sum_{i=1}^{n} \{\Delta[Cu^{2+}]_i - \Delta[Cu^{2+}]_i\}^2 \qquad (3)$$

where the notation is analogous to that in expression (2). The revised model form and least squares estimates of its parameters are shown in Table 2. Minimisation of expression (3) was carried out using the method of Hooke and Jeeves[25]. In each iteration of the estimation process, the model was solved for values of $\hat{\Delta}[Cu^{2+}]$ by the method of successive substitution.

TABLE 2

FINAL FORM OF THE KINETIC MODEL

AND LEAST SQUARES ESTIMATES OF ITS PARAMETERS

$$\Delta[Cu^{2+}] = k_1 t \frac{[\text{LIX 65N}]^{a_1} \; [Cu^{2+}]^{a_2}}{[H_2SO_4]^{a_3} \; \Delta[Cu^{2+}]^{a_4}} + k_2 t \, \Delta[Cu^{2+}]^{a_5}$$

where $\Delta[Cu^{2+}]$ = $[CuR_2]$, the copper chelate concentration, mole l^{-1}

$[Cu^{2+}]$ = initial aqueous cupric ion concentration, mole l^{-1}

$[H_2SO_4]$ = initial aqueous sulphuric acid concentration, mole l^{-1}

[LIX 65N] = initial organic oxime concentration, mole l^{-1}

t = reaction time, min.

Parameter Estimates	Approximate Standard Error	95% Confidence Interval
$k_1 = 0.011$	0.016	±0.034
$k_2 = 0.049$	0.049	±0.102
$a_1 = 3.50$	0.66	±1.38
$a_2 = 1.80$	0.43	±0.90
$a_3 = 1.25$	0.14	±0.28
$a_4 = 1.97$	0.08	±0.17
$a_5 = 0.56$	0.38	±0.79

Residual sum of squares = 5.96×10^{-4}

Residual mean square = 2.98×10^{-5}

Standard error = 5.46×10^{-3}

Adequacy of the final model

The individual residuals from the final model were analysed to reveal any non-random tendencies, and also to ensure that the assumptions upon which the least squares estimation is based were not violated.

A plot of each residual against the corresponding predicted change in aqueous copper concentration (Fig.1), provides no evidence to suggest that the variance of the residuals is not constant. A time sequence plot of the

residuals is shown in Fig.2, and provides no indication of any remaining time trends in the data.

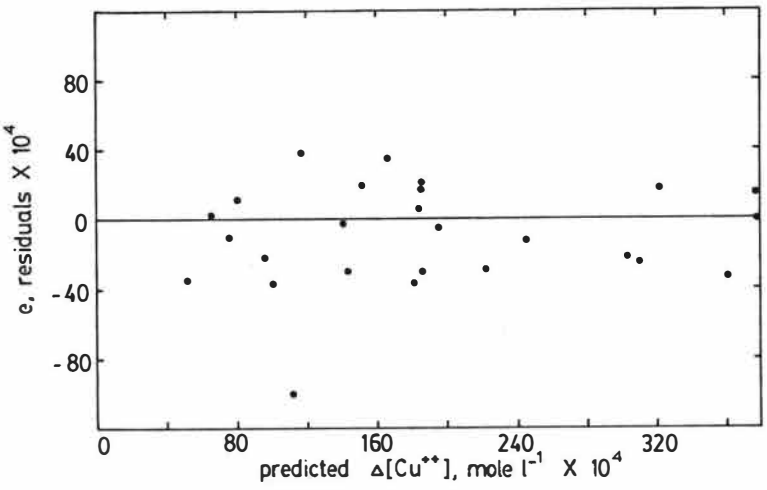

FIG.1

Residuals vs. predicted change in aqueous copper concentration

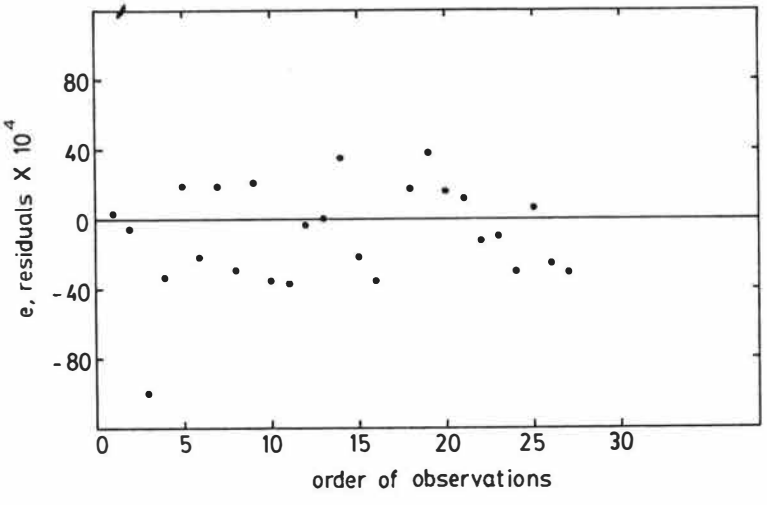

FIG.2

Residuals vs. order of observations

Further analysis of the adequacy of the fitted kinetic model involved a test for "lack of fit"[26], to check whether or not the residuals can be explained on the basis of experimental or "pure" error alone.

The mean square for pure error is the total "within repeats" sum of squares divided by its associated degrees of freedom. The mean square due to lack of fit can be obtained by subtracting the pure error sum of squares from the residual sum of squares and dividing this result by $n_r - n_e$. For the fitted model, the ratio

$$\frac{\text{Mean square due to lack of fit}}{\text{Mean square due to pure error}} = \frac{3.22 \times 10^{-5}}{8.15 \times 10^{-6}} = 3.95$$

can be compared with the statistic F(.95, 18, 2) = 19.40. Since ratio value 3.95 is much smaller than 19.40, there is no apparent lack of fit and thus no reason to doubt the adequacy of the model. The expression

$$\Delta[Cu^{2+}] = 1.05 \times 10^{-2} \frac{t\,[\text{LIX 65N}]^{3.50}\,[Cu^{2+}]^{1.80}}{[H_2SO_4]^{1.25}\,\Delta[Cu^{2+}]^{1.97}} + 4.89 \times 10^{-2}\, t\,[Cu^{2+}]^{0.56} \qquad (4)$$

is therefore considered to be an adequate representation of the measured values of the change in aqueous copper concentration. It fits the experimental data with a standard error of 5.46×10^{-3} mole l^{-1}.

Precision of the parameter estimates

The precision of the least squares parameter estimates of the fitted model can be expressed in terms of both approximate standard errors and approximate 95% confidence intervals for each parameter (Table 2). These values were calculated from an approximate variance-covariance matrix for the parameter estimates. The fact that the confidence intervals for k_1, k_2, and a_5 enclose zero is indicative of the complexity of the reactions which are taking place in the copper(II)-LIX 64N extraction.

An approximate correlation matrix for the parameter estimates is given in Table 3. The results suggest that with the exception of parameters, k_2 and a_5, there is little association between the parameter estimates of model (4).

TABLE 3

CORRELATION MATRIX FOR THE PARAMETER ESTIMATES OF THE FITTED MODEL

	Parameter						
Parameter	k_1	k_2	a_1	a_2	a_3	a_4	a_5
k_1	1.00	-0.61	0.83	0.50	-0.40	-0.42	-0.59
k_2	-0.61	1.00	-0.74	-0.39	-0.11	-0.08	0.98
a_1	0.83	-0.74	1.00	0.14	-0.15	-0.29	-0.73
a_2	0.50	-0.39	0.14	1.00	-0.02	0.11	-0.41
a_3	-0.40	-0.11	-0.15	-0.02	1.00	0.02	-0.13
a_4	-0.42	-0.08	-0.29	0.11	0.02	1.00	-0.07
a_5	-0.59	0.98	-0.73	-0.41	-0.13	-0.07	1.00

DISCUSSION

Complex kinetics, involving both chemical reaction and mass transfer, are indicated by the fitted model (4) for the system LIX 64N, Escaid 100/copper sulphate, sulphuric acid in the range of oxime concentrations investigated (5 to 15% by volume LIX 64N). The reaction rate dependencies

are particularly significant not only in the case of the concentration of the active β-hydroxyoxime in LIX 64N, but also in the case of the extracted complex concentration. It should be noted, however, that the reaction orders appearing in the model are not in themselves indicative of all that is occurring in the extraction process. The 95% confidence intervals for the parameter estimates (Table 2) suggest that the kinetics are such that several competing reactions take place with the nature of these reactions being dependent on the relative population of the various possible solution species, especially in the organic phase.

The observed reaction order with respect to the bulk LIX 65N concentration indicates that polymerised LIX 65N molecules take part in the overall reaction mechanism. In conjunction with the observed reaction order for the bulk aqueous cupric ion concentration, the LIX 65N rate dependence suggests that a possible rate controlling chemical step involves a chemical reaction in which dimerised LIX 65N molecules participate. In addition, this reaction does not appear to be interfacial, in agreement with the fact that expression (4) fits the measured copper extraction rates in the absence of any knowledge of the aqueous/organic interfacial area. Such a reaction probably occurs in a reaction zone on the organic side of the interface. This suggestion is consistent with the approximate 1/2 order dependence observed for the diffusion of the extracted complex from the reaction zone into the bulk organic phase, a process which also appears to play an important role in determining the rate of copper extraction.

The formation of LIX 65N aggregates in various diluents, including Escaid 100, at LIX 64N concentrations similar to those employed in this investigation has been established[20,27,28]. On the other hand, very little has been published to indicate that dimerised or other polymerised copper-LIX 65N complexes are formed (at similar LIX 64N concentrations) during the course of the copper extraction reaction.

Fleming et al.[16] reported the formation of an intermediate copper-LIX 65N-LIX 63 complex in chloroform solutions which contained less than 0.015M LIX 65N and similar concentrations of the oxime LIX 63. Flett et al.[12] had previously interpreted copper extraction rates by dilute LIX 64N solutions in terms of a mechanism which involved the formation of such a complex as the rate determining step. Although copper complexation by LIX 65N molecules in dilute LIX 64N solution might involve formation of intermediate copper-LIX 65N-LIX 63 complexes, and such might also be the case at higher LIX 65N concentrations depending on the diluent, species of this type would not appear to be involved in the rate controlling chemical step in cases where significant LIX 65N aggregation occurs, such as in the system LIX 64N/Escaid 100.

The formation of intermediate copper-LIX 65N complexes, and their involvement in the rate determining chemical reaction, is therefore inferred from the results of this investigation, a conclusion which is consistent with the observed reaction orders.

From the modelling of copper extraction rates alone, and in the absence of other data, it is not completely clear how dimerised or other polymerised copper-LIX 65N complexes might form during the process of copper complexation. At present it can only be suggested that such complexes probably result under the following conditions: (1) when a significant aggregation of nonchelated LIX 65N occurs, and (2) in the presence of an excess concentration of cupric ions in the aqueous phase relative to the organic LIX 65N

concentration.

Formation of the species CuR^+ would appear to be the initial step in copper complexation and such a step probably involves a fast chemical reaction between cupric ions and LIX 65N monomers, as is generally accepted. The site of this initial reaction might be either the aqueous/organic interface[11,12,15] or an aqueous reaction zone adjacent to the interface[19,20]. Further reaction of CuR^+ complexes with LIX 65N monomers probably occurs but to a limited extent, as such a reaction is undoubtedly affected by the presence of polymerised LIX 65N molecules at or near the interface, and by the reduced availability of LIX 65N monomers which themselves react rapidly with the excess cupric ions. The reaction of LIX 65N aggregates with CuR^+ species appears possible under such conditions, leading to the formation of intermediate polymerised copper-LIX 65N complexes. It should be noted that CuR^+ and other copper-LIX 65N complexes are not likely to be soluble in aqueous solution. Therefore any reactions involving such complexes probably occur in the organic phase and not at the aqueous/organic interface.

CONCLUSIONS

This statistical modelling study of the extraction of copper in the system LIX 64N, Escaid 100/copper sulphate, sulphuric acid has underlined the complexity of the extraction kinetics. The fitted kinetic model suggests that the kinetics can involve both chemical reaction and mass transfer, with the rate determining chemical step incorporating dimerised LIX 65N molecules and the possible formation of intermediate copper-extractant complexes. This reaction quite likely occurs in the organic phase and not at the aqueous/organic interface.

The confidence intervals for the parameter estimates suggest that the fitted model is not the only and ultimate representation of the extraction rate data. There are indications that a number of competing reactions are taking place with these reactions being dependent on the relative abundance of the different complex species which are to be found especially in the organic phase.

REFERENCES

1. Rydberg, J., Acta Chem. Scand., 23, 647 (1969).

2. Anderson, C., S.O. Anderson, J.O. Liljenzin, H. Reinhardt and J. Rydberg, Acta Chem. Scand., 23, 2781 (1969).

3. Johansson, H. and J. Rydberg, Acta Chem. Scand., 23, 2797 (1969).

4. Reinhardt, H. and J. Rydberg, Chem. Ind., 50, 488 (1970).

5. Baumgartner, F. and L. Finsterwalder, J. Phys. Chem., 74, 108 (1970).

6. Farbu, L., H.A.C. McKay and A.G. Wain, Proc. Intl. Solvent Extraction Conf., Lyon, 1974; pub. Soc. Chem. Ind., London, 2427 (1974).

7. Whewell, R.J., M.A. Hughes and C. Hanson, J. Inorg. Nucl. Chem., 37, 2303 (1975).

8. Lewis, J.B., Chem. Eng. Sci., 3, 248 (1954).

9. Lewis, J.B., Chem. Eng. Sci., 3, 262 (1954).

10. Lewis, J.B., Chem. Eng. Sci., 8, 295 (1958).

11. Spink, D.R. and D.N. Okuhara, "International Symposium on Hydrometallurgy", Ed. D.J.I. Evans and R.S. Shoemaker, AIME, New York, N.Y., 497 (1973).

12. Flett, D.S., D.N. Okuhara and D.R. Spink, J. Inorg. Nucl. Chem., 35, 2471 (1973).

13. Whewell, R.J., M.A. Hughes and C. Hanson, J. Inorg. Nucl. Chem., 38, 2071 (1976).

14. Hughes, M.A., J.S. Preston and R.J. Whewell, J. Inorg. Nucl. Chem., 38, 2067 (1976).

15. Atwood, R.L., D.N. Thatcher and J.D. Miller, Met. Trans., 6B, 465 (1975).

16. Fleming, C.A., M.J. Nicol, R.D. Hancock and N.P. Finkelstein, Proc. Intl. Solvent Extraction Conf., Toronto, 1977; pub. Cdn. Inst. Min. Met. (CIM SV-21), Montreal, 193 (1979).

17. Murray, K.J. and C.J. Bourboulis, Eng. Min. Journal, 174 (7), 74 (1973).

18. Rice, N.M. and M. Nedved, Hydrometallurgy, 2, 361 (1976/77).

19. Hanson, C., M.A. Hughes and J.G. Marsland, Proc. Intl. Solvent Extraction Conf., Lyon, 1974; pub. Soc. Chem. Ind., London, 2401 (1974).

20. Whewell, R.J., M.A. Hughes and C. Hanson, Proc. Intl. Solvent Extraction Conf., Toronto, 1977; pub. Cdn. Inst. Min. Met. (CIM SV-21), Montreal, 185 (1979).

21. Ritcey, G.M. and B.H. Lucas, CIM Bull., 67, 87 (Feb. 1974).

22. Barkley, D.J., Paper presented at 14th Annual Conf. of Metallurgists, Aug. 24-27, 1975, Edmonton, Canada.

23. Box, G.E.P. and D.W. Behnken, Technometrics, 2, 455 (1960).

24. Boag, I.F., D.W. Bacon and J. Downie, Can. J. Chem. Eng., 54, 107 (1976).

25. Hooke, R. and T.A. Jeeves, J. Assoc. Computer Machines, 8, 272 (1961).

26. Draper, N.R. and H. Smith, "Applied Regression Analysis", John Wiley & Sons, Inc., New York, 1966.

27. Whewell, R.J. and M.A. Hughes, Hydrometallurgy, 4, 109 (1979).

28. Whewell, R.J., M.A. Hughes and P.D. Middlebrook, Hydrometallurgy, 4, 125 (1979).

COMPARING SCALE-UP METHODS FOR SOLVENT EXTRACTION MIXERS

John Roberts
Department of Chemical Engineering
University of Newcastle
New South Wales, 2308
Australia.

Operating data from large industrial mixers are now becoming available which indicate that lower stage efficiencies are probable when scale-up is based solely on constant tip speed. Conversely, much higher stage efficiencies are possible if scale-up is based on power per unit volume or $n^3D_i^2$. Recent work concluded that (i) tip speed for a required stage efficiency be determined in a laboratory mixer; (ii) relative impeller/tank size for this mixer be optimised at this tip speed to minimise entrainment losses; and (iii) scale up to commercial size mixer using geometric similarity on the basis of equal $n^3D_i^2$.

Only Treybal seems to have considered the overall problem of optimising process variables and scale-up geometry in obtaining a minimum cost design. Most recent references explore the effect of tip speed and power input on mass transfer coefficient (k.a), specific surface area (a), and stage efficiency (η), for a number of impeller/tank ratios, usually for batch systems in one size of mixer. However, in terms of mass transfer rate (N), or value of metal recovered per unit time, no one has considered the ultimate objective of maximising these quantities. Here $N = k.a.\ \Delta c.\eta$ where Δc = concentration difference between extract and raffinate. Thus while (k.a.) might decrease with increase in mixer size, stage efficiency (η) may increase, resulting in a maximum mass transfer rate (N) at some intermediate vessel size.

In summary, computer calculations carried out involved exploring the effect of impeller tip speed, $n^3D_i^2$, change in equilibrium distribution coefficient and droplet coalescence on the parameters noted.

Implications of Findings

If scale-up from small laboratory units ($D_T \sim 10$ cm) to large commercial units (D_T 2 to 5 m) is based solely on constant tip speed, then (i) $n^3D_i^2$ may be too low in the full scale unit; (ii) stage efficiency could be significantly lower, depending on droplet coalescence properties within the mixer; and (iii) mass transfer rate could be 2 to 7 times smaller in the commercial unit.

However, for scale-up based on similar $n^3D_i^2$ then (i) stage efficiency will be marginally improved and (ii) mass transfer rate could be similar to or up to 5 times more than that of the small pilot unit, again depending on droplet coalescence phenomena in the mixer.

To obtain best mass transfer rate in the full scale mixer, non-coalescent droplets are required. This can be partially achieved by improved mixing, or circulation by adding another impeller at about mid depth and/or altering the interfacial tension by modifying the liquid properties to promote more stable droplets in the mixer.

MODEL OF DISPERSION BAND IN A CENTRIFUGAL CONTACTOR

R. A. Leonard, G. J. Bernstein,

R. H. Pelto and A. A. Ziegler

Argonne National Laboratory
9700 South Cass Avenue
Argonne, Illinois 60439 USA

A model of the dispersion band in a centrifugal contactor used in solvent extraction has been developed to enable prediction of separating capacity. The model applies specifically to contactors in which the separating rotor rotates about its vertical axis. Separated light (organic) phase is discharged over an inner circular weir, and separated heavy (aqueous) phase flows through underflow passages near the periphery of the rotor and over its weir. The dispersion band is located between the organic weir and the aqueous underflow and may be positioned by applying air pressure to the aqueous weir (1). Maximum separating capacity is reached when the dispersion band extends from organic weir to aqueous underflow.

In the model of the dispersion band, a hydraulic force balance is used to find the theoretical interface between completely coalesced phases. This is combined with the volume of the dispersion band to find the actual boundaries of the dispersion band. A new dimensionless dispersion number (2) related to the overall operation of the contactor is used to determine the volume of the dispersion band. This model was tested, with good agreement between predicted and experimental results, using 20-mm diameter and 94-mm diameter centrifugal contactors which have annular mixing zones (3).

REFERENCES

(1) D. S. Webster, A. S. Jennings, A. A. Kishbaugh, and H. K. Bethmann, "Performance of Centrifugal Mixer-Settler in the Reprocessing of Nuclear Fuel," CEP Symposium Series, Nuclear Engineering--Part XX, No. 94, Vol. 65, 70-77 (1969).

(2) R. A. Leonard, G. J. Bernstein, R. M. Pelto, and A. A. Ziegler, "Liquid-Liquid Dispersion in Turbulent Couette Flow," 72nd Annual A.I.Ch.E. Meeting, San Francisco, California, November 25-29, 1979.

(3) G. J. Bernstein, D. E. Grosvenor, J. F. Lenc, and N. M. Levitz, Nuclear Technology, 20, 200-202 (1973).

EXPERIMENTAL AND THEORETICAL INVESTIGATION OF FILM FLOW ON A TILTED PLATE AS THE BASIS OF A SETTLER DESIGN

Prof. Dr.-Ing. E. Blaß
Dipl.-Ing. D. Rautenberg

Lehrstuhl A für Verfahrenstechnik,
TU München

D-8000 München 2,
Bundesrepublik Deutschland

The design of mixer-settlers is with regard to the settler still very uncertain. Existing calculations are unsatisfactory because the coalescence is essentially influenced by surface active agents at the interface, which cannot be involved in the mathematical models. Therefore we aspire to avoid the influence of the surfactants by offering the drops really clean interface for coalescence. We generate this interface with the help of tilted plates on which the disperse phase coalesces, so that there arises a permanent film flow of original disperse phase.

Thereby the phase boundary is permanently renewed. An important viewpoint therefore is the film flow on a tilted plate. From the equilibrium of shear- and buoyancy forces we derived the one dimensional differential equation of motion of a laminar film. At the film phase boundary we take into account the momentum transport to the second liquid phase. For the velocity profile w(y) we obtained:

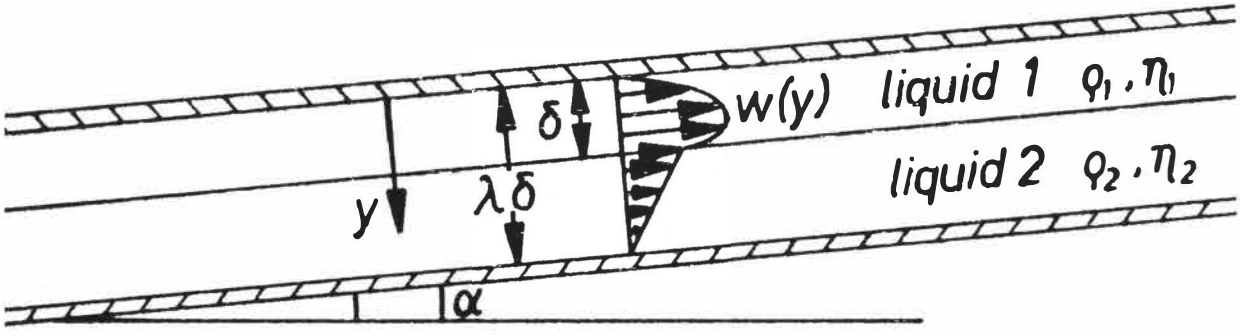

$$w(y) = \frac{\Delta\rho \cdot g \cdot \sin\alpha}{2\eta_1} \left(y \cdot \delta \cdot \frac{2\eta_1 \cdot (\lambda-1) + \eta_2}{\eta_1 \cdot (\lambda-1) + \eta_2} - y^2 \right)$$

We can now calculate the mean velocity, the film thickness and the specific throughput of a tilted plate, which is needed for the design of a settler at steady state operation. Experimental measurements of the film thickness showed good agreement with the theoretical values.

If the film is created by coalescing drops we get an upper limit for the angle of inclination. The drops roll down the plate and cannot wet it. The examination of the coalescence mechanism on tilted plates is the matter of separate experiments, they will be presented later.

THE DISPERSION MODEL : CONCENTRATION PROFILES IN AND DESIGN OF ROTATING DISC CONTACTORS

Dipl.Ing. Bernd WOLSCHNER
Prof.Dr.Ing. Rolf MARR
Institut für Grundlagen der
Verfahrenstechnik, TU Graz
Kopernikusg. 24, A-8o1o Graz
Austria

When comparing laboratory columns with industrial columns, it was seen throughout that columns with a larger diameter need a much greater column height for the same selectivity.

This phenomenon refers to axial mixing effects in the continous as well as in the dispersed phase; its influence on mass transfer can be registered with the so called dispersion model. For both phases a convective flow, a dispersion flow and a source respectivly a sink are put into the continiuty equations. The numerical solution, and with it the concentration profils and the height of the column can be arrived at with the help of the difference-method, the Jacobimatrix and the Thomas procedure.

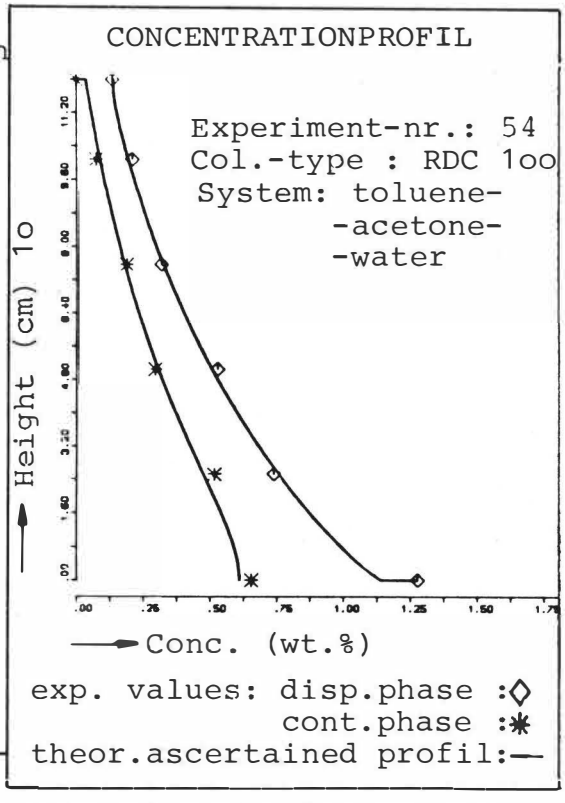

To prove the accuracy of the concentration profiles theoretically ascertained in this way, mass transfer experiments were carried out on a 5o mm RDC column (rotating disc contactor) and a 1oo mm geometrically similar RDC column. The parameters used for the calculation are obtained by means of the drop size distribution and the residence time distribution [1]. The experimental registration of the concentration profiles were carried out with a newly developed sample taking system, with which the dispersed and the continous phase were taken directly, separatly and at constant flow from the column [2]. The concentration profiles got from these experiments corresponded well with the theoretically ascertained concentration profiles(FIG.). Hence it follows that, after getting the single parameters from a laboratory column or from existing correlations, avoiding the use of experiments on pilot plants, exact scaling up of extraction columns with the help of the dispersion model is possible.

REFERENCES:

[1] Wolschner,B. : Dissertation, TU Graz (in preparation)
[2] Wolschner,B;Sommeregger,E.;Marr,R. : VDI-GVC Jahrestreffen Nürnberg,26.-28.9.1979

BATCH AND CONTINUOUS PILOT PLANT STUDIES, LEADING TO FULL-SCALE MIXER DESIGN FOR CONTINUOUS COUNTERCURRENT EXTRACTION.

Dr. James Y. Oldshue
Vice President, Mixing Technology
Mixing Equipment Company
Div. of General Signal

Rochester, New York, USA

Data were obtained on a 150 mm diameter single mixing stage,operated both batch and continuous, and in a 600 mm diameter mixing stage, operated batchwise. Two different impeller types were used, both radial flow, to see whether any marked differences in extraction rate could be observed in single-stage

By studying a process batchwise in the laboratory and pilot plant, it is possible to study many more mixing and extraction variables. However, it is important to be able to relate the effect of these variables to the effect they will have on a continuous process.

By looking at the mass transfer coefficient, it is possible to relate mixing variables to the overall process.

In dealing with a liquid-liquid equilibrium process without reaction, batch tests and continuous tests are compared. Data were taken on a liquid-liquid system which included a chemical reaction, and the relationship is more involved.

Methods of evaluating batch and continuous pilot plant experiments are discussed in terms of both full-scale mixer settler operation as well as full-scale continuous countercurrent, multistage mixing columns.

MODELLING OF BREAKAGE AND COALESCENCE IN A MIXING TANK

H.Sovová and J.Procházka
Institute of Chemical Process
Fundamentals
Czechoslovak Academy of Sciences
Prague, Czechoslovakia

Power functions of drop volumes are proposed as a mathematical model of breakage and coalescence frequencies in a stirred dispersion. The ability of this model to describe the behaviour of real systems is demonstrated by comparing the calculated drop size distributions in a batch mixing tank with those obtained experimentally[1].

According to the model the breakage frequency is given by

$$g(v) \sim v^a, \qquad a\varepsilon \langle 0;2\rangle, \qquad (1)$$

the coalescence frequency by

$$\omega(v,v') \sim (v+v')^b, \qquad b\varepsilon\langle -1;1\rangle \qquad (2)$$

or

$$\omega(v,v') \sim (v.v')^{b/2}, \qquad b\varepsilon\langle -2;2\rangle. \qquad (3)$$

By each breakage event the droplet of volume v formes two new droplets the volumes of which are: i) equal (distribution function β_1); ii) normally distributed (β_2); iii) homogeneously distributed with the range $\langle 0;v\rangle$ (β_3).

Variance σ^2 of the dimensionless volume distribution $A_v(d/d_{32})$ corresponding to the model can be approximated as a function of e = a-b and β (Fig.1), whereas the first moment is almost constant. Fig.2 compares curves calculated for σ = 0.23 with the experimental distribution[1].

FIG.1
Correlation σ vs. e=a-b

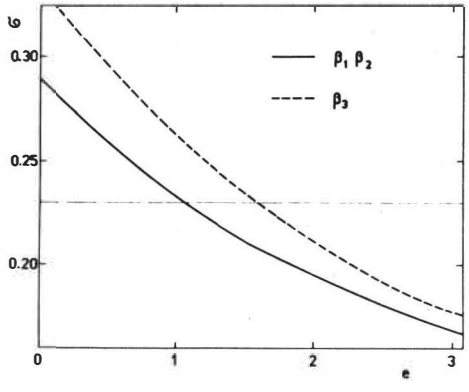

FIG.2
Comparison with experimental distribution

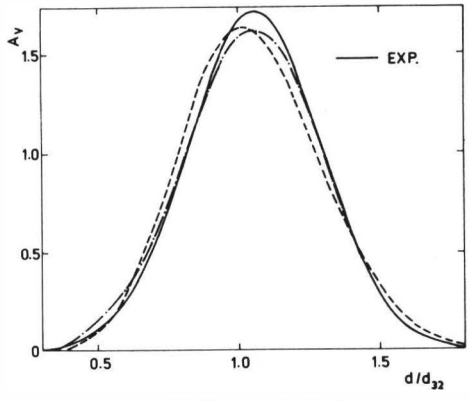

REFERENCE

1. Chen H.T. and Middleman S., A.I.Ch.E.J. 13, 989 (1967).

DYNAMIC BEHAVIOUR OF MIXER-SETTLERS

APPLICABILITY OF THE ORTHOGONAL COLLOCATION METHOD

G. Aly

Dept of Chemical Engineering
Box 740
S-220 07 Lund, Sweden

Difficulties in obtaining accurate dynamic response measurements which are not encountered in steady state analyses have held back experimental work in the field of extraction dynamics. Burns and Hanson in experimental studies of the dynamic response of a 5-stage mixer-settler unit applied the tedious "stop-start" procedure in order to overcome the volumetric transient caused by the removal of samples. They were able to achieve only discrete measurements of the aqueous phase concentration. The applicability and suitability of the AKUFVE measuring technique, based on the use of radioactive tracers, was tested by Aly et. al. This experimental technique enabled the collection of large amount of response data describing the dynamic behaviour of a 4-stage mixer-settler unit. Step and PRBS input signals were applied in the four control variables, i.e. the inlet concentrations and flow rates.

Aly developed and tested some relatively simple linearized models and a large amount of experimental evidence was presented which shows that models of this type adequately simulate the dynamic behaviour of mixer-settler units. These models did not involve any specific hydrodynamic lags or settler flow patterns.

When the complexity of the mathematical model increases, it becomes increasingly important to apply efficient numerical techniques. The orthogonal collocation method has been applied to solve certain problems in chemical reaction engineering, where it proved to be very efficient. One of the main objectives in this work is to illustrate where advantages might be obtained by usage of this method to solve more sophisticated models describing the dynamic behaviour of mixer-settlers. The Runge-Kutta method with variable step length was also used for comparison. The Ingham model with allowance for entrainment backmixing of the two phases, non-linear equilibrium, and mixing in the settler compartments was used. It was however modified to accomodate for hydrodynamic lags.

An "exact" solution was generated using 3 collocation points and was used to compare the response of the other methods. The simulation results show that Runge-Kutta method consumes less CPU-time while numerical stability of the orthogonal collocation method is superior.

Using the Ingham model together with experimental data, it was possible to identify some unknown process variables such as backmixing coefficients and settler flow pattern parameters.

Fundamentals and chemistry of solvent extraction
Session 6

Co-chairmen : A.S. van der Zeeuw (Shell Lab., Amsterdam, The Netherlands)
G. Duyckaerts (University of Liège, Belgium)

6A

80-9 Chemically based synergic solvent extraction model for the system Nd $(NO_3)_3$-HDEPH-TBP-benzene.
Ying-Chu Hoh, Maw-Chwain Lee and R. Bautista, Institute of Nuclear Energy Research, Lung-Tan, Taiwan (China), Ames Laboratory and Iowa State University, Ames, U.S.A.

80-51 Extraction of UO_2^{2+} and other metalyl (+2) ions with ß-diketones.
R. Lundqvist, Chalmers University of Technology, Göteborg, Sweden.

80-6 Crown ethers as size-selective synergists in solvent extraction systems.
W.J. Mc Dowell, W.F. Kinard and R.R. Shoun, Oak Ridge National Laboratory, Tennessee, U.S.A.

80-48 Solvent extraction of trivalent lanthanides by dibutyl phenacylphosphonate.
J. Alstad, B. Ceccaroli, J.P. Brunette and M.J.F. Leroy, University of Oslo, Norway and Ecole Nationale Supérieure de Chimie, Strasbourg, France.

80-147 Solvent extraction of lanthanides by 2-ethylhexylphosphonic acid mono-2-ethylhexyl ester.
Ma Enxim, Yan Xiaamin, Wang Sanyi, Wang Guoliang and Yuan Chengye, Shangai Institute of Organic Chemistry, Academia Sinica, China.

80-185 The extraction of lanthanoides and americium by benzyldialkylamines and benzyltrialkylammonium nitrates from the nitrate solutions, structure and aggregation of their salts.
V. Jedinakova, J. Zilkova, Z. Dvorak and M. Hanova, Institute of Chemical Technology, Prague, Czechoslovakia.

80-236 Comparative studies on the metal extraction with different chelating extractants.
P. Mühl and K. Gloe. Zentralinstitut für Festkörperphysik und Werkstofforschung der Akademie der Wissenschaften der DDR, Dresden, German Democratic Republic

6B

80-206 Quarantum-chemical description of proton affinity of molecules of nitrogen bases.
Yu. A. Panteleev and A.A. Lipovskii, V.G. Khlopin Radium Institute, Leningrad, U.S.S.R.

80-203 NMR ^{31}P ans IR investigation of interactions between UO_2 $(D2EHP)_2$, TBP and UO_2SO_4 in benzene.
E.S. Stoyanov, V.A. Mikhailov, V.G. Torgov and T.V. Us, Siberian Branch of the Acad. of Sc., Novosibirsk, U.S.S.R.

80-15 Chemistry of extraction of copper, cobalt and nickel with substituted 8-sulphonamidoquinolines.
M. Cox and W. van Bronswijk, The Hatfield Polytechnic, Hertfordshire, U.K. and Western Australia Institute of Technology, London, Australia.

80-53 Characterization of the complexes of Ni (II) with LIX63 oxime.
K. Osseo-Asare and M.E. Keeney, Pennsylvania State University, University Park, Pennsylvania, U.S.A.

80-204 Linear correlations of free energies as a tool for comparating information on extraction equilibra. V. S. Shmidt, G. A. Mezhov and K. A. Rybazov, USSR, Atomic Commitee, Moscow, USSR.

CHEMICALLY BASED SYNERGIC SOLVENT EXTRACTION MODEL FOR THE SYSTEM $Nd(NO_3)_3$-HDEHP-TBP-BENZENE

Ying-Chu Hoh and Maw-Chwain Lee*
Institute of Nuclear Energy Research,
Lung-Tan, Taiwan, China and

Renato G. Bautista
Ames Laboratory** and Department of Chemical
Engineering, Iowa State University,
Ames, IA 50011, U.S.A.

ABSTRACT

A chemically based synergic solvent extraction model has been developed for the system $Nd(NO_3)_3$-HDEHP-TBP-Benzene. The model equation for the distribution ratio can be written as $D_c = K_1\alpha_o((HG)_2)_{org}^3(TBP)_{org}^3(H^+)_w^{-3}$, where K_1 is the effective equilibrium constant containing the quotient of the activity coefficients of the reacting species and α_o is the degree of formation of the neodymium complex in the equilibrated aqueous phase. $((HG)_2)_o$, $(TBP)_o$, and $(H^+)_w$ denote the equilibrated HDEHP, TBP, and aqueous hydrogen ion concentrations, respectively. Experimental equilibrium distribution data generated in this work were used to test the model equation. Correlation coefficients between the experimental data and the predicted values are in the range of 0.899 to 0.983.

INTRODUCTION

The separation of rare earths by solvent extraction system using di-2-ethylhexyl phosphoric acid as the organic complexing agent gives very small separation factors which in effect requires more stages to produce the individual rare earth of the highest purity. In order to improve the efficiency of the solvent extraction process, the chemistry of the separation of the rare earths must be modified to increase their distribution ratios and separation factors. In this work, the extraction of neodymium is enhanced by using a complexing mixture of an acid chelate di-2-ethylhexyl phosphoric acid (HDEHP) and a neutral ligand tri-n-butyl phosphate (TBP) in the presence of an inert diluent benzene.

The enhancement of the solvent extraction of metals by the use of a second metal organic complexing reagent has been reviewed in the literature.(1) Hoh and Wang(2) recently extended the chemically based models to predict the distribution ratios and separation factors previously reported by

*Visiting Scientist at the Ames Laboratory, 1978.

**Operated for the U.S. Department of Energy by Iowa State University under contract No. W-7405-Eng-82. This research was supported in part by the Assistant Secretary for Energy Research, Office of Basic Energy Sciences, WPAS-KC-03-02.

Bautista and coworkers(3-8) to a synergic solvent extraction system using the experimental data reported by Hayden, Gerow, and Davis.(9) In this paper is reported the successful application of the synergic model equation to the system $Nd(NO_3)_3$-HDEHP-TBP-Benzene system.

MODEL DEVELOPMENT AND APPLICATION

The synergic effect in mixtures of neutral organic compounds with acids is frequently explained by the formation of mixed complexes according to an addition mechanism.(1,10)

$$M_w^{n+} + n\ HG_{org} + q\ S_{org} \rightleftharpoons MG_n\ q\ S_{org} + n\ H_w^+ \qquad (1)$$

where M^{n+} denotes a metal ion with a charge of +n, HG and S represent an acid and a neutral organic ligand respectively, q is the neutral ligand stoichiometric coefficient and the subscripts w and org denote the aqueous and organic phases respectively. The kinetics of the extraction of uranium (VI) by a synergic mixture of di-2-ethylhexyl phosphoric acid (HDEHP) and tri-n-butyl phosphate (TBP) has been reported by Formin, et al.(11). The interaction of TBP with HDEHP was assumed to proceed according to the reaction

$$(HG)_{2\ org} + TBP_{org} \rightleftharpoons (HG)_2 \cdot TBP_{org} \qquad (2)$$

where $(HG)_2$ represents the HDEHP dimer. On the basis of Equations 1 and 2, the extraction of neodymium by a synergic mixture of HDEHP and TBP can be assumed to be represented by the reaction

$$Nd_w^{3+} + 3\ (HG)_{2\ org} + 3\ TBP_{org} \rightleftharpoons Nd(HG_2)_3 \cdot 3\ TBP_{org} + 3\ H_w^+ \qquad (3)$$

A synergic solvent extraction equilibrium model for the distribution ratio, D_c, was developed following the same modeling procedure previously described by Bautista and coworkers(3-8) and by Hoh and Wang(2). The model equation is given by

$$D_c = K_1\ \alpha_0\ ((HG)_2)_{org}^3 (TBP)^3\ (H^+)_w^{-3} \qquad (4)$$

where the parentheses represent the concentration for each species and α_0 is the degree of formation. The degree of formation is defined by the equation

$$\alpha_0 = \frac{1}{1 + \sum_i \beta_i (A)^i} \qquad (5)$$

where β_i is the stability constant for the ith species and A is the ligand. K_1 is defined as the effective equilibrium constant given by the equation

$$K_1 = \frac{K_{ex}}{K_\gamma} \qquad (6)$$

where $\underline{K_{ex}}$ is the extraction equilibrium constant and K_γ is the quotient of the activity coefficients. It is assumed that K_γ varies slightly with concentration and therefore has an approximately constant value.

The equilibrium solvent extraction data on the system $Nd(NO_3)_3$-HDEHP-TBP-Benzene are given in Table 1. Based on the extraction mechanism given by Equations (1) and (3), Goto(12) and Lenz and Smutz(13) calculated the equilibrated hydrogen ion concentrations on the $RE(NO_3)_3$-HDEHP-Amsco systems from the equation

$$(H^+)^E = (H^+)^i + 3\ (RE)_o \tag{7}$$

where RE represents the rare earths and the superscripts E and I denote equilibrium and initial concentrations respectively. The equilibrated hydrogen ion concentration in this work was estimated from Equation (7).

O'Brien and Bautista(14) correlated the relationship between the equilibrated aqueous $(Nd^{+3})_w$ and $(NO_3^-)_w$ by using a nitrate ion-selective electrode to measure the aqueous nitrate ion concentration. The equation describing the relationship is given by Equation (8)

$$\ln (NO_3^-)_w = -2.54 + 4.41\ (Nd^{+3})_w - 3.05\ (Nd^{+3})_w^2 + 0.77\ (Nd^{+3})_w^3 \tag{8}$$

where the subscript w represents the aqueous phase. Equation 8 was used to calculate the equilibrated aqueous nitrate ion concentration, $(NO_3^-)_w$, in this work. The equilibrium nitrate ion data are also given in Table 1.

The stability constants for this system have been correlated by O'Brien and Bautsita(14) using Krumholtz's(15) data. These are given in Equations (9) and (10)

$$\ln \beta_1 = 0.6347 - 0.6128\ I + 0.0804\ I^2 - 0.0033\ I^3 \tag{9}$$

$$R^2 = 0.955$$

$$\ln \beta_2 = -0.7568 - 0.0421\ I + 0.0233\ I^2 - 0.00025\ I^3 \tag{10}$$

$$R^2 = 0.790$$

where β_1 and β_2 denote the stability constants for the species $Nd(NO_3)^{+2}$ and $Nd(NO_3)_2^{+1}$ respectively and I represents the ionic strength. The stability constant for the neutral species $Nd(NO_3)_3$ was considered to be negligible since this species is assumed to be present only at lanthanide nitrate concentrations approaching the solubility limit. This assumption is based on the outer sphere nature of the lanthanide nitrate complexes(16) which in effect reduces the ionic bond strength of the complex. Equations 9, 10 and 5 were used to calculate β_1, β_2 and α_o, respectively. In Table 2 are given the results.

The effective equilibrium constant K_1 was then calculated by using Equation 4 along with the equilibrium data in Table 1 and the calculated values of α_o in Table 2. Linear regression analysis was applied to obtain the regressed values of K_1 at different conditions. The experimental values of the equilibrated HDEHP and TBP concentrations were assumed to have changed very little during the extraction. This is further substantiated by the experimental neodymium concentration in the organic phase after equilibration which were for the most part constant at around 10^{-3} M.

Table 1. Equilibrium Solvent Extraction Data for the $Nd(NO_3)_3$-HDEHP-TBP-BENZENE System

Initial Conditions					Equilibrium Conditions				
Aqueous Phase			Organic Phase		Aqueous Phase			Organic Phase	
pH	Nd M	I* M	HDEHP M	TBP M	(H^+)** M	Nd M	(NO_3^-)*** M	Nd M	D_c
0.46	0.0607	0.364	0.222	0.0	0.3469	0.0604	0.09	0.0003	0.0045
0.46	0.1143	0.68	0.222	0.0	0.3496	0.1131	0.135	0.0012	0.0106
0.46	0.1950	1.17	0.222	0.0	0.3502	0.1936	0.18	0.0014	0.0074
0.46	0.2799	1.68	0.222	0.0	0.351	0.2783	0.23	0.0016	0.0057
0.46	0.0607	0.364	0.222	0.108	0.3475	0.0602	0.09	0.0005	0.0076
0.46	0.1143	0.68	0.222	0.108	0.3499	0.1130	0.135	0.0013	0.0115
0.46	0.1950	1.17	0.222	0.108	0.3510	0.1934	0.18	0.0016	0.0083
0.46	0.2799	1.68	0.222	0.108	0.3559	0.2765	0.23	0.0033	0.0120
0.46	0.0607	0.764	0.222	0.324	0.3502	0.0593	0.09	0.0014	0.0236
0.46	0.1143	0.68	0.222	0.324	0.3505	0.1128	0.135	0.0015	0.0133
0.46	0.1950	1.17	0.222	0.324	0.3556	0.1918	0.18	0.0032	0.0167
0.46	0.2799	1.68	0.222	0.324	0.3628	0.2743	0.23	0.0056	0.0204
1.0	0.0639	0.383	0.222	0.0	0.112	0.0599	0.09	0.0040	0.0668
1.0	0.1143	0.68	0.222	0.0	0.116	0.1088	0.13	0.0055	0.0506
1.0	0.2057	1.234	0.222	0.0	0.124	0.1977	0.18	0.0080	0.0405
1.0	0.2914	1.748	0.222	0.0	0.1333	0.2803	0.235	0.0111	0.0396
1.0	0.0639	0.383	0.222	0.108	0.113	0.0595	0.09	0.0044	0.0739
1.0	0.1143	0.68	0.222	0.108	0.117	0.1086	0.13	0.0057	0.0525
1.0	0.2057	1.234	0.222	0.108	0.1324	0.1948	0.18	0.0108	0.0554
1.0	0.2914	1.748	0.222	0.108	0.1441	0.2767	0.23	0.0147	0.0531
1.0	0.0639	0.383	0.222	0.324	0.114	0.0592	0.09	0.0047	0.0794
1.0	0.1143	0.68	0.222	0.324	0.1201	0.1076	0.13	0.0067	0.0623
1.0	0.2057	1.234	0.222	0.324	0.1381	0.1930	0.18	0.0127	0.0653
1.0	0.2914	1.748	0.222	0.324	0.1534	0.2736	0.23	0.0178	0.0651

* I : ionic strength

** Calculated by Equation 7

*** Calculated by Equation 8

The predicted equilibrium distribution ratio were calculated by using the corresponding values of K_1 and the equilibrium extraction data. Table 3 presents the regressed values of the effective equilibrium constant, K_1, the calculated distribution ratios, D_c (model), and the experimentally determined distribution ratios. The correlation coefficients, R^2, defined as

$$R^2 = \frac{\text{total sum of square due to regression}}{\text{total (corrected) sum of square}} \qquad (11)$$

between the calculated and experimental distribution ratios are also given

in Table 3. The results calculated from the model equation are in reasonably good agreement with the experimentally determined distribution ratio. These results are also shown in Fig. 1.

Table 2. The Calculated Stability Constants and Degrees of Formation for the System $Nd(NO_3)_3$-HDEHP-TBP-Benzene

I	$(NO_3^-)_w$	β_1	β_2	α_o
M	M			
0.364	0.09	1.52	0.46	0.8767
0.68	0.135	1.289	0.461	0.8457
1.17	0.18	1.027	0.461	0.8330
1.68	0.23	0.844	0.466	0.820
0.383	0.09	1.470	0.46	0.8803
0.68	0.13	1.289	0.461	0.8508
1.234	0.18	0.999	0.461	0.8369
1.748	0.235	0.824	0.467	0.8200

Table 3. Comparison of the Model and Experimental Distribution Ratios and the Calculated Effective Equilibrium Constants for the System $Nd(NO_3)_3$-HDEHP-TBP-Benzene

D_c	K_1	K_1	D_c	R^2
(Data)		(Regressed)	(Model)	
0.0045	0.00243		0.0074	
0.0106	0.00593		0.0072	
0.0074	0.00433	0.00402	0.0069	0.9056
0.0057	0.00342		0.0067	
0.0076	4.16		0.01033	
0.0115	6.61		0.0099	
0.0083	4.89	5.67	0.0096	0.9408
0.0120	7.49		0.0091	
0.0236	0.40		0.0202	
0.0133	0.234		0.0194	
0.0167	0.330	0.3422	0.0173	0.9607
0.0204	0.41		0.0170	
0.0668	0.00121		0.0622	
0.0506	0.00105		0.0539	
0.0405	0.00104	0.001126	0.0438	0.9834
0.0396	0.00120		0.0370	
0.0739	1.374		0.0806	
0.0525	1.121		0.0702	
0.0554	1.744	1.5	0.0476	0.9399
0.0531	2.199		0.0363	

Table 3 (continued)

D_c (Data)	K_1	K_1 (Regressed)	D_c (Model)	R^2
0.0794	0.05034		0.099	
0.0623	0.0478		0.082	
0.0653	0.0774	0.06287	0.053	0.8994
0.0651	0.10790		0.0380	

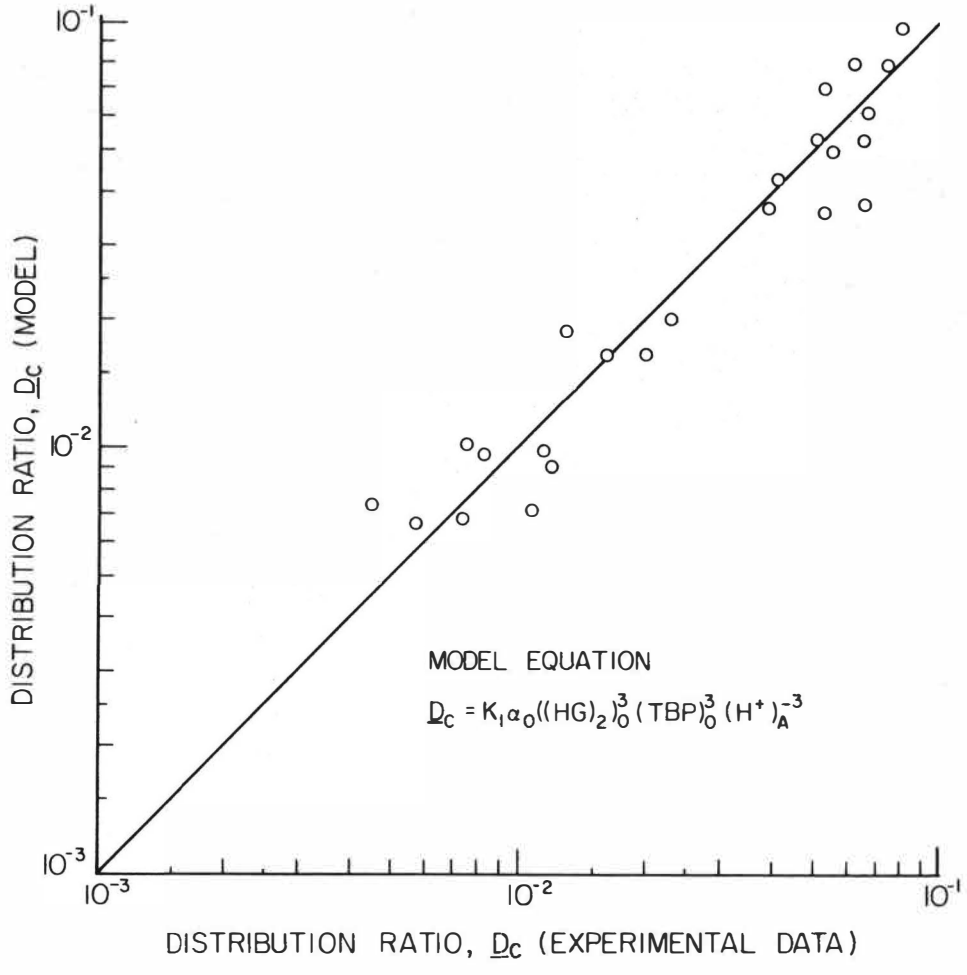

FIG. 1

Comparison of the calculated distribution ratio from the model equation to that obtained experimentally for the synergic solvent extraction system $Nd(NO_3)_3$-HDEHP-TBP-Benzene.

SUMMARY AND CONCLUSION

This paper has successfully applied a simple chemically based model to describe and predict the distribution ratio of a solvent extraction system in the presence of two synergic metal-organic complexing reagents. The method used in the development of the predictive model is an extension of the successful models previously applied to various single, binary, and ternary metal-organic complexing systems. The information needed for the development of the model equation are the solvent extraction mechanism, the equilibrium constant for the extraction reaction, the complexes formed in the aqueous phase, the stability constants or the degree of formation of the various inorganic complexes, and the initial and the equilibrium aqueous and organic phase concentrations of the components taking part in the extraction reaction. The assumption of a constant quotient of the activity coefficients appears to be sufficiently satisfied in this system, if the main consideration is the estimation of a distribution ratio.

ACKNOWLEDGMENT

This research was supported in part through the Traineeship Award to one of the authors (M.C.L.) by the Institute of Nuclear Energy Research, Chinese Atomic Energy Council, Taiwan, Republic of China, and the U.S. Department of Energy, Assistant Secretary for Energy Research, Office of Basic Energy Sciences, WPAS-KC-03-02.

REFERENCES

(1) Duyckaerts, G. and Desreux, J. F., Proc. ISEC 77, CIM Special Volume 21, 1979, Lucas, B. H., Ritcey, G. M. and Smith, H. W., Eds., Vol. 1, 73-86.

(2) Hoh, Y. C. and Wang, W. K., Hydrometallurgy, 1980,

(3) Nevarez, M. and Bautista, R. G., AIChE Symp. Series No. 173, 1978, Chapman, T. W., Tavlarides, L. L., Hubred, G. L. and Wellek, R. M., Eds., Vol. 74, 97-106.

(4) Hoh, Y. C., Nevarez, M. and Bautista, R. G., I and EC Process Design and Develop., 1978, 17, 88-91.

(5) Hoh, Y. C. and Bautista, R. G., Met. Trans. B, 1978, 9B, 69-74.

(6) Hoh, Y. C. and Bautista, R. G., I and EC Process Design and Develop., 1979, 18, 446-453.

(7) Hoh, Y. C. and Bautista, R. G., Proc. ISEC 77, CIM Special Volume 21, 1979, Lucas, B. H., Ritcey, G. M., and Smith, H. W., Eds., Vol. 1, 273-278.

(8) Hoh, Y. C. and Bautista, R. G., J. Inorg. Nucl. Chem., 1979, 41, 1787-1792.

(9) Hayden, J. G., Gerow, I. H., and Davis, M. W., Separation Science, 1974, 9, no. 4, 317-350.

(10) Zangen, V., J. Inorg. Nucl. Chem., 1963, 25, 581-594.

(11) Fomin, A. V., Yagodin, C. A., and Tarasou, V. V., Soviet Radiochemistry, 1977, 19, no. 5, 532-535.

(12) Goto, T., J. Inorg. Nucl. Chem., 1968, 30, 3305-3315.

(13) Lenz, T. G. and Smutz, M., J. Inorg. Nucl. Chem., 1968, 30, 621-637.

(14) O'Brien, W. G. and Bautista, R. G., ACS Adv. Chem. Series No. 177, Furter, W. F., Ed., 1979, 299-321.

(15) Krumholtz, P., Advances in the Chemistry of Coordination Compounds, Kirshner, S., Ed., 1961, MacMillan Co., NY.

(16) Choppin, G. R. and Strazik, W. F., Inorg. Chem., 1965, 9, 1250-1254.

EXTRACTION OF UO_2^{2+} AND OTHER METALYL (+2) IONS WITH β-DIKETONES

Robert Lundqvist

Department of Nuclear Chemistry
Chalmers University of Technology

412 96 Göteborg , Sweden

ABSTRACT

The extraction of UO_2^{2+} with acetylacetone (HAA) was studied and the extraction mechanism under various conditions could be described with the existence of the following species: UO_2^{2+}, $UO_2(AA)^+$, $UO_2(AA)_2$ and $UO_2(AA)_2HAA(org)$. K_{ex} for the distribution equilibria

$$UO_2^{2+}(aq) + 3HAA(org) \rightleftharpoons UO_2(AA)_2HAA(org) + 2H^+(aq)$$

and formation constants β_n were determined for several organic solvents and ionic strenghts. The various types of compounds formed with different β-diketones and other metalyl (+2) ions are reviewed and discussed. The thermodynamics of the extraction process of the uranylacetylacetonate adducts is derived from its temperature dependency.

INTRODUCTION

In a series of distribution studies of oxygenated metal ions MO_x^{2+}, different types of complexes are observed [1-5]. E.g. PaO^{2+} and HfO^{2+} form bisacetylacetonates $MO(AA)_2$ with acetylacetone (HAA), whereas with benzoylacetone (HBA) or thenoyltrifluoroacetone (HTTA) the same metals form complexes of the type $M(BA)_4$ or $M(TTA)_4$ [6]. The uranyle ion differs from PaO^{2+} and HfO^{2+} in that adduct compounds $UO_2(AA)_2HAA$ or $UO_2(BA)_2HBA$ are extractable [7,8]. Furthermore, complexes formed in an extraction system is not always identical to the preferred solid complexes [9,10] (e.g. $HfO(AA)_2$ is extracted while $Hf(AA)_4$ or $Hf(AA)_3Cl$ may be formed in solid state [11,12]). Table 1 summarizes the extractable species formed for PaO^{2+}, HfO^{2+}, UO_2^{2+} and VO^{2+}. Attempting to explain the underlying reasons for the formation of a particular metalyl compound, the uranyl ion is an important member because the oxygens are exceptionally firmly bound. Both the HAA and the HBA extraction systems have been investigated before [7,8], but the systematic difference in the observed behavior of the two systems has not been explained. We have therefore undertaken a reinvestigation of the uranyl system starting with acetylacetone; this would also be the most suitable for modelling experiments of an adduct system.

EXPERIMENTAL

Apparatus. The extraction experiments were carried out with the use of the continous extraction equipment AKUFVE [13,14], and batch technique. Distribution measurements of U^{233} were made with a Packard Tri Carb liquid scintilla-

tion spectrometer. pH measurements were performed with specially treated glass-calomel electrode combinations as described previously for batch experiments[1] and AKUFVE experiments[14]. The accuracy was ±0.01 pH unit.

Chemicals. Stock solution of 10 mg ^{233}U/ml in 3 M HNO_3 was supplied from Amersham, England. $NaClO_4$ and acetylacetone were purified as previously[1] and other reagents or solvents were of p.a. quality.

TABLE 1.
Extractable β-diketone complexes of bivalent metalyl ions.*

	HAA acetylacetone	HBA benzoylacetone	HTTA 2-thenoyl-trifluoroacetone	HPMBP 1-phenyl-3-methyl-4-benzoyl-pyrazolone-5	HDM dibenzoylmethane
$H^+(pK_a)$ [e]	9.05 [b]	8.24 [19]; 8.55 [18]	6.23 [10]	4.11 [20]	9.35 [10, f]
$\log K_d$ [e]	0.68 [b]	2.97	1.73 [18]	3.01 [20]	5.35 [f]
HfO^{2+}	$HfO(AA)_2$ [4, 5]	$Hf(BA)_4$ [3]	$Hf(TTA)_4$ [10]	$Hf(PMBP)_4$ [26]	—
PaO^{2+}	$PaO(AA)_2$ [1]	$Pa(BA)_4$ [3]	$Pa(TTA)_4$ [6]	—	—
	$PaOH(AA)_3$ [2, a]				
UO_2^{2+}	$UO_2(AA)_2HAA$ [7, b]	$UO_2(BA)_2HBA$ [8]	$UO_2(TTA)_2$ [21, c, d]	$UO_2(PMBP)_2$ [23, 24]	$UO_2(DM)_2HDM$
VO^{2+}	—	—	—	$VO(PMBP)_2$ [20, 25]	—

a) presence of Na_2SO_4 b) this work c) adducts formed with TBP and TOPO d) $UO_2(TTA)_2HTTA$ at high HTTA conc. [11]
e) 1 M $NaClO_4$, 25°C (benzene) f) μ = 0.1 *) possible H_2O adducts omitted

Extraction procedure. (a) Batch experiments were carried out in a closed 50 ml glass vesse[1] under argon gas atmosphere. The extraction system was stirred with a magnetic spinner and was thermostated (± 0.05 °C). 15 ml of sodium perchlorate solution and 15 ml organic phase containing ^{233}U tracer and acetylacetone were added. After equalibration 15-20 min. samples (1.31 ± 0.005 ml) of each phase were taken and the activity from ^{233}U content measured. The pH was then lowered by addition of $HClO_4$ + $NaClO_4$ mixture of proper ionic strength and the procedure repeated. The organic phase was prepared by preextraction in the following manner: 12.9 ml acetylacetone solvent solution was shaked with 1.27 ml 1M $NaClO_4$+6 drops of 1 M NaOH + 2 drops ^{233}U stock solution. In this way the uranium concentration in the organic phase became $<1 \cdot 10^{-4}$ M.

(b) AKUFVE experiments were carried out with 500 ml organic solvent and 500 ml 1 M $NaClO_4$ at constant temperature of 25 °C. 1 ml ^{233}U from diluted stock solution and 20 ml 1 M $HClO_4$ were added. Acetylacetone was added and the first point in the run was taken. pH was then increased with addition of NaOH. When pH about 8 was reached the procedure was reversed by making the system more acidic with $HClO_4$.

GENERAL DESCRIPTION OF THE EXTRACTION OF UO_2^{2+} WITH ACETYLACETONE

The extraction of the uranyl ion with acetylacetone involves the formation of complexes of the general composition $M_mL_n(OH)_p\ B_q(HL)_r(org)_s(H_2O)_t$ where M = UO_2^{2+}, HL = acetylacetone and org = solvent molecule. B is another complexant than acetylacetone but here we can assume that B is absent (although there is a weak complexation with the ionic media). Neglecting also hydrating and solvent interaction, we can simplify the formula to $M_m(HL)_xH_{-y}$ where x = n + r and y = n + p. The extractable species must have certain composition to obey electroneutrality and therefore they are written $M_c(HL)_aH_{-b}$.

The distribution ratio of uranyl ion can hence be described by

$$D = \frac{\sum_{c,a,b} \left[M_c(HL)_aH_{-b}\ (org)\right]}{\sum_{m,x,y} \left[M_m(HL)_xH_{-y}\right]} \qquad (1)$$

$$D = \frac{\sum_{c,a,b} \lambda_{c,a,b}\, \beta_{c,a,b} [HL]^a [H]^{-b} [M]^c}{\sum_{m,x,y} \beta_{m,x,y} [HL]^x [H]^{-y} [M]^m} \qquad (2)$$

where λ represents the distribution constants for the species $M_c(HL)_aH_{-b}$ and β denotes the formation constants of the uranyl complexes.

RESULTS AND ANALYSIS

Distribution mechanism. The distribution of UO_2^{2+} between benzene solutions containing HAA and 1 M $NaClO_4$ was determined for a wide range of acetylacetone concentration (0.01-7 M) and pH (1-8), FIG. 1. All curves has a limiting slope $\delta\log D/\delta pH = +2$ at sufficiently low pH and reaches a maximum plateau distribution D_λ value at higher pH. Furthermore the D_λ values increase with acetylacetone concentration thus indicating adduct formation with acetylacetone itself. It can be found that $\delta\log D_\lambda/\delta\log [HAA]^\circ_{org} = +1$ and that $\delta\log D/\delta\log [HAA]^\circ_{org} = +3$ for sufficiently low pH from analysis of FIG. 1. In FIG. 2 these statements are easier to see since the logD is plotted directly as a function of $\log [HAA]^\circ_{org}$, where $[HAA]^\circ_{org}$ is the original concentration of HAA in the organic phase. Also it follows that $\delta\log D/\delta\log [HAA]^\circ_{org} = +1$ for different solvents; benzene, chloroform and cyclohexane. We may now return to eq (1) and conclude that $a - x = 3$ and $+(b - y) = +2$. Assuming only mononuclear species to be formed, which is supported by the invariance of D with varying uranyl concentration 10^{-5} — 10^{-3} M, we can deduce that at sufficiently low pH where the uranyl ion must be uncomplexed ($x = 0$, $y = 0$) in aqueous phase a complex of the type $M(HL)_3H_{-2}$ is extracted. The extraction reaction with the equilibrium constants K_{ex}, may be written

$$UO_2^{2+} + 3\ HAA(org) \rightleftharpoons UO_2(AA)_2HAA(org) + 2\ H^+ \qquad (3)$$

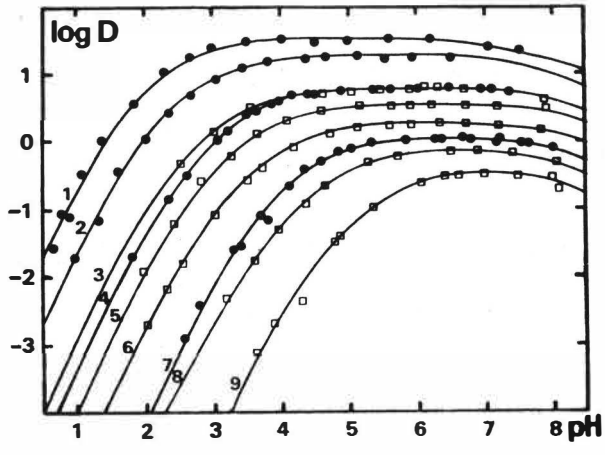

FIG. 1

The distribution of U(VI) between benzene solutions of acetylacetone (HAA) and I M $NaClO_4$, as a function of pH at 25°C. (●) batch- or (□) AKUFVE-technique.

$[HAA]^\circ_{org}$ M	7.34	2.81	0.96	0.79	0.48	0.23	0.101	0.061	0.010
curve nr	1	2	3	4	5	6	7	8	9

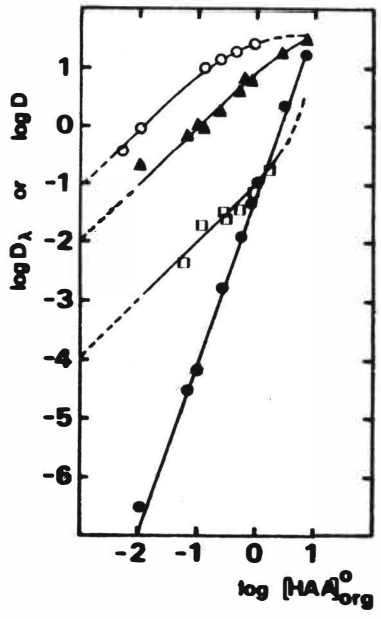

FIG. 2

The influence of the initial concentration of acetylacetone $[HAA]^o_{org}$ on the plateau distribution value D_λ of U(VI) for some organic solvents and I M $NaClO_4$ at 25°C. The influence on the distribution D of U(VI) at pH 2 is also shown.

$CHCl_3$ ▲ C_6H_6 □ cyclohexane ○ C_6H_6, pH 2

The relationship $\delta \log D_\lambda / \delta \log [HAA]^o_{org} = +1$ which holds for sufficiently low HAA concentrations (a too high HAA concentration changes for properties of the diluent) tells us that there must be on the average one molecule more of HAA in the uranyl complex in the organic phase than in the aqueous phase. Thus since $UO_2(AA)_2HAA$ is dominating in organic phase according to eq. 3 we conclude that $UO_2(AA)_2$ is dominating in aqueous phase at the plateaus. Now let's test the obtained information using eq. 2:

Assume first that the dominating uranyl species $UO_2(AA)_2HAA$ in the organic phase is formed by the reaction $UO_2(AA)_2$(org) + HAA(org) with the adduct formation constant k(org). We may then divide both sides in eq 2 with $[HAA]_{org}$

$$\frac{D}{[HL]_{org}} = \frac{\sum_{a,b} \lambda_{a,b} \beta_{a,b} [HL]^{a-1} [H]^{-b}}{K_D \sum_{x,y} \beta_{x,y} [HL]^{x} [H]^{-y}} \qquad (4)$$

where K_D is the distribution constant of HL ($HL \rightleftarrows HL(org)$). This new expression is shown in FIG. 3 where the relation $\log(D/[HAA]_{org})$ is plotted as a function of pAA = $-\log[AA^-]$. The remarkable result is that all data for various pH and of the very different acetylacetone concentrations (0.06–7 M $[HAA]_{org}$) coincide to a common curve, FIG. 3. There is some spread in the data ± 0.2 log units in logD over the entire pAA range but there is no correlation with $[HAA]_{org}$ that should indicate any hydrolysis (separation of the plateau-values). Moreover the data are obtained by two techniques: AKUFVE and batch giving the same result. The line has a limiting slope $\delta \log(D/[HAA]_{org})/\delta pAA = -2$ which means that $-(a-1-x) = -2$ or that because $x = 0$ (UO_2^{2+} dominates) $a-1 = 2$. Because the electroneutrality of the distributed complex $a-1 = b$, i.e. $a = 3$: $b = 2$.

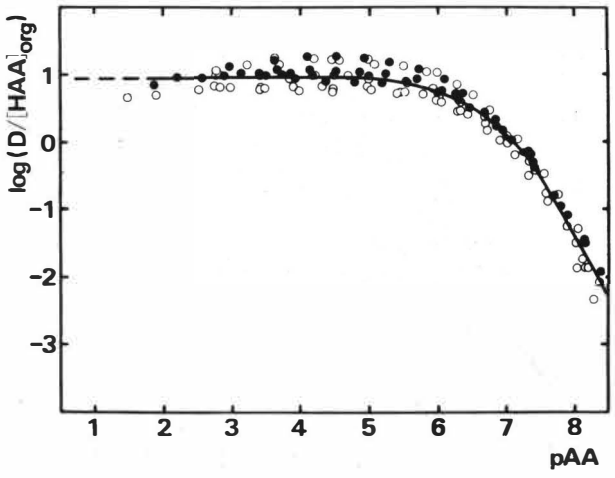

FIG. 3

Normalized distribution function of the U(VI)-acetylacetone-adduct extraction system. Log (D/$[HAA]_{org}$) is plotted as a function of pAA (= - log $[AA^-]$) for benzene solvent and I M $NaClO_4$ aqueous phase, 25°C. $[HAA]^0_{org}$ = 0.06I — 7.34M Full drawn curve is calculated from determined equilibrium constants.

(●) AKUFVE experiments (○) batch experiments

Equation (4) can now be rewritten

$$\frac{D}{[HL]_{org}} = \frac{\lambda_{3,2}\,\beta_{3,2}\,[HL]^2\,[H]^{-2}}{K_D \sum_{x,y} \beta_{x,y}\,[HL]^x\,[H]^{-y}} = \frac{\lambda'_2\,\beta_2\,[L]^{-2}}{\sum_n \beta_n\,[L]^{-n}} \qquad (5)$$

where $\lambda'_2 = \lambda_2 \cdot k(org)$ and β_n are the formation constants ($UO_2^{2+} + nAA^- \rightleftharpoons UO_2(AA)^{2-n}$). From the curve in FIG. 3, the formation constants were found to be $\log \beta_1 = 7.5 \pm 0.4$ and $\log \beta_2 = 13.7 \pm 0.4$. K_{ex} according to eq. 3 was calculated to $\log K_{ex} = -4.8 \pm 0.2$ The plateau of the normalized curve gives the value of λ'_2 which is the product of $\lambda_2 \cdot k(org)$. However since the adduct species $UO_2(AA)_2HAA$ is dominating in the organic phase for all tested HAA concentrations, it is impossible to resolve λ'_2 into its components.

Solvent influence regularities. The distribution of UO_2^{2+} with acetylacetone was investigated with a number of solvents at different ionic strengths of $NaClO_4$ (0; 1; 4; 6 M). Typical distribution curves are shown in FIG. 4. The obtained plateau values $\log D_\lambda$, for a given HAA concentration were then plotted as a function of $\log K_D$ as is shown in FIG. 5. From the theory of regular solutions, modifying the procedure by Omori and co-workers,[16,17] can be shown that the relation:

$$\log D_\lambda = n \log K_D + \text{const.} \qquad (6)$$

is valid for a constant concentration of HAA. n is equal to the ratio between the molar volume of the extracted uranyl complex and acetylacetone. From the slopes of the lines in FIG. 5 it follows that n = 3.0 ± 0.1 for tested ionic strengths 0, 1 and 6 M. Thus one concludes that the volume of the extracted species is 3.0 times the volume of HAA, or 309 ml since the volume of HAA is 103 ml[17] .

Effect of ionic strenght. The influence of the ionic strenght on the

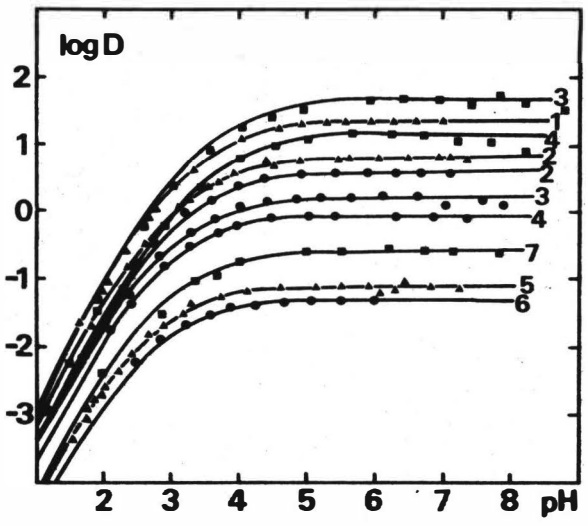

FIG. 4

The distribution of U(VI) between aqueous perchlorate and acetylacetone solutions in various organic diluents.
(●) 0 M $NaClO_4$ (▲) I M $NaClO_4$ (■) 6 M $NaClO_4$, $[HAA]^{o}_{org}$ = 0.76 M , 25°C
I=$CHCl_3$, 2= C_6H_6, 3=toluene, 4=CCl_4, 5=cy lohexane, 6=n-hexane, 7=n-heptane

distribution of U(VI) is shown in FIG. 6 , where logD = f(pH) is plotted for 0; 1; 4 and 6 M ionic strenght. The curves were all obtained for the same initial acetylacetone concentration (0.76 M) in benzene. Since K_D for HAA is decreasing with μ (Table 2), this should lead to a decrease of the D_λ-values according to eq.(6). However the plateau values shows an increase with increased [HAA] which is due to a dominating salting out effect. The values of β_n and

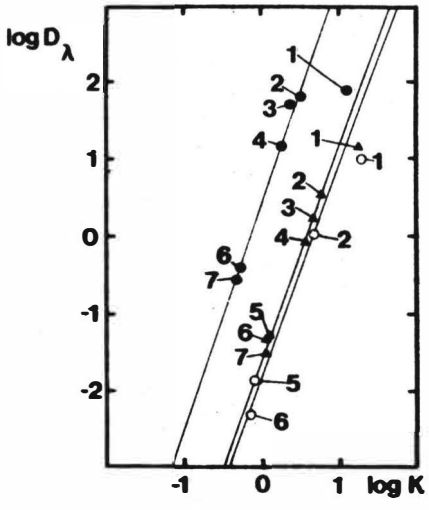

FIG. 5

The relation between the distribution, log D_λ, of the uranylacetonato complex and the partition constant, log K , of acetylacetone. The D_λ corresponds to the plateau value of the distribution, at identical initial acetylacetone concentration, between an aqueous $NaClO_4$ phase and the organic phase.

μ « » $[HAA]^{o}_{org}$	6 M $NaClO_4$	I M $NaClO_4$	0 M $NaClO_4$
	0.76 ●	0.76 ▲	0.12 ○

I=$CHCl_3$, 2=C_6H_6, 3=toluene, 4=CCl_4, 5=cy lohexane, 6=n-hexane, 7=n-heptane

K_{ex} calculated for the different ionic strenghts are listed in Table 2 together with thermodynamic constants for the distribution. The β_n values are almost equal for 0 and 1 M $NaClO_4$ and increases for higher ionic strenght.

TABLE 2.
Equilibrium constants of the uranyl extraction system [i]: UO_2^{2+}, HAA(benzene)/(Na,H)ClO_4, 25°C.

μ mol —	K	pK_a mol	$\log K_{ex}$ mol^{-1}	$\log \beta_1$ [viii] mol^{-1}	$\log \beta_2$ [viii] mol^{-2}	$\log \lambda_2'$ —	$\Delta H (\lambda_2')$ $kJmol^{-1}$	$\Delta S (\lambda_2')$ $Jmol^{-1}deg^{-1}$
0	6.53 ± 0.60 [ii]	8.81 ± 0.03 [iii]	-4.74 ± 0.06	7.5 ± 0.2	13.78 ± 0.10 [v]	0.73 ± 0.06	7.9 ± 0.7	40.6 ± 2.2
1	4.80 ± 0.20 [ii]	9.05 ± 0.01 [iii]	-4.69 ± 0.06 [iv]	7.7 ± 0.2 [v]	13.78 ± 0.10 [vi]	1.00 ± 0.06 [vii]	3.7 ± 1.2	28.3 ± 4.2
4	3.35 ± 0.10 [ii]	9.85 ± 0.03 [iii]	-4.59 ± 0.06	7.9 ± 0.2	14.58 ± 0.10	1.58 ± 0.08	-4.4 ± 1.6	16.4 ± 5.5
6	2.7 ± 0.2 [ii]	10.48 ± 0.01 [iii]	-4.52 ± 0.06	8.5 ± 0.2	15.45 ± 0.10	1.85 ± 0.09	-14.9 ± 1.9	-10.5 ± 6.1

i) $[HAA]^{o}_{org}$ = 0.77 M
ii) determined by spectrophotometry of Fe(III)complex, K is independent of temp. (and of [HAA] ≤ 6-8 M at 1 M $NaClO_4$)
iii) determined by potentiometric titration, temp. dependency will be reported sv
iv) -4.8 ± 0.2 from all benzene data ([HAA(org)] = 0.01-7 M)
v) 7.5 ± 0.5 — " —
vi) 13.70± 0.45 — " —
vii) 0.93± 0.25 — " —
viii) 50% dioxane [27] ($\log \beta_1$ = 9.32, $\log \beta_2$ = 16.92) ; 0.1 M $NaClO_4$ [7] ($\log \beta_1$ = 6.8, $\log \beta_2$ = 13.1) ; PaO^{2+}, 1 M $NaClO_4$ [1] ($\log \beta_1$ = 6.1 ± 0.3, $\log \beta_2$ = 13.15 ± 0.13) ; HfO^{2+}, 1 M $NaClO_4$ [4] ($\log \beta_1$ = 7.79 ± 0.03, $\log \beta_2$ = 14.27 ± 0.21)

Temperature dependence. In order to investigate the thermodynamics of the distribution of U(VI), the temperature effect on the plateau values D_λ was measured for benzene solutions of constant HAA concentration, see FIG. 7. The influence of temperature (5-70°C) was very small in the investigated range of ionic strenght 0-6 M. The transport of a neutral complex from aqueous to organic phase can be treated as a set of thermodynamic processes as was described previously [5]. In addition we have adduct formation in the organic phase which complicates the interpretation. We shall not try to make such an inter-

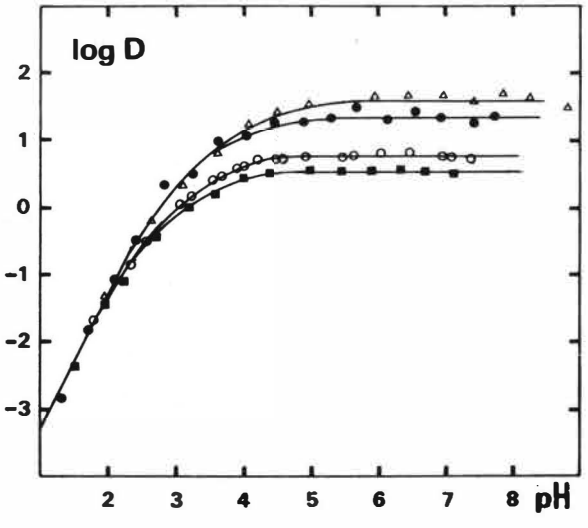

FIG. 6

Influence of ionic strenght on the distribution curves, log D = f(pH), for U(VI). Initial concentration of acetylacetone in benzene equals 0.76 M. Solid curves are calculated from estimated equilibrium constants. 25°C
(■) 0 M $NaClO_4$ (○) I M $NaClO_4$ (●) 4 M $NaClO_4$ (△) 6 M $NaClO_4$

pretation but merely give (Table 2) the calculated thermodynamic constants ΔH and ΔS for the distribution of U(VI) as described by λ_2'

$$UO_2(AA)_2(aq) \rightleftharpoons UO_2(AA)_2HAA(org) \qquad (7)$$

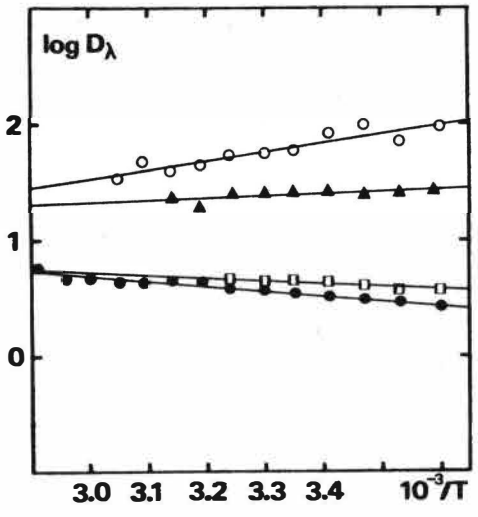

FIG. 7

Temperature dependence on the distribution D_λ , $UO_2(AA)_2 \rightleftharpoons UO_2(AA)_2HAA$(benzene), at different ionic strenghts. Initial acetylacetone is 0.76 M, 5 — 70 °C.

(●) 0 M $NaClO_4$ (□) I M $NaClO_4$ (▲) 4 M $NaClO_4$ (○) 6 M $NaClO_4$

DISCUSSION

The present investigation has shown that the extraction of U(VI) with HAA under the used conditions can be described with the following minimum of existing species: UO_2^{2+}, $UO_2(AA)^+$, $UO_2(AA)_2$ and $UO_2(AA)_2HAA$(org). Due to the sufficiently high concentration at HAA employed any hydrolysis was completely suppressed. In order to detect hydrolysis it can be calculated from estimated hydrolysis constants that it is necessary to decrease $[HAA]_{org}$ below 0.01 M so that the complexation of UO_2^{2+} with AA^- and OH^- becomes comparable. The extent of complexing with AA^- is proportional to the product $K/K_a/\beta_n$. Using this relation one can explain why Rydberg[7] in his treatment of the UO_2^{2+}, 0.01-1 M HAA($CHCl_3$)/0.1 M (Na,H)ClO_4 extraction system was able to calculate hydrolysis constants because K in his system was larger by a factor of 4.9. A more drastic difference in the susceptibility for hydrolysis is obtained for benzoylacetone HBA. Stary[8] studied the extraction of U(VI) with HBA in CCl_4 for which the number $K/K_a/\beta_2$ is about 18 times greater than the corresponding number for the present HAA extraction system. This means that $|HBA|_{org} > 0.18$ M would be required to suppress hydrolysis. Since the highest HBA concentration used by Stary was 0.1 M, hydrolysis remarkably changed the extraction curves: no broad plateau values were obtained but maxima. Hydrolysis not only of UO_2^{2+} but also of mixed hydroxy-β-diketone complexes must be considered. However at sufficiently low pH, the similiar adduct extraction mechanism as for HAA was observed:

$$UO_2^{2+} + 3\ HBA(org) \rightleftharpoons UO_2(BA)_2HBA(org) + 2\ H^+ \qquad (8)$$

In order to verify that $UO_2(AA)_2HAA$ was the dominating species in the organic phase a series of stochiometric analysis of the composition of the extracted species were made. Thus when extracting macro amounts of UO_2^{2+} into $CHCl_3$ it was found that $UO_2(AA)_2HAA$ always was extracted, both in excess and deficit of HAA relative to the original uranium content in aqueous phase. The analysis were made by determining the uranium content by igniting crystallized complexes to U_3O_8.

The calculated β_n values seems resonable in magnitude by comparing with other determinations for UO_2^{2+}, PaO^{2+} and HfO^{2+} considering the different conditions (ionic media etc), Table 2. The HAA complexation increases in the order $PaO^{2+} < UO_2^{2+} < HfO^{2+}$.

In Table 1 summarized information is given about the extractable complexes of various β-diketones with bivalent metalyl ions. No obvious reason why the different types of complexes are extracted can be concluded. For instance why doesn't thenoyltrifluoroacetone (HTTA) and 1-phenyl-3-methyl-4-benzoyl--pyrazolone-5 (HPMBP) forme adducts like HAA, HBA and HBM (dibenzoylmethane) do. Much more future studies on various extraction systems is needed to reveal those questions. A systematic study of a series of β-diketone derivatives and other metalyl ions VO^{2+}, TiO^{2+} and ZrO^{2+} must be made.

Acknowledgement. Dr. S.O.Andersson is thanked for initializing this studies and ing. Eva Jomar and fil.kand. Anna Selme for skilful experimental help. Ing. Monika Bengtsson was very helpful in typing and figure drawing wich is greatfully acknowledged. This work was supported by the Swedish Natural Science Council.

REFERENCES

1. Lundqvist, R. Acta Chem. Scand. A28 (1974) 243.
2. Lundqvist, R. and Rydberg, J. Acta Chem. Scand. A28 (1974) 399.
3. Lundqvist, R. Acta Chem. Scand. A29 (1975) 231.
4. Lundqvist, R. To be published.
5. Allard, B., Johnson, S., Narbutt, J. and Lundqvist, R., Proc. Int. Solvent Extraction Conf., ISEC-77. Toronto, sept. 9-16 1977, Canadian Inst. of Mining and Metallurgy, special vol.21 (1979) 150.
6. Guillaumont, R. Comp. Rend. Acad. Sci. Paris 260 (1965) 1416.
7. Rydberg, J., Arkiv Kemi 8 (1955) 113.
8. Stary, J., Coll. Czech. Chem. Comm. 25 (1960) 890.
9. Mehrotra, R.C., Bohra, R. and Gaur, D.P. "Metal β-diketones and allied derivatives". Academic Press, 1978.
10. Stary, J. "The Solvent Extraction of Metal Chelates", Pergamon 1964.
11. Larsen E.M., Terry, G. and Leddy, J. J. Am. Chem. Soc. 75 (1953) 5107.
12. Pinnavaia, T.J. and Fay R.C., Inorg. Chem. 7 (2968) 502.
13. Rydberg, J. Acta. Chem. Scand. 23 (1969) 647.
14. Andersson, C., Andersson, S.O., Liljenzin, J.O., Reinhardt, H. and Rydberg, J. Acta Chem. Scand. 23 (1969) 2781.
15. Rydberg, J. Arkiv Kemi 8 (1955) 101.
16. Wakahayshi, T., Oki, S., Omori, T. and Suzuki, N. J. Inorg. Nucl. Chem. 26 (1964) 2555.
17. Omori, T., Wakahayashi, T., Oki, S. and Suzuki, N. J. Inorg. Nucl. Chem. 26 (1964) 2565.

18. Sekine, T., Hasegawa, T. and Ihara, N , J. Inorg. Nucl. Chem. 35 (1973) . 3968.
19. Peshkova, V.M., Melchakova, N.V. and Zhemchuzin S.G., Russ. J. Inorg. Chem. 6 (1961) 639.
20. Zolotov, Yu.A. and Kozmin, N.M. "Extraction of metal acetyl-pyrazolones" Nauka, Moscow, 1977, in russian.
21. Akiba, K., Suzuki, N., Asano, H. and Kanno, T., J. Radioanal. Chem. 7 (1971) 203.
22. Peterson, S., J. Inorg. Nucl. Chem. 14 (1960) 126.
23. Jensen. B.S., Acta Chem. Scand. 13 (1959) 1890.
24. Bacer, W. and Keller, C., J. Inorg. Nucl. Chem. 32 (1970) 1679.
25. Krasnjanskaya, N.A., Jevjentova, I.I., Melchakova, N.V. and Pechkova, N.M. Zh. anal. Khim. 27 (1972) 1842.
26. Navratil, O. and Jensen, B.S J. Radioanal. Chem. 5 (1970) 313.
27. Bryant, B.E., J. Phys. Chem. 58 (1954) 573.

SIZE-SELECTIVE SYNERGISM BY CROWN ETHERS IN THE EXTRACTION OF ALKALI METALS BY DI(2-ETHYLHEXYL)PHOSPHORIC ACID*

W. J. McDowell, W. F. Kinard,† and R. R. Shoun

Chemical Technology Division
Oak Ridge National Laboratory
Oak Ridge, Tennessee 37830

ABSTRACT

Although the macrocyclic polyethers, known as crown ethers, complex metal ions and do so preferentially according to the size correspondence between the ion and the crown ether cavity, their usefulness as liquid-liquid extraction reagents has been limited by the necessity of solubilizing the anion in the organic phase. The common mineral acid anions are difficult to transfer to the organic phase, and organophilic anions are expensive or impractical. A method is described that avoids this problem by combining organic-soluble cation exchangers with the crown ethers in the organic phase. The resulting mixtures show synergistic extraction for cations, and for the alkali metal ions the synergistic effect is size selective. The size dependence of the synergistic extraction in the system di(2-ethylhexyl)phosphoric acid/crown ethers parallels the extraction of picrate salts of the alkali metals and of the complex formation of the alkali picrates with crown ethers. A preliminary evaluation of concentration dependencies in the extraction of potassium by di(2-ethylhexyl)phosphoric acid–dicyclohexo-18-crown-6 mixtures in benzene suggests an organic-phase complex containing two alkyl phosphoric acid groups and one crown ether per potassium.

INTRODUCTION

Although the existence of cyclic polyether compounds has been known for several decades, Pedersen (1-4) was the first to systematically synthesize and investigate the properties of these unusual molecules. The most notable of these properties is their ability to form complexes with alkali metal salts and to form the strongest complexes when there is good correspondence between the size of the alkali metal ion and the cavity in the cyclic polyether. Pedersen synthesized a large number of polyethers with cavity sizes appropriate for all the alkali metals. He called these compounds "crown" ethers because of their structural resemblance to a crown and created a trivial nomenclature in which the number of atoms in the polyether ring was denoted by a number followed by the word *crown*, followed by the number of ether oxygens. Thus, 18-crown-6 is an 18-atom ring consisting of 12 carbon atoms and six oxygen atoms.

Stability constants for many alkali metal-crown ether complexes have been measured by various methods both in water solution and in methanol solution (5). These measurements show the expected tendency for the crown ether-alkali metal pairs with the best size correspondence to be most stable. They also show the stability in the presence of water to be less, indicating competition between the crown ether complexing and ion hydration. Because

*Research sponsored by the Division of Chemical Sciences, U.S. Department of Energy under contract W-7405-eng-26 with the Union Carbide Corporation.

†Currently at College of Charleston, Charleston, South Carolina.

most of the crown ethers were organophilic to some degree and because they would complex and solubilize a variety of alkali metal salts into organic phases, they were used to transfer to organic phases catalytic agents that are normally soluble only in an aqueous phase. This procedure is referred to as phase-transfer catalysis. The possibility of using crown ethers as liquid-liquid extraction (solvent extraction) reagents in analytical and hydrometallurgical applications was quickly recognized.

Frensdorff used solvent extraction of alkali metal picrates by chloroform solutions of crown ethers as a means of evaluating the relative strength of crown ether complexes (6). Size selectivity was observed as expected. Distribution coefficients, D_M (organic-phase metal concentration/aqueous-phase metal concentration), were very low but were larger when the large organophyllic picrate anion was used than when mineral acid anions such as sulfate, chloride, or nitrate were used. The difficulty of solubilizing the mineral acid anions in nonpolar organic phases is a primary problem in applying the size-selective properties of crown ethers to hydrometallurgical or analytical extraction problems since economics and practicality often dictate the use of the common mineral acids. A process for the separation of potassium chloride from other metal chlorides in a brine solution has been developed using the concept of an anion-solvating diluent (7). A polar solvent, *m*-cresol, was found suitable for solvating the chloride anion and enhancing the extraction of the potassium-chloride ion pair into the organic phase.

McDowell and Shoun have used a different approach to the problem of anion solvation (8). In their work, they mixed an organic-phase-soluble cation exchanger with the crown ether so that the necessity of transferring the inorganic anion to the organic phase is eliminated. In this system the cation in the aqueous phase is exchanged at the interface for the hydrogen of the organic-phase acid. The metals then exist as an organic-phase-soluble salt with which the crown ether can easily coordinate. Large and dramatic effects by dicyclohexo-18-crown-6 on the order of extraction of alkali metals by di(2-ethylhexyl)phosphoric acid (HDEHP) have been observed and reported (8,9). This study expands upon these early observations and reports a systematic examination of the extraction behavior of the alkali metals with several crown ethers mixed with HDEHP.

EXPERIMENTAL

Crown ethers were obtained from Parish and Aldrich Chemical companies at stated purities of $\geq$99% and were used without further purification. No attempts were made to separate the structural isomers of the dicyclohexo-substituted crown ethers, and the results reported thus represent a compositional average of the two isomers. The HDEHP was purified by copper(II) precipitation and molecular distillation according to published procedures (10,11). The didodecylnaphthalene sulfonic acid (HDDNS) was prepared in this laboratory, and the neocarboxylic acid (V-Acid) was obtained from Shell Development Laboratories and purified by molecular distillation.

All alkali metal salts used were reagent grade. The radionuclides were obtained from New England Nuclear Company. Their radiochemical purity was verified by gamma spectrometry. The nuclides used were ^{22}Na, ^{42}K, ^{86}Rb, and ^{134}Cs; these were chosen to ensure the absence of radioactive daughters that might interfere with the experiment. Lithium was determined by atomic emission spectrometry using a Perkin-Elmer Model 460 atomic absorption spectrophotometer. Reagent-grade benzene was used as the diluent in all experiments.

The organic phase for the liquid-liquid extractions was prepared by diluting the appropriate, weighed amount of reagent with benzene. In the systematic studies, where extraction reagents were used separately or combined, the formal concentration of crown ether was 0.250 *M* and that of HDEHP was 0.125 *M*. In these tests, the experimental procedure involved the equilibration of approximately 10 ml of the aqueous phase with approximately 10 ml of the organic extractant phase. The pH of the solution was adjusted to near 6 using a 0.125 *M* solution of the metal hydroxide under study. The radioactive tracer was added, and the phases were mixed for 5 min to ensure that equilibrium was obtained. Mixing was accomplished in a 30-ml vial using a magnetic stirrer, and the aqueous-phase pH was monitored with an Orion Model 801 digital pH meter. Dilute nitric acid was added incrementally by a microburet to titrate the solutions to lower pH values. After each acid addition and equilibration, stirring was stopped and the phases were allowed to separate. Aliquots of 0.200 ml of each phase were removed for analysis and counted on a single-channel Packard Auto-Gamma scintillation spectrometer. Counting times were adjusted to give statistical counting errors of less than 1% with the exception of extremely low counting samples. Titration-equilibrations were performed with crown ether alone, HDEHP alone, and with the two reagents mixed.

Phase separation was poor above a pH of about 5.5 when HDEHP was present because of the conversion of a large fraction of HDEHP to the interface-active alkali metal salts above this pH. Extraction coefficients at pH values below 2.5 for systems containing HDEHP and at all pH values when using crown ethers alone were very low ($D_M \leq 10^{-4}$); thus the counting rates obtained in the organic layer in these equilibrations were near the analytical limit.

RESULTS AND DISCUSSION

Preliminary Tests

Crown ethers were tested in combination with a variety of available extractants, including tributylphosphate, trioctylphosphine oxide, a secondary and tertiary alkyl amine, a carboxylic acid, a sulfonic acid, and HDEHP. Cations and associated anion systems that were known to give moderate extraction were chosen, and a crown ether was chosen for test that had a cavity to match the ion diameter. No synergistic effect was noted with the neutral phosphorus extractants and only a slight synergistic effect with the amines. All the extractants that were cation exchangers showed sizable synergistic effects (see Table 1). Di(2-ethylhexyl)phosphoric acid was chosen for further systematic examination because of the existence of a large body of data on the extraction of alkali metals by this reagent.

Table 1. Liquid cation exchanger-crown ether synergism

System	Aqueous phase	Element	Distribution coefficient	Synergistic factor
V-Acid + DC18C6[a]	10^{-4} *M*, pH 6	K	0.01	300
HDDNS + DC18C6[b]	10^{-4} *M*, pH 1	K	20	50
HDEHP + DC18C6	10^{-4} *M*, pH 4	K	1.4	370
HDEHP + C15C5	10^{-4} *M*, pH 6	Na	3.0	30

[a] V-Acid = a neocarboxylic acid, 15 to 19 carbon atoms on the alkyl groups.

[b] HDDNS = didodecylnaphthalene sulfonic acid.

Size-Selective Synergism

A typical illustration of the synergistic effect of the crown ether on alkali metal extraction by HDEHP is shown in Fig. 1. The effect varies with pH, and the synergistic factor (distribution coefficient for the mixture, divided by the sum of the distribution coefficients for the individual components used alone) is a maximum at about pH 4. In all equilibrations where the crown ether was used alone, distribution coefficients for the alkali metals were $\leq 10^{-4}$, and there was no dependence on aqueous-phase pH within experimental detection. The lack of pH dependence (Item 5, Table 2) is as would be expected for this reagent because the crown ether should extract by neutral molecule association and not by cation exchange.

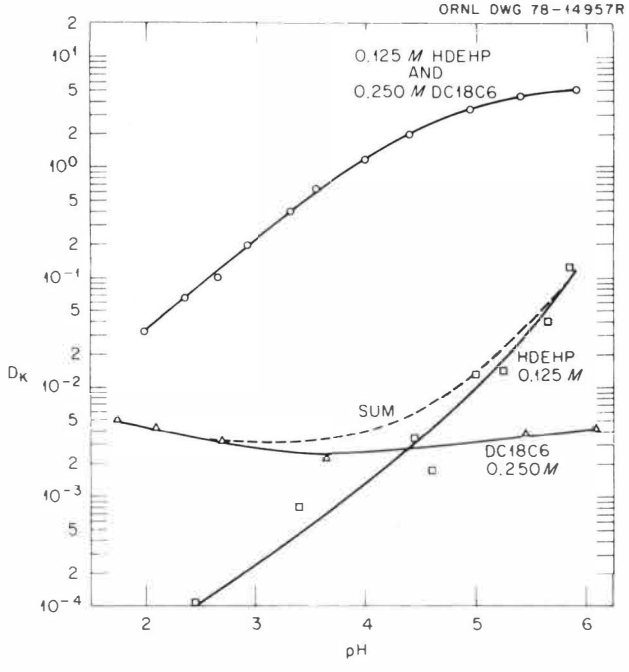

FIG. 1

Extraction of potassium from nitrate medium by 0.250 *M* DC18C6, by 0.125 *M* HDEHP, and by a solution of these two reagents together at the same concentrations all as a function of aqueous-phase pH. The synergistic factor is the ratio of the distribution coefficient obtained with the mixture to the sum of those obtained by the reagents when used alone.

Table 2. Stoichiometric ratios for the crown ether-HDEHP extraction system

Item	Reactant varied	Li	Na	K	Rb	Cs
1	Metal ion concentration		1.15	1.00	0.95	0.92
2	HDEHP concentration		0.96	0.92	1.12	0.92
3	DC18C6 concentration		0.80	0.70	0.84	0.62
4	pH dependence (HDEHP + DC18C6)[a]	0.96	0.84	0.58	0.67	0.93
5	pH dependence (DC18C6 alone)[a]	0.05	-0.02	-0.01	0.00	0.01
6	pH dependence (HDEHP alone)[a]	0.91	0.96	0.84	0.86	0.94

[a]Range of pH = 2 to 6.

The extraction of alkali metals by HDEHP is a cation exchange process, and a plot of log D_M versus pH should have a slope of 1 as has been demonstrated by earlier work (12). The data shown in Items 4 and 6, Table 2 and in the lower group of curves in Fig. 2 are in reasonable agreement with this idea and show further that under the conditions of this work (trace metal ion; no competition for extraction) there is little difference in the extraction coefficients for the various alkali metals.

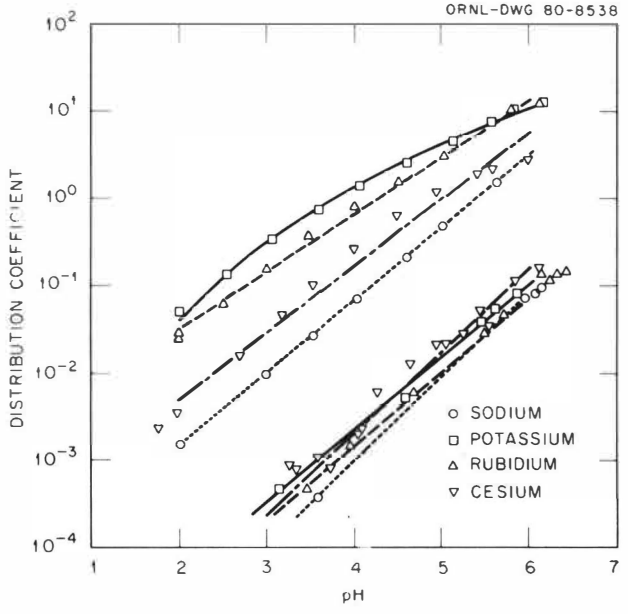

FIG. 2

The effect of 0.250 *M* DC18C6 on the extraction of the alkali metals from nitrate solutions by 0.125 *M* HDEHP as a function of aqueous-phase pH.

The upper group of curves in Fig. 2 shows the effect of adding 0.25 *M* DC18C6 to the HDEHP solution. The extraction of all the alkali metals is synergized, with potassium extraction being synergized most strongly, as would be expected from the correspondence in ion and cavity size. Synergistic factors were calculated using corresponding data for each of the crown ethers tested plus data for extraction by the crown ether alone, taking them in sets like that in Fig. 1 and smoothing the data by least-squares. The resulting set of curves of synergistic factor vs pH for DC21C7-HDEHP mixtures may be seen in Fig. 3. Rubidium extraction is synergized most strongly. Table 3 lists the synergistic factors obtained at pH 4 and the extraction coefficient at that pH for the synergistic mixture 0.125 *M* HDEHP + 0.25 *M* crown ether for the alkali metals lithium through cesium. The crown ethers C15C5, DC18C6, and DC21C7 synergize most strongly an alkali metal expected to fit the crown ether cavity (see synergistic factors in Table 3 and sizes in Table 4). However, the extraction of lithium and cesium is not synergized most strongly by 12C4 and DC24C8, respectively, as would be expected from size considerations; instead, the strongest synergistic effect is on sodium and potassium for 12C4 and on potassium for DC24C8, although these effects are small. It appears further that DC18C6 produces the strongest interaction for every alkali metal except sodium, for which C15C5 is most effective. Several possible reasons may be cited for

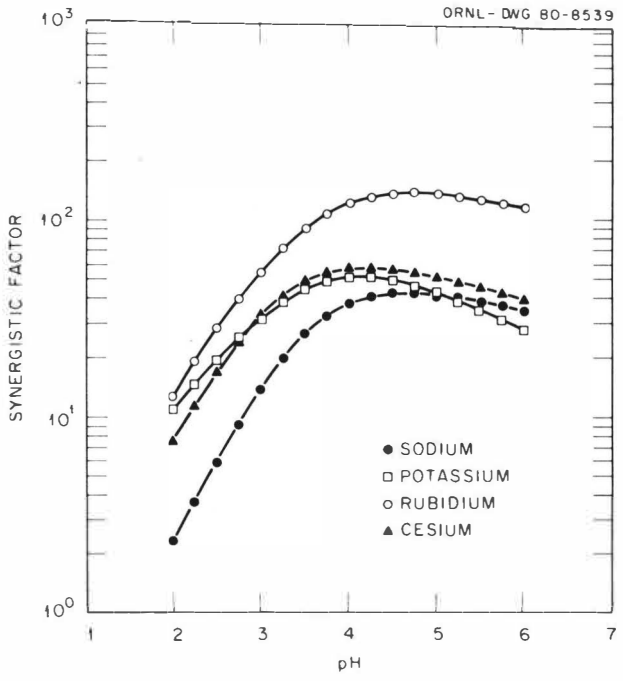

FIG. 3

Synergistic factors produced by the mixture 0.25 *M* DC21C7 + 0.125 *M* HDEHP as a function of aqueous-phase pH.

Table 3. Distribution coefficients (*D*) and synergistic factors (SF) for the extraction of the alkali metals by crown ethers (0.25 *M*) and HDEHP (0.125 *M*) in benzene from dilute aqueous solutions at pH 4.0

Crown ether	Li		Na		K		Rb		Cs	
	D	SF	*D*	SF	*D*	SF	*D*	SF	*D*	SF
12C4	0.0124	1	0.005	5	0.011	5	0.0033	2	0.0042	2
C15C5	0.038	3	0.221	160	0.166	65	0.156	85	0.0724	30
DC18C6	0.081	6	0.070	50	1.44	400	1.01	360	0.267	100
DC21C7			0.055	40	0.180	50	0.261	120	0.151	60
DC24C8	0.059	4	0.051	30	0.256	95	0.126	60	0.209	70

Table 4. Size parameters for alkali metal ions and macrocyclic polyethers

Alkali metal	Ionic diameter[a] (Å)	Crown ether	Cavity diameter[a] (Å)
Li	1.36	14-crown-4	1.2-1.5
Na	1.94	15-crown-5	1.7-2.2
K	2.66	18-crown-6	2.6-3.2
Rb	2.94	21-crown-7	3.4-4.3
Cs	3.34	24-crown-8	4.5-5.6

[a]Ionic diameters and cavity diameters through 21-crown-7 are from ref. 5. The 24-crown-8 cavity diameter was measured using CPK molecular models.

the above observed interactions. Lithium is a highly hydrated ion, and competition of water for the coordinative bonding may hinder the formation of crown ether complexes. In addition, 12C4 is somewhat water soluble (we do not have a quantitative measurement), and a direct comparison with the less aqueous-soluble C15C5 and DC18C6 may not be appropriate. For the heavier alkalis, a lower charge density may reduce their ability to complex with crown ethers, and the uncertainty of the effective cavity size in the larger, flexible polyether rings may attenuate the size-selective effect in adduct formation.

Comparison with Picrate Extraction

Although these experiments represent a system that is quite different from the one used by Frensdorff, the relationships between the distribution coefficients found in our work are similar to the relationships of the distribution coefficients reported for the picrate system (see Table 5). Figure 4 shows the ratio of the distribution coefficient of the alkali metals (scaled according to their ionic diameter on the abscissa) to that of the alkali metal expected to interact most strongly with a given crown ether because of size considerations. Data for both the present work and Frensdorff's work are included. Although the extraction of picrate salts does show the selectivity of the crown ethers, the distribution coefficients obtained were extremely low when calculated on the basis of total metal ion concentration. Frensdorff's experiments involved the extraction of 7×10^{-5} *M* alkali metal picrate solutions by an equal concentration of crown ether. However, the total metal ion concentration in eac' case was 0.1 *M* because the extractions were made using a 0.1 *M* metal hydroxide solution as the aqueous phase. The use of the cation-exchanger HDEHP in the present study maintained the selectivity of the crown ethers while increasing the distribution coefficients by a factor of over one thousand in many cases.

The synergistic extraction data are in agreement with the alkali picrate extraction data of Frensdorff in regard to the size-selective behavior of the crown ethers. For dicyclohexo-24-crown-8, both this work and the earlier work of Frensdorff found a stronger interaction with potassium than with cesium. For 12-crown-4, the possible aqueous solubility of the complex combined with the strong interaction of lithium with HDEHP precluded any definitive determination of size effects. It should be noted

Table 5. Distribution coefficients of crown ethers with alkali metal ions

System	Li	Na	K	Rb	Cs
12C4 + HDEHP	1.24E-2[a]	5.05E-3	1.10E-2	3.28E-3	4.20E-3
Di-(t-BuC)14C4[b] + picrate	7.70E-5				0
C15C5 + HDEHP	3.76E-2	2.21E-1	1.66E-1	1.56E-1	7.24E-2
t-BuC15C5[b] + picrate	1.12E-5	1.38E-4	6.09E-5		2.80E-5
DC18C6 + HDEHP	8.09E-2	6.96E-2	1.44E00	1.10E00	2.67E-1
DC18C6[b] + picrate	2.31E-5	1.79E-4	5.45E-4		3.09E-4
DC21C7 + HDEHP		5.53E-2	1.80E-1	2.61E-1	1.51E-1
DC24C8 + HDEHP	5.87E-2	5.06E-2	2.56E-1	1.26E-1	2.09E-1
DC24C8[b] + picrate	2.03E-5	6.23E-5	1.41E-4		1.27E-4

[a] Read as 1.24×10^{-2}.

[b] Calculated from values given in ref. 6.

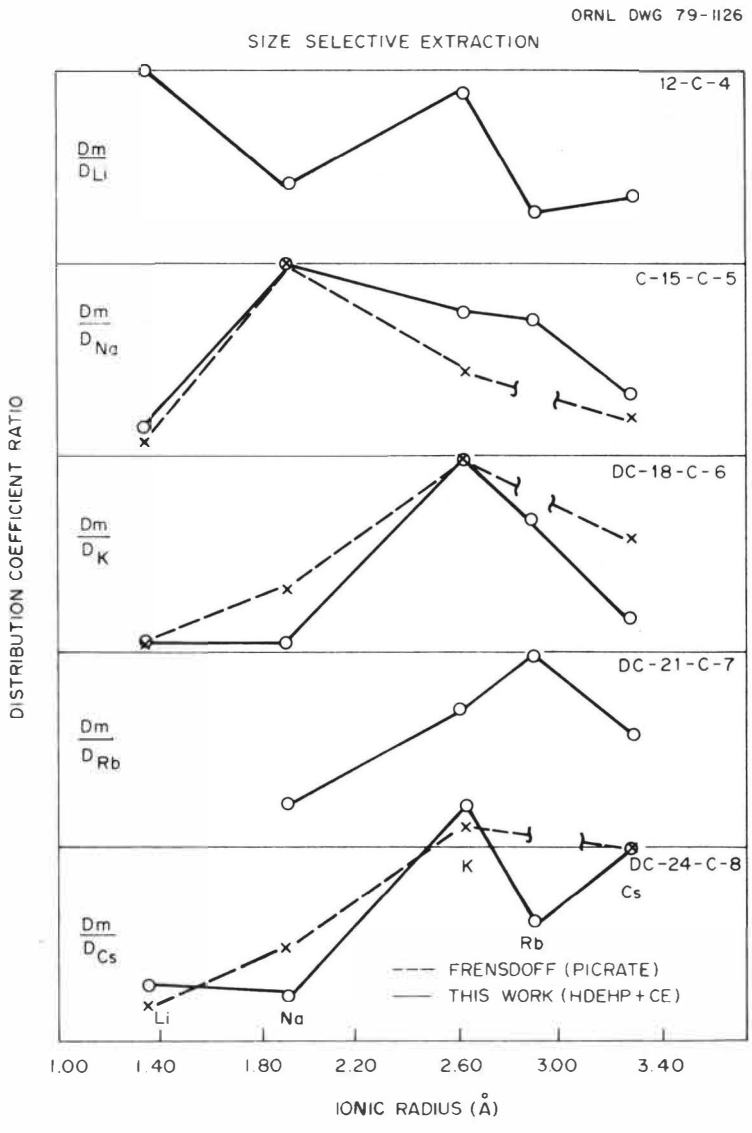

FIG. 4

A comparison of the crown ether-HDEHP extraction of alkali metals with their extraction by crown ethers as the picrates. The ratio of the distribution coefficient for a given metal to that of the metal expected to be best extracted by that crown ether (because of size) is presented vs ionic diameter.

that while the interaction of the crown ethers with certain "best-fit" alkali metals is size selective, it is not specific in that the extraction of other alkali metals is also synergized, although not as strongly.

A major result of this investigation is the demonstration that the crown ethers can be used to synergize the liquid-liquid extraction (or phase transfer) of ions by organophilic cation exchange extractants in a size-selective manner. This result suggests the possibility that this principle can be applied to all cation exchange extraction systems. Thus, a new parameter is made available in the continuing endeavor to develop extraction systems more specific for a given ion. Possibilities for new extraction systems with entirely new selectivities thus exist by mixing these size-selective synergistic agents with familiar cation exchangers. Work is currently under way to explore these possibilities.

Stoichiometry of the Complex

The DC18C6-HDEHP system was chosen for further study to try to establish the stoichiometry of the organic-phase species. A general reaction for the extraction of the alkali metals by the extraction system crown ether-HDEHP can be written as follows:

$$M^{+n} + x/r(\overline{CE})_r + y/s(\overline{HDEHP})_s \rightleftharpoons \overline{M(DEHP)_n(HDEHP)_m(CE)_x} + nH^+ , \quad (1)$$

where the overlined species represent organic soluble compounds. Because loading curve experiments exhibited an initial slope of 1.0 (Table 2) indicating that the extracted species was mononuclear (assuming a mononuclear aqueous-phase metal ion), the following equilibrium quotient can be written for the reaction:

$$Q = \frac{[\overline{M(DEHP)_n(HDEHP)_m(CE)_x}][H^+]^n}{[M^{+n}][\overline{HDEHP}]^{y/s}[CE]^{x/r}} . \quad (2)$$

The distribution coefficient is defined as the concentration of the metal in the organic phase divided by the concentration of the metal in the aqueous phase:

$$D = \frac{[\overline{M(DEHP)_n(HDEHP)_m(CE)_x}]}{[M^{+n}]} . \quad (3)$$

Therefore, substitution of the distribution coefficient into the equilibrium expression and rearrangement of terms yields:

$$\log D = \log Q + n\text{pH} + y/s \log [\text{HDEHP}] + x/r \log [\text{CE}] . \quad (4)$$

In order to determine the stoichiometric coefficients for each of the reactants in Eq. 1, a series of experiments was run in which only one of the concentration parameters was varied and all of the other conditions were held as nearly constant as feasible. From the slope of log D versus the logarithm of the concentration of the reactant varied, as determined by a least-squares fit, coefficients were obtained for Eq. 4, and these are listed in Table 2, Items 2, 3, and 4.

As expected, the pH dependence of the extraction by crown ether alone was zero. The expected value for the slope of the crown ether dependence with HDEHP present was 1.0 assuming the crown ether to be monomeric in solution (r = 1), but there appears to be a substantial deviation toward lower values. Values of x/r less than 1 could result from competing equilibria consuming crown ether, partial association of the crown ether, or significant solubility of the complex in the aqueous phase.

When used alone, HDEHP is known to be a dimer in benzene at the concentrations used in these experiments [s = 2 in Eq. (1)]; therefore, the values of y/s which were essentially 1.0 indicate a value of $n + m = 2$ and of m = 1, suggesting that there is one neutral HDEHP solvating the metal ion in the organic phase. When HDEHP alone is the extractant, it has been shown that the alkali metals can be coordinated by at least three additional neutral HDEHP molecules (12). All of these parameters taken together suggest

an extracted species of the stoichiometry

M[DEHP][HDEHP][crown ether] . (5)

Further work needs to be done to examine the possibility of crown ether-HDEHP interaction in the organic phase and to define distribution of the crown ether to various aqueous phases before a firm conclusion about complex stoichiometry can be made.

REFERENCES

1. C. J. Pedersen, *J. Am. Chem. Soc.* 89: 7017 (1967).
2. C. J. Pedersen, *J. Am. Chem. Soc.* 89: 2495 (1967).
3. C. J. Pedersen, *J. Am. Chem. Soc.* 92: 391 (1970).
4. C. J. Pedersen, *J. Am. Chem. Soc.* 92: 386 (1970).
5. J. M. Lehn, in *Structure and Bonding, No. 15*, J. D. Dunitz et al., Eds., Springer-Verlag, New York, 1973, pp. 1-69.
6. H. K. Frensdorff, *J. Am. Chem. Soc.* 93: 4674 (1971).
7. Y. Marcus and L. E. Asher, *J. Phys. Chem.* 82: 1246 (1978).
8. *Chemical Technology Division Annual Progress Report Period Ending March 31, 1977*, ORNL-5295, Oak Ridge National Laboratory, pp. 30-31.
9. *Separation Science and Technology*, special issue in press.
10. W. J. McDowell, P. T. Perdue, and G. N. Case, *J. Inorg. Nucl. Chem.* 38: 2127 (1976).
11. J. A. Partridge and R. C. Jensen, *J. Inorg. Nucl. Chem.* 31: 2587 (1969).
12. W. J. McDowell, *J. Inorg. Nucl. Chem.* 33: 1067 (1971).

SOLVENT EXTRACTION OF TRIVALENT LANTHANIDES BY DIBUTYL PHENACYLPHOSPHONATE.

J. ALSTAD, B. CECCAROLI
Department of Nuclear Chemistry, University of Oslo,
Boks 1033 - Blindern, OSLO 3, NORWAY.

J.P. BRUNETTE, M.J.F. LEROY,
Laboratoire de Chimie Minérale, Ecole Nationale
Supérieure de Chimie, 1, rue Blaise-Pascal,
67008 - STRASBOURG CEDEX, FRANCE.

ABSTRACT

The extraction of gadolinium from aqueous thiocyanate and perchlorate media by dibutylphenacylphosphonate, HDBPP has been studied. The extractant acts like TBP in the thiocyanate system whereas in the perchlorate medium HDBPP is found to be an acidic extracting agent. The hypothesis of chelation of extracted metals is supported by infrared measurements. The separation of lanthanum and the fourteen lanthanides by HDBPP has been studied by extraction from 1M $NaClO_4$, $|H^+| < 2\ 10^{-4}$M medium. A plot of $\log\alpha_{Z/La}$ vs.Z shows that the series is divided in four subgroups.

INTRODUCTION

The β-ketophosphonates have been studied during the last years because of their potential extraction abilities (1)-(6) Firstly, these compounds have an asymmetric donor power due to the P=O and C=O groups. Secondly their enolic tautomer gives them an acidic and chelating character. The previous results with dibutylphenacylphosphonate HDBPP and various metals have mostly shown the extraction by solvation through the P=O group (3)-(5). Evidence for the extraction from perchlorate medium by compound formation or acidic extraction (chelation has been suggested) has been found for U(VI) and Th(IV) (3) and (5). But in the U(VI) case the acidic extraction coexists with the neutral extraction. This work describes the extracting ability of HDBPP for Gd (III) and the separation by extracting the trivalent lanthanides from a perchlorate aqueous solution.

EXPERIMENTAL

Distribution measurements : They were performed in a thermostated vessel at (20±0.1)°C. The determination of the distribution ratio was made by γ-counting using a NaI(Tl) well type scintillation detector for the exhaustive study of Gd extraction. A Ge(Li) detector combined with a multichannel analyser was used in the case of simultaneous extraction of several elements. The radioactive tracers are reported in table I.

Chemicals : HDBPP was prepared and purified as described previously (3).

Table I. Nuclides and energies of the γ-lines used for determinations.

Nuclide	$t_{\frac{1}{2}}$	Eγ keV
^{140}La	40.27 h	487.00 1596.17
^{144}Ce	284.4 d	133.53
^{142}Pr	19.2 h	1575.80
^{147}Nd	11.1 d	91.11 531.02
^{151}Pm	28 h	168
^{149}Pm	53 h	285.90
^{151}Pm	28 h	340
^{153}Sm	46.5 h	103.18
^{152}Eu	12 y	121.78 344.27
^{153}Gd	242 d	97.43 103.18
^{160}Tb	72.3 d	86.79 298.57 879.36 962.00 966.15 1177.93
^{165}Dy	2.36 h	94.68
^{166}Ho	27 h	80.57
^{171}Er	7.5 h	124.00 295.91 308.30
^{170}Tm	127 d	84.25
^{169}Yb	32 d	109.78 130.51 177.18
^{177}Lu	6.71 d	208.36

RESULTS AND DISCUSSION

The figures 1, log D=f(log $|SCN^-|$)and 2, log D= f(log $|H^+|$) show that Gd is extracted by HDBPP from thiocyanate medium as by tributylphosphate (TBP) and probably forms an additional complex by bonding the neutral salt $Gd(NCS)_3$ through the donor P=O group. The slope of the curve log D=f(log $|SCN^-|$) is approximately +2 indicating that the predominant complex in the aqueous phase is $Gd(NCS)^{2+}$. The high concentration of the extractant enables the observation of the extraction of $Gd(ClO_4)_3$ and $Gd(BF_4)_3$ at the lower thiocyanate concentration. Figure 2 shows that the distribution of the metal is almost independant of pH when the extraction of thiocyanic acid can be neglected.

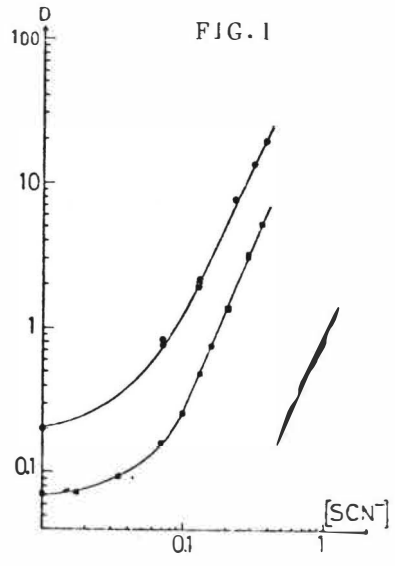

FIG.1

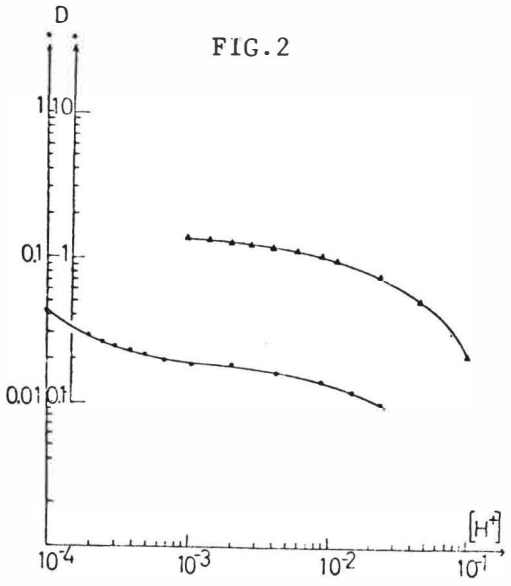

FIG.2

FIG.1

Thiocyanate ion dependence of the extraction of gadolinium.

- 0.94M HDBPP, toluene, 1M(NH_4^+, H^+, ClO_4^-, SCN^-), pH $\leq$ 3, 25°C ;
- 1.1M HDBPP, toluene, 1M(NH_4^+, H^+, BF_4^-, SCN^-), pH $\leq$ 3, 25°C ;
- 0.3M TBP, n-octane, 2M(NH_4^+, H^+, ClO_4^-, SCN^-), pH = 2, 20°C.

FIG.2

Hydrogen ion dependence of the extraction of gadolinium from a perchlorate-thiocyanate medium.

- 0.3M TBP, n-octane, 1M NH_4SCN, 1M(NH_4^+, H^+, ClO_4^-), 20°C ;
- 0.1M HDBPP, solvesso 150, 0.7M NH_4SCN, 0.3M (NH_4^+, H^+, ClO_4^-), 20°C.

From these results we conclude that the behaviour of HDBPP towards the trivalent lanthanides is very similar to that observed with other metal ions in thiocyanate medium (4). The extraction is described by the following equilibrium :

$$M^{3+} + 3SCN^- + x\ \overline{HDBPP} \rightleftharpoons \overline{M(NCS)_3 . xHDBPP} \qquad (1)$$

where x is probably 3 or 4. (Overlined symbols for organic phase species).

In order to find evidence for the acidic extraction, the perchlorate medium, which is less complexing than thiocyanate, was used. Also salts of tetraborofluorate (BF_4^-) are proposed as a low complexing electrolyte. As figure 3 shows the acidic extraction is obtained under the chosen experimental conditions when $|H^+| < 2.10^{-4}$M. At higher concentrations the distribution of metal becomes almost independent of pH, indicating that the neutral extraction becomes predominant. The weak decrease of the curve in these concentration regions suggests the existence of mixed complexes.

The slope of the curve (fig. 4) log D=f (log$|\overline{HDBPP}|$) is exactly equal to +3 in the case of the acidic extraction while it tends towards 3.4 in the case of the neutral extraction. It should be pointed out that the lat-

FIG.3

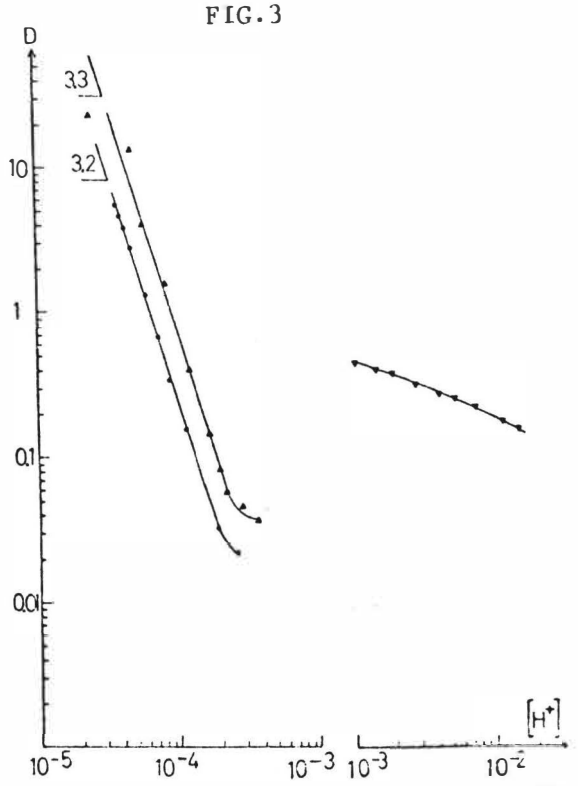

FIG.4

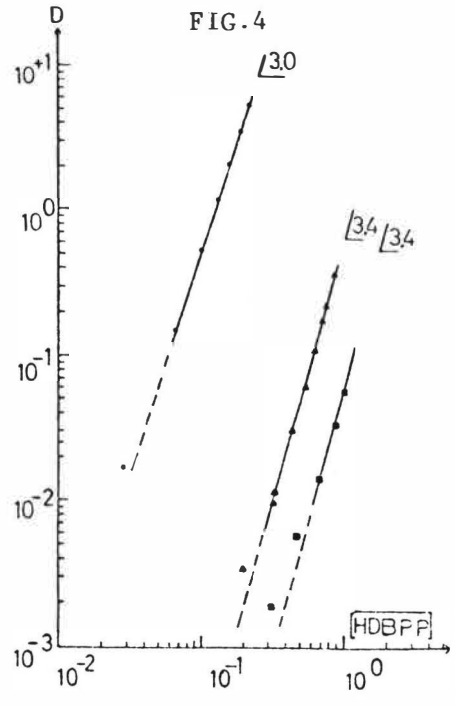

FIG.3

Hydrogen ion dependence of the extraction of gadolinium from a perchlorate aqueous solution.

- ● 0.23M HDBPP, solvesso 150, 1M(H^+, Na^+, ClO_4^-), 20°C ;
- ▲ 0.45M HDBPP, solvesso 150, 1M(H^+, Na^+, ClO_4^-), 20°C ;
- ▼ 0.94M HDBPP, toluene, 1M(H^+, NH_4^+, ClO_4^-), 25°C ;

FIG.4

Extractant dependence of the extraction of gadolinium.

- ● solvesso 150, 1M(H^+, Na^+, ClO_4^-), $|H^+| = (4\pm0.5).10^{-5}$, 20°C ;
- ▲ toluene, 1M(H^+, NH_4^+, ClO_4^-), $|H^+| > 10^{-3}$M, 25°C ;
- ■ toluene, 1M(H^+, NH_4^+, BF_4^-), $|H^+| > 10^{-3}$M, 25°C.

-ter is very unfavourable in ClO_4^- and BF_4^- media in comparison with the former. The ratio between them at a constant concentration of extractant is of the order of 10^3.

In conclusion we suggest that the following equilibrium describes the extraction of lanthanides from BF_4^- and ClO_4^- media :

$$M^{3+} + pX^- + (x+3-p)\overline{HDBPP} \underset{}{\overset{K_{3-p,x}}{\rightleftharpoons}} \overline{MX_p(DBPP)_{3-p}.xHDBPP} + (3-p)H^+ \quad (2)$$

where $X^- = ClO_4^-$ or BF_4^-, $0 \leqslant p \leqslant 3$, $0 \leqslant x \leqslant 4$, p and x are dependent of each other through the total coordination number. For Gd we have p = 0 and x = 0 when $|H^+| < 2\ 10^{-4}$M. The infrared spectra of the organic phases from acidic extractions of Er and Eu show new absorption bands near 1510 (C⋯O), 1400 (C⋯C) and 1160 (P⋯O) cm^{-1}, supporting the hypothesis of chelation (17).

It seemed to be interesting to investigate the separation of the rare earths when the metal is complexed by the enolate, since the best separation between them are obtained with organophosphoric acids like HDEHP or β-diketones like HTTA (7).

Table II. Separation factors and equilibrium extraction constants $K_{ex} = [M(DBPP)_3][M^{3+}]^{-1}[H^+]^3[HDBPP]^{-3}$ Solvesso 150 - 1M(H^+,Na^+,ClO_4^-)

Z	$\alpha_{Z,Z-1}$	$\alpha_{Z,La}$	- log K_{ex}
La			
Ce	4.4±0.3	4.4±0.3	
Pr	1.36±0.04	6.0±0.5	
Nd	1.18±0.04	7.1±0.5	
Pm	1.67±0.04	12±1	
Sm	1.93±0.04	23±2	
Eu	1.23±0.02	28±2	
Gd	0.77±0.02	21±2	10.5±0.2
Tb	1.83±0.02	39±3	
Dy	1.38±0.04	54±5	
Ho	1.09±0.03	60±5	
Er	1.16±0.02	71±6	
Tm	1.83±0.04	130±10	
Yb	2.08±0.02	271±21	
Lu	1.07±0.03	300±25	

Table III. Comparison of HDBPP with HTTA and HDEHP

Extractant	$\alpha_{Lu,La}$	$\alpha_{Z,Z-1}$	logK_{ex} (Gd)	ref.
HDBPP	$3 \cdot 10^{+2}$	1.7	-10.5 ±0.2	Present work
HTTA	$3 \cdot 10^{+3}$	1.8	-8.40±0.04	[14]
HTTA	$5.5 \cdot 10^{+3}$	(2.7)	-7.57	[15]
HDEHP	$9.78 \cdot 10^{+4}$	2.4±0.9		[16]

In order to determine the separation factor of the elements with a maximum of precision, distribution experiments with several elements admixed were performed. The 15 elements were divided in the four following groups, employing at least one common element from one group to another.

i) La, Ce, Pr, Nd, Pm, Sm, Eu, Tb.
ii) Gd, Tb, Tm, Yb.
iii) Dy, Ho, Er, Tm, Lu.
iv) Gd, Ho, Er, Tm, Lu.

Energies of γ-lines that were used to determine the distribution ratio are given in Table I. The separation factors between adjacent elements $\alpha_{Z/Z-1}$, between lutetium and lanthanum $\alpha_{Lu/La}$ and K_{ex} values for each lanthanide are given in Table II. These results show a lower distribution ratio for Gd than for Eu and Sm. The separation factor between Lu and La is approximately $3 \cdot 10^2$ and the mean separation factor between adjacent elements approximately 1.7. Table III compares these values to those obtained with other well known extractants.

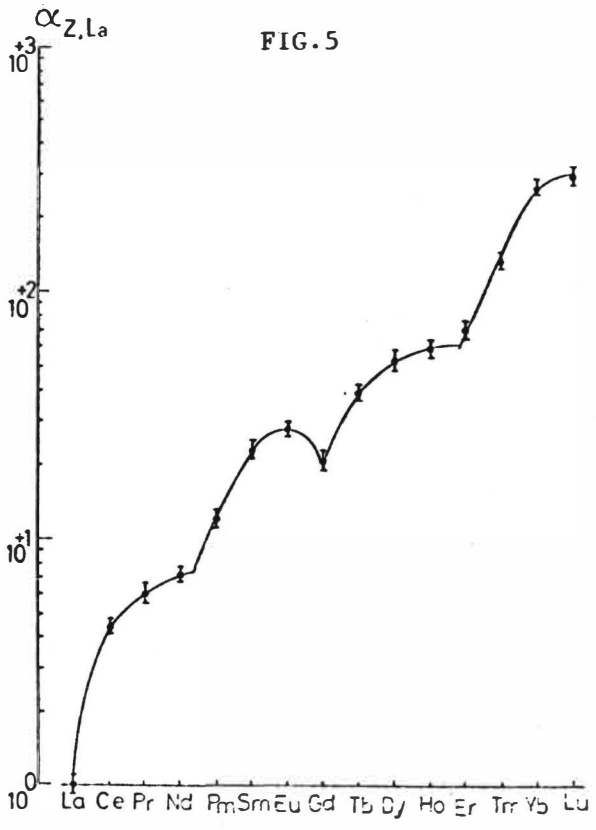

FIG.5

FIG.5
Variation of logarithm of separation factors with atomic number.
0.1 - 0.25 M HDBPP, solvesso 150, 1M (H^+, Na^+, ClO_4^-), $|H^+| < 2.10^{-4}$M, 20°C.

In a plot of log $K_{3,0}$ or log $\alpha_{Z/La}$ vs. Z (fig.5) division of the series into four "tetrades" appears distinctly (8)-(9), while a plot of $\alpha_{Z/Z-1}$ vs. $|Z-1, Z|$ fits well into the regularities of the so-called double-double effect (10)-(11). These experimental facts have been observed in several liquid-liquid extraction systems and are interpreted to some extent as a disclosure of the nephelauxetic effect in the 4f series (12)-(13). This effect is in general distinctly observed when the ligand is strongly bonded to the central atom forming an inner sphere complex. The exceptional low value of $\alpha_{Gd/La}$ in regard to Sm and Eu may suggest a change in the coordination number throughout the lanthanides series; compounds like $M(DBPP)_3$ and $M(DBPP)_3.(HDBPP)$ are expected with $Z \geq 64$ and $Z < 64$ respectively.

REFERENCES

1) D. Sevdic and H. Meider-Gorican : J. Less. Common metals, 37,103 (1974).

2) P. Bronzan and H. Meider-Gorican : J.Less, Common Metals, 29,407 (1972).

3) J.L.Martin and M.J.F.Leroy : J.Chem.Res. (S) 88 (1978) (M) 1113 (1978).

4) J.P.Brunette, M.J.F.Leroy, B.Ceccaroli and J.Alstad : Acta Chem.Scand., A32, 415 (1978).

5) B.Allard, J.P.Brunette, U.Olofsson and A.Selme : To be published.

6) J.P.Brunette, U.Olofsson, A.Selme and B.Allard : To be published.

7) Y.Marcus and A.S.Kertes : Ion Exchange and Solvent Extraction of Metal complexes, Wiley-Interscience,(1969), 509 and 945.

8) D.F.Peppard, G.W.Mason and S. Lewey : Solvent Extraction Research (Edited by A.S. Kertes and Y.Marcus), Wiley-Interscience, New-York (1969), 49.

9) D.F.Peppard, C.A.A.Bloomquist, E.P.Horwitz, S.Lewey and G.W.Mason : J. Inorg. Nucl. Chem. 32, 339 (1970).

10) S.Siekierski and I.Fidelis : J. Inorg. Nucl. Chem. 33, 3191 (1971).

11) S.Siekierski : J. Inorg. Nucl. Chem. 33, 377 (1971).

12) C.K.Joergensen : J. Inorg. Nucl. Chem. 32, 3127 (1970).

13) L.J.Nugent : J. Inorg. Nucl. Chem. 32, 3485 (1970).

14) J.Alstad, J.H.Augustson and L.Farbu : J. Inorg. Nucl.Chem. 36, 899 (1974).

15) Y.Marcus and A.S.Kertes : Ref. 7, 509.

16) T.B.Pierce and P.F. Peck : Analyst 88, 217 (1963).

17) F.A. Cotton and R.A.Schunn : J. Am. Chem. Soc. 85, 2314 (1963).

SOLVENT EXTRACTION OF LANTHANIDES BY 2-ETHYLHEXYLPHOSPHONIC ACID MONO-2-ETHYLHEXYL ESTER

Ma Enxin Yan Xiaomin Wang Sanyi
Long Haiyan Yuan Chengye

Shanghai Institute of Organic Chemistry,
Academia Sinica, Peoples Republic of China.

The chemistry of extraction of lanthanide and yttrium by 2-ethylhexylphosphonic acid mono-2-ethylhexyl ester (HL) in n-dodecane from nitric acid was described. By MW determination, NMR and the slope method, the extraction reaction was studied. Based upon elementary analyses, IR, NMR as well as MW determination, the compositions of the complexes formed by saturation of HL with $La(NO_3)_3$ and $Nd(NO_3)_3$ were studied. Both the standard enthalpy changes ($-\Delta H^{o}$) as well as the relative free energy and entropy changes ($-\Delta Z_T^{o}$) (ΔS_T^{o}) of the extraction reaction were also estimated. The regularity of the variation of Kex(concentration equilibrium constant), $-\Delta Z_T^{o}$ and ΔS_T^{o} reveales the tetrad effect. The average separation factor of adjacent lanthanides was calculated to be as high as 3.04.

The acidic organophosphorous compounds for extraction of lanthanides have been studied extensively with di-(2-ethylhexyl) phosphoric acid (D2EHPA) (1,2). As indicated by earlier reports from our laboratory, on substituting a P-C bond for a P-O-C in D2EHPA molecule, the pKa value of the resulted compound 2-ethylhexylphosphonic acid mono-2-ethylhexyl ester (simplized as mono-isooctyl isooctylphosphonate and denoted as HL) increases owing to the weakened effect of negativity of alkoxy group and the distribution ratio of lanthanide by this extractant decreases respectively. Besides this, mono-isooctyl isooctylphosphonate possesses notable properties in extracting medium and heavy rare earths in less acidic solution(2). Nevertheless, there are only a few reports dealing with extraction behaviours of mono-alkyl alkylphosphonate for lanthanides(3-6). For mono-isooctyl isooctylphosphonate, it has been described only for extraction of promethium, uranium and curium in the chloride system(3), and thorium in the nitrate system(7). However, the degree of aggregation(8a), IR(8b) and NMR(9) studies of this extractant have heen reported.

The extraction of lanthanides(except promethium) and yttrium by mono-isooctyl isooctylphosphonate in n-dodecane from nitric acid is described in detail in this paper. The aggregation of this extractant in an aliphatic diluent was determined by vapor pressure osmometry and proton nuclear magnetic resonance spectra. From the slope method, the extraction equation was also deduced. The solid complexes of mono-isooctyl isooctylphosphonate with lanthanum and neodymium nitrate were prepared by the saturation method.

Based upon elementary analyses, IR, NMR spectra as well as MW determi-

nation, the composition of these species was estimated. The extraction equilibrium constants(Kex) at various temperatures(10-60°C) were calculated. Besides these, both the standard enthalpy changes($-\Delta H^{o}$)and the free energy changes($-\Delta Z^{o}_{r}$) as well as the entropy changes(ΔS^{o}_{r}) related to lanthanum for all other lanthanides of this extraction reaction were also estimated. On the basis of general physico-chemical concepts and the lanthanide contraction, the regularity of the variation of the concentration equilibrium constants and these thermodynamic functions were examined and discussed.

EXPERIMENTAL

1. REAGENTS

2-Ethylhexylphosphonic acid mono-2-ethylhexyl ester was synthesized in our laboratory and purified through its copper salt. A product with more than 99% purity was determined by potentiometric titration. The purity of the extractant was also checked by elementary analyses. Found C, 62.71; H, 11.51; P, 10.11 compared with C, 62.68; H, 11.42; P, 9.73 calculated for $C_{16}H_{35}O_3P$. n-Dodecane was used as BDH reagent. Lanthanides(except cerium)and yttrium solutions were prepared from nitrates, converted from S.P. grade oxides. Cerium was used as nitrate with high purity. Other reagents were A.P. grade.

2. METHODS

A. Extraction Equilibrium: Equal volumes of organic and aqueous phases were shaken for 30 minutes in a separatory funnel at 25°C. For the study of temperature effect, the separatory funnels with a water jacket connected to a thermostat were used. All data are the average values of at least two experimental results.

B. Preparation of Solid Complexes: Equal volumes of mono-isooctyl isooctylphosphonate 0.1M in n-dodecane solution and aqueous solution of 0.1M lanthanide nitrate were sufficiently mixed by shaking in a separatory funnel. In the mixing process, the pH value of aqueous layer must be adjusted to neutrality by adding continuously 1M ammonium hydroxide sol. to the system. After the establishment of equilibrium, the aqueous phase was discharged. The saturation and equilibrium experiments were repeated until the concentration of lanthanide did not change after three operations as shown above. A waxy solid was obtained by centrifugation of the saturated organic phase followed by desiccation in a Abderhalden vacum drying apparatus for four hours at 80°C.

3. ANALYSES

Concentrations of lanthanide were determined either volumetrically by EDTA titration with xylenol orange as indicator(10) or spectrophotometrically by ArsenazonIII(11). In the case of low distribution ratios in extration, the concentration of the rare earths was estimated in the organic phase in order to minimize experimental errors in analysis. The content of lanthanide in solid complexes was also determined from its solution in n-dodecane by stripping with nitric acid. The nitrate ion and phosphorus contents in the solid complex were analysed by the spectrometrical method with phenol diphenylsulfonate(12a) and phosphomolybdic blue(12b), respectively. The organic material in the solid complex was decomposed by ignition with a mixture of concentrated nitric acid and sulfuric acid. The water content was determined by Karl-Fisher method(13).

4. INSTRUMENTS

A. Hitachi 115 model molecular weight apparatus. Dibenzoyl acetone (MW 210.2) as standard.

B. Perkin-Elmer 557 IR spectrometer. Samples were made as liquid film or CsI pellet.

C. JEOL PS-100 model NMR apparatus. CCl_4 as solvent and HMDS as reference.

RESULTS AND DISCUSSIONS

1. EXTRACTION EQUILIBRIUM

By VPO method, the molecular weight of mono-isooctyl isooctylphosphonate was found to be 636.8, supporting the existence of a dimer in an aliphatic solvent . The NMR spectra of mono-isooctyl isooctylphosphonate show the chemical shift of associated proton at 12 ppm, which disappears upon deuterium exchange.The dimer of mono-isooctyl isooctylphosphonate is denoted as $(HL)_2$ in this paper.

The solvent extraction of a lanthanide in less acidic solution with acidic phosphoric(phosphonic) ester can be considered as a cation exchange process. In the extraction system: Ln(0.01M),(Na,H)NO_3(1M), various acidity/HL(0.5F), n-dodecane, the plot of $LogD/[(HL)_2]^3_{org}$ versus $Log[H^+]_{aq}$ was found to be a straight line for each lanthanide with the slope near to -3 except for lanthanum (FIG.1a).

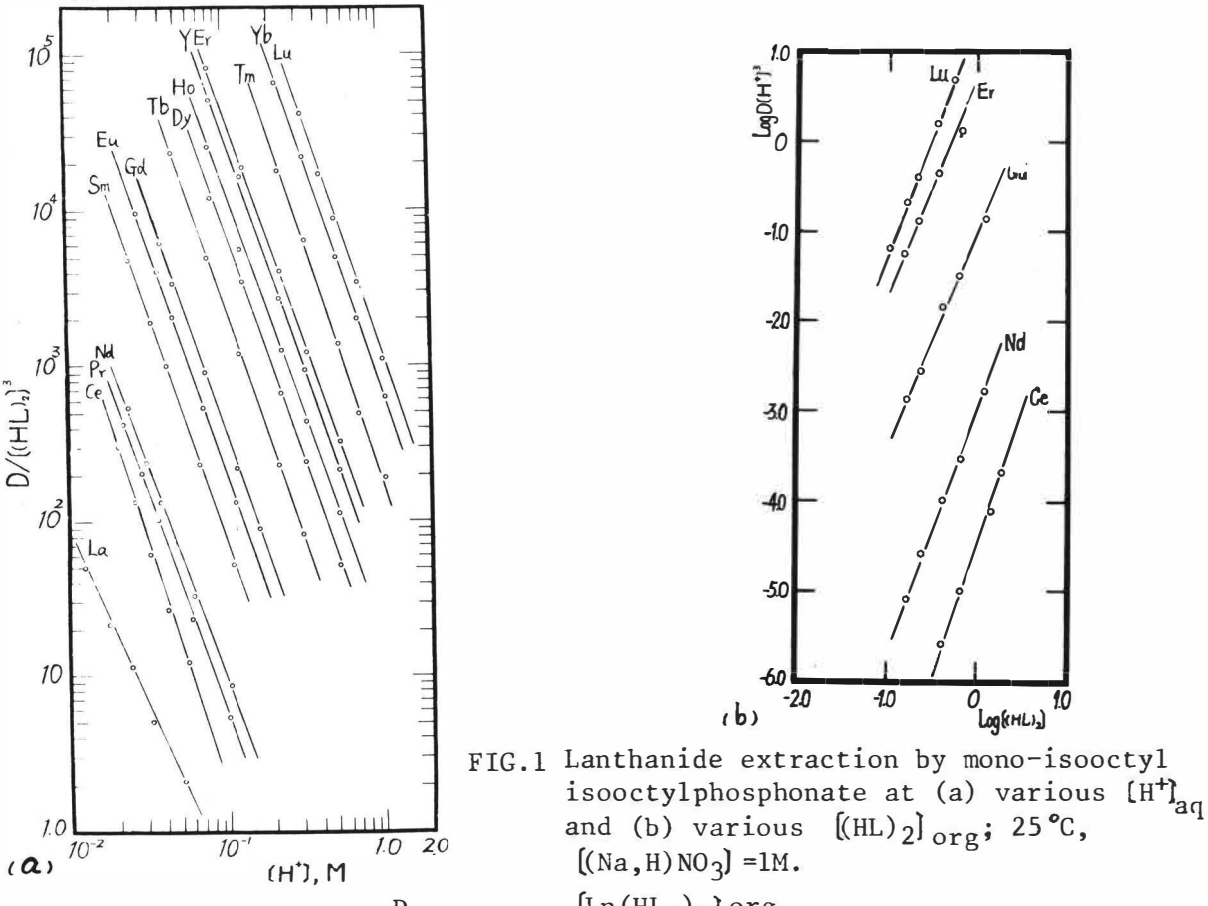

FIG.1 Lanthanide extraction by mono-isooctyl isooctylphosphonate at (a) various $[H^+]_{aq}$ and (b) various $[(HL)_2]_{org}$; 25 °C, $[(Na,H)NO_3]$ =1M.

We define: $$D' = \frac{D}{[(HL)_2]^3_{org}} = \frac{[Ln(HL_2)_3]_{org}}{[Ln^{3+}]_{aq}\,[(HL)_2]^3_{org}}$$

In this equation, all terms are experimental values with $[(HL)_2]_{org} = 0.5/2 - 6x[Ln(HL_2)_3]_{org}$. $[H^+]_{aq}$ is denoted as acidity of the aqueous phase in equilibrium.

In the extraction system: Ln(0.01M),(Na,H)NO_3(1M)/HL(various conc.), n-dodecane, the plot of $LogD\,[H^+]^3_{aq}$ versus $Log\,[(HL)_2]_{org}$ was found to be a straight line. For Ce, Nd, Gd, Er and Lu as lanthanides,the slope is close to 3(FIG.1b).

Thus, the extraction reaction of lanthanide nitrate by mono-isoctyl isooctylphosphonate could be written as the following equation:

$$Ln^{3+}_{aq} + 3(HL)_{2org} \rightleftharpoons Ln(HL_2)_{3org} + 3H^+_{aq} \qquad (1)$$

The thermodynamic equilibrium constant is then

$$K = \frac{[Ln(HL_2)_3]_{org}\,[H^+]^3_{aq}}{[Ln^{3+}]_{aq}\,[(HL)_2]^3_{org}} \cdot \frac{\gamma_{Ln(HL_2)_3}\cdot\gamma^3_{H^+}}{\gamma_{Ln^{3+}}\cdot\gamma^3_{(HL)_2}} \qquad (2)$$

As the aqueous ionic strength was constant (1M) in the experiments, the product of activity coefficients may be assumed constant.

The concentration equilibrium constant then becomes

$$Kex = \frac{[Ln(HL_2)_3]_{org}\,[H^+]^3_{aq}}{[Ln^{3+}]_{aq}\,[(HL)_2]^3_{org}}$$

2. THE COMPOSITION AND STRUCTURE OF SOLID COMPLEXES

The prepared solid complexes of mono- isooctyl isooctylphosphonate with lanthanum or neodymium nitrate are waxy solids with a white and purplish colour, respectively. They are practically insoluble in water and mineral acids, soluble very little in ethanol and acetone and slightly soluble in chloroform, carbon tetrachloride, benzene, n-hexane and n-dodecane(<1%). The melting points of these waxy solids are higher than 400°C.

The elementary analysis of the solid complexes, shows the presence of NO_3 groups on the basis of the nitrogen content. From the results in TAB.1 the composition of the solid complex may be considered as a mixture of LnL_3 and $Ln(NO_3)L_2$. The saturated extraction for the preparation of complexes has been carried out in neutral medium, which favours the formation of the complex with a NO_3 group. Hence, we assume that there are two reactions going on in the saturated extraction.

$$Ln^{3+}_{aq} + 3/2(HL)_{2org} \rightleftharpoons LnL_{3org} + 3H^+_{aq}$$

$$Ln^{3+}_{aq} + NO^-_{3aq} + (HL)_{2org} \rightleftharpoons Ln(NO_3)L_{2org} + 2H^+_{aq}$$

TABLE. 1 The elemertary analysis of the solid complexes (%).

Element	C	H	N	P	Ln	P/Ln	NO_3/Ln
Found (La Complex)	52.72	9.25	0.47	8.39	14.0	2.7	0.33
Calcd. as LaL_3	54.64	9.74		8.81	13.17		
Calcd. as $La(NO_3)L_2$	47.35	8.44	1.73	7.63	17.11		
Found (Nd Complex)	51.33	9.13	0.65	7.73	14.36	2.5	0.38
Calcd. as NdL_3	54.36	9.70		8.76	13.60		
Calcd. as $Nd(NO_3)L_2$	47.04	8.39	1.71	7.58	17.66		

The molecular weight of these solid complexes were measured in organic solutions showing a very high values; for both lanthanum complex, 22400 (n-hexane), 40800(chloroform) and neodymium complex, 17100(n-hexane), 39900 (chloroform). The solution of complexes existed as a viscous liquid and converted to silky form after evaporation of the solvent. These results clearly indicate that these solid complexes are polymers in nature with the degree of aggregation ranging from 20 to 40. The water content of these solid complexes were found to be 0.63% and 0.95% for lanthanum and neodymium complexes, respectively.

The IR spectra of the complexes are given in FIG.2 with the sampling form of liquid film which gives more clear spectra than with CsI pellets.

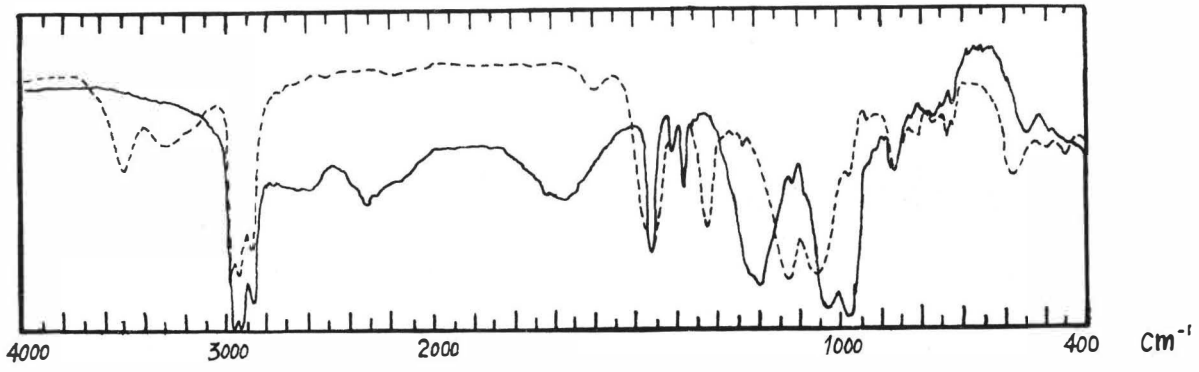

FIG.2 IR spectra(film) of mono-isooctyl isooctylphosphonate (solid line) and its complex with lanthanum(dashed line).

By comparing the IR spectra of the lanthanum complex with the parent compound mono-isooctyl isooctylphosphonate , some obvious differences are shown as follows :

4000-3000cm^{-1} : H_2O absorption bands at 3500-3300cm^{-1} for the complex were observed.

3000-1500cm^{-1} : The broad absorption bands(2600, 2300 and 1680 cm^{-1}) of the associated OH group existing in the parent ligand disappeared in the complex.

1500-1000cm^{-1} : The band at 1460cm^{-1} due to CH_2 and CH_3 broadened in the complex probably due to the overlap of the asymmetric stretching absorption band of a coordinated NO_3 group. The new absorption band appearing at 1322cm^{-1} may be assigned to the symmetric stretching absorption. With the disapearance of the original P=O sharp absorption (1200cm^{-1}) and P-O-C absorption (1040, 985 cm^{-1}) in the complex, the asymmetric absorption (1125cm^{-1}) and symmetric absorption (1050cm^{-1}) of $P\begin{smallmatrix}O\\O\end{smallmatrix}^{-}$ occur.

The absorption band at 1322cm^{-1} in the complex is approximately near the vibration absorption of a ionic NO_3^- group. However, we tend to assign this absorption as symmetric of coordinated NO_3 group for the broadened band at 1460cm^{-1} of CH absorption. In the IR spectra of the neodymium complex, the occurrence of a new absorption band at 1490cm^{-1} assigned to a coordinated NO_3 group is more appearent (FIG. 3). Besides this, the new absorption is stronger than that at 1322cm^{-1}.

Only very small variation was observed in the IR spectra between the lanthanum complex and the neodymium complex. The IR spectrum of the lanthanum complex with mono-isooctyl isooctylphosphonate prepared from a chloride medium does not reveal the absorption band at 1322cm^{-1} and also the broad absorption

band at 1460 cm^{-1} for CH_2 and CH_3. Based on these observations, we can conclude that the NO_3 group exists in a coordinated form in the prepared complexes with the asymmetric stretching absorption ν_1 and asymmetric stretching absorption ν_4 at 1490 and 1322cm^{-1}, respectively. It may still be considered that the NO_3 group is a bidentate bonded to the lanthanide due to $\nu_1-\nu_4$= 168cm^{-1} (14).

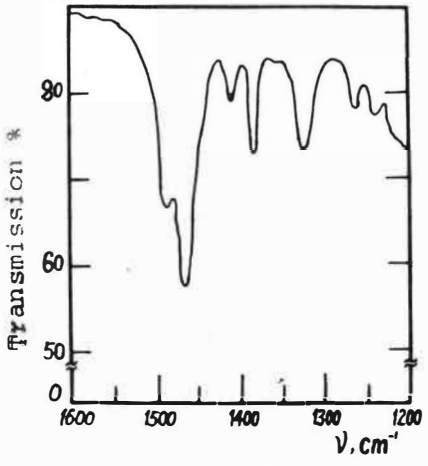

FIG.3 The characteristic frequencies of the NO_3 group in the complex of mono-isooctyl isooctylphosphonate with neodymium.

The proton nuclear magnetic resonance spectra of the complex of lanthanum with mono-isooctyl isooctylphosphonate indicate the disappearance of the hydrogen chemical shift(δ=12ppm) of the hydroxyl group which has been exchanged by the metal ion and the lines are as broad as found in the parent compound (FIG. 4).

The chemical structure of the two kinds of complex may be considered as $[La(NO_3)_{0.3}L_{2.7}\cdot mH_2O]_n$ and $[Nd(NO_3)_{0.4}L_{2.6}\cdot mH_2O]_n$,

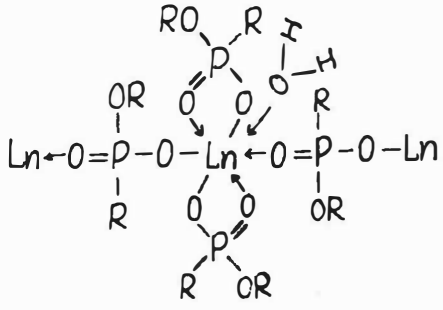

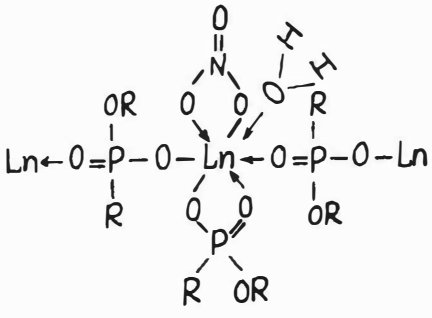

3. DETERMINATION OF THE THERMODYNAMIC FUNCTIONS ΔH^o, ΔZ_r^o AND ΔS_r^o

The concentration equilibrium constants of lanthanide nitrate extraction in n-dodecane at 10, 25, 40 and 60°C were estimated. The original lanthanide concentration,(Ln) is equal to 0.01M. The equilibrium aqueous acidity for La, Ce-Nd, Sm-Gd, Tb-Dy, Ho-Er and Y, and Tm-Lu is 0.015, 0.05, 0.16 0.4, 0.7, and 1.9M, respectively. The total nitrate concentration in aqueous phase for La-Er and Y, and Tm-Lu is 1 and 1.9M, respectively. The plot of LogKex versus 1/T was found to be a straight line for all lanthanides(FIG.5) There is no obvious change in the extraction for La, Ce,Pr and Nd at various temperatures. According to the inversion equation of Clapeyron-Clausius equation ΔLogKex Δ1/T = $-\Delta H^o/2.303R$, the enthalpy changes ΔH^o of the extraction equilibrium reaction were estimated by the least-square method(TAB.2). The ΔH^o values for various acidity of the gadolinium nitrate solution were estimated as identical.

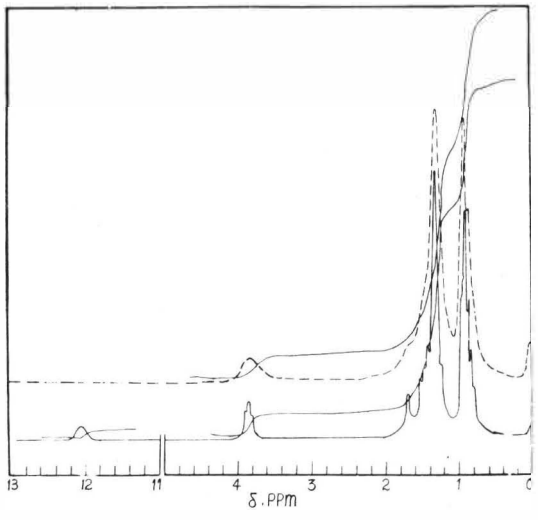

FIG.4 NMR spectra of mono-isooctyl isooctylphosphonate(solid line) and its complex with lanthanum (dashed line).

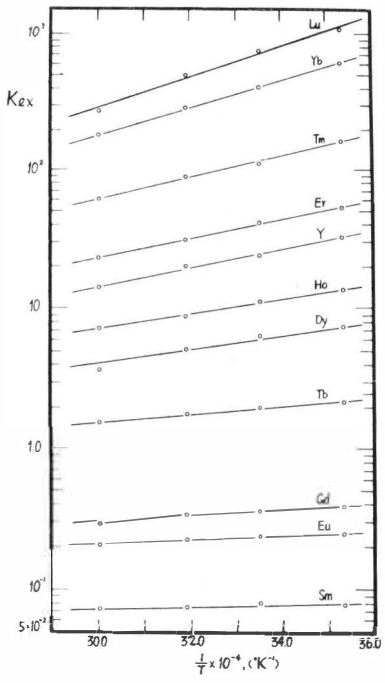

FIG.5 Kex values of lanthanides extraction by HL at various temperature.

TABLE 2 Concentration equilibrium constants, separation factors, thermodynamic functions for lanthanides extraction with mono-isooctyl isooctylphosphonate in n-dodecane from nitric acid

Element	Kex	D'*	$\alpha^{**}_{z+1/z}$	$\alpha_{Ln/La}$	ΔZ^o_r Kcal/Mole	ΔH^o Kcal/Mole	ΔS^o_r Cal/Mole·deg
La		2.3					
Ce	2.21×10^{-3}	16.4	7.13	7.13	-1.16		3.89
Pr	4.73×10^{-3}	40.8	2.49	17.7	-1.70		5.70
Nd	6.93×10^{-3}	59.5	1.46	25.9	-1.93		6.47
(Pm)***		1.60×10^{2}	2.69	69.6	-2.51		8.41
Sm	7.42×10^{-2}	5.7×10^{2}	3.56	2.48×10^{2}	-3.27	-0.31	9.89
Eu	0.201	1.65×10^{3}	2.89	7.17×10^{2}	-3.90	-0.66	10.86
Gd	0.366	3.1×10^{3}	1.88	1.35×10^{3}	-4.27	-0.97	11.06
Tb	2.47	2.0×10^{4}	6.45	8.70×10^{3}	-5.38	-1.29	13.71
Dy	8.04	6.3×10^{4}	3.13	2.72×10^{4}	-6.05	-2.11	13.21
Ho	15.6	1.16×10^{5}	1.86	5.04×10^{4}	-6.42	-2.41	13.44
Er	48.2	3.7×10^{5}	3.19	1.61×10^{5}	-7.11	-3.11	13.40
Tm	2.07×10^{2}	2.2×10^{6}	5.95	9.6×10^{5}	-8.17	-3.78	14.71
Yb	7.64×10^{2}	7.2×10^{6}	3.27	3.13×10^{6}	-8.87	-4.51	14.62
Lu	1.26×10^{3}	1.32×10^{7}	1.83	5.74×10^{6}	-9.23	-5.15	13.68
Y	33.8	2.5×10^{5}		1.07×10^{5}	-6.88	-2.99	13.04

*D'=Distribution ratio(extrapolated value) at 0.05M (H^+) and 1M (HL).
**α =Spearation factor(extrapolated value) at 0.05M (H^+) and 1M (HL).
***Values referred to Pm are extrapolated values.

The relationship between the standard free energy change(ΔZ^{o}) of the extraction equilibrium reaction and K is $\Delta Z^{o}=-RTLnK$. The relative free energy change of each lanthanide, ΔZ_r^o can be expressed by the following equation: $\Delta Z_r^o=\Delta(\Delta Z^{o})=-RTLnKz/Kz'=-RTLn\alpha$, where α is the separation factor for two lanthanides. Assuming that the product of activity coefficients is identical for all lanthanides we obtain: $\alpha = Kex,z/Kex,z' \sim D'z/D'z'$, where D' was estimated by regressing the line to $\{H^{+}\}=0.05M$ from FIG.1. Thus, we can estimate the free energy changes related to lanthanum for each lanthanide, ΔZ_r^o. Relating ΔZ_r^o to ΔH^{o}, the relative entropy change can also be calculated.

4. REGULARITIES OF THE VARIATION OF THE EXTRACTION EQUILIBRIUM PARAMETERS AND THE THERMODYNAMIC FUNCTIONS WITH ATOMIC NUMBER OF LANTHANIDES

The plots of estimated thermodynamic functions, ΔZ_r^o, ΔH^{o} and ΔS_r^o, as well as Kex versus atomic number of lanthanides are shown in FIG.6 and FIG.7. As indicated by these figures, the Kex values and the absolute values of relative free energy change increase with the increase in atomic number of the lanthanides. These plots reveal obvious tetrad effect(15). All lanthanides may be divided into four subgroups: La-Ce-Pr-Nd, (Pm)-Sm-Eu-Gd, Gd-Tb-Dy-Ho, Er-Tm-Yb-Lu. Gd lies both in the second and the third subgroup. Y locates between Ho and Er d to the appropriate ionic radius.

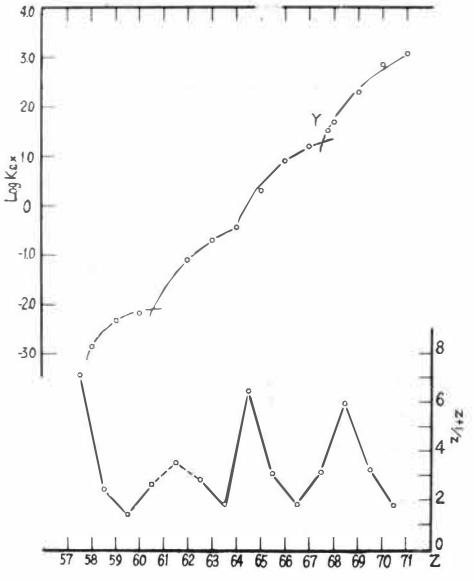

FIG.6 Relationship between the extraction parameters(Kex, $\alpha_{z+1/z}$) and atomic number of lanthanides.

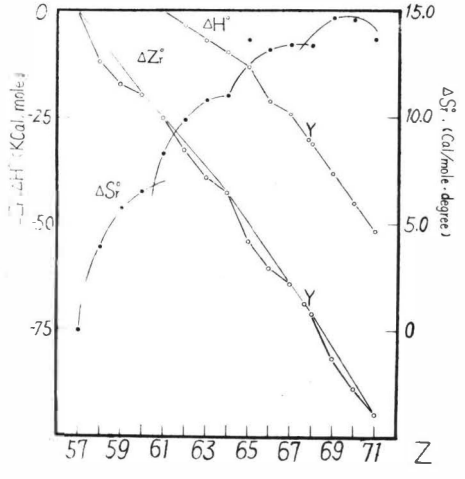

FIG.7 Relationship between the thermodynamic functions and atomic number of lanthanides.

The absolute value of the enthalpy change, $-\Delta H^{o}$ for lanthanide extraction by mono-isooctyl isooctylphosphonate increases with increasing of atomic number of the lanthanide. It means that the released heat increases in the reaction with atomic number. Fidelis(16-18) showed that the regularities of the variation of enthalpy change of lanthanide extraction by tributylphosphate and other extractants reveal the tetrad effect. But the behaviour of extraction by mono-isooctyl isooctylphosphonate has not been reported.

The relative entropy change of the extraction reaction increases with the increasing of atomic number of the lanthanides. (The value for Tb shows some deviation). It shows the fact that the entropy change as well as the enthalpy change increase with the atomic number favours the extraction reaction. The regularity of the variation of ΔSr^{o} with the atomic number also reveals a tetrad effect.

The separation factor between the first and the second element in each group is the largest and that between the third and the fourth element is the smallest (FIG.4). The following is noteworthy. The average separation factor of adjacent lanthanides for this extraction system was calculated to be as high as 3.04 which is higher than that for all reported extraction systems for lanthanides.

The extraction equilibrium and the free energy change, an energy function directily related to the extraction reaction, increases with the increasing of atomic number. As the free energy change is composed of two parts,the enthalpy change ΔH^{O} and the entropy change $\Delta S^{\bullet}$, the extraction reaction of a lanthanide can be considered as a process in which the hydrated trivalent lanthanide ion is converted to chelated molecules soluble in the organic solvent (FIG.8). The lanthanide ion is a "hard acid" having a serious tendency of hydration in aqueous solution. The entropy change is assumed to depend on the energy change of the rearrangement of the particles in the reaction and reflects the difference in bond energy between the hydrated lanthanide ion and chelated lanthanide. As the ionic radius of the lanthanide decreases with the increase of the atomic number, the hydration ability of lanthanide ions increases with the increase in atomic number. In the process of formation of similar chelated molecules, the released heat (enthalpy change - ΔH^{O}) also increases with the increase of atomic number of lanthanides. The entropy change ΔS^{O} is concerned with the degree of disorder of the system in the reaction. In the extraction process, the coordinated water molecules are converted to free water molecules and the total number of particles in this system increases. Both of them cause the increase in the entropy change. Owing to the enlargement of configurational entropy, the formed chelates are more stable. Thus, the entropy change of the extraction reaction favours the reaction. As the hydration ability of the lanthanide increases with the atomic number, the relative entropy of extraction also increases with the increase of the lanthanides atomic number.

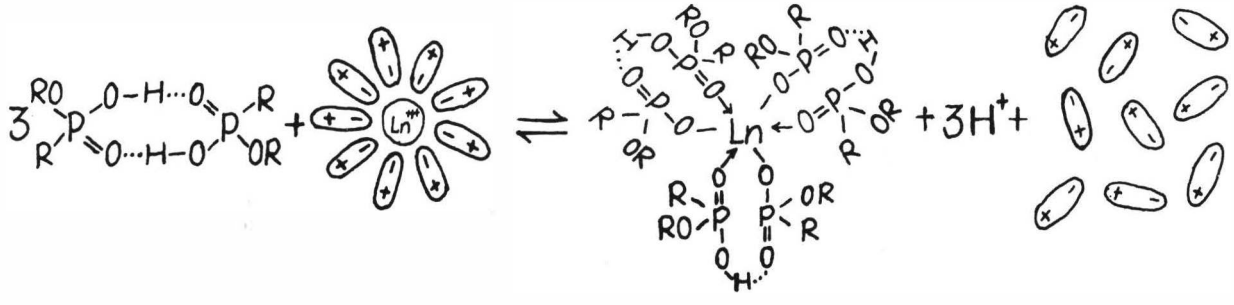

FIG.8 Schematic diagram for the extraction process of lanthanide with mono-isooctyl isooctylphosphonate.

As far as authors are aware of ,the tetrad effect between atomic number of lanthanides and entropy change (ΔS) of the extraction reaction in any systems has not yet been reported in the literature (15). Further study on the regularity of variation of thermodynamic functions in the process of extraction with the atomic number of lanthanides would be helpful in shedding light on the intrinsic nature of the tetrad effect.

REFERENCES

1. Weaver, B., in"Progress in the Science and Technology of the Rare Earths", (ed. Eyring, L.), Pergamon, 1968, Vol.3, 129.
2. Yuan Chengye. Kexue Tongbao 11, (1977), 465.
3. Peppard, D. F., & Mason, G. W., Hucher, I., J. Inorg. Nucl. Chem., 18, (1961), 245.
4. Peppard, D. F., Mason, G. W., & Lewey, S., J. Inorg. Nucl. Chem., 27, (1965), 2065.
5. Mikhalin, E. B., Glimboski, A. V. et al. Izv. Vyssh. Ucheb. Zaved., Tsvetn. Metall., 6 (1976), 62.
6. Radosevic, J., Jagodic, V., & Herak, M. J., J. Inorg. Nucl. Chem., 39, (1977), 2053.
7. Peppard, D. F., Namboodri, M. N., & Mason, G. W., J. Inorg. Nucl. Chem., 24, (1962), 979.
8. Peppard, D. F., Ferraro, J. R., & Mason, G. W., J. Inorg. Nucl. Chem., (a) 7, (1958), 231; (b) 12, (1959), 60.
9. Ferraro, J. R., & Peppard, D. F., J. Phys. Chem., 67, (1963), 2639.
10. Kinnuen, J., & Wennerstrand, B., Chemist Analyst, 46, (1957), 92.
11. Savin, S.B., Zavod. Lab., 29, (1963), 131.
12. (a) Boltz, D. F., & Taras, M. J., in "Colorimetric Determination of Nonmetals", 2 ded., (ed. Boltz, D. F., & Howell, J. A.), A Wiley-interscience Publication John Wiley & Sons, New York, 1978, 222. (b) Boltz, D. F., Lueck, C. H., & Jakubiec, R. J., in ibid., 1978, 343.
13. Mitchel, J., & Smith, D. M., "Aquametry", Interscience Publishers Inc., New York, 1948, 65.
14. Curtis, N. F., & Curtis, Y. M., Inorg. Chem., 4, (1965), 804.
15. Peppard, D.F., Mason, G. W., & Lewey, S., in "Solvent Extraction Research", (ed. Kertes, A. S. & Marcus, Y.), Wiley-interscience, New York, 1969, 49.
16. Fidelis, I., Siekierski, S., in "Proceedings of the Tenth Rare Earth Research Conference", (ed. Kevane, C. J., Moeller, T.), Carefree, Arizona, 1973, Vol. II, 919.
17. Fidelis, I., in "Proceedings International Solvent Extraction Conference", S. C. I., London, 1974, Vol. II, 1073.
18. Fidelis, I., & Krejzler, J., J. Radioanal. Chem., 31, (1976), 45.

THE EXTRACTION OF LANTHANIDES AND AMERICIUM BY BENZYLDIALKYLAMIDES AND BENZYLTRIALKYLAMMONIUM NITRATES FROM THE NITRATE SOLUTIONS, STRUCTURE AND AGGREGATION THEIR SALTS.

Jedináková Věra, Žilková Jana,
Dvořák Zdeněk, Vojtíšková Marta
Department of Nuclear Fuel
Technology and Radiochemistry,
Institute of Chemical Technology
Prague, Czechoslovakia.

Benzyldialkylamine and benzyltrialkylammonium nitrates were used for the extraction of lanthanides and americium from aqueous nitrate solutions. The difference in distribution coefficients can be used for the separation of the lanthanides from americium.

The positive extraction properties of benzyldimethyldodecylammonium nitrate (further $BDMLNNO_3$) were confirmed in investigating the extraction of lanthanides(1-3) and americium (4) from acidic nitrate solutions. Other long-lived nuclear fission and corrosion products (Cs, Sr, Zr, Fe) which are also significant from the concentration point of view are practically not extracted (Cs, Sr, Fe) or if at all, then significantly less than Zr (5). Separation factors $\alpha_{Ln/Cs,Sr,Fe}$ reach values of 10^2 up to 10^3 and $\alpha_{Ln/Zr}$ reach values of tens.

When investigating the extraction of americium by benzyldibutylamine (BDBuN), it was found that for comparable compositions of the organic and aqueous phases, the distribution ratio for Am(III) is very similar to that of Eu(III), both with regard to the effect of concentration and to that of the nature of salting-out reagent and solvent (Figure 1).

Therefore, we have paid more attention to the extraction of Am(III) by benzyltrialkylammonium salts, i.e. benzyldimethyldodecylammonium nitrate ($BDMLNNO_3$) (Figure 2) and benzyltrioctylammonium nitrate ($BTONNO_3$) (Figure 3).

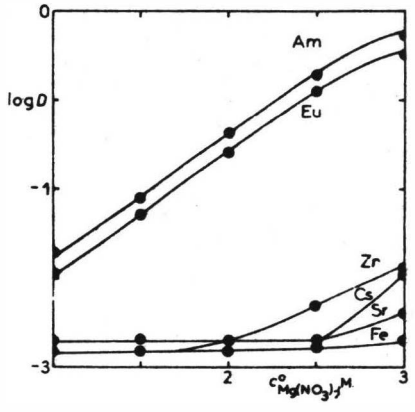

FIG. 1

Dependence of the distribution ratios on the concentration of magnesium nitrate

$C^{o}_{Eu(NO_3)_3}$ = 0.02 M , $C^{o}_{Am(NO_3)_3}$ = 1.10^{-7} M, $C^{o}_{Fe(NO_3)_3}$ = 0.008M, $C^{o}_{Zr(NO_3)_2}$ = 0.007 M, $C^{o}_{CsNO_3}$ = 0.005 M, $C^{o}_{HNO_3}$ = 0.5 M, C_{BDBuN} = 0.5 M (in benzene), $C_{C_{16}H_{33}OH}$ = 0.04 M.

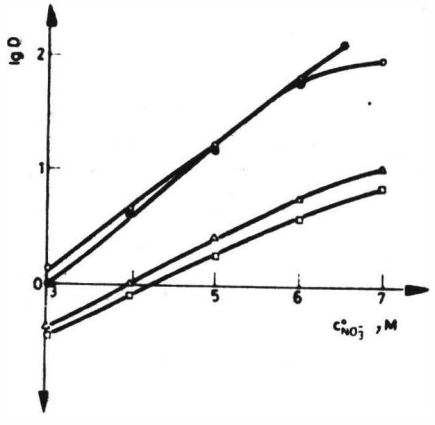

FIG. 2

Extraction of $Am(NO_3)_3$ by $BDMLNNO_3$, as a function of the concentration of salting-out agents.

$C^{o}_{HNO_3}$ = 0.3 M, $C^{o}_{Am(NO_3)_3}$ = 1.10^{-7}, $C_{BDMLNNO_3}$ = 0.5 M (in benzene)

1 - $Mg(NO_3)_2$; 2 - $LiNO_3$; 3 - $Ca(NO_3)_2$; 4 - $NaNO_3$.

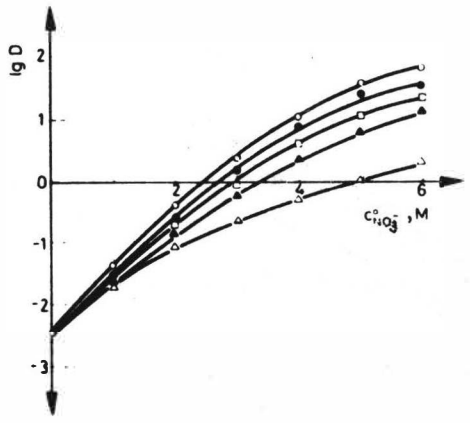

FIG.3

Extraction of Am(III) by $BTOANO_3$ as a function of the concentration of salting-out agents.
$C^o_{HNO_3}$ = 0.1 M, $C^o_{Am(NO_3)_3}$ = 1.10^{-7} M, C_{BTONNO_3} = 0.5 M (in benzene)
1 - $LiNO_3$; - 2 - $Mg(NO_3)_2$; 3 - $Al(NO_3)_3$; 4 - $Ca(NO_3)_2$; 5 - $NaNO_3$.

For both reagents, high values of distribution ratios are achieved, also when lower concentrations of salting-out agents are used.

In comparison with BDBuN, the quaternary ammonium salts are more suitable for the extraction of both Am(III) and the lanthanides. In the case of $BDMLNNO_3$ the distribution ratios for the extraction of Am(III) are in the order of tens to hundreds, whereas in the case of BDBuN, it is in the range of units up to tens.

Similar chemical properties of lanthanides and transplutonium elements come also to the fore in their similar extraction properties. It can therefore be expected that higher concentrations of lanthanides in the aqueous phase will suppress the extraction of americium. For that reason, we investigated the effect of the presence of lanthanides on the extraction of americium from aqueous nitric acid solutions by $BDMLNNO_3$, using a total metal concentration of 8.195 M. Of the lanthanides investigated (Ce(III), Pr(III), Nd(III), Sm(III), Eu(III) and Y(III)), the least extractable ones (Eu and Y) have the least influence on the extraction of Am(III) (Figure 4), whereas in the presence of La, Ce and Pr salts, the distribution ratios for Am(III) are reduced by more than one order of magnitude (Figure 5). There occurs a marked drop in the distribution ratios D_{Am} in comparison with the extraction of Am(III) by $BDMLNNO_3$ without the presence of lanthanides. The great difference in the concentrations of Am(III) and lanthanides in the aqueous extracted solutions is the reason for the extraction of low concentrations of Am(III) to be controlled by the extraction properties of lanthanides. This effect is especially pronounced for Eu(III) (Figure 5).

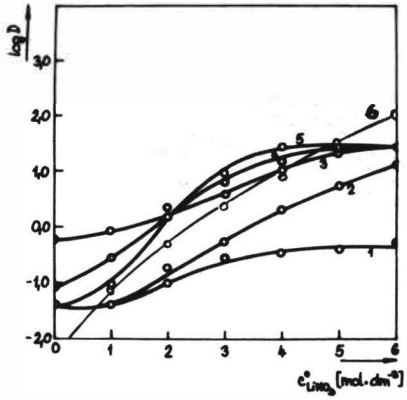

FIG. 4

The dependence of the extraction of americium by $BDMLNNO_3$ on the concentration of $LiNO_3$.

1 - $Y(NO_3)_3$; 2 - $Sm(NO_3)_3$; 3 - $Nd(NO_3)_3$; 4 - $Pr(NO_3)_3$; 5 - $Ce(NO_3)_3$; 6 - $Am(NO_3)_3$.

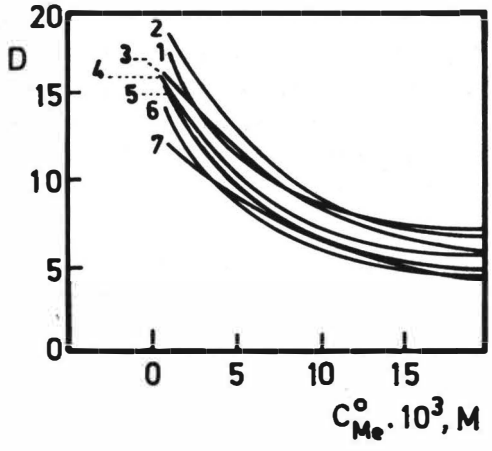

FIG. 5

Extraction of Am(III) by $BDMLNNO_3$ in the presence of lanthanides

$C^{o}_{HNO_3}$ = 0.5 M, $C^{o}_{LiNO_3}$ = 6 M, $C^{o}_{Am(NO_3)_3} = 1.10^{-7}$ M,

$C_{BDMLNNO_3}$ = 0.5 M (in benzene).

1 - $Y(NO_3)_3$; 2 - $Eu(NO_3)_3$; 3 - $Sm(NO_3)_3$; 4 - $Nd(NO_3)_3$; 5 - $Pr(NO_3)_3$; 6 - $Ce(NO_3)_3$.

Separation factors $\alpha_{Am/Ln}$ evaluated for individual elements (Table 1) indicate the possibility of separating Am(III) from light lanthanides like La(III), Ce(III), Pr(III) and Nd(III) which are extracted best by $BDMLNNO_3$ without any further addition of complex forming agents. A very low value for the separation factor was found in the system Am:Eu. This can be explained on the basis of the very similar properties, caused by the identical electron configuration in the valence spheres of both ions.

The same effects, albeit less pronounced, are also found when $BTONNO_3$ is applied. Here the values are 8.34 for D_{Eu} and 12.4 for D_{Am}.

Considering the extraction of metal salts from acidic nitrate solutions by tertiary amines, it is obvious that amine nitrates (generally, $[(R_3N)_t(HNO_3)_v(H_2O)_x]_y$ are formed, in addition to the complexes of the amines with the metal Me^{a+} (generally, $[(R_3N)_t(HMe(NO_3)_{a+1})_u(HNO_3)_v(H_2O)_x]_y$. In order to obtain the stoichiometry of these complex systems, it is necessary to know how the various components of the extraction system aggregate. Solid benzyldibutylamine nitrate was therefore prepared, and the aggregation of this salt in benzene was measured. The calculated constants indicate that in benzene, only one single aggregated species is present i.e. the tetramer, with log β_4 values of 5.70 $\pm$ 0.01, 5.58 $\pm$ 0.02 and 5.09 $\pm$ 0.01 at 5.5, 25 and 37°C, respectively. As shown in tables the experimental results are fitting in the best with the assumption of the presence of the sole tetramer.

Comparing the aggregation of benzyldibutylamine nitrate and of trioctylamine nitrate (6), it appears that the highest aggregation occurs with the first mentioned reagent ; for the second, on the contrary, the existence of dimers or trimers comes out from interpretation by means of the Letagroup (6-8) or MOP program ; the values obtained for the aggregation constants are the following : log β_2 = 1.80 ; log β_3 = 2.35 (7), log β_2 = 0.90 ; log β_3 = 2.48 (8), or log β_2 = 2.22, log β_4 = 5.52 (9).

In the infrared spectrum of benzyldibutylamine nitrate, the NH bands are shifted to higher wavenumbers, which indicates a weaker NH bond in the aggregate. This fits with the finding (6,9,10) that a weakening of the NH bond leads to the formation of a higher aggregation.

TABLE 1

The separation factors $\alpha_{Am/Ln}$

$c^{o}_{Am(NO_3)_3} = 1.10^{-7}$ mol.dm^{-3} = konst, $c^{o}_{HNO_3}$ = 0,5 M, $c_{BDMLNNO_3}$ = 0,5 M (in benzene)

$c^{o}_{Ln(NO_3)_3}$ (mol.dm^{-3})	$\alpha_{Am/Ln}$						
	Y	La	Ce	Pr	Nd	Sm	Eu
1.10^{-3}	1.46	0.10	0.12	0.20	0.30	0.33	0.57
2.10^{-3}	1.90	0.10	0.12	0.24	0.29	0.45	0.69
4.10^{-3}	3.20	0.12	0.23	0.29	0.41	0.59	1.13
6.10^{-3}	4.12	0.15	0.28	0.33	0.44	0.71	1.23
8.10^{-3}	3.73	0.17	0.28	0.37	0.50	0.78	1.19
10.10^{-3}	3.60	0.19	0.30	0.38	0.55	0.78	1.20
20.10^{-3}	3.06	0.22	0.35	0.51	0.78	0.77	1.10

TABLE 2

Association Constants of Benzyldibutylamine Nitrate in Benzene

n-mer	$\log \beta_n$	U_{min} [a]
	5.5°C	
Trimer	4.37 ± 0.17	$1.69 \cdot 10^{-2}$
Tetramer	5.70 ± 0.01	$7.49 \cdot 10^{-4}$
Pentamer	7.22 ± 0.15	$1.67 \cdot 10^{-2}$
Hexamer	8.81 ± 0.38	$2.01 \cdot 10^{-2}$
Dimer + tetramer	$\beta_2 = 0$	
	$\beta_4 = 5.76 \pm 0.07$	$2.32 \cdot 10^{-4}$
Tetramer + hexamer	$\beta_4 = 4.89 \pm 0.43$	
	$\beta_6 = 6.72 \pm 0.23$	$3.45 \cdot 10^{-1}$
	25°C	
Trimer	4.21 ± 0.21	$2.41 \cdot 10^{-2}$
Tetramer	5.58 ± 0.02	$8.26 \cdot 10^{-3}$
Pentamer	7.10 ± 0.09	$5.79 \cdot 10^{-2}$
Hexamer	8.61 ± 0.11	$4.34 \cdot 10^{-2}$
Octamer	12.10 ± 0.2	$4.87 \cdot 10^{-1}$
Dimer + Tetramer	$\beta_2 = 0$	
	$\beta_4 = 5.62 \pm 0.05$	$7.30 \cdot 10^{-4}$
Tetramer + hexamer	$\beta_4 = 4.48 \pm 0.11$	
	$\beta_6 = 6.42 \pm 0.11$	$3.86 \cdot 10^{-2}$
	37°C	
Dimer	30.68 ± 2.8	$1.76 \cdot 10^{-2}$
Trimer	4.00 ± 0.1	$2.88 \cdot 10^{-3}$
Tetramer	5.09 ± 0.01	$9.43 \cdot 10^{-6}$
Pentamer	6.40 ± 0.01	$5.42 \cdot 10^{-4}$
Hexamer	7.79 ± 0.07	$1.58 \cdot 10^{-3}$
Heptamer	9.26 ± 0.32	$2.53 \cdot 10^{-4}$
Octamer	11.92 ± 0.9	1.26
Tetramer + hexamer	$\beta_4 = 4.52 \pm 0.13$	
	$\beta_6 = 7.10 \pm 0.16$	$8.26 \cdot 10^{-2}$

[a] U_{min} = sum of deviations squares.

REFERENCES

1. Jedináková V.: Czech. 180505
2. Jedináková V., Cibulková J., Teplý J.: J,Radioanal.Chem. 52, 69 (1979)
3. Jedináková V., Cibulková J.: Sb. Vys. Šk. Chemico-Technol., Prague, in press
4. Jedináková V., Cibulková J., Kuča L.: Collection Czechoslov. Chem. Commun. 44, 1900(1979)
5. Jedináková V., Žilková J. in the book: Issledavanija v Oblasti Pererabotki Obluchennogo Topliva, Vol.II p.180, Materialy IV.Simpoziuma SEV, Karlovy Vary 28.3. - 1.4. 1977
6. Jedináková V., Högfeldt E.: Chem. Scripta 9, 178 (1976)
7. Baskol S.: Thesisi METU, Ankara 1968
8. Markovits G., Kertes A.S. in the book: Solvent Extraction Chemistry (J.Dyrssen, O. Liljenzin, J.Rydberg, Eds), p.390, North-Holland, Amsterdam 1967
9. Mamoun A. Muhamed: Aggregation Equilibria Involving Trilaurylamine, n-Octanol and Hydrochloric Acid in Benzene, p. 32, Published by KTH, Stockholm 1975
10. Jedináková V., Högfeldt E.: Chem. Scripta 9, 171 (1976)

COMPARATIVE STUDIES ON THE METAL EXTRACTION WITH DIFFERENT CHELATING EXTRACTANTS

P. Mühl and K. Gloe
Zentralinstitut für Festkörperphysik
und Werkstofforschung der Akademie
der Wissenschaften der DDR,
Dresden
German Democratic Republic

A number of complex forming agents, which form with metal ions stabile chelate rings, has been studied with regard to their extraction properties.

The use of chelating extraction agents leads to a considerable increase of stability of the formed metal complexes. This is the result of the chelating action and is caused by the circumstance that several donor atoms contained in the molecule can coordinate the metal ion. Naturally, simultaneous coordination of the different donor atoms must be sterically possible, and these should not be arranged too far from one another in the chelating agents because the chelating effect is particularly high in the formation of 5-or-6-membered chelate rings. Furthermore, such envelopment of the metal leads to a rise of the solubility properties in the organic solvent. The sequence of stability constants for a number of bivalent 3d metals, and also of extraction due to their proportionality with the extraction constant, correlates with the so-called Irving-Williams Series which follows approximately the course of the ionization potentials of the metals /1/:

$Mn(II) < Fe(II) < Co(II) < Ni(II) < Cu(II) > Zn(II)$.

This sequence, however, is not absolute and is subject to a number of influencing factors. In general, the following possibilities of influencing the extractability and separation selectivity of an extraction system are obtained when one considers the organic phase:

- variation of the type of structure
- introduction of different donor atoms
- substituent variation
- utilization of steric factors
- use of different diluents

There can be no doubt that the discussed aspects represent important criteria for the extraction system, but one must always bear in mind that the decisive precondition of extraction is the presence of corresponding metal ions with the capability to complex formation with organic ligands, and that the composition and chemistry of the aqueous phase are decisive process parameters which can bring about specific separating effects. Some of these questions shall be discussed on the basis of practical examples.

Extraction Properties of Chelates with O,N-Donor Atoms

Chelating compounds with O,N-donors have been known as analytical extraction agents for many years /2/. As could be expected, when one considers the Irving-Williams Series, different compounds show particularly towards copper(II) a high extractability.

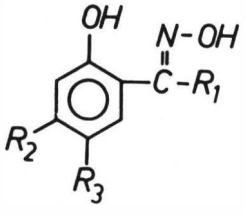

R_1 = CH_3.C_2H_5.C_6H_5
R_2 = CH_3.$C_6H_{13}O$.$C_{10}H_{21}O$.
$C_{16}H_{33}O$.H
R_3 = H.$C_{10}H_{21}O$

2 - hydroxyoximes

Aromatic 2-hydroxyoximes and substituted hydroxyquinolines have proved to be particularly excellent agents for extraction of copper(II) from acid solution /3/. The hydroxyoxime system is also suited for nickel(II) /4/, and palladium(II) /5/. Extraction studies with alkoxylated 2-hyroxyoximes revealed good extraction properties for copper in the acid pH range /6/.

Fig. 1 shows on the basis of an example that the differences in the extraction properties are relatively small, by changing

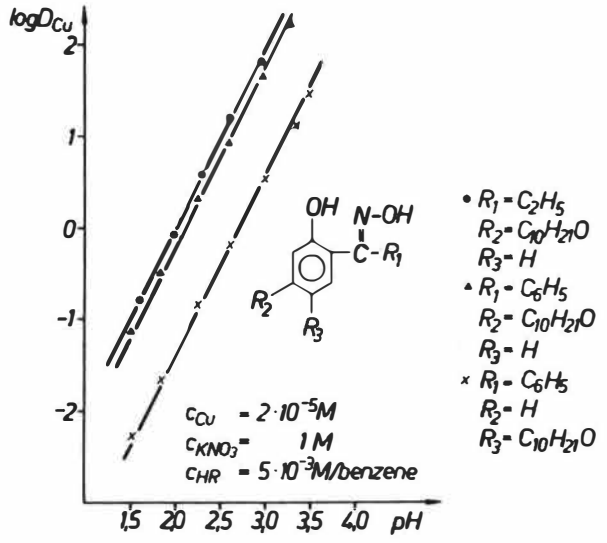

Fig. 1 Extraction of copper(II) with 2-hydroxyoximes in dependence on substitution

the listed substituents. Larger differences were only observed in the arrangement of the alkoxy group in 5-position where both solubility effects as well as electronic influences are responsible for this significant decline. Analogous phenomena can be observed also with iron(III) extraction, but the distribution ratio is lower by two orders of magnitude, thus allowing copper-iron separation with high separation factors. The influence of the diluent on extraction is much greater than the influence of substitution variation (Fig. 2).

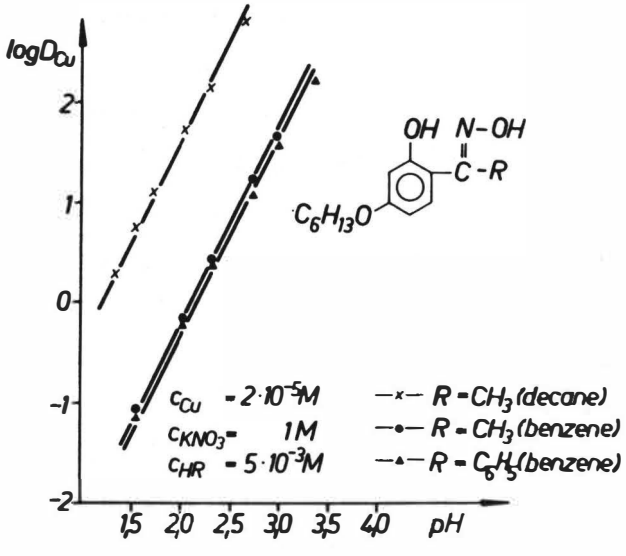

Fig. 2 Extraction of copper(II) in dependence on diluents

The rate of increase for copper extraction is clearly smaller at the transition from benzene to n-decane than in the case of iron(III). But this also means that the separation factors copper/iron are smaller. In view of the fact that both metal ions have marked kinetic differences, separation does not present any problems. Other bivalent transition metal ions are extracted with 2-hydroxyoximes, only at much higher pH values, so that they do not influence copper extraction. Adequate solubility of both the extraction agent and of the formed metal complexes in organic solvents is of great significance for technical application. In this particular case, it is greatly influenced by substituent variation. Contrary to the 2-hydroxyoximes alkyl substituted in 5-position /7/, the solubility of the metal compounds declines considerably in case of the 2-hydroxyoximes alkoxylated in 4-position compared with the hydroxyoximes itself.

The increase of the ring number of a certain chelate structure enhances the stability of the chelate as show by CALVIN and BAILES on the basis of the salicylaldimine chelates /8/.

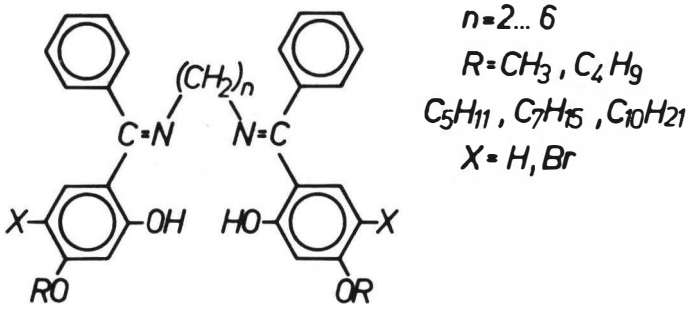

schiff bases

Four dendate Schiff bases form with metal ions 3-ring complexes. The extraction of different metal ions with such Schiff bases exhibits a pronounced tendency for copper(II), but the extraction of iron(III) is much better (Fig. 3). This makes copper-iron separation more difficult, but due to the large kinetic differences, it is not impossible. An advantage of this class of compounds is the formation of 1:1 complexes with bivalent metal ions. This has a positive effect on the capacity of the extraction agent.

As opposed to the salicylaldehyde derivates - their extraction properties were studied by STRONSKI et al. /9/ - the investigated benzophenone derivates have much higher solubilities

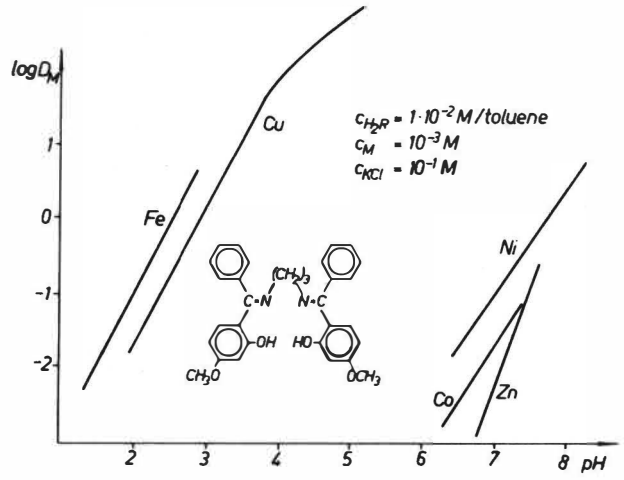

Fig. 3 Extraction of various metal ions with a four-dentate Schiff base

in non-polar organic solvents, thus making this class of compounds applicable for liquid-liquid extraction. The copper extraction with these Schiff bases (Fig. 4) indicates that an increase of the number of bridge carbon atoms in the central chelate ring from n=2 to 6 leads to a marked decline of extractability. This fact illustrates that the complex-forming tendency of such a macrocyclic ring system depends considerably on the ring sequence of the formed metal complex. For the investigated compounds, the sequence 6-5-6 shows the highest complex forming tendency and also the highest copper extraction.

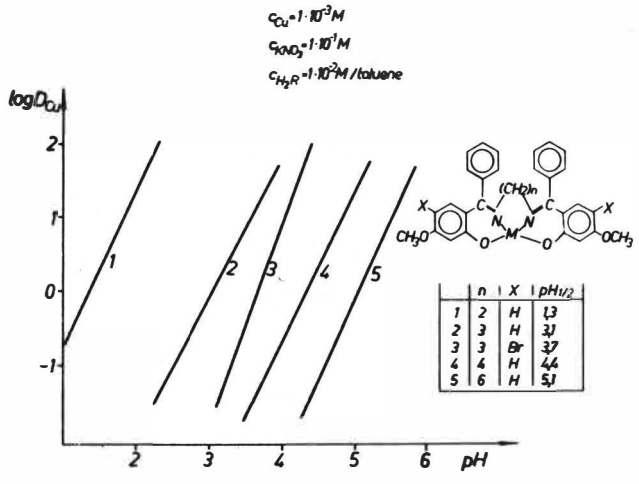

Fig. 4 Extraction of copper(II) with four-dendate Schiff bases in dependence on tne size of central cnelate ring

Stability of this ethylene diimino compound, however, is markedly limited, so that it is less suitable as extraction agent. Thus, the propylene diimino compound of this series has optimal extraction properties. The influence of substituents at the Schiff bases on extraction is similarly to hydroxyoximes only negligible. This is due to the large distance from the reaction centre. The slow rate of the reaction equilibrium during the extraction of all studied metal ions is far more pronounced than with the hydroxyoximes. This is due to the formation of such a complicated ring system. Here, a high increase of the extraction rate for copper(II) can be achieved by adding an accelerator.

Extraction Properties of Chelates with O,S-Donor Atoms

Transition to extraction agents containing a sulphur donor atom must lead to a change of the selective properties in extraction in conformity with the known coordination behaviour. Extraction studies were carried out with acylthioacetamides /10/ and acylthioureas /11/ on a number of transition metal and noble metal ions. The introduction of a sulphur atom revealed that also metals with a greater tendency towards covalent bonding can be extracted from an acid solution compared with the chelates with O,N-donor atoms. For instance, this applies to such ions as Pd(II), Pt(II), Au(III), Hg(II), Ag(I) as well as to Zn(II) and Cd(II).

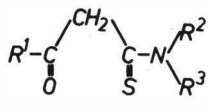

acylthioacetamides

$R^1 = CH_3, C_6H_5$
$R^2 = H, n\text{-}C_4H_9$
$R^3 = C_6H_5, n\text{-}C_4H_9$

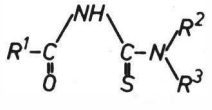

acylthioureas

$R^1 = C_6H_5$
$R^2 = R^3 = n\text{-}C_4H_9, i\text{-}C_4H_9, n\text{-}C_6H_{13}$
$R^2 = C_6H_5$; $R^3 = H, CH_3$

Fig. 5 shows the curves, in a log D-pH diagram, for a number of metal ions with benzoylthioacetanilide as extraction agent. The sequence of extraction proceeds according, to the series Cu(II) > Zn(II) > Ni(II) > Co(II) > Cd(II). Fe(III) is not extracted within the pH-region of ≤ 3. The series of

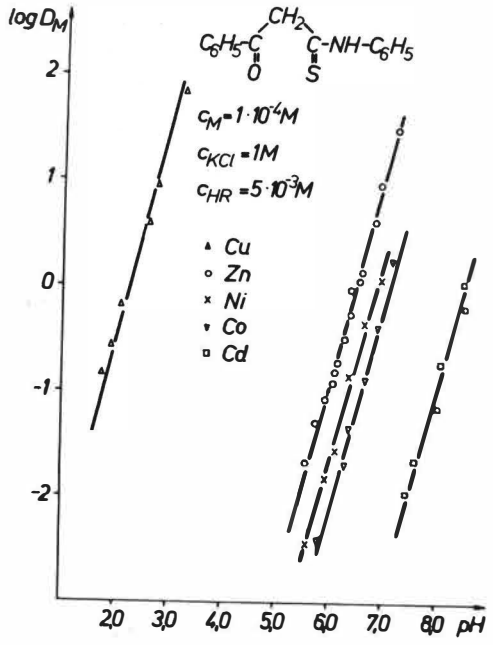

Fig. 5 Extraction of various metal ions with benzoylthioacetanilide

decreasing extractability correlates with the decrease of the determined constants of complex formation. The position of copper in this connection is not so dominant as it was for the extraction agents with O,N-donor atoms. The difference between cadmium and zinc, on the other hand, makes possible effective zinc-cadmium separation due to the greater stability of the cadmium chloro-complexes, preferably in a chloride solution. The influence of the substituents on extraction is shown in Fig. 6 taking zinc(II) as an example. The change in the R^1-position leads only to a negligible shift, whereas a modification of substitution at the nitrogen of the amide group strongly influences the extraction. In this connection, a significant role is played by the dissociation constant of the compound which is extremely small for N,N-dibutyl-substituted benzoylthioacetamide. Furthermore, there is a marked difference also of the distribution constants of the extraction agents. The influence of diluents in this systems is negligible.

The replacement of the CH_2 group present in the acylthioacetamides between the carbon atoms linked to the O- and S-donor atoms by an NH group leads to a decisive change of the electron structure of the compounds. This is reflected by large differences in the constants of dissociation and

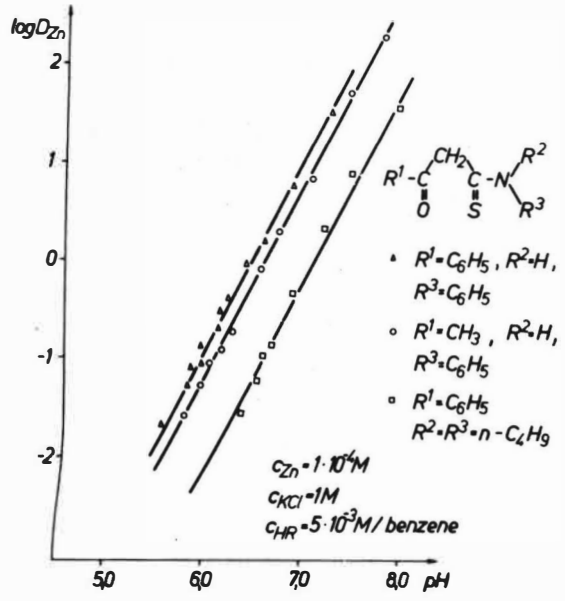

Fig. 6 Extraction of zinc(II) in dependence on substitution

stability. Thus, the acylthioureas extract metal ions in a lower pH range than the corresponding acylthioacetamides. This means that copper extraction becomes possible in the same pH ranges as with hydroxyoximes under comparable conditions (Fig. 7). The series of decreasing extractability is the following :

Cu(II) > Fe(III) > Ni(II) > Zn(II) > Cd(II) > Co(II).

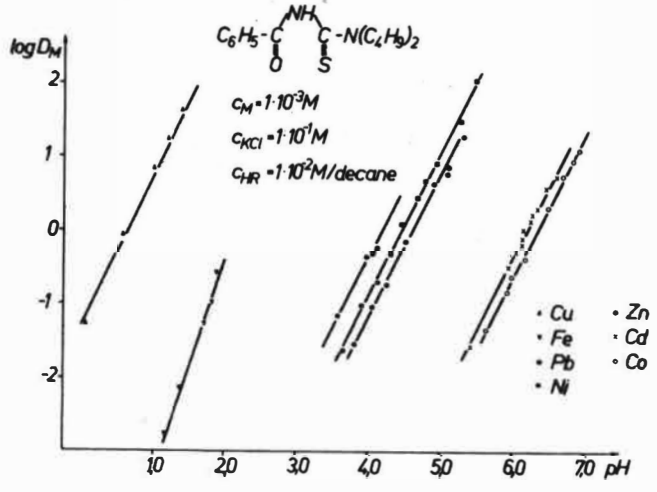

Fig. 7 Extraction of various metal ions with N,N-dibutyl-N-benzoylthiourea

Accordingly the extraction of nickel and zinc from acid solution also becomes possible, and effective possibilities of separation are obtained for the metal pairs Ni/Co and Zn/Cd. This sequence is in agreement with the variation of the constants of complex stability. It is noticeable that the position of zinc differs from that in the two series showed above. This fact is closely related with the electron structure of Zn^{2+} which has a $3d^{10}$ orbital configuration. Comparison of the two systems with O,S-donor atoms dealt with here, reveals the remarkable chemical stability of the thioureas, particularly also in a strong acid solution. It is obvious that this is related with the favourable electronic structure.

Extraction Properties of Macrocyclic Crown Ethers.

Pedersen's polyethers /12/ or Lehn's cryptates /13/ represent a class of compounds in which the chelating effect is combined in an interesting manner with the principle of stereoselectivity. Crown ethers are complexing agents which can even successfully extract alkali and alkaline-earth metal ions. The pronounced steric effect is caused by the generally resulting arrangement of the metal ion in the cavity of the crown ether ring. By influencing optimatically the complex stability by choosing the size of the ring, and by the number, position and kind of donor atoms, it becomes possible to obtain extremely selective metal ion separations. Extraction studies has been carried out with four crown ethers. Both the ring diameter of the crown, as well as the substitution at the ring, were varied. Fig. 8 shows that the extraction of different alkali metal nitrates with DBC-18 under the same experimental conditions is clearly a function of the metal ion diameter : $K^+ > Rb^+ > Cs^+ > Na$.

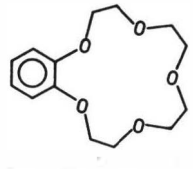

benzo-15-crown-5
(BC-15)

dibenzo-18-crown-6
(DBC-18)

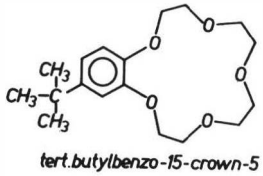

tert.butylbenzo-15-crown-5
(BuBC-15)

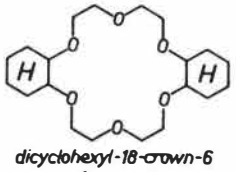

dicyclohexyl-18-crown-6
(DCC-18)

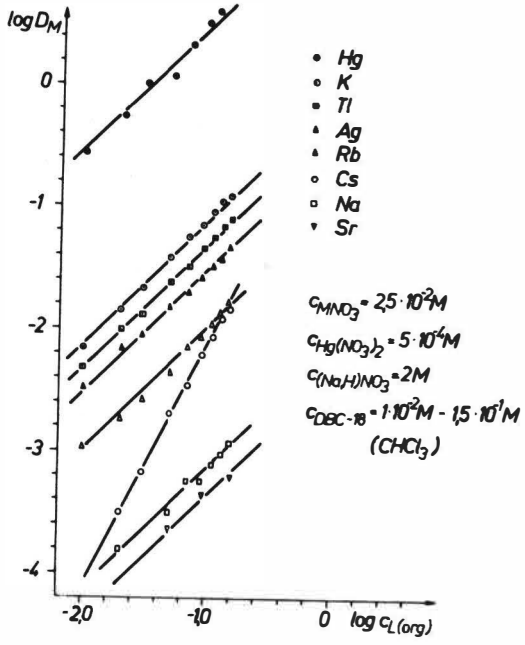

Fig. 8 Extraction of various metal nitrates with DBC-18

Tl^+ and Ag^+ /14/ are integrated accordingly. The alkaline-earth metal nitrates of Ca^{2+}, Ba^{2+} and Sr^{2+}, on the other hand, give a much lower extraction. Both the solubility effect as well as the high dehydratation energies of these salts are responsible for this behaviour /15/. When compared to all other metals, the greater slope of the curve for Cs^+ extraction in Fig. 8 must be attributed to the formation of a sandwich complex. The reason lies in the fact that the cesium cation has a larger ion diameter than the cavity of the crown ether with the result that the arrangement of the cation in the crown ether cavity, feasible in other examples, is not possible /16/.

The distribution ratios obtained with DBC-18 shows values which are unsuitable for separating processes. The principal reason for this is the low solubility of the crown ether as well as of the corresponding metal complexes. The anion, necessary as counter ion in the organic phase, plays an important role in this connection. Thus, large and easily polarized anions favour extraction. From the point of view of application, however, the smaller anions NO_3^-, Cl^- and SO_4^{2-} are of greater interest.

The conditions are more favourable by using DCC-18. The distribution ratios rise generally for the investigated metals. Fig. 9 shows a comparison of extraction of K^+ and Sr^{2+}

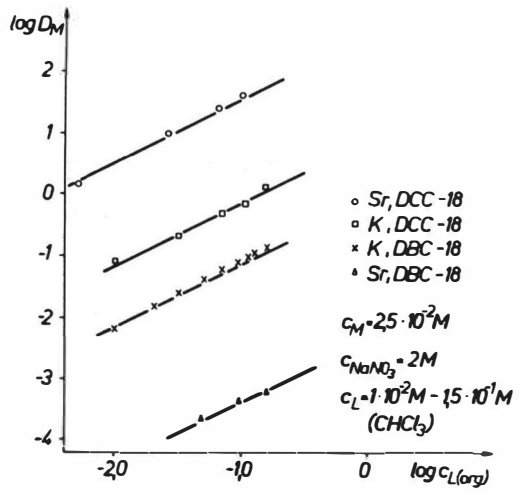

Fig. 9 Extraction of potassium and strontium nitrates with DBC-18 and DCC-18

with DBC-18 and DCC-18. The distribution ratios for K^+ rose by about one order of magnitude, while an increase by 4 orders of magnitude was observed with Sr^{2+}. This means that Sr^{2+} is extracted more effectively than K^+, a fact which is in relation with the increase of the complex stability /16/.

A high extractability was observed for Hg^{2+}, both with DBC-18 and with DCC-18. But the solubility of the formed mercury complexes is not extraordinarily high. Nevertheless, these results could gain significance for removing mercury traces from aqueous waste solutions.

As is to be expected, the transition from an 18-crown-6 to a 15-crown-5, i.e. reduction of the cavity of the ring, leads to a rise of the extraction of smaller metal ions (e.g. Na^+), and to a reduction of the larger ones. Fig. 10 shows this on the example of K^+ and Na^+ for DBC-18 and BC-15. Since K^+ forms a sandwich complex in the case of BC-15, its extraction still remains higher, as to be expected. The influence of a tertiary-butyl group at BuBC-15 on extraction is only slightly negative.

The fact that extraction with crown ethers transfers ion pairs into the organic phase affords a second possibility of metal separation which is independent of the radius of the metal ions. This is based on the fact that metal ions forming stable anion complexes can be extracted in this form as counter ion into a selected crown ether-metal complex. Thus, high distribution ratios are obtained, e.g. for $AuCl_4^-$ and $FeCl_4^-$ from KCl solutions with DBC-18.

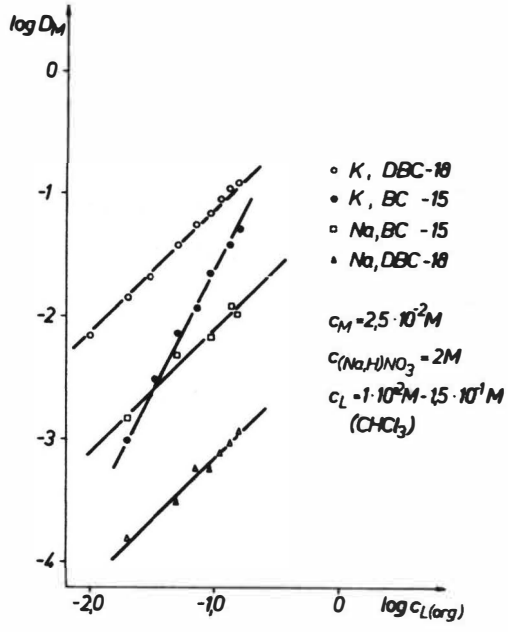

Fig. 10 Extraction of potassium and sodium nitrate with DBC-18 and BC-15

With this class of compounds, a series of separation possibilities are indicated which can be modified in various directions. By variation of the diluent and the addition of compounds which especially increase anion solvation, it is possible to increase still further the extraction of metal nitrates, but also of chlorides and sulphates.

The results reported in this paper were achieved by co-operation with J. BEGER and H.-J. BINTE from the Bergakademie Freiberg concerning 2-hydroxyoximes, with E. UHLIG and U. DINJUS from the Universität Jena concerning SCHIFF bases, with E. HOYER and L. BEYER from the Universität Leipzig concerning acylthioureas, with E. UHLEMANN and E. LUDWIG from the Pädagogische Hochschule Potsdam concerning acylthioacetamides, with L.M. GINDIN and A.I. KHOLKIN from the Institute of Inorganic Chemistry, Novosibirsk, and J. BEGER concerning crown ethers.

References

/1/ H. IRVING, R.I.P. WILLIAMS, Nature 162 (1948) 746

/2/ Ju.A. ZOLOTOV, Extraction of Chelate Compounds, Ann-Arbor-Humphrey Science Publishers, Ann Arbor, London 1970

/3/ A.W. ASHBROOK, Coord. Chem. Rev. 16 (1975) 285

/4/ N.M. RICE, M. NEDVED, G.M. RITCEY, Hydrometallurgy 3 (1978) 35

/5/ M.J. CLEARE, P. CHARLESWORTH, D.J. BRYSON, J. appl. Chem. Biotechnol. 29 (1979) 210

/6/ K. GLOE, P. MÜHL, J. BEGER, H.-J. BINTE, 9. Radiochemical Conference, Piestany (CSSR) 1978

/7/ A.J. VAN DER ZEEUW, Erzmetall 30 (1977) 139

/8/ M. CALVIN, R.M. BAILES, J. Amer. Chem. Soc. 68 (1946) 949

/9/ I. STRONSKI, A. ZIELINSKI, Isotopenpraxis 2 (1966) 291

/10/ E. LUDWIG, K. GLOE, P. MÜHL, E. UHLEMANN
5. Intern. Symp. High Purity Materials, Dresden 1980

/11/ P. MÜHL, K. GLOE, L. BEYER, F. DIETZE, E. HOYER
5. Intern. Symp. High Purity Materials, Dresden 1980

/12/ C.F. PEDERSEN, H.K. FRENSDORFF, Angew. Chem. 84 (1972) 16

/13/ J.-M. LEHN, Acc. Chem. Res. 11 (1978) 49

/14/ K. GLOE, A.I. CHOLKIN, P. MÜHL et al. Z. Chem. 19(1979) 382

/15/ H.K. FRENSDORFF, J. Amer. Chem. Soc. 93 (1971) 4684

/16/ J.J. CHRISTENSEN, D.I. EATOUGH, R.M. IZATT, Chem. Rev. 74 (1974) 351

QUANTUM-CHEMICAL DESCRIPTION OF PROTON AFFINITY OF MOLECULES OF NITROGEN BASES

Yu. A. Panteleev, A. A. Lipovskii

V. G. Khlopin Radium Institute

Leningrad, USSR

The proton affinity of the nitrogen bases is due to the presence of electron lone pair (LP) of nitrogen atom.

One of the ways for determination of the directions for electrophilic attack and a site of proton binding is based on calculation of molecular electrostatic field maps. The calculations were perfomed in CNDO/2 approximation. For the molecules of pyridine row, a correlation between the depth of electrostatic minimum near nitrogen LP and calculated protonation energy has been obtained. The correlation coefficient is equal to R = 0,978, what is higher than R = 0,898 obtained for correlation-effective charge on nitrogen atom and protonation energies. So, the charge on nitrogen is less indicative of proton affinity, because it is characteristic for only one center, while the depth of minimum is determined by effect of the whole electronic structure of the base. Analysis of the maps has shown that the substituent effect is very obvious. Apparently the field characteristics can be also used for discussion of extraction properties of organic bases in dependence on their structure. While Hammet constants for example estimate only the summary effect, the electrostatic maps make it possible to detail the picture of polar effect of substituents and will be useful for explaining the complex steric effects of the substituents.

The other way for description of proton affinity of the bases is connected with consideration of molecular orbital (MO) nature of nitrogen electron LP. For estimation of LP nucleophilic properties, two parameters of its donor activity have been suggested which are determined by coefficients at LP wave functions in occupied MO's and MO energies. Strong correlations between these parameters and protonation energies have been obtained. For the pyridine row R = 0,983 and - 0,942; for the heterocyclic amines R = 0,996 and - 0,986; for the aliphatic amines R = 0,935.

The bases calculated by us may be considered only as the models of the molecules-extractants, which are convenient from computating point of view. However, it is believed that the methods suggested for estimating the proton affinity can be recomended for usable extractants.

NMR ^{31}P AND IR INVESTIGATION OF INTERACTIONS BETWEEN $UO_2(D2EHP)_2$, TBP and UO_2SO_4 IN BENZENE.

E.S. Stoyanov, V.A. Mikhailov,
V.G. Torgov, T.V. Us.

Institute of Inorganic Chemistry,
Siberian Branch of the Academy of
Sciences of the USSR
Novosibirsk, 630090, USSR.

Uranyl di-2-ethylhexylphosphate (UO_2R_2) in benzene solution is a long chain polymer. The mixture of UO_2R_2 with TBP |1,2| can extract uranyl sulphate from its aqueous solutions directly in the form of UO_2SO_4. The present paper deals with the composition and structure of links formed by addition of UO_2SO_4 to $(UO_2R_2)_p$ in the presence of TBP and with the interaction between $(UO_2R_2)_p$ and TBP in the absence of UO_2SO_4.

Interaction with TBP. In NMR spectra of UO_2R_2 solution in C_6H_6 only one signal P_o is observed. At low TBP concentrations a new signal P_1 appears in addition to the signal P_o and that from TBP itself, while further adding of TBP leads to two more signals (P_2 and P_3). We distinguish the uranium atoms in a polymer chain joined with n molecules of TBP as occupied (O), all the rest being free (F). Assignments of the signals has been made according to the scheme (1) (arrows indicate occupied uranium atoms). Signal P_1 is assigned to phosphor atoms places

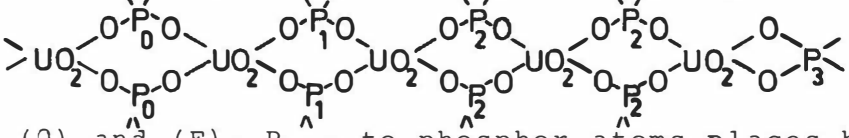

(1)

between (O) and (F), P_2 - to phosphor atoms places between two atoms (O) and P_3 - to end-line sites. The value of n determined from NMR and quantitative IR-spectroscopy data is found to equal 1.

Extracts of uranyl sulphate. In NMR spectra of extracts, one observes signal P_o that is due to TBP as well as both signals P_1 and P_2. Besides, two new signals (P_4 and P_5) appear. Signal P_4 is assigned to phosphor atoms placed between two uranium atoms one of which is free, the other being occupied by UO_2SO_4, signal P_5 - to phosphor atoms placed between two uranium atoms, both being occupied by UO_2SO_4. The results show, that one link of a polymer chain is charged with one molecule of UO_2SO_4. Using quantitative IR-spectroscopy, every thus charged links has been determined to carry either one (at low TBP concentration) or two molecules of TBP. Thus the structure of a link charged by UO_2SO_4 must correspond to scheme 2.

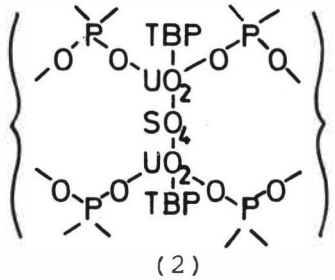

(2)

REFERENCES

1. V.A. Mikhailov, V.G. Torgov, T.V. Us, Dokl. AN SSSR, 214, 1121 (1974).
2. V.G. Torgov, T.V. Us, V.A. Mikhailov, A.V. Nikolaev, Dokl. AN SSSR, 227, 635 (1976).

CHEMISTRY OF EXTRACTION OF COPPER, COBALT AND NICKEL WITH SUBSTITUTED 8-SULPHONAMIDOQUINOLINES

M. Cox, School of Natural Sciences,
The Hatfield Polytechnic, Hatfield,
Hertfordshire U.K.

W.J. van Bronswijk, Western Australia
Institute of Technology, Perth, Australia.

This paper reports the results of a study of the coordination and extraction chemistry of a series of model compounds related to the commercially available reagent LIX34 (Henkel Corporation). The structure of this reagent disclosed at ISEC77 is shown in the figure and the model compounds used here have R = methyl, phenyl, p-tolyl and p-dodecylbenzene. These were obtained as colourless crystalline solids from toluene, with the exception of the p-dodecylbenzene derivative which was a pale yellow liquid.

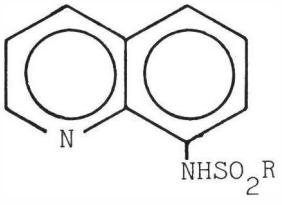

Equilibrium extraction performance: The reagents in toluene solution were contacted with the appropriate metal ion in an aqueous solution of constant ionic strength. The results obtained from equilibrium studies agree with the suggestion that the compounds behave as mono-acidic extractants giving linear plots of log D vs pH with slopes approximately equal to 2. The variation of R in the model compounds has little effect on the extraction and data for all reagents with a particular metal can be fitted on the same plot within experimental error. The pH_{50} values for the three metals examined are: copper 1.7 ± 0.2; cobalt 4.2 ± 0.2; nickel 8.0 ± 0.5.

Stereochemistry: Solid derivatives of the extractants were obtained which analysed satisfactorily for a 1:2 metal:ligand complex; these were subjected to spectroscopic investigation to try to elucidate their stereochemistry. Infra-red studies of the solid derivatives confirm the behaviour of these compounds as mono-acidic extractants in that the -NH vibration present in the free ligand is lost on coordination. The visible spectra and magnetic susceptibilities were measured in solution and in the solid state the results indicating the same basic coordination was maintained in both cases. The data to be presented from nmr and visible spectal studies indicate, in the case of cobalt and nickel, a rapid stereochemical rearrangement is taking place in solution. This rearrangement is suggested as being tetrahedral ⟷ square planar with very little, if any, contribution from octahedral species under the conditions used to date. This stereochemical arrangement may clarify the problem of oxidation of cobalt(II) during extration with coordinating ligands. In this study cobalt(II) showed little tendency to oxidise and this will be compared with the performance of other chelating extractants.

CHARACTERIZATION OF THE COMPLEXES OF Ni(II) WITH LIX63 OXIME

M. E. Keeney and K. Osseo-Asare
Metallurgy Section, Department of Materials
Science and Engineering
The Pennsylvania State University
University Park, PA 16802, USA

Previous published reports on the nickel-LIX63 oxime (H_2Ox) system have included only indirect characterization of the extracted metal complexes. Several complexes resulting from the extraction have been isolated, purified and characterized by a variety of analytical techniques including spectral (IR,NMR,ESR,UV-Vis, Mass Spec), elemental, and magnetic susceptibility analyses. The results indicate that nickel forms a variety of complexes with H_2Ox depending upon the solution conditions including: $[Ni(Ox)]_n$; $[Ni(HOx)_2]$; $[Ni(HOx)_2(H_2Ox)]$ and $[Ni(H_2Ox)_3]^{2+}$

$[Ni(Ox)]_n$ is an amorphous, polymeric olive powder insoluble in polar solvents. The complex exhibits low magnetic susceptibility indicative of anti-ferromagnetic interactions. VPO results indicate a degree of association (n) of approximately 7-9.

$[Ni(HOx)_2]$ is a viscous, orange diamagnetic liquid at room temperature which is thermally unstable. The complex slowly decomposes after undergoing a coordinated rearrangement of the oxime ligands. $[Ni(HOx)_2]$ is preferentially formed in solution under extraction conditions of intermediate to high pH (pH>5), and in extraction from ammoniacal solutions. $[Ni(HOx)_2(H_2Ox)]$ is a pale blue complex formed slowly by prolonged contact of $[Ni(HOx)_2]$ with excess H_2Ox in solution.

$[Ni(H_2Ox)_3]SO_4$ is a blue, paramagnetic crystalline solid which appears to exist in both hydrated and dehydrated forms(i.e. $[Ni(H_2Ox)_3]SO_4 \cdot nH_2O$). The hydrated form (n~2-3) is soluble in non-polar organic solvents forming extremely viscous solutions. The complex undergoes a slow dehydration in the solid state and a rapid dehydration in polar solvents to form an insoluble polymeric species.

ACKNOWLEDGEMENTS

This work was supported by the National Science Foundation. M.E. Keeney acknowledges the award of a fellowship by the Mining and Mineral Resources Research Institute, The Pennsylvania State University.

LINEAR CORRELATIONS OF FREE ENERGIES AS A TOOL FOR COMPACTING INFORMATION ON EXTRACTION EQUILIBRIA.

V.S. Shmidt, E.A. Mezhov and K.A. Rybakov

USSR Atomic Energy Committee

Moscow, USSR.

It is demonstrated that equations based on LCE are an effective tool for shortening the designation of large files of constants which describe the extraction equilibria.

1) Extraction by tertiary amines

$\log K_{HNO_3} = 5.03 - 3.48\,\Sigma\sigma^* + 1.55\,\Sigma E_s^*$ (10 systems)

$\log \bar{K}_{HNO_3} = -0.20 - 0.28\,\Sigma\sigma^* + 0.79\,\Sigma E_s^*$ (15 systems)

$\log KHCl = 6.47 - 0.76\,\Sigma\sigma^* + 1.93\,\Sigma E_s^*$ (6 systems)

$\log K_{Pu} = 8.02 - 0.33\,\Sigma\sigma^* + 2.24\,\Sigma E_s^*$ (16 systems)

$\log D_{Am} = -0.21 - 1.06\,\Sigma\sigma^* + 1.02\,\Sigma E_s^*$ (20 systems)

$\log D_{Cm} = -0.60 - 1.25\,\Sigma\sigma^* + 0.99\,\Sigma E_s^*$ (30 systems)

$\log D_{Cf} = -0.51 - 1.41\,\Sigma\sigma^* + 0.78\,\Sigma E_s^*$ (20 systems)

$\log D_{Es} = -0.55 - 2.28\,\Sigma\sigma^* + 1.04\,\Sigma E_s^*$ (20 systems)

$\log \bar{K}_{HNO_3} = -0.315 - 0.28\,\Sigma\sigma^* + 0.68\,\Sigma E_s^* + 0.52\,(\Sigma E_s^* + 1.34)\,BP$, ($\sim$ 50 systems)

$\log K_{HA} = 16.37 + 1.20\,BP^* + 0.18\,\Delta G_{hydr}$ (for trioctylamine) (30 systems)

$\log K_{HA} = 12.76 + 1.47\,BP^{x+} + 0.148\,\Delta G_{hydr}$ (for trilaurylamine) (20 systems)

2) Anion exchange (cation : trioctyloctadecylammonium)

$\log K_x^y = 0.236\,(\Delta G_x - \Delta G_y)$ (50 systems)

3) Extraction by extractants containing phosphoryl groups

$\log \bar{K}_{HNO_3} = -1.60 - 0.724\,\Sigma\sigma\phi + 0.009\,BP - 0.202\,BP\Sigma\sigma\phi$ (30 systems)

$\log K_{Pu} = -0.18 - 3.03\,\Sigma\sigma\phi + 0.33\,BP\Sigma\sigma\phi$ ($\sim$ 35 systems)